

**Protective microglial activation in
Alzheimer's disease pathogenesis**

Patrick Jarmo Paasila

Discipline of Pathology
School of Medical Sciences
Faculty of Medicine and Health
The University of Sydney

A thesis submitted in fulfilment of the requirements
for the degree of Doctor of Philosophy (Medicine)

August 2021

Statement of originality

This is to certify that the content of this thesis is my own work. This thesis has not been submitted for any other degree or purpose.

I certify that the intellectual content of this thesis is the product of my own work and that all the sources and assistance received in its preparation have been acknowledged.

A solid black rectangular box used to redact the signature of the author.

Patrick Jarmo Paasila

30th June 2021

Dedication

To beautiful people everywhere. And the family :P

Abstract

The burden of Alzheimer's disease (AD) is rapidly increasing due to an ageing population and a lack of disease-modifying therapeutics. The symptoms of AD reflect irreversible neuronal loss and treatments ideally need to be implemented during its presymptomatic stage. One major paradigm for modelling the spread of A β plaques and tau-associated neurofibrillary degeneration—the hallmark pathologies of AD—in post-mortem tissue is to determine the prevalence of their deposition in different brain regions across the clinical spectrum of the disease. This approach was used by diagnosticians in the early 1990s to predict the hierarchical involvement of functionally connected brain regions through the natural course of the disease and today forms the basis of the most up to date recommendations for the post-mortem neuropathological diagnosis of AD, which predict heavy involvement of association cortices and relative sparing of primary cortices. These hallmark pathologies coincide at sites termed neuritic plaques and are associated with microgliosis. Microglia are further implicated in the pathogenesis of AD in mouse models and genome-wide association studies.

Here it was of interest to determine the spatiotemporal relationships between A β , tau, and microglial pathological changes in post-mortem human AD brains by comparing brain regions that were expected to be differentially affected by the disease as set out by the established diagnostic schema. Immunohistochemistry and immunofluorescence histochemistry targeting A β , total tau, and the pan-microglia marker ionised calcium binding adaptor molecule 1 (Iba1) was performed in three regions of decreasing pathological severity: inferior temporal cortex, superior frontal cortex, and primary visual cortex of ten controls, five controls with Alzheimer changes (CAc), and eight AD cases. Following a validated modified disector sampling approach, using manual and corroborative automated methods, the results showed that activated microglia predominated in the inferior temporal cortex of CAc. AD brains were characterised by increased clustering of activated microglia in the primary visual cortex and a loss of clustering and ramified healthy microglia in the inferior temporal cortex. Brain pH was found to be an important effector of microglial dystrophy suggesting antemortem (agonal) factors may confound post-mortem investigations of microglia morphology. Although the inferior temporal cortex showed significant atrophy and loss of neurons, it did not differ in hallmark pathological load to the primary visual and superior frontal cortices. Therefore, no clear inferences as to the sequence of pathological changes could be made. To address this,

tissue from the primary motor cortex of the same cohort was sourced and examined. The primary motor cortex showed no atrophy or neuronal loss, including no degeneration of prominent layer Vb pyramidal Betz cells, and showed a significantly reduced A β and tau load compared to the inferior temporal cortex. Further, clustering of microglia was significantly greater in the mildly affected primary motor cortex compared to the severely affected inferior temporal cortex which showed a relatively impaired microglial clustering response. These clusters coincided with the deposition of A β but before tau-positive neuritic dystrophy was evident, suggesting that the activation of microglia is upstream of tau-associated neurofibrillary degeneration. Nevertheless, the phagocytic potential of microglia in the context of AD was confirmed by both conventional confocal microscopy in the primary motor cortex and super-resolution ground-state depletion microscopy in available sections from the superior frontal cortex.

The prominence of microglial clustering at A β plaques in the more mildly affected regions of the AD brain and the widespread activation of microglia in CAC suggested that microglial functional responses may differ with regard to the maturity of A β pathology. To investigate this, a gene expression study of microglial functional changes in response to treatment with different doses of synthetic A β monomers and mature fibrils was undertaken. Murine organotypic brain slice cultures showed an upregulation of markers involved in microglia-mediated phagocytosis and a major anti-inflammatory pathway in response to treatment with A β monomers. Conversely, extended treatments with fibrillar species of A β induced gene transcriptional changes similar to pro-inflammatory, phagocytically active neurotoxic microglia described in some mouse studies. Overall, findings presented here suggest that the activation of microglia in response to monomeric A β may be neuroprotective. This activation is seen most prominently in CAC and mildly affected regions of the AD brain, with culture models suggesting that A β monomers may induce neuroprotective activation, whereas fibrillar A β , in concert with neurofibrillary pathology and likely neurotoxic A β oligomers and fibrils, induces a phagocytic, neurodegenerative phenotype.

Acknowledgements

There are a number of people who I would like to thank for helping me at different times during my candidature. First, a big thank you to my supervisor Greg Sutherland for all of the support throughout. I really appreciate the opportunity Greg gave me to do a PhD in his group, particularly since I was out from medical school at another university. Greg always showed good humour and enviable wit—I'm still secretly working on how to steal it. I enjoyed our many arguments and discussions; may they ever continue in our future work. I'd also like to thank Claire Goldsbury and Danielle Davies with whom I worked for my first two publications. Both were very welcoming and always open to having a chat. I'd like to thank Markus Hofer for having me a short while in his lab to do the culture work and Barney Viengkhou for teaching me various culture techniques. Many thanks also to Joe Ciccotosto at The University of Melbourne for getting me started on using the notorious A β peptide; Manuel Graeber for giving me the proverbial professorial kick every once in a while—I look forward to working more with Manuel in the future; and the many other friendly faces, including Shelley Forrest, Caine Smith, Clair De Sousa, Julia Lim, and Hamish Mundell. I'd also like to thank all past, present, and future brain donors for the amazing gift you leave behind; your contribution makes all of this possible. Finally, to the family—thanks for all your love and support!

List of publications

First author publications

Paasila, P. J., Davies, D. S., Kril, J. J., Goldsbury, C., & Sutherland, G. T. (2019). The relationship between the morphological subtypes of microglia and Alzheimer's disease neuropathology. *Brain Pathol.* doi:10.1111/bpa.12717

Paasila, P. J., Davies, D. S., Goldsbury, C., & Sutherland, G. T. (2020). Clustering of activated microglia occurs before the formation of dystrophic neurites in the evolution of A β plaques in Alzheimer's disease. *Free Neuropathol.* doi:10.17879/freeneuropathology-2020-2845

Paasila, P. J., Fok, S. Y. Y., Flores-Rodriguez, N., Sajjan, S., Svahn, A. J., Dennis, C. V., Holsinger, R. M. D., Kril, J. J., Becker, T. S., Banati, R. B., Sutherland, G. T., & Graeber, M. B. (2021). Ground state depletion microscopy as a tool for studying microglia-synapse interactions. *J Neurosci Res.* doi:10.1002/jnr.24819

Other published contributions

Guennewig, B., Lim, J., Marshall, L., McCorkindale, A. N., **Paasila, P. J.**, Patrick, E., Kril, J. J., Halliday, G. M., Cooper, A. A., & Sutherland, G. T. (2021). Defining early changes in Alzheimer's disease from RNA sequencing of brain regions differentially affected by pathology. *Sci Rep*, 11(1), 4865. doi:10.1038/s41598-021-83872-z

List of conference proceedings

Paasila, P. J., & Sutherland, G. T. (2019). *Neuroprotective activation of microglia in the pathogenesis of Alzheimer's disease.* Presentation at the Biology Domain Seminar Series, Camperdown NSW Australia: The University of Sydney.

Paasila, P. J., Davies, D. S., Goldsbury, C., & Sutherland, G. T. (2019). *Microglial activation in the motor cortex of Alzheimer's disease cases and inferior temporal cortex of non-demented individuals with high Alzheimer's-type pathology.* Poster presented at the Alzheimer's Association International Conference, Sydney NSW Australia: Alzheimer's Association.

Paasila, P. J., Davies, D. S., Goldsbury, C., & Sutherland, G. T. (2019). *Microglial activation in the motor cortex of Alzheimer's disease cases and inferior temporal cortex of non-demented individuals with high Alzheimer's-type pathology.* Presentation at the Back to Basics Workshop—Understanding the Molecular basis of Alzheimer's disease, North Ryde NSW Australia: Macquarie University.

Paasila, P. J., Davies, D. S., Goldsbury, C., & Sutherland, G. T. (2018). *Microglial subtypes in differentially affected areas of the Alzheimer's disease brain.* Poster presented at the Australian Dementia Forum, Sydney NSW Australia: NHMRC National Institute for Dementia Research.

Paasila, P. J., Davies, D. S., Goldsbury, C., Kril, J. J., & Sutherland, G. T. (2017). *Spatiotemporal relationships between pathological changes and microglial subtypes in differentially affected areas of the Alzheimer's disease brain.* Poster presented at the ANS 37th Annual Meeting, Sydney NSW Australia: Australasian Neuroscience Society.

List of awards

Winnett Specialist Group Scholarship Programme, 2021.

Brain Pathology, Top 10 Most Accessed Articles in 2019, published in 2019.

Professor John Irvine Hunter Prize for Research in Anatomical Sciences, 2019.

Figures and tables

List of figures

Figure 1. Preparations of A β ₄₂ peptides, pg. 175.

Figure 2. Isolation of neonatal mouse brain slice cultures, pg 177.

Figure 3. cPCR of genes of interest, pg 179.

Figure 4. ddPCR assay output, pg 182.

Figure 5. References genes for mouse BSCs, pg 185.

Figure 6. Genes of interest for mouse BSCs, pg 186.

Figure 7. Gene amplification studies in the PreC and PVC of AD and control brains, pg 188.

List of tables

Table 1. Murine genes of interest, pg 179.

Table 2. Human genes of interest, pg 183.

List of abbreviations

5-HT _n	5-hydroxytryptamine; <i>n</i> denotes [receptor] type
AA	Alzheimer's Association
ABC	Amyloid- β plaque Thal phases, Braak neurofibrillary tau staging, and the Consortium to Establish a Registry for Alzheimer's disease protocol for neuritic plaques combination scoring system for the neuropathological diagnosis of Alzheimer's disease
ABS	Australian Bureau of Statistics
ACH	Amyloid cascade hypothesis
ACh	Acetylcholine
AD	Alzheimer disease
AICD	Amyloid precursor protein intracellular domain
AIHW	Australian Institute of Health and Welfare
ALS	Amyotrophic lateral sclerosis
APOE	Apolipoprotein E
APP	Amyloid precursor protein
APPs α	Secreted amyloid precursor protein ectodomain α
APPs β	Secreted amyloid precursor protein ectodomain β
ATP	Adenosine triphosphate
A β _n	β -amyloid; <i>n</i> indicates peptide length in number of amino acid residues
A β DP	A β -degrading protease
BDNF	Brain derived neurotrophic factor
BBB	Blood brain barrier
BSC	Brain slice culture
bvFTD	Frontotemporal dementia, behavioural variant
CAA	Cerebral amyloid angiopathy
CAn	<i>Cornu Ammonis</i> ; <i>n</i> indicates the number of the hippocampal subfield
CBD	Corticobasal degeneration
CD	Cluster of differentiation
CDR	Clinical dementia rating
CERAD	Consortium to Establish a Registry for Alzheimer's disease
COX	Cyclooxygenase

CPC	Clinicopathological correlation
CSF	Cerebrospinal fluid
CSF1R	Colony stimulating factor 1 receptor
CTE	Chronic traumatic encephalopathy
C-terminal	Carboxyl terminal
CX ₃ CR1	CX ₃ C chemokine receptor 1
DALY	Disability-adjusted life years
DAMP	Damage/danger-associated molecular pattern
ddPCR	Droplet digital polymerase chain reaction
DEG	Differentially expressed gene
DIAN	Dominantly Inherited Alzheimer Network
DIAD	Dominantly inherited Alzheimer's disease
DMT	Disease-modifying therapeutic
DN	Dystrophic neurite
DNA	Deoxyribonucleic acid
<i>En</i>	<i>n</i> th day of embryonic development
EC	Entorhinal cortex
EM	Electron microscopy
EOAD	Early-onset AD
fAD	Familial AD
FDA	Food and Drug Administration
FDG	Fluorodeoxyglucose
FTD	Frontotemporal dementia
GABA	γ aminobutyric acid
GBD	Global Burden of Disease
GVB	Granulovacuolar degeneration body
GWAS	Genome-wide association study
HLA	Human leucocyte antigen
HMWO	High molecular weight (A β) oligomers
H&E	Haematoxylin and eosin
HS	Hippocampal sclerosis
Iba1	Ionised calcium-binding adaptor molecule 1
IF	Immunofluorescence

IHC	Immunohistochemistry
IL	Interleukin
ITC	Inferior temporal cortex
KO	Knock-out
LB	Lewy body
LBD	Lewy body dementia
LMWO	Low molecular weight (A β) oligomers
LOAD	Late-onset AD
LPS	Lipopolysaccharide
MAP	Microtubule associated protein
MAPK	Mitogen-activated protein kinase
MAPT	Microtubule associated protein tau
MHC	Major histocompatibility complex
MRI	Magnetic resonance imaging
mRNA	Messenger ribonucleic acid
MTL	Medial temporal lobe
nAChR	Nicotinic acetylcholine receptor
NEP	Neutral endopeptidase [also, neprilysin]
NFT	Neurofibrillary tangle
NF- κ B	Nuclear factor κ B
NIA	National Institute on Aging
NLR	NOD-like receptor
NMDA	N-methyl-D-aspartate
NO	Nitric oxide
NOD	Nucleotide binding and oligomerisation domain
NP	Neuritic plaque
NT	Neuropil thread
N-terminal	Amino terminal
PAF	Platelet-activating factor
PAMP	Pathogen-associated molecular pattern
PD	Parkinson's disease
PET	Positron emission tomography
PHF	Paired helical filament

Phosphotau	Hyperphosphorylated tau
PMC	Primary motor cortex
PMI	Post-mortem interval
PMT	Post-translational modification
PNFA	Progressive non-fluent aphasia
PPA	Primary progressive aphasia
PreAD	Preclinical Alzheimer's disease
PreC	Precuneus
PRR	Pattern recognition receptor
<i>PSEN1/2</i> [<i>PS_n</i>]	Presenilin gene [<i>n</i> denotes subtype]
PSF	Point spread function
PSP	Progressive supranuclear palsy
p-tau _{<i>n</i>}	Phosphorylated tau; <i>n</i> indicates the amino acid site of phosphorylation
PVC	Primary visual cortex
RIP	Regulated intramembrane proteolysis
RNA-Seq	RNA sequencing
ROS	Reactive oxygen species
scRNA-Seq	Single-cell RNA sequencing
SD	Standard deviation
SDS	Sodium dodecyl sulphate
SF	Straight filament
SFC	Superior frontal cortex
SiTH	Signal transduction hypothesis [an acronym proposed here]
SMLM	Single molecule localisation microscopy
snRNA-Seq	Single-nuclei RNA sequencing
Syp	Synaptophysin
TDP43	Transactive response DNA-binding protein 43
TNF	Tumour necrosis factor
TGFβ	Transforming growth factor
TLR	Toll-like receptor
TMEM119	Transmembrane protein 119
TREM2	Triggering receptor expressed on myeloid cells 2
Trk	Tropomyosin receptor kinase

TTau	Total tau
TTX	Tetrodotoxin
VIP	Vasoactive intestinal peptide
α CTF	α APP carboxyl-terminal fragment
β CTF	β APP carboxyl-terminal fragment

Table of Contents

Statement of originality.....	ii
Dedication.....	iii
Abstract	iv
Acknowledgements.....	vi
List of publications	vii
List of conference proceedings	viii
List of awards.....	ix
Figures and tables.....	x
List of figures	x
List of tables	x
List of abbreviations.....	xi
Chapter 1: Introduction.....	1
1.1 Epidemiology of dementia	1
1.1.1 Frequency	1
1.1.2 Societal impact	2
1.1.3 Risk factors.....	3
1.1.4 Protective factors.....	4
1.2 Diagnostics of Alzheimer's disease	5
1.2.1 Clinical diagnosis	5
1.2.2 Neuropathological diagnosis	8
1.2.3 Clinicopathological correlations	13
1.3 Major proteinopathies of Alzheimer's disease	15
1.3.1 β -amyloid	15
1.3.2 Tau.....	20
1.4 Other neuropathological features	25
1.4.1 Atrophy.....	25
1.4.2 Loss of neurons and synapses	25
1.4.3 Gliosis.....	26
1.4.4 Cerebral amyloid angiopathy	26
1.4.5 Granulovacuolar degeneration bodies	27
1.4.6 Hirano bodies	27
1.4.7 White matter hyperintensities.....	28

1.5	Genetics of Alzheimer's disease	28
1.5.1	Familial disease	28
1.5.2	Sporadic disease	29
1.6	Microglia	31
1.6.1	Historical perspectives	31
1.6.2	Ontogeny of microglia	32
1.6.3	Morphological study of microglia.....	33
1.6.4	Molecular characteristics.....	38
1.6.5	Physiology	46
1.6.6	Involvement in Alzheimer's disease	49
1.7	Hypotheses of Alzheimer's disease pathophysiology	51
1.7.1	Amyloid cascade hypothesis	51
1.7.2	Tau propagation hypothesis	52
1.7.3	Inflammation hypothesis	53
1.7.4	Neurotransmitter hypotheses.....	53
1.7.5	Other hypotheses	54
1.8	Experimental paradigms	55
1.8.1	Experimental neuropathology	55
1.8.2	Organotypic slice culture	56
1.9	Thesis overview.....	57
1.9.1	Hypotheses	57
1.9.2	Experimental aims.....	58
1.9.3	Further details.....	59
 Chapter 2: The relationship between the morphological subtypes of microglia and Alzheimer's disease neuropathology.....		
		60
2.1	Preamble	60
2.2	Authorship attribution statement	61
2.3	Published manuscript	61
2.4	Published supplementary material	77
2.5	Application for the Professor John Irvine Hunter Prize for Research in Anatomical Sciences	88
 Chapter 3: Clustering of activated microglia occurs before the formation of dystrophic neurites in the evolution of Aβ plaques in Alzheimer's disease		
		109
3.1	Preamble	109
3.2	Authorship attribution statement	110
3.3	Published manuscript	110

Chapter 4: Ground state depletion microscopy as a tool for studying microglia-synapse interactions.....	129
4.1 Preamble	129
4.2 Authorship attribution statement	130
4.3 Published manuscript	130
4.4 Published supplementary material	149
Chapter 5: Gene amplification studies	169
5.1 Preamble	169
5.2 Authorship attribution statement	170
5.3 Introduction	171
5.4 Methods	172
5.4.1 Animal handling	172
5.4.2 Preparation of A β solutions.....	173
5.4.3 Isolation of brain slices	176
5.4.4 Culture procedures	177
5.4.5 ddPCR of mouse samples.....	178
5.4.6 Human cohort	181
5.4.7 ddPCR of human samples	182
5.4.8 Statistics	184
5.5 Results	184
5.5.1 ddPCR of mouse BSCs	184
5.5.2 ddPCR of human samples	186
5.6 Discussion	187
Chapter 6: Discussion	196
6.1 Summary of key findings.....	196
6.1.1 Activation of microglia in PreAD and loss of healthy microglia in AD	196
6.1.2 Activation of microglia precedes NFD	197
6.1.3 Increased phagocytosis of (pre-)synapses in AD	198
6.1.4 Microglia react more potently to monomers than fibrils of A β	198
6.1.5 Immune activation and phagocytosis coincides with mild AD	198
6.2 Contextualisation of findings.....	199
6.2.1 Neuropathology	199
6.2.2 Relationships between microglia and AD neuropathology	200
6.2.3 Immune activation and phagocytosis in mild AD	202
6.3 Strengths and weaknesses.....	204
6.3.1 Post-mortem human brain tissue	204
6.3.2 Quantitative neuropathology	204
6.3.3 Gene amplification studies	205

6.4	Conclusions	206
	References	207
	Appendix	287

Chapter 1: Introduction

1.1 Epidemiology of dementia

1.1.1 Frequency

Alzheimer's disease (AD) is the commonest cause of dementia, comprising 60–80% of all cases (Alzheimer's Association, 2020; Brookmeyer et al., 2011). Currently, one in 10 Australians over the age of 65 and three in 10 over 85 are living with dementia. The total estimated number of people with dementia in Australia is 459,000, but with an additional 250 diagnoses being made per day, which is predicted to increase to 650 by 2056 (Brown et al., 2017), this is expected to more than double to over one million by 2058 (Dementia Australia, 2018). Deaths due to dementia numbered 13,963 in 2018, an increase of 68.6% since 2009, making it the second leading cause of death in Australia after ischaemic heart disease (ABS, 2019).

Globally, the total number of people living with dementia increased by 20.2 million in 1990 to 43.8 million in 2016 (Nichols et al., 2019). The increase in the number of dementia sufferers by Global Burden of Disease (GBD) region is largely driven by population growth, ageing populations, and longer survival with dementia (Prince et al., 2016). Evidence on the trends of the age-standardised prevalence of dementia over time is very mixed and varies by GBD region (Stephan et al., 2018). For instance, Nichols et al. (2019) reported a minor increase of 1.7% in the global prevalence of dementia from 1990 to 2016, whereas at least three other reviews have indicated minor decreases over roughly the same time period, particularly in high income countries with improved living conditions, education, and healthcare (Prince et al., 2016; Roehr et al., 2018; Wu et al., 2017). More importantly, however, Nichols et al. (2019) also identified that 6.4 million of the estimated 28.8 million disability-adjusted life years (DALY) due to dementia were attributable to modifiable risk factors including obesogenic diets, sugar-sweetening, and smoking, meaning that current trends in the overall burden of disease can be significantly reduced even in the absence of any new disease-modifying therapeutics (DMTs).

1.1.2 Societal impact

Economic cost

The total annual direct cost of dementia in Australia was AUD \$8.8 billion in 2016 and \$9.1 billion in 2017. These costs, which include medical expenses for hospitalisations, general practitioner (GP) and specialist consultations, medications, aged care, and transportation, are expected to rise to \$24.1 billion by 2056. Indirect costs due to dementia include the loss of productivity and income of patients and carers and amounted to approximately \$5.6 billion in 2017. Over the next 40 years the total direct and indirect economic cost of dementia in Australia is projected to be in excess of \$1 trillion, in constant 2016 dollar terms (Brown et al., 2017).

The total estimated worldwide cost of dementia was USD \$604 billion in 2010 and \$818 billion in 2015, accounting for ~1.09% of aggregate global gross domestic product (GDP). Assuming current trends, the total cost of dementia will likely reach \$2 trillion by 2030 (Wimo et al., 2013; Wimo et al., 2017). It is important to recognise that the advent of any new DMTs will not necessarily result in absolute cost savings because of costs associated with treatment, care, and prolonged DALY. Cost effectiveness with regard to societal ‘willingness to pay’ per gained quality-adjusted life years (QALY) is therefore a more reasonable measure for consideration when modelling the economic impact of newly developed DMTs (Wimo et al., 2020).

Burden of disease and comorbidity

The age-standardised burden of disease measured in DALY due to dementia in Australia jumped from 12th in 2003 to 5th in 2015 (due in part to changes in practices of coding deaths) (AIHW, 2019a). Dementia disproportionately affects the elderly and is one of the three biggest causes of disease burden in both men and women over the age of 75 (AIHW, 2019a). People with dementia experience more hospitalisations, including for non-neurological symptoms such as hip fractures (Scandol et al., 2013) and unintentional poisoning (Mitchell et al., 2015), are more likely to develop nosocomial complications such as pneumonia and ulcers (Bail et

al., 2015), and require a higher level of care than non-demented patients, particularly as the disease progresses and its clinical complexity increases (AIHW, 2019b).

Dementia also indirectly contributes to the overall burden of disease through associated psychiatric and non-psychiatric comorbidities. Psychiatric disorders which include anxiety, depression, bipolar disorder, schizophrenia, and psychosis are all well recognised comorbidities of dementia (Casanova et al., 2011; Garcez et al., 2015; Muliya & Varghese, 2010; Starkstein et al., 2008). Late-life psychological distress also carries with it an increased risk of dementia-related mortality (Rosness et al., 2016). Further, spousal or other caregivers of persons with dementia are also at a higher relative risk of developing an anxiety or depressive disorder (Cuijpers, 2005; Joling et al., 2015). Dementia is also associated with a host of somatic (non-psychiatric) comorbidities (Bunn et al., 2014; Duthie et al., 2011; Nelis et al., 2019) such as glaucoma (Mancino et al., 2018), bone fracture (Harvey et al., 2017), osteoporosis (Downey et al., 2017), and sleep apnoea (Emamian et al., 2016). Dementia, along with depression, has also been found to be the commonest comorbidity of cerebrovascular disease, musculoskeletal disease, diabetes, and other diseases of the nervous system in a review of the Australian permanent aged care population (Hillen et al., 2017).

1.1.3 Risk factors

There are many known non-genetic risk factors for AD, the largest group of which is cerebrovascular disease and its own antecedent risk factors. These include cardiovascular disease, smoking, hypertension, type 2 diabetes mellitus, obesity—although questionably (Qizilbash et al., 2015), and dyslipidaemia (Reitz & Mayeux, 2014). Among the proposed mechanisms by which some of these factors might lead to dementia include post-stroke amnesic syndromes due to site-specific parenchymal damage and the elevation of β -amyloid ($A\beta$) pathology by hypoxia-induced overexpression of the cyclin-dependent kinase 5/activator protein 25 system which leads to increased β -secretase 1 (BACE1) levels and thus higher amyloid precursor protein (APP) catabolism (Camins et al., 2006; Mayeux & Stern, 2012) or through impaired $A\beta$ clearance due to hyperinsulinaemia in the case of

diabetes (Farris et al., 2003). Refer to section 1.3.1 for more information on APP and A β metabolic pathways.

Other independent factors which have been linked to an increased risk of developing AD include depression (Ownby et al., 2006); midlife psychological distress (Skogen et al., 2015); dysthyroidism (Tan & Vasan, 2009); frailty (Borges et al., 2019); midlife insomnia and late-life prolonged sleep (Sindi et al., 2018); traumatic head injury (Fleminger et al., 2003; Franz et al., 2003); excessive alcohol consumption, and air pollution (Livingston et al., 2020). The 2020 report of the Lancet Commission argues that by modifying 12 key dementia risk factors—including tackling inequality—as much as 40% of future dementias can be delayed or prevented (Livingston et al., 2020).

1.1.4 Protective factors

Epidemiological studies show that there are many non-genetic factors which protect against AD or provide symptomatic relief. These include consumption of a Mediterranean diet which is high in fruit, vegetables, cereals, nuts, legumes, seeds, fish, and olive oil and low in red and processed meats and poultry (Cremonini et al., 2019; Petersson & Philippou, 2016; Yusuf et al., 2017); high educational attainment, particularly in developed countries (Sharp & Gatz, 2011); having a strong social network (Fratiglioni et al., 2004); participation in cognitively stimulating activities in old age (Wilson et al., 2010) and greater cognitive activity during midlife, particularly in apolipoprotein E (APOE) ϵ 4 carriers (Carlson et al., 2008); long-term physical exercise (Meng et al., 2020); and meditation (Russell-Williams et al., 2018). It will be important to ensure that awareness and knowledge of ways to prevent dementia continue to increase to reduce its future incidence (Pickett et al., 2018).

1.2 Diagnostics of Alzheimer's disease

1.2.1 Clinical diagnosis

All-cause dementia

The National Institute on Aging (NIA) and the Alzheimer's Association (AA) workgroup provides the most up to date criteria for the diagnosis of all-cause and AD dementia (McKhann et al., 2011). The original criteria were set out by the Neurological and Communicative Disorders and Stroke and the Alzheimer Disease and Related Disorders Association (NINCDS-ADRDA) workgroup (McKhann et al., 1984). These criteria proved reliable over time (Galasko et al., 1994; Lim et al., 1999), but were updated to include advances in neuropsychological assessment, brain imaging, neuropathology, and biomarker and genetic screening. The core clinical criteria for all-cause dementia is the presence of cognitive or behavioural symptoms that: (1) interfere with the ability to function at work or during other daily activities; (2) represent a deterioration from a previous level of performance; (3) are not caused by delirium or other psychiatric disease; (4) are detectable through formal history-taking and cognitive testing; and (5) include at least two of the following: (i) memory impairment, (ii) executive impairment—including poor decision making and planning of complex activities, (iii) visuospatial impairment—including the inability to operate simple tools, recognise faces or objects, or orient clothing, (iv) language impairment—including simple grammatical errors, poor recall of words, or hesitation in speech, or (v) altered personality—including mood swings, apathy, or social withdrawal.

Alzheimer's disease dementia

The NIA-AA workgroup proposed the following classifications for individuals with AD dementia: (1) Probable AD dementia, (2) Possible AD dementia, and (3) Probable or Possible AD dementia with evidence of the AD pathophysiological process. The lattermost being reserved mainly for the purposes of research. Probable AD dementia is diagnosed when the patient meets the criteria for all-cause

dementia and displays: (i) an onset of symptoms over months or years, (ii) a clear and progressive deterioration in cognition by report or observation, and (iii) initially and most prominently presents with either (a) amnesia and impairment of one other domain of all-cause dementia outlined above, or (b) a non-amnestic condition including deficits in either language, visuospatial ability, or executive function with concurrent impairment in at least one other domain. The diagnosis of Probable AD dementia cannot be made where there is substantial cerebrovascular disease or extensive white matter rarefaction seen as hyperintensities on magnetic resonance imaging (MRI), evidence for another neurological or non-neurological disease with cognitive sequelae, or core features of another dementia such as Lewy Body Dementia (LBD) or frontotemporal dementia (FTD), including its behavioural variant (bvFTD), primary progressive aphasia (PPA), progressive non-fluent aphasia (PNFA), or related tauopathies such as corticobasal degeneration (CBD), progressive supranuclear palsy (PSP), Pick's disease, argyrophilic grain disease (AGD), multiple system tauopathy with dementia, neurofibrillary tangle dementia, and amyotrophic lateral sclerosis (ALS) (Rabinovici & Miller, 2010). Further, a diagnosis of Probable AD dementia with increased level of certainty can be made where the cognitive decline has been documented in the context of either formal clinical evaluations or standardised mental status examinations. Possible AD dementia is diagnosed when the core clinical criteria for AD dementia are satisfied but where the course of the dementing syndrome is atypical (such as rapid onset), there is insufficient historical detail or documentation of cognitive decline, evidence of mixed disease such as concomitant cerebrovascular disease or another dementing condition, or evidence of any other comorbidity, medication, or substance that might have a significant impact on cognition (McKhann et al., 2011).

The NIA-AA clinical diagnostic criteria provide two further categories to reflect the full continuum of the AD pathophysiological process. Preclinical AD (PreAD), also termed 'asymptomatic at-risk state for AD' and 'presymptomatic AD' (Dubois et al., 2010), refers to individuals who exhibit AD-type biomarker changes in the absence of any clinically detectable dementia syndrome (Sperling et al., 2011). Although the presence of AD-type biomarkers confers increased longitudinal risk of AD (Shim & Morris, 2011), this designation is mainly reserved for research purposes and future drug testing as it rests on what is ultimately the hypothetical

progression of such people to AD dementia. Mild cognitive impairment (MCI) is the final set of criteria to describe the complete clinical disorder that is AD. This designation may be applicable where a patient displays a deterioration of cognition which does not significantly impact their independence or functional ability. Cognitive testing is the best means to determine the presence of MCI which typically presents as 1 to 1.5 standard deviations below age and education-matched peers (Albert et al., 2011).

Biomarkers of Alzheimer's disease

In vivo biomarkers of the AD pathophysiological process include different imaging modalities and fluid analytes. The five most widely used were formally incorporated in the NIA-AA criteria and are only intended to complement the clinical diagnostic criteria (Jack et al., 2011). The preferred biomarkers in the criteria are those that are tied most closely to the pathological criteria for AD. As such they are divided into two broad categories: (1) biomarkers of A β accumulation—including decreased cerebrospinal fluid (CSF) A β ₄₂ and increased Pittsburgh compound B (PiB) binding to fibrillar A β deposits in the brain on positron emission tomography (PET) imaging, and (2) biomarkers of neuronal degeneration or injury—including elevated CSF tau (both total and phosphorylated forms), decreased fluorodeoxyglucose (FDG) uptake on PET imaging in a specific topographic pattern involving the temporoparietal cortex, and thirdly ventricular enlargement and atrophy of medial, basal, and lateral temporal lobe areas and medial and lateral parietal cortices on structural MRI. The onset and progression of AD biomarkers likely follows an ordered temporal pattern beginning with changes to A β markers followed by alterations to markers of neurodegeneration (Craig-Schapiro et al., 2009; Fagan et al., 2009; Jack et al., 2010; Mattsson-Carlsson et al., 2020; Perrin et al., 2009). Notwithstanding the apparent sequence of changes there is insufficient data to establish a clear hierarchical system to arbitrate between the presence and absence of different combinations of biomarkers in individual cases (McKhann et al., 2011).

In addition to those outlined above, there are many other potential biomarkers for AD. These include non-A β and non-tau-based proteomics (Park et al., 2020); quantitative-MRI techniques such as resting state functional network connectivity MRI (Buckner et al., 2005), diffusion tensor imaging (Bozzali et al., 2016), and proton-nuclear magnetic resonance spectroscopy (Kantarci, 2007); electroencephalography (EEG) (Vecchio et al., 2018); and most recently a new blood serum test for phosphorylated tau-threonine 217 (p-tau₂₁₇) (Barthélemy et al., 2020b; Barthélemy et al., 2020a). Serum p-tau₂₁₇ distinguishes controls from AD patients, in whom it is 5.7–8 times higher, with an accuracy of 90–99% in cases positive for A β on PET imaging. It can also distinguish AD dementia from non-AD dementias, including primary tauopathies such as bvFTD, PPA, PNFA, PSP, and CBD, with an accuracy of up to 96%; soundly outperforming the accuracy of other commonly used biomarkers such as p-tau₁₈₁ (Janelidze et al., 2020), neurofilament light chain, and imaging markers (Palmqvist et al., 2020). Serum p-tau₂₁₇ also has the potential to identify PreAD individuals as it has been shown to be elevated roughly 20 years before the onset of symptoms in cases of dominantly inherited AD (DIAD) sourced from the Dominantly Inherited Alzheimer Network (DIAN) (Barthélemy et al., 2020c). This result was similarly demonstrated in a study of individuals from the Colombian Autosomal-Dominant AD Registry, who carry the presenilin-1 (*PSEN1*) E280A mutation (Paisa mutation), in which p-tau₂₁₇ was significantly higher by 25 years of age compared to non-carriers; again occurring roughly 20 years before the average age of onset of dementia in Paisa mutation carriers (Palmqvist et al., 2020).

1.2.2 Neuropathological diagnosis

The NIA-AA provides the most up to date recommendations (Hyman et al., 2012) for the post-mortem neuropathological assessment of AD, which remains the gold-standard for confirmatory diagnosis. A β plaques and neurofibrillary tangles (NFTs) are the *sine qua non* of AD neuropathological changes. Immunohistochemistry (IHC) targeting A β and tau, or p-tau, are the preferred methods for assessing diffuse non-neuritic A β plaques and NFTs respectively. The preferred method for detecting neuritic plaques (NPs), a subset of A β plaques that are associated with dystrophic neurites (DNs), is Thioflavin S or modified Bielschowsky silver staining. In

addition to these, other methods for visualising A β deposits (although also non- A β amyloids ; refer to Benson et al. (2018) for a definition of ‘amyloid’) have also been described, including, Thioflavin T (Biancalana & Koide, 2010; Vassar & Culling, 1959), Congo red—which exhibits apple-green birefringence (Howie et al., 2008; Yakupova et al., 2019), and many other silver impregnation techniques for NPs by Bodian, Campbell-Switzer, Cross, Gallyas, Grocott-Gömöri, and Naoumenko-Feigin (Lamy et al., 1989; Uchihara, 2007). Other neuropathological features of AD include the loss of synapses and neurons, atrophy, gliosis, cerebral amyloid angiopathy (CAA), white matter degeneration, hippocampal granulovacuolar degeneration and actin-immunoreactive Hirano bodies, transactive response DNA-binding protein 43 (TDP43) inclusions, and Lewy bodies (LBs). It is also important to recognise that all of the aforementioned neuropathological characteristics, including plaques and tangles, are not exclusively seen in AD but are commonly found in healthy aged brains (Berg et al., 1998; Davis et al., 1999; Guillozet et al., 2003; Hof et al., 1996; Knopman et al., 2003; Price et al., 2009; Sengoku, 2020; Xekardaki et al., 2015).

ABC score

The NIA-AA also provides practical guidelines for the neuropathological assessment of AD (Montine et al., 2012). These guidelines set out an ‘**ABC**’ scoring system of AD changes which combines scores from three previously described schema: (1) A β plaque phases (Thal et al., 2002), (2) Braak staging of NFTs (Braak & Braak, 1991), and (3) the Consortium to Establish a Registry for AD (CERAD) protocol for NPs (Mirra et al., 1991). A stepwise approach to a set of minimum recommended brain regions for the assessment of A β plaques is suggested, beginning with the superior and middle temporal gyri, middle frontal gyrus, inferior parietal lobule, and occipital cortex. It is also suggested that leptomeningeal and parenchymal vessels are screened for CAA. If A β plaques are identified in these primary cortical regions then it is recommended that secondary regions are examined, including, the hippocampus, entorhinal cortex (EC), and basal ganglia including the nucleus basalis of Meynert at the level of the anterior commissure are screened next, followed by tertiary regions: cerebellar cortex, dentate nucleus, and midbrain including the substantia nigra. The minimum recommended regions for

assessing the spread of NFTs and NPs include the primary regions stipulated above for A β plaques, but critically with the inclusion of the hippocampus and EC. It is also recommended that haematoxylin and eosin (H&E) stains are performed to screen for hippocampal sclerosis (HS) and vascular brain injury in all of the minimum recommended regions. Lastly, IHC or H&E for LBs might also be performed following a similar stepwise approach beginning with the medulla, pons, midbrain, and amygdala followed by at least one of the anterior cingulate, middle frontal gyrus, superior and middle temporal gyri, inferior parietal lobule, or the hippocampus and EC.

A – A β plaque phases

Scores for each of the major pathognomonic entities are determined according to their respective staging scheme and then adapted to a four-point scale as set out in the NIA-AA 2012 criteria. The phases of A β plaque deposition used in these criteria were set out by Thal et al. (2002). In Phase 1, A β deposits are found in the frontal, parietal, temporal, or occipital cortices. In Phase 2, plaques appear in the EC, *Cornu Ammonis 1* (CA1) subfield of the hippocampus, insular cortex, and start to appear in the cingulate gyrus, amygdala, presubiculum, and in the molecular layer of the fascia dentata. Phase 3 is characterised predominantly by the occurrence of A β deposits in subcortical structures such as the basal forebrain nuclei, caudate nucleus, claustrum, hypothalamus, lateral habenular nucleus, putamen, substantia innominata, thalamus, and white matter areas. In Phase 4, A β deposits are seen in brainstem structures such as the inferior and superior colliculi, inferior olivary nucleus, periaqueductal gray, red nucleus, reticular formation, and substantia nigra. Finally, Phase 5 includes further involvement of brainstem structures such as the locus coeruleus and raphe nuclei, and lastly the molecular layer of the cerebellum. Each of these phases correspond to one of four A scores: Phases 1 and 2 to A1; Phase 3 to A2; Phase 4 and 5 to A3. The absence of A β plaques is scored A0.

B – Braak stages of NFTs and NTs

For the staging of NFTs and neuropil threads (NTs), Braak and Braak (1991) described three major stages—labelled Transentorhinal, Limbic, and Isocortical—which were each divided into two further substages based on the severity of neurofibrillary changes seen in the regions defined by each major stage. The Transentorhinal stages I and II are characterised by the mild involvement of Pre- α neurons that follow an oblique course through the transitional cortical area between the EC proper and the adjoining temporal cortex. Isolated NFTs may also occur in CA1, basal forebrain, and anterodorsal nucleus of the thalamus. The Limbic stages III and IV are characterised by the continued involvement of Transentorhinal stages, including the formation of ‘ghost tangles’ (extracellular NFTs which represent corpses of dead neurons), and the development of NFTs in multipolar neurons of sectors CA2 to CA4 of the hippocampus. Additionally, NFTs begin to form in pyramidal cells in the subiculum and there may also be sparse involvement of basal portions of frontal, temporal, and occipital association areas, magnocellular forebrain nuclei, anterodorsal and reuniens nuclei of the thalamus, amygdala, tuberomammillary nucleus of the hypothalamus, claustrum, putamen, and nucleus accumbens. Finally, the Isocortical stages represent the first major involvement of the cerebral cortex (also termed the isocortex, neocortex, or neopallium). All association cortices are susceptible to NFTs, with primary cortices remaining relatively spared except for a dense network of NTs in layer V of sensory core fields which develops in Stage VI. However, the presence of globose NFTs in granule cells of the fascia dentata in Stage VI most easily distinguishes it from Stage V. Each of the major Braak stages correspond to one of four **B** scores in NIA-AA criteria: Transentorhinal stages to B1; Limbic stages to B2; Isocortical stages to B3. The absence of NFTs and NTs is scored B0.

C – CERAD protocol for NPs

The scoring system for NPs as set out by CERAD (Mirra et al., 1991) comprises the final score in the NIA-AA ABC criteria. The CERAD protocol recommends the use of either Thioflavin S or modified Bielschowsky silver staining in sections from the superior and middle temporal gyri, middle frontal gyrus, and inferior parietal

lobule to semiquantitatively assess the load of NPs in given individuals. Consideration for testing the hippocampus, EC, and occipital cortex is also suggested by the NIA-AA 2012 criteria. It is recommended that microscopic fields are examined using a 100× objective where the density of NPs is maximal. A CERAD score for NPs may be ‘none’, ‘sparse’, ‘moderate’, or ‘frequent’ and assigned a C score of C0, C1, C2, or C3 respectively. Once a complete ABC score has been generated, a designation of ‘Not’, ‘Low’, ‘Intermediate’, or ‘High’ AD neuropathological change is assigned according to the rubric set out in the NIA-AA 2012 criteria.

Mixed pathology

Although AD neuropathological changes are commonest of any single disease at post-mortem, it is rarely found in isolation (Boyle et al., 2018; Jellinger, 2020; McAleese et al., 2020). Cerebrovascular lesions, which represent a heterogeneous group of diseases underlined by cardiovascular disease risk factors, are the most frequent coincidental finding in AD (DeTure & Dickson, 2019; Kalaria, 2016; Perl, 2010; Rodríguez García & Rodríguez García, 2015). As outlined by the NIA-AA diagnostic recommendations, other common co-pathologies include LBs (Hamilton, 2000), TDP43 (Josephs et al., 2015), and hippocampal sclerosis (Murray et al., 2014). Other diseases that have been reported to overlap with AD include Parkinson’s disease (PD) and the rarer Creutzfeldt-Jakob disease, Gerstmann-Straussler-Scheinker syndrome, and Niemann-Pick disease (Armstrong et al., 2005). A review of the prevalence of mixed pathology suggests that it represents between 10 and 74% of aged brains investigated at post-mortem (Rahimi & Kovacs, 2014), with higher values represented by community-based, as opposed to more biased clinic-based, cohorts (Schneider et al., 2007). Consideration for the high prevalence of mixed pathology, particularly in the community setting, will be of great importance in the management and treatment of AD as the dementing syndrome will likely be caused by the cumulative effect of a number of coincident pathologies (Kapasi et al., 2017; Thomas et al., 2020).

Macroscopic features

Macroscopic features of neurodegenerative diseases (including AD) are not necessarily diagnostic but are often readily appreciable (Jellinger, 2020; Perl, 2010; Serrano-Pozo et al., 2011a). Such features include reduced brain weight and hydrocephalus *ex vacuo* which is seen as an enlargement of the frontal and especially temporal horns of the lateral ventricles secondary to symmetrical atrophy predominantly affecting the medial temporal lobes (MTLs) with relative sparing of the primary motor, somatosensory, and visual cortices. Microinfarcts in the cortex and lacunar infarcts in the basal ganglia, pons, or white matter may be visible in the presence of significant CAA. Usually there is no discolouration of the substantia nigra unless there is a significant number of LBs present.

1.2.3 Clinicopathological correlations

The subject of clinicopathological correlations (CPC) in AD has been described as ‘*critically important*’ but ‘*sometimes-controversial*’ (Nelson et al., 2012). The general applicability and validity of CPCs identified in studies using post-mortem human brain are limited based on numerous potential sources of data variability which might weaken any identifiable correlation between cognitive status and neuropathological load. These include, biased cohorts sourced from the clinic or hospital settings—which have traditionally been over-representative of older middle and upper income class people of West Eurasian ancestry; disease heterogeneity associated with mixed pathologies and a non-uniform pattern of molecular, anatomical, and clinical changes which are difficult to model statistically, especially where data is not parametrically distributed and the sample size is relatively low; an over-reliance on ordinal variables which may obscure more nuanced clinicopathological relationships; variation in the elapsed time between final clinical evaluation and death; and, variation and evolution of clinical and autopsy practices—including the use of semi-quantitative measures, different brain regions, and different laboratory techniques (Nelson et al., 2012). Indeed, some argue that the neuropathological changes seen in AD are actually epiphenomena of aging and therefore should not necessarily be used to define the disease (Castellani

et al., 2008; Chen et al., 2011; Herrup, 2010; Lee et al., 2005; Maltsev et al., 2011; Mondragón-Rodríguez et al., 2010; Whitehouse et al., 2011).

However, evidence from independent research institutes across the globe strongly supports the existence of a specific neurodegenerative disease defined by the presence of A β plaques and hyperphosphorylated tau (phosphotau)-associated neurofibrillary degeneration (NFD)—including NFTs, NTs, and DNs (Nelson et al., 2009a; Nelson et al., 2011). There is also strong evidence demonstrating the potential neurotoxicity of both A β (De Felice et al., 2008; Mattson, 2004; Selkoe & Hardy, 2016; Shankar et al., 2008) and phosphotau (Delacourte, 2008; Iqbal et al., 2009; Johnson & Stoothoff, 2004; Pei et al., 2008; Pritchard et al., 2011; Takashima, 2008). Both NPs and NFTs are known to correlate with the severity of dementia (Baner et al., 1996; Crystal et al., 1993; McKee et al., 1991; Nelson et al., 2007; Tiraboschi et al., 2004). However, most CPC studies indicate that the burden of NFTs better correlates with cognitive impairment than do NPs and diffuse A β plaques; the lattermost generally having the weakest relationship of these entities to cognitive status (Nelson et al., 2012; Qiu et al., 2018). This may be due in part to the brain's natural ability to reabsorb A β plaques throughout life (Bennett et al., 1993; Holmes et al., 2008; Oide et al., 2006) and that the burden of A β plaques plateaus earlier in the disease time course meaning any linear relationship to dementia would fall away at later stages of the disease (Ingelsson et al., 2004; Serrano-Pozo et al., 2011b). The single best correlate and most likely physical basis of cognitive impairment is the loss of synapses (DeKosky et al., 1996; Terry et al., 1991). Synaptic loss is appreciable in the hippocampus early in the disease time course, especially with electron microscopy (EM) but also synaptophysin IHC of pre-synapses (Scheff et al., 2006). Despite this the hippocampus is often excluded from CPC studies due to strong '*floor and ceiling*' effects when quantifying the relative load of pathologies (Nelson et al., 2012). Notwithstanding the essential importance of synaptic loss in potentiating cognitive impairment (Scheff & Price, 2006), it cannot be described as a hallmark pathology as it does not represent a feature of brain degeneration that is unique to AD (Scheff et al., 2014).

1.3 Major proteinopathies of Alzheimer's disease

1.3.1 β -amyloid

APP

A β is derived from the large type I transmembrane protein APP which has its amino terminus extending into the extracellular space and its carboxyl terminus within the cell (Dyrks et al., 1988; Kang et al., 1987). In non-polarised cells, APP undergoes a constant cycle of trafficking through the cellular endomembrane system: it is first routed from the endoplasmic reticulum to the plasma membrane, Golgi apparatus, or trans-Golgi network; in transit nascent APP is post-translationally modified by glycosylation, phosphorylation, and sulphation; the small proportion of APP that reaches the plasma membrane is endocytosed within minutes and recycled or degraded in lysosomes (Haass et al., 2012). In polarised cells such as neurons, as for non-polarised cells, APP is transported from the endoplasmic reticulum to the Golgi apparatus or trans-Golgi network, but is then packaged in post-Golgi transport vesicles and conveyed by the microtubule motor protein kinesin-1 (Kins et al., 2006) to dendrites and within axons, along the fast axonal transport system (Goldsbury et al., 2006; Koo et al., 1990; Sisodia et al., 1993).

APP may be proteolytically cleaved by γ -secretase and either α - or β -secretase (the name 'secretase' refers to the secretion of cleaved substrates) (Haass et al., 2012). β -secretase, a transmembrane enzyme with its active site in the extracellular space, initiates the amyloidogenic pathway responsible for the generation of A β peptides. β -secretase cleaves APP to form the secreted APP ectodomain (APPs β) and the membrane-bound APP carboxyl-terminal fragment (β CTF) which is subsequently cleaved by γ -secretase within the plasma membrane or the endosomal/lysosomal system (Haass, 2004). The cleavage of β CTF occurs within the hydrophobic domain of the plasma membrane in a process termed 'regulated intramembrane proteolysis' (RIP) (Lichtenthaler et al., 2011). RIP by γ -secretase can occur at several sites; labelled the ϵ -, ζ -, and γ -site. These sites do not necessarily denote a single cleavage location, rather sequential cleavage sites that are responsible for the production of

A β peptides of varying lengths from A β ₃₇ to A β ₄₉ (Haass et al., 2012). This is of relevance to AD as A β _{39/40} are the predominant composites of CAA (see also section 1.4.4) (Prelli et al., 1988; Suzuki et al., 1994) and the slightly longer A β _{42/43} are more prone to aggregation and are thought to be the essential constituents of the neurotoxic oligomers which cause AD (Haass & Selkoe, 2007; Saito et al., 2011; Selkoe & Hardy, 2016).

It should be stressed that limiting investigations to the A β ₄₀ and A β ₄₂ species is a simplification since peptides isolated from AD brains show significant heterogeneity in their biochemistry due in part to differing lengths at both the amino and carboxyl terminuses (Masters & Selkoe, 2012). Indeed, longer peptides with cleavage sites up to residue 55 have also been reported; for instance in a presenilin-1 mutant case report (Van Vickle et al., 2008). Further, A β is subject to a number of different post-translational modifications (PMTs) including glycosylation, isomerisation, N-homocysteinylation, nitration, oxidation, phosphorylation, pyroglutamylation, and racemisation (Kummer & Heneka, 2014; Moro et al., 2018). It is not known precisely how such PMTs affect the chemical dynamics of A β aggregation nor its toxicity (Schaffert & Carter, 2020). Following γ -secretase activity A β is released into the extracellular space. A second by-product, the APP intracellular domain (AICD), is released into the cellular cytosol where it may have a role in nuclear signalling (von Rotz et al., 2004). The breakdown of APP can also follow a similar step-wise proteolytic routine that does not produce pathological A β peptides—the non-amyloidogenic pathway. This pathway is initiated by α -secretase, on the cell surface or within the trans-Golgi network, where it cleaves APP at a locus close to the middle of its A β region (Esch et al., 1990; Sisodia et al., 1990). The two resulting by-products are an extended secreted APP ectodomain (APPs α) and a truncated carboxyl-terminal fragment (α CTF), the latter of which is further cleaved into the AICD (as for the amyloidogenic pathway) and the non-pathological p3 peptide (Haass et al., 1993).

Biochemistry of A β

Glenner and Wong first isolated and sequenced A β from meningeal blood vessel walls in Down's syndrome (Glenner & Wong, 1984a) and AD (Glenner & Wong, 1984b). Efforts were then made to isolate and sequence A β in NP cores (Allsop et al., 1983; Masters et al., 1985; Selkoe et al., 1986). These early biochemical studies established that the subunit of fibrils isolated from the meningeal vasculature and NP cores was a relatively small (~4 kDa) hydrophobic peptide with a high propensity to self-aggregate into dimers, trimers, tetramers, higher oligomers, and finally larger fibrils. A β plaques observed at post-mortem are composed of extracellular fibrils with a high cross- β sheet content (Masters & Selkoe, 2012). The conversion of α -helical conformers to β -sheet rich structures in AD shares striking similarity to protein misfolding in prion diseases and is a common motif in degenerative diseases of the brain (Lauwers et al., 2020; Rasmussen et al., 2017; Vaquer-Alicea & Diamond, 2019; Walker et al., 2016). Cryo-EM structures of A β fibrils purified from the meninges of AD patients has allowed for their detailed conformational modelling which shows marked differences to synthetic A β fibrils formed *in vitro* (Kollmer et al., 2019).

A β monomers represent the basic building block of a short list of aggregates of increasing size. These range from soluble low and high molecular weight oligomers (LMWOs or HMWOs, respectively) and protofibrils (~4 nm in diameter) to the classical fibrils seen at post-mortem (8–22 nm in diameter) (Close et al., 2018). A β in its monomeric form has been found to have neurotrophic effects on undifferentiated and mature neurons *in vitro* (Giuffrida et al., 2009; Yankner et al., 1990; Zou et al., 2002; Zou et al., 2003). LMWOs—including dimers, trimers (Larson & Lesné, 2012), and tetramers—along with HMWOs (dodecamers or larger) are stable substrates in sodium dodecyl sulphate (SDS)–urea solutions (Lesné et al., 2006; McLean et al., 1999). They are thought to be the responsible neurotoxic molecules in AD (De Felice et al., 2004; Ferreira & Klein, 2011; Jana et al., 2016; Selkoe & Hardy, 2016). The level of dimers in blood and the frontal cortex of AD cases has been shown to correlate with cognitive impairment (McDonald et al., 2010; Villemagne et al., 2010). However, trimers and tetramers are known to be the more potent oligomeric species (Harmeier et al., 2009; Ono et al.,

2009; Townsend et al., 2006). Overall, there remains uncertainty as to the relative pathogenicity of soluble A β as it is known that their concentrations are significantly higher in young adults compared to the elderly (van Helmond et al., 2010). A β protofibrils (100–150 kDa) are curvilinear intermediate aggregates comprised of 15–40 monomers. These structures have only been described *in vitro* (Harper et al., 1999; Kaye et al., 2009; Kirkitadze et al., 2001). Thus their relevance to AD, and even existence in the brain, are as yet unresolved questions.

Degradation of A β

A β is subject to degradation by a group of peptidases known as A β -degrading proteases (A β DPs) (Saido & Leissring, 2012). Bateman et al. (2006) have shown that the rates of A β production and clearance can be measured in the CSF and subsequently demonstrated that reduced clearance, but not increased production, characterised sporadic AD (Mawuenyega et al., 2010). However these results were unable to distinguish cause from effect. One of the earliest studies that examined A β degradation in living animal identified neutral endopeptidase (NEP; neprilysin) as a key A β DP, which if inhibited resulted in increased A β ₄₂ pathology (Iwata et al., 2000). Conversely, transgenic overexpression of NEP in an APP mouse model significantly reduced A β levels and prevented the formation of plaques and downstream cytopathology (Leissring et al., 2003). Further, the delivery of NEP to presynaptic sites in the hippocampus of NEP-deficient APP mice has been shown to abolish continued deposition of A β (Iwata et al., 2004). In this study, the deposition of A β was also significantly attenuated in the contralateral hippocampal formation of young APP mice. In addition to NEP there have been a large number of A β DPs identified to date. These can be classified according to their enzymological type, including, aspartyl, cysteine, and serine proteases, and metalloproteases (e.g. NEP); all of which can also be further subclassified by the subcellular compartment they inhabit (Saido & Leissring, 2012). Finally, the modulation of A β DPs, along with the upstream proteases responsible for the generation of A β , represents an auspicious therapeutic target for preventing the progression of preclinical AD.

Aβ plaques

Filamentous aggregates of Aβ are observed as plaques at post-mortem neuropathological investigation (historically the term ‘plaque’ was used to describe flat disk- or patch-like objects) (Walker, 2020). The term ‘Aβ plaque’ refers to a multiplicity of brain lesions associated with deposits of Aβ. Several classification schemes have been proposed for these (Armstrong, 1998; Dickson & Vickers, 2001; Duyckaerts et al., 2009; Ikeda et al., 1989; Thal et al., 2000; Wisniewski et al., 1989; Yamaguchi et al., 1988), but there is as yet no universally accepted system for their categorisation (Walker, 2020). Morphological subtypes of Aβ plaques include diffuse (also, ‘primitive’ or ‘immature’), fibrillar, dense-cored (also just ‘cored’, ‘classical’, or ‘mature’ plaques), and burned-out (also, ‘core-only’) plaques. NPs are a minority subset of Aβ plaques that are most often associated with phosphotau-positive dystrophic neurites (DNs). Phosphotau-positive DNs are comprised of helical filaments identical to those in NFTs (Iqbal et al., 2009). DNs can also be tau-negative, in which case require detection by silver stains, thioflavin S, or IHC targeting p62, ubiquitin, neurofilament proteins, or APP (Nelson et al., 2012; Price et al., 2009; Thal et al., 2000; Thal et al., 2006). DNs are elongated or globular in morphology and represent both degenerating axonal terminals (Yasuhara et al., 1994) and dendrites (Shi et al., 2020). Fibrillar and dense-cored plaques are more likely to be associated with DNs compared to diffuse plaques in AD (Dickson & Vickers, 2001; Serrano-Pozo et al., 2011a). Notably, non-AD tauopathies usually lack NPs, suggesting they are not an inevitability of tau pathology (Nelson 2012). The recently described ‘coarse-grained’ plaques in early-onset AD (EOAD), which are associated with Aβ₄₀, *APOE* ε4 homozygosity and CAA, are also often accompanied by DNs (Boon et al., 2020).

Diffuse plaques can include small stellate or ball-shaped structures which are homogeneously labelled and often profusely scattered throughout the parenchyma (Dickson & Vickers, 2001; Walker, 2020). Other diffuse plaque subtypes include subpial sheet-like bands (Thal et al., 2000), large ‘cotton-wool’ plaques which feature most prominently in a presenilin-1 mutant of autosomal dominant AD (Houlden et al., 2000), and large cribriform ‘lake-like’ patches in the subicular complex (Wisniewski et al., 1998). Like dense-cored plaques, fibrillar plaques

exhibit a central mass of A β but with ‘spoke-like’ extensions leading to the outer rim of diffuse A β (Dickson & Vickers, 2001). Dense-cored plaques have a ‘core-space-corona’ pattern of A β staining which produces the classical bulls-eye appearance (Walker, 2020). Burned-out plaques are a small subset of plaques which have the appearance of dense-cored plaques but lack the surrounding corona of A β . These plaques have previously been considered the end-stage of the natural evolution of A β plaques through the disease process (Wisniewski et al., 1989).

A β plaques occur in the vast majority of the elderly but are not universal (Braak et al., 2011; Davies et al., 1988; Jicha et al., 2012). A β plaques are not sufficient to cause AD, however there is a strong association between their formation and the development of AD. Genetic risk factors, including *APOE* (see section 1.5.2), account for 50–58% of heritability, and up to 79% in a best-fitting model, of late-onset AD (LOAD) (Bertram et al., 2010; Gatz et al., 2006). The combination of genetic, biochemical, longitudinal biomarker, and histopathological investigations have theoretically strong mechanistic implications for the role of A β as a prime aetiological factor in AD. In spite of this there has been repeated failure of A β -related pharmacological agents to attenuate the progression of disease (Panza et al., 2019). Therefore it will be important to continue to investigate other avenues of potential treatment.

1.3.2 Tau

Structure of tau

The microtubule associated protein tau (MAPT), or simply ‘tau’, is the subunit protein which when hyperphosphorylated polymerises to form NFTs, NTs, and tau-positive DNAs. Whilst extracellular A β was first identified by molecular cloning (Kang et al., 1987), intracellular tau in the form of NFTs was first identified by antibody reactivity (Brion et al., 1985; Grundke-Iqbal et al., 1986; Kosik et al., 1986; Wood et al., 1986). Tau is a member of the Type 2 microtubule associated protein (MAP) family. It is a highly soluble protein which is unfolded in its native state (Mandelkow et al., 2007; Schweers et al., 1994). It is expressed as six alternatively spliced isoforms with 0, 1, or 2 amino (N)-terminal inserts of 29

residues each (0N, 1N, or 2N; derived from exons 2 and 3) and 3 or 4 carboxyl (C)-terminal repeats of 31–32 residues (3R or 4R; derived from exon 10) (Goedert et al., 1988; Goedert et al., 1989). Thus the smallest and largest isoforms are 0N3R tau and 2N4R tau, respectively (Iqbal et al., 2010). The full length protein can be divided into an N-terminal ‘projection domain’, which projects away from the microtubule surface, followed by a C-terminal ‘assembly domain’ which is further subdivided into a proline-rich region, the microtubule-binding repeats, and a C-terminal tail (Mandelkow & Mandelkow, 2012). Tau contains 85 potential serine, threonine, and tyrosine phosphorylation sites, most of which reside in the proline-rich region and the C-terminal tail (Noble et al., 2013). Tau exhibits many structural conformations, biochemical modifications, and the ability to interact with a number of different protein types, including cytoskeletal proteins, motors, kinases, phosphatases, and chaperones (Mandelkow & Mandelkow, 2012). Unlike *APP*, mutations in *MAPT* cause FTD, but not AD (Hutton et al., 1998).

Tau and microtubules

Microtubules are dynamic protein polymers with diverse tasks including involvement in the assembly of the mitotic spindle, maintaining cell morphology, and serve as intracellular highways for the transportation of cellular material by motor proteins (Goodson & Jonasson, 2018). The repeat regions in tau’s assembly domain are responsible for its binding to $\alpha\beta$ -heterodimers of tubulin, which has been demonstrated in vitro, unfortunately without the ability to determine the exact binding site (Gustke et al., 1994; Makrides et al., 2004). Binding of microtubules to tau and other MAPs improves their stability and promotes further self-assembly. However MAPs, including tau, are not essential for the formation and structure of microtubules (Mandelkow & Mandelkow, 2012). Indeed, the abundance of intraneuronal tau ($\sim 1\ \mu\text{M}$) compared to tubulin ($20\text{--}40\ \mu\text{M}$) appears substantially substoichiometric (Cleveland et al., 1977; Hiller & Weber, 1978).

Tau’s role to promote the formation and stabilisation of microtubules is regulated by the degree of its phosphorylation (Weingarten et al., 1975). AD brains do not show increased normal tau protein or upregulation of tau messenger ribonucleic acid (mRNA) (Mah et al., 1992). However diseased brains contain four to eightfold

more phosphotau than do normal brains (Khatoon et al., 1992, 1994). This suggests that the increase in total tau likely results from reduced turnover following hyperphosphorylation (Poppek et al., 2006). Polymerised tau in the form of NFTs and NTs does not appear to bind tubulin or promote the assembly and stabilisation of microtubules (Alonso et al., 2006; Iqbal et al., 1994).

Biochemistry of tau

The most likely cause of tau dysfunction and aggregation is its hyperphosphorylation (Alonso et al., 1994; Grundke-Iqbal et al., 1986). Other disease related properties and biochemical changes include missorting to the somatodendritic compartment, acetylation, glycation, glycosylation, methylation, nitration, oxidation, ubiquitination, and truncation (Ittner & Ittner, 2018; Mandelkow & Mandelkow, 2012). Aggregations of phosphotau likely occur first as oligomers which further aggregate to form fibrils (Maeda et al., 2007). Soluble oligomeric species of tau form early in the pathogenesis of AD and arguably represent the neurotoxic substrate of tau, rather than the relatively inert and insoluble tau fibrils (Lasagna-Reeves et al., 2012; Ward et al., 2012). Tau fibrils occur as straight filaments (SFs) or paired helical filaments (PHFs) which are ultrastructural polymorphs that contain all six isoforms of tau (Fitzpatrick et al., 2017). SFs and PHFs serve as the structural subunits of NFTs, NTs, and tau-positive DN. At least one essential factor for tau's fibrillisation is its tendency for β -sheet structure in its repeat subdomain (von Bergen et al., 2000). Disruption of these repeats impairs tau's propensity to aggregate *in vitro* and in cell and animal models. Oppositely, the promotion of β -sheet structure accelerates aggregation, as seen in the dK280 'proaggregation' mutant (Mocanu et al., 2008). Inducers of tau fibrillisation within neurons are not known, however acidic cofactors are likely to be involved (Mandelkow & Mandelkow, 2012).

Degradation of tau

Tau is susceptible to cleavage by a number of different proteases, including, aminopeptidases, calpains, caspases, human high temperature requirement serine protease A1 (HTRA1), and thrombin (reviewed by Chesser et al., 2013). However,

bulk clearance of normal and pathological tau is through the ubiquitin–proteasomal system for monomeric forms and autophagy–lysosomal degradative system for larger aggregates (Lee et al., 2013; Tang et al., 2019). Importantly, fragments of tau generated proteolytically by calpains, caspases, and thrombin are potentially cytotoxic and exhibit a greater propensity to self-associate (Chesser et al., 2013). Therefore, therapeutic strategies aimed at modulating the clearance of tau must balance proteolytic processing with the proteasome and broad scale autophagy–lysosomal degradation. Autophagy inducers, such as trehalose (Schaeffer et al., 2012), methylene blue (Congdon et al., 2012), rapamycin (Majumder et al., 2011), and lithium (Shimada et al., 2012), have all been used with positive effect to facilitate the degradation of pathological tau and impair the formation of NFTs in various models of tauopathy.

Neurofibrillary degeneration

NFD in AD is defined by three lesions—NFTs, NTs, and DN—each associated with insoluble tau fibrils. These histopathological entities likely represent end-stage lesions which appear to be inert markers of earlier pathological changes to soluble monomeric and oligomeric species of tau (Iqbal et al., 2009; Lasagna-Reeves et al., 2012; Ward et al., 2012). However, the density and anatomical spread of NFD remain essential for diagnostic and staging purposes. NFTs and NTs have also proved useful for describing the related sequence of cytoskeletal changes in AD (Braak et al., 1994). Five groups of neuronal and extraneuronal structures are described according to their AT8 immunoreactivity (*which is commonly used to label a pathogenic form of phosphotau; S199/S202/T205 epitopes*) and sensitivity to silver impregnation. Group 1 neurons show initial pre-argyrophilic changes characterised by the complete labelling of axons, dendrites, and soma with AT8 immunoreactive granules without any morphological alterations. These granules represent viscous ‘pretangle’ material that strongly tends to convert to silver stain-positive fibrils (Braak & Del Tredici, 2015a). Group 2 neurons are characterised by alterations to cellular processes. The terminal tuft of the apical dendrite may be fragmented or replaced by tortuous fibres and coarse granules. Distal dendrites may also be thickened and associated with appendages. Thickened dendrites and the soma may harbour intense homogeneously labelled rod-like inclusions which may

also be argyrophilic. Group 3 neurons show pronounced alterations to their distal dendritic field and soma, whereas the intermediate field loses its AT8 immunoreactivity. AT8 material in the distal field and soma show up as NTs and classical NFTs, respectively, in silver stains. Group 4 structures are marked by the further accumulation of coarse extracellular AT8 granules which represent early ghost tangles. Lastly, group 5 structures represent late ‘tombstone’ ghost tangles in the extracellular space which are sensitive to silver staining but not necessarily AT8 immunolabelling.

The morphology of NFTs is region specific and dependant on the affected type of neuron; ranging from globose/compact in granule cells in the fascia dentata and modified pyramidal cells in CA4 to large flame-like shapes in cortical pyramidal cells and slender tangles with long extensions through the apical dendrites of subicular neurons (Braak & Braak, 1991). The fibrillary material of ghost tangles is occasionally less tightly packed than intracellular tangles; a tentative marker of turnover (Nelson et al., 2012), possibly by astrocytic engulfment and degradation (Braak & Braak, 1991). NTs are elongated in shape and frequently occur in dendrites of tangle-bearing neurons and show a patchwork of deposition throughout the neuropil, contributing considerably to the total load of NFD (Braak & Braak, 1988; Yamaguchi et al., 1990).

Tau dysfunction is sufficient to cause neurodegeneration, but which is not necessarily representative of AD (Buée et al., 2000; Goedert, 2004). Indeed, in many circumstances, such as prion disease, chronic traumatic encephalopathy (CTE), certain brain tumours, and viral encephalitides, NFD is a secondary marker of the primary insult (Nelson et al., 2012). Modest numbers of NFTs are universal in the MTL of people over 70 years of age (Bouras et al., 1994) and they are also near universal in certain brainstem nuclei. The occurrence of NFD in non-thalamic subcortical nuclei may in fact represent the earliest neuropathological changes in AD that can arise even before puberty (Braak & Del Tredici, 2011; Braak et al., 2011; Braak & Del Tredici, 2015b; Grinberg et al., 2009; Iqbal & Grundke-Iqbal, 2005; Iqbal et al., 2009; Simic et al., 2009). However, NFD limited to subcortical structures is often asymptomatic and cognitive impairment only occurs where there is substantial involvement of the cerebral cortex (Nelson et al., 2012).

1.4 Other neuropathological features

1.4.1 Atrophy

AD is characterised by atrophy of anatomically discrete brain regions (Halliday et al., 2003). These can be broadly sorted by severity into two groups. The most severely atrophic regions tend to occur where the load of NFTs is greatest, whereas less atrophic regions tend to be those where NPs predominate. Examples of severely atrophic regions include the fusiform gyrus, temporal pole, superior and middle frontal gyri, hippocampus and entorhinal cortex, and the amygdala and inferior temporal gyrus. Less atrophic regions, in descending order, include the middle temporal gyrus, angular gyrus, superior temporal and posterior cingulate cortices, anterior cingulate cortex, frontal pole, occipital lobe and supramarginal gyrus, superior parietal lobule, and the insula. Regions unaffected by atrophy include the orbital and inferior frontal gyri, post-central gyrus, and the posterior parahippocampus. This pattern of grey matter atrophy is markedly different from the loss of brain volume with age, which is by and large confined to the white matter (Piguet et al., 2009).

1.4.2 Loss of neurons and synapses

Neuronal loss appears to be the main pathological substrate of atrophy. The regional and laminar pattern of loss corresponds with, but importantly exceeds, the load of NFTs (Gomez-Isla et al., 1996; Gomez-Isla et al., 1997). This suggests at least two broad mechanistic categories of neuronal loss in AD involving non-tangle-bearing and tangle-bearing neurons, which can house a tangle for up to two decades (Bussière et al., 2003; Hof et al., 2003). The loss of pre- and post-synapses also contributes to atrophy, likely precedes neuronal loss, and is associated with a compensatory enlargement of remaining boutons (Serrano-Pozo et al., 2011a). The loss of synapses remains the strongest correlate of cognitive impairment in AD (DeKosky & Scheff, 1990; DeKosky et al., 1996; Masliah et al., 1989, 1991, 2001; Reddy et al., 2005; Scheff et al., 1990, 1993, 2001, 2006, 2007; Scheff & Price, 1993; Terry et al., 1991). This is also supported by gene expression studies showing

involvement of trafficking and release of synaptic vesicles, post-synaptic density scaffolding, and neuromodulatory systems, including neurotransmitter receptors (Overk & Masliah, 2014). Notably, a meta-analysis of synaptic pathology concluded pre-synapses are more affected than post-synapses in AD (de Wilde et al., 2016). Synaptophysin—involved in soluble N-ethylmaleimide-sensitive factor [NSF] attachment protein [SNAP] receptor (SNARE) assembly—is the most abundant pre-synaptic vesicle protein (Clare et al., 2010) and the most affected in AD, with synaptopodin representing the most affected post-synaptic marker (Reddy et al., 2005).

1.4.3 Gliosis

The association of astrocytes and microglia at A β plaques in human tissue has been referred to as the ‘reactive glial net’ (Bouvier et al., 2016). Reactive gliosis in AD has been intensively researched over many decades. A cursory search of PubMed using the terms: ‘Alzheimer* Disease* AND (Microglia* OR Astrocyt*)’; yielded 10,125 articles since 1960; almost two thirds of which were published in the last 10 years. Yet critical work remains in order to resolve the precise nature of the astrocytic and microglial responses in AD and how best to modulate various aspects of their respective capabilities as potential therapeutics (Björkqvist et al., 2009; McGeer et al., 2016). Characterising certain aspects of the microglial response in AD is the subject of this thesis. Refer to section 1.6 and 1.6.6 for further background information on microglia and their involvement in AD, respectively.

1.4.4 Cerebral amyloid angiopathy

CAA involves the deposition of A β in the interstices of the tunica media of blood vessel walls, usually affecting capillaries, small arterioles, and intermediate arteries of the brain and leptomeninges (Serrano-Pozo et al., 2011a). Factors that cause the termination of A β at or before position 41 tend to favour vascular over parenchymal deposition of A β , with the more soluble A β ₄₀ being the major constituent of CAA (Greenberg et al., 2020). CAA is present in 80% to over 90% of AD cases, with higher severity in those with more severe AD neuropathological changes (Arvanitakis et al., 2011; Brenowitz et al., 2015). Brain injuries secondary to CAA

most likely arise from blood vessel dysfunction; either by haemorrhage or ischaemia (Greenberg et al., 2014). ‘Definite CAA’ represents the highest level of diagnostic certainty and is made on the basis of post-mortem neuropathology demonstrating CAA with lobar, cortical, or cortical–subcortical haemorrhage in the absence of other diagnostic lesions (Greenberg & Charidimou, 2018).

1.4.5 Granulovacuolar degeneration bodies

Granulovacuolar degeneration bodies (GVBs) were first described in the hippocampus of AD brains over 100 years ago (Grzybowski et al., 2017; Simchowicz, 1911). GVBs are clear membrane bound lysosomal structures which measure 3–5 μm in diameter and contain a dense core, or ‘granule’, which measures 0.5–1.5 μm in diameter (Wiersma et al., 2020). GVBs mainly occur in the soma and can number from 1 to dozens in a single neuron. GVBs can be visualised in routine H&E sections or silver stains (Tomlinson & Kitchener, 1972). Immunoreactivity of GVBs include neurofilament proteins, tau, and tubulin. The formation of GVBs is thought to be an early response to tau aggregation and their presence constitutes the neuropathological feature termed granulovacuolar degeneration—withstanding the use of this terminology, it is unknown as to whether GVBs represent a protective or degenerative cellular response (Wiersma et al., 2020).

1.4.6 Hirano bodies

Hirano bodies were first described in a post-mortem evaluation of ALS-Parkinsonism/Dementia complex of Guam (Guam disease) over 50 years ago (Hirano et al., 1966) and were subsequently found in normal brains (Ogata et al., 1972) and other pathological conditions including AD (Hirano et al., 1968). Hirano bodies are eosinophilic, haematoxylinophilic intraneuronal inclusions that predominantly occur in CA1. They are spheroidal when cut transversely (up to 15 μm in diameter) and fusiform when cut longitudinally (up to 30 μm in length) (Gibson & Tomlinson, 1977). Hirano bodies are primarily composed of actin filaments, actin-associated proteins (Galloway et al., 1987b), and tau (Galloway et al., 1987a), but also accumulate other molecules such as bromodomain plant homeodomain [PHD] finger transcription factor (BPTF) (Jordan-Sciutto et al.,

1998) and AICD (Ha et al., 2011)—through which they may modulate cell death (Spears et al., 2014).

1.4.7 White matter hyperintensities

Severe disability in LOAD is associated with white matter hyperintensities (Ble et al., 2006). Leukoaraiosis, seen in white matter rarefaction due to ischaemia or haemorrhage, presents as hypodensities on computerised tomography (CT) and hyperintensities on T2-weighted MRI. These hyperintensities are often the result of cerebrovascular pathology caused by CAA or other common vascular comorbidities of AD such as atherosclerosis (including thromboembolism) and small vessel disease (including arteriosclerosis, arteriolosclerosis, and lipohyalinosis) which often affect arteries in the basal ganglia and white matter (Grinberg & Thal, 2010). CAA affects both leptomeningeal and intracerebral arteries and is a sufficient cause of lacunar infarcts, microinfarcts, microhaemorrhage, and white matter lesions more broadly (Kalaria, 2016).

1.5 Genetics of Alzheimer’s disease

1.5.1 Familial disease

Familial AD (fAD), or DIAD, accounts for ~1% of all cases (Bateman et al., 2012). fAD can occur as either EOAD (before 65 years of age) or LOAD and is caused by mutations in the *APP*, *PSEN1*, or *PSEN2* genes. fAD accounts for 10–15% of EOAD (Kamboh, 2018), which might be diagnosed where at least two first degree relatives are also affected (Lanoiselée et al., 2017). The discovery of an *APP* missense mutation segregated with fAD (Goate et al., 1991) led to the amyloid cascade hypothesis (ACH) which posits A β as the prime aetiological factor of AD, including for the majority sporadic disease (Hardy & Higgins, 1992). The subsequent discoveries of mutations in *PSEN1* (Clark et al., 1995) and *PSEN2* (Rogaev et al., 1995)—genes responsible for encoding γ -secretase subunits—and a protective *APP* ‘Icelandic’ variant associated with reduced A β production (Jonsson et al., 2012; Peacock et al., 1993) lent further credibility to the theory. However

no A β -based experimental therapies have proved effective to date (Huang et al., 2020). There are at least 68 known unique mutations of *APP* (Alzforum, a). *APP* is a 20 exon gene located on chromosome 21 (21q21.3), which accounts for the gene-dose dependent effect on brain A β levels observed in individuals with trisomy 21 (Gomez et al., 2020). Mutations are most common in *PSEN1* (14q24.2) with some 322 described (Alzforum, b) (Dai et al., 2018) while 64 have been described in *PSEN2* (14q42.13) (Alzforum, c).

1.5.2 Sporadic disease

APOE

Sporadic AD comprises ~99% of all cases and like fAD can be divided into EOAD and LOAD. EOAD accounts for 4–6% of all AD cases (Zhu et al., 2015). EOAD differs from LOAD in numerous ways, including higher association with low cardiovascular fitness and cognitive reserve, history of CTE, depression, a more aggressive natural history, and a lower association with diabetes, obesity, and the *APOE* ϵ 4 allele (Mendez, 2017). The *APOE* (19q13.32) gene contains 6 exons and has three known alleles: ϵ 2, ϵ 3, ϵ 4. APOE is a secreted glycoprotein which binds cholesterol and phospholipids and has a central role in lipid metabolism (Huang & Mahley, 2014). It is produced in the liver and brain—predominantly by astrocytes under physiological conditions. Interestingly, APOE immunoreactivity at dense-cored A β plaques is associated with pericytes (Blanchard et al., 2020) and reactive microglia but not astrocytes (Uchihara et al., 1995), an observation supported by single-nuclei RNA-sequencing (snRNA-Seq) (Mathys et al., 2019). APOE is broadly implicated in AD by its direct effects on A β , microglia, astrocytes, the blood brain barrier (BBB), and indirect effects on tau. The ϵ 4 allele is the strongest known genetic risk factor for sporadic LOAD, conferring 3.7 \times increased risk in heterozygotes and 12 \times in homozygotes (Serrano-Pozo et al., 2021; Verghese et al., 2011). The ϵ 2 allele represents the strongest protective genetic factor, associated with an odds ratio of 0.39 in heterozygotes and 0.13 in homozygotes compared to ϵ 3 homozygotes (Reiman et al., 2020)—associated with neutral risk for AD; except for the rare ‘Christchurch’ polymorphism first identified in a fully penetrant though cognitively intact Paisa mutation carrier (Arboleda-Velasquez et al., 2019).

Christchurch homozygosity appeared to inhibit A β oligomerisation, binding of APOE to low-density lipoprotein receptor, and APOE binding affinity to heparan sulphate proteoglycans, which may exert a pathological effect through interactions with A β (Lorente-Gea et al., 2017; Snow et al., 1994). Incidentally, homozygosity of ϵ 2 and ϵ 2 ϵ 3 is associated with extreme longevity compared to neutral ϵ 3 homozygosity (Sebastiani et al., 2019).

Genome-wide association studies

The origins of sporadic LOAD is in an admixture of genetic and lifestyle factors, with genetics accounting for a marginally greater proportion of total phenotypic variance: 50–58% according to best estimates, but up to 79% in one study (Andrews et al., 2020; Bertram et al., 2010; Gatz et al., 2006; Ridge et al., 2016). Genome-wide association studies (GWAS) involving hundreds or thousands of participants have so far identified 40 susceptibility loci in sporadic LOAD (Andrews et al., 2020). GWAS have traditionally only captured common genetic risk variants, but with the aid of imputation ably capture low allelic frequencies—down to 0.1% (McCarthy et al., 2016). Functional genomic analyses have associated these susceptibility loci with genes of interest; including: *CR1*, *BIN1*, *INPP5D*, *HLADRB1*, *TREM2*, *CD2AP*, *PILRA*, *AGFG2*, *EPHA1*, *CLU*, *PTK2B*, *PSMC3*, *MS4A6A*, *PICALM*, *SORL1*, *STYX*, *SLC2A4A*, *ADAM10*, *IQCK*, *ABCA7*, and *CASS4* (Jansen et al., 2019; Kunkle et al., 2019). Most of these have a relatively high allelic frequency, but confer only very small risk of developing LOAD (Lane et al., 2018). Consequently, a substantial proportion of the estimated heritability of LOAD remains unaccounted for after the summation of their cumulative effect (Bertram et al., 2010; Bertram & Tanzi, 2019). This ‘missing heritability’ is referred to as the ‘dark matter’ of GWAS (Manolio et al., 2009). Notwithstanding the minor effect of individual genes, a common polygenic risk score (plus age, sex, and *APOE* status) predicts LOAD with an accuracy of 78.2% (Escott-Price et al., 2015). Finally, pathway analyses of these genes implicates APP processing, endolysosomal-vesicle recycling pathways, lipid metabolism, and immune response pathways—particularly microglial phagocytosis (Podleśny-Drabiniok et al., 2020)—in the pathogenesis of LOAD (Pimenova et al., 2018).

1.6 Microglia

Microglia are a type of mononuclear phagocyte of mesodermal origin and as such share many characteristics with other myeloid cells of the body. They are the major innate immune sentinel of the central nervous system (CNS), but are also responsible for maintaining homeostasis of key elements of neuronal and synaptic activity. However, unlike other myeloid cells, such as macrophages, microglia persist *in situ* without the need for replenishment from circulating monocytes (Prinz et al., 2014). An extensive review of the physiology of microglia is provided by Kettenmann et al. (2011). Microglia mobilise and react to brain injury by upregulating activities such as cytokine production. These ‘activated’ microglia have been heavily implicated in a number of neurodegenerative (Hickman et al., 2018) and psychiatric diseases (Tay et al., 2017a) including AD, PD, Huntington’s disease, prion diseases, ALS, FTD, CTE, bipolar disorder, major depressive disorder, and schizophrenia.

1.6.1 Historical perspectives

Descriptions of glia have their beginnings in 1856 when Rudolf Virchow described the ‘nervenkitt’, or ‘nerve cement’, a type of brain connective tissue he termed ‘neuroglia’ (Kettenmann & Verkhratsky, 2008). Later W. Ford Robertson introduced the term ‘mesoglia’ in reference to their derivation from mesodermal elements. However these were eventually shown to be ‘macroglia’, namely astrocytes and oligodendrocytes (Rezaie & Male, 2002). The first description of microglia per se came from Franz Nissl in the late 19th century in his work on ‘stabchenzellen’, reactive rod cells with the ability to migrate, phagocytose, and proliferate (Ginhoux et al., 2013). Santiago Ramón y Cajal coined the term ‘the third element’ to distinguish these cells from neurons and neuroglia. Finally, Pío del Río Hortega introduced the term ‘microglial cell’ in his work to differentiate the cells of the ‘third element’ based on functional and morphological differences (Río Hortega, 1919, 1939). Eventually research on microglia would enter a ‘dark age’—wherein their existence was seriously questioned—at the outbreak of World War 2, lasting until the 1960s when Blinzinger, Kreutzberg, and others revitalised interest

in microglia as immune effector cells (Blinzinger & Kreutzberg, 1968; Rezaie & Male, 2002; Svahn et al., 2014).

1.6.2 Ontogeny of microglia

The investigation of microglial ontogeny has been performed most extensively in the mouse embryo. Reviews of embryonic haematopoiesis are provided by Cumano and Godin (2007) and Orkin and Zon (2008). An in depth review of the embryological origin of microglia is provided by Ginhoux and Prinz (2015). ‘Definitive haematopoiesis’ is characterised by the generation of haematopoietic stem cells in the aorta–gonad–mesonephros region of the embryo at around E10.5. These stem cells then migrate to the liver and bone marrow wherein they differentiate into cells of the myeloid and lymphoid lineages. Before this, ‘primitive haematopoiesis’ begins the transient production of primitive macrophages and erythrocytes in blood islands (of mesodermal origin) of the yolk sac (of endodermal origin) at E8.5. Microglia can be observed in the developing neuroepithelium as early as E9.0 (Alliot et al., 1991; Alliot et al., 1999; Ashwell, 1990), strongly suggesting their progenitors originate from the yolk sac after spreading through blood circulation (Koushik et al., 2001)—itself under ongoing development from around E8.5. This hypothesis was confirmed in a later fate mapping study (Ginhoux et al., 2010) and others which also showed microglia are derived from c-kit⁺ erythromyeloid precursors via Pu.1 and Irf8 dependent pathways (Kierdorf et al., 2013) without the need for the myeloblastosis (Myb) transcription factor, unlike CD11b^{high} monocytes and macrophages (Schulz et al., 2012). Finally, extravasation of circulating monocytes may contribute to the microglial population in the adult murine cerebrum with an intact BBB (Lawson et al., 1992)—though this remains a topic of significant contention given the proliferative potential of the resident cells (Réu et al., 2017), among other reasons (Ginhoux et al., 2013). In contrast, it is generally accepted that the recruitment of non-local cells occurs during CNS inflammation (Ladeby et al., 2005; Mildner et al., 2007; Vallières & Sawchenko, 2003).

1.6.3 Morphological study of microglia

Microglia constitute a highly dynamic and morphologically heterogeneous cell population of the CNS (Hanisch & Kettenmann, 2007; Lawson et al., 1990). Microglia are the most morphologically plastic cells of the brain (Hristovska & Pascual, 2015) and it was through the study of morphology that they were originally implicated in diseases of the CNS (Kettenmann et al., 2011; Streit et al., 2014). The morphology of microglia is influenced by numerous factors, including diet and gut flora (Cope et al., 2018; Graham et al., 2016); drug (Burkovetskaya et al., 2020) and alcohol (Marshall et al., 2020) consumption; infection and traumatic injury (Giordano et al., 2021); psychiatric disease (Kreisel et al., 2014; Wohleb et al., 2014); sex and ageing (Brawek et al., 2021); sleep deprivation (Wadhwa et al., 2017); sleep–wake cycles (Nakanishi et al., 2021); and systemic and autoimmune diseases (Aw et al., 2020). Assessment of morphology can be made on the basis of both manual (Lawson et al., 1990; Vela et al., 1995) and automated statistical methods (Davis et al., 2017; Salamanca et al., 2019; Verdonk et al., 2016). There is no universally accepted nomenclature for the morphological categorisation of microglia. However, they may be grouped based on three broad categories of morphology: ramified, activated, and dystrophic. Ramified microglia are highly branched cells with a small spherical soma (Kettenmann & Verkhratsky, 2008; Kettenmann et al., 2011). Activated (also ‘reactive’) microglia are hypertrophied cells with either a loss or gain of branching complexity. Activated microglia present with a range of morphologies, from bushy in appearance to rod-shaped or enlarged and amoeboid (Streit et al., 1999). Dystrophic microglia show a loss of processes with the remainder showing significant tortuosities, fragmentation, and the formation of spheroids (Streit et al., 2004).

Interpretation of morphological changes

Microglia with a ramified morphology represent the healthy cell population (Almolda et al., 2013; Boche et al., 2013; Cho & Choi, 2017; Lawson et al., 1990; Ling & Wong, 1993; Perry, 2016; Prinz & Priller, 2014; Tremblay, 2011; Tremblay et al., 2011). Ramified microglia have previously been termed ‘resting’ or ‘quiescent’ to contrast ‘activated’ or ‘reactive’ microglia. However, they are in fact

highly motile, constantly retracting and extending their processes in order to monitor their surrounding environment (Nimmerjahn et al., 2005). Ramified microglia are characterised by long, thin, highly branched cellular processes with relatively equal distribution around a small, spherical soma. Ramified microglia tend to be evenly distributed throughout the grey matter, where they are more numerous than in the white matter and form an extensive tile-like pattern of cells which are subject to a tightly regulated process of turnover (Askew et al., 2017; Tay et al., 2017b).

The activation of microglia is associated with hypertrophy of the soma and cellular processes, with either deramification or hyperramification (Streit et al., 1999). Microglia which demonstrate these morphological changes might be referred to as ‘deramified’, ‘hyperramified’, or ‘bushy’. Deramified microglia have been described in the inferior temporal cortex and anterior cingulate cortex of AD and aged brains (Davies et al., 2017). These microglia showed reduced branch length, number of branches and junctions, and coverage of the neuropil. Deramified microglia have also been described in mouse models: APP/PSEN1 [PS1] (Holloway et al., 2020), anorexia (Reyes-Ortega et al., 2020), sphingosine 1-phosphate dependent activation (Karunakaran et al., 2019), repetitive TBI (Rowe et al., 2019), the resolution phase of activation following systemic challenge with lipopolysaccharides (LPS) (Norden et al., 2016), depression following TBI (Fenn et al., 2014), focal cerebral ischaemia (Morrison & Filosa, 2013), and repeated social defeat (Wohleb et al., 2011); in rats: early postpartum period (Eid et al., 2019) and following cerebral injection of neuraminidase wherein the extent of deramification correlated with the expression of IL1 β (Fernández-Arjona et al., 2019); and in manganese neurotoxicity *in vitro* (Kirkley et al., 2017). Hyperramified microglia have been described in post-mortem AD (Bachstetter et al., 2015), aged human brains (Streit & Sparks, 1997), and neurocognitive controls (Torres-Platas et al., 2014), but are more commonly described in mice. For instance, hyperramified murine microglia have been associated with wakefulness (Nakanishi et al., 2021); chronic stress (Tynan et al., 2010); acute challenge with p-chloramphetamine (Wilson & Molliver, 1994); early life stress (Rowson et al., 2016; Zetter et al., 2021); chronic depression (Hellwig et al., 2016); premature ageing (Hui et al., 2018); food restriction (Ganguly et al., 2018); and diffuse TBI

(Ziebell et al., 2017). Hyperramified microglia are morphologically similar to ramified microglia but have an enlarged soma and thickened processes. This category of cells has been proposed as an intermediate level of activation between ramified and deramified microglia (Streit et al., 1999). As such, they have also been termed ‘primed’ microglia (Torres-Platas et al., 2014). Bushy microglia have been described mainly in rat models of cerebral trauma (Soltys et al., 2001), focal ischaemia (Zhan et al., 2008), and sleep deprivation (Hsu et al., 2003) and in mice following neuronal ablation with trimethyltin (Kraft et al., 2016), hypoglossal axotomy (Yamada & Jinno, 2013), and in a model of ALS (Ohgomori et al., 2016). Bushy microglia display numerous short, poorly ramified processes of differing diameter which form bundles around an enlarged soma. Importantly, ‘activated’ (also, ‘hypertrophic’) microglia of at least these three morphological kinds—deramified, hyperramified, and bushy—have been proposed as neuroprotective and proregenerative following mouse facial nerve axotomy (Streit, 2002, 2005).

Rod-shaped or bipolar microglia are another morphological subcategory of activated cells which have been described in normal white matter and in the grey matter of a number of pathological conditions (Giordano et al., 2021; Graeber, 2010; Tam & Ma, 2014). Rod-shaped microglia have been identified clinically in AD, DLB, HS, normal ageing (Bachstetter et al., 2015, 2017) and various encephalopathies: neurosyphilis, subacute sclerosing panencephalitis, viral encephalitides, and Rasmussen’s encephalitis (Au & Ma, 2017; Holloway et al., 2019; Wirenfeldt et al., 2009). They have also been described in experimental models of diffuse TBI (Bachstetter et al., 2013; Cao et al., 2012; Taylor et al., 2014; Ziebell et al., 2012). Microglia that have reached an advanced stage of activation appear macrophage-like and amoeboid in morphology (Hendrickx et al., 2017; Li et al., 2019; Satoh et al., 2016). Amoeboid microglia have been described in AD and PD patients (Doorn et al., 2014; Sheng et al., 1997), but occur much more prominently in AD where there is concomitant HS (Bachstetter et al., 2015). Amoeboid microglia have also been described in mice. For instance, they appear epileptogenic with phagocytic and proliferative capability and express lysosomal genes before significant induction of proinflammatory pathways (Zhao et al., 2018). They have also been described as proinflammatory in a somatic mutation causing neurodegeneration (Mass et al., 2017); prominent in the developing brain,

particularly in the white matter (Kaur et al., 2017); associated with TBI (Caplan et al., 2020); and associated with myelinogenesis and the maintenance of oligodendrocyte progenitors (Hagemeyer et al., 2017). Amoeboid microglia show an enlarged soma with no or very few processes and display enhanced phagocytosis *in vitro* compared to ramified cells (Levtova et al., 2017).

All of the aforementioned morphologies—deramified, hyperramified, bushy, amoeboid, and rod-shaped (in most circumstances)—can be grouped under the umbrella term ‘activated microglia’ (Streit et al., 1999, 2014). Clusters of activated microglia are associated with NPs in AD (Serrano-Pozo et al., 2013; Walker et al., 2020a). The number of microglia that cluster at an A β plaque appears to increase linearly throughout the disease time course, even though the total number of plaques plateaus relatively early (Serrano-Pozo et al., 2011b). Interestingly, clusters are a very prominent feature in the brain of mouse models of AD but are much less common in human tissue (Sanchez-Mejias et al., 2016). The activation and clustering of microglia does not necessarily equate to ‘diseased’ microglia which implies a degree of incapacitation or aberrant functionality (Streit et al., 2014). In fact, clusters of activated microglia may have a neuroprotective effect by promoting the formation of dense-cored plaques (Huang et al., 2021).

Dystrophic microglia represent the diseased cell population which likely have impaired homeostatic function due to severe morphological disruption (Streit et al., 2004, 2014; Streit, 2006). Dystrophic microglia may be induced by soluble phosphotau (Sanchez-Mejias et al., 2016) and have been closely associated with NFD in post-mortem tissue (Streit et al., 2009). Thus, the concept of microglial incapacitation over the course of AD has come under increasing focus (Navarro et al., 2018; Streit et al., 2020). Dystrophic microglia may represent cells undergoing pyroptosis, which would be consistent with reports of ‘neuroinflammation’ in the context of AD (Gomez-Nicola & Boche, 2015; Hanslik & Ulland, 2020; Heneka & O'Banion, 2007; Heneka et al., 2013, 2014, 2015a, 2015b). Dystrophic microglia are characterised by processes which are asymmetrically distributed, fewer in number, tortuous, and often beaded or discontinuous in single label immunostains (Davies et al., 2017). The apparent fragmentation of cell processes likely represents the redistribution of the selected marker as they remain contiguous when viewed

with multiple markers using EM (Tischer et al., 2016). Therefore, the beaded or discontinuous immunostaining of processes in the context of single immunolabelling would be more aptly referred to as ‘pseudo-fragmentation’.

Ultrastructural morphology

In addition to the morphologies described above from studies using diffraction-limited light microscopy, EM studies have also investigated microglia at the ultrastructural level (Savage et al., 2019). Microglia can be distinguished from other cells of the CNS using EM without antibody-based techniques (Savage et al., 2018). Typically, they display a small soma, a bean-shaped nucleus with a distinct heterochromatin pattern, long stretches of endoplasmic reticulum, mitochondria, Golgi saccules, and lysosomes. Gitter cell-like microglia are filled with cellular debris and are described in the contexts of Werner syndrome mouse models (Hui et al., 2018); loss of sensory function with age in mice (Tremblay et al., 2012); cerebellum of young rats (Das, 1976); and in white matter of cats (Innocenti et al., 1983). Dark microglia are the most recently described cell type using EM whose name is derived from their electron-dense cytoplasm and nucleoplasm making them as dark as mitochondria. This sign of oxidative stress is also accompanied by the remodelling of nuclear chromatin. Dark microglia appear much more active than normal microglia and are rarely present under homeostatic conditions, but are abundant during chronic stress, ageing, and in CX₃C chemokine receptor 1 (CX₃CR1) knock-out (KO) and APP-PS1 mice (Bisht et al., 2016). Finally, the investigation of the ultrastructural features of microglial morphology is also possible using single-molecule localisation microscopy (SMLM). SMLM achieves sub-diffraction-limited light microscopy by reducing the total number of fluorescent emitters in a single timeframe and then super-localising active emitters by taking advantage of their point spread function (PSF) (Galbraith & Galbraith, 2011). Nanoscale resolution using SMLM has been successfully applied to eukaryotic cells (Lalkens et al., 2012) and bacteria (Coltharp & Xiao, 2012). However there remains a paucity of studies demonstrating its use in biological tissues (Badawi & Nishimune, 2020; Dani et al., 2010; Sigrist & Sabatini, 2012; Vaziri et al., 2008) and in archival human brain samples, in particular.

1.6.4 Molecular characteristics

Delineation of myeloid cells

Due to their mesodermal origin, microglia express a number of markers in common with macrophages and other myeloid cells, including F4/80, Fc receptors, and cluster of differentiation (CD)11b in human brain (Akiyama & McGeer, 1990). The ionised calcium-binding adaptor molecule 1 (Iba1) is a common macrophage marker but also a very effective pan-microglial marker (Ito et al., 1998). Iba1-labelled microglia are readily distinguished from perivascular or meningeal cells of myeloid lineage based on morphology and microanatomical separation (Ito et al., 2001; Kettenmann et al., 2011). Other common myeloid markers which are used to detect microglia in routine neuropathology include, CD169 (sialoadhesin, siglec-1), CD204 (MSR), β -glucan receptor dectin-1, CD206 (mannose receptor), and CD16 (Kettenmann et al., 2011). Activated microglia have been detected in AD brains using immunohistochemistry targeting the pan-microglia marker Iba1 (Ito et al., 1998, 2001); P2RY12—traditionally considered a marker of resting microglia (Walker et al., 2020a); major histocompatibility complex (MHC)I/II proteins, human leucocyte antigen (HLA)-A/B/C and HLA-DR and the lysosomal membrane protein CD68 (macrosialin) (Hendrickx et al., 2017; Tooyama et al., 1990); CD11a, CD11b, CD11c, CD18 (Akiyama & McGeer, 1990); CD33 (Walker et al., 2015); CD163 (scavenger receptor M130, ED2) (Pey et al., 2014); immunoglobulin Fc receptors, *e.g.* CD32 (Swanson et al., 2020) and CD64 (Minett et al., 2016); colony stimulating factor 1 receptor (CSF1R) (Akiyama et al., 1994); toll-like receptor (TLR)-2/3/4 (Walker et al., 2018); ferritin (Grundke-Iqbal et al., 1990); transmembrane protein 119 (TMEM119)—another marker traditionally used for homeostatic microglia (Walker, 2020b); and TREM2—involved in microglia-mediated phagocytosis and implicated in LOAD (Lue et al., 2015). Other inflammatory markers that may be upregulated in activated microglia include cyclooxygenase (COX) 2, monocyte chemoattractant protein 1, tumour necrosis factor (TNF) α , interleukin (IL) 1 β , and IL16 (Akiyama et al., 2000; Glass et al., 2010).

Murine microglia also express common macrophage markers, including *Csf1r*, inhibitory immune receptor *Cd200r*, tyrosine-protein phosphatase non-receptor type substrate 1 (also, *Cd172α*), and the fractalkine receptor *Cx3cr1* (Prinz & Mildner, 2011). Resident microglia are distinguishable from infiltrating monocytes and perivascular macrophages in the murine CNS using *Cd39* (Butovsky et al., 2012), *Tmem119* (Bohnert et al., 2020), *P2ry12* (Walker et al., 2020a), *Fcrls*, *Olfml3*, *Hexb*, *Tgfb1*, *Gpr34*, *Sall1* (Butovsky et al., 2014) and lower expression of the pan-haematopoietic marker *Cd45* (Gautier et al., 2012) and haemoglobin scavenger receptor *Cd163* (Serrats et al., 2010). A number of these are also demonstrated in human microglia (Bennett et al., 2016). Other transcriptomic analyses have also proved useful for the discrimination of microglial patterns of gene expression from other myeloid cells (Chiu et al., 2013; Hickman et al., 2013). Whilst all important, the utility of each of these markers may change in different disease settings and across different species (Masuda et al., 2019).

Mass cytometry and transcriptomics

The understanding of the molecular signatures of microglia has been expanded considerably over the last decade (Prinz et al., 2019). The transcriptome and epigenome of microglia have been described in the adult mouse brain (Gosselin et al., 2014; Lavin et al., 2014) as well as at different stages of development (Matcovitch-Natan et al., 2016; Varol et al., 2017). These were followed by single-cell mass cytometry (Ajami et al., 2018; Mrdjen et al., 2018) and single-cell RNA-Seq (scRNA-Seq) (Mathys et al., 2017) of murine microglia in health and disease. Further, scRNA-Seq of mouse models was used to identify neuroprotective disease-associated microglia (DAM) (Keren-Shaul et al., 2017), the microglial neurodegenerative phenotype (MGnD) (Krasemann et al., 2017), and the differential effect of immune training (exacerbator) and immune tolerance (attenuator) on cerebral Aβ deposition (Wendeln et al., 2018). The transcriptome and epigenome of human microglia (Gosselin et al., 2017) have also been described. Most recently, mass cytometry (Böttcher et al., 2019) and scRNA-Seq (Masuda et al., 2019) have also been used to describe the signature of microglia in post-mortem human brain or from surgical resections for the treatment of epilepsy.

Membrane channels

The following information organised under the subheadings membrane channels, membrane transporters, and receptor systems is in large part a summary of the extensive review by Kettenmann et al. (2011). Microglia are electrically non-excitable cells, though they are certainly not precluded from expressing a full complement of plasmalemmal ion channels, including those that are voltage gated. These include calcium (Ca^{2+}), sodium (Na^+), and potassium (K^+) ions, anions, and protons. Ca^{2+} signalling mechanisms are present in most living cells and are controlled by phylogenetically ancient molecular cascades for its transportation across lipid membranes and intracellular storage and buffering (Case et al., 2007; Petersen et al., 2005). Ca^{2+} ions are heavily involved in physiological signalling pathways and act as important triggers of apoptosis and necrosis (Nagano et al., 2006; Nicotera et al., 2007). The presence of Na^+ ion channels is disputed. Black et al. (2009) demonstrated that the inhibition of Na^+ channels in LPS-activated microglia by phenytoin or tetrodotoxin (TTX) decreased phagocytosis, secretion of $\text{IL1}\alpha$, $\text{IL1}\beta$, and $\text{TNF}\alpha$, and impaired adenosine triphosphate (ATP)-induced cellular motility *in vitro*. However, other labs have been unable to replicate Na^+ ion currents in a variety of microglial preparations (Bordey & Spencer, 2003; Boucsein et al., 2000; McLarnon et al., 1997) and treatment with TTX does not affect the motility of microglial processes *in vivo* (Nimmerjahn et al., 2005). The other aforementioned ion channels have also been closely studied in various preparations, each subserving particular functions in microglia (Kettenmann et al., 2011): K^+ ion channels are a marker for mobile microglia and are downregulated in stationary cells; Cl^- ion channels regulate intracellular water volume; and voltage-gated H^+ channels reduce extracellular pH—important following rapid extracellular alkalosis caused by neuronal activity.

Aquaporins and connexons are two other plasma membrane channels that have been identified in microglia (Kettenmann et al., 2011). There are 11 types of aquaporins in mammals which are responsible for maintaining water balance and play a role in the regulation of cell migration (Verkman, 2009). In the brain, aquaporins are mainly expressed by astrocytes, but can be induced in microglia by LPS injection (Tomás-Camardiel et al., 2004). Connexons are comprised of six connexin subunits

and form gap junctions which allow for intercellular coupling. For instance, gap junctions are critical in the formation of astrocytic syncytia (Ma et al., 2016). The subtype connexin 36 is expressed in murine neurons and microglia (Iacobas et al., 2007). Studies of gap junctions by the injection of dye into resting or activated microglia showed no intracellular coupling *in vivo* (Wasseff & Scherer, 2014) or only low levels *in vitro* (Eugenín et al., 2001). Lastly, gap junctions may form during CNS inflammation and under other pathological circumstances such as AD (Kielian, 2008).

Membrane transporters

Microglia express a number of different plasmalemmal transporters (Kettenmann et al., 2011). These include ion pumps, the ATP-binding cassette (ABC) transporters, and transporters for glucose, monocarboxylate, and glutamate. The glutamate–cystine antiporter Xc is almost exclusively responsible for the exchange of extracellular cystine with substantial quantities of intracellular glutamate following the activation of microglia by fibrillar A β ₄₀ (Qin et al., 2006), APPs α/β (Barger & Basile, 2001), or LPS (Barger et al., 2007)—potentially contributing to cerebral excitotoxicity. However, microglial involvement in overall glutamate homeostasis accounts for <10% of astrocytic function under physiological conditions (Persson et al., 2006). Microglia express the glucose transporter 5 (GLUT5) for the exchange of fructose, rather than glucose as for other GLUTs (Payne et al., 1997). Monocarboxylate transporters are expressed by endothelial cells, neurons, and astrocytes under normal conditions (Pierre & Pellerin, 2005). These transporters are proton dependent and allow for the transportation of energy substrates, such as lactate and ketone bodies. They may also be significantly upregulated in microglia following compression induced ischaemia in rats (Moreira et al., 2009). ABC transporters comprise seven subtypes (labelled ‘A’ through ‘G’; associated with further numerical subdivisions) (Jones & George, 2004). High expression of ABCG4—involved in cholesterol transport and lipid metabolism—was found in microglia associated with NPs in human AD tissue (Uehara et al., 2008). Lastly, microglia also express transporters for inorganic ions, including Cl[−] (Zierler et al., 2008), bicarbonate (Faff et al., 1996), and the H⁺/K⁺ pump (Shirihai et al., 1998). Interestingly, proton pump inhibition in combination with a non-

steroidal anti-inflammatory drug (NSAID) has been proposed as a treatment for broad spectrum neurodegeneration associated with microglial activation (Hashioka et al., 2009).

Receptor systems

The activation of microglia is triggered by ‘On’ and ‘Off’ receptor mediated signalling (Biber et al., 2007; Block et al., 2007; Hanisch & Kettenmann, 2007; Kettenmann et al., 2011). On signals are defined by those molecules which induce alterations to the functions of microglia upon receptor binding. Off signals are constitutively active systems which induce the activation of microglia only upon the interruption of their supply. Off signals differ from active suppressors (*e.g.* IL10) of microglia in that they do not necessarily inhibit the homeostatic activity of microglia. In this way microglia have the potential to react to local insults without the need of a recognisable danger signal (Kettenmann et al., 2011). On and off molecular signals come in the form of cytokines, alarmins, pathogen-associated molecular patterns (PAMPs), inorganic ions, neurotransmitters, neuromodulators, and neurohormones. Examples of On signals include cytokines, PAMPs, and alarmins; examples of Off signals include ligand–receptor pairs such as CD200–CD200R (Barclay et al., 2002), CX₃C ligand 1 (L1)–R1 (Cardona et al., 2006), and CD172 α –CD47 (Brooke et al., 2004).

Neurotransmitter receptors expressed by microglia include purinoceptors and adrenergic, cholinergic, dopaminergic, γ aminobutyric acid (GABA)-ergic, and glutamatergic receptors (Kettenmann et al., 2011). Purines and pyrimidines are ubiquitous extracellular signalling molecules. ATP and its derivatives are the nervous system’s principal purinergic signalling molecule (Abbracchio et al., 2009). ATP is released in large quantities in response to cellular damage, due to its particularly high cytosolic concentration. Microglia express ionotropic and metabotropic purinoceptors (Färber & Kettenmann, 2006) whose concentrations are dependent on the cellular activation status (Möller et al., 2000a). Binding of ATP to microglial purinoceptors has the potential to trigger a rapid response characterised by membrane ruffling, outgrowth of processes and convergence on a site of injury, and the release of proinflammatory cytokines. Microglia express α_{1A} ,

α_2A , β_1 , and β_2 adrenoreceptors which show anti- and proinflammatory effects under different circumstances (Kettenmann et al., 2011). Adrenoreceptors may be important in regulating the motility and phagocytic potential of microglia, which may be impaired in AD due to the early degeneration of the locus coeruleus, the brain's major production centre of noradrenaline (Heneka et al., 2010). Cholinergic pathways acting on the α_7 nicotinic acetylcholine receptor ($\alpha_7nAChRs$) exert global anti-inflammatory effects in the brain (Wang et al., 2003). Loss of cholinergic systems in AD may be responsible for the disinhibition of inflammatory pathways in microglia (Carnevale et al., 2007; Shytle et al., 2004). Dopaminergic receptors enhance the migratory capability of microglia and reduce the secretion of nitric oxide (NO) following LPS stimulation (Färber et al., 2005). GABA is the brain's main inhibitory neurotransmitter and has known neuroprotective effects (Fern et al., 1995). Stimulation of GABA_B receptors causes K^+ and Ca^{2+} ion currents and the reduced secretion of ILs from LPS stimulated microglia (Kuhn et al., 2004). Activation of microglial ionotropic α -amino-3-hydroxy-5-methyl-4-isoxazolepropionic acid (AMPA) glutamatergic receptors leads to the rapid and substantial reorganisation of the cytoskeleton (Christensen et al., 2006). The stimulation of metabotropic glutamatergic receptors induces a neurotoxic phenotype characterised by the activation of nuclear factor $\kappa\beta$ (NF- $\kappa\beta$) and the release of TNF α (Kaushal & Schlichter, 2008).

Microglia are sensitive to a number of neurohormones and neuromodulators (refer to Hoyle (1985) for general definitions). These include angiotensin II, bradykinin, cannabinoids, corticosteroids, endothelin, histamine, neurokinin (substance P), neurotrophins, opioids, platelet-activating factor (PAF), somatostatin, and vasoactive intestinal polypeptide (VIP) (Kettenmann et al., 2011). Angiotensin II receptors type 1 and 2 are expressed by microglia. The inhibition of type 1 receptors impairs morphological changes associated with activation and reduces the production of NF- $\kappa\beta$, IL1 β , and NO (Miyoshi et al., 2008). Bradykinin acts as a microglial chemokine and the stimulation of bradykinin receptors B₁ and B₂ have neuroprotective effects by attenuating the release of cytokines (Noda et al., 2007). Cannabinoid receptors enhance proliferation (Carrier et al., 2004) and reduce the neurotoxicity of microglia (Stella, 2009). The activation of microglia is also associated with the upregulation of cannabinoid receptors (Stella, 2010), the

stimulation of which reduces the production of NO and cytokines (Cabral & Marciano-Cabral, 2005). Corticosteroid receptors, including glucocorticoid and mineralocorticoid receptors are expressed by microglia. Activation of glucocorticoid receptors impairs proliferation and enhances the formation of lysosomes (Tanaka et al., 1997). Neurokinin receptors stimulated by substance P may trigger the activation of NF- κ B (Rasley et al., 2002), increase IL1 production (Martin et al., 1993), and enhance inflammatory responses in the context of bacterial infection (Rasley et al., 2004). Neurotrophins—nerve growth factor (NGF), brain-derived neurotrophic factor (BDNF), and neurotrophin 3 and 4 (NT3; NT4) exert their effects through tropomyosin receptor kinase (Trk) tyrosine kinase receptors and the p75 neurotrophin receptor (Kaplan & Miller, 2000; Patapoutian & Reichardt, 2001). A subclass of Trk receptors, the truncated tropomyosin-related kinase receptor are expressed by microglia and their activation by BDNF results in increased Ca²⁺ ion currents and decreased release of NO from activated microglia (Mizoguchi et al., 2009). Stimulation of κ -opioid receptors triggers morphological activation (Dobrenis et al., 1995), migration (Horvath & DeLeo, 2009), and promotes NO release from invertebrate microglia (Liu et al., 1996). These receptors appear important in regulating the immune response in human immunodeficiency virus 1 (HIV1) encephalopathy and dementia (Chao et al., 1996). Neuronal PAF binds microglial G protein and mitogen-activated protein kinase (MAPK)-coupled PAF receptors to produce a potent chemotactic response (Aihara et al., 2000). The activation of somatostatin receptors induces protein phosphorylation and impairs proliferation (Feindt et al., 1998). Finally, the activation of VIP/pituitary adenylate cyclase-activating peptide receptors 1 and 2 (VPAC_{1/2}) is known to be anti-inflammatory and immunosuppressive (Arranz et al., 2008; Leceta et al., 2007). Activation of VPAC₁ by VIP strongly inhibits the production of TNF α via cyclic adenosine monophosphate (cAMP) (Kim et al., 2000); reduces COX2 and prostaglandin E₂ via downregulation of NF- κ B (Gonzalez-Rey & Delgado, 2008); and reduces secretion of IL1 β , IL6, and NO (Delgado et al., 2003).

Microglial activities are heavily influenced by the receptor binding of cytokines (Kettenmann et al., 2011). These receptors include TNF α receptors; IL receptors; and chemokine receptors: CCR, CXCR, and CX₃CR. Stimulation of TNF α receptor types 1 and 2 is a potent effector of microglial activation (Bruce et al., 1996;

MacEwan, 2002); increases TNF α secretion—setting up a positive feedback loop (Kuno et al., 2005); and enhances phagocytic capability (von Zahn et al., 1997). Microglia express many types of IL receptors, *e.g.* types 1-RI/RII, 5, 6, 8, 9, 10, 12, 13, and 15 (Lee et al., 2002). ILs may exert trophic (Monif et al., 2016), inflammatory (Pinteaux et al., 2002; Sawada et al., 1995), or inhibitory effects—as seen with IL10 (Sawada et al., 1999)—on microglia. Chemokines such as CCL2, CCL21, and CX₃CL1 are released by neurons to signal neighbouring microglia of local endangerment or injury (Biber et al., 2008). The intracellular effects of these molecules are mediated by G protein coupled receptors linked to several enzymatic cascade systems, including adenylate cyclase, phospholipases, guanosine triphosphatases (GTPases), MAPK, and phosphatidylinositol 3-kinase (Baggiolini et al., 1997). Chemokines exert migratory effects and alter sensitivity to anti- or pro-inflammatory signals (Cardona et al., 2006; Prinz & Priller, 2010). There is also some evidence that AD involves aberrant chemokine signalling (Gebicke-Haerter et al., 2001).

Microglia express pattern recognition receptors (PRRs) for the detection of bacterial and viral infection and to assist with control of adaptive immunity (Padovan et al., 2007; Palm & Medzhitov, 2009). PRRs include the DNA-sensing absent in melanoma 2 (AIM2)-like receptor (ALR) (Keating et al., 2011); C-type lectin receptors (CLRs), *e.g.* dectin-1 (also, CLEC7A) and mannose receptors (Chiffolleau, 2018; Geijtenbeek & Gringhuis, 2009); nucleotide binding and oligomerisation domain (NOD)-like receptors (NLRs) (Fritz et al., 2006); retinoic acid-inducible gene I (RIG-I)-like receptors (RLRs) (Rehwinkel & Gack, 2020); and TLRs (Kawasaki & Kawai, 2014). TLRs are essential for the successful mobilisation of the body's innate immune system and exert their effects through complex signalling pathways that end at either, or both of, the activator protein 1 (AP1) or NF- κ B transcription factors (Hansson & Edfeldt, 2005; Jin & Lee, 2008). Pharmacological modulation of certain TLR mediated processes presents a potential avenue of neuroprotection in the context of trauma, infection, and non-infectious diseases of the CNS, including AD (Hanisch et al., 2008). PRRs are instrumental for the detection of PAMPs during invasion of the CNS by exogenous pathogens and a subset, namely the TLRs, are also capable of detecting endogenous molecules produced during tissue injury. These molecules are referred to as

alarmins, which together with PAMPs form the larger family of damage- or danger-associated molecular patterns (DAMPs) (Bianchi, 2007). The detection of DAMPs by microglia informs on homeostatic perturbations or overt tissue injury by infectious agents, trauma, radiation, chemical insult, hypoxia, or the accumulation of neuropathological peptides (Kono & Rock, 2008; Matzinger, 2007).

Microglia also express a range of other receptor systems in addition to the aforementioned. These include calcium receptors—for Ca^{2+} homeostasis (Brown & MacLeod, 2001); leukotriene receptors—linked to the secretion of ATP (Ballerini et al., 2005); notch-1 receptors—regulators of the production of cytokines and NO (Grandbarbe et al., 2007); complement receptors—implicated in the control of microglial motility impaired phagocytosis in AD (Crehan et al., 2012); thrombin receptors—linked to the secretion of NO, chemokines, $\text{TNF}\alpha$, and ILs (Möller et al., 2000b); macrophage colony-stimulating factor receptors—promotes phagocytosis and secretion of NO and cytokines (Mitrasinovic & Murphy, 2003); epidermal growth factor receptors—linked to motility (Nolte et al., 1997); CD200R—an important Off signal receptor as mentioned earlier (Wang et al., 2007; Wright et al., 2003); lysophosphatidic acid receptors—linked to membrane ruffling and upregulation of BDNF (Fujita et al., 2008); formyl peptide receptors—able to bind non-fibrillar $\text{A}\beta_{42}$, causing chemotaxis and the production of reactive oxygen species (ROS) (Tiffany et al., 2001); and finally, sigma receptors—suppressors of microglial inflammation and migration (Hall et al., 2009).

1.6.5 Physiology

Motility

In vivo two-photon microscopy of microglia in mice has demonstrated a constant ‘baseline’ or ‘surveillance’ motility (Nimmerjahn et al., 2005). Although only 5% of microglia showed migration of their soma at a velocity of 1–2 μm per hour, their cellular processes showed a continual cycle of extension and retraction at averages of 1.47 ± 0.1 μm per minute and 1.47 ± 0.08 μm per minute, respectively. The estimated fraction of total brain volume sampled each hour by moving processes was $14.4 \pm 1.6\%$. Given that the extracellular space accounts for ~20% of cortical

volume (Lehmenkühler et al., 1993), the authors suggested that the total volume of extracellular space is sampled by microglia every few hours. Further, the sampling fraction could be augmented by the application of the GABA receptor blocker bicuculline. Microglial processes were shown to directly contact astrocytes, blood vessels, and neuronal somata. Disruption of the BBB around capillaries by highly localised laser lesions induced an immediate response by mostly adjacent microglia, characterised by a switch from random to targeted movement of processes towards the site of injury. This form of motility contrasts with the stochasticity of baseline motility and is often referred to as ‘directed’ or ‘chemotactic’ motility. As outlined earlier, chemotactic motility can be induced in microglia by a number of chemokines (Biber et al., 2008) and ATP (Davalos et al., 2005).

Membrane ruffling and cellular migration is underpinned by the rearrangement of cytoskeletal proteins (Ramaekers & Bosman, 2004). Microglia display a single layered lining of actin microfilaments beneath the cell membrane termed the ‘cell cortex’. Rearrangement of the cell cortex to form lamellipodia, filopodia, and uropods controls motility and migration (Franco-Bocanegra et al., 2019). Lamellipodia are thin membrane enclosed sheets filled with a dense network of actin filaments at the leading edge of the direction of movement. Filopodia are the foremost protrusions of a ruffling lamellipodium, whilst the uropod represents the contractile trailing end of the migrating cell (Blanchoin et al., 2014; Hind et al., 2016). Nucleation of globular actin monomers into oligomers and their subsequent polymerisation into larger filaments are the first steps in the formation of microfilaments. This is followed by branching (controlled by the actin related protein [Arp]2/3 complex) and crosslinking with other actin filaments. The most notable crosslinking protein of actin filaments in microglia is Iba1 (Sasaki et al., 2001). Iba1 is essential for actin bundling—the parallel alignment of actin filaments—which is necessary for membrane ruffling, cellular migration, and phagocytosis (Bartles, 2000; Ohsawa et al., 2000; Ohsawa et al., 2004).

Summary of physiological functions

Microglial dynamics are conferred by their expression of membrane channels, transporters, receptor systems, and signalling molecules (Madry & Attwell, 2015).

Their key functions can be categorised into three broad domains: contributions during brain development, maintenance of CNS homeostasis, and innate immunity (Kierdorf & Prinz, 2017; Prinz et al., 2019; Shemer et al., 2015; Tremblay et al., 2011). Microglia display an amoeboid morphology in the developing mouse embryo (Perry et al., 1985) and are actively involved in phagocytosis and tissue remodelling (Matcovitch-Natan et al., 2016). In fact, in the absence of other glial cells during prenatal development, microglia appear critical for the control of neuronal progenitor numbers (Frost & Schafer, 2016), the establishment of neuronal architecture (Zhan et al., 2014), and synaptic pruning (Paolicelli et al., 2011). Further, they have also been shown to contact neuronal somata resulting in reduced spontaneous activity in zebrafish larvae (Li et al., 2012). Microglia also control neovascularisation in the mouse retina and zebrafish (Fantin et al., 2010). They also support other cells, including oligodendrocytes and their precursors during myelogenesis of the mouse CNS (Włodarczyk et al., 2017). Microglia are also essential for the masculinisation of the developing neonatal rat brain through oestradiol-induced upregulation of prostaglandin E₂ (Lenz et al., 2013). Many of these functions also persist into adulthood. Microglia continue to modulate neuronal activity (Tremblay et al., 2011), reorganise neuronal circuits (Tremblay, 2011), perform efferocytosis (Sierra et al., 2010), and remain important for the maintenance of oligodendrocyte progenitors and myelogenesis (Hagemeyer et al., 2017). Finally, microglia represent the major innate immunocompetent cells of the CNS (see reviews: Aloisi, 2001; Jin & Yamashita, 2016; Kaur et al., 2010; Lehnardt, 2010; Lenz & Nelson, 2018; Rivest, 2009; Yang et al., 2010). Microglia are active sensors of infection, mechanical trauma, ischaemia, and neuropathological lesions. Microglia initiate innate responses following the activation of cytokine, chemokine, growth factor, and other receptors or PRRs, *e.g.* NLRs and TLRs. The effects of immune activation in the brain may include increased antigen-presenting capacity; further expression of proinflammatory mediators; opsonic mediators and phagocytosis; permeability of the BBB; plasma leakage into the cerebral interstices—associated with risk of cerebral oedema; margination and extravasation of peripheral leucocytes; and the initiation of adaptive immune responses and tissue repair.

1.6.6 Involvement in Alzheimer's disease

The involvement of the innate immune system in AD has been known since at least the 1980s (Dickson et al., 1988; Eikelenboom & Stam, 1982; Eikelenboom et al., 1989; Itagaki et al., 1989; McGeer et al., 1989). These studies were followed by additional descriptions of clusters of activated microglia associated with A β plaques (Perlmutter et al., 1990; Sanchez-Mejias et al., 2016; Sasaki et al., 1997; Serrano-Pozo et al., 2011b; Serrano-Pozo et al., 2013; Walker et al., 2020a) and the correlation of inflammatory markers with the loss of synapses (Lue et al., 1996). *In vivo* imaging of GFP-labelled microglia in APP/PS1 mice has demonstrated their ability to migrate at an average of 5–9 mm/month and are thus capable of reaching a developing plaque in 1–2 days (Bolmont et al., 2008). As mentioned earlier, dystrophic microglia have also been closely associated with NFD in AD (Streit et al., 2009). It appears that the binding of A β to PRRs, including NLRs (Halle et al., 2008), the receptor for advanced glycation end-products (RAGE), scavenger receptors, formyl peptide receptors, and TLRs (Salminen et al., 2009)—among other mechanisms—is sufficient to cause neurotoxic activation of microglia in various disease models (Heneka et al., 2015b, 2015b). A number of mechanisms by which neurotoxic microglia exert their effects have been proposed, including the release of proinflammatory cytokines such as TNF α and ILs associated with suppression of long-term potentiation (LTP) (Kummer et al., 2011); reduced trophic factors, *e.g.* transforming growth factor β (TGF β) and BDNF (Heneka et al., 2015b; Parkhurst et al., 2013; Tarkowski et al., 2003); inhibition of mitochondrial respiration (Heneka et al., 2015a); phagoptosis—the direct phagocytosis of phosphatidylserine-presenting neurons by microglia (Neniskyte et al., 2011); and exacerbation of existing neuropathological lesions, resulting in a chronic feedback loop (Heneka et al., 2015b; Heneka et al., 2015a).

More recently the field of genetics has strongly implicated microglia in the pathogenesis of LOAD (Jones et al., 2015). A number of GWAS of AD have been performed (Harold et al., 2009; Hollingworth et al., 2011; Lambert et al., 2009; Naj et al., 2011)—mostly in European populations—with subsequent meta-analyses (Jun et al., 2010; Lambert et al., 2013). Many of the genes of putative significance are expressed by myeloid cells and microglia in particular, including, *CR1* (c1),

TREM2 (c6), *TREML2* (c6), *PILRB* (c7), *MS4A4A* (c11), *MS4A6A* (c11), *SPI1* (c11), *PLCG2* (c16), *ABI3* (c17), and *CD33* (c19) (Pimenova et al., 2018). A few of these are described in brief here. For instance, *SPI1* is a myeloid enhancer, encoding the transcription factor PU.1 which has a major role in the development and cell type-specific gene expression of myeloid cells. Reduced *SPI1* expression has been associated with delayed onset of AD (Huang et al., 2017). Genes involved in microglial phagocytosis represent an emerging theme in AD GWAS (Podleśny-Drabiniok et al., 2020). These include *CD33*, *TREM2*, *MS4A* and *CR1*, among others (Sierra et al., 2013). *CD33* is also expressed by myeloid cells and is involved in anti-inflammatory immune responses. It has been associated with AD through a polymorphism in its promoter region. *Cd33* has been shown to inhibit A β ₄₂ uptake in mouse primary microglia culture and its ablation in APP/PS1 mice was associated with reduced plaque pathology (Griciuc et al., 2013). Further, *ex vivo* monocytes from *CD33* risk allele carriers showed increased *CD33* expression which was associated with reduced A β internalisation and increased plaque load (Bradshaw et al., 2013). The R47H *TREM2* (Triggering receptor expressed on myeloid cells 2) variant more than doubles the risk of AD (Guerreiro et al., 2013; Jonsson et al., 2013), making it the strongest genetic risk factor for LOAD after *APOE*. Variants of *TREM2* reduce the expression of the full-length protein resulting in reduced apolipoprotein binding and uptake by microglia, thereby also reducing the uptake of A β (Yeh et al., 2016). Of note too is that the *MS4A* gene family risk alleles—4A and 6A—are key regulators of cellular activation (Eon Kuek et al., 2016) and levels of soluble *TREM2* (Deming et al., 2019). *CR1* (complement receptor 1) is a phagocytic receptor, recognising complement proteins C1q, C3b, C4b, and C3b/4b and C3b/C3b complexes. Reduced expression of *CR1* results in reduced clearance of A β and confers significant risk of AD in individuals who express a copy-number variant that increases the number of C3b/C4b binding sites (Brouwers et al., 2012; Villegas-Llerena et al., 2016)—corresponding to the CR1-S isoform.

In addition to GWAS, gene network analysis and proteomics also suggest microglia and myeloid cells play a causal role in AD. Gene-regulatory networks of brain tissue from LOAD patients and nondemented controls have demonstrated the differential regulation of immune-related genes governed by *TYROBP*, which is expressed by

microglia and associated with, though not critically to, TREM2 signalling pathways (Audrain et al., 2021; Zhang et al., 2013). Finally, a study of protein networks in cortical AD tissue also supports the role of microglia in AD (Seyfried et al., 2017). In this study the enrichment of microglial and astrocytic markers occurred in symptomatic AD cases, suggesting these cells are also important effectors of cognitive decline during the end-phase of the disease.

1.7 Hypotheses of Alzheimer's disease pathophysiology

A very brief overview of a number of different hypotheses for the pathophysiology of AD are provided here. Among them include the ACH, tau propagation, neurotransmitter, inflammation, neurovascular disruption, and mitochondrial cascade hypotheses. These hypotheses vary widely in their origin and evolution over time but are not necessarily independent of each other. Brief mention will also be made in section 1.7.1 on the progress of clinical trials to date—which have been overwhelmingly unconvincing in support of the popular ACH. So long as this is true, the exact nature of AD remains obscure. Liu et al. (2019a) have provided a good summary of the current hypotheses and related clinical trials in the field.

1.7.1 Amyloid cascade hypothesis

The ACH remains the predominant hypothesis in the field. It originated in the early 1990s with the discovery of a missense mutation in *APP* (Goate et al., 1991; Hardy & Allsop, 1991; Hardy & Higgins, 1992; Selkoe, 1991) and has been adapted over time (Hardy & Selkoe, 2002; Selkoe & Hardy, 2016). The essential formulation is as follows: generation of A β (soluble or fibrillar) \rightarrow NFD \rightarrow neuronal loss. The ACH is based on sound biochemical, biomarker, genetic, and neuropathological evidence (Selkoe, 2019). However, the vast majority of A β -based therapies have failed in clinical trials (Cummings et al., 2014, 2019; Forester et al., 2020; Huang et al., 2020; Hyman & Sorger, 2014; Karran & Hardy, 2014; Panza et al., 2019). In very recent news, the monoclonal antibody aducanumab which targets neurotoxic oligomeric species of A β (Arndt et al., 2018) received approval for use in the United States. The United States Food and Drug Administration (FDA) approved its use

for the treatment of AD under an *‘accelerated approval pathway, which provides patients suffering from a serious disease earlier access to drugs when there is an expectation of clinical benefit despite some uncertainty,’* (FDA, 2021, Jun 7). This news came in spite of their Peripheral and Central Nervous System Drugs Advisory Committee voting overwhelmingly against regulatory approval last year (FDA, 2020, Nov 6). There also remains significant debate as to whether or not the 0.39 point difference between the treatment group and controls on the clinical dementia rating–sum of boxes (CDR–SB) test reaches a minimum clinically important difference (MCID) (Alexander et al., 2021; Cummings et al., 2021; ICER, 2021, May 5; Knopman et al., 2021)—especially considering this effect only reached statistical significance in a post-hoc analysis of the EMERGE trial but not in the concurrent and identically designed ENGAGE companion trial (Kuller & Lopez, 2021; Liu et al., 2021). It is interesting to note that given the weight of numbers, a chance positive result from ACH-based trials would be increasingly likely over time as predicted by Castellani and Smith (2011). Thus, there still remain many unanswered and very significant questions as to the validity of the ACH (Morris et al., 2018).

1.7.2 Tau propagation hypothesis

The tau propagation hypothesis (also, signal transduction hypothesis—?SiTH) was proposed over a decade after the ACH (Frost et al., 2009; Iqbal & Grundke-Iqbal, 2005) and recently updated (Arnsten et al., 2021). It posits a more multifactorial concept of AD pathophysiology, starting with an admixture of environmental exposures; metabolic abnormalities—which may involve glucose, cholesterol, or ROS; age-related impairments of plasma membrane fluidity or glial support; and genetic factors, including mutations in transmembrane proteins such as *APP*, *PSEN1*, and *PSEN2* which set up two parallel running pathological processes defined by the accumulation of phosphotau in the one and A β in the other (Small & Duff, 2008). Given the complexity of the disease it is not unreasonable to expect that a combination of therapies targeting several lines of pathological processes will be necessary for its successful management (Salloway et al., 2020).

1.7.3 Inflammation hypothesis

As described earlier, the involvement of the immune system in AD has been known for decades. The inflammation hypothesis is generally posited as a downstream process of A β and tau pathological changes (Calsolaro & Edison, 2016; Hashioka et al., 2020; Heneka et al., 2015b). The binding of misfolded A β or phosphotau to PRRs expressed by microglia and astrocytes initiates a sustained, self-propagating neurotoxic process of cellular activation, release of proinflammatory mediators, the potential recruitment of blood-borne leucocytes, aberrant phagocytosis, and the induction of apoptosis in neurons. Factors that modulate this process of sterile inflammation include systemic inflammation, obesity, TBI, and the degeneration of the locus coeruleus and cholinergic system which exert potently anti-inflammatory effects throughout the brain. Notwithstanding, clinical trials involving immunotherapy or anti-inflammatory therapy have broadly failed to prevent the progression of MCI to AD (Heneka et al., 2015b)—however may require initiation earlier in the disease time course as has been argued for anti-A β immunotherapies, albeit with no record of success.

1.7.4 Neurotransmitter hypotheses

The cholinergic hypothesis is one of the oldest in the field (Davies & Maloney, 1976). In the original study of Davies and Maloney, the concentration of ACh at synapses was reduced in AD due to the reduced activity of choline acetyltransferase—an enzyme required for its synthesis—in the amygdala, hippocampus, mid-brain, pons, and sensory, parietal, and frontal cortices of AD brains. Acetylcholinesterase inhibitors prevent the breakdown of ACh and are able to modestly, but not indefinitely, alleviate the symptoms of AD (Knight et al., 2018). Other neurotransmitters of interest are glutamate and 5-hydroxytryptamine (5-HT). Glutamate is the major excitatory neurotransmitter of the brain and appears responsible for mediating excitotoxicity in AD via extrasynaptic N-methyl-D-aspartate (NMDA) receptors (Liu et al., 2019b; Wang & Reddy, 2017). Memantine is a non-competitive antagonist of glutamatergic NMDA receptors (Johnson & Kotermanski, 2006). Blockade of these receptors reduces the risk of pathological Ca²⁺ currents responsible for excitotoxicity. Memantine also appears to disinhibit

the activity of α -secretase which results in reduced production of A β . It is also an antagonist of nAChRs (*n.b.* it is not an acetylcholinesterase inhibitor) and 5-HT₃ receptors. The role of 5-HT in depression, ageing, and AD has been under investigation for some time (Meltzer et al., 1998) such that selective serotonin (5-HT) reuptake inhibitors, *e.g.* fluoxetine, have been proposed as treatments for AD (Liu et al., 2019a).

1.7.5 Other hypotheses

There are also a number of other hypotheses in the field each of which are under active investigation in clinical trials (Liu et al., 2019a). The neurovascular disruption hypothesis is based on the observation that vascular dysfunction can lead to brain dysfunction (de la Torre, 2018; Iadecola, 2004; Scheffer et al., 2021; Zlokovic, 2005) and that the cerebral microvasculature is damaged in AD (Buée et al., 1994) before the onset of symptoms (Knopman & Roberts, 2010). The mitochondrial cascade hypothesis was contributed by Swerdlow and Khan (2004). The central contention of this hypothesis is that the accumulation of ROS in mitochondria leads to damage of associated DNA, RNA, lipids, and proteins. Oxidative damage may also induce soluble proteins to adopt insoluble β -pleated sheet structure, giving rise to fibrillar A β and tau. The diabetes hypothesis centres on insulin-resistance and deficiency not as a risk factor or secondary to either type 1 or 2 diabetes mellitus, but as a distinct pathological entity within the brain which causes AD—hence the coinage of ‘type 3 diabetes’ as a synonym of AD (Arnold et al., 2018; de la Monte, 2019; Mittal et al., 2016). Other hypotheses include the exercise and inactivity hypothesis (De la Rosa et al., 2020); infection hypotheses—which are also amongst the oldest hypotheses, having started with Sjogren et al. (1952) with updates until the present time (Seaks & Wilcock, 2020; Sochocka et al., 2017); metal ion hypotheses—which started with Bush et al. (1994) and are often closely related to the ACH (Spinello et al., 2016; Yang et al., 2019); calcium dysregulation hypotheses—also very old (Khachaturian, 1994) and often presented in association with other hypotheses, *e.g.* ACH, SiTH, or neurotransmitter hypotheses (Cascella & Cecchi, 2021); and meningeal lymphatic (Da Mesquita et al., 2018) and glymphatic (Mentis et al., 2021; Reeves et al., 2020) system

impairment hypotheses which revolve around the impaired clearance of A β from the brain.

1.8 Experimental paradigms

The work presented in this thesis falls within two broad paradigms of neuroscientific research. The first is experimental neuropathology which entails the use of post-mortem human brain tissue sections to characterise and make inferences about pathophysiological processes and their sequence of events during life—in addition to performing regular diagnostic procedures. The second is the use of organotypic brain slice cultures as a 3D culture model of the brain with which to perform prospective molecular studies of health, disease, and treatment. The following two sections will summarise the key concepts of each and provide examples of their application to answering important questions in the field of AD research. This will be of relevance to understanding the hypotheses and experimental aims presented in section 1.9.

1.8.1 Experimental neuropathology

One of the key concepts of experimental neuropathology is in making inferences about the pattern of spread of pathology through the brain based on its presence across a series of brain regions in a given cohort. This conceptual framework was employed by Braak and Braak (1991) for the staging of NFD and Thal et al. (2002) for the staging of A β plaques. The hierarchical sequence of neuropathological changes across brain regions rests on the argument that regions involved early in the disease time course by and large retain the build-up of pathological changes during life until post-mortem investigation. Importantly, this does not necessarily make assumptions about the pattern of accumulation of neuropathological lesions—whether linear, exponential, logarithmic, or other—over the natural history of the disease. Indeed, it is the extent of spread and not the load of pathology *per se* which is stressed in the staging schema. Thus, regions showing the most extensive pathological changes in the sample population represent the earliest affected areas in the disease time course and regions showing the least pathology represent more

belatedly affected areas. Reassuringly, longitudinal PET imaging studies of NFD (Schöll et al., 2016; Schwarz et al., 2016) and A β (Jelistratova et al., 2020)—though with less certainty (Fantoni et al., 2020)—have broadly recapitulated the patterns of spread as hypothesised according to the respective autopsy series.

Extending this concept, it is therefore theoretically possible to select regions based on the staging schema to represent earlier and later stages of the disease process with the aim of inferring the relative timing of other pathological events in relation to the deposition patterns of NFD and A β . In this way the natural history of certain aspects of the disease can be recapitulated within individual brains by comparing differentially affected brain regions. The regions of interest selected for investigation in the work presented here are based on the AD staging schema (Braak & Braak, 1991; Mirra et al., 1991; Thal et al., 2002) and a volumetric study (Halliday et al., 2003). These include the inferior temporal cortex (ITC)—an earlier and severely affected brain region, representative of end-stage AD at post-mortem; and the superior frontal cortex (SFC) and precuneus (PreC)—two intermediately affected brain regions; and the primary visual cortex (PVC) and primary motor cortex (PMC)—two belatedly and lesser affected brain regions, representative of earlier phases of AD at post-mortem. Furthermore, and based on the linear progression proposed by the ACH, the belatedly affected regions of the neocortex will have A β pathology, some NFD pathology but little or no neuronal loss. Theoretically they represent sites for observing early neuronal dysfunction and targets for treatment prior to irreversible neuronal loss (Sutherland et al., 2011).

1.8.2 Organotypic slice culture

Organotypic brain slice cultures (BSCs) have been in widespread use in neuroscientific research for over 50 years (Humpel, 2015) and have found good utility in the research of neurodegeneration in particular. The major advantages of using BSCs is that they retain a 3D structure with the same mix of cells found *in vivo* and eliminate the requirement for living animals to experience severe morbidity. Further, these *ex vivo* cells remain representative of their *in vivo* counterparts (Beach et al., 1982; Croft et al., 2019b; Daria et al., 2017; del Rio et

al., 1991; Hailer et al., 1996; Hutter-Schmid et al., 2015; Staal et al., 2011). BSCs have been successfully applied to studying A β and tau molecular pathology as well as microglia-mediated clearance of A β and synaptic loss (Croft et al., 2019a); the lattermost being inconsistently observed in transgenic models of AD (Wirths & Bayer, 2010). BSCs were used here to investigate how monomeric and fibrillar species of A β ₄₂ impact the expression of a number of candidate genes.

1.9 Thesis overview

This thesis includes a three-part neuropathological study—each published separately—of microglial morphological changes and phagocytic activity in cortical regions of non-demented controls with minimal AD-type pathology; non-demented controls with a high level of AD-type pathology—termed controls with Alzheimer changes (CAc), which are representative of PreAD; and AD brains differentially affected by the load of A β , tau, and neuronal loss. It also includes gene amplification studies in mouse BSCs and published results from human tissues. The principal aim of this thesis is to argue that early microglial changes represent a neuroprotective response to the development of AD neuropathological insults.

1.9.1 Hypotheses

- i. Microglia react to the deposition of fibrillar species of A β and tau during the preclinical phase of AD by exhibiting morphological features consistent with activation at earlier stages and dystrophic changes only during the symptomatic end-stage of disease.
- ii. Microglial activation follows the deposition of A β but precedes NFD in cortical regions of PreAD and AD brains.
- iii. Aberrant phagocytosis of presynaptic elements by microglia is upregulated during the symptomatic end-stage of AD but not during PreAD.
- iv. Microglia in mouse BSCs treated with synthetic preparations of A β monomers will upregulate activation markers while treatment with fibrils

will upregulate phagocytic markers. Here monomers and fibrils represent earlier and later phases of A β -dependent AD pathophysiology, respectively.

- v. Markers of immune activation and phagocytosis will be upregulated in the minimally-affected PVC and moderately-affected PreC which represent early phases of AD.

1.9.2 Experimental aims

- i. To use Iba1 IHC of tissue sections from the ITC, SFC, and PVC of control, PreAD, and AD brains to enumerate total microglia and morphological subtypes both manually and with automated morphometric image analysis. Immunofluorescence (IF) histochemistry to quantify the load A β and TTau pathology. Cresyl violet stains to enumerate total neurons and measure cortical thinning.
- ii. To use Iba1, A β , and TTau double IF-labelling of tissue sections from the ITC and PMC of control, PreAD, and AD brains to determine the relative sequence of microglial, A β , and TTau pathological changes.
- iii. To use SMLM of Iba1 and synaptophysin (Syp) double IF-labelled sections from the SFC of control, PreAD, and AD brains to investigate the potential internalisation (phagocytosis) of presynaptic elements by microglia.
- iv. To use ddPCR to quantify myeloid/microglial constitutive (*Aif1*, *Itgam*, *Ptpnc*) and phagocytic (*Cd68*, *Trem2*) markers, and the expression of a major anti-inflammatory markers (*Chrna7*) from mouse BSCs treated with two and 10 μ M synthetic A β monomer and fibril solutions for eight and 72 hours.
- v. To use droplet digital polymerase chain reaction (ddPCR) gene amplification to quantify microglial *CXCR4*, *MS4A6A*, *SLC7A2* and *TREM2* and other AD-related genes (*SST*, *IGF1R*, and *INSR*) in the PreC and PVC of control and AD brains.

1.9.3 Further details

Chapter 1 of this thesis presented a general introduction to microglia and AD and a basis for the hypotheses explored here. Chapters 2–5 present the four Methods and Results sections. The first three Results chapters are all first-author publications in peer-reviewed scientific journals: *Brain Pathology* (Paasila et al., 2019), *Free Neuropathology* (Paasila et al., 2020), and *Journal of Neuroscience Research* (Paasila et al., 2021). Chapter 2 addresses the first hypothesis and aim; Chapter 3 addresses the second; Chapter 4 addresses the third; Chapter 5 is presented as a traditional thesis chapter and addresses the fourth and fifth listed hypotheses and aims. The ddPCR assays of candidate gene amplification studies in the PreC and PVC of human tissues presented in Chapter 5 were performed by the candidate and have also been published in the journal *Scientific Reports* (Guennewig et al., 2021). Each of the Results chapters is presented with a preamble, an authorship attribution statement and attestation, the published manuscript, and any published supplementary material. Chapter 2 also concludes with the successful application submitted to the Discipline of Anatomy and Histology, School of Medical Sciences, The University of Sydney, for the Professor John Irvine Hunter Prize for Research in the School of Medical Sciences for the most influential paper by a HDR student. Chapter 6 is a general discussion of all findings presented here. References cited in the published works are presented at the end of each manuscript. References cited in Chapters 1, 5, and 6 are listed at the end of this thesis.

Chapter 2: The relationship between the morphological subtypes of microglia and Alzheimer's disease neuropathology

2.1 Preamble

This chapter presents a manuscript published by Brain Pathology, the official journal of the International Society of Neuropathology. Here it was of interest to investigate the spatiotemporal relationships between microglia and their morphological changes in relation to the evolution of AD neuropathology through differentially affected regions of the brain. This was particularly relevant given conflicting reports from post-mortem human studies which showed significant heterogeneity in microglial phenotypes in AD. Further, the results from human pathological studies reflect markedly different microglial responses from those seen in mouse models which show widespread activation. It was hypothesised that the activation of microglia would be associated with the appearance of A β plaques in mildly affected brain regions, whilst microglia in severely affected brain regions would exhibit features of cellular dystrophy—as suggested by a past qualitative neuropathological study of limited sample size. The aim of this investigation was to undertake a much larger sampling of total microglia through different cortical regions of the AD brain—including the ITC, SFC, and PVC—and to then correlate these findings with quantitative data on neuronal numbers, cortical atrophy, and A β and NFD pathological changes. These procedures were performed both manually and also validated by automated image analysis with the potential for significant upscaling in future work. The brain regions were selected based on the semi-quantitative AD staging schema and a previous volumetric study undertaken by one of the co-authors—JJK. All AD cases presented in this thesis were diagnosed and rated by CDR during life and then neuropathologically confirmed at post-mortem. This work was done in collaboration with Dr. Claire S. Goldsbury and Danielle S. Davies at the Brain and Mind Centre, The University of Sydney.

2.2 Authorship attribution statement

Chapter 2 of this thesis is published as ‘The relationship between the morphological subtypes of microglia and Alzheimer’s disease neuropathology’ (Paasila et al., 2019). The manuscript was authored by Patrick J. Paasila, Danielle S. Davies, Jillian J. Kril, Claire S. Goldsbury, and Greg T. Sutherland (corresponding author). PJP co-designed the study, collected all the data except the tau data, analysed all the data, and wrote the manuscript. DSD collected and helped analyse the tau data. JJK and CSG co-designed the study. GTS designed the study and analysed the data. All authors contributed to editing the manuscript.

Attestation

In addition to the statement above, permission to include the published material has been granted by the corresponding author.

Patrick J. Paasila

Candidate

June 2021



Greg T. Sutherland

Corresponding author

June 2021

2.3 Published manuscript

The published manuscript begins on the next page.

RESEARCH ARTICLE

The relationship between the morphological subtypes of microglia and Alzheimer's disease neuropathology

Patrick Jarmo Paasila¹; Danielle Suzanne Davies²; Jillian June Kril ¹; Claire Goldsbury²; Greg Trevor Sutherland ¹

¹ Discipline of Pathology, Faculty of Medicine and Health, The University of Sydney, Sydney, Australia.

² The University of Sydney Brain & Mind Centre, Sydney, Australia.

Keywords

Alzheimer's disease, brain pH, microglia, post-mortem human brain, quantitative neuropathology.

Corresponding author:

Greg Trevor Sutherland, Charles Perkins Centre, The University of Sydney, Rm 6211 Level 6W, Sydney, NSW 2006, Australia (E-mail: g.sutherland@sydney.edu.au)

Received 11 December 2018

Accepted 18 February 2019

Published Online Article Accepted

25 February 2019

doi:10.1111/bpa.12717

Abstract

Microglial associations with both the major Alzheimer's disease (AD) pathognomonic entities, β -amyloid-positive plaques and tau-positive neurofibrillary tangles, have been noted in previous investigations of both human tissue and mouse models. However, the precise nature of their role in the pathogenesis of AD is debated; the major working hypothesis is that pro-inflammatory activities of activated microglia contribute to disease progression. In contrast, others have proposed that microglial dystrophy with a loss of physiological and neuroprotective activities promotes neurodegeneration. This immunohistochemical study sought to gain clarity in this area by quantifying the morphological subtypes of microglia in the mildly-affected primary visual cortex (PVC), the moderately affected superior frontal cortex (SFC) and the severely affected inferior temporal cortex (ITC) of 8 AD cases and 15 age and gender-matched, non-demented controls with ranging AD-type pathology. AD cases had increased β -amyloid and tau levels compared to controls in all regions. Neuronal loss was observed in the SFC and ITC, and was associated with atrophy in the latter. A major feature of the ITC in AD was a decrease in ramified (healthy) microglia with image analysis confirming reductions in arborized area and skeletal complexity. Activated microglia were not associated with AD but were increased in non-demented controls with greater AD-type pathology. Microglial clusters were occasionally associated with β -amyloid- and tau-positive plaques but represented less than 2% of the total microglial population. Dystrophic microglia were not associated with AD, but were inversely correlated with brain pH suggesting that agonal events were responsible for this morphological subtype. Overall these novel findings suggest that there is an early microglial reaction to AD-type pathology but a loss of healthy microglia is the prominent feature in severely affected regions of the AD brain.

INTRODUCTION

The clinical diagnosis of Alzheimer's disease (AD) is probabilistic and typically supported by an abbreviated form of a neuropsychological evaluation such as the Clinical Dementia Rating (CDR) (36). Confirmation of AD can only be made at autopsy where the most comprehensive diagnostic schema is provided by the National Institute of Aging-Alzheimer's Association work-group (35). This diagnostic schema incorporates previously described semi-quantitative criteria for (A) β -amyloid (A β) immunostaining (60), (B) Braak staging of neurofibrillary tangles (NFTs) (6) and (C) CERAD neuritic plaque score (33) to generate an "ABC" score. An intermediate or high "ABC" score being considered sufficient to confirm AD in a demented individual. Yet, this pathological diagnosis is also probabilistic caused by the common finding of AD-type pathology, albeit at lower levels, in

similarly aged but non-demented individuals (4). A β pathology appears first in the cortex before spreading more ventrally; whereas neurofibrillary pathology, including NFTs, begins in the medial temporal lobe, then spreads more dorsally and laterally throughout the limbic system and cortex with relative sparing of primary cortices (6).

Along with A β plaques and NFTs, the pathology of AD is characterized by neuronal loss and gliosis (59). Microglial activation has been considered a key pathomechanism in AD, with activated microglia associating with neuritic plaques and subsequently producing a neurotoxic milieu that contributes to neuronal degeneration (30, 41, 46). Single-nucleotide polymorphisms in genes exclusively or largely expressed in microglia are associated with increased AD risk including *TREM2*, *CD33*, *CRI*, *ABCA7* and *SHIP1* (31). Microglial activation in AD appears to be A β -dependent; with A β binding to NLR

Family Pyrin Domain Containing 3 (16), and pattern recognition receptors such as RAGE, scavenger receptors (44) and toll-like receptors (TLR2, TLR4 and TLR6) (8) being sufficient to cause microglial activation in mouse models of AD.

In the past, microglia were regarded as quiescent cells that only responded to brain injury. It is now known that microglia are physiologically active, surveying their territory by continually extending and retracting their processes (38). Extensive *in vitro* and animal studies of microglia demonstrate their ability to sample their surrounding microenvironment and are particularly involved in synaptic homeostasis (26) throughout life by pruning of synapses in the developing CNS (47) and mediating remodeling in the adult brain (40). Microglia are functionally dynamic cells as evidenced by the wide range of morphologies observed in the brain under normal and pathological states (11). There have been a number of attempts to categorize microglia into distinct subtypes but there is little consensus on what constitutes each subtype or the nomenclature used to describe them.

Briefly, in studies using human post-mortem brain tissue, ramified (healthy) microglia (previously called “resting” or “quiescent” microglia) are characterized by equally distributed, long, thin, ramified processes attached to a small, spherical soma (5). The terms “activated,” “reactive,” “bushy” and “hypertrophic” have been used to describe microglia that are responding to injury or potentially injurious events. Activated microglia display significantly hypertrophic soma and processes with some degree of deramification (hence the use of the term “deramified” by some authors) (3, 45). Fully activated microglia, with enlarged soma and lacking processes entirely, are termed “amoeboid” and have enhanced phagocytic capabilities (52). “Dystrophic” microglia are characterized by highly tortuous, asymmetrical and truncated processes and may demonstrate discontinuous or beaded immunostaining. Such dystrophic microglia may also be termed “pseudo-fragmented” as electron microscopy studies have revealed that apparent discontinuities in their cellular processes represent a redistribution of the selected marker, with the processes remaining contiguous when visualized using multiple markers (61). Other features of dystrophic microglia that occur variably include the formation of spheroids and condensation within the nucleus, possibly indicative of pyknosis (56). Streit and colleagues found that dystrophic microglia preceded neurofibrillary pathology in AD (54) raising the possibility that a loss of microglial function may be as, or more, important than a gain of toxic function in AD pathophysiology.

In this immunohistochemical investigation, microglia were identified by their expression of ionized calcium binding adaptor molecule 1 (IBA1), which is known to be an effective pan-microglial marker that is independent of “activation” states compared to other commonly used markers (23, 54). In our previous work, we had demonstrated greater densities of dystrophic microglia in severely affected cortical areas of the AD brain, namely the inferior temporal cortex (ITC) and the anterior cingulate

cortex (9). Here, this work has been extended by quantifying the morphological subtypes of microglia by manual and automated methods in AD cases and controls with variable amounts of AD-type pathology in three neocortical areas – the primary visual cortex (PVC), superior frontal cortex (SFC) and ITC. AD pathology and particularly tau pathology are known to spread in a stereotypical fashion through the cortex (2, 6, 13, 60). Furthermore, the density of NFTs is inversely correlated with surviving neurons in the AD cortex (14). These three regions were chosen to reflect the reported spread of tau pathology, with the PVC being one of the last regions to be affected (6). This is also reflected by a volumetric study where the severely affected ITC undergoes ~35% atrophy and the PVC ~15% in AD cases compared to gender-matched controls (17), a scenario that potentially allows regional comparisons to model disease progression within cases (58). The aim here was to gain a greater understanding of spatiotemporal relationships between the morphological subtypes of microglia and AD progression.

METHODS

This immunohistochemical study of microglial subtypes using human post-mortem brain tissue from AD patients and non-demented controls was approved by the University of Sydney’s Human Research Ethics Committee (HREC #2015/477). All tissue samples for this study along with demographics, clinical and pathological diagnosis were supplied by the New South Wales Brain Tissue Resource Centre (NSW BTRC) and the Sydney Brain Bank (SBB), collectively referred to as NSW Brain Banks (NSWBB) following clearance from their Scientific Advisory Committee. APOE ϵ 4 genotyping was also carried out as previously described (32). NSWBB measure brain pH on a frozen (-80°C) segment of the lateral cerebellar hemisphere which has previously been shown to be representative of the whole brain pH (51) and may be used as a marker of the length and severity of events in the pre-mortem period (12, 34). The demographic and clinicopathological characteristics of the cohort are listed in Table 1.

Immunohistochemistry

Immunohistochemistry (IHC) was performed on free-floating $45\text{-}\mu\text{m}$ fixed sections from the PVC, SFC and ITC of cognitively normal individuals with variable AD-type pathology (CDR = 0–0.5; $n = 15$) and AD patients (CDR 2–3; $n = 8$) to quantify the morphological subtypes of microglia. Heat-induced epitope retrieval was performed by baking sections in a 60°C oven overnight using a $0.95\text{ mmol}\cdot\text{L}^{-1}$ sodium citrate (pH 8.5) buffer. Sections were washed with 50% ethanol followed by endogenous peroxidase block using 0.9% H_2O_2 (50% ethanol diluent). Standard blocking was performed for 30 minutes in 10% normal goat serum (NGS; Gibco, Life Technologies Australia Pty Ltd., Mulgrave, Australia) diluted using a $0.05\text{ mol}\cdot\text{L}^{-1}$

Table 1. Cohort details.

Case ID (n = 23)	Age	Sex	Status	Cause of death	Disease duration (years)	PMI (hours)	Brain pH	Fixation (months)	CDR	ABC score	AD likelihood	APOE genotype
M01	69	Male	Control	Cardiac failure	–	16	6.6	97	–	A3 B1 C3	Low	E3/E4
M02	74	Female	Control	Cancer	–	20	6.59	19	–	A3 B1 C3	Low	E3/E4
M03	76	Female	AD	Cardiorespiratory failure	11	3	5.98	35	3	A3 B2 C3	Intermediate	E3/E4
M04	77	Male	AD	Aspiration pneumonia	9	26	6.34	12	2	A3 B3 C2	High	E4/E4
M05	78	Female	Control	Respiratory failure	–	11	6.3	78	–	A0 B0 C0	Low	E3/E3
M06	78	Female	Control	Toxicity	–	45	6.05	58	–	A0 B1 C0	Low	E3/E4
M07	81	Male	Control	Cardiac failure	–	29	6.57	26	–	A0 B2 C0	Low	E3/E3
M08	80	Male	Control	Respiratory failure	–	12	6.5	9	–	A0 B0 C0	Low	E3/E3
M09	80	Female	AD	Alzheimer's disease	10	32	6.54	25	3	A3 B3 C3	High	E3/E4
M10	82	Female	Control	Respiratory failure	–	7.5	6.45	102	–	A3 B1 C2	Low	E3/E3
M11	83	Male	AD	Cerebrovascular	5	25	6.26	70	3	A3 B3 C3	High	E4/E4
M12	83	Female	AD	Uraemia	7	3	5.88	61	3	A3 B3 C2	High	E3/E4
M13	84	Female	AD	Aspiration pneumonia	13	6	6.32	64	3	A3 B3 C3	High	E3/E4
M14 ^a	85	Male	Control	Cancer	–	9	6.57	61	–	A2 B2 C3	Intermediate	E3/E3
M15	85	Female	Control	Respiratory failure	–	10	6.63	34	–	A2 B1 C0	Low	E3/E3
M16	85	Female	Control	Pneumonia	–	23	6.44	73	0	A2 B0 C1	Low	E3/E3
M17	85	Female	AD	Cardiorespiratory failure	5	10	5.91	15	3	A3 B3 C3	High	E3/E3
M18 ^a	87	Female	Control	Cancer	–	5	6.38	34	–	A2 B2 C0	Intermediate	E3/E4
M19 ^a	92	Female	Control	Pancytopenia	–	5	6.08	34	0	A2 B2 C2	Intermediate	E3/E3
M20	93	Female	Control	Cardiac failure	–	21	6.96	81	0.5	A1 B0 C0	Low	E3/E3
M21 ^a	87	Female	Control	Acute peritonitis	–	24	–	–	0	A3 B2 C1	Intermediate	–
M22	98	Female	AD	Cerebrovascular	6	11	6.11	18	3	A3 B3 C2	High	E3/E3
M23 ^a	102	Female	Control	Acute renal failure	–	5	5.92	35	0	A2 B2 C2	Intermediate	E2/E3

^aHigh-pathology controls.^bAs per NIA-AA diagnostic criteria (35).

tris-buffered saline ($1 \times$ TBS; pH 7.4) wash buffer solution with additional Triton-X₁₀₀ detergent (0.1%). Sections underwent primary antibody (IBA1; 1:1000, rabbit monoclonal; 019-1974, Wako Pure Chemical Industries, Japan) incubation at 4°C overnight. All incubations were followed by three washes with gentle agitation for five minutes using $1 \times$ TBS. Negative control sections incubated without primary antibodies were run concomitantly during each staining procedure. Secondary antibody incubation (biotinylated anti-rabbit IgG (H+L), 1:200; BA-1000, Vector Laboratories, Burlingame, CA, USA) was performed at room temperature (RT) for one hour followed by an hour in avidin-biotin-peroxidase complex solution (1:100; Vectastain Elite ABC, Universal). DAB (0.7 mg/mL; SigmaFast™ 3, 3'-diaminobenzidine tablets, Merck & Company, Inc., Kenilworth, NJ, USA) in an aqueous solution containing urea hydrogen peroxide tablet (0.67 mg/mL; H₂O₂ equivalence, 0.24 mg/mL) was applied for 15 seconds. Regressive counterstaining involving sequential immersion into hematoxylin (28), followed by acid alcohol (two second immersion) and Scott's blueing solution (45 seconds) was performed prior to cover slipping using DPX mounting media (06522-Sigma Pharmaceuticals, Rowville, VIC, Australia).

Quantification of microglia

Microglia were quantified from images acquired by an Olympus VS-120 slide scanner following an adapted stereological approach (27). Briefly, images of three 500- μ m wide strips of the full cortical thickness were acquired from areas where the gray matter was at its thinnest and strictly parallel to the gray matter-white matter boundary. An eyepiece graticule at $200 \times$ magnification (0.25 mm²) with defined inclusion and exclusion lines was used as an unbiased counting frame. IBA1 + cells were counted if a nucleus and surrounding soma could be identified. Inter-rater reliability was established between two experienced raters on 10% of sections with >95% concordance for both microglial and neuronal counts. All counts were expressed as densities and adjusted to account for cortical atrophy in AD by multiplying raw densities by the fraction of the mean cortical width of each case by the mean cortical width of all controls for each region. Total microglia were enumerated and microglia also subdivided into one of three subtypes based on their morphology: ramified, activated or dystrophic. Ramified cells were defined on the basis of their thin, highly branched processes and spherical soma. Activated microglia were defined by somal enlargement with either hyper-ramification or a reduced number of thickened processes. Microglia that were amoeboid in shape, large and lacking processes were counted as activated cells as they occurred infrequently. Dystrophic cells were identified by spheroidal swellings, fragmentation of cellular processes and reduced ramification (57). In addition, microglial clusters were also counted; arbitrarily defined as three or more cell bodies that could fit within a 50 μ m² graticule sub-region.

Immunofluorescence

Immunofluorescent (IF) double labeling was performed to investigate relationships between microglia and A β - and tau-positive pathology. Antigen retrieval was as described above, followed by a 12-minute formic acid (90%) incubation at RT to optimize A β immunoreactivity. All incubations were followed by three washes for five minutes with gentle agitation using 0.01molL⁻¹ PBS (pH 7.4). Sections were co-incubated in antibodies for IBA1 (1:1000) and A β (1:500; mouse monoclonal; M0872, Dako, Santa Clara, CA, USA) at 4°C overnight. Sections were co-incubated in secondary antibodies (1:200; AlexaFluor 488, goat anti-mouse IgG (H+L); A11001, Invitrogen, Waltham, MA, USA); (1:200; AlexaFluor 568, goat anti-rabbit IgG (H+L); A11011, Invitrogen) for 72 hours with gentle agitation at 4°C in the dark and wrapped in aluminum foil. Autofluorescence caused by lipofuscin and aldehydes was minimized by washing sections for 10 minutes in 0.1% Sudan Black B (B.D.H Laboratory Chemicals Group) (70% ethanol diluent). Sections were mounted with DAPI Fluoroshield™ medium (F6057; Merck & Company, Inc., Kenilworth, NJ, USA) before coverslipping. Tau immunolabeling was performed as previously described (9). Briefly, Heat-induced epitope retrieval was performed with sodium citrate (pH 6.0), before permeabilizing, blocking with BSA and overnight incubation in primary antibodies: total tau (1:500; Dako, K9JA) and IBA1 (1:50; Millipore, MABN92). Sections were co-incubated in secondary antibodies (1:200; AlexaFluor 555 and 647, anti-mouse and anti-rabbit IgG (H+L), respectively; A21424 and A21244, respectively, Invitrogen). The total tau antibody has been previously shown to immunostain NFTs, neuritic plaques and neuropil threads and is comparable to phospho-tau (Ser262; 12E8) immunoreactivity (42). Hoechst 33342 was added to label nuclei and sections were mounted in Prolong Gold (Invitrogen).

A β and tau imaging

Researchers were blind to section status throughout the staining and imaging process. A β IF slides were imaged using a Zeiss LSM 510 Meta confocal microscope at the Advanced Microscopy Facility (AMF), Bosch Institute, The University of Sydney. A β was quantified in three cortical strips using a $20\times/0.8$ objective. These regions of interest (ROIs) were located at random while visualizing DAPI staining. Cortical strips were constructed of serial images (450 μ m²) from the surface to the gray-white boundary; moving inward sequentially. Individual images were maximum intensity projections (MIPs) of three z-slices (z-step = 5 μ m) centered at the area with the most intense level of staining and were thresholded manually. Widefield images of total tau IF slides were captured using an Olympus VS-120 slide scanner. Whole section overviews using DIC and fluorescence were taken with the $10 \times$ objective to clearly identify gray matter and overall level of staining. Four ROIs of 500 μ m² (totaling 1 mm² per section) were systematically mapped out within mid-cortical layers (II-V) distributed throughout the entire section. A

6- μ m deep z-stack comprised of seven z-slices of each ROI was obtained using a 40 \times /0.95 objective. ROIs chosen were representative of the overall level of tau staining throughout the gray matter, allowing for an accurate assessment of tau pathology within the cortex. All slide scanner image files (.vsi) were opened in Fiji using the BioFormats Importer. A MIP was produced and saved as a .tif file for subsequent thresholding and positive pixel analysis. Tau-positive plaques and tangles within all ROIs of each case were manually counted.

Neuronal staining and quantification

Neurons were quantified on 10- μ m formalin-fixed paraffin-embedded (FFPE) sections stained with 0.1% cresyl violet acetate. Sections were dewaxed in xylene and hydrated through a series of graded ethanol solutions. Cresyl violet solution was applied for eight minutes followed by a deionized water rinse. Differentiation was achieved by briefly washing sections in absolute ethanol. The appropriate level of staining was confirmed by light microscopy before sections were cleared in xylene for nine minutes and mounted with DPX for cover slipping. Neuronal counts were performed using an Olympus BX50 microscope at 200 \times magnification.

Image analysis

Image analysis was performed using *Fiji* (NIH, Bethesda, MD, USA). A β and tau areal fraction, a more accurate indicator of pathology load than quantifying individual entities because of size variation, was determined by expressing a positive pixel count as a percentage of total pixels (Supplementary Figure S1). However, to enumerate the percentage of A β -immunopositive plaques (A β plaques) that were associated with a microglial cluster, the density of A β plaques was also calculated for each region. Given the subjective nature of microglial subtype classification, automated morphometric image analyses were also performed to complement traditional, qualitative cell counts. Cortical strip images of IBA1-stained IHC sections were used and underwent color deconvolution and manual thresholding where two primary parameters were measured: (i) “arborised area” which was determined by summing the area of all convex hull polygons overlaying each cell mask and (ii) “structural complexity” which was assessed using the Skeletonize 2D/3D ImageJ plugin (1) which provided total branch length, total number of branches and total number of junctions (Supplementary Figure S2).

Statistical analyses

The normality of all data was tested using the Shapiro-Wilk test. Group differences were determined using either a Welch's T test or a Mann-Whitney U test where data were not normally distributed, or chi-squared test. Regional differences were compared using either one-way analysis

of variance (ANOVA) with Games-Howell test for pairwise comparisons or Kruskal-Wallis test with Dunn's test for pairwise comparisons using SPSS statistics 24 (SPSS Inc., Chicago, IL, USA). *P*-values < 0.05 were considered statistically significant. Potential confounders including brain pH, APOE genotype, post-mortem interval (PMI) and fixation period along with age and sex were investigated by univariate analysis. Factors that were significantly associated with microglial subtypes, arborised area or skeletal analysis parameters were included in multivariate models along with case-control status using JMP 10 (SAS Institute Inc., Cary, NC, USA). Microglial parameters that survived multivariate testing were further investigated by calculating Pearson's *r* or Spearman's ρ for relationships with tau or A β . All graphs presented here show significant findings following multivariate testing and were produced using GraphPad Prism 7.00 (GraphPad Software Inc., La Jolla, CA, USA).

RESULTS

Clinicodemographic characteristics

Pathologically confirmed AD cases and non-demented controls were matched for age and sex. The AD cases were more likely to carry the APOE ϵ 4 allele (*P* = 0.04), had greater AD-type pathology according to the ABC scoring system (35) and Braak staging (7) and had lower brain pH (*P* = 0.03) and brain weight (*P* = 0.04) (Table 2).

Neuropathology

Cortical thickness differed between AD cases (2.1 \pm 0.3 mm) and controls (2.6 \pm 0.5 mm, *P* = 0.01) in the ITC, whereas cortical thinning was not observed in the PVC (2.2 \pm 0.2) or SFC (2.8 \pm 0.4) of AD cases compared to controls (PVC = 2.2 \pm 0.2, *P* = 0.6;

Table 2. Demographic, clinical and pathological characteristics of cohort.^a

	Control (n = 15)	AD (n = 8)	<i>P</i> -value
Sex (male/female)	4, 11	2, 6	0.9
Age (years)	83.9 \pm 8.1	83.3 \pm 6.8	0.9
Disease duration (years)	–	8.3 \pm 3.0	–
ABC score (Low, intermediate, high)	10, 5, 0	0, 1, 7	<0.0001
Braak stages (0/I/II, III/IV, V/VI)	11, 4, 0	0, 2, 6	0.0002
Brain pH	6.4 \pm 0.27	6.2 \pm 0.24	0.03
PMI (hours)	16.2 \pm 11.1	14.5 \pm 11.5	0.8
Fixation (months)	52.9 \pm 29.7	37.5 \pm 23.9	0.2
Brain weight (g)	1241 \pm 150.7	1086 \pm 163	0.04
APOE ϵ 4 (no/yes)	10, 4 ^b	2, 6	0.04

^aMean \pm standard deviation throughout.

^bAPOE genotype of one control case missing (M21).

SFC = 2.7 ± 0.4 , $P = 0.8$). Neuronal loss was observed in the SFC (145.8 ± 63.5 cells) and ITC (132.9 ± 29.6) of AD cases compared to controls (SFC = 207.2 ± 35.1 ; ITC = 220.7 ± 69.2) (Figure 1A). A β areal fraction in the PVC ($1.2 \pm 0.5\%$), SFC ($1.6 \pm 1.5\%$) and ITC ($1.8 \pm 0.6\%$) of AD cases was greater compared to controls (PVC = $0.3 \pm 0.5\%$, $P = 0.0004$; SFC = $0.5 \pm 0.6\%$, $P = 0.02$; ITC = $0.6 \pm 0.8\%$, $P = 0.002$) (Figure 1B). Similarly, the density of A β plaques in the PVC (22.2 ± 17.8 plaques/mm²), SFC (37.1 ± 28.6) and ITC (40.6 ± 19) of AD cases was higher compared to controls (PVC = 6.6 ± 12.8 , $P = 0.003$; SFC = 11.5 ± 15.8 , $P = 0.01$; ITC = 14.4 ± 20.9 , $P = 0.008$) (Figure 1C). Tau areal staining in the mid-cortical layers was significantly greater in AD cases (PVC = $1.4 \pm 0.6\%$; SFC = $1.9 \pm 0.8\%$; ITC = $1.8 \pm 0.6\%$) compared to controls (PVC = $0.01 \pm 0.03\%$, $P < 0.0001$; SFC = $0.07 \pm 0.2\%$, $P < 0.0001$; ITC = $0.1 \pm 0.2\%$, $P < 0.0001$) across all three regions (Figure 1D). The density of cortical tau-positive neuritic plaques was significantly higher in the PVC (18.8 ± 12.5 plaques/mm²), SFC (8.4 ± 6.0) and ITC (7.4 ± 9.4) of AD cases compared to controls (PVC = 0.2 ± 0.8 , $P < 0.0001$; SFC = 0.4 ± 1.4 , $P = 0.0001$; ITC = 0.4 ± 0.8 , $P = 0.002$) (Figure 1E). Cortical NFT density was significantly greater in AD cases (PVC = 9.4 ± 8.7 NFTs/mm²; SFC = 25.4 ± 13.9 ; ITC = 21.9 ± 20.4) compared to controls (PVC = 0.2 ± 0.6 ,

$P < 0.0001$; SFC = 0.8 ± 3.1 , $P < 0.0001$; ITC = 0.7 ± 1.9 , $P < 0.0001$) in all regions (Figure 1F). Pathological load did not differ significantly between any of the three regions in AD or control cases.

Loss of healthy microglia in the ITC of AD brains

Total IBA1-immunopositive microglia and commonly defined morphological subtypes: ramified (Figure 2A), activated and dystrophic were quantified in the three cortical regions of AD cases and controls. A range of phenotypes within the activated (Figure 2B,C) and dystrophic (Figure 2D,E) subtypes were seen within all individuals as well as clusters made up of activated microglia in those individuals with AD pathology (Figure 2F). Total microglia were lower in the ITC of AD cases compared to controls. This was exclusively caused by a reduction in the number of ramified microglia in the ITC of AD cases (Table 3). In contrast, neither activated nor dystrophic microglia differed in total number, or as a percentage of total microglia, between AD cases and controls in any of the three regions. Microglial clusters were relatively rare in all regions but were seen more frequently in the PVC of AD cases compared to controls. There was no difference in the density of clusters in the SFC or ITC between AD cases and controls.

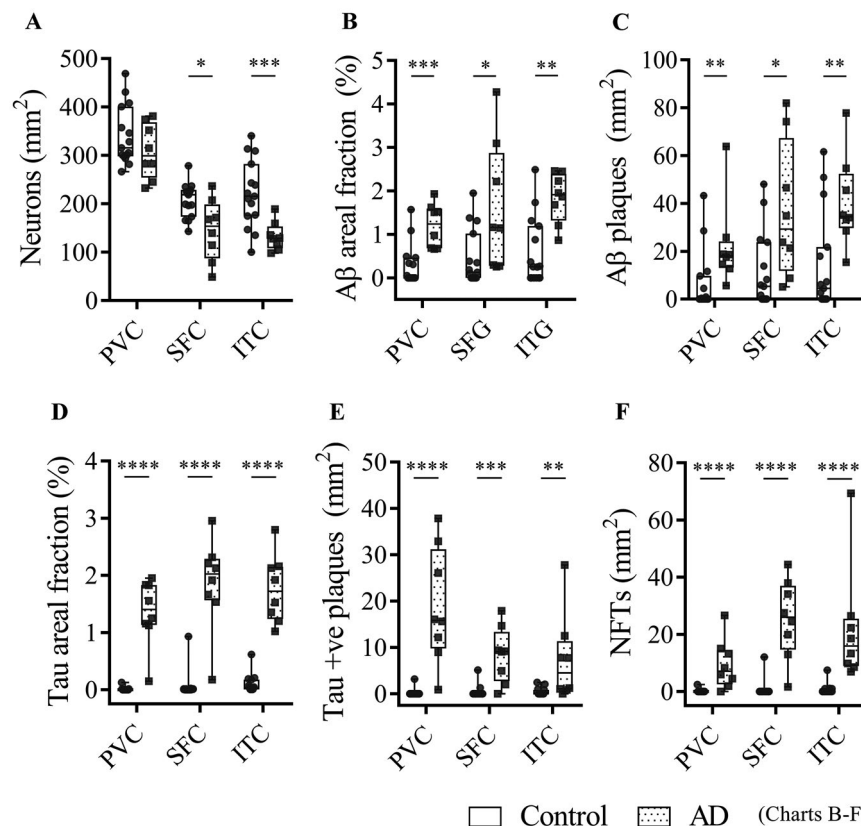


Figure 1. Neuropathological characterization. Box and whisker plots show mean values for: cortical neuronal density (A), cortical A β areal fraction (percentage of positive pixels stained) (B), A β plaque density

(C), cortical tau areal fraction (D), tau-positive neuritic plaque density (E) and NFT density (F). * $P < 0.05$; ** $P < 0.01$; *** $P < 0.001$; **** $P < 0.0001$. Error bars indicate SD throughout.

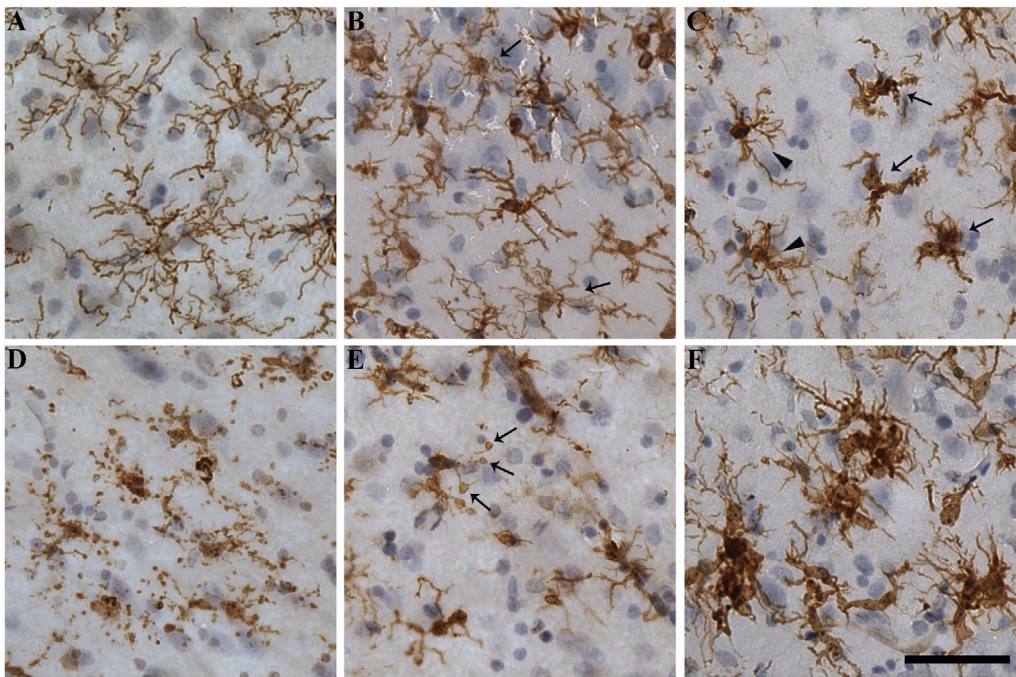


Figure 2. *Microglial morphologies.* Representative photomicrographs from the ITC show exemplars of microglial subtypes quantified here. **A.** Ramified microglia seen in a control case (M20) have small, spherical soma and symmetrically distributed, thin, highly branched processes. **B.** Activated microglia in an AD case (M09) that are hypertrophied and have reduced branching compared to ramified microglia. Arrows indicate ramified microglia for comparison. **C.** Activated microglia that are

ameboid in morphology (arrows) are seen among other activated cells (arrow heads) in another AD case (M11). **D.** Dystrophic microglia that are pseudo-fragmented with discontinuous IBA1 staining of processes in the same AD case (M11). **E.** A dystrophic microglia that is deramified and has spheroidal swellings at the end of its processes (arrows) from an AD case (M13). **F.** Clusters of activated microglia seen in an AD case (M09). Nuclei counterstained with hematoxylin. Scale bar = 50 μ m.

Table 3. Quantification of the morphological subtypes of microglia.

	Control (cells/mm2)	%	AD	%	P-value
PVC					
Total Microglia	140.7 \pm 45.2		139.6 \pm 43.1		0.95
Ramified microglia	55.3 \pm 34	39.3	39.5 \pm 25	28.3	0.26
Activated microglia	55 \pm 29.3	39.1	64 \pm 27.4	45.8	0.48
Dystrophic microglia	30.4 \pm 17.3	21.6	36 \pm 19.9	25.8	0.48
Microglial clusters	0.7 \pm 1.9		2.8 \pm 2.3		0.03
SFC					
Total Microglia	188.4 \pm 59.6		187.1 \pm 62		0.96
Ramified microglia	70.8 \pm 36.9	37.6	49.1 \pm 23.8	26.2	0.15
Activated microglia	81.6 \pm 47	43.3	90.4 \pm 42.9	48.3	0.67
Dystrophic microglia	36 \pm 23.4	19.1	47.6 \pm 24.3	25.4	0.28
Microglial clusters	0.8 \pm 1.1		3.2 \pm 3		0.05
ITC					
Total Microglia	205 \pm 66		128 \pm 52.2		0.01
Ramified microglia	77.3 \pm 47.2	37.7	13.8 \pm 8.9	10.8	0.001
Activated microglia	86.6 \pm 42.4	42.2	70.6 \pm 60.4	55.2	0.46
Dystrophic microglia	41.1 \pm 23.3	20.0	43.7 \pm 30.5	34.1	0.82
Microglial clusters	1.1 \pm 1.3		1.9 \pm 2.1		0.28

Non-demented, higher pathology-controls have increased activated microglia

The control cases were sub-divided into five “high-pathology control cases” (HPCs), whose levels of AD-type pathology were similar to the AD cases and 10 “low-pathology control cases” (LPCs) with low or no AD pathology (Table 2). ITC gray matter of HPCs was thicker compared to LPCs ($P = 0.01$; Figure 3A). A β positive immunostaining ($P = 0.02$; Figure 3B) and cortical tau immunostaining ($P = 0.01$; Figure 3C) was also increased compared to LPCs. This also coincided with more total ($P = 0.02$) and activated microglia ($P = 0.01$) in HPCs compared to LPCs (Figure 3D). Group differences presented here survived multivariate testing (see Supplementary tables ST1 and ST2 for univariate and multivariate tests that included data for control cases only).

Reduced microglial arborized area and structural complexity in AD

A reduction in the arborized area was observed in the SFC and ITC of AD cases compared to controls, but not in the PVC (Figure 4A; Table 4). Similarly, a standard positive pixel analysis showed these same effects (Figure 4B). A skeletal analysis showed that the total branch length,

the total number of branches and the total number of junctions were significantly reduced in AD cases compared to controls in the ITC (Table 4). Total junctions were also significantly reduced in the SFC of AD cases compared to controls, but there were no changes in any of these parameters in the PVC.

Microglial clustering was not a major feature of the AD cortex

Clusters of microglia (three or more cell bodies within a 50- μm^2 graticule field) were occasionally found near cored and diffuse A β plaques and tau-positive plaques in both the control (Figure 5A–F) and AD groups (Figure 5G–O). These microglia were predominantly activated or, less commonly, dystrophic in morphology (Figure 5G–I). There was no difference between the percentage of A β plaques associated with a microglial cluster between the AD and control groups in any of the three regions: PVC

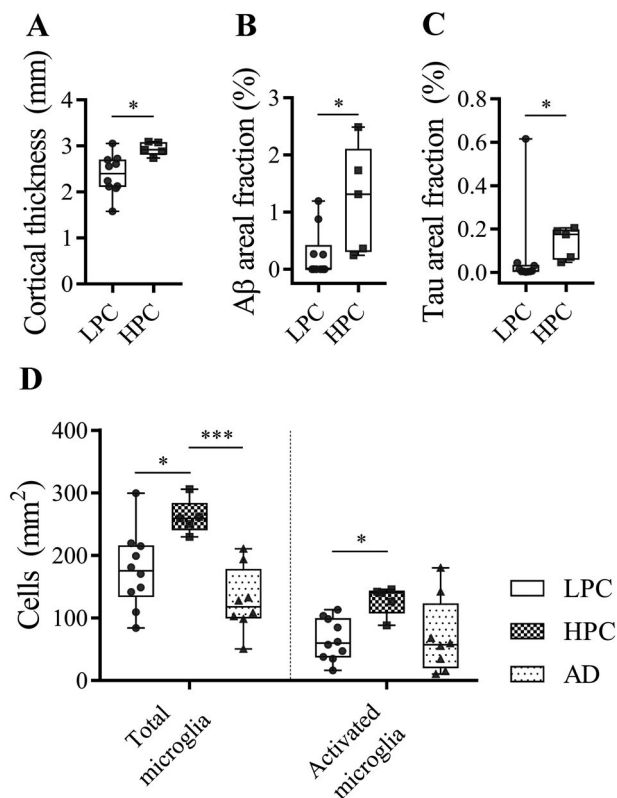


Figure 3. Comparisons between low pathology controls (LPCs) and high-pathology controls (HPCs). A. HPCs had thicker cortices, elevated A β (B) and tau areal fraction (C) compared to LPCs in the ITC. D. Total and activated microglia were also higher in HPCs compared to LPCs.

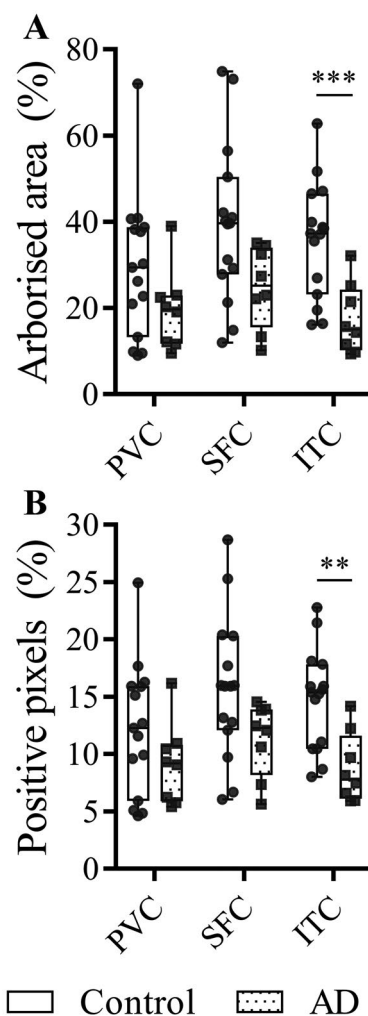


Figure 4. Microglial arborized area. Box and whisker plots demonstrating the area of tissue covered by microglial processes as determined using the convex hull analysis (A) and IBA1 positive pixel analysis (B) in the PVC, SFC and ITC of AD cases and controls.

Table 4. Microglial structural complexity.

	Control	AD	P-value
<i>Arborized area (%)</i>			
PVC	29.3 ± 16.7	19.7 ± 9.4	0.09
SFC	39.6 ± 18.5	24.8 ± 9.4	0.02
ITC	35.8 ± 13.4	17.5 ± 8.1	0.0006
<i>Positive pixels (%)</i>			
PVC	12.2 ± 5.7	9.2 ± 3.6	0.2
SFC	15.8 ± 6.2	11.3 ± 3.3	0.03
ITC	14.8 ± 4.4	8.8 ± 3.1	0.001
<i>Summary of skeletal analyses (mm²)</i>			
		PVC	
Total branch length (mm)	47.2 ± 33.8	32.9 ± 29.3	0.06
Total #branches	3873 ± 1406	3042 ± 805	0.14
Total #junctions	1114 ± 524.2	756.1 ± 312.1	0.09
		SFC	
Total branch length (mm)	78.6 ± 68.6	44.6 ± 36	0.1
Total #branches	5385 ± 1873	3949 ± 1139	0.06
Total #junctions	1762 ± 854.5	1031 ± 426.2	0.03
		ITC	
Total branch length (mm)	65.7 ± 50.9	21.9 ± 8.8	0.0002
Total #branches	5480 ± 2091	2665 ± 1110	0.002
Total #junctions	1685 ± 757.6	625.2 ± 386.6	0.001

(AD = 16.8 ± 14.4%, control = 12.2 ± 23.4; $P = 0.15$), SFC (AD = 12.4 ± 12.7, control = 5.8 ± 5.5; $P = 0.28$) and ITC (AD = 5.4 ± 6.5, control = 17.2 ± 19.9; $P = 0.25$) (Figure 5J–L) or tau-positive plaques (Figure 5M–O) in either the AD cases or controls.

Morphological changes of microglia correlate with tau pathology

Potential confounders of microglial parameters including brain pH, PMI and fixation time were investigated by univariate analyses (Supplementary table ST3) and those that were or approached significance were included in multivariate analyses with case status for the three regions. Neuronal loss in the SFC and ITC, and reduced arborized area, IBA1 positive pixels, total branch length, total number of branches and number of ramified microglia in the ITC, as well as increased density of microglial clusters in the PVC remained significantly different following multivariate testing (Table 5; refer to Supplementary table ST4 for all multivariate statistics).

Those microglial parameters associated with AD status were further investigated for associations with either tau or A β pathology (Table 6). In the ITC, neurons, arborized area, IBA1 positive pixels and ramified microglia were all inversely correlated with the level of tau staining. There was also an inverse correlation between total branch length and A β in the ITC. Microglial clusters were positively correlated with both A β and tau staining in the SFC, and only tau staining in the PVC.

Brain pH is an important effector of microglial dystrophy

Among the potential confounders, brain pH was inversely correlated with a number of different microglial parameters; most notably the presence of dystrophic microglia (Table 7). The exception was ramified microglia in the SFC where a positive correlation was observed. A combined analysis of cases and controls showed that dystrophic microglia were inversely correlated with brain pH in all three regions (Figure 6).

DISCUSSION

This study undertook to provide clarity on how microglia relate temporally to the progression of Alzheimer's disease by comparing morphological subtypes in differentially affected areas of post-mortem brain tissue. Unlike previous studies, our findings showed that activated microglia were only increased in high-pathology controls while clustering of microglia with A β plaques was uncommon and highest in the mildly affected PVC (~17%), suggesting that there is an early microglial reaction to A β but this is prior to the onset of dementia. Whereas only 12% and 5% of A β plaques were associated with a microglial cluster in the SFC and ITC, respectively. Second, the severely affected ITC, was characterized by a reduced number of ramified (healthy) microglia. Third, dystrophic microglia were not associated with AD status or pathology, but rather brain pH.

As expected, AD cases had greater quantities of A β and tau-positive plaques and neurofibrillary pathology compared to non-demented controls. The ITC showed a reduction in the number of neurons and AD-related cortical thinning, consistent with a more advanced stage of AD than the SFC, which had reduced neurons but no cortical atrophy and the PVC in which neither of these measures was affected. Therefore, changes seen in the PVC can be viewed as representative of earlier disease mechanisms; with previous pathological and molecular studies also suggesting that the amount of tau pathology in the PVC has minimal effects on the neurons in this region (22, 28). Intra-regional differences in cortical pathology was not as extensive as predicted here from staging schema and volumetric studies. The commonly used ABC staging criteria for AD is semi-quantitative in nature, stressing the spread of pathology rather than the quantity of pathology, specifically as it pertains to each defined phase or stage of the criteria (21). Indeed, it is quite rare to find studies that have systematically quantified AD pathology across cortical regions, with those that have, describing significant heterogeneity in the accumulation of plaques and NFTs within regions and limited regional differences (37, 64).

The working hypothesis for how microglia contributes to AD pathogenesis has been that activated cells associate with plaques and produce a neurotoxic milieu that culminates in neuronal degeneration (30, 41, 46). Others have suggested that astrocytes may be equally or more prominent in this area (48, 49, 63), while Liddel and colleagues

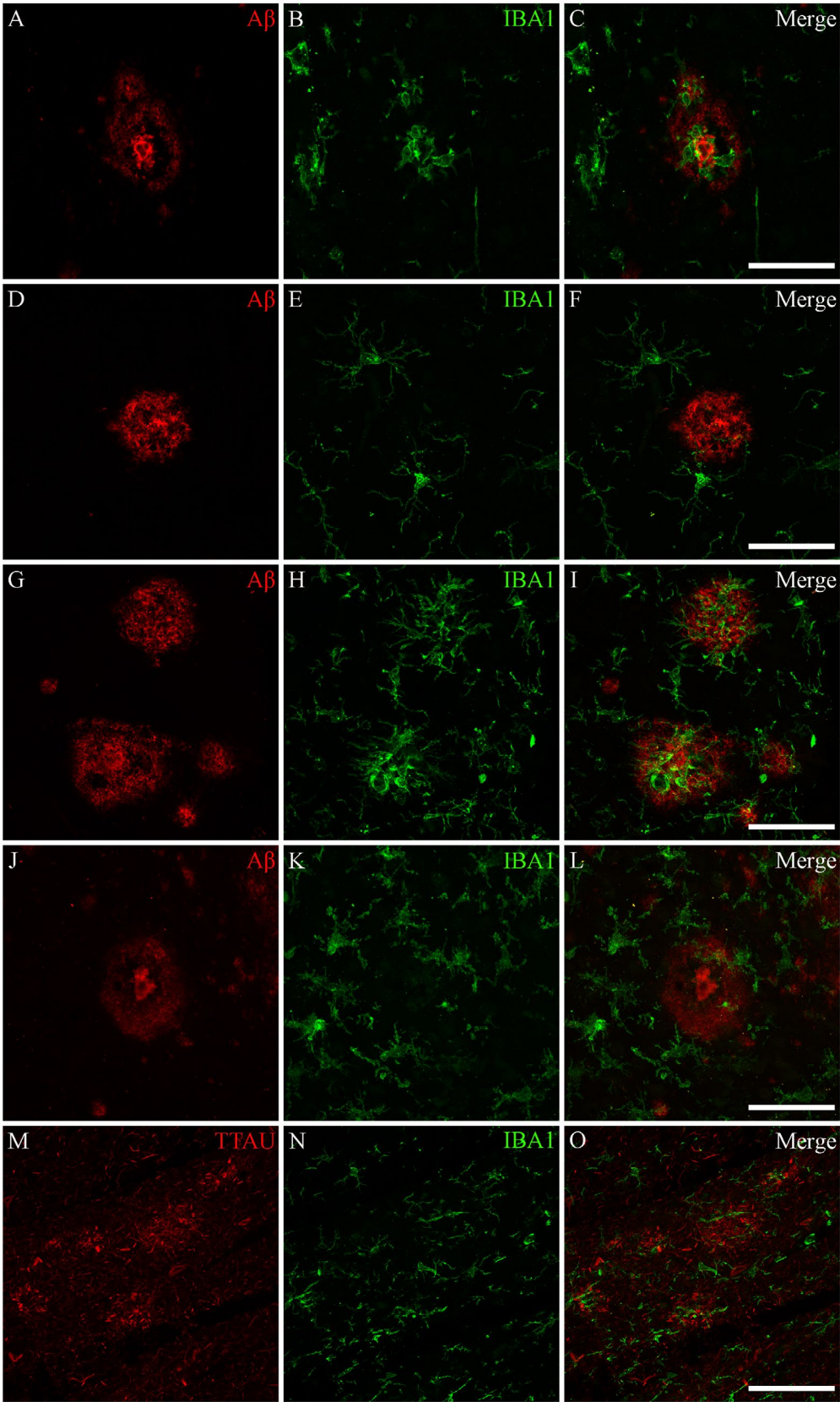


Figure 5. Associations between microglia and AD plaques. Microglia were found to only occasionally cluster around tau-positive plaques and A β -immunopositive diffuse and cored plaques in both AD and control cases. Photomicrographs of immunofluorescent labeling for A β (A), IBA1 (B) and the merged image (C) from a control case with elevated AD-type pathology (M23) demonstrates a cluster of amoeboid microglia associated with a cored A β plaque. D–F. Ramified microglia and no microglial activation associated with a cored plaque of another control case (M19). Similarly, for AD cases, microglia were found to only

occasionally cluster around A β plaques; as seen in the photomicrographs from an AD case (M09) demonstrating both significant clustering around diffuse and cored A β plaques (G–I), and an absence of microglial clustering (J–L). M–O. Tau-positive plaques from the same AD case demonstrating an absence of microglial clustering. All photomicrographs were acquired using a Zeiss LSM 800 confocal microscope (40 \times /1.3 Oil). Scale bars = 50 μ m.

Table 5. Summary of multivariate analyses (case-control differences).

	PVC		SFC		ITC	
	R^2	P-value	R^2	P-value	R^2	P-value
Neurons			0.26	0.01	0.36	0.003
Arborized area					0.36	0.003
IBA1 positive pixels					0.35	0.004
Total branch length					0.22	0.03
Total #branches					0.12	0.04
Ramified microglia					0.39	0.002
Microglial clusters	0.2	0.04				

Table 6. Neuropathological correlations.^a

		PVC		SFC		ITC	
		R^2	P-value	R^2	P-value	R^2	P-value
Neurons	Tau ^b					0.27	0.01
Arborized area	Tau					0.2	0.03
IBA1 positive pixels	Tau					0.18	0.04
Total branch length	A β ^b					0.2	0.03
Ramified microglia	Tau					0.27	0.01
Microglial clusters	A β ^b			0.4	0.001		
	Tau ^b	0.27	0.01	0.12	0.04		

^aAll correlations presented in this table include variables that are significantly different between groups and remained so following multivariate analysis (excluding microglial clusters in the SFC, where $P = 0.05$).

^bIndicates most significant correlation determined by multivariate analysis that included both A β and tau areal fractions (following univariate analyses demonstrating correlations with both pathologies).

recently showed that the interplay between microglia and astrocytes is critical by demonstrating that microglia-derived cytokines induce a neurotoxic phenotype in astrocytes (29). In contrast, work begun by Streit, Graeber and

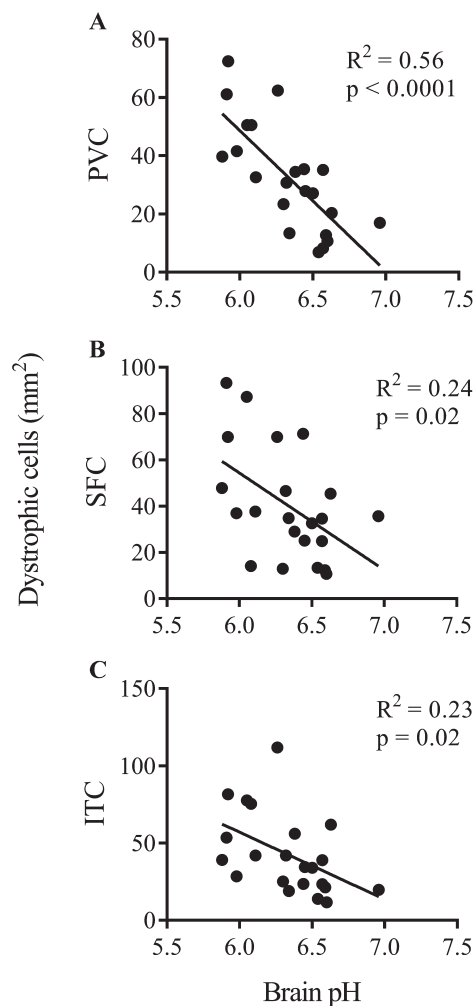
Kreutzberg (55) and continued by Stevens, Barres and colleagues opined that a loss of microglial function and particularly a deficit in their role in synaptic maintenance may be more important in AD pathogenesis (18). Streit and colleagues suggested that dystrophic microglia were an early and prominent feature of AD (54), an idea which may also be relevant to other neurodegenerative diseases such as Dementia with Lewy bodies (3).

Yet, rather than confirming the predominance of either activated or dystrophic microglia in the AD cortex, the major finding here was a reduction in ramified microglia in the ITC only, and that this loss occurred in the absence of a commensurate increase in either the activated or dystrophic subtypes. In contrast, activated microglia were significantly greater in controls with sufficient AD pathology (35) to be pathologically diagnosed with AD. If these “high pathology” controls are representative of the proposed preclinical AD phenotype (53) then microglial activation may be an early driver of the disease. However, the fact remains that microglial reactivity seen in this group was not associated with dementia and so could alternatively be considered a protective mechanism against the neurotoxic effects of relatively high AD-type pathology, an idea consistent with transition events of protective disease-associated microglia (DAM) occurring at early stages of the disease process (25). Furthermore, as DAM are known to localize closely around plaques, the possibility that this activation is associated with neuroprotective mechanisms is further strengthened by the observation of increased microglial clustering in PVC, an area that may be considered representative of earlier stages in the disease process caused by the milder effects of AD observed here.

Given the turnover of microglia in the adult human brain (43), the loss of microglia could represent a decrease in proliferation or increase in cell death. Alternatively, it may represent a loss of IBA1 immunoreactivity caused by the downregulation of this calcium binding protein. The latter has important implications for microglial functionality as reduced IBA1 would result in impaired mobility and phagocytosis (24). Additional pan-microglial markers are required to differentiate between these two scenarios. Indeed, previous investigations have observed significant increases in other markers, such as MHC II, with at least one identifying an IBA1/MHC II⁺ subpopulation (48). However, this phenotypic subpopulation represented a minority of cells in that study. Alternatively, this question could be approached with proliferative and apoptotic markers but our experience with the proliferative marker Ki-67 (10) and the apoptotic marker, cleaved caspase 3

Table 7. Brain pH effects on microglial morphology.

	PVC		SFC		ITC	
	R^2	P -value	R^2	P -value	R^2	P -value
Arborised area	0.24	0.02	0.37	0.003		
IBA1 positive pixels	0.22	0.03	0.4	0.002		
Total #branches					0.44	0.0008
Total #junctions			0.4	0.002	0.45	0.0006
Ramified microglia			0.64	<0.0001		
Dystrophic microglia	−0.56 ^a	<0.0001	−0.55 ^a	0.008	−0.56 ^a	0.006

^aSpearman's ρ .**Figure 6.** Dystrophic microglia and brain pH. Scatter plots and regression lines show the inverse relationships between dystrophic microglia and brain pH in the PVC (A), SFC (B) and ITC (C).

(unpublished data) are that these are rare events in the adult brain and a single “point in time” assay may not be informative for a chronic disease such as AD.

As A β is widely regarded as a precursor to tau pathology, further temporal information on the role of microglial

subtypes in AD pathogenesis was sought by determining the relative associations with A β or tau load. Microglial clusters were correlated with both A β and tau pathology in the PVC and SFC (univariate testing), representing early microglial reactivity that may be associated with neuro-protective processes and potentially corresponding with DAM that have been investigated elsewhere (25). Microglial arborized area, IBA1 positive pixels and the number of ramified microglia were inversely correlated with the level of tau in the ITC, which is indicative of the neurodegenerative stage of the disease and is consistent previous reports of microglial degeneration following phagocytosis of AT8 and/or AT100-positive phospho-tau species (45).

The other major finding here was an inverse correlation between brain pH and dystrophic microglia in all three regions. A low brain pH is often indicative of a severe and prolonged agonal period (12, 34), common in patients with neurodegenerative diseases. The antemortem factors and events that comprise a patient's agonal period impact a patient's brain pH. These factors include: duration of hospitalization, coma, respiratory illness and need for ventilation, systemic inflammation and duration of terminal phase. Unlike the work of Streit and colleagues, there were no differences in the number of dystrophic microglia, including in a sub-cohort excluding samples with pH < 6.0. It is unclear whether previous studies proposing a link between microglial dystrophy and progression of AD considered differences in brain pH (54); however, the loss of healthy microglia in the ITC here still supports a loss of function hypothesis for the role of microglia in AD. More widely the prominence of immune signaling pathways in omic studies using post-mortem brain tissue could similarly represent the influence of brain pH rather than a general inflammatory mechanism in brain disease (15, 50, 62, 65).

This investigation had three important limitations. Namely, the subjective categorization of the morphological subtypes of microglia, the use of a single microglial marker, IBA1 and the small cohort size. Microglial activation does not follow a monophasic (“all-or-nothing”) process, rather these cells respond to changes in their surroundings in a calibrated manner, thereby allowing for a wide range of morphological presentations that can be difficult to categorize. Microglia are rapidly responsive cells operating in time scales of hours and days unlike AD, the archetypal chronic brain disease. This response time may well account

for the relationship between dystrophic microglia and brain pH, a proxy for agonal period. Although IBA1 is recognized as an effective pan-microglial marker (23), more subtle changes in activation including phagocytic status may have been missed. For example, other human post-mortem studies have demonstrated upregulation of major histocompatibility complex class II (MHC II) and cluster of differentiation 68 (CD68), markers of activation and phagocytosis, respectively; see review (19).

Study strengths include the use of well-characterized tissue and a previously verified stereological approach that ensured a quantitative exploration across the entire cortical strip for pathology, residual neurons and microglia (27). This stereological approach ensured that the sampling area is sufficient to generate data that is representative of the tissue section under investigation and by selecting cortical strips at areas where the cortical thickness is at its thinnest, oblique cuts made during tissue sectioning do not inflate thickness measurements. Furthermore, the largely subjective morphological characterization of microglia was corroborated by automated “skeletal” analysis which validated our previous observations of reductions in structural complexity and arborized area in the more severely affected ITC (9). A validated approach for normalization of cortical atrophy (39) was also employed, although this may still have underestimated the true loss of cells in the ITC of AD patients as atrophy in the rostrocaudal dimension is not taken into consideration. Reassuringly, a previous study has indicated that shrinkage in this dimension is minimal (20).

Overall, the novel findings here suggest that ramified microglia are lost in more advanced stages of AD. The loss of the surveillance and support of microglia may cause neurons to be more susceptible to tau-related degeneration. While activation, as seen in higher pathology controls and as an increase in the clustering of microglia in the PVC of AD cases, may be seen as key processes in preventing conversion to dementia. Future studies on morphological changes in microglia in human AD brain tissue must account for the patient's brain pH as a potential confounder for dystrophic microglia. Further immunohistochemical studies with functional markers will be required to determine the more nuanced aspects of microglia dysfunction in AD, but the current findings suggest that strategies aiming to augment microglial function are likely to be more effective as a treatment than those attenuating their pro-inflammatory activities, particularly in earlier phases of the disease.

DATA ACCESSIBILITY STATEMENT

All data pertinent to this study is contained within the manuscript or supplementary tables and figures.

ACKNOWLEDGMENTS

The authors would like to thank the donors and their families for their kind gift. This work was funded by a Sydney Medical School Foundation Fellowship (GS). Brain tissue was received from the NSW Brain Tissue Resource

Centre and Sydney Brain Bank. These brain banks are supported by the NHMRC of Australia, The University of New South Wales, Neuroscience Research Australia and the National Institute of Alcohol Abuse and Alcoholism [NIH (NIAAA) R28 AA012725].

REFERENCES

1. Arganda-Carreras I, Fernandez-Gonzalez R, Munoz-Barrutia A, Ortiz-De-Solorzano C (2010) 3D reconstruction of histological sections: application to mammary gland tissue. *Microsc Res Tech* **73**(11):1019–1029.
2. Arriagada PV, Growdon JH, Hedley-Whyte ET, Hyman BT (1992) Neurofibrillary tangles but not senile plaques parallel duration and severity of Alzheimer's disease. *Neurology* **42**(3 Pt 1):631–639.
3. Bachstetter AD, Van Eldik LJ, Schmitt FA, Neltner JH, Ighodaro ET, Webster SJ, *et al* (2015) Disease-related microglia heterogeneity in the hippocampus of Alzheimer's disease, dementia with Lewy bodies, and hippocampal sclerosis of aging. *Acta Neuropathol Commun* **3**:1–16.
4. Bennett DA, Wilson RS, Boyle PA, Buchman AS, Schneider JA (2012) Relation of neuropathology to cognition in persons without cognitive impairment. *Ann Neurol* **72**(4):599–609.
5. Boche D, Perry VH, Nicoll JA (2013) Review: activation patterns of microglia and their identification in the human brain. *Neuropathol Appl Neurobiol* **39**:3–18.
6. Braak H, Braak E (1991) Neuropathological staging of Alzheimer-related changes. *Acta Neuropathol* **82**(4):239–259.
7. Braak H, Braak E (1995) Staging of Alzheimer's disease-related neurofibrillary changes. *Neurobiol Aging* **16**(3):271–278; discussion 278–284.
8. Cameron B, Tse W, Lamb R, Li X, Lamb BT, Landreth GE (2012) Loss of interleukin receptor-associated kinase 4 signaling suppresses amyloid pathology and alters microglial phenotype in a mouse model of Alzheimer's disease. *J Neurosci* **32**(43):15112–15123.
9. Davies DS, Ma J, Jegathees T, Goldsby C (2017) Microglia show altered morphology and reduced arborization in human brain during aging and Alzheimer's disease. *Brain Pathol* **27**(6):795–808.
10. Dennis CV, Sheahan PJ, Graeber MB, Sheedy DL, Kril JJ, Sutherland GT (2014) Microglial proliferation in the brain of chronic alcoholics with hepatic encephalopathy. *Metab Brain Dis* **29**(4):1027–39.
11. Dubbelaar ML, Kracht L, Eggen BJL, Boddeke E (2018) The kaleidoscope of microglial phenotypes. *Front Immunol* **9**:1753.
12. Durrenberger PF, Fernando S, Kashefi SN, Ferrer I, Hauw JJ, Seilhean D, *et al* (2010) Effects of antemortem and postmortem variables on human brain mRNA quality: a BrainNet Europe study. *J Neuropathol Exp Neurol* **69**(1):70–81.
13. Giannakopoulos P, Hof PR, Michel JP, Guimon J, Bouras C (1997) Cerebral cortex pathology in aging and Alzheimer's disease: a quantitative survey of large hospital-based geriatric and psychiatric cohorts. *Brain Res Brain Res Rev* **25**(2):217–245.
14. Gomez-Isla T, Hollister R, West H, Mui S, Growdon JH, Petersen RC, *et al* (1997) Neuronal loss correlates with but exceeds neurofibrillary tangles in Alzheimer's disease. *Ann Neurol* **41**(1):17–24.

15. Gupta S, Ellis SE, Ashar FN, Moes A, Bader JS, Zhan J, *et al* (2014) Transcriptome analysis reveals dysregulation of innate immune response genes and neuronal activity-dependent genes in autism. *Nat Commun* **5**:5748.
16. Halle A, Hornung V, Petzold GC, Stewart CR, Monks BG, Reinheckel T, *et al* (2008) The NALP3 inflammasome is involved in the innate immune response to amyloid-beta. *Nat Immunol* **9**(8):857–865.
17. Halliday GM, Double KL, Macdonald V, Kril JJ (2003) Identifying severely atrophic cortical subregions in Alzheimer's disease. *Neurobiol Aging* **24**(6):797–806.
18. Hong S, Beja-Glasser VF, Nfonoyim BM, Frouin A, Li S, Ramakrishnan S, *et al* (2016) Complement and microglia mediate early synapse loss in Alzheimer mouse models. *Science* **352**(6286):712–716.
19. Hopperton KE, Mohammad D, Trepanier MO, Giuliano V, Bazinet RP (2018) Markers of microglia in post-mortem brain samples from patients with Alzheimer's disease: a systematic review. *Mol Psychiatry* **23**(2):177–198.
20. Hyman BT, Gomez-Isla T, Irizarry MC (1998) Stereology: a practical primer for neuropathology. *J Neuropathol Exp Neurol* **57**(4):305–310.
21. Hyman BT, Phelps CH, Beach TG, Bigio EH, Cairns NJ, Carrillo MC, *et al* (2012) National Institute on Aging-Alzheimer's Association guidelines for the neuropathologic assessment of Alzheimer's disease. *Alzheimers Dement* **8**(1):1–13.
22. Iacono D, O'Brien R, Resnick SM, Zonderman AB, Pletnikova O, Rudow G, *et al* (2008) Neuronal hypertrophy in asymptomatic Alzheimer disease. *J Neuropathol Exp Neurol* **67**(6):578–589.
23. Ito D, Imai Y, Ohsawa K, Nakajima K, Fukuuchi Y, Kohsaka S (1998) Microglia-specific localisation of a novel calcium binding protein, Iba1. *Brain Res Mol Brain Res* **57**(1):1–9.
24. Kanazawa H, Ohsawa K, Sasaki Y, Kohsaka S, Imai Y (2002) Macrophage/microglia-specific protein Iba1 enhances membrane ruffling and Rac activation via phospholipase C-gamma -dependent pathway. *J Biol Chem* **277**(22):20026–20032.
25. Keren-Shaul H, Spinrad A, Weiner A, Matcovitch-Natan O, Dvir-Szternfeld R, Ulland TK, *et al* (2017) A unique microglia type associated with restricting development of Alzheimer's disease. *Cell* **169**(7):1276–1290.e17.
26. Kettenmann H, Hanisch UK, Noda M, Verkhratsky A (2011) Physiology of microglia. *Physiol Rev* **91**(2):461–553.
27. Kril JJ, Halliday GM, Svoboda MD, Cartwright H (1997) The cerebral cortex is damaged in chronic alcoholics. *Neuroscience* **79**(4):983–998.
28. Liang WS, Dunckley T, Beach TG, Grover A, Mastroeni D, Ramsey K, *et al* (2008) Altered neuronal gene expression in brain regions differentially affected by Alzheimer's disease: a reference data set. *Physiol Genomics* **33**(2):240–256.
29. Liddelow SA, Guttenplan KA, Clarke LE, Bennett FC, Bohlen CJ, Schirmer L, *et al* (2017) Neurotoxic reactive astrocytes are induced by activated microglia. *Nature* **541**(7638):481–487.
30. Lue LF, Brachova L, Civin WH, Rogers J (1996) Inflammation, A beta deposition, and neurofibrillary tangle formation as correlates of Alzheimer's disease neurodegeneration. *J Neuropathol Exp Neurol* **55**(10):1083–1088.
31. Malik M, Parikh I, Vasquez JB, Smith C, Tai L, Bu G, *et al* (2015) Genetics ignite focus on microglial inflammation in Alzheimer's disease. *Mol Neurodegener* **10**:52.
32. Mills JD, Sheahan PJ, Lai D, Kril JJ, Janitz M, Sutherland GT (2014) The alternative splicing of the apolipoprotein E gene is unperturbed in the brains of Alzheimer's disease patients. *Mol Biol Rep* **41**(10):6365–6376.
33. Mirra SS, Heyman A, McKeel D, Sumi SM, Crain BJ, Brownlee LM, *et al* (1991) The Consortium to Establish a Registry for Alzheimer's Disease (CERAD). Part II. Standardization of the neuropathologic assessment of Alzheimer's disease. *Neurology* **41**(4):479–486.
34. Monoranu CM, Apfelbacher M, Grunblatt E, Puppe B, Alafuzoff I, Ferrer I, *et al* (2009) pH measurement as quality control on human post mortem brain tissue: a study of the BrainNet Europe consortium. *Neuropathol Appl Neurobiol* **35**(3):329–337.
35. Montine TJ, Phelps CH, Beach TG, Bigio EH, Cairns NJ, Dickson DW, *et al* (2012) National Institute on Aging-Alzheimer's Association guidelines for the neuropathologic assessment of Alzheimer's disease: a practical approach. *Acta Neuropathol* **123**(1):1–11.
36. Morris JC (1997) Clinical dementia rating: a reliable and valid diagnostic and staging measure for dementia of the Alzheimer type. *Int Psychogeriatr* **9**(Suppl. 1):173–176; discussion 177–178.
37. Nelson PT, Abner EL, Scheff SW, Schmitt FA, Kryscio RJ, Jicha GA, *et al* (2009) Alzheimer's-type neuropathology in the precuneus is not increased relative to other areas of neocortex across a range of cognitive impairment. *Neurosci Lett* **450**(3):336–339.
38. Nimmerjahn A, Kirchhoff F, Helmchen F (2005) Resting microglial cells are highly dynamic surveillants of brain parenchyma in vivo. *Science* **308**(5726):1314–1318.
39. Oorschot DE (1994) Are you using neuronal densities, synaptic densities or neurochemical densities as your definitive data? There is a better way to go. *Prog Neurobiol* **44**(3):233–247.
40. Parkhurst CN, Yang G, Ninan I, Savas JN, Yates JR 3rd, Lafaille JJ, *et al* (2013) Microglia promote learning-dependent synapse formation through brain-derived neurotrophic factor. *Cell* **155**(7):1596–1609.
41. Perlmuter LS, Barron E, Chui HC (1990) Morphologic association between microglia and senile plaque amyloid in Alzheimer's disease. *Neurosci Lett* **119**(1):32–36.
42. Rahman T, Davies DS, Tannenberg RK, Fok S, Shepherd C, Dodd PR, *et al* (2014) Cofilin rods and aggregates concur with tau pathology and the development of Alzheimer's disease. *J Alzheimers Dis* **42**(4):1443–1460.
43. Réu P, Khosravi A, Bernard S, Mold JE, Salehpour M, Alkass K, *et al* (2017) The lifespan and turnover of microglia in the human brain. *Cell Rep* **20**(4):779–784.
44. Salminen A, Ojala J, Kauppinen A, Kaarniranta K, Suuronen T (2009) Inflammation in Alzheimer's disease: amyloid-beta oligomers trigger innate immunity defence via pattern recognition receptors. *Prog Neurobiol* **87**(3):181–194.
45. Sanchez-Mejias E, Navarro V, Jimenez S, Sanchez-Mico M, Sanchez-Varo R, Nunez-Diaz C, *et al* (2016) Soluble phospho-tau from Alzheimer's disease hippocampus drives microglial degeneration. *Acta Neuropathol* **132**(6):897–916.

46. Sasaki A, Yamaguchi H, Ogawa A, Sugihara S, Nakazato Y (1997) Microglial activation in early stages of amyloid beta protein deposition. *Acta Neuropathol* **94**(4):316–322.
47. Schafer DP, Lehrman EK, Kautzman AG, Koyama R, Mardinly AR, Yamasaki R, *et al* (2012) Microglia sculpt postnatal neural circuits in an activity and complement-dependent manner. *Neuron* **74**(4):691–705.
48. Serrano-Pozo A, Gomez-Isla T, Growdon JH, Frosch MP, Hyman BT (2013) A phenotypic change but not proliferation underlies glial responses in Alzheimer disease. *Am J Pathol* **182**(6):2332–2344.
49. Serrano-Pozo A, Mielke ML, Gomez-Isla T, Betensky RA, Growdon JH, Frosch MP, *et al* (2011) Reactive glia not only associates with plaques but also parallels tangles in Alzheimer's disease. *Am J Pathol* **179**(3):1373–1384.
50. Seyfried NT, Dammer EB, Swarup V, Nandakumar D, Duong DM, Yin L, *et al* (2017) A multi-network approach identifies protein-specific co-expression in asymptomatic and symptomatic Alzheimer's disease. *Cell Syst* **4**(1):60–72.e4.
51. Sheedy D, Say M, Stevens J, Harper CG, Kril JJ (2012) Influence of liver pathology on markers of postmortem brain tissue quality. *Alcohol Clin Exp Res* **36**(1):55–60.
52. Sheng JG, Mrak RE, Griffin WS (1997) Neuritic plaque evolution in Alzheimer's disease is accompanied by transition of activated microglia from primed to enlarged to phagocytic forms. *Acta Neuropathol* **94**(1):1–5.
53. Sperling RA, Aisen PS, Beckett LA, Bennett DA, Craft S, Fagan AM, *et al* (2011) Toward defining the preclinical stages of Alzheimer's disease: recommendations from the National Institute on Aging-Alzheimer's Association workgroups on diagnostic guidelines for Alzheimer's disease. *Alzheimers Dement* **7**(3):280–292.
54. Streit WJ, Braak H, Xue QS, Bechmann I (2009) Dystrophic (senescent) rather than activated microglial cells are associated with tau pathology and likely precede neurodegeneration in Alzheimer's disease. *Acta Neuropathol* **118**(4):475–485.
55. Streit WJ, Graeber MB, Kreutzberg GW (1988) Functional plasticity of microglia: a review. *Glia* **1**(5):301–307.
56. Streit WJ, Sammons NW, Kuhns AJ, Sparks DL (2004) Dystrophic microglia in the aging human brain. *Glia* **45**(2):208–212.
57. Streit WJ, Xue QS, Tischer J (2014) Bechmann I. Microglial pathology. *Acta Neuropathol Commun* **2**:142.
58. Sutherland GT, Janitz M, Kril JJ (2011) Understanding the pathogenesis of Alzheimer's disease: will RNA-Seq realize the promise of transcriptomics? *J Neurochem* **116**(6):937–946.
59. Sutherland GT, Kril JJ (2012) Alzheimer's Disease: Approaches to Pathogenesis in the Genomic Age, Neuroscience - Dealing With Frontiers. InTech.
60. Thal DR, Rub U, Orantes M, Braak H (2002) Phases of A beta-deposition in the human brain and its relevance for the development of AD. *Neurology* **58**(12):1791–1800.
61. Tischer J, Krueger M, Mueller W, Staszewski O, Prinz M, Streit WJ, *et al* (2016) Inhomogeneous distribution of Iba-1 characterizes microglial pathology in Alzheimer's disease. *Glia* **64**(9):1562–1572.
62. van Kesteren CF, Gremmels H, de Witte LD, Hol EM, Van Gool AR, Falkai PG, *et al* (2017) Immune involvement in the pathogenesis of schizophrenia: a meta-analysis on postmortem brain studies. *Transl Psychiat* **7**(3):e1075.
63. Vehmas AK, Kawas CH, Stewart WF, Troncoso JC (2003) Immune reactive cells in senile plaques and cognitive decline in Alzheimer's disease. *Neurobiol Aging* **24**(2):321–331.
64. Vermersch P, Frigard B, Delacourte A (1992) Mapping of neurofibrillary degeneration in Alzheimer's disease: evaluation of heterogeneity using the quantification of abnormal tau proteins. *Acta Neuropathol* **85**(1):48–54.
65. Warden A, Erickson E, Robinson G, Harris RA, Mayfield RD (2016) The neuroimmune transcriptome and alcohol dependence: potential for targeted therapies. *Pharmacogenomics* **17**(18):2081–2096.

SUPPORTING INFORMATION

Additional supporting information may be found in the online version of this article at the publisher's web site:

Figure S1. *Quantification of A β and tau areal fraction.* **A.** Confocal photomicrograph showing A β positive immunofluorescent plaques in the ITG of an AD case (M09). **B.** The corresponding digitally generated mark up used to calculate areal fraction with an ImageJ positive pixel algorithm. Scale bars = 50 μ m.

Figure S2. *Quantification and analysis of microglial territoriality and skeletal structure.* **A.** Photomicrograph demonstrating a single field of view with IBA1 + microglia and hematoxylin counterstained nuclei from an AD case (M09). ImageJ color deconvolution plugin was used to separate DAB (**B**) and hematoxylin (**C**) stains; with the third component (**D**) representing the remainder of the subtractive mixing algorithm. The image of the isolated DAB staining was manually thresholded, with the digitally generated mark up (**E**) allowing for the convex hull area to be calculated by summing all polygons bounded in green (**F**) and the production of tagged skeletal frames of each cell mask (**G**) that could be used to calculate total branch length, total number of branches and total number of junctions. Scale bar = 100 μ m.

2.4 Published supplementary material

The published supplementary material begins on the next page.

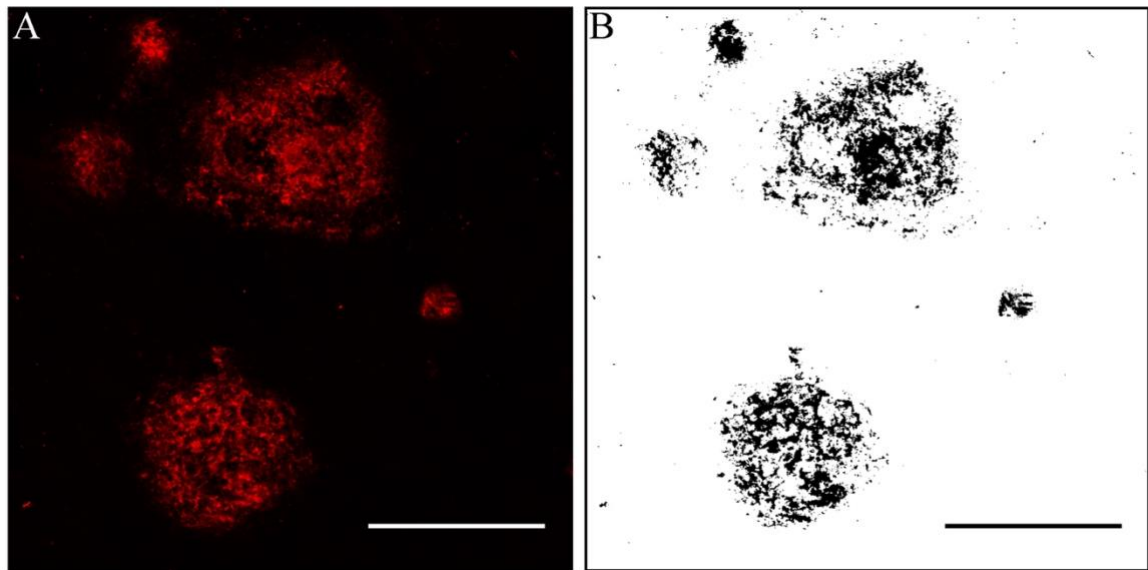


Figure S1. Quantification of A β and TTau areal fraction.

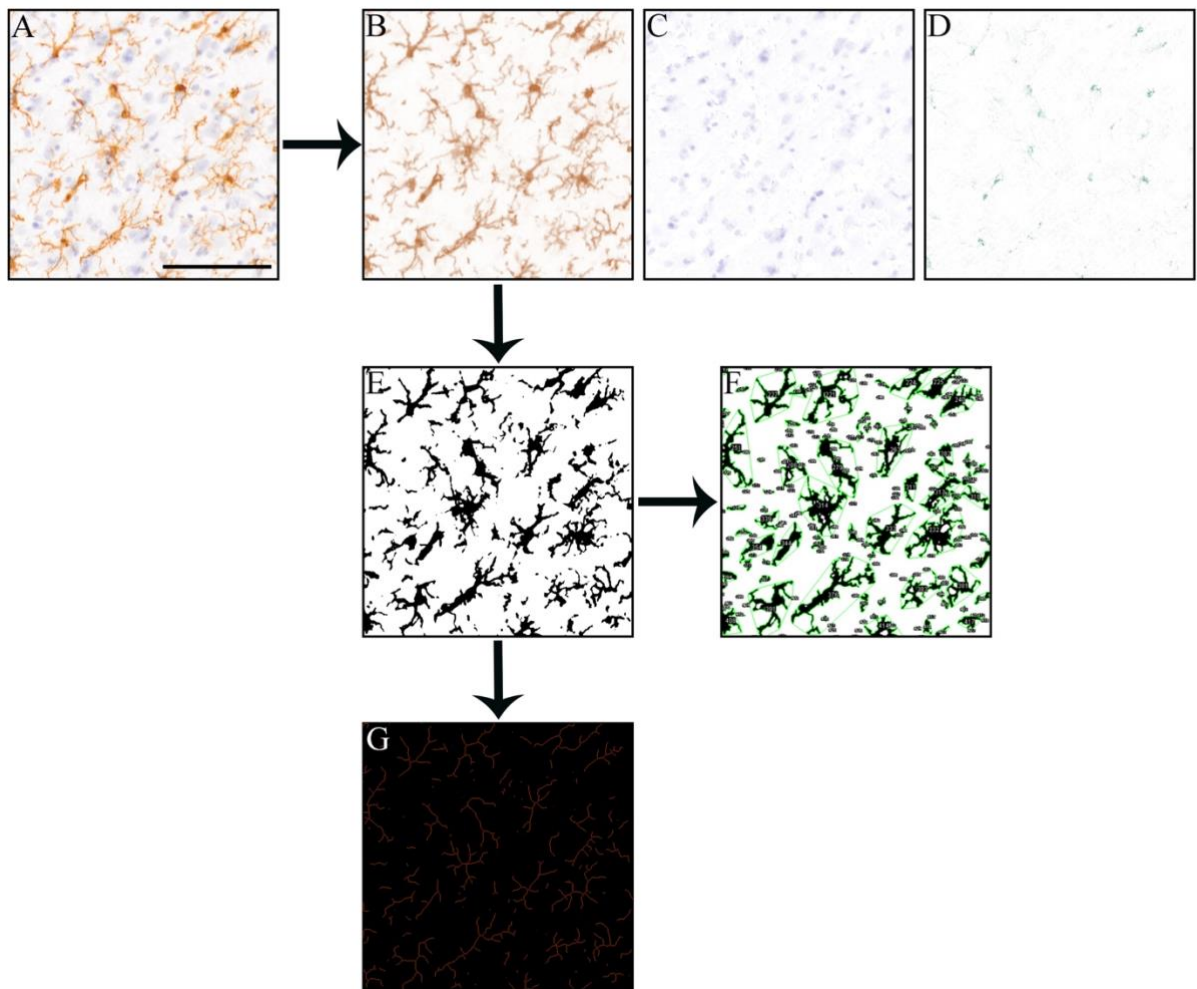


Figure S2. Quantification and analysis of microglial territoriality and skeletal structure.

ST1. Univariate analyses (control cases):		
	ITC	
Aβ	R ²	P-value
Case v control	6	0.02
Age	0.45	0.09
Sex	19	0.72
APOE genotype	16.5	0.63
Fixation time	0.03	0.93
Brain pH	-0.03	0.92
PMI	-0.17	0.55
Tau		
Case v control	5	0.01
Age	0.21	0.44
Sex	18	0.66
APOE genotype	11	0.24
Fixation time	0.24	0.42
Brain pH	-0.35	0.22
PMI	-0.2	0.46
Cortical thickness		
Case v control	0.38	0.01
Age	0.02	0.65
Sex	0.17	0.14
APOE genotype	0.0009	0.93
Fixation time	0.18	0.13
Brain pH	0.27	0.1
PMI	0.26	0.05
A β	0.07	0.35
Tau	0.09	0.28
Total microglia		
Case v control	0.51	0.003
Age	0.25	0.06
Sex	0.0001	0.98
APOE genotype	0.16	0.27

Fixation time	0.04	0.47
Brain pH	0.03	0.59
PMI	0.34	0.02
A β	0.12	0.2
Tau	0.05	0.45
Activated microglia		
Case v control	0.62	0.001
Age	0.33	0.02
Sex	0.15	0.33
APOE genotype	0.17	0.4
Fixation time	0.06	0.38
Brain pH	0.16	0.16
PMI	0.32	0.03
A β	0.1	0.25
Tau	0.01	0.68

ST2. Multivariate analyses (control cases):			
		ITC	
	Rank	R ²	P-value
Cortical thickness			
LPC v HPC	1	0.38	0.01*
PMI	2	0.07	0.22
Total microglia			
LPC v HPC	1	0.52	0.002**
PMI	2	0.08	0.15
Age	3	0.02	0.47
Activated microglia			
LPC v HPC	1	0.39	0.01*
PMI	2	0.12	0.12

ST3. Univariate analyses:						
	PVC		SFC		ITC	
Aβ (areal)	Spearman's ρ	P-value	Spearman's ρ	P-value	Spearman's ρ	P-value
Case v control	10 ^b	0.0004	24 ^b	0.02	15 ^b	0.002
Age	0.03	0.88	0.13	0.56	0.14	0.54
Sex	49 ^b	0.91	49 ^b	0.9	49 ^b	0.9
APOE genotype	31 ^b	0.05	38 ^b	0.15	30.5 ^b	0.05
Fixation time	-0.15	0.5	0.03	0.9	-0.05	0.83
Brain pH	-0.55	0.009	-0.24	0.29	-0.36	0.1
PMI	-0.15	0.49	0.02	0.93	-0.16	0.47
Aβ plaques	Spearman's ρ	P-value	Spearman's ρ	P-value	Spearman's ρ	P-value
Case v control	16 ^b	0.003	23 ^b	0.01	20 ^b	0.008
Age	0.05	0.84	0.13	0.55	0.05	0.81
Sex	44 ^b	0.64	50 ^b	0.96	44 ^b	0.64
APOE genotype	34 ^b	0.08	35 ^b	0.1	29 ^b	0.04
Fixation time	-0.28	0.2	-0.02	0.92	-0.19	0.4
Brain pH	-0.52	0.01	-0.19	0.41	-0.38	0.09
PMI	-0.17	0.45	-0.02	0.91	-0.15	0.51
Tau (areal)	Spearman's ρ		Spearman's ρ		Spearman's ρ	
Case v control	0 ^b	<0.0001	1 ^b	<0.0001	0 ^b	<0.0001
Age	0.14	0.51	0.01	0.95	-0.04	0.86
Sex	38 ^b	0.39	39 ^b	0.43	47 ^b	0.81
APOE genotype	41 ^b	0.13	36 ^b	0.07	25 ^b	0.01
Fixation time	-0.11	0.62	-0.06	0.78	-0.16	0.49
Brain pH	-0.45	0.04	-0.3	0.16	-0.49	0.02
PMI	-0.36	0.09	-0.11	0.62	-0.04	0.85
Tau +ve plaques	Spearman's ρ		Spearman's ρ		Spearman's ρ	
Case v control	1 ^b	<0.0001	10.5 ^b	0.0001	16.5 ^b	0.002
Age	-0.06	0.79	-0.27	0.22	-0.11	0.61
Sex	43 ^b	0.54	45.5 ^b	0.68	39 ^b	0.39
APOE genotype	34 ^b	0.05	34 ^b	0.02	42 ^b	0.22
Fixation time	-0.23	0.3	-0.03	0.9	-0.09	0.7
Brain pH	-0.54	0.01	-0.47	0.03	-0.37	0.09

PMI	-0.11	0.63	-0.17	0.43	-0.04	0.87
Tau +ve tangles	Spearman's ρ		Spearman's ρ		Spearman's ρ	
Case v control	9 ^b	<0.0001	1 ^b	<0.0001	1 ^b	<0.0001
Age	0.3	0.17	-0.29	0.18	-0.2	0.35
Sex	39 ^b	0.38	42.5 ^b	0.52	42 ^b	0.54
APOE genotype	40 ^b	0.13	31 ^b	0.01	25 ^b	0.01
Fixation time	-0.1	0.65	-0.17	0.45	-0.17	0.45
Brain pH	-0.47	0.03	-0.3	0.17	-0.3	0.17
PMI	-0.12	0.58	0.06	0.79	0.15	0.5
Neurons	R ²		R ²		R ²	
Case v control	0.09 ^c	0.23	0.41 ^c	0.03	0.47 ^c	0.0004
Age	0.0005	0.92	0.06	0.25	0.002	0.84
Sex	0.03 ^c	0.43	0.04 ^c	0.36	0.1 ^c	0.16
APOE genotype	0.02 ^c	0.58	0.22 ^c	0.03	0.04 ^c	0.36
Fixation time	0.06	0.29	0.001	0.88	0.18	0.05
Brain pH	0.004	0.78	0.0001	0.96	0.003	0.82
PMI	0.13	0.09	0.0002	0.95	0.03	0.42
A β	0.05	0.3	0.009	0.66	0.19	0.04
Tau	0.14	0.1	0.38	0.002	0.25	0.02
Arborised area	Spearman's ρ		R ²		R ²	
Case v control	0.13 ^c	0.09	0.17 ^c	0.02	0.37 ^c	0.0006
Age	0.35	0.11	0.18	0.04	0.07	0.23
Sex	43 ^b	0.61	0.002 ^c	0.85	0.02 ^c	0.54
APOE genotype	0.21 ^c	0.03	0.27 ^c	0.01	0.18 ^c	0.05
Fixation time	-0.06	0.81	0.01	0.65	0.0004	0.93
Brain pH	0.42	0.05	0.37	0.003	0.24	0.02
PMI	-0.09	0.68	0.0001	0.96	0.01	0.64
A β	-0.32	0.13	0.08	0.17	0.04	0.38
Tau	-0.1	0.66	0.18	0.04	0.2	0.03
IBA1 +ve pixels	R ²		R ²		R ²	
Case v control	0.08 ^c	0.2	0.2 ^c	0.03	0.44 ^c	0.001
Age	0.09	0.17	0.16	0.06	0.05	0.31
Sex	0.0003 ^c	0.94	0.002 ^c	0.82	0.02 ^c	0.48

APOE genotype	0.2 ^c	0.04	0.26 ^c	0.02	0.16 ^c	0.07
Fixation time	0.005	0.76	0.007	0.7	0.00007	0.97
Brain pH	0.22	0.03	0.4	0.002	0.23	0.02
PMI	0.03	0.42	0.001	0.88	0.007	0.7
A β	0.09	0.17	0.04	0.35	0.08	0.18
Tau	0.07	0.21	0.15	0.07	0.18	0.04
Total branch length	Spearman's ρ		Spearman's ρ		Spearman's ρ	
Case v control	31 ^b	0.06	34 ^b	0.1	7 ^b	0.0002
Age	0.26	0.23	0.53	0.01	0.2	0.37
Sex	46 ^b	0.76	41 ^b	0.52	51 ^b	>0.99
APOE genotype	0.35 ^c	0.02	25 ^b	0.02	26 ^b	0.02
Fixation time	0.23	0.3	-0.1	0.66	0.14	0.53
Brain pH	0.31	0.16	0.35	0.11	0.43	0.04
PMI	0.04	0.85	0.18	0.41	0.26	0.22
A β	-0.53	0.01	-0.03	0.89	-0.45	0.03
Tau	-0.28	0.19	-0.24	0.27	-0.62	0.002
Total #branches	R ²		R ²		R ²	
Case v control	0.1 ^c	0.14	0.16 ^c	0.06	0.37 ^c	0.002
Age	-0.1 ^a	0.65	0.07	0.23	0.002	0.77
Sex	0.0001 ^c	0.96	0.1 ^c	0.14	0.02 ^c	0.52
APOE genotype	0.09 ^c	0.18	0.17 ^c	0.05	0.17 ^c	0.06
Fixation time	0.17 ^a	0.45	0.003	0.83	0.001	0.87
Brain pH	0.49 ^a	0.02	0.42	0.001	0.44	0.0008
PMI	-0.2 ^a	0.37	0.0002	0.95	0.0007	0.9
A β	-0.48 ^a	0.02	0.001	0.86	0.19	0.04
Tau	-0.12 ^a	0.6	0.11	0.13	0.25	0.01
Total #junctions	R ²		R ²		R ²	
Case v control	0.13 ^c	0.09	0.2 ^c	0.03	0.39 ^c	0.001
Age	0.01	0.59	0.13	0.09	0.02	0.51
Sex	0.004 ^c	0.78	0.03 ^c	0.4	0.01 ^c	0.59
APOE genotype	0.18 ^c	0.05	0.21 ^c	0.03	0.22 ^c	0.03
Fixation time	0.02	0.52	0.008	0.69	0.002	0.83
Brain pH	0.26	0.01	0.4	0.002	0.45	0.0006

PMI	0.05	0.31	0.0006	0.91	0.001	0.89
A β	0.17	0.05	0.008	0.68	0.18	0.04
Tau	0.09	0.17	0.17	0.05	0.28	0.009
Total microglia	R ²		R ²		R ²	
Case v control	0.0002 ^c	0.95	0.0001 ^c	0.96	0.28 ^c	0.01
Age	0.03	0.44	0.13	0.08	0.07	0.23
Sex	0.02 ^c	0.48	0.08 ^c	0.19	0.001 ^c	0.87
APOE genotype	0.0001 ^c	0.96	0.06 ^c	0.29	0.11 ^c	0.14
Fixation time	0.000002	0.99	0.03	0.46	0.0004	0.93
Brain pH	0.005	0.76	0.03	0.43	0.06	0.27
PMI	0.06	0.27	0.006	0.73	0.05	0.3
A β	0.02	0.54	0.03	0.4	0.01	0.6
Tau	0.002	0.85	0.01	0.6	0.12	0.1
Ramified microglia	R ²		R ²		R ²	
Case v control	0.06 ^c	0.26	0.1 ^c	0.15	0.4 ^c	0.001
Age	0.03	0.45	0.03	0.47	0.003	0.8
Sex	0.03 ^c	0.44	0.2 ^c	0.03	0.07 ^c	0.23
APOE genotype	0.004 ^c	0.79	0.02 ^c	0.58	0.12 ^c	0.11
Fixation time	0.05	0.3	0.02	0.54	0.05	0.33
Brain pH	0.34	0.004	0.64	<0.0001	0.34	0.004
PMI	0.01	0.64	0.007	0.7	0.01	0.64
A β	0.1	0.13	0.26	0.06	0.13	0.09
Tau	0.07	0.21	0.07	0.23	0.27	0.01
Activated microglia	R ²		R ²		R ²	
Case v control	0.02 ^c	0.48	0.009 ^c	0.7	0.03 ^c	0.46
Age	0.02	0.53	0.21	0.03	0.05	0.32
Sex	0.09 ^c	0.17	0.01 ^c	0.64	0.09 ^c	0.19
APOE genotype	0.0005 ^c	0.92	0.04 ^c	0.39	0.01 ^c	0.61
Fixation time	0.06	0.28	0.01	0.67	0.05	0.31
Brain pH	0.003	0.82	0.01	0.61	0.0003	0.94
PMI	0.008	0.69	0.003	0.81	0.04	0.38
A β	0.13	0.09	0.11	0.12	0.01	0.59
Tau	0.006	0.73	0.001	0.9	0.0003	0.93

Dystrophic microglia	R²		Spearman's ρ		Spearman's ρ	
Case v control	0.02 ^c	0.48	34 ^b	0.1	57 ^b	0.87
Age	0.24	0.02	0.38	0.07	0.51	0.01
Sex	0.09 ^c	0.4	37 ^b	0.35	36 ^b	0.32
APOE genotype	0.01 ^c	0.63	0.003 ^c	0.81	0.0003 ^c	0.95
Fixation time	0.0003	0.94	-0.002	0.99	-0.04	0.87
Brain pH	0.56	<0.0001	-0.55	0.008	-0.56	0.006
PMI	0.07	0.22	-0.09	0.69	-0.39	0.06
A β	0.03	0.47	0.21	0.33	0.08	0.72
Tau	0.06	0.24	0.24	0.27	0.1	0.63
Microglial clusters	Spearman's ρ		Spearman's ρ		Spearman's ρ	
Case v control	14 ^b	0.001	30 ^b	0.05	44 ^b	0.32
Age	-0.23	0.29	-0.01	0.96	-0.03	0.9
Sex	45 ^b	0.7	45 ^b	0.71	50 ^b	0.97
APOE genotype	26 ^b	0.02	32 ^b	0.07	0.15 ^c	0.17
Fixation time	-0.23	0.29	-0.2	0.38	-0.06	0.78
Brain pH	-0.21	0.35	-0.14	0.54	0.34	0.12
PMI	-0.05	0.81	0.07	0.74	-0.16	0.47
A β	0.62	0.002	0.57	0.005	0.4	0.06
Tau	0.61	0.002	0.44	0.03	0.36	0.09

^aSpearman's ρ

^bMann-Whitney U

^c η^2

ST4. Multivariate analyses:									
		PVC			SFC			ITC	
	Rank	R ²	P-value	Rank	R ²	P-value	Rank	R ²	P-value
Aβ (areal)									
Case v control	1	0.62	<0.0001****				1	0.46	0.0005***
APOE genotype	2	0.02	0.36				2	0.02	0.39
Aβ plaques									
Case v control	1	0.36	0.003**				1	0.42	0.001**
APOE genotype							2	0.03	0.27
Brain pH	2	0.01	0.46						
Tau (areal)									
Case v control	1	0.8	<0.0001****				1	0.82	<0.0001****
APOE genotype							2	0.007	0.36
Brain pH	2	0.02	0.17				3	0.003	0.52
Tau +ve plaques									
Case v control	1	0.62	<0.0001***	1	0.53	0.0001***			
Brain pH	2	0.06	0.08	2	0.03	0.25			
Tau +ve tangles									
Case v control	1	0.46	0.0005***	1	0.67	<0.0001***	1	0.44	0.0008***
APOE genotype	2	0.002	0.83	2	0.06	0.06	2	0.02	0.42
Arborised area									
Case v control				4	0.0001	0.92	1	0.36	0.003**
Age				2	0.33	0.0002***			
APOE genotype	2	0.16	0.04*	3	0.01	0.35			
Brain pH	1	0.24	0.02*	1	0.37	0.003**	2	0.06	0.18
Neurons									
Case v control				1	0.26	0.01*	1	0.36	0.003**
APOE genotype				2	0.02	0.47	2	0.005	0.71
IBA1 +ve pixels									
Case v control				3	0.01	0.51	1	0.35	0.004**
APOE genotype	2	0.15	0.05	2	0.18	0.009**			
Brain pH	1	0.22	0.03	1	0.4	0.002**	2	0.05	0.21
Total branch length									
Case v control							1	0.22	0.03
APOE genotype				1	0.21	0.03*	3	0.07	0.16

Brain pH							2	0.08	0.16
Age				2	0.01	0.62			
Total #branches									
Case v control							2	0.12	0.04*
Brain pH							1	0.44	0.0008***
Total #junctions									
Case v control				3	0.0003	0.92	3	0.45	0.16
APOE genotype				2	0.14	0.03	2	0.15	0.02
Brain pH				1	0.4	0.002	1	0.04	0.0006
Ramified microglia									
Case v control							1	0.39	0.002**
Sex				2	0.05	0.11			
Brain pH				1	0.64	<0.0001****	2	0.12	0.048*
Dystrophic microglia									
Case v control									
Age	2	0.11	0.02*				2	0.11	0.09
Brain pH	1	0.56	0.0001***				1	0.23	0.02*
Microglial clusters									
Case v control	1	0.2	0.04*						
APOE genotype	2	0.07	0.18						

2.5 Application for the Professor John Irvine Hunter Prize for Research in Anatomical Sciences

The manuscript presented in Chapter 2 was submitted in a successful application to the Discipline of Anatomy and Histology, Faculty of Medicine and Health, The University of Sydney for the Professor John Irvine Hunter Prize for Research in Anatomical Sciences (2019). A presentation of the work to the Discipline was also done as part of the assessment process. The application, which also contains relevant information on the conceptual underpinnings of the research presented in this chapter, begins on the next page.

Application for the Professor John Irvine Hunter Research Prize (2019).

Applicant: Patrick Jarmo Paasila.

Position: PhD student (full-time); Discipline of Pathology.

SID: 430162637.

Supervisor: Greg Sutherland.

Article Title: The relationship between the morphological subtypes of microglia and Alzheimer's disease neuropathology.

DOI: 10.1111/bpa.12717

Authors: Patrick Jarmo Paasila¹; Danielle Suzanne Davies²; Jillian June Kril¹; Claire Goldsbury²; Greg Trevor Sutherland¹.

¹Discipline of Pathology, Faculty of Medicine and Health, The University of Sydney.

²Discipline of Anatomy and Histology, Faculty of Medicine and Health, The University of Sydney.

Overview:

- i. **Significance of the research in the context of the Discipline of Anatomy and Histology;**
- ii. **Outline of the impact and contribution of the research in the field;**
- iii. **Outline of the contribution of each author;**
- iv. **Manuscript (including supplementary figures and tables); and**
- v. **Comments from referees and responses from authors prior to publication.**

i. Significance of the research in the context of the Discipline of Anatomy and Histology.

The research that I present in this application was done in collaboration with Dr Claire Goldsbury and Ms Danielle Davies of the Discipline of Anatomy and Histology and is a histological investigation using post-mortem human brain tissue that examines the spatiotemporal associations of microglial morphological changes with the development of Alzheimer's disease (AD) neuropathology. Three differentially affected cortical regions of the AD brain – the inferior temporal, superior frontal and primary visual cortices – were selected based on established diagnostic criteria and a previous volumetric study¹. It is my view that the research presented here strongly aligns with the major themes of the Discipline of Anatomy and Histology. The discipline is of course widely recognised for its focus on the structure and development of the human body in both normal and pathological contexts. Research carried out in the discipline is done so through a number of laboratories that focus on the use of immunohistochemistry and immunofluorescence, advanced microscopy, and computing for image analysis to generate both qualitative and quantitative data in order that the microscopic and macroscopic organisation of human body structures might be better understood. Importantly for this application, each of these areas of interest within the discipline are also relevant in the research presented here, which has been published in *Brain Pathology*, the medical journal of the International Society of Neuropathology. Following a previously validated stereological approach² which involves sufficient sampling of cell numbers across all six cortical laminae of the human neocortex, we have thus been able to characterise the cortical thickness, density of total neurons, density of total microglia and the associated morphological subtypes, and the load of AD-type pathology in three cortical regions of the normally aged brain and clinicopathologically confirmed AD cases.

Briefly, immunohistochemistry utilising the pan-microglia marker IBA1 was performed on 45 µm thick post-mortem human brain tissue sections in order to enumerate total microglia and for the characterisation of microglial morphological subtypes in age and gender matched controls and AD cases. Double-labelled immunofluorescence stains using markers for β-amyloid/IBA1 and Total Tau/IBA1 were also performed in order to examine the potential associations between IBA1+ microglia and the major pathognomonic entities of AD. Nissl staining using cresyl violet acetate of 10 µm thick sections was also performed in order to quantify the cortical thickness of each region and for the enumeration of total neurons. Sections were analysed by brightfield (Stereo Investigator) and confocal microscopy (Zeiss LSM 510) at the Bosch Institute's Advanced Microscopy Facility. The data collected included both manual counts for neurons and microglia, which were also supplemented by automated morphometric analyses, including quantification of microglial branch length, number of branches, number of branch junctions and total arborised area as a measure of microglial territorial coverage. Additionally, quantitative data on the load of AD-type neuropathology in normal ageing and AD was also generated from automated image analyses but also included manual counts to determine the density of neurofibrillary tangles.

¹ Halliday, G. M., Double, K. L., Macdonald, V., & Kril, J. J. (2003). Identifying severely atrophic cortical subregions in Alzheimer's disease. *Neurobiol Aging*, 24(6), 797-806. doi: 10.1016/s0197-4580(02)00227-0

² Kril, J. J., Halliday, G. M., Svoboda, M. D., & Cartwright, H. (1997). The cerebral cortex is damaged in chronic alcoholics. *Neuroscience*, 79(4), 983-998. doi: 10.1016/s0306-4522(97)00083-3

ii. Outline of the impact and contribution of the research in the field.

The research presented here has addressed a number of important technical and conceptual issues relating to the involvement of microglia in AD and to the development of both β -amyloid and tau pathology. The inclusion of non-demented control cases with a sufficiently high AD-type pathological load to satisfy the neuropathological diagnosis of AD ('high pathology controls') as well as the use of differentially affected neocortical regions have allowed for the temporal modelling of the disease in human post-mortem tissue. Additionally, the use of a more thorough, previously validated stereological sampling protocol has ensured the reliability of the quantitative neuronal, microglial and neuropathological data generated by this investigation.

This investigation sought to model the AD time course using post-mortem tissue through the inclusion of high pathology controls and differentially affected neocortical regions. High pathology controls demonstrated an elevation in the density of activated microglia in the inferior temporal cortex compared to low pathology controls and confirmed AD cases. Suggesting that microglial activation, in contrast to the animal models, occurs early in the disease time course and is not associated with cognitive impairment. This finding was also recapitulated in regional comparisons within the AD group, where the primary visual cortex – a belatedly affected region of the AD brain that may be hypothetically used as a marker of earlier AD-related pathophysiological processes – demonstrated a higher density of microglial clustering around β -amyloid plaques compared to the severely affected inferior temporal cortex, which may be thought of as representing end-stage AD, which was characterised by an impaired microglial clustering response and a loss of IBA1+ microglia.

The generation of quantitative neuronal, microglial, and neuropathological data for comparisons across multiple cortical regions is also an important contribution to the field of AD research. Our findings demonstrate a great heterogeneity in the accumulation of A β and tau throughout the neocortex, which contrasts with the suggestion made from semi-quantitative staging schema, that are used in the routine neuropathological diagnosis of AD, that the spread of AD-type pathology occurs in a stereotypical fashion. Furthermore, correlations between microglial morphological subtypes and the level of AD-type pathology were also possible. For instance, the number of clusters of activated microglia was shown to be correlated with the level of tau pathology in the primary visual cortex, suggesting that microglia actively respond to the deposition of pathology in AD, but only during earlier stages of the disease. Interestingly, we have also shown that 15/15 of the controls investigated here had some level of tau pathology, 11/15 showed clustering of activated microglia and only 9/15 show any deposition of A β . This differential in the prevalence of each of these pathological changes might suggest that the deposition of tau is an earlier event in AD, followed by clustering of activated microglia and finally the accumulation of insoluble A β plaques.

Here we also used a previously validated stereological approach that ensured equal representation of all cortical laminae and required that a higher number of total cells were counted in order to ensure the accuracy of the estimates generated. Previously, stereological investigations would assess the reliability of estimates by examining the ratio between the mean of the squared coefficients of error and the squared coefficient of variation, with the suggestion that if the ratio is less than .5, which can be achieved by counting between 50 and 100 objects per individual³, as is commonly done, then the estimate of the mean can be considered reliable. However subsequent investigations using computer simulations have demonstrated that this method of reliability testing is unsound and that much higher counts, e.g. 700-1000 objects per individual, are required for reliable estimates⁴. Here the average number of counted objects (e.g. neuronal and microglial cells) was between this range, giving us greater confidence in the estimates of cell numbers generated in this study.

³ Gundersen, H. J. G. (1986). Stereology of arbitrary particles*. *Journal of Microscopy*, 143(1), 3-45. doi: 10.1111/j.1365-2818.1986.tb02764.x

⁴ Schmitz, C., & Hof, P. R. (2000). Recommendations for straightforward and rigorous methods of counting neurons based on a computer simulation approach. *J Chem Neuroanat*, 20(1), 93-114. doi: 10.1016/S0891-0618(00)00066-1

iii. Outline of the contribution of each author.

PJP carried out all experiments and microscopy relating to the quantification of A β , microglia and neurons, performed all computational morphometric analyses and statistical analyses, co-designed the study, and prepared the draft manuscript. DSD assisted with experiments and microscopy relating to the quantification of tau. JJK advised on the stereological techniques and brain region selection. CG advised on microglial morphometry and interpretation of results. GTS co-designed the study and supervised the analysis and interpretation of results. All authors contributed to the final manuscript.

iv. Manuscript:

- Starting on the next page.
- Supplementary figures and tables appended at the end.
- **Note (June 2021):** These have been omitted for the purposes of presentation in this thesis.—PJP

v. Comments from referees and responses from authors prior to publication.

- Starting on the next page.



THE UNIVERSITY OF
SYDNEY

Greg T Sutherland BVSc. PhD
A/Prof, Discipline of Pathology

Prof Seth Love,
Editor, Brain Pathology,
Institute of Clinical Neurosciences
Bristol University
United Kingdom.

25th January 2019,

Dear Prof Love,

Re: Revision of Manuscript BPA-18-12-RA-219

Thank you to the Reviewers and Brain Pathology Editorial staff for your time and efforts in reviewing our article entitled "*The Relationship between Microglial Subtypes and Alzheimer's Disease Neuropathology*".

We have addressed the concerns of the two Reviewers and incorporated these into our revised manuscript, that is now entitled "*The Relationship between the Morphological Subtypes of Microglia and Alzheimer's Disease Neuropathology*". A point-by-point rebuttal is provided immediately below and as an attached document along with the revised manuscript, figures and supplementary tables.

Please contact me if you require further information.

Yours sincerely

Greg Sutherland (on behalf of the authors)

Point-by-point rebuttal of Reviewers comments (in bold):

Reviewer 1:

- 1. The manuscript reports microglial morphological subtypes in relation to brain area in Alzheimer's disease, but does not add any new findings on the role of microglia in Alzheimer's disease.**

We agree with Reviewer 1 that some of our findings are consistent with those in the previous literature. However, we would also like to respectfully point out what we consider are novel findings although some of these may been understated in our original manuscript. As such we have added the following as the first paragraph in the revised 'Discussion' (Page 21):

- *'This study undertook to provide clarity on how microglia relate temporally to the progression of Alzheimer's disease by comparing morphological subtypes in differentially affected areas of post-mortem brain tissue. Unlike previous studies, our findings showed that activated microglia were only increased in high-pathology controls while clustering of microglia with A β plaques was uncommon and highest in the mildly affected PVC (~17%), suggesting that there is an early microglial reaction to A β but this is prior to the onset of dementia. Whereas only 12% and 5% of A β plaques were associated with a microglial cluster in the SFC and ITC respectively. Second, the severely affected ITC, was characterised by a reduced number of ramified (healthy) microglia. Third, dystrophic microglia were not associated with AD status or pathology, but rather brain pH.'*

Introduction

- 2. The introduction is unclear as whether the information provided are sourced from in vitro, animal or human studies. This is an important point as some information from experimental studies might not be relevant to the human disease.**

We agree with Reviewer 1 that information on sources would make the report clearer. In the revised manuscript we have made the followings changes:

- i. Page 3; paragraph 2; final line: '*...in mouse models of AD.*'
- ii. Page 3; paragraph 3; line 3: '*Extensive in vitro and animal studies of microglia demonstrate their ability to...*'
- iii. Page 4; paragraph 1; line 3: '*There have been a number of attempts to categorise microglia into distinct subtypes but there is little consensus on what constitutes each subtype or the nomenclature used to describe them.*'
- iv. Page 4; paragraph 2; line 1: '*Briefly in studies using human post-mortem brain tissue, ramified (healthy)...*'
 - Page 4; paragraph 2 – all citations are now from human tissue studies and one review (that examined human tissue where applicable; Ref. 6)
- v. Page 4; paragraph 2; line 6: '*...processes with either some degree of deramification (hence the use of the term deramified by some authors) or hyper-ramification (3, 47).*'
- vi. Other minor changes in the 'Introduction':
 - a. Page 3; paragraph 2; line 8: '*...and...such as RAGE, scavenger receptors...*'
 - b. Page 3; paragraph 3; line 1: moved '*only*' to precede '*responded*'
 - c. Page 4; paragraph 1; line 1: '*phenotypic*' changed to '*morphologies*'
 - d. Page 4; paragraph 2; line 2: removal of '*...represent healthy cells and...*'
 - e. Page 4; paragraph 2; line 4: '*... 'bushy' ...*' (moved from line 8)
 - f. Page 4; paragraph 2; line 6: '*hypertrophied*' changed to '*hypertrophic*'
 - g. Page 4; paragraph 2; line 17: added '*found*'
 - h. Page 5; paragraph 1; line 17: moved '*within cases*' to the end of the sentence.

3. All acronyms should be explained once in the main text e.g. ITC, PVC, SFC, PMI

As suggested, the revised manuscript has been updated to include the expanded terms for the above acronyms at their first use in the main text (as opposed to the Abstract):

- i. Page 5; paragraph 1; line 6: ‘...*inferior temporal cortex (ITC)*...’
- ii. Page 5; paragraph 1; line 9: ‘...*primary visual cortex (PVC)*, *superior frontal cortex (SFC)*...’
- iii. Page 13; paragraph 1; line 7: ‘...*post-mortem index (PMI)*...’
- iv. Other:
 - a. Abbreviation ‘*Aβ*’ removed from ‘Abstract’ and replaced with ‘*beta-amyloid*’; the first instance of the use ‘*Aβ*’ now occurs in the ‘Introduction’ (Page 2; line 6)
 - b. Acronym ‘*HIER*’ removed from Pages 8 (line 4) and 10 (lines 2 and 15)

Methods

4. The presentation of the methodology should be clearer with additional subheadings e.g. quantification, NeuN detection.

The additional subheadings have been added to the ‘Methods’ in the revised manuscript:

- i. Page 9: ‘*Quantification of microglia*’
- ii. Page 11: ‘*Aβ and tau imaging*’
- iii. Page 12: ‘*Neuronal staining and quantification*’
- iv. Other minor changes in the ‘Methods’:
 - a. Page 6; line 1: changed ‘*utilising*’ to ‘*using*’
 - b. Page 6; line 3: changed ‘*specimens*’ to ‘*samples*’
 - c. Page 6; line 7: added ‘*genotyping*’
 - d. Page 6; line 9: removed ‘*(3g) taken at autopsy and*’ and replaced with ‘*which has previously been shown...whole brain pH*’

5. The brain area investigated should be justified with regards to the CERAD or ABC scoring system.

We agree with Reviewer 1 that these staging schemes are important for benchmarking our findings. The brain areas chosen for investigation were done so on the basis of a previous volumetric study from our laboratory that demonstrated incremental atrophy in the three areas chosen (PMID: 2927762) and also incrementally increased tau load as described by the original AD staging paper by Braak and Braak (PMID: 1759558) and for A β , this same paper and a follow-up study by Thal and colleagues (PMID: 12084879). We have now amended the 'Introduction' in the revised manuscript to more clearly define our choice of regions:

- Page 5; line 10: '[Starting] *AD pathology and particularly tau pathology...* [Ending] *compared to gender-matched controls (19)...*'

However, as we discuss in our paper the AD staging schemes are not without their issues. Both the CERAD and (combinatorial) ABC scoring systems are based on a semi-quantitative appraisal across very few cortical areas, basal ganglia and midbrain for A β immunostaining ('A'), entorhinal cortex, hippocampus and inferior temporal cortex for neurofibrillary tangles ('B') and the inferior temporal gyrus alone to derive an age-related neuritic plaque score ('C'). In contrast, the few studies that have quantitatively compared cortical areas in the AD brain (e.g. PMID: 19010392), along with our current study, give evidence that conflicts with the relative pathological load predicted by the staging schema, and tau load in particular.

6. The cohort summary should be attached to the case description rather as a result.

We agree and have moved Table 2 from the 'Results' to the 'Methods' section (Page 7) and renumbered and renamed it 'Table 1. Cohort details' and added the following sentence:

- Page 6; final line: *'The demographic and clinicopathological characteristics of the cohort are listed in Table 1.'*

7. Dementia duration should be added as an important parameter, especially with regards to the view that PVC could be used as representative of earlier disease mechanisms.

Disease duration been added to the Table 1 (Page 7) and Table 2 (Page 14) in the revised manuscript.

8. What is the justification of performing Iba1 quantification on DAB staining and then double staining for microglia with A β or Tau to quantify the neuropathology?

DAB staining and light microscopy was preferred for microglial quantification as the fine processes of the microglia were more readily visualised on DAB sections compared with IF sections. Double labelling for IBA1 with A β or tau was necessary to investigate relative localisation with microglia.

9. The calculation of the Iba1+ cell density is unclear. Do the author mean number of cells per field or percent?

Cell density is expressed in terms of cells/mm² (please refer to Table 3; Page 17) and Figure 3D. Table 3 also includes columns marked with '%' to indicate the proportion of the total microglial population that is comprised of a particular morphological subtype. Where findings are expressed as percentages e.g. A β -, tau- and IBA1-positive pixels, then we have included '%' to indicate this.

10. A neuron-specific marker such as NeuN or Hu should be used to quantify the neurons instead of a cresyl violet.

Thank you for this suggestion. In our experience NeuN does not stain all cortical neurons, e.g. Cajal-Retzius cells (PMID: 9545178). Therefore, in our opinion, cresyl violet is a better pan-neuronal marker.

Results

11. Overall, the quantification data (Figures 1, 3 and 4) should be presented as scattered plot to reflect the human variability.

We agree with Reviewer 1; the histograms presented in Figures 1, 3 and 4 have been changed to box-and-whisker plots accordingly in the revised manuscript (see attached files for updated figures).

12. Figure 2 is confusing and not consistent with the definition of the different subtypes described in the introduction. In Figures 2B, 2D and 2F, the microglia do not appear “deramified” as ramifications are present.

As described in the ‘Introduction’ (Page 4, paragraphs 1 & 2) the nomenclature describing the microglial morphological subtypes vary considerably in the literature. Nevertheless, we agree with Reviewer 1 that the definition of the ‘activated’ morphological subtype could still be clearer and we have added the following to the ‘Introduction’ of the revised manuscript:

- Page 4; paragraph 2; line 6: ‘...*hypertrophic soma and processes with some degree of deramification (hence the use of the term ‘deramified’ by some authors) (3, 47).*’

All the microglia seen in Figures 2B and 2F are considered activated (except those indicated by arrows) as they are hypertrophic and have reduced, though not an absence of, branching compared to ramified microglia. Microglia in Figure 2D represent dystrophic microglia due to the discontinuities seen in the IBA1 staining. Figure 2 legend (i) and the associated main text (ii) have been updated to improve clarity:

- i. Page 32; ‘Figure Legends’; ‘Fig. 2 Microglial morphologies’: ‘**Fig. 2 Microglial morphologies.** Representative photomicrographs from the ITC show exemplars of microglial subtypes quantified here. **A.**

Ramified microglia seen in a control case (M20) have small, spherical soma and symmetrically distributed, thin, highly branched processes. B. Activated microglia in an AD case (M09) that are hypertrophied and have reduced branching compared to ramified microglia. Arrows indicate ramified microglia for comparison. C. Activated microglia that are amoeboid in morphology (arrows) are seen among other activated cells (arrow heads) in another AD case (M11). D. Dystrophic microglia that are pseudo-fragmented with discontinuous IBA1 staining of processes in the same AD case (M11). E. A dystrophic microglia that is deramified and has spheroidal swellings at the end of its processes (arrows) from an AD case (M13). F. Clusters of activated microglia seen in an AD case (M09). Nuclei counterstained with haematoxylin. Scale bar = 50 μ m'

- ii. Minor changes:
 - a. Page 4; paragraph 2; line 12: parentheses around the clause beginning with '*Such dystrophic microglia...*' have been removed.
 - b. Page 9; *Quantification of microglia* subsection; line 17: sentence revised by the removal of '*cytorrhesis*' and replacement of '*deramification*' with '*reduced ramification*'.

13. Figure 2C does not represent dystrophic microglia as described by Streit, but rather illustrate reactive microglia.

Thank you for pointing out this error. These cells are 'activated' and the figure legend (Page 32; Fig. 2) has been updated in the revised manuscript accordingly (see Point 12 (i) for updated Figure 2 legend).

14. Dystrophic microglia are present in figures 2D and 2E. Additionally, Figure 2D and 2E could be part of the same process.

As suggested by Reviewer 1 the microglia in both Figures 2D and 2E are dystrophic. The word '*dystrophic*' has been added to part D of the of Figure 2 legend to clarify that both images represent the morphological characteristics of microglia that are considered, and were counted as, dystrophic.

- 15. We do not know yet whether these different morphologies reflect different states or function of microglia. The authors should clarify whether the images were taken from an AD or control case and how often these features were observed between the 2 groups.**

We agree with Reviewer 1 that there remains a knowledge gap in understanding the functional consequences of the various subtypes, and indeed within subtypes. As suggested we have clarified which individual and their case status pertains to each image in the figure legend for Figure 2 (see Point 12 (i) for updated Figure 2 legend). We have also made this clearer in the main text with the following:

- Page 16; line 2: ‘...(Fig. 2A)...[line 3] A range of phenotypes within the activated (Fig. 2B, C) and dystrophic (Fig. 2D, E) subtypes were seen within all individuals as well as clusters made up of activated microglia in those individuals with AD pathology (Fig. 2F).’

- 16. Microglial clusters in AD usually relate to neuritic plaques. The authors did not observe any microglial clusters in the SFC and ITC area in the AD cases which is quite unusual (observation on the DAB or immunofluorescent slides?). Would this reflect an absence of neuritic plaques in these area or a technical problem due to the length of the fixative that can affect the quality of the microglial staining or the double staining?**

Thank you for this comment. Microglial clusters were observed in all three regions on both the DAB and IF sections with the latter showing co-localisation with A β and tau pathologies when they were present. These findings are presented in Table 3, but to make this point clearer to readers we have made the following to the ‘Results’ sub-section entitled ‘*Loss of healthy microglia in the ITC of AD brain*’ in the revised manuscript:

- i. Page 16; line 4: removed ‘...however no differences were seen in the PVC or SFC (Table 3).’
- ii. Page 16; line 7: added ‘(Table 3).’

- iii. Page 16; final line: added '*...of AD cases compared to controls. There was no difference in the density of clusters in the SFC or ITC between AD cases and controls.*'

In addition, neuritic plaques (tau-positive) were found in all regions and the fixation period did not adversely affect the quality or amount of staining (see univariate analyses in Supplementary Table ST3.)

17. Page 12 line 10, “Neuronal loss was observed in the SFC”.

Corrected. (Page 15; line 4)

18. Figure 3 should have the word “controls” in the title.

Corrected. (Page 33; Figure 3 Title)

19. Figure 6 should contain the R2 and P value.

Corrected.

Discussion

20. The authors state that they are using the model of tau spreading to make inferences about microglial function over time. This first paragraph would be more suitable for the introduction.

As suggested by Reviewer 1 the first paragraph of the 'Discussion' has been removed and largely incorporated into the 'Introduction' of the revised manuscript:

- i. Page 5; line 10: '[Starting] *AD pathology*...[Ending] *gender-matched controls (19)*...'
- ii. Other minor changes to the 'Discussion' of the revised manuscript:
 - a. Page 22; paragraph 2; line 1: added '*A β and tau-positive*'

- b. Page 22; paragraph 2; line 5: sentence now ends '*in which neither of these measures was affected*'

21. To consider PVC as a representative of an earlier disease mechanisms might be an overinterpretation. Is there a justification for this?

Thank you for this question. These references (PMID: 18520776; PMID: 18270320) show relatively less pathology and/or mild effects on the neurons in the PVC, providing support for our hypothesis. Thus the following clause has been added to the second paragraph of the 'Discussion' in the revised manuscript:

- Page 22; paragraph 2; line 6: '*...with previous pathological and molecular studies also suggesting that the amount of tau pathology in the PVC has minimal effects on the neurons in this region (24, 30).*'

Reviewer 2:

In this new paper, the authors use the same technical approach to further investigate the microglia phenotype in AD. This time they chose to study again inferior temporal cortex, and in addition, primary visual cortex and superior frontal cortex. The choice is clever in that these 3 regions are known to show different degrees of AD pathology, which the authors confirm. This allow the authors to make additional novel observations. However, some of their conclusions doesn't seem to go in line with their previous publication and would need clarification.

- 1. It would be best if the title and abstract clearly state that the studied microglia subtypes correspond to 'microglia morphology' subtypes.**

The 'Title', 'Abstract', 'Introduction' and 'Discussion' of the paper have been updated to include the word '*morphological*':

- i. 'Title' now reads: '*The relationship between the morphological subtypes of microglia and Alzheimer's disease neuropathology.*'
 - The phrase '*microglial morphological subtypes*' has been changed to '*the morphological subtypes of microglia*' throughout the revised manuscript:
- ii. 'Abstract'; Page 1; line 8
- iii. Page 5; lines 7 and 18
- iv. Page 8; line 3
- v. Page 17; Table 3 Title
- vi. Page 19; *Morphological changes of microglia correlate with tau pathology* subsection
- vii. Page 25; paragraph 2; line 2

2. Please reconsider to call 'ramified' microglia as 'healthy' microglia. A more objective and appropriate term, if necessary, would be non-disease associated microglia, or more specifically here, non-AD microglia.

'Ramified microglia' is the term commonly used in the literature to refer to normally functioning microglia. For consistency with the literature we would like to retain the word 'ramified'. Please note that term '*Ramified (healthy)*' is present in the 'Abstract' (Page 2; line 4) and now in the 'Introduction' (Page 4, paragraph 2, line 1) and 'Discussion' (Page 22; paragraph 1; line 2) of the revised manuscript.

3. Please explain why you find less total microglia density in the ITC now, and not in your previous paper. What changed?

In our previous paper (PMID: 27862631) we noted a trend towards a reduction in microglial density in AD cases compared to controls in the ITC. We consider that the inclusion of 10 additional cases was the major reason that a significant reduction was demonstrated in the current study.

4. Same as point 3, regarding no differences in the density of dystrophic microglia in the ITC now, while you reported an increase of them in the previous paper.

As correctly observed by Reviewer 2, our previous study reported increased dystrophic microglia in AD cases. We consider that the inclusion of brain pH in multivariate analyses as the major factor for the lack of difference in the current study. Brain pH, a known confounder of molecular studies utilising post-mortem human brain tissue, is highly correlated with the length and severity of the agonal period; which could conceivably affect microglial morphology as they react to their immediate environment, as shown in this study. Importantly, other parameters such as deramification and a reduction in the arborised area were similarly correlated with AD in both studies.

5. You say that the majority of microglia clusters were not associated with Abeta plaques in AD or controls. Could you provide quantification to support this claim? And, what is the percentage of plaques that are associated with microglia clusters?

We agree with Reviewer 2 that quantification of A β plaques, as opposed to just areal fraction, would provide more clarity on the degree to which microglia associate with plaques. As such we have now quantified A β -immunopositive plaques and added the following to the revised manuscript:

‘Methods’, *Image analysis* subsection:

- i. Page 12; paragraph 2; line 2: ‘...a more accurate indicator of pathology load than quantifying individual entities because of size variation...’
- ii. Page 12; paragraph 2; line 4: ‘However, to enumerate the percentage of A β -immunopositive plaques (A β plaques) that were associated with a microglial cluster the density of A β plaques was also calculated for each region.’

‘Results’, *Neuropathology* subsection:

- i. Page 15; line 2: ‘... $p = 0.01$ [typo in original manuscript; changed from 0.02 to 0.01]) in the ITC whereas cortical thinning was not observed in the PVC (2.2 ± 0.2) or SFC (2.8 ± 0.4) of AD cases

compared to controls (PVC = 2.2 ± 0.2 , $p = 0.6$; SFC = 2.7 ± 0.4 , $p = 0.8$).'

- ii. Page 15; line 8: '*Similarly, the density of A β plaques in the PVC (22.2 ± 17.8 plaques/mm²), SFC (37.1 ± 28.6) and ITC (40.6 ± 19) of AD cases was higher compared to controls (PVC = 6.6 ± 12.8 , $p = 0.003$; SFC = 11.5 ± 15.8 , $p = 0.01$; ITC = 14.4 ± 20.9 , $p = 0.008$) (Fig. 1C).'*'
- iii. Removed Figure 1A (cortical thickness ratio).
 - Figures 1B (Page 15; line 5) and 1C (Page 15; line 8) renumbered 1A and 1B respectively.
- iv. Added new Figure 1C (A β plaques; see updated figures).

'Results', *Microglial clustering was not a major feature of the AD cortex* subsection:

- i. Page 19; line 4: '*There was no difference between the percentage of A β plaques associated with a microglial cluster between the AD and control groups in any of the three regions: PVC (AD = $16.8 \pm 14.4\%$, control = 12.2 ± 23.4 ; $p = 0.15$), SFC (AD = 12.4 ± 12.7 , control = 5.8 ± 5.5 ; $p = 0.28$) and ITC (AD = 5.4 ± 6.5 , control = 17.2 ± 19.9 ; $p = 0.25$) (Fig. 5J-L) or tau-positive plaques (Fig. 5M-O) or tau-positive plaques (Fig. 5M-O) in either the AD cases or controls.'*
- ii. Error correction: Page 19; paragraph 1; line 1: '*two*' changed to '*three*' (criteria for a cluster is also included in the 'Methods' section; Page 9; *Quantification of microglia* subsection; last sentence).
 - Additionally; '*subregion*' changed to '*field*' (Page 19; paragraph 1; line 1).

Figure 1 legend:

- i. Page 32; removed: '*...the ratio of AD cortical thickness to mean control thickness (A).*'
- ii. Added: '*...A β plaque density (C)...*'
- iii. Figures 1B and 1C renumbered 1A and 1B respectively.
- iv. Minor changes to Figure 5 legend (Page 33:

- a. Line 2: added '*immunopositive*'
- b. Line 2: replaced '*neuritic*' with '*cored*'
- c. Line 5: added '*A β* '

Chapter 3: Clustering of activated microglia occurs before the formation of dystrophic neurites in the evolution of A β plaques in Alzheimer's disease

3.1 Preamble

This chapter presents a manuscript published by Free Neuropathology, a non-commercial journal operated and peer-reviewed by neuropathologists. Although the regions presented in Chapter 1 were differentially affected by neurodegenerative changes—including neuronal loss and atrophy—they did not show the expected differences in neuropathological load, with the PVC exhibiting similar levels of AD pathology as the ITC. Therefore another primary cortical area, the PMC, was selected based on the suggestion in the staging schema that it also appears to be an area minimally affected by AD pathology. The objective here was to find an area with significantly reduced levels of pathology compared to the most severely affected area previously investigated, namely the ITC, with aim of determining the relative sequence of neuropathological and microglial changes in the evolution of AD pathology in the cerebral cortex. Given the results presented in Chapter 1 showed that morphological markers of activation were more associated with the deposition of A β and that microglial dystrophy and loss of cell number coincided with advanced NFD, it was hypothesised that the activation of microglia follows the deposition of A β but occurs before NFD. This work was also done in collaboration with Dr. Claire S. Goldsbury and Danielle S. Davies.

Corrigendum (Aug 2021): Figure 3a in the published manuscript is missing a figure legend. The figure legend which should appear is the same one presented with Figure 1a–c.

3.2 Authorship attribution statement

Chapter 3 of this thesis is published as ‘Clustering of activated microglia occurs before the formation of dystrophic neurites in the evolution of A β plaques in Alzheimer’s disease’ (Paasila et al., 2020). The manuscript was authored by Patrick J. Paasila, Danielle S. Davies, Greg T. Sutherland, and Claire S. Goldsbury (corresponding author). PJP co-designed the study, collected all the data except the tau data, analysed all the data, and wrote the manuscript. DSD collected and helped analyse the tau data. GTS and CSG co-designed the study and analysed the data. All authors contributed to editing the manuscript.

Attestation

In addition to the statement above, permission to include the published material has been granted by the corresponding author.

Patrick J. Paasila

Candidate

June 2021

Claire Goldsbury

Claire S. Goldsbury

Corresponding author

June 2021

3.3 Published manuscript

The published manuscript begins on the next page.

Original Paper

Clustering of activated microglia occurs before the formation of dystrophic neurites in the evolution of A β plaques in Alzheimer's disease.

Patrick Jarmo Paasila², Danielle Suzanne Davies¹, Greg Trevor Sutherland², Claire Goldsbury¹

¹ *Discipline of Anatomy and Histology, School of Medical Sciences, Faculty of Medicine and Health, The University of Sydney, NSW 2006, Australia*

² *Discipline of Pathology, School of Medical Sciences, Faculty of Medicine and Health, The University of Sydney, NSW 2006, Australia*

Corresponding author:

Dr Claire Goldsbury PhD · Brain and Mind Centre · 94 Mallett Street · Camperdown, NSW 2050 · Australia · Tel +61 2 9351 0878
claire.goldsbury@sydney.edu.au

Submitted: 16 June 2020 · Accepted: 29 July 2020 · Copyedited by: Jeffrey Nirschl · Published: 04 August 2020

Abstract

Alzheimer's disease (AD) is a late-onset disease that has proved difficult to model. Microglia are implicated in AD, but reports vary on precisely when and how in the sequence of pathological changes they become involved. Here, post-mortem human tissue from two differentially affected regions of the AD brain and from non-demented individuals with a high load of AD-type pathology (high pathology controls) was used to model the disease time course in order to determine how microglial activation relates temporally to the deposition of hallmark amyloid- β (A β) and hyperphosphorylated microtubule associated protein tau pathology. Immunofluorescence against the pan-microglial marker, ionised calcium-binding adapter molecule 1 (IBA1), A β and tau, was performed in the primary motor cortex (PMC), a region relatively spared of AD pathological changes, and compared to the severely affected inferior temporal cortex (ITC) in the same cases. Unlike the ITC, the PMC in the AD cases was spared of any degenerative changes in cortical thickness and the density of Betz cells and total neurons. The clustering of activated microglia was greatest in the PMC of AD cases and high pathology controls compared to the ITC. This suggests microglial activation is most prominent in the early phases of AD pathophysiology. Nascent tau inclusions were found in neuritic plaques in the PMC but were more numerous in the ITC of the same case. This shows that tau positive neuritic plaques begin early in AD which is likely of pathogenic importance, however major tau deposition follows the accumulation of A β and clustering of activated microglia. Importantly, findings presented here demonstrate that different states of microglial activation, corresponding to regional accumulations of A β and tau, are present simultaneously in the same individual; an important factor for consideration if targeting these cells for therapeutic intervention.

Keywords: Alzheimer's disease, Inferior temporal cortex, Microglia, Post-mortem human brain tissue, Primary motor cortex

Introduction

Alzheimer's disease (AD) is neuropathologically characterised by inclusions of microtubule-associated protein tau (tau) and extracellular deposits of β -amyloid (A β). Intraneuronal tau pathology includes neurofibrillary tangles (NFTs) in the cell soma and neuropil threads (NTs), which occur mostly in the dendritic compartment, but also in the axonal domain though to a lesser extent (1, 2). NFTs and NTs are both comprised of paired helical filaments and straight filaments of polymerised hyperphosphorylated tau protein (3, 4). The extent of tau pathology follows a predictable spatiotemporal progression through functionally integrated brain regions (5, 6) and there is an extensive body of literature that demonstrates an inverse correlation between the accumulation of NFTs and cognitive status (7) such that the spread and regional level of NFTs reflects the severity of dementia with time (8).

Contrastingly, A β plaques follow a seemingly more haphazard regional pattern of accumulation throughout the neocortex, indeed plateauing relatively early in the disease time course (9, 10), and therefore correlate poorly with disease status until substantial argyrophilic neuritic tau pathology is also present (5, 7, 11). Whilst A β load may be an unreliable indicator of disease severity, it is generally accepted that the extent of its spread, in combination with tau pathology, is useful for staging purposes (9). A β plaques can be classified with immunostaining into at least three morphologically distinct categories: diffuse, fibrillar, or dense-cored. Diffuse plaques have long been proposed to be a structural precursor of other plaque forms, but whether these categories represent separate entities with independent mechanisms of development or are temporally linked is still unclear. Neuritic plaques (NPs) are those A β plaques that also feature dystrophic neurites (DNs) with silver staining. DNs can occur in all these morphological subtypes of A β plaques, though more commonly in dense-cored and fibrillar plaques than morphologically diffuse plaques (12). Most DNs are tau-positive and morphologically similar to NTs which are elongated in shape, but may also be globular, and possibly represent swollen presynaptic (axonal) terminals

(13). NPs that retain sparse DNs but show minimal A β staining have previously been described and were termed 'remnant plaques' which were proposed to result from glial phagocytosis of insoluble A β (14).

There remains significant debate as to the sequence of the neuropathological changes that precede the onset of AD symptomatology. The amyloid cascade hypothesis posits A β , and in particular the soluble, oligomeric, non-fibrillar fraction, as the initiating factor (15-20). A competing view is offered by others who contend that the sequence of pathological events begins with neurofibrillary pathology (21, 22) which precedes the formation of insoluble A β pathology (23). Indeed, there is evidence that tau pathology occurs prior to A β pathology as it is more common in the brains of non-demented individuals (21) but this might represent a non-AD scenario described as primary age-related tauopathy (PART) (24). Notwithstanding the order of events, both hypotheses suggest that an activated glial response is an integral component of the pathogenesis of AD.

The study of microglia morphology in post-mortem human brain tissue presents a simple method with which to gauge the involvement of microglia in instances of changed physiological conditions or to the development of a disease. Microglia with a ramified morphology, characterised by thin, evenly distributed, highly branched processes with a small, spherical soma, represent the healthy cell population (25-27). Activated microglia are characterised by reduced morphological complexity including hypertrophy of the soma and processes and may also display the formation of distal phagosomes (23, 25, 28). Dystrophic microglia display features consistent with cellular senescence (29), including a loss of processes, tortuosity of remaining processes, and discontinuous IBA1-immunolabelling (30-32). Lastly, clusters of activated microglia in AD have been noted previously in post-mortem human brain tissue and represent the direct interaction between microglia and A β and tau pathology (10, 32, 33).

By investigating brain regions differentially affected by AD-type pathology in non-demented and demented individuals it may be possible to model the sequence of pathological changes in the dis-

ease, in particular the activated microglial response. Previously we demonstrated an increased density of activated microglia in the inferior temporal cortex (ITC) of non-demented controls with similar levels of AD-type pathology ('high pathology controls' – HPCs) as clinically and neuropathologically-confirmed AD cases (26). This suggested that the microglial response occurs in the preclinical phases of AD but we wished to confirm this finding in a belatedly affected region of the AD brain, the primary motor cortex (PMC), compared to an earlier and more severely affected region, the ITC, of the same cases. Further, we wished to determine the sequence of A β , tau, and microglia pathological changes that occur in the cortex. The findings here

demonstrate that nascent NTs and DNPs in the PMC begin early in the pathogenesis of AD, but follow the clustering of activated microglia. By contrast, looking at the severely affected ITC in the same cases, findings suggest that microglial clustering at plaques dissipates once tau and A β pathology is long established and there is also a substantial loss of IBA1-immunoreactivity (26, 34). Although an early toxic microglial gain of function cannot be ruled out, these findings appear most consistent with a scenario where microglial activation is neuroprotective early in the pathogenesis of AD. We suggest that this is followed by a gradual exhaustion of microglial function that contributes to cognitive deterioration in the AD brain.

Table 1. Cohort characteristics.

Case ID	Age	Sex	Status	Cause of death	AD duration (years)	CDR	ABC score	AD likelihood
M03	76	Female	AD	Cardiorespiratory failure	11	3	A3 B2 C3	Intermediate
M04	77	Male	AD	Aspiration pneumonia	9	2	A3 B3 C2	High
M09	80	Female	AD	Alzheimer's disease	10	3	A3 B3 C3	High
M11	83	Male	AD	Cerebrovascular	5	3	A3 B3 C3	High
M12	83	Female	AD	Uraemia	7	3	A3 B3 C2	High
M13	84	Female	AD	Aspiration pneumonia	13	3	A3 B3 C3	High
M17	85	Female	AD	Cardiorespiratory failure	5	3	A3 B3 C3	High
M22	98	Female	AD	Cerebrovascular	6	3	A3 B3 C2	High
M14	85	Male	HPC	Cancer	-	-	A2 B2 C3	Intermediate
M18	87	Female	HPC	Cancer	-	-	A2 B2 C0	Intermediate
M19	92	Female	HPC	Pancytopenia	-	0	A2 B2 C2	Intermediate
M21	87	Female	HPC	Acute peritonitis	-	0	A3 B2 C1	Intermediate
M23	102	Female	HPC	Acute renal failure	-	0	A2 B2 C2	Intermediate
M01	69	Male	Control	Cardiac failure	-	-	A3 B1 C3	Low
M02	74	Female	Control	Cancer	-	-	A3 B1 C3	Low
M05	78	Female	Control	Respiratory failure	-	-	A0 B0 C0	Not
M06	78	Female	Control	Toxicity	-	-	A0 B1 C0	Not
M07	81	Male	Control	Cardiac failure	-	-	A0 B2 C0	Not
M08	80	Male	Control	Respiratory failure	-	-	A0 B0 C0	Not
M10	82	Female	Control	Respiratory failure	-	-	A3 B1 C2	Low
M15	85	Female	Control	Respiratory failure	-	-	A2 B1 C0	Low
M16	85	Female	Control	Pneumonia	-	0	A2 B0 C1	Low
M20	93	Female	Control	Cardiac failure	-	0.5	A1 B0 C0	Low

Methods

This study was approved by the University of Sydney's Human Research Ethics Committee (HREC#2015/477). All tissue samples for this study, as well as demographic and clinical information, were supplied by the New South Wales Brain Tissue Resource Centre (NSWBTRC) and the Sydney Brain Bank (SBB), collectively the New South Wales Brain Banks (NSWBB), following approval from their Scientific Advisory Committee. Methods for case ascertainment and tissue preparation by NSWBB have been previously published (35). The demographic and clinicopathological characteristics of the cohort (Table 1) and data from the ITC have been previously published (26).

Immunofluorescence

Immunofluorescence staining procedures were performed on free-floating 45 µm fixed sections derived from the caudal aspect of the superomedial area of the PMC of controls ($n = 10$), HPCs ($n = 5$), and pathologically confirmed AD cases ($n = 8$) as previously described (26). Double-labelled sections using antibodies against A β , total tau (TTau), and the pan-microglial marker ionised calcium-binding adapter molecule 1 (IBA1), were used for the quantification of A β and tau loads and microglial morphological subtypes.

For A β and IBA1 quantification, heat-induced epitope retrieval was performed using a sodium citrate solution (pH 8.5) at 60°C overnight, followed by a 12-minute formic acid (90%) incubation at room temperature. Blocking was performed in 10% normal goat serum (Gibco #16210072), and primary (mouse A β , 1:1000, BioLegend 803002; rabbit IBA1, 1:1000, Wako 019-19741) and secondary (1:200; Thermo Scientific: Alexa Fluor (AF) 488 goat anti-mouse, #A11001; AF 568 goat anti-rabbit, #A11011) antibody incubations were performed at 4°C with gentle agitation. Nuclear counterstaining was performed in the last 40 minutes of the secondary antibody incubation by the addition of Hoechst 33342 dye (1 µg/mL; Thermo Scientific 62249). Sections were mounted using Prolong Diamond Antifade (Invitrogen P36961). Double-immunolabelling of TTau (rabbit; 1:500; Dako K9JA/A0024) and IBA1 (mouse; 1:50; Millipore

MABN92) was carried out as previously described (34). TTau immunostaining of NFTs, NTs, and DNs has previously been demonstrated to give comparable immunostaining to standard phosphotau antibodies (12E8 and AT8) (36). Briefly, heat-retrieval was performed with sodium citrate (pH 6.0) for 10 minutes at 100°C, before permeabilising, blocking with BSA, and incubating in primary antibodies for three hours at room temperature or overnight at 4°C, and finally incubating in secondary antibodies (1:200; Invitrogen: AF555 goat anti-mouse, A214424; AF647 goat anti-rabbit, A21244). Hoechst 33342 was added to counterstain nuclei and sections were mounted in ProLong Gold Antifade.

Image acquisition and analysis

A β and IBA1 double-labelled sections were imaged using a Zeiss LSM 800 confocal microscope using the 'tile scan' function at the Advanced Microscopy Facility, Bosch Institute, The University of Sydney. A previously validated modified disector sampling approach that utilises one section per individual was used here for the analysis of the A β and IBA1 immunostained sections (37). Briefly, a total of three cortical strips per section from areas where the pial surface and the grey-white boundary were strictly in parallel were acquired for the quantification of microglia, A β plaques and A β -positive pixels. These cortical strips were constructed of serial images 500 µm in width, 6 µm in z-depth with three z-slices (z-step = 3 µm), spanning all of the cortical laminae of the PMC using a 20 \times /0.8 numerical aperture (NA) objective. Clusters of microglia and individual microglia, which were categorised as having either a ramified, activated, or dystrophic morphology as previously described (26), were enumerated in image analysis software (Fiji; NIH). The terminology used to describe the different populations of morphologically diverse populations of microglia was informed by previous investigations (25, 28, 30). Microglia with thin, highly branched processes, and a spherical nucleus were categorised as 'Ramified'. 'Activated' microglia (previously termed 'deramified' (34)) included those cells that displayed hypertrophy of the soma or processes with retraction of secondary or tertiary processes. 'Dystrophic microglia' were identified on the basis of a loss of processes with the

remaining processes displaying significant tortuosities or discontinuous IBA1-immunolabelling with or without blebbing or punctate IBA1-labelling (previously dystrophic microglia were subcategorised as either 'punctate' or 'discontinuous' to reflect these observations (34)). A 'Cluster of microglia' was counted if three or more soma occurred within, or were touching the margins of, a 20 μm^2 virtual graticule subregion. Larger clusters were counted as one cluster if the graticule subregion could be moved and still incorporate at least three somata. Clusters were counted whilst visualising only the 568 nm (IBA1-positive) channel to distinguish these from individual microglia and to minimise potential false-positive counts in the presence of either A β - or TTau-immunostaining. The total number of microglia counted per section averaged 519 with a coefficient of error (CE) of ≤ 0.2 for all counts of morphological subtypes, with the exception of microglial clusters (CE ≤ 0.3) which were relatively rare and displayed significant variance between cases.

Quantification of TTau was carried out using an Olympus VS120 slide scanner at the Sydney Microscopy and Microanalysis, Brain and Mind Centre, The University of Sydney. Whole section DIC and fluorescence overviews of a single section from each case were generated using a 10 \times objective and were used to systematically map out four representative 500 μm^2 regions of interest (= 1mm² per section) within the mid-cortical laminae (III-V) for manual counts of NFTs and for the quantification of TTau-positive pixels. Individual images were captured using a 40 \times /0.9 NA objective and were comprised of seven z-slices with a depth of 6 μm (z-step = 1 μm). Image analysis was performed in Fiji using manually thresholded images. Positive pixel counts were generated for A β and TTau staining and expressed as a percentage of total pixels (% A β and % TTau respectively). High resolution imaging of all immunolabelled sections were carried out using a Nikon A1R or Zeiss LSM 710 confocal microscope (Sydney Microscopy and Microanalysis, Charles Perkins Centre and Brain and Mind Centre, The University of Sydney). Features were imaged with either a 40 \times /0.95 NA or 100 \times /1.4 NA objective and shown as maximum intensity projections.

Nissl staining

Nissl stains of free-floating 45 μm thick formalin-fixed sections were performed for the meas-

urement of cortical thickness and neuronal counts. Sections were incubated in 0.1% cresyl violet acetate (0.02% glacial acetic acid; added immediately before use) for 15 minutes at 60°C. Differentiation was achieved by sequentially washing sections for three minutes in 70% and 95% ethanol. The final level of staining was adjusted by briefly dipping sections in 100% ethanol and confirmed by light microscopy before clearing in xylene for ten minutes and mounting in DPX. Cortical thickness measurements and neuronal counts were performed on three cortical strips from one section per individual using an eyepiece graticule on an Olympus BX50 microscope using a 20 \times /0.75 NA objective. A height measure of 45 μm was used in determining density estimates to eliminate artefactual tissue shrinkage during staining; with the microtome accuracy to cut precise sections having been previously validated (37). CEs using the modified disector technique outlined above were <0.1 for cortical thickness and <0.15 for the density of Betz cells and total neurons.

Statistical analyses

The normality of data was tested using the Shapiro-Wilk test. Equality of variances was tested using Brown-Forsythe test. Group differences were investigated by either Welch's analysis of variance or Kruskal-Wallis test for non-Gaussian distributions, with either Games-Howell or Dunn's test, respectively, for pairwise comparisons. Regional differences to the previously reported ITC (26) were investigated by either Welch's T test or Wilcoxon rank-sum test for non-Gaussian distributions. The Pearson correlation coefficient (r) and coefficient of determination (r^2), or Spearman rho (ρ) for non-Gaussian distributions, were calculated for univariate correlations to investigate relationships between AD-type pathology, microglial morphologies, and APOE $\epsilon 4$ status. Stepwise regression models which included age, sex, brain pH, post-mortem interval, and fixation period were performed to exclude effects of potential confounders. A p-value <0.05 was considered statistically significant. All statistical analyses were performed using JMP Pro 14 (SAS Institute Inc). Graphs were produced using Microsoft Excel.

Results

The Alzheimer's disease primary motor cortex exhibits mild tau and β -amyloid deposition but no evidence of neurodegeneration

This study involved 23 autopsy cases that had previously been clinicopathologically characterised as 'probable AD' or controls based on ABC score and clinical dementia rating (Table 1) (39). AD cases (n=8) included individuals with an intermediate–high likelihood of AD dementia following routine neuropathological diagnostic testing (38) and who presented with typical AD dementia prior to death. 'High pathology controls' (HPC) (n=5) were grouped as such on the basis of no cognitive impairment but satisfied a diagnosis of intermediate AD likelihood on post-mortem examination. Controls (n=10) included individuals with a range of ABC scores (A0–3; B0–2; C0–3), though only satisfying a 'Not' or 'Low' outcome after diagnostic testing.

There was no cortical atrophy (Fig. 1a) or neuronal loss (Fig. 1b), including the prominent layer Vb Betz cells (Fig. 1c), in the PMC of AD cases or HPCs compared with controls. Following a positive pixel analysis, grey matter A β areal fraction (% A β) was higher in the PMC of AD cases compared to controls ($p = 0.0005$), but not HPCs ($p = 0.07$). The density of total A β plaques, fibrillar, and dense-cored plaques was also significantly higher in AD cases compared to controls (Total $p = 0.003$; Fibrillar $p = 0.002$; Dense-cored $p = 0.004$) but not HPCs (Total $p = 0.1$; Fibrillar $p = 0.06$; Dense-cored $p = 0.2$). Total tau areal frac-

tion (% TTau) and the density of NFTs was higher in the PMC of AD cases compared to controls (%TTau $p = 0.001$; NFT $p = 0.001$) and HPCs (%TTau $p = 0.007$; NFT $p = 0.01$) (Table 2).

Amongst the AD cases, the PMC had significantly reduced % A β ($p = 0.006$), total A β plaques (0.001), and fibrillar plaques ($p = 0.0002$), but not dense-cored plaques ($p = 0.2$) compared to the ITC. The % TTau ($p = 0.02$) and the density of NFTs ($p = 0.02$) were also significantly reduced in the PMC compared to the ITC of AD cases. Amongst controls the % TTau was significantly reduced in the PMC compared to the ITC ($p = 0.04$). There were no other regional differences in terms of pathological load in controls, including amongst HPCs (Table 3).

In the ITC, all of the control, HPC, and AD cases had neuritic tau pathology at varied levels. A β pathology in the ITC occurred in 4/10 controls, and all HPCs and AD cases. The clustering of activated microglia in the ITC was apparent in 6/10 controls (including three with only tau pathology), and all of the HPCs and AD cases except one (M12) (ITC case data is shown in Fig. 1d). In the PMC, neuritic tau pathology was present in 7/10 controls, 4/5 HPCs, and all AD cases, while A β deposition in the PMC occurred in 6/10 controls, 4/5 HPCs, and all AD cases. Microglial clustering in the PMC was observed in 5/10 controls, and all of the HPCs and AD cases, with the exception of one case (M12) (PMC case data is shown in Fig. 1e). In controls, the % TTau correlated with age in the PMC ($r^2 = 0.44$, $p = 0.04$) but not in the ITC, which was near significant ($r^2 = 0.39$, $p = 0.05$).

Table 2. Summary of neuronal and neuropathological data of the primary motor cortex^a

	Control	HPC	AD	P-value ^b
Cortical thickness (mm)	2.7 \pm 0.4	3 \pm 0.5	3 \pm 0.4	0.3
Total neurons ('000/mm ³) ^c	24.8 \pm 5.9	35.6 \pm 12.1	33.1 \pm 8	0.05
Betz cells (/mm ³) ^d	726.8 \pm 372.5	943.7 \pm 148.8	636.8 \pm 265.7	0.2
% A β	0.1 \pm 0.1	0.3 \pm 0.3	0.7 \pm 0.2	0.0009
Total A β plaques (/mm ³)	3.1 \pm 4.8	4.6 \pm 3.6	13.7 \pm 4.7	0.003
Fibrillar (/mm ³)	1.6 \pm 2.2	2.2 \pm 2.4	7.7 \pm 4.3	0.001
Dense-cored (/mm ³)	1.5 \pm 3.2	2.2 \pm 2.2	6 \pm 2.8	0.006
% TTau	0.003 \pm 0.003	0.002 \pm 0.003	0.9 \pm 0.6	0.004
NFTs (mm ³)	0 \pm 0	0 \pm 0	11.8 \pm 10.2	0.0004

^aMean \pm standard deviation.

^bANOVA results; see text for p-values of pairwise comparisons.

^cInclusive of Betz cells.

^dDensity of Betz cells in layer V.

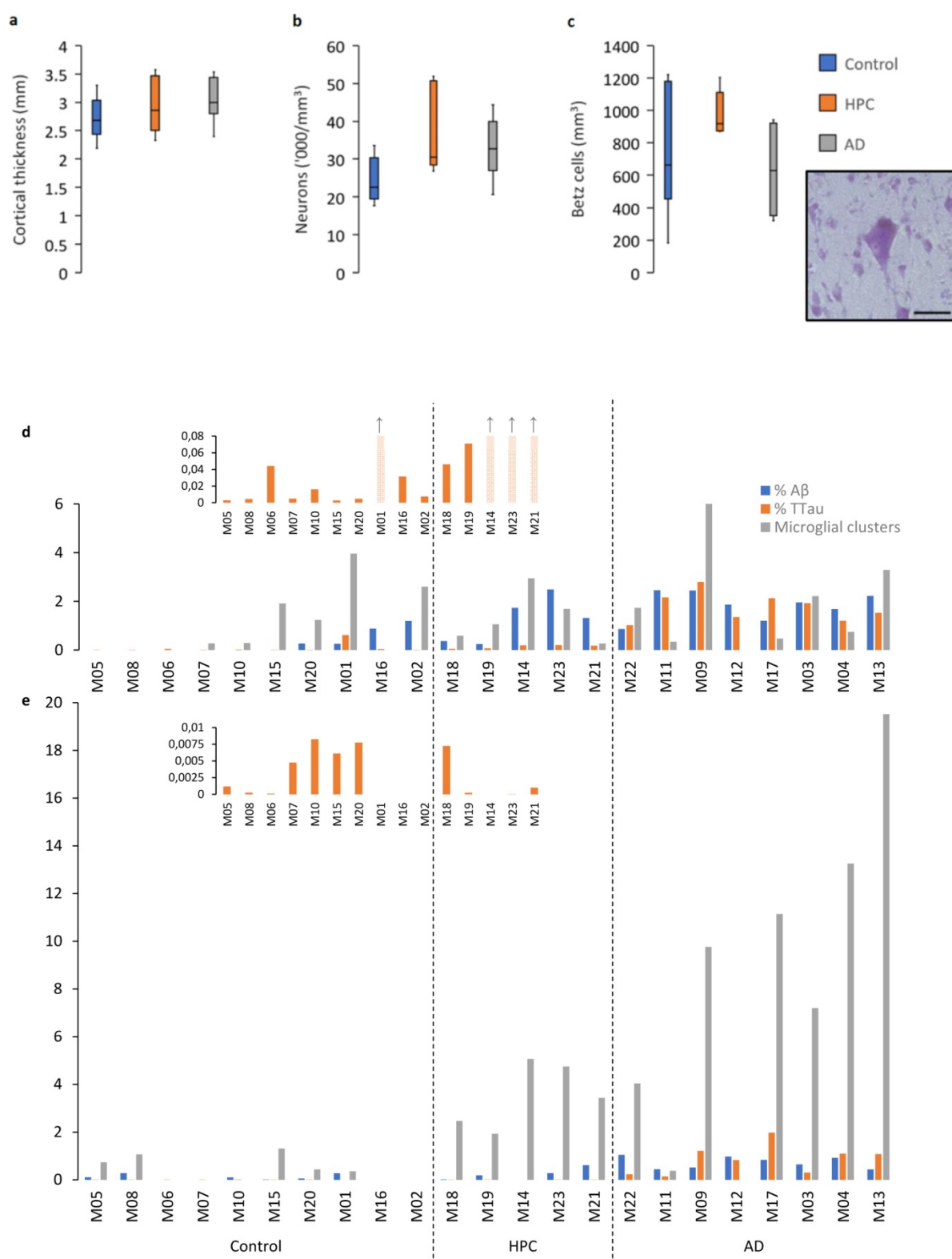


Figure 1 Characteristics of the PMC and regional neuropathological comparisons. **a–c** The PMC is spared of AD-related neurodegenerative changes as measured by cortical thickness (**a**), total neuronal density (**b**), and the density of layer Vb Betz cells (inset demonstrates a pyramidal Betz cell with multiple asymmetrically distributed perisomatic neurites, a prominent nucleolus, and a dark dense deposit of cytoplasmic lipofuscin) (**c**). **d–e** A cohort wide comparison of the percentage of Aβ and Ttau immunolabelling and microglial clustering in the ITC (**d**) and PMC (**e**) demonstrates age-related tau build-up in a majority of control brains in both regions and an early build-up of Aβ in HPCs (that were scored as A2-3, B2, C0-3 on diagnostic slides) with a concomitant microglial clustering response that is more prevalent in the PMC compared to the ITC and which appears to dissipate with severe AD pathology in the ITC. Scale bar = 50 μm (**c**)

Table 3. Regional neuropathological comparisons^a.

Tau		Control		
		PMC	ITC	P-value
	% TTau	0.003 ± 0.003	0.1 ± 0.2	0.04
	Tangles (/mm ²)	0 ± 0	0.9 ± 2.2	0.5
		HPC		
	% TTau	0.002 ± 0.003	0.1 ± 0.1	0.06
	Tangles (/mm ²)	0 ± 0	0.4 ± 0.5	0.5
		AD		
	% TTau	0.9 ± 0.6	1.8 ± 0.6	0.02
	Tangles (/mm ²)	11.8 ± 10.2	21.9 ± 19.1	0.02
Aβ		Control		
	% Aβ	0.1 ± 0.1	0.3 ± 0.4	0.8
	Total Aβ plaques (/mm ²)	3.1 ± 4.8	7.2 ± 13.4	0.9
	Fibrillar	1.6 ± 2.2	5.7 ± 11.3	0.9
	Dense-cored	1.5 ± 3.2	1.5 ± 2.4	>0.9
		HPC		
	% Aβ	0.3 ± 0.3	1.2 ± 0.8	0.2
	Total Aβ plaques (/mm ²)	4.6 ± 3.6	29 ± 23.3	0.08
	Fibrillar	2.2 ± 2.4	22.5 ± 21.9	0.1
	Dense-cored	2.2 ± 2.2	6.5 ± 4.9	0.2
		AD		
	% Aβ	0.7 ± 0.2	1.8 ± 0.5	0.006
	Total Aβ plaques (/mm ²)	13.7 ± 4.7	40.6 ± 17.7	0.001
	Fibrillar	7.7 ± 4.3	35.5 ± 17.8	0.0002
	Dense-cored	6 ± 2.8	5.1 ± 3.2	0.2

^aMean ± standard deviation.

Clusters of activated microglia are more commonly found in the PMC than the ITC of HPCs and AD cases

The density of individual activated (Fig. 2a–e), ramified (Fig. 2f), dystrophic (Fig. 2g–h), or total microglia did not differ between any of the three groups in the PMC (Table 4). Microglial clusters (Fig. 2i–j), although a small proportion of total microglia, were significantly more common in HPCs (Fig. 2k) and AD (Fig. 2l) cases compared to controls in the PMC (^{HPC}p = 0.01; ^{AD}p = 0.04).

Clusters in the PMC were also higher than in the ITC of HPCs (p = 0.02) and AD cases (p = 0.03) (Fig. 3a), whilst the density of total (p = 0.04) and

ramified microglia (p = 0.002) were reduced in the ITC compared to the PMC of AD cases. Immunofluorescent double-labelling for Aβ and IBA1 in the PMC showed that the clusters of activated microglia, occurred preferentially within the boundaries of fibrillar Aβ plaques, with a significant correlation in a combined analysis of control and AD brains (Spearman ρ = 0.54, p = 0.006; Fig. 3a). The percentage of Aβ plaques associated with a cluster of activated microglia in the PMC ranged from a mean of 41% in controls and 43% in AD cases to 60% in HPCs, with one control (M15), two HPCs (M14 and M18), and one AD case (M13) having a higher density of microglial clusters than Aβ plaques.

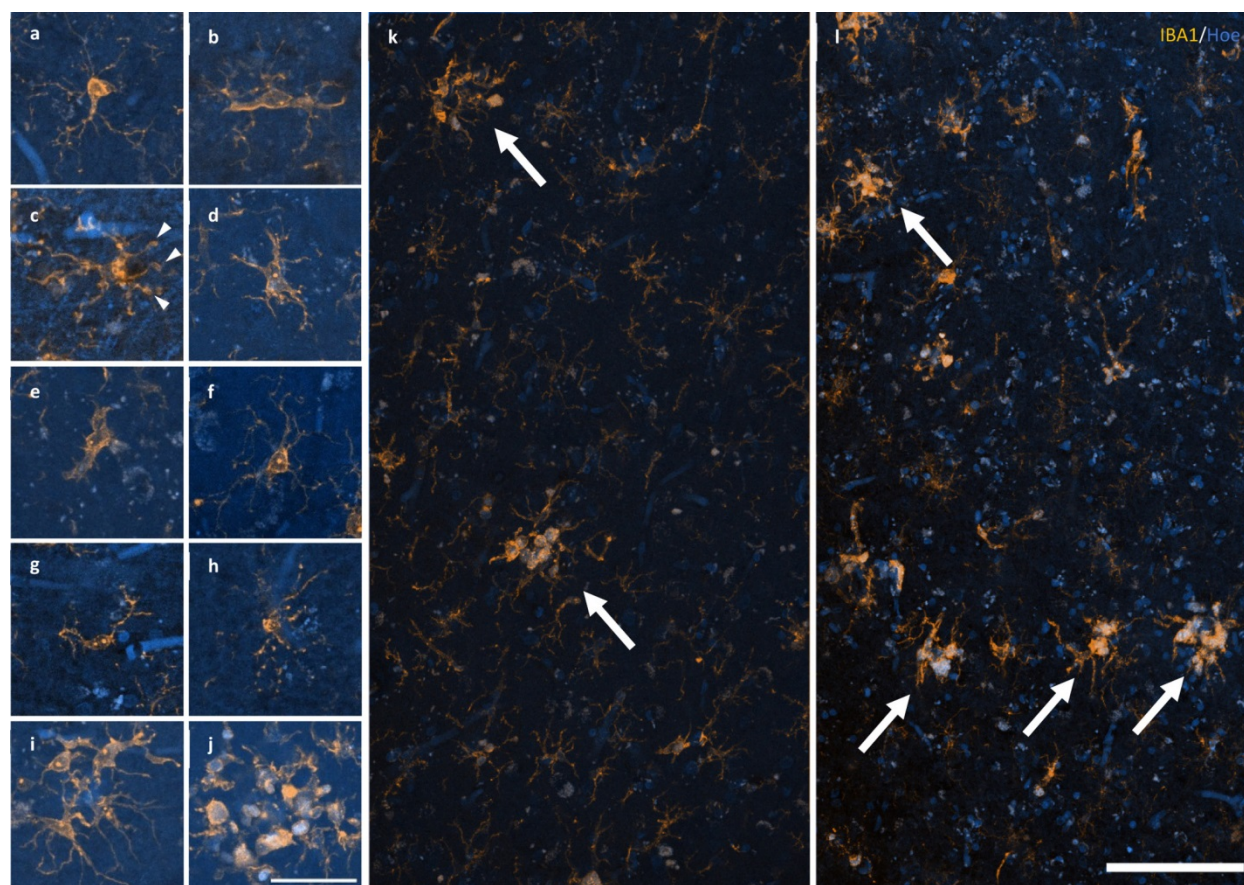


Figure 2 Response of microglia to AD pathology. **a–e** A spectrum of microglial activation can be identified by a series of morphological changes including an enrichment of IBA1 labelling of the soma and primary processes (**a**), hypertrophy of the primary processes (**b**), retraction of tertiary processes ± the formation of morphological features consistent with phagosomes (arrow heads) (**c**), further retraction of secondary processes (**d**), until amoeboid in shape (**e**). **f–h** Healthy ramified microglia have a small, spherical soma and thin, evenly distributed processes (**f**), contrasting with dystrophic microglia that have either deramified and tortuous processes (**g**) or pseudo-fragmentation of processes when marked with IBA1 (**h**). **i–j** Microglia that form a cluster within the boundary of an Aβ plaque may be either dystrophic or have reached a phase of early (**i**) or late/amoeboid (**j**) activation. **k–l** Mosaics of IBA1 staining demonstrating the size and distribution of microglial clusters (arrows), defined as three or more somata occurring within, or touch the boundaries of, a 20 μm² virtual graticule subregion, in the PMC of an HPC (**k**; M23) and AD case (**l**; M13). Scale bar in **j** = 40 μm (**a–j**); in **l** = 100 μm (**k–l**)

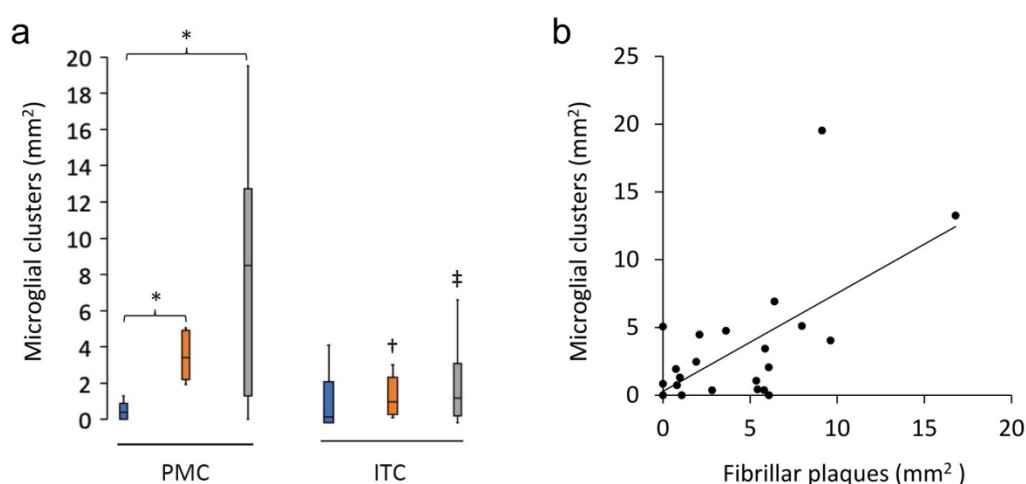


Figure 3 Characteristics of microglial clustering in the PMC. **a** The density of microglial clusters was significantly greater in the PMC of HPCs and AD cases compared to controls. **b** Microglial clusters were more frequently associated with fibrillar neuritic plaques in a combined group analysis; Spearman $\rho = 0.54$, $p = 0.006$. [†]Significantly reduced compared to PMC of HPCs; [‡]Significantly reduced compared to PMC of AD cases. ^{***} $p < 0.05$.

Table 4. Quantification of the morphological subtypes of microglia in the primary motor cortex^a

	Control	HPC	AD	P-value ^b
Total microglia	177.4 ± 44.9	224.8 ± 67.1	195.1 ± 60.1	0.3
Ramified microglia	77.4 ± 47.3	78.3 ± 43.2	59.1 ± 27.8	0.6
Activated microglia	57 ± 31.5	96.4 ± 35.9	76.9 ± 40.9	0.1
Dystrophic microglia	43 ± 27.1	50.1 ± 26.9	59.2 ± 14.9	0.2
Microglial clusters	0.5 ± 0.5	3.5 ± 1.4	8.2 ± 6.7	0.01

^aCells/mm²; mean ± standard deviation.

^bANOVA results; see text for p-values of pairwise comparisons of microglial clusters.

A graded extent of neuritic tau pathology and clustering of microglia occurs within nascent Aβ plaques, with the persistence of dystrophic neurites and the loss of IBA1-immunoreactivity and Aβ-immunoreactivity occurring in established neuritic plaques

All of the Aβ plaques examined in the ITC, and a majority in the PMC, contained DNs. However, the extent of the accumulated neuritic tau pathology within each plaque was lower in the PMC (Fig. 4a) than the ITC of the same case (Fig. 4b). Both Aβ deposits and globular DNs were seen perivascularly (Fig. 4c), consistent with previous observations (39). The density of DNs was greatest in the ITC of AD cases (Fig. 4c), which also had the highest density of remnant plaques characterised by accumulations of DNs associated with weak or absent Aβ-immunoreactivity (Fig. 4d). In the ITC a diffuse lattice of elongated NTs occurred throughout the neuropil and independently of Aβ plaques (Fig. 4e). DNs appeared radially projecting from Aβ plaques (Fig. 4e) and showed either elongated or globular morphology (Fig. 5a). Hoechst dye marked cell nuclei around the periphery of Aβ plaques and also partly stained the fibrillar deposits of Aβ (Fig. 5a). Hoechst has previously been reported to stain Aβ plaques in transgenic mice (40). Immunofluorescent double-labelling showed no colocalisation of Aβ and Ttau (Fig. 5b).

Microglia cell processes exhibiting evidence of phagocytic activity are interspersed around the periphery and core of Aβ plaques

Microglia that occurred in proximity to diffuse, fibrillar, and cored plaques commonly displayed structures morphologically consistent with phagosomes on distal processes with enriched IBA1 im-

munolabelling that closely associated with the Aβ element in the periphery and core of plaques (Fig. 6a; Fig. 7a). As previously reported for the ITC, superior frontal gyrus, and primary visual cortex, the overall density of dystrophic microglia was inversely correlated with brain pH in the PMC ($r^2 = 0.3$, $p = 0.01$) (26). However, it was also noted that individual plaques with dense DNs, that were associated with weak or absent Aβ staining which were more abundant in the ITC, were associated with dystrophic microglia (Fig. 6b) rather than a cluster of activated microglia which more commonly occurred where the extent of DNs was not yet fully developed (Fig. 6c–d). Confocal views showed colocalisation of microglial cell processes with Aβ in AD (Fig. 7a–b), but no co-localisation with tau pathology (Fig. 7c–d).

Discussion

AD is a uniquely human disease with a long prodrome and has proved difficult to model. The combination of using different regions of post-mortem brain tissue from individuals with or without dementia and with variable amounts of AD-type pathology may allow the pathological sequence of events to be elucidated. For example, the level of disease severity could be ordered from lowest to highest as follows: PMC-controls < ITC-controls < PMC-HPC < ITC-HPC < PMC-AD < ITC-AD. In particular, regions such as the ITC in HPCs and the PMC in AD cases could harbour the pre-symptomatic targets required to therapeutically delay or prevent AD. Prior to using this model to understand the role of microglia in AD, a quantitative neuropathological analysis of the PMC was carried out to ensure that it met expectations for being a relatively unaffected region of the AD brain.

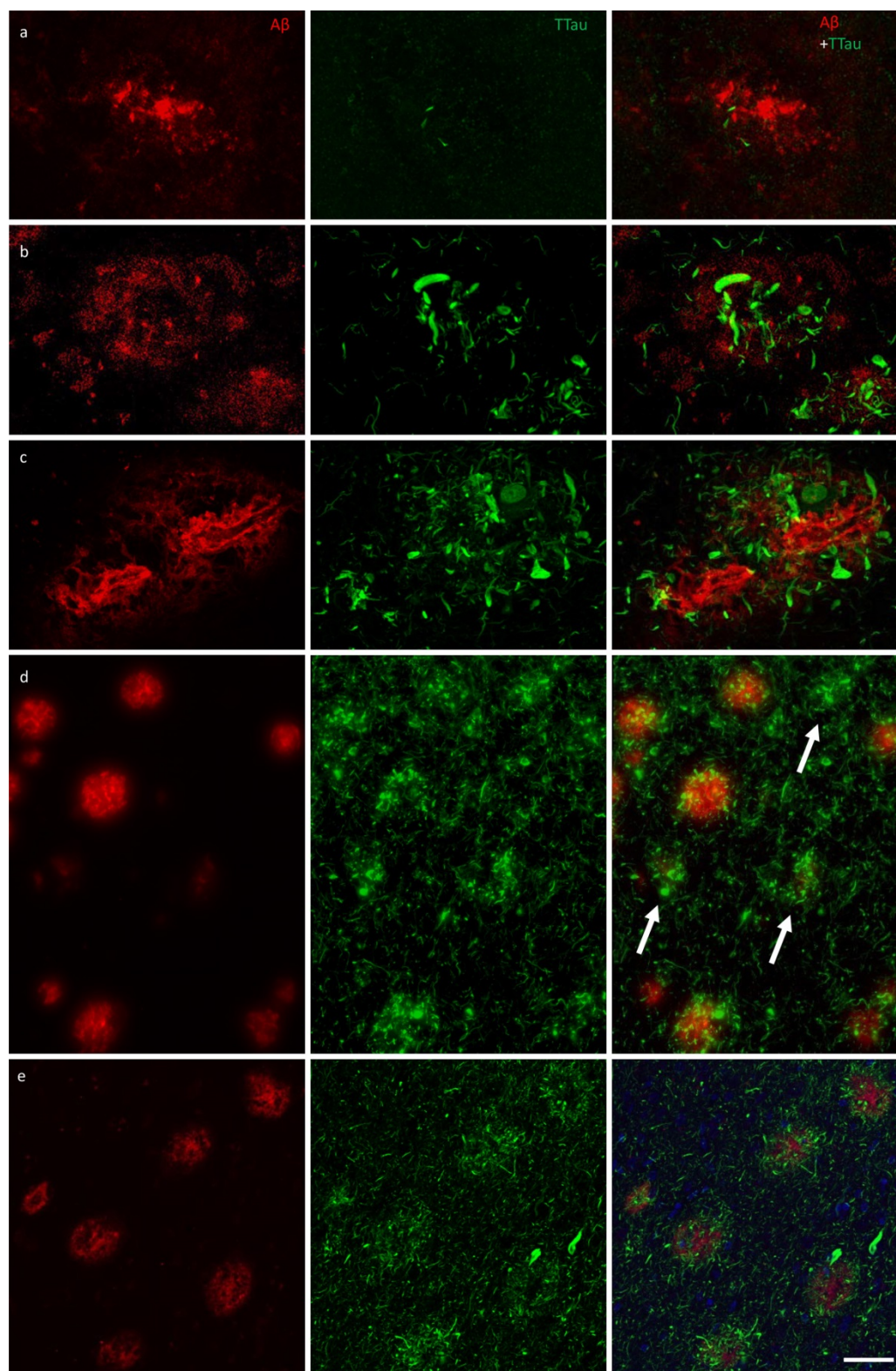


Figure 4 Immunofluorescent double-labelling for A β and Ttau. **a–c** The majority of A β plaques examined here were associated tau-positive dystrophic neurites, with a clear gradation visible between the PMc (**a**) and ITC (**b**) in controls (M01 pictured in **a** and **b**) and AD cases (ITC of M09 pictured in **c**). AD cases had the most extensive build-up of DNs in fibrillar and dense-cored plaques, as well as perivascular (capillary) A β deposits (**c**). **d** Remnant plaques (arrows) are characterised by absent or weak A β staining and dense accumulations of tau pathology and were much more common in the ITC than the PMc (also seen in **b**). **e** Severely affected regions of the AD brain, such as the ITC, showed a diffuse network of elongated NTs throughout the parenchyma as well radially projecting DNs. Scale bar = 20 μ m (**a–c**), 60 μ m (**d**), 40 μ m (**e**)

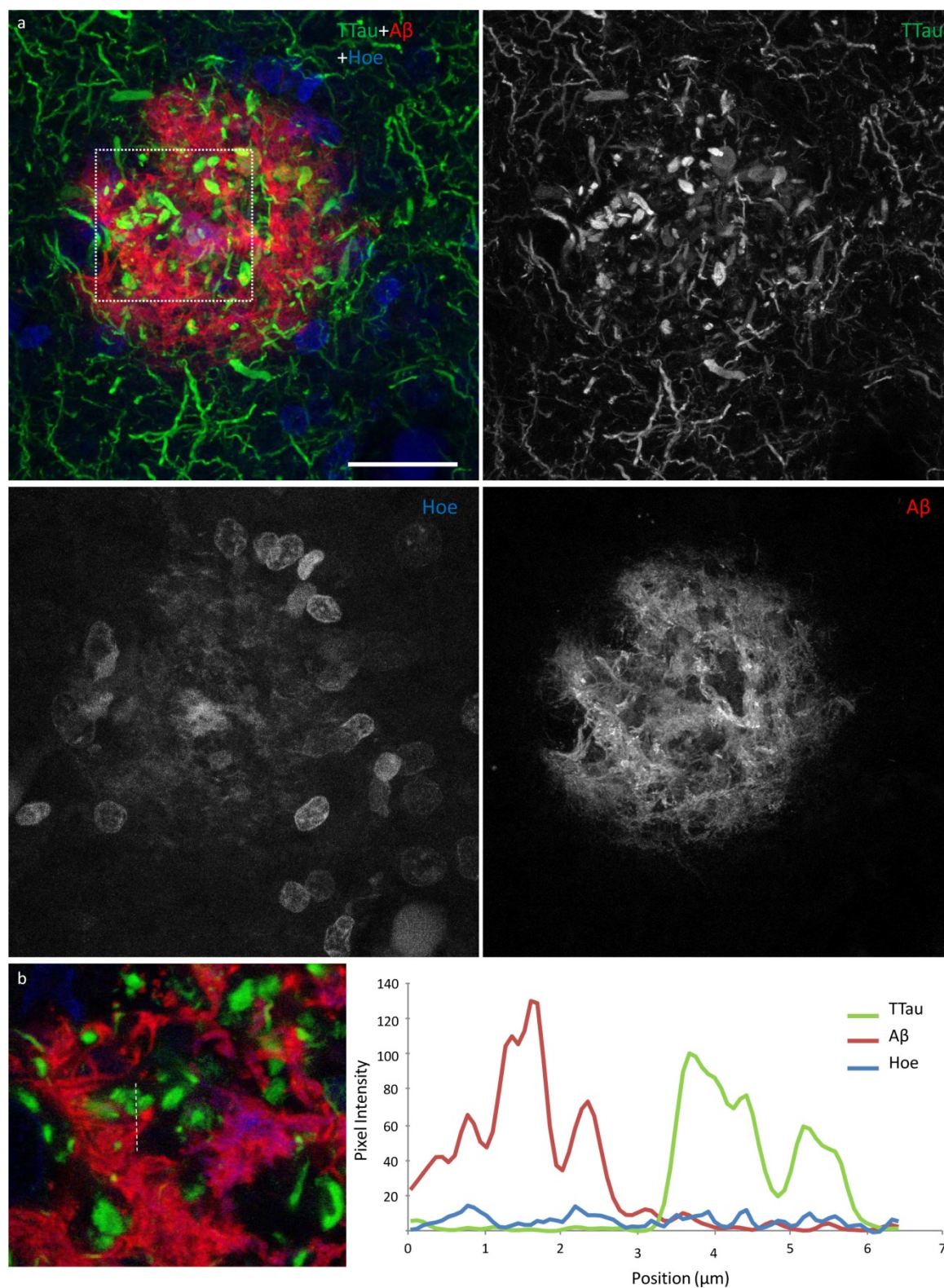


Figure 5 High power image of an Aβ plaque in AD. **a** Image panel showing a fibrillar neuritic plaque in an AD case (M03) with globular and threadlike DNs distributed throughout the plaque, which is also surrounded by a network of NTs (dotted box in merged image demonstrates ROI shown in **b**). Hoechst staining labelled cell nuclei around the periphery of the plaque as well as the fibrillar Aβ component inside the plaque. **b** Colocalisation study showed no coincidence Aβ and Ttau staining in any of the sections examined here (dotted line represents a 6.5 μm length along which pixel intensities have been compared in this exemplar ROI). Scale bar = 20 μm (**a**)

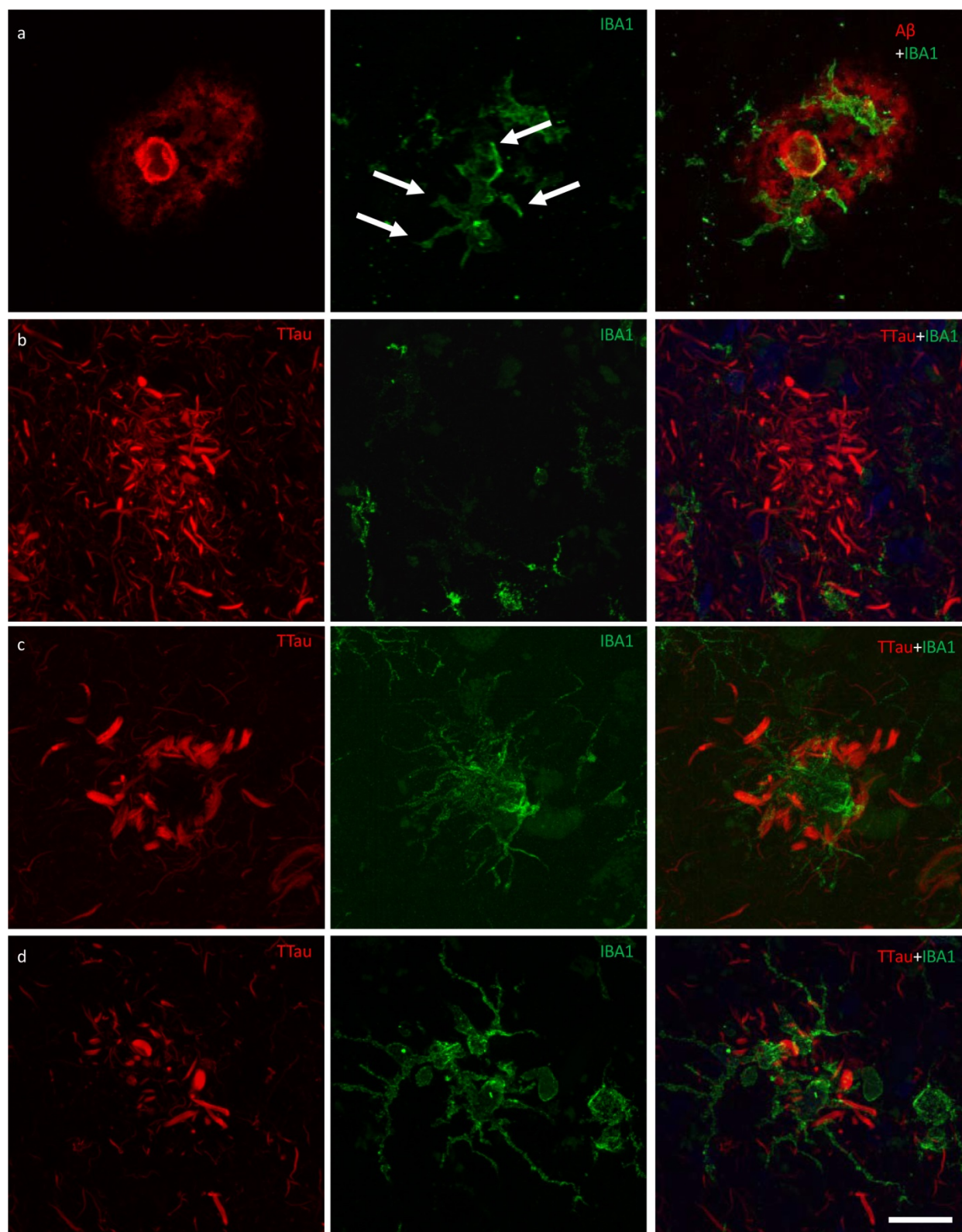


Figure 6 Responses of microglia to AD neuropathology. **a** The ITC of a control case (M01) demonstrating activated microglia with morphological features consistent with the formation of phagosomes (arrows) responding to peripheral and core elements of an A β plaque. **b** In the ITC of AD cases (M17 pictured), dystrophic microglia were more commonly associated with plaques that contained dense accumulations of dystrophic neurites, however the overall density of dystrophic microglia was inversely correlated with brain pH and not with AD. **c–d** Conversely, plaques with a lower density of dystrophic neurites were more commonly associated with a cluster of activated microglia (M01 pictured) in both the PMC (**c**) and ITC (**d**). Scale bar = 20 μ m (**a–d**)

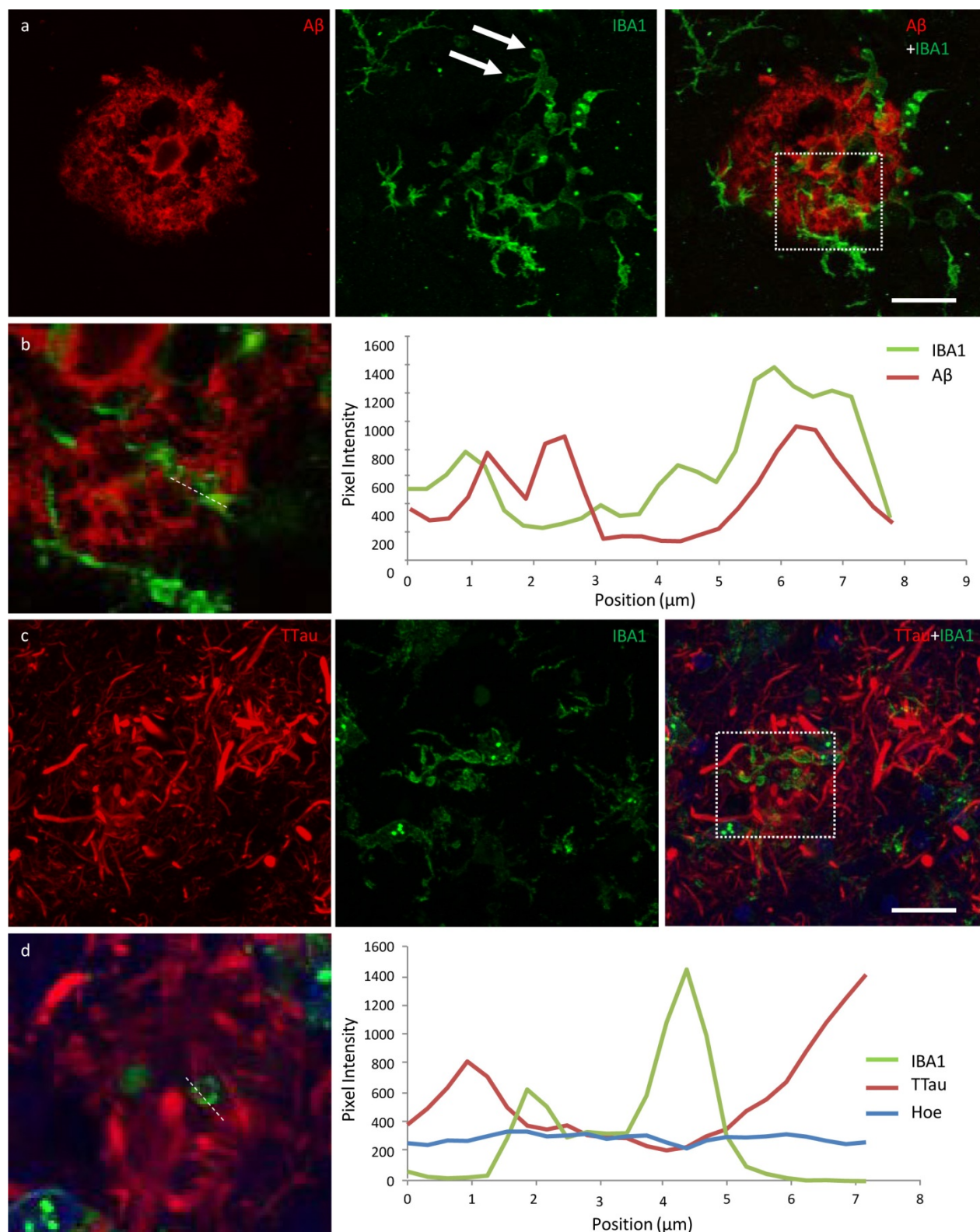


Figure 7 Exemplars from an investigation into the potential internalisation of Aβ and tau pathology by microglia. **a** Activated microglia in an Aβ plaque in the ITC of a control case with morphological features consistent with the formation of phagosomes (arrows) (M01; dotted box represents region of interest in **b**). **b** Coincidence of Aβ and IBA1 pixel intensities along a 7.8 μm length (dotted line) suggests potential internalisation of Aβ by microglia. **c** Activated microglia in close proximity to tau-positive DNs in the ITC of an AD case (M17; dotted box represents region of interest in **d**). **d** There was no evidence of the internalisation of tau pathology by microglia in any of the sections investigated here; exemplar shows Aβ and TTau staining intensities over a 7.2 μm length (dotted line). Scale bar 20 μm (**a**, **c**)

As expected, the PMC of AD cases had a significantly higher % A β , A β plaque count, % TTau, and NFT density compared controls. There were no NFTs observed in the PMC of controls and HPCs, which also had very similar levels of % TTau (which correlated with increasing age), but differed in their level of % A β . HPCs were defined according to standard neuropathological diagnostic criteria – having an intermediate ABC score (38). Incidentally, HPCs and AD cases (intermediate–high ABC scores) were similar in their A β load but differed in their tau levels in both regions. In contrast to the primary visual cortex previously investigated (26), the PMC in AD did have significantly reduced levels of A β and overall tau pathology, including NFTs as well evidenced elsewhere (41–46), compared to the ITC of the same cases. Overall there was no evidence of neurodegeneration in the PMC of AD cases, unlike the ITC, with cortical thickness, number of total neurons, and giant layer Vb pyramidal Betz cells remaining unchanged as expected (47, 48).

Examination of the microglial morphologies in the PMC using the previously validated modified disector sampling approach across all cortical laminae yielded no significant differences between controls, HPCs, and AD cases. However, group differences could be seen locally around AD-type pathology within the cortex with an increase in clustering of activated microglia in the PMC of HPCs compared to controls, and in the PMC compared to the ITC of AD cases. Moreover, a higher percentage of plaques contained clusters of microglia in HPCs than in AD cases and also a portion of microglia clusters that were not spatially associated with A β . The presence of a strong microglial clustering response in the PMC of AD cases and in the HPCs aligns with PET imaging studies demonstrating early activation of microglia in preclinical AD cases (49). Although the presence of clusters unrelated to A β pathology may be a non-specific observation, it is interesting to note that a previous animal study using a 5 \times FAD model also reported the presence of microgliosis prior to the formation of insoluble A β plaques (50), with another mouse model also indicating microglial activation in relation to synaptic dysfunction prior to A β deposition (51).

Here it is suggested that clusters of activated microglia in the PMC represent a neuroprotective

response correlating with the deposition of A β . We have demonstrated clusters of activated microglia that display phagocytic capabilities in the mildly affected PMC before the development of extensive tau pathology. It is conceivable that once the phagocytic potential of microglia is overwhelmed, a transition to a more neurotoxic proinflammatory phenotype occurs and that this represents a pivotal moment preceding tau-related neurofibrillary degeneration. Studies in mouse models of A β overexpression suggest proinflammatory microglia, which may be induced by the binding of oligomeric and fibrillar A β species to NLR Family Pyrin Domain Containing 3, Receptor for Advanced Glycation Endproducts, Scavenger receptors, and Toll-like receptors, among others (52–58), are associated with poorer cognitive and survival outcomes, have impaired phagocytic capabilities (59), and are capable of secreting an expansive complement of neurotoxic compounds including reactive oxygen species, nitric oxide, peroxynitrite, tumour necrosis factor α , interleukin 1 β , and prostaglandin-E2 (60). However A β -independent mechanisms of microglia activation or exhaustion in human AD cannot be excluded and require further research considering the so far limited efficacy of the pharmacological clearance of A β in clinical trials (61, 62).

Activated microglia tended to be associated with fibrillar NPs, and higher resolution confocal photomicrographs showed evidence of A β internalisation by microglia in both regions. The latter may explain the remnant plaques observed here (that contain weak or absent A β -immunolabelling; in which higher levels of A β were associated with activated microglia, but dystrophic microglia where A β -immunoreactivity was very minimal or absent, particularly where dystrophic neurites were extensive) and described elsewhere (14) and is potentially relevant to the proposed dynamic equilibrium between soluble A β oligomers and insoluble fibrils (63). However, it will be important to confirm the internalisation of A β by microglia with super resolution techniques such as direct stochastic optical reconstruction microscopy (dSTORM). In contrast, microglia did not specifically cluster around any of the three forms of tau pathology, NFTs, NTs and DN, nor did they appear to internalise tau in co-localisation studies, although processes of microglia were coincidentally found adjacent to DN. The

microglial clustering response dissipated over the modelled disease course with advanced stages, represented by the ITC of AD cases, being characterised by reduced IBA1 immunoreactivity, as reported elsewhere (31, 64). This suggests a process of microglial incapacitation in the context of increased tau load, a concept which is supported by a growing body of literature (65, 66). From these results it is hypothesised that the activation of microglia coincides with cortical A β deposition. Neuritic inclusions of tau in the cortex are evident early in the disease process, represented here by the PMC of AD cases, but mainly develop after the deposition A β and the activation of microglia.

This sequence of pathological changes is ostensibly consistent with the amyloid cascade hypothesis for AD pathogenesis (19) given the presence of elevated A β in the PMC of HPCs, however it should be stressed that the levels of A β and tau pathology were present at similar levels in the PMC of confirmed AD cases. Therefore it could be argued that insoluble A β and tau deposits begin forming concurrently in the cerebral cortex of AD brains. This would be consistent with those arguing in favour of the pathogenetic importance of tau deposition (22, 23, 67, 68) and the possibility that it in fact acts as a causative factor behind AD-related microglial activation (69). Certainly, animal models suggest that microglial activation augments tau pathology and specifically tau phosphorylation (70). This scenario would then be consistent with our observation that microglial activation wanes with increased tau deposition and with the idea that ageing impairs the housekeeping functions of microglia (71). Finally, even in the presence of extensive tau pathology, the increased presence of remnant plaques in the ITC suggests that microglia retain the ability to clear A β peptides.

Understanding the functional significance of these dynamic spatiotemporal changes in microglial activity along the time course of AD pathophysiology will be critical before new treatments targeting these cells can be imagined. Given that microglia of different brain regions display different activation states simultaneously depending on the graded extent of AD-type pathology present, the implementation of either anti- or pro-inflammatory microglia-based therapies would presumably be

beneficial in one brain region but detrimental in another. In future work the genetic characterisation of subjects investigated here may also provide further insight into how genotype affects individual susceptibility to differential microglial function, represented by the highly variable clustering response of microglia in HPCs and AD cases in particular. Overall, findings from the post-mortem model used here suggest that the clustering of activated microglia occurs concomitantly with the formation of A β plaques, and that tau-related neuritic degeneration follows these changes along with a loss of clustering.

Acknowledgements

The authors would like to thank the donors and their families for their kind gift. Brain tissue was received from the NSW Brain Tissue Resource Centre and Sydney Brain Bank. These brain banks are supported by the NHMRC of Australia, The University of New South Wales, Neuroscience Research Australia, and the National Institute of Alcohol Abuse and Alcoholism (NIH (NIAAA) R24AA012725). The authors also acknowledge the facilities used at The Bosch Institute and Microscopy Australia at the Australian Centre for Microscopy & Microanalysis both at The University of Sydney.

Data availability statement

The data that support the findings of this study are available from the corresponding author upon reasonable request.

References

1. Braak E, Braak H, Mandelkow EM. A sequence of cytoskeleton changes related to the formation of neurofibrillary tangles and neurofil threads. *Acta Neuropathol.* 1994;87(6):554-67.
2. Perry G, Kawai M, Tabaton M, Onorato M, Mulvihill P, Richey P, et al. Neurofil threads of Alzheimer's disease show a marked alteration of the normal cytoskeleton. *J Neurosci.* 1991;11(6):1748-55.
3. Barghorn S, Davies P, Mandelkow E. Tau paired helical filaments from Alzheimer's disease brain and assembled in vitro are based on beta-structure in the core domain. *Biochemistry.* 2004;43(6):1694-703.
4. Fitzpatrick AWP, Falcon B, He S, Murzin AG, Murshudov G, Garringer HJ, et al. Cryo-EM structures of tau filaments from Alzheimer's disease. *Nature.* 2017;547(7662):185-90.
5. Braak H, Braak E. Neuropathological staging of Alzheimer-related changes. *Acta Neuropathol.* 1991;82(4):239-59.
6. Franzmeier N, Neitzel J, Rubinski A, Smith R, Strandberg O, Ossenkoppele R, et al. Functional brain architecture is associated with the rate of tau accumulation in Alzheimer's disease. *Nat Commun.* 2020;11(1):347.
7. Nelson PT, Alafuzoff I, Bigio EH, Bouras C, Braak H, Cairns NJ, et al. Correlation of Alzheimer disease neuropathologic changes with cognitive status: a review of the literature. *J Neuropathol Exp Neurol.* 2012;71.
8. Arriagada PV, Growdon JH, Hedley-Whyte ET, Hyman BT. Neurofibrillary tangles but not senile plaques parallel duration and severity of Alzheimer's disease. *Neurology.* 1992;42(3 Pt 1):631-9.
9. Thal DR, Rub U, Orantes M, Braak H. Phases of A beta-deposition in the human brain and its relevance for the development of AD. *Neurology.* 2002;58(12):1791-800.
10. Serrano-Pozo A, Mielke ML, Gomez-Isla T, Betensky RA, Growdon JH, Frosch MP, et al. Reactive glia not only associates with plaques but also parallels tangles in Alzheimer's disease. *Am J Pathol.* 2011;179(3):1373-84.
11. Mirra SS, Heyman A, McKeel D, Sumi SM, Crain BJ, Brownlee LM, et al. The Consortium to Establish a Registry for Alzheimer's Disease (CERAD). Part II. Standardization of the neuropathologic assessment of Alzheimer's disease. *Neurology.* 1991;41(4):479-86.
12. Dickson TC, Vickers JC. The morphological phenotype of beta-amyloid plaques and associated neuritic changes in Alzheimer's disease. *Neuroscience.* 2001;105(1):99-107.
13. Yasuhara O, Kawamata T, Aimi Y, McGeer EG, McGeer PL. Two types of dystrophic neurites in senile plaques of Alzheimer disease and elderly non-demented cases. *Neurosci Lett.* 1994;171(1-2):73-6.
14. Oide T, Kinoshita T, Arima K. Regression stage senile plaques in the natural course of Alzheimer's disease. *Neuropathol Appl Neurobiol.* 2006;32(5):539-56.
15. Yu L, Petyuk VA, Tasaki S, Boyle PA, Gaiteri C, Schneider JA, et al. Association of Cortical beta-Amyloid Protein in the Absence of Insoluble Deposits With Alzheimer Disease. *JAMA Neurol.* 2019.
16. Lesne SE, Sherman MA, Grant M, Kuskowski M, Schneider JA, Bennett DA, et al. Brain amyloid-beta oligomers in ageing and Alzheimer's disease. *Brain.* 2013;136(Pt 5):1383-98.
17. Lue LF, Kuo YM, Roher AE, Brachova L, Shen Y, Sue L, et al. Soluble amyloid beta peptide concentration as a predictor of synaptic change in Alzheimer's disease. *Am J Pathol.* 1999;155(3):853-62.
18. McLean CA, Cherny RA, Fraser FW, Fuller SJ, Smith MJ, Beyreuther K, et al. Soluble pool of A beta amyloid as a determinant of severity of neurodegeneration in Alzheimer's disease. *Ann Neurol.* 1999;46(6):860-6.
19. Selkoe DJ, Hardy J. The amyloid hypothesis of Alzheimer's disease at 25 years. *EMBO Mol Med.* 2016;8(6):595-608.
20. Hardy J, Selkoe DJ. The amyloid hypothesis of Alzheimer's disease: progress and problems on the road to therapeutics. *Science.* 2002;297(5580):353-6.
21. Braak H, Del Tredici K. The pathological process underlying Alzheimer's disease in individuals under thirty. *Acta Neuropathol.* 2011;121(2):171-81.
22. Braak H, Thal DR, Ghebremedhin E, Del Tredici K. Stages of the pathologic process in Alzheimer disease: age categories from 1 to 100 years. *J Neuropathol Exp Neurol.* 2011;70(11):960-9.
23. Streit WJ, Braak H, Del Tredici K, Leyh J, Lier J, Khoshbouei H, et al. Microglial activation occurs late during preclinical Alzheimer's disease. *Glia.* 2018;66(12):2550-62.
24. Crary JF, Trojanowski JQ, Schneider JA, Abisambra JF, Abner EL, Alafuzoff I, et al. Primary age-related tauopathy (PART): a common pathology associated with human aging. *Acta Neuropathol.* 2014;128(6):755-66.
25. Kettenmann H, Hanisch UK, Noda M, Verkhratsky A. Physiology of microglia. *Physiol Rev.* 2011;91.
26. Paasila PJ, Davies DS, Kril JJ, Goldsbury C, Sutherland GT. The relationship between the morphological subtypes of microglia and Alzheimer's disease neuropathology. *Brain Pathol.* 2019.
27. Bachstetter AD, Van Eldik LJ, Schmitt FA, Neltner JH, Ighodaro ET, Webster SJ, et al. Disease-related microglia heterogeneity in the hippocampus of Alzheimer's disease, dementia with Lewy bodies, and hippocampal sclerosis of aging. *Acta Neuropathol Commun.* 2015;3:32.
28. Streit WJ, Walter SA, Pennell NA. Reactive microgliosis. *Prog Neurobiol.* 1999;57(6):563-81.
29. Streit WJ, Sammons NW, Kuhns AJ, Sparks DL. Dystrophic microglia in the aging human brain. *Glia.* 2004;45(2):208-12.
30. Streit WJ, Braak H, Xue QS, Bechmann I. Dystrophic (senescent) rather than activated microglial cells are associated with tau pathology and likely precede neurodegeneration in Alzheimer's disease. *Acta Neuropathol.* 2009;118(4):475-85.
31. Tischer J, Krueger M, Mueller W, Staszewski O, Prinz M, Streit WJ, et al. Inhomogeneous distribution of Iba-1 characterizes microglial pathology in Alzheimer's disease. *Glia.* 2016;64(9):1562-72.
32. Sanchez-Mejias E, Navarro V, Jimenez S, Sanchez-Mico M, Sanchez-Varo R, Nunez-Diaz C, et al. Soluble phospho-tau from Alzheimer's disease hippocampus drives microglial degeneration. *Acta Neuropathol.* 2016;132(6):897-916.
33. Walker DG, Tang TM, Mendsaikhana A, Tooyama I, Serrano GE, Sue LI, et al. Patterns of Expression of Purinergic Receptor P2RY12, a Putative Marker for Non-Activated Microglia, in Aged and Alzheimer's Disease Brains. *Int J Mol Sci.* 2020;21(2).
34. Davies DS, Ma J, Jegathees T, Goldsbury C. Microglia show altered morphology and reduced arborization in human brain during aging and Alzheimer's disease. *Brain Pathol.* 2017;27(6):795-808.
35. Sutherland GT, Sheedy D, Stevens J, McCrossin T, Smith CC, van Rooijen M, et al. The NSW brain tissue resource centre: Banking for alcohol and major neuropsychiatric disorders research. *Alcohol.* 2016;33-9.

36. Rahman T, Davies DS, Tannenberg RK, Fok S, Shepherd C, Dodd PR, et al. Cofilin rods and aggregates concur with tau pathology and the development of Alzheimer's disease. *J Alzheimers Dis*. 2014;42(4):1443-60.
37. Kril JJ, Halliday GM, Svoboda MD, Cartwright H. The cerebral cortex is damaged in chronic alcoholics. *Neuroscience*. 1997;79(4):983-98.
38. Montine TJ, Phelps CH, Beach TG, Bigio EH, Cairns NJ, Dickson DW, et al. National Institute on Aging-Alzheimer's Association guidelines for the neuropathologic assessment of Alzheimer's disease: a practical approach. *Acta Neuropathol*. 2012;123(1):1-11.
39. Hansra GK, Popov G, Banaczek PO, Vogiatzis M, Jegathees T, Goldsbury CE, et al. The neuritic plaque in Alzheimer's disease: Perivascular degeneration of neuronal processes. *Neurobiology of Aging*. 2019.
40. Uchida Y, Takahashi H. Rapid detection of A β deposits in APP transgenic mice by Hoechst 33342. *Neurosci Lett*. 2008;448(3):279-81.
41. Murray ME, Graff-Radford NR, Ross OA, Petersen RC, Duara R, Dickson DW. Neuropathologically defined subtypes of Alzheimer's disease with distinct clinical characteristics: a retrospective study. *Lancet Neurol*. 2011;10(9):785-96.
42. Arendt T, Bruckner MK, Gertz HJ, Marcova L. Cortical distribution of neurofibrillary tangles in Alzheimer's disease matches the pattern of neurons that retain their capacity of plastic remodelling in the adult brain. *Neuroscience*. 1998;83(4):991-1002.
43. Geula C, Mesulam MM, Saroff DM, Wu CK. Relationship between plaques, tangles, and loss of cortical cholinergic fibers in Alzheimer disease. *J Neuropathol Exp Neurol*. 1998;57(1):63-75.
44. Golaz J, Bouras C, Hof PR. Motor cortex involvement in presenile dementia: report of a case. *J Geriatr Psychiatry Neurol*. 1992;5(2):85-92.
45. Petersen C, Nolan AL, de Paula Franca Resende E, Miller Z, Ehrenberg AJ, Gorno-Tempini ML, et al. Alzheimer's disease clinical variants show distinct regional patterns of neurofibrillary tangle accumulation. *Acta Neuropathol*. 2019;138(4):597-612.
46. Suva D, Favre I, Kraftsik R, Esteban M, Lobrinus A, Miklossy J. Primary motor cortex involvement in Alzheimer disease. *J Neuropathol Exp Neurol*. 1999;58(11):1125-34.
47. Arnold SE, Hyman BT, Flory J, Damasio AR, Van Hoesen GW. The topographical and neuroanatomical distribution of neurofibrillary tangles and neuritic plaques in the cerebral cortex of patients with Alzheimer's disease. *Cereb Cortex*. 1991;1(1):103-16.
48. Genç B, Jara JH, Lagrimas AKB, Pytel P, Roos RP, Mesulam MM, et al. Apical dendrite degeneration, a novel cellular pathology for Betz cells in ALS. *Scientific reports*. 2017;7:41765-.
49. Shen Z, Bao X, Wang R. Clinical PET Imaging of Microglial Activation: Implications for Microglial Therapeutics in Alzheimer's Disease. *Front Aging Neurosci*. 2018;10:314-.
50. Boza-Serrano A, Yang Y, Paulus A, Deierborg T. Innate immune alterations are elicited in microglial cells before plaque deposition in the Alzheimer's disease mouse model 5xFAD. *Scientific Reports*. 2018;8(1):1550.
51. Hong S, Beja-Glasser VF, Nfonoyim BM, Frouin A, Li S, Ramakrishnan S, et al. Complement and microglia mediate early synapse loss in Alzheimer mouse models. *Science*. 2016;352(6286):712-6.
52. Cameron B, Tse W, Lamb R, Li X, Lamb BT, Landreth GE. Loss of Interleukin Receptor-Associated Kinase 4 Signaling Suppresses Amyloid Pathology and Alters Microglial Phenotype in a Mouse Model of Alzheimer's Disease. *The Journal of Neuroscience*. 2012;32(43):15112-23.
53. Halle A, Hornung V, Petzold GC, Stewart CR, Monks BG, Reinheckel T, et al. The NALP3 inflammasome is involved in the innate immune response to amyloid-beta. *Nat Immunol*. 2008;9(8):857-65.
54. Salminen A, Ojala J, Kauppinen A, Kaarniranta K, Suuronen T. Inflammation in Alzheimer's disease: amyloid-beta oligomers trigger innate immunity defence via pattern recognition receptors. *Prog Neurobiol*. 2009;87(3):181-94.
55. Heneka MT, Kummer MP, Stutz A, Delekate A, Schwartz S, Vieira-Saecker A, et al. NLRP3 is activated in Alzheimer's disease and contributes to pathology in APP/PS1 mice. *Nature*. 2013;493(7434):674-8.
56. Heneka MT, Golenbock DT, Latz E. Innate immunity in Alzheimer's disease. *Nat Immunol*. 2015;16(3):229-36.
57. Heneka MT, Kummer MP, Latz E. Innate immune activation in neurodegenerative disease. *Nat Rev Immunol*. 2014;14(7):463-77.
58. Hanisch U-K, Kettenmann H. Microglia: active sensor and versatile effector cells in the normal and pathologic brain. *Nat Neurosci*. 2007;10(11):1387-94.
59. Koenigsknecht-Talboo J, Landreth GE. Microglial phagocytosis induced by fibrillar beta-amyloid and IgGs are differentially regulated by proinflammatory cytokines. *J Neurosci*. 2005;25(36):8240-9.
60. Block ML, Zecca L, Hong JS. Microglia-mediated neurotoxicity: uncovering the molecular mechanisms. *Nat Rev Neurosci*. 2007;8(1):57-69.
61. Howard R, Liu KY. Questions EMERGE as Biogen claims aducanumab turnaround. *Nature Reviews Neurology*. 2020;16(2):63-4.
62. Cummings J, Lee G, Ritter A, Sabbagh M, Zhong K. Alzheimer's disease drug development pipeline: 2019. *Alzheimers Dement (N Y)*. 2019;5:272-93.
63. Wang ZX, Tan L, Liu J, Yu JT. The Essential Role of Soluble A β Oligomers in Alzheimer's Disease. *Mol Neurobiol*. 2016;53(3):1905-24.
64. Minett T, Classey J, Matthews FE, Fahrenhold M, Taga M, Brayne C, et al. Microglial immunophenotype in dementia with Alzheimer's pathology. *J Neuroinflammation*. 2016;13(1):135.
65. Streit WJ, Khoshbouei H, Bechmann I. Dystrophic microglia in late-onset Alzheimer's disease. *Glia*. 2020;68(4):845-54.
66. Navarro V, Sanchez-Mejias E, Jimenez S, Muñoz-Castro C, Sanchez-Varo R, Davila JC, et al. Microglia in Alzheimer's Disease: Activated, Dysfunctional or Degenerative. *Front Aging Neurosci*. 2018;10:140.
67. Iqbal K, Liu F, Gong CX, Alonso Adel C, Grundke-Iqbal I. Mechanisms of tau-induced neurodegeneration. *Acta Neuropathol*. 2009;118(1):53-69.
68. Grinberg LT, Rub U, Ferretti RE, Nitrini R, Farfel JM, Polichiso L, et al. The dorsal raphe nucleus shows phospho-tau neurofibrillary changes before the transentorhinal region in Alzheimer's disease. A precocious onset? *Neuropathol Appl Neurobiol*. 2009;35(4):406-16.
69. Felsky D, Roostaei T, Nho K, Risacher SL, Bradshaw EM, Petyuk V, et al. Neuropathological correlates and genetic architecture of microglial activation in elderly human brain. *Nature Communications*. 2019;10(1):409.
70. Ising C, Venegas C, Zhang S, Scheiblich H, Schmidt SV, Vieira-Saecker A, et al. NLRP3 inflammasome activation drives tau pathology. *Nature*. 2019;575(7784):669-73.
71. Vogels T, Murgoci AN, Hromadka T. Intersection of pathological tau and microglia at the synapse. *Acta neuropathologica communications*. 2019;7(1):109.

Chapter 4: Ground state depletion microscopy as a tool for studying microglia-synapse interactions

4.1 Preamble

This chapter presents a manuscript published by the Journal of Neuroscience Research. Chapters 2 demonstrated increased activation of microglia in PreAD and greater clustering of activated microglia in more mildly affected brain regions. Chapter 3 demonstrated that the activation of phagocytically active microglia occurs after the deposition of A β but before the formation of DNs in A β plaques. Here it was of interest to determine if phagocytic microglia internalise synapses in the context of PreAD and AD. It was hypothesised that microglia display increased phagocytosis of synapses during the symptomatic end-stage of the disease but not in PreAD—despite the latter having increased activated microglia. This was based on past pathological studies showing strong correlations between synaptic density and severity of symptoms. This was investigated using Iba1/Syp double IF-labelling and SMLM which allows for the super-resolution of individual fluorescent emitters. Syp-immunolabelling of pre-synapses was performed as optimisation trials suggested it was the most amenable of a number of different pre- and post-synaptic markers for use in archival brain tissue with extended fixation periods. Additionally, a previous meta-analysis also concluded that pre-synapses are more affected in AD than post-synapses as described earlier.

4.2 Authorship attribution statement

Chapter 4 of this thesis is published as ‘Ground state depletion microscopy as a tool for studying microglia-synapse interactions’ (Paasila et al., 2021). The manuscript was authored by Patrick J. Paasila, Sandra Y. Y. Fok, Neftali Flores-Rodriguez, Sujata Sajjan, Adam J. Svahn, Claude V. Dennis, R. M. Damian Holsinger, Jillian J. Kril, Thomas S. Becker, Richard B. Banati, Greg T. Sutherland, and Manuel B. Graeber (corresponding author). PJP co-designed the study, collected and analysed data, and wrote the manuscript. SYF collected and analysed data and wrote the manuscript. SS, AJS, CVD, NFR, RMDH, JJK, TSB, and RBB collected and analysed data. GTS collected and analysed data and wrote the manuscript. MBG designed the study, collected and analysed data, and wrote the manuscript. All authors contributed to editing the manuscript.

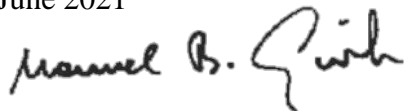
Attestation

In addition to the statement above, permission to include the published material has been granted by the corresponding author.

Patrick J. Paasila

Candidate

June 2021



Manuel B. Graeber

Corresponding author

June 2021

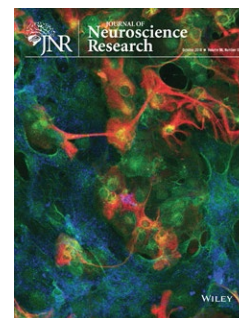
4.3 Published manuscript

The published manuscript begins on the next page.

TECHNICAL REPORT

Ground state depletion microscopy as a tool for studying microglia–synapse interactions

Patrick Jarmo Paasila¹ | Sandra Y. Y. Fok² | Neftali Flores-Rodriguez³ |
 Sujata Sajjan⁴ | Adam J. Svahn⁴ | Claude V. Dennis¹ |
 R. M. Damian Holsinger⁴ | Jillian J. Kril¹ | Thomas S. Becker⁴ |
 Richard B. Banati^{4,5} | Greg T. Sutherland¹ | Manuel B. Graeber⁴



¹Faculty of Medicine and Health, Charles Perkins Centre and School of Medical Sciences, The University of Sydney, Camperdown, NSW, Australia

²Biomedical Imaging Facility, Mark Wainwright Analytical Centre, University of New South Wales Sydney, Kensington, NSW, Australia

³Charles Perkins Centre, Sydney Microscopy and Microanalysis, The University of Sydney, Camperdown, NSW, Australia

⁴Faculty of Medicine and Health, Brain and Mind Centre, The University of Sydney, Camperdown, NSW, Australia

⁵Life Sciences, Australian Nuclear Science and Technology Organisation, Kirrawee, NSW, Australia

Correspondence

Manuel B. Graeber, Faculty of Medicine and Health, Brain and Mind Centre, The University of Sydney, 94 Mallett St., Camperdown, Sydney, NSW 2050, Australia. Email manuel.graeber@sydney.edu.au

Funding information

Faculty of Medicine and Health, The University of Sydney; Australian Research Council; National Institute of Alcohol Abuse and Alcoholism

Abstract

Ground state depletion followed by individual molecule return microscopy (GSDIM) has been used in the past to study the nanoscale distribution of protein co-localization in living cells. We now demonstrate the successful application of GSDIM to archival human brain tissue sections including from Alzheimer's disease cases as well as experimental tissue samples from mouse and zebrafish larvae. Presynaptic terminals and microglia and their cell processes were visualized at a resolution beyond diffraction-limited light microscopy, allowing clearer insights into their interactions *in situ*. The procedure described here offers time and cost savings compared to electron microscopy and opens the spectrum of molecular imaging using antibodies and super-resolution microscopy to the analysis of routine formalin-fixed paraffin sections of archival human brain. The investigation of microglia–synapse interactions in dementia will be of special interest in this context.

KEYWORDS

Alzheimer disease, ground state depletion followed by individual molecule return microscopy, microglia, post-mortem archival human brain tissue, super-resolution microscopy, synapses, zebrafish, RRID:AB_141874, RRID:AB_2199013, RRID:AB_2286948, RRID:AB_2534072, RRID:AB_2534076, RRID:AB_2535731, RRID:AB_2536183, RRID:AB_2633277, RRID:AB_324660, RRID:AB_839504, RRID:SCR_013726, RRID:SCR_001622, RRID:SCR_002285, RRID:SCR_002798, RRID:SCR_013673

1 | INTRODUCTION

Advances in microscopy research have facilitated the development of various techniques of super-resolution microscopy which overcome the diffraction limits of light that constrain confocal and two-photon

microscopy (Galbraith & Galbraith, 2011). Single molecule localization microscopy (SMLM) techniques perform two basic operations for image reconstruction: (a) the super-localization of single emitters within the nanometer range and (b) the active control of emitters to reduce the concentration of fluorescing molecules at any one time

Patrick Jarmo Paasila and S. Y. Y. Fok contributed equally.

Edited by Christopher Anderson and Junie Warrington. Reviewed by Eamonn Dickson, Bryan Heit, and Mike Jackson.

This is an open access article under the terms of the Creative Commons Attribution-NonCommercial-NoDerivs License, which permits use and distribution in any medium, provided the original work is properly cited, the use is non-commercial and no modifications or adaptations are made.

© 2021 The Authors. *Journal of Neuroscience Research* published by Wiley Periodicals LLC.

thus ensuring minimal overlap across a sequence of imaging frames. Single-molecule active control microscopy (SMACM) is a term applied to the various techniques whereby the active control of fluorescent molecules is achieved for the generation of pointillist images (Fölling et al., 2008; Schermelleh et al., 2010; Thompson et al., 2012).

Ground state depletion followed by individual molecule return microscopy (GSDIM) represents one such method of active control and is capable of achieving resolutions down to 20 nm in the lateral dimension (Bretschnneider et al., 2007; Hell, 2007; Moerner, 2012). This translates into an approximately 10-fold improvement over the power of resolution of conventional confocal methods. In conventional confocal microscopy, molecules are driven from the ground state into a singlet excited state followed by a dark triplet state that lasts on the order of milliseconds, a period which is too short to ensure a low enough density of active emitters required for SMACM (Thompson et al., 2012). In GSDIM, sufficiently high power is applied to molecules cycling through the standard energy levels in order to drive them into a longer-lived dark state which lasts on the order of seconds, thereby reducing the number of molecules returning to the ground state from which they can be activated once more (hence “ground state depletion”) and thus satisfying the conditions required for SMACM. The “blinking” events of single molecules that cycle through energy levels and stochastically return to their ground state with the emission of fluorescent light are recorded over time for image reconstruction (Fölling et al., 2008; Watanabe et al., 2014).

SMACM has been successfully used to study the nanoscale distribution of proteins and their co-localization, revealing molecular interactions that form part of biological processes in eukaryotic cells (Lalkens et al., 2012) and bacteria (Coltharp & Xiao, 2012). However, to date few studies have been performed on multicellular biological samples (Dani et al., 2010; Sigrist & Sabatini, 2012; Vaziri et al., 2008). In this study we present the results of the successful application of GSDIM to tissue from different species: frozen and formalin-fixed paraffin-embedded sections (mouse; human), as well as whole mounts of zebrafish larvae. Our focus is on human brain tissue and specifically the interaction of microglia and synapses in dementia.

Microglia originate from the yolk sac during early embryonic development (Ginhoux et al., 2013), although a small portion, derived from bone marrow precursors, enter the central nervous system (CNS) postnatally (Chen et al., 2010). Microglia in their normal state exhibit a ramified morphology with a territorial coverage of 30%–40% on average in the human cortical parenchyma (Paasila et al., 2019). Microglia are not part of the glial syncytium—they lack gap junctions and thus electrophysiological coupling between individual cells (Eugenín et al., 2001; Wasseff & Scherer, 2014). Microglia are the resident tissue macrophages of the CNS and act as sensors of pathology (Kreutzberg, 1996). However, this is not their most important function because they do not display a macrophage phenotype in healthy normal brain (diseases are exceptional states and not the norm). Maintenance of synaptic integrity appears to be their normal function (Graeber, 2010). Microglia are dynamic cells whose processes are continuously in motion, monitoring their local microenvironment (Nimmerjahn et al., 2005), and intermittently contact neighboring synapses (Nimmerjahn et al., 2005; Schafer et al., 2013;

Significance

We present the use of super-resolution microscopy to detect the internalization of presynaptic material by microglia in the brain of different species *in situ*. Here we demonstrate that the methodology can be applied to routine formalin-fixed paraffin-embedded archival sections of human brain allowing for the study of synapses at high resolution without the need for electron microscopy. Brain tissue from Alzheimer's disease cases and non-demented controls with or without Alzheimer's disease-type pathology are employed to demonstrate this powerful approach. The best studied model of post-traumatic synaptic plasticity, the rodent facial nucleus paradigm, is used for comparison and processes of mouse microglia surrounding axotomized motor neurons are shown to contain focal synaptophysin immunoreactivity. In addition, we illustrate that whole mounts of zebrafish larvae are amenable to the application of this technique. Importantly, we also show enhanced co-localization at a resolution of 20 nm/pixel demonstrating increased intracellular uptake of presynaptic material into microglia cell processes in Alzheimer's disease.

Wake et al., 2009). They respond rapidly to changes in their local environment and may also migrate to sites of tissue injury where they are capable of clearing cellular debris. Thus, microglia have a key role in CNS tissue maintenance and repair as well as in defense mechanisms and notably in inflammatory responses. Importantly, however, microglial activation is not synonymous with neuroinflammation (Svahn et al., 2014). The latter term is highly ambiguous (Graeber, 2014) and thus best avoided, a view also supported by the finding that microglial activation is independent of TSPO, the 18-kDa translocator protein situated on the outer mitochondrial membrane (Banati et al., 2014). In contrast, the normal role of microglia in the development of synaptic connections (synaptic pruning) (Paolicelli et al., 2011) and in the maintenance of synaptic integrity, their apparent normal function (Graeber, 2010) is increasingly appreciated (Ji et al., 2013; Lim et al., 2013; Miyamoto et al., 2013; Parkhurst et al., 2013; Tremblay et al., 2010; Wu et al., 2015; Zhan et al., 2014). Here we have used GSDIM to visualize interactions between microglia and synapses in physiological and pathological conditions.

2 | METHODS

2.1 | Sample preparation

2.1.1 | Human tissue sections

Immunofluorescence staining

Following ethics approval from University of Sydney Human Research Ethics Committee (HREC #2019/531), seven micrometer

thick formalin-fixed paraffin-embedded sections of the superior frontal gyrus from four Alzheimer's disease cases (AD), four non-AD control brains, and three non-demented controls with Alzheimer's changes (Cac) that satisfied a Braak stage III or IV were obtained from the NSW Brain Tissue Resource Centre and mounted on glass coverslips (Table 1). One additional non-AD case where the tissue block was exposed to just 24 hr (hrs) fixation (non-AD PC 1) was supplied and is included here as a positive control for comparison to other archival sections examined here with variable fixation periods (Table 1). Blind ID numbers which were written on 6-well plates for free-floating sections were assigned to each section by the experimenter who remained blind to cases and controls until after completing image analysis. Preparation of human brain tissue was performed as previously published (Sutherland et al., 2016). Sections were dewaxed in three, 5-min washes in xylene, and rehydrated by washing for 5 min in 100%, 95%, 70%, and 50% ethanol. Sections underwent heat-induced epitope retrieval in 10 mM Tris/1 mM EDTA (pH 8.5) at 110°C for 30 min in a decloaking chamber (DC2002, BioCare medical, Concord, United States). Aldehyde-related fluorescence was quenched by washing sections twice for 5 min on ice in freshly prepared, effervescent 0.1% sodium borohydride diluted in 0.01 M (1×) PBS. Sections were subsequently washed five times for 5 min in 1× PBS containing 0.3% tween-20 (PBST; pH 7.4). Blocking was performed in 10% NGS (Cat# 16210-072, Thermo Fisher Scientific, Waltham, Massachusetts, United States) diluted in 1× PBST followed by primary antibody incubation (anti-ionized calcium-binding adaptor molecule 1 (Iba1), 1:1,000, Cat# 019-19471, FUJIFILM Wako Pure Chemical Corporation, Osaka, Japan, RRID:AB_839504; anti-synaptophysin (Synp), 1:200, Cat# M0776,

Dako, Denmark, RRID:AB_2199013), and secondary antibody incubation (1:500; Alexa Fluor (AF) 532 goat anti-rabbit, Cat# A32728, RRID:AB_2534076; Alexa Fluor 647 goat anti-mouse, Cat# A11009, RRID:AB_2633277; ThermoFisher Scientific), both in 1% NGS at 4°C overnight with gentle agitation. Sections were then washed five times for 5 min in 1× PBS. Previously, sections for GSDIM (imaged according to old gold-standard acquisition settings) were stained as described here but incubated in AF 647 (1:200, donkey anti-rabbit, Cat# A-31573, ThermoFisher Scientific, RRID:AB_2536183) and AF 568 (1:200; goat anti-mouse, Cat# A11004, ThermoFisher Scientific, RRID:AB_2534072) and quenched using 0.1% Sudan Black B (BDH Laboratory Chemical Group, United Kingdom) in 70% ethanol for 4 min, then stored in 1× PBS at 4°C until imaging. Further methodological information can be found in the Supporting Information Methods. Table 2 lists all antibodies used here.

2.1.2 | Brain tissue from mice

Mice were held in a secure licensed facility at the Australian Nuclear Science and Technology Organisation (ANSTO, Kirrawee DC NSW 2232, Australia; Licensing body, NSW Department of Primary Industries) in accordance with regulations set out by the Animal Care and Ethics Committee (ACEC). Mice were housed in a temperature-controlled room which was maintained under a 12-hr light/dark cycle. The housing density of mice was 1–5 per cage, depending on behavior. Food and water were made available to the mice *ad libitum* as well as appropriate bedding and environmental enrichment (Supplier, Gordon's Specialty Stockfeed).

TABLE 1 Basic clinical data of human cases used in this study

Case	Age	Sex	Cause of death	ABC score ^a	Post-mortem Interval (hrs)	Fixation time (wks)	Brain pH
AD 1	83	F	Uremia	A3 B3 C2	3	265	5.9
AD 2	77	M	Aspiration pneumonia	A3 B3 C2	26	52	6.3
AD 3	85	F	Cardiorespiratory failure	A3 B3 C3	10	60	5.9
AD 4 ^b	78	F	Cardiac failure	A ^d B3 C ^d	6	3	6.6
Non-AD Control 1 ^c	59	M	Pulmonary emboli	A0 B0 C0	29	17	6.6
Non-AD Control 2	69	M	Atherosclerotic cardiac disease	A3 B1 C3	16	421	6.6
Non-AD Control 3	78	F	Pulmonary fibrosis	A0 B0 C0	11	339	6.3
Non-AD Control 4	74	F	Breast and liver cancer with bone metastases	A3 B1 C3	20	83	6.6
Cac 1	85	M	Colorectal cancer and severe cachexia	A2 B2 C3	9	265	6.6
Cac 2	87	F	Metastatic breast cancer	A2 B2 C0	5	148	6.4
Cac 3	102	F	Acute renal failure	A2 B2 C2	5	152	5.9
Non-AD PC 1	94	F	Cardiorespiratory arrest	^d	43	24 (hr)	^d

^aAccording to the National Institute on Aging-Alzheimer's Association guidelines (Hyman et al., 2012; Montine et al., 2012).

^bExcluded from the Iba1/Syp co-localization study due to missing data and tissue availability.

^cExcluded from the Iba1/Syp co-localization study due to tissue availability.

^dData unavailable.

TABLE 2 List of antibodies

Name	Immunogen	Origin	Concentration
Anti-Ionized calcium binding adaptor molecule 1 (Iba1)	Synthetic peptide corresponding to the C-terminus of Iba1	Manufacturer: Wako Catalogue: 019-19471 RRID:AB_839504 Host species: Rabbit Target: Human Iba1 Type: Primary, polyclonal	1:1,000
Anti-Synaptophysin (Syp)	A recombinant protein fragment corresponding to the C-terminal cytoplasmic domain of human Syp	Manufacturer: Dako (now Agilent) Catalogue: M0776 RRID:AB_2199013 Host species: Mouse Target: Human Syp Type: Primary, monoclonal (SY38)	1:200
Anti-Syp	Synaptophysin presynaptic vesicles	Manufacturer: AbD Serotec (now Bio-Rad) Catalogue: 8479-0004 RRID:AB_2286948 Host species: Rabbit Target: Mouse Syp Type: Primary, monoclonal (SY38)	1:100
Anti-Cluster of differentiation 11b (Cd11b)	T cell enriched splenocytes from B10 mice	Manufacturer: AbD Serotec (now Bio-Rad) Catalogue: MCA74GA RRID:AB_324660 Host species: Rat Target: Mouse Cd11b Type: Primary, monoclonal (5C6)	1:100
Alexa Fluor 532	Structure: Whole antibody; gamma immunoglobins Heavy and Light chains	Manufacturer: ThermoFisher Scientific Catalogue: A-11009 RRID:AB_2534076 Host species: Goat Target: Anti-rabbit IgG Type: Secondary, polyclonal	1:500
Alexa Fluor 647	Structure: Whole antibody; gamma immunoglobins Heavy and Light chains	Manufacturer: ThermoFisher Scientific Catalogue: A32728 RRID:AB_2633277 Host species: Goat Target: Anti-mouse IgG Type: Secondary, polyclonal	1:500

(Continues)

TABLE 2 (Continued)

Name	Immunogen	Origin	Concentration
Alexa Fluor 568	Structure: Whole antibody; gamma immunoglobins Heavy and Light chains	Manufacturer: Molecular Probes, Invitrogen; now ThermoFisher Scientific Catalogue: A-11077 RRID:AB_141874 Host species: Goat Target: Anti-rat IgG Type: Secondary, polyclonal	1:200
Alexa Fluor 633	Structure: Whole antibody; gamma immunoglobins Heavy and Light chains	Manufacturer: Molecular Probes, Invitrogen; now ThermoFisher Scientific Catalogue: A-21070 RRID:AB_2535731 Host species: Goat Target: Anti-rabbit IgG Type: Secondary, polyclonal	1:200
Alexa Fluor 647	Structure: Whole antibody; gamma immunoglobins Heavy and Light chains	Manufacturer: Molecular Probes, Invitrogen; now ThermoFisher Scientific Catalogue: A-31573 RRID:AB_2536183 Host species: Donkey Target: Anti-rabbit IgG Type: Secondary, polyclonal	1:200
Alexa Fluor 568	Structure: Whole antibody; gamma immunoglobins Heavy and Light chains	Manufacturer: ThermoFisher Scientific Catalogue: A-11004 RRID:AB_2534072 Host species: Goat Target: Anti-mouse IgG Type: Secondary, polyclonal	1:200

Facial nerve axotomy was carried out in accordance with a surgical protocol approved by the University of Sydney Animal Ethics Committee (AEC 2013/5856). In brief, mice were anaesthetized using isoflurane and the right facial nerve transected at its exit from the stylomastoid foramen (for review see [Moran & Graeber, 2004]). After different survival times (Sajjan et al., 2014), the brain stem was removed, embedded in Tissue-Tek® O.C.T compound (Cat# IA018, ProSciTech, Kirwan, Queensland, Australia) and stored at -70°C until further processing. Sixteen micrometer thick coronal sections were cut on a Leica cryostat and collected on coverslips (ProSciTech). Coverslips were immersed in 3.7% methanol-stabilized formaldehyde in 1 × PBS followed by 2-min long incubations in cold acetone (50%, 100%, and 50%). For the reproduction experiment (Graeber et al., 1988) shown in Figure 1, a 1-year-old male mouse was sacrificed 3 days after the operation (Banati et al., 2014). Sections were incubated in a mixture of anti-CD11b (1:100, Cat# MCA74GA, AbD Serotec, Oxford, United Kingdom, RRID:AB_324660) and

anti-Syp antibodies (1:100, Cat# 8479-0004, AbD Serotec, RRID:AB_2286948) for 2 hr in a humidified chamber at room temperature. Sections were then rinsed twice in 1× PBS and a secondary antibody mixture (AF 568, Cat# A-11077, RRID:AB_141874; AF 633, Cat# A-11031, RRID:AB_2535731; Molecular Probes, Oregon, United States) was applied for 1 hr at room temperature. Finally, sections were rinsed twice in 1× PBS and stored at 4°C until imaged.

2.1.3 | Whole mounts of zebrafish larvae

Zebrafish larvae were maintained under optimal conditions (Westerfield, 2000) and in accordance with experimental protocols approved by the University of Sydney Animal Ethics Committee (AEC 2013/5591). Adult fish were housed in 4 L tanks maintained at 28.5°C on a 14/10 hr light/dark cycle with twice daily feeding of artemia and protein pellets. Larvae were obtained from natural

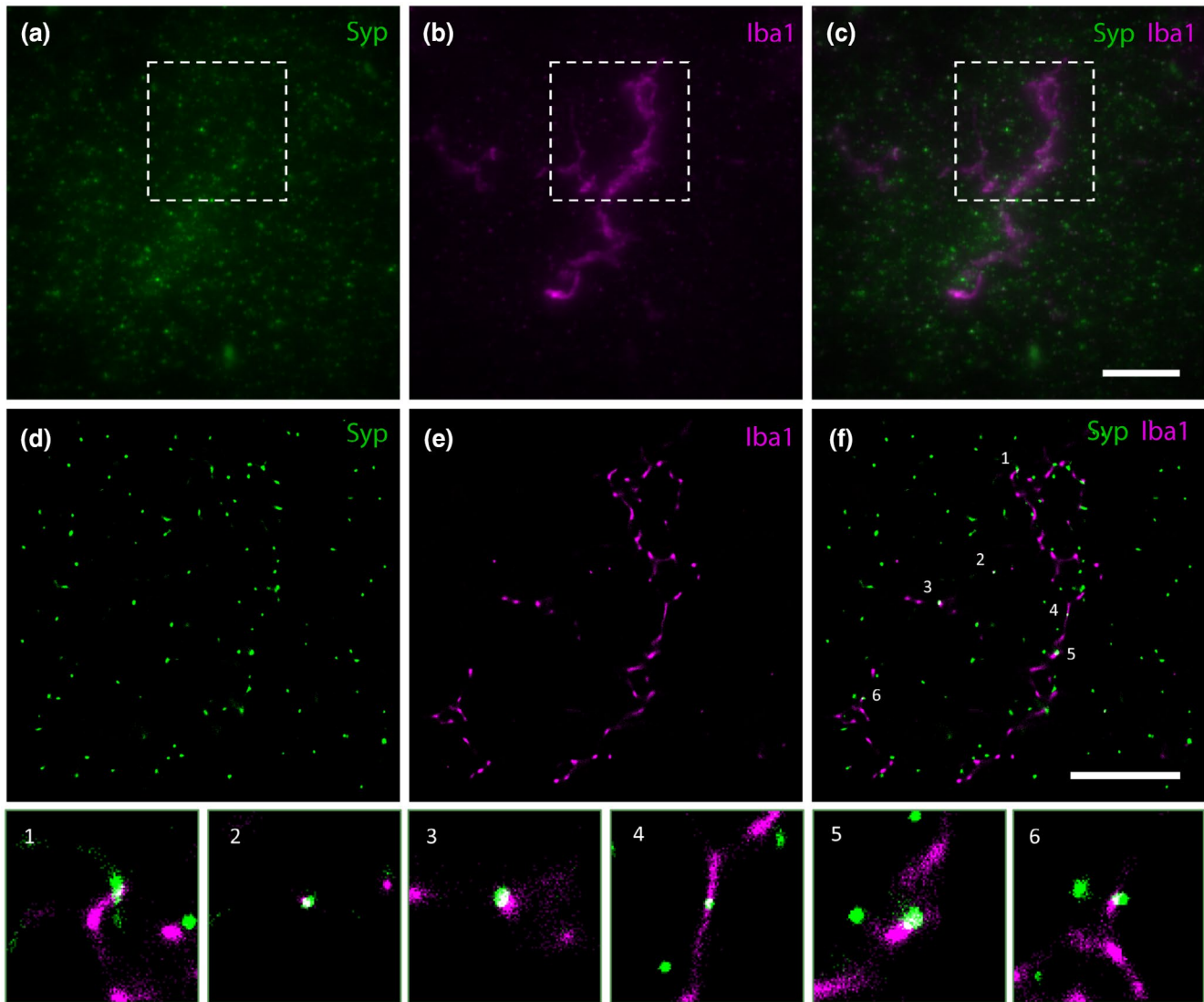


FIGURE 1 (a–c) Widefield epifluorescence images of (a) Syp-immunostaining of presynaptic boutons, (b) Iba1-immunostaining of a microglia profile, and (c) the composite image (case AD 1). Widefield images are shown as maximum intensity projections of 35 z-slices with a depth of 6.65 μm ; insets outline the fields of view corresponding to GSDIM reconstructions in the following row (d–f). (d–f) GSDIM reconstruction demonstrating the ability of the technique to display very high resolution images of (d) Syp-immunostaining, (e) Iba1-immunostaining, and (f) the composite image. The numbered spots in (f) highlight overlapping signal (white), that is, Syp-positive presynaptic material inside Iba1-positive microglial cell processes. Scale bar in c = 10 μm (a–c), in f = 5 μm (d–f)

crossing and eggs were maintained at 28.5°C in E3 medium on a 14/10 hr light/dark cycle. 0.005% 1-Phenyl-2-thiourea (PTU) was added to the E3 medium at 24 hr post-fertilization (pf) to prevent pigmentation. From 5 days pf larvae were fed with paramecia from a culture raised in the facility. Zebrafish sex is indeterminate at embryonic and early larval stages and therefore was not considered as a biological variable here.

For confocal studies, transgenic zebrafish lines expressing mpeg1:mCherry-CAAX were crossed with HCRT:Syp-eGFP resulting in larvae expressing both mpeg1:mCherry-CAAX and HCRT:Syp-eGFP. Larvae expressing both mCherry and eGFP were selected at 3 days pf. For GSDIM studies, transgenic zebrafish expressing mpeg1:eGFP were used 6 days pf. Larvae were euthanized and fixed

with 4% paraformaldehyde (pH 7.2) in 1× PBS at room temperature for 2.5 hr and rinsed/stored in 1× PBS at 4°C until use. A total of six larvae were included for GSDIM. Of these, photoswitching was successfully replicated in three.

2.2 | Imaging

2.2.1 | Confocal microscopy

Whole zebrafish larvae were embedded in 1% low melting point agarose. Confocal imaging was performed on a Zeiss LSM 710 confocal microscope using a W Plan-Apochromatic 20×/1.0 NA DIC objective

with 1 airy unit (AU). mCherry was excited with a 568 nm laser line and emission captured on a spectral detector from 570 to 700 nm.

2.2.2 | Ground state depletion followed by individual molecule return microscopy

Mouse and human sections collected onto coverslips were immunolabeled as described above and stored in 1× PBS until imaging. Prior to imaging, sections were first mounted onto “ultracleaned” glass coverslips (Cat# 0107032; 1.5H 18 mm × 18 mm high precision, ±5 µm tolerance; Marienfeld Superior, Lauda-Königshofen, Germany; refer to the Supporting Information Methods for coverslip preparation for GSDIM), and allowed to dry for 10 min before being mounted on depression slides (Cat# 1-6293, neoLab, Heidelberg, Germany) in 100 mM β-mercaptoethylamine (MEA; Sigma, Cat# 30070-10G; dissolved in 36 mM HCl, pH adjusted 8.5; aliquoted and stored at −80°C until imaging), and sealed with silicon glue, Twinsil® (Cat# 13001000, Picodent, Wipperfurth, Germany) or with Bondic® (preferred method; Bondic, Niagara Falls, New York, United States). GSDIM imaging was performed on a Leica SR 3D Ground State Depletion microscope with a Leica HCX PL APO 160×/1.43 NA CORR GSD objective (Leica Microsystems, Wetzlar, Germany). Drift and chromatic aberration are regularly checked on the GSDIM system used here (Sydney Microscopy and Microanalysis, The University of Sydney), and were also checked before and after experiments using 100 nm TetraSpeck™ microspheres (Cat# T7279, ThermoFisher Scientific) imaged using the 488, 532, and 642 nm laser lines. An additional test for drift was also performed using 40 nm FluoSpheres™ (Cat# F8789, ThermoFisher Scientific) and the 642 nm laser line (Supporting Information Methods).

Human brain

Image acquisition parameters were further optimized for imaging human AD archival tissue. For optimal results, the GSDIM system was turned on at least 1 hr before imaging. At least three regions of interest per case, selected at random within the cortical gray matter, were acquired using widefield epifluorescence and GSDIM. Widefield z-stacks (up to 7 µm z-depth) were acquired using the 160 × GSD objective described above and visualized as maximum intensity projections (z-step = 0.19 µm). For GSDIM, an exposure of 11.7 ms, EM gain of 200, and low laser power (2%, 532 nm channel; 4%, 647 nm channel) as for typical super-resolution imaging was used. No pumping or back-pumping was required. Images were acquired over 1 to 3 min, depending on the photo-switching characteristics observed during imaging; with the first 10–30 s being omitted in post-processing using LAS X to eliminate background autofluorescence. A detection threshold of 30 photons/pixel was used for visualization of all GSDIM reconstructions. 3D GSDIM images (0.77 µm z-depth) were also acquired using a cylindrical astigmatism lens and following calibration of the Leica GSD system using 80 nm gold beads using the LAS X software wizard. The Z-position

of single emitters was determined by taking advantage of the morphology of their astigmatic point spread function by comparing to known morphologies obtained using the gold beads. Internalization of Syp-positive presynaptic material by Iba1-immunolabeled microglia was confirmed by visualizing image reconstructions with orthogonal views for the XZ and YZ dimensions. Negative-primary antibody sections were prepared and viewed concomitantly. Refer to the Supporting Information Methods for further methodological information.

Co-localization study

Here a study was undertaken to investigate the co-localization of Syp- and Iba1-immunolabeling. Eight regions of interest sampled at random between cortical layers III and V from the available three AD cases (AD 1–3 in Table 1), three CAC (CAC 1–3), and three controls (Non-AD Controls 2–4) were acquired from each individual. GSDIM reconstructions were exported as.tif files with a dynamic range set to 0–10 gray values. The 532 and 647 nm channels were then separated and converted to a binary image. Corresponding color channels were then multiplied and filtered to remove “salt and pepper” noise using the “despeckle” algorithm in Fiji in order to find all co-localized positive pixels. Results were displayed as the average percentage of co-localized positive pixels of eight 18 µm² regions of interest per case. Image analysis was performed blinded using batch-processing in Fiji (National Institutes of Health, Bethesda, Maryland, United States, RRID:SCR_002285). LAS X was used to export all event lists (in.ascii format) to determine the full width at half maximum (FWHM) of structures of interest, photon counts, localization precision, and for co-cluster analysis.

Mouse and zebrafish

The focus drive on the Leica GSD system is limited to 200 µm. Therefore, in order to prepare whole mounts of zebrafish larvae for GSDIM imaging, a thin layer of head tissue was sliced off with a razor blade under a dissection microscope as the region of interest was slightly deeper than the focus depth of the objective; this also facilitated the diffusion of the MEA buffer into the tissue. The fish larva was then embedded in a drop of 1% low melting point agarose on a depression slide. Once the agarose had set, 100 mM MEA, pH 7.4 was added followed by cover slipping and sealing the sample with Twinsil®. eGFP was excited using a 488 nm laser (excitation bandpass filter 488/10, dichroic longpass mirror 496, and emission bandpass filter 555/100). AF 532 was excited using a 532 laser (excitation bandpass filter 532/10, dichroic longpass mirror 541, and emission bandpass filter 600/100). AF Fluor 647 was excited using a 642 nm laser (excitation bandpass filter 642/10, dichroic longpass mirror 649, and emission bandpass filter 710/100). For GSDIM acquisition, the respective area of interest was “pumped” in epifluorescence mode until molecules began blinking. Acquisition of photons representing molecules returning from the long-lived dark state was carried out in epifluorescence mode and reconstruction of the final GSDIM image was completed

using the Leica Application Suite X (LAS X; Leica Microsystems, RRID:SCR_013673).

2.3 | Statistics

For the aforementioned co-localization study, three AD cases, three CAC, and three controls were included as per tissue availability. Blinding was established by assigning each individual with a random alphanumeric identifier. Blinding was maintained until after statistical analyses had been completed. For the co-localization study, the data were expressed as the mean percentage (of eight regions of interest) of co-localized pixels per standard $18 \mu\text{m}^2$ (900 pixels^2) field of view per individual. Quantile–quantile (Q–Q) plots of each group were visualized and the normality was tested using the Shapiro–Wilk test. Equality of variances was tested using the Brown–Forsythe test. Group differences were tested by Welch's analysis of variance (ANOVA) (W) with Dunnett's T3 test for multiple comparisons. The mean and standard deviation (SD) were determined for each group and a post hoc power analysis to determine effect size (f) was performed using G*Power (F test, post hoc ANOVA: fixed effects, omnibus, one-way; RRID:SCR_013726). Groups were controlled for age, sex (which was not disaggregated due to the small group sizes), fixation time, post-mortem index, and brain pH. Spearman ρ was calculated to identify potential correlations between the percentage of co-localized Iba1/Syp pixels and the aforementioned factors. A p value < 0.05 was considered statistically significant. Statistical analyses and scatterplots were performed in GraphPad Prism (GraphPad Software; San Diego, California, United States, RRID:SCR_002798). Event lists (exported from LAS X as .ascii files) were handled using MATLAB (MathWorks, Natick, Massachusetts, United States, RRID:SCR_001622), which was also used to produce the line graphs of photon counts. Table 3 lists all software tools used here.

3 | RESULTS

3.1 | GSDIM as a tool to study the localization of synapses in archival sections of human cerebral cortex

Widefield epifluorescence images (Figure 1a–c) are presented alongside their respective super-resolved pointillist reconstructions

(Figure 1d–f), demonstrating the suitability of GSDIM as a tool for studying synapses at high resolution. FWHM of a representative structure of interest in widefield and GSDIM micrographs demonstrates the ability of the GSDIM system used here to achieve super-resolved images (Figure 2a–c). GSDIM reconstructions had a horizontal resolution of 20 nm/pixel and an axial resolution of 50 nm/pixel. Internalization of Syp-immunoreactive presynaptic material by Iba1-positive microglia was demonstrated in AD cortical samples using 3D GSDIM (Figure 3) (Supporting Information Movie 1 and 2 show the 3D GSDIM projection and the corresponding wide-field fluorescence image, respectively, of this region of interest). Images showing spurious co-localization in widefield and more certain co-localization in a GSDIM reconstruction of cortical tissue from a control case have also been provided for comparison (Figure 4). Additional images, including a positive-control section from tissue fixed for 24 hr (sample, Non-AD PC 1, Table 1) and TetraSpeck™ microsphere controls are provided in the Supporting Information (Figures S1–S4).

3.2 | Study of Iba1/Syp co-localization

Previously we have shown morphological changes in cortical microglia in AD and CAC post-mortem brain tissue (Paasila et al., 2019, 2020). Here it was of interest to investigate the potential of microglia to internalize pre-synaptic material in AD and CAC cases. AD cases ($n = 3$, mean percentage of co-localized pixels = $0.04\% \pm 0.006 \text{ SD}$) showed a higher level of Iba1/Syp signal co-localization compared to CAC ($n = 3$, mean = $0.006 \pm 0.0008 \text{ SD}$, $p = 0.02$) and controls ($n = 3$, mean = 0.006 ± 0.005 , $p = 0.006$; Welch's ANOVA: $n = 9$, $W(2.0, 2.8) = 36.1$, $p = 0.01$; effect size (f) = 0.8) (Figure 5). Groups did not differ by the percentage of area stained for Iba1 ($n = 9$, $W(2.0, 2.8) = 8.2$, $p = 0.1$) or Syp ($n = 9$, $W(2.0, 3.4) = 4.5$, $p = 0.1$). Plots of the number of localizations and photons for both the 532 and 647 nm channels in AD cases, CAC, controls, and background fluorescence can be found in Figure 6a,b. The summary statistics are also presented in Table 4. The frame correlation rate during image acquisition was between 0.25 and 0.5. Exclusion of the first 10–30 s of imaging for GSDIM reconstructions significantly reduced the level of background fluorescence. To further test the quality of reconstructions, a filtration step to exclude all localizations in 10 or more and 2 or more consecutive frames was applied. This resulted in a loss of ~11.1% and ~17.6% of localizations compared to the original reconstruction (which was generated without filtration of localizations occurring in consecutive frames), respectively. Importantly, the overall effect this had on the test reconstructions was minimal compared to the original reconstruction (Figure 7a–e).

The impact of blood vessel in co-localization analyses was negligible as they were not present in the 647 nm channel reconstructions (Figure S5; see also Figure 7 and Figure S4). Autofluorescence due to lipofuscin deposits displayed variable photoswitching characteristics depending on its signal intensity, with only low intensity deposits impacting reconstructions of both channels. Therefore, all

TABLE 3 List of software tools

Software	RRID
MATLAB	RRID: SCR_001622
Fiji	RRID: SCR_002285
G*Power	RRID: SCR_013726
GraphPad Prism	RRID: SCR_002798
Leica Application Suite X	RRID: SCR_013673

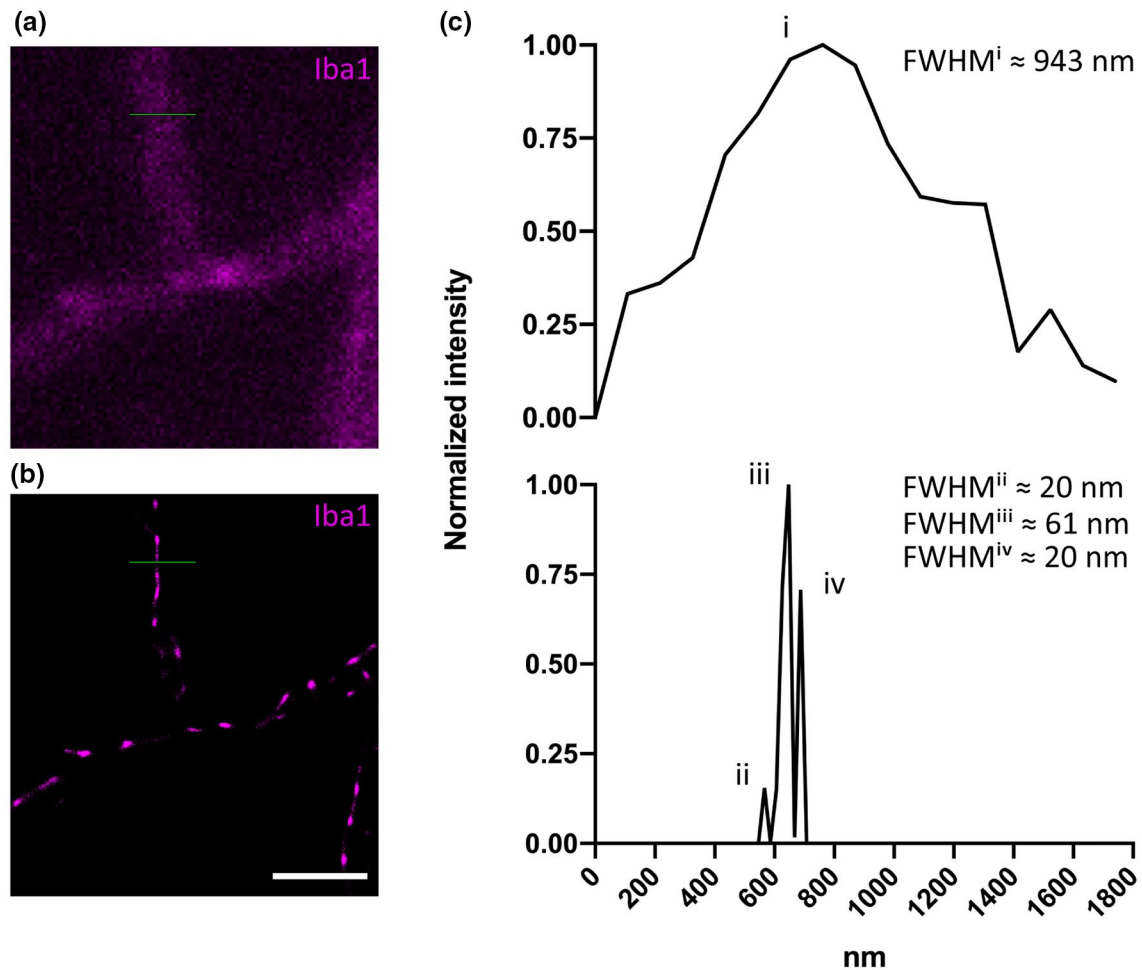


FIGURE 2 (a–b) A representative Iba1-positive (magenta) microglial cell with a typical perpendicularly branching cell process imaged in (a) widefield and (b) GSDIM mode, respectively. (c) Normalized pixel intensity values are plotted against the diameter of the cell process measured in nanometers as marked by the corresponding green line of interest in (a) and (b), respectively. Full width at half maximum (FWHM) of the single peak in the upper chart (marked “i”) corresponds to ~943 nm for the widefield image. FWHM of the first (“ii”), second (“iii”), and third (“iv”) peak corresponding to the GSDIM reconstruction in (b) is ~20, 61, and 20 nm, respectively. Scale bar = 2.5 μ m (a,b)

regions of interest imaged here were selected to exclude the presence of lipofuscin. Sudan Black B staining to block lipofuscin autofluorescence was not included here as it was found to significantly impair photoswitching of fluorophores which resulted in non-cycling noise during imaging and greater “smearing” in GSDIM reconstructions (Figure S6).

3.3 | Post-traumatic synaptic stripping in the rodent facial nucleus at super-resolution

GSDIM is less time consuming than conventional transmission electron microscopy (EM). Here GSDIM was employed to examine the mouse facial nucleus 3 days following axotomy to determine whether the technique is suitable for visualizing the involvement of microglial cells in synaptic stripping (Blinzinger & Kreutzberg, 1968). GSDIM revealed occasional microglia containing presynaptic material predominantly within their perineuronal cell processes (Figure 8,

insets). The frequency of this observation was in keeping with published EM results indicating that uptake of presynaptic material by microglial cells during synaptic stripping is not a readily discernible phenomenon.

3.4 | Whole mounts of zebrafish larvae are amenable to GSDIM

We further tested whether it was possible to perform GSDIM on whole mounts of transgenic zebrafish larvae. A zebrafish larva expressing mpeg1:eGFP in microglia was subjected to high laser power to induce the long-lived triple dark state and emitter blinking in MEA buffer. We observed that longer pumping times at lower laser intensity were more effective; it took on average 20 min for eGFP to start blinking. Figure 9a represents a GSDIM image reconstruction of a tectal microglia cell. The inset seen in Figure 9a shows an mpeg1-expressing microglial cell at confocal

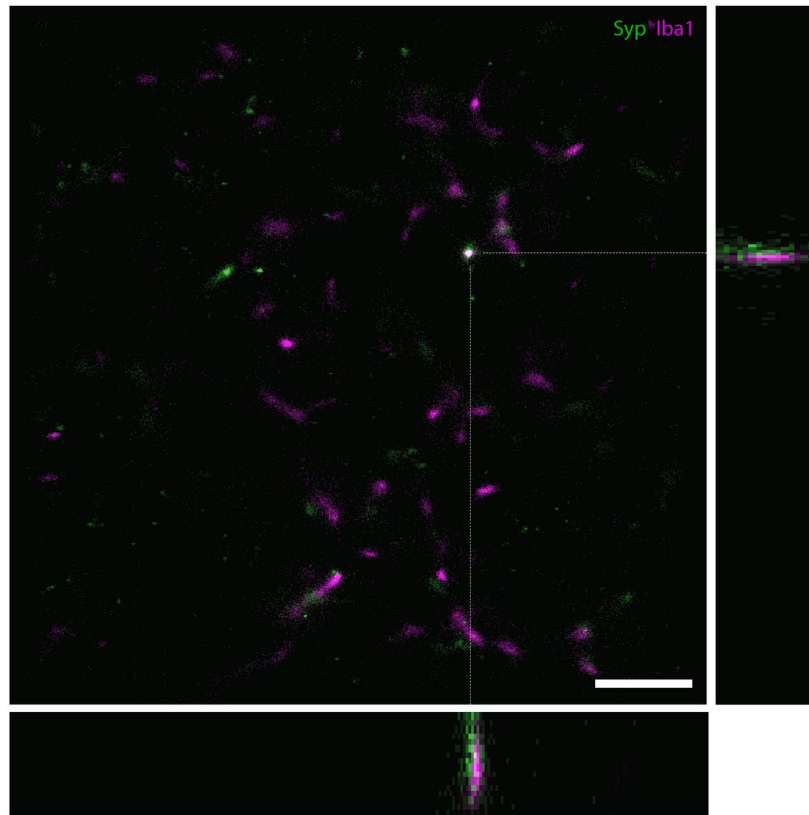


FIGURE 3 A 3D GSDIM reconstruction of part of a microglial cell from case AD 2 with a z-depth of 0.77 μm shown as a maximum intensity projection, with orthogonal views of the XZ and YZ dimensions on the bottom and left of the image, respectively. The orthogonal views have been magnified by 1.99 \times and cropped for better visualization (each view represents a space that is 0.77 μm in the Z-direction \times 5.17 μm in the X- and Y-direction, respectively). Scale bar = 2.5 μm (XY image only)

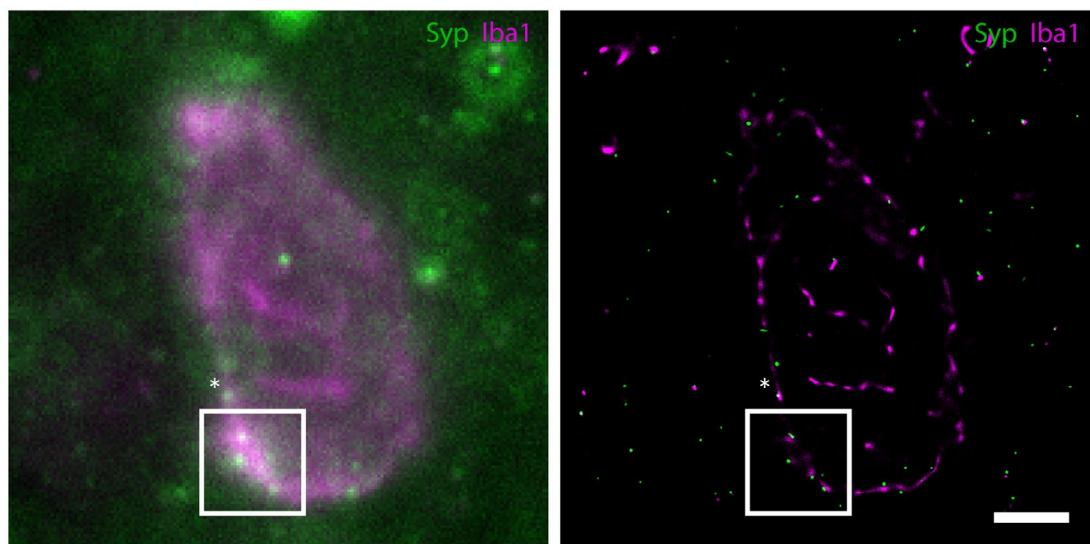


FIGURE 4 A widefield (left) and corresponding GSDIM reconstruction (right) demonstrating Iba1- (magenta) and Syp- (green) immunoreactivity in the dorsolateral prefrontal cortex of control human brain tissue (Non-AD Control 2). The areas marked by the asterisk (*) and within the white box in the widefield image indicate instances of potential co-localization of signals (white, merge color). The GSDIM reconstruction of the corresponding area (white box, right) better able resolves the Iba1- and Syp-positive signals, illustrating the need for GSDIM resolution. The area marked by the asterisk (*) in the GSDIM reconstruction represents an instance of true signal overlap (Syp inside a microglial process; white, merge color). Examples of overlap regions (white) in the GSDIM reconstruction are indicative of Iba1 and Syp molecules that are closer than 20 nm. Scale bar = 2.5 μm

resolution for comparison. Figure 9b–e illustrates selected areas at higher magnification of images captured with GSDIM compared to widefield fluorescence.

4 | DISCUSSION

The technical ability to visualize the spatial relationships of multiple proteins in tissues at super-resolution represents a major capability

in the field of microscopy. Applications for studying biological structure with super-resolution microscopy have grown considerably in the last few years (Birk, 2019; Fang et al., 2018; Garcia et al., 2017; Mockl et al., 2014; Schermelleh et al., 2019; Sieben et al., 2018; Sreedharan et al., 2017; Stracy & Kapanidis, 2017; Xu & Liu, 2019) and new advances in the field are predicted to improve our understanding as the potential of the technology is further realized. In the past, studies of microglia in brain tissue were typically conducted using immunocytochemistry in combination with brightfield, epifluorescence widefield, or confocal microscopy (Sarmiento, 2013). However, if more detailed information on cell-cell interactions was required, such as the precise spatial relationships between microglial processes and synaptic boutons, then tissue samples had to be processed for EM. With the invention of super-resolution microscopy, the diffraction limit imposed by conventional light microscopy no longer applies and biological structures can be viewed at a resolution closer to that offered by EM with essentially the same effort that is required for conventional confocal microscopy. Here we have demonstrated the use of GSDIM to show increased co-localization of Iba1-positive microglia and Syp-positive presynaptic material in AD compared to CAC and normal controls.

4.1 | Super-resolution imaging of formalin-fixed paraffin-embedded sections of human cerebral cortex

EM is the traditional method for obtaining ultrastructural information on brain tissue, but samples have to be perfusion-fixed ideally and dissected into small pieces measuring only 1–2 mm³. As a result, images may not be representative due to their small size, necessitating additional experiments. Post-fixation, embedding into plastic, ultrathin sectioning, and contrasting are all labor intensive, costly, and time consuming. Furthermore, while mouse and zebrafish tissue can be easily procured and processed for EM, fresh human tissue samples are much

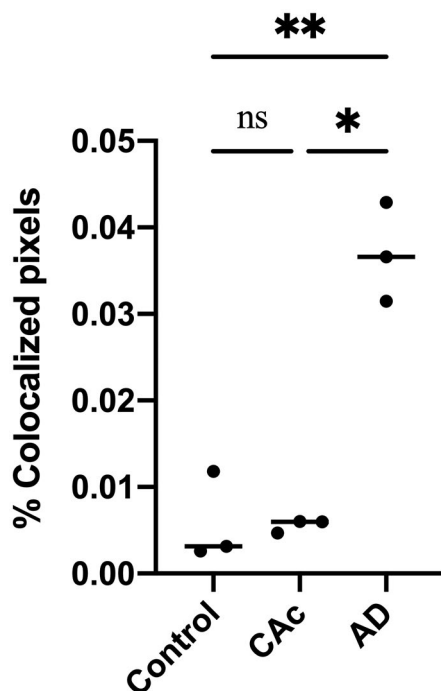


FIGURE 5 Scatterplot demonstrating an elevated average percentage of co-localized pixels per 18 μm^2 (900 pixels²) standard region of interest in AD compared to CAC and controls. * $p < 0.05$; ** $p < 0.01$; ns (not significant), $p > 0.99$

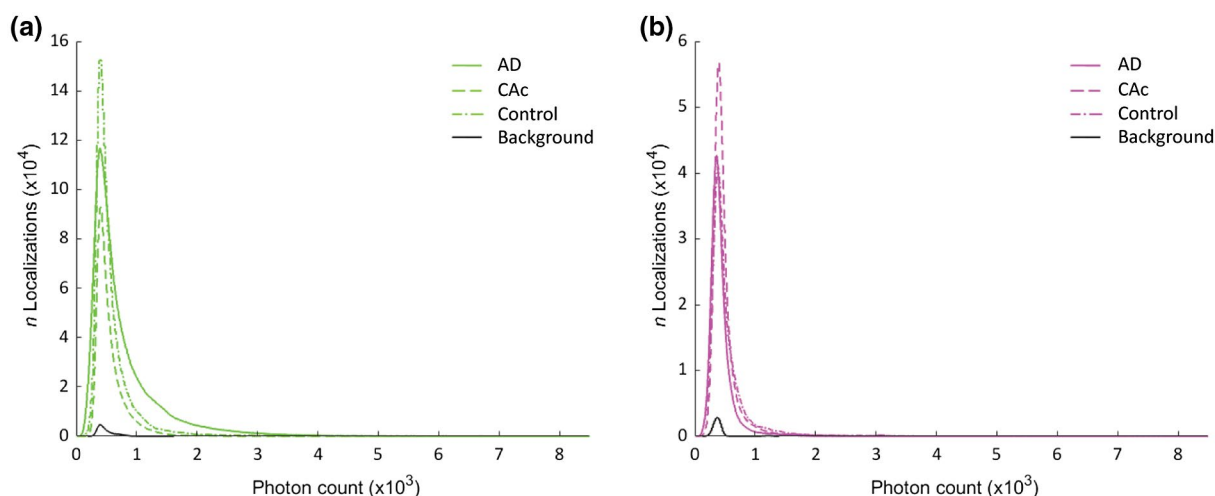


FIGURE 6 (a,b) Plots showing the number of localizations by photon count in both the (a) 647 nm (green) and (b) 532 nm (magenta) channels from Alzheimer's disease (AD) cases, Controls with Alzheimer's changes (CAC), normal controls, and background. Table 2 shows the summary statistics

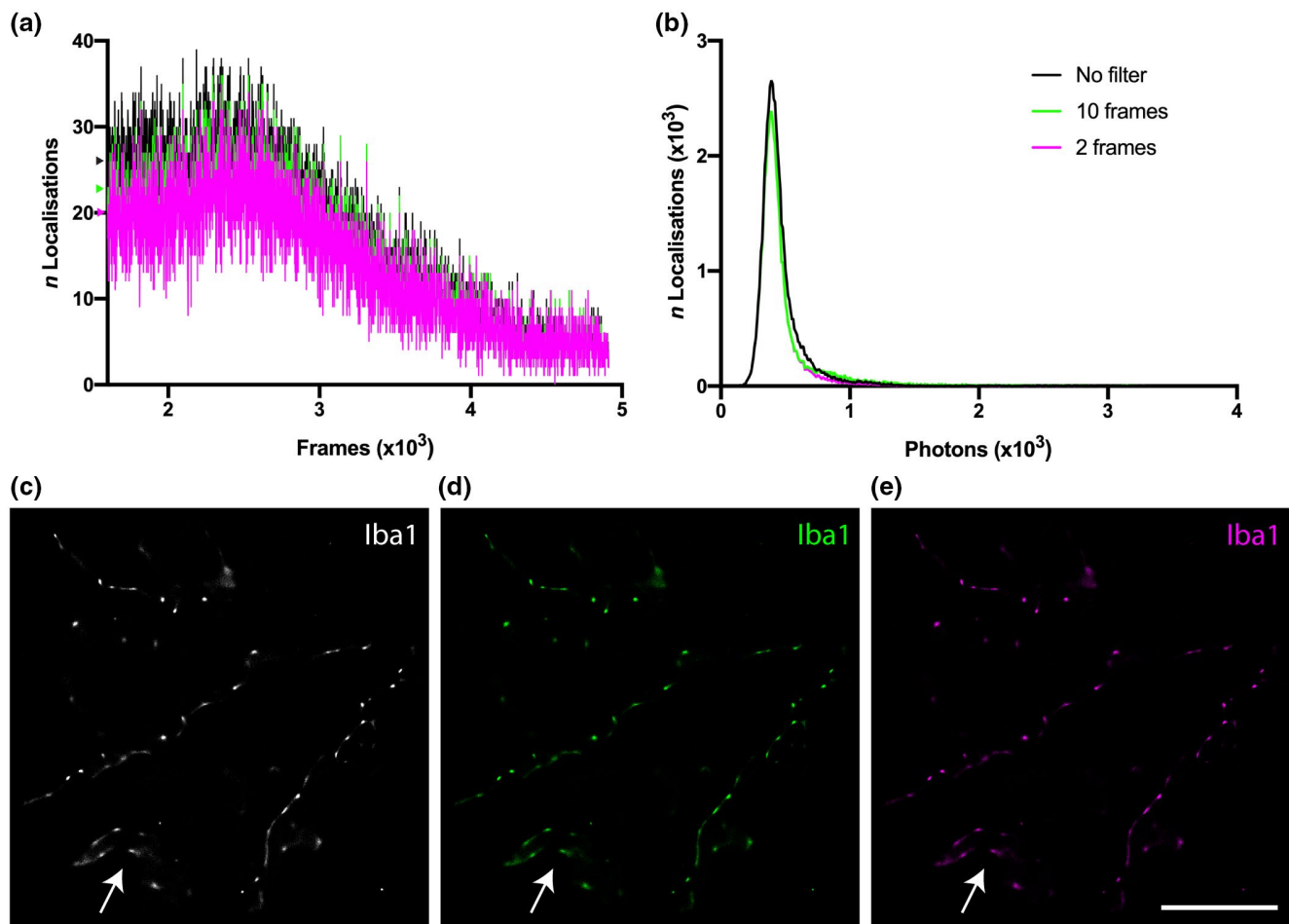


FIGURE 7 A test of the quality of GSDIM reconstructions from unfiltered data was performed in order to determine the impact of localizations that occurred through consecutive imaging frames. (a) “Blinking” events over several thousand frames in unfiltered data (black) and filtered data excluding localizations that occurred in 10 or more (green) and 2 or more (magenta) consecutive frames (the colored markers on the y axis show the shift in the average number of localizations in the first 2×10^3 frames for each filter group). (b) The total number of localizations in the unfiltered data set was 55,006 (black), 48,913 after removing localizations occurring in 10 or more consecutive frames (green), and 45,347 after removing localizations in 2 or more consecutive frames (magenta). c–e GSDIM reconstructions of the respective event lists for (c) unfiltered data (white), and thresholds at (d) 10 (green) and (e) 2 (magenta) consecutive frames were not substantially different (arrow heads indicate Iba1-positive staining in a likely blood vessel—shown in each image). Scale bar = 5 μ m (c–e)

harder to obtain. However, archives of human brain tissue exist worldwide in neuropathology departments and brain banks in the form of collections of brain tissue retained in fixative and paraffin blocks left over from routine diagnostic procedures. This is of relevance as extended storage in aldehyde fixatives reduces the suitability of CNS tissue for EM (Liu & Schumann, 2014). Therefore, being able to perform GSDIM on routine human paraffin sections opens up new avenues for research. In particular, the approach described in this paper enables the spectrum of molecular imaging methods using antibodies and super-resolution microscopy to be used for high-throughput analyses of common brain diseases and at cheaper cost compared to EM even if tissue has been stored for several years.

Microglia–synaptic interactions in physiological and diseased states are increasingly appreciated. A preprint of one study using confocal microscopy demonstrated increased co-localization of the endosomal/

lysosomal marker CD68, expressed by myeloid cells including microglia, and the presynaptic marker synapsin-I in post-mortem human tissue (Tzioras et al., 2019). Here we have used GSDIM to demonstrate increased co-localization of presynaptic material by microglia in post-mortem human AD tissue compared to healthy controls and other non-demented controls with high levels of AD-type pathology. It has long been known that neuronal loss exceeds the burden of neurofibrillary tangles in AD (Gomez-Isla et al., 1997), that microglia neuronal toxicity can be elicited in cell culture (Giulian et al., 1996), and that the loss of synapses best correlates with the severity of dementia (Terry et al., 1991), but there remains a paucity of evidence linking these observations in human studies. Here we show the direct involvement of microglia in synaptic loss in AD. Discontinuities in the Iba1-positive cellular processes, particularly in AD cases seen here (termed “pseudo-fragmentation”), has been previously noted (Paasila et al., 2019, 2020;

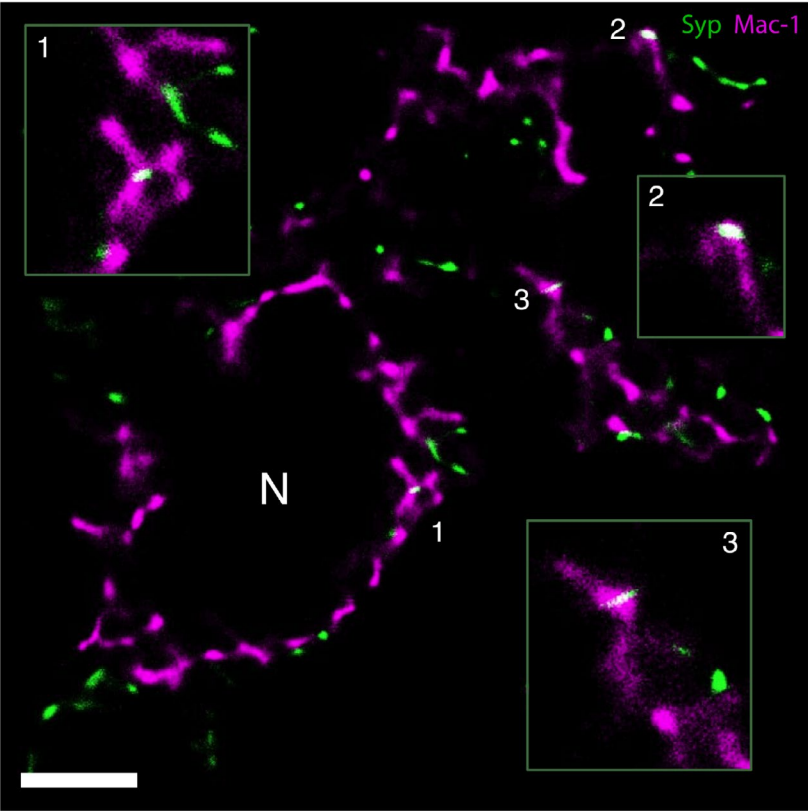


FIGURE 8 GSDIM demonstrates Syp-immunoreactive presynaptic material (green) inside perineuronal microglial processes (Mac-1, magenta) in the axotomized mouse facial nucleus 3 days following axotomy. Examples of stripped synapses (white, merge color) are magnified in the insets. Numbered regions represent the magnified areas in the insets. N marks a cross-sectioned motor neuron. Scale bar = 2.5 μ m

TABLE 4 Photon counts and total number of localizations

	AD (AF 532)	AD (AF 647)	CAC (AF 532)	CAC (AF 647)	Control (AF 532)	Control (AF 647)	Background (AF 532)	Background (AF 647)
Mean (n photons)	432.6940	777.1586	500.1218	566.3529	531.1901	635.8538	394.1738	491.7849
Median (n photons)	388.1000	569.5000	428.5000	480.2000	433.0000	478.3000	372.2000	449.6000
Minimum (n photons)	13.8000	18.5000	53.2000	58.9000	23.9000	32.9000	136.5000	190.7000
Maximum (n photons)	5,222.6000	8,065.3000	12,822.0000	15,146.6000	16,630.6000	14,520.4000	1,393.0000	1,610.9000
SD (n photons)	218.6298	616.6569	341.7096	332.1231	393.3020	675.1907	156.7882	153.1452
SEM	0.1465	0.2407	0.2856	0.1998	0.3478	0.4360	1.0304	0.4703
n localizations	2,226,894	6,562,200	1,431,497	2,762,082	1,278,972	2,398,669	23,153	106,033
n ROIs	24	24	24	24	24	24	5	5

Abbreviations: n, number of; ROIs, regions of interest; SEM, standard error of the mean.

Streit et al., 2009). In fact, such processes remain intact when visualizing cells with an additional marker as has been demonstrated in an EM investigation performed elsewhere (Tischer et al., 2016). Given a recent two-photon imaging study in mice showed that microglia work in concert with astrocytes to phagocytose neuronal apoptotic debris (Damisah et al., 2020) it will also be interesting to see in a larger cohort

of AD cases if a similar cooperative underpins physiological synaptic pruning and how this might also interact with a human life-span synaptome architecture (LSA) as described in mouse (Cizeron et al., 2020). Co-localization studies are commonly employed in biology in order to study spatial relationships between structures or molecules of interest. In broad terms, co-localization of signals can

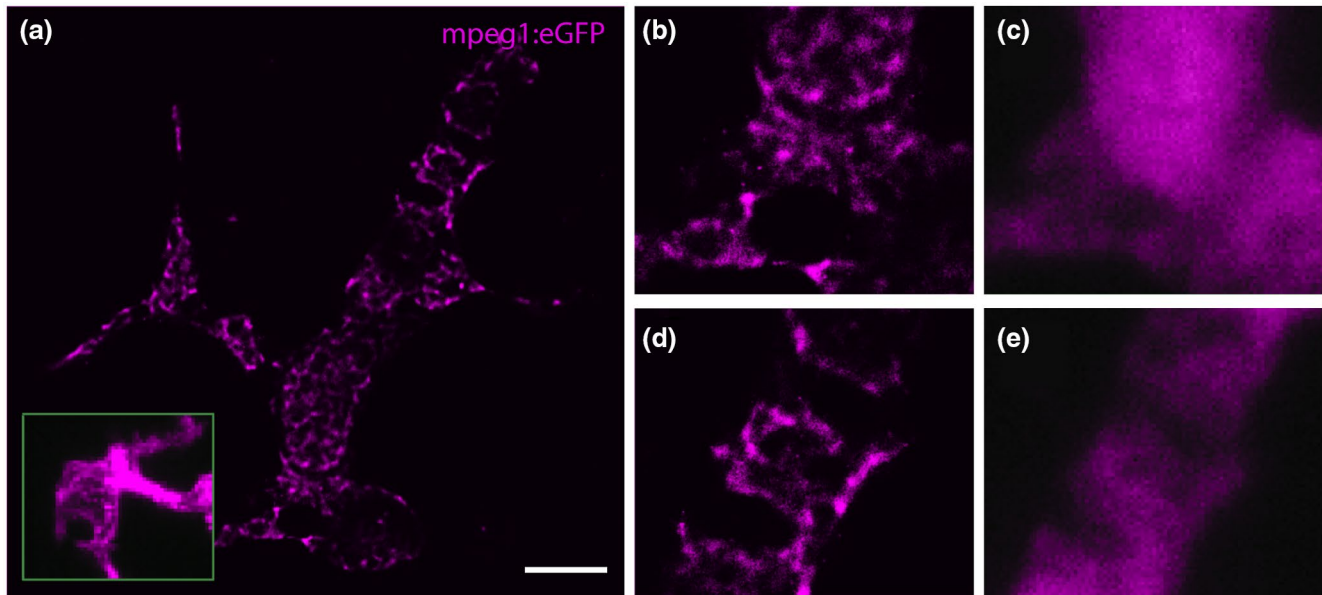


FIGURE 9 (a) GSDIM reveals the intracellular distribution of mpeg1:eGFP (magenta) in microglia in the optic tectum of a zebrafish larva. Inset in a shows an mpeg1:eGFP expressing microglial cell captured with confocal microscopy for comparison. (b,d) Magnified areas from a showing the intracellular distribution of eGFP with their widefield fluorescence images in (c) and (e), respectively. Scale bar = 5 μ m (a)

be investigated by pixel-based or object-based methods (Bolte & Cordelières, 2006). Pixel-based methods rely on finding correlations between signal intensities whereas object-based methods first segment images and then apply an overlap procedure. Here a simple object-based strategy was pursued to quantify the relative occurrence of Iba1/Syp co-localization (at a resolution of 20 nm/pixel) in AD, CAC, and normal aged brain. However, it is important to note that other advanced spatial interaction analyses for investigating co-localization also exist. Such strategies robustly account for accidental overlap, post-processing errors, and offer additional statistics-based inferences about spatial relationships between objects of interest (Helmuth et al., 2010). Software packages for these types of cluster analyses, such as Mosaic segmentation and Dual parameter Optimization in Histograms (QuASIMODOH) (Paparelli et al., 2016) and MosaicIA (Shivanandan et al., 2013), are freely available for use in image analysis software such as Fiji, but were outside the scope of this investigation. A recent review also covers many other plugins for processing and analyzing image data acquired from various imaging modalities for use in Fiji (Linde, 2019).

4.2 | GSDIM enables studies of pathological synaptic turnover

Peripheral axotomy of the rodent facial nerve leads to well-characterized changes in its central nucleus of origin. The extrinsic facial motor neurons respond to the loss of their distal axon by activating a cellular regeneration program (Moran & Graeber, 2004). Surrounding facial nucleus glial cells also become involved. Microglia respond by expressing the CR3 complement receptor within hours

of the axotomy (Graeber et al., 1988) and undergo mitotic cell division (Yamamoto et al., 2010) after a few days. Astrocytes upregulate their expression of the glial fibrillary acidic protein (GFAP) and reshape their cell processes. Accompanying the axonal reaction, microglial cells engage in a process known as “synaptic stripping” (Blinzinger & Kreutzberg, 1968; Graeber, 2010). This process has two components, an initial detachment of afferent axonal endings from the neuronal somatic membrane and dendrites, followed by the displacement of the detached terminals by microglial cells. It is the latter process followed by astroglial insulation of neurons (Graeber & Kreutzberg, 1988) that appears to be responsible for the long-lasting functional deficit observed in patients with Bell's palsy (Graeber et al., 1993). In functional terms, a facial nerve transection results in what equates to a structural and functional split of the face from the brain. Importantly, the fate of the large number of “stripped” axon terminals is not known in detail. Typical phagocytic macrophages are absent during the entire regeneration period although synaptic boutons have been seen being displaced and even engulfed by microglial processes at the EM level. However, systematic EM studies are costly and very time consuming and therefore specific EM studies to elucidate the fate of the stripped axon terminals have so far not been performed. It is assumed that retraction of afferent neurites plays a major role in the disappearance of free-lying axon boutons during post-traumatic synaptic plasticity in the axotomized rodent facial nucleus. This view is supported by the results of the present study, as the rather limited uptake of synaptic material by microglia in GSDIM is incompatible with large-scale phagocytosis.

A number of studies implicate microglia in synaptic remodeling, internalization, and plasticity in healthy and pathological conditions (Graeber, 2010; Hong et al., 2016; Ji et al., 2013; Lim et al., 2013;

Miyamoto et al., 2013; Paolicelli et al., 2011; Parkhurst et al., 2013; Schafer et al., 2012; Svahn et al., 2014; Tremblay et al., 2010; Tzioras et al., 2019; Vasek et al., 2016; Wake et al., 2009; Wang et al., 2020; Weinhard et al., 2018; Zhan et al., 2014). The majority of studies monitoring microglial interactions with synapses have been conducted using confocal and two-photon microscopy. The advantages of using confocal and two-photon microscopy are that the cellular components in microglia can also be directly labeled and observed, and microglial interactions can even be studied *in vivo*. However, resolution of these microscopic techniques is limited by the diffraction limit of light (Schermerle et al., 2010). To further elucidate their physiological roles, EM studies of microglia combined with serial sectioning had to be employed, providing new insights into the interaction of microglia and excitatory synapses. For instance, it was discovered that microglia are involved in synaptic plasticity following mere alterations in sensory experience (Tremblay et al., 2010).

4.3 | Super-resolution imaging of transgenic zebrafish larvae

Super-resolution microscopy may be utilized for cultured cells or tissue sections ranging from nanometers to micrometers in thickness by direct or indirect labeling with fluorescent dyes. Fluorophore selection will depend on compatibility with the embedding media used. As demonstrated in this paper, active control of fluorescent probes labeling tissue sections that are several micrometers in thickness can be successfully performed (Galbraith & Galbraith, 2011). Here we demonstrate that molecules expressed *in situ* in whole mount preparations of transgenic zebrafish larvae can be imaged as well. However, it is worth noting that fluorophores linked to antibodies are clearly preferred for the visualization of expressed gene products because endogenously expressed fluorescent proteins yield a much lower intensity in GSDIM (Ries et al., 2012).

In this example, eGFP expressed in microglia was used as the *in situ* expression of fluorophores as it is suitably bright and photostable (Fernandez-Suarez & Ting, 2008). GFP is known for its “blinking properties” (Dickson et al., 1997) and a sizeable population of expressing microglia are consistently present in the tectal region (Svahn et al., 2013). Having an easy to define and comparatively bright cell population minimizes the influence of background fluorescence and out of focus light from neighboring tissue areas which allows for the relatively straightforward reconstruction of super-resolved mpeg1:eGFP microglia. Importantly, this study along with others demonstrates that eGFP, a widely used fluorescent marker, can also be used in super-resolution microscopy (Rankin et al., 2011).

5 | CONCLUSIONS

In this study, we have demonstrated that GSDIM can be used to investigate microglia-synapse interactions in conventional, readily prepared cryostat sections of mouse brain, in whole mount

transgenic zebrafish larvae and, most importantly, in 7 μ m post-mortem formalin-fixed paraffin-embedded human brain tissue. We have also shown that the uptake of synaptic material is elevated in AD. Continued use of GSDIM will benefit from addressing certain limitations encountered here: reducing background fluorescence, for example, by using thinner tissue sections or by the deactivation of out-of-focus fluorophores as has been demonstrated elsewhere (Dani et al., 2010); by taking greater advantage of the total internal reflection fluorescence (TIRF) capability of the system used here to limit the focal depth of the lasers; by fitting the microscope with a motorized stage and expanding the available software features to include a tilescan and quick spiral functionalities to enable larger previews and automated sampling methodologies as the manual stage operation of the system used here would make it difficult to undertake a larger sampling regime; and increasing sample size with additional consideration for the impact of biological variables such as sex. Lastly, the methods presented here allowed for imaging of human brain samples even with extended storage and the unequivocal identification of Syp/Iba1 co-localized puncta as evidence of contact between synapses and microglia processes.

DECLARATION OF TRANSPARENCY

The authors, reviewers and editors affirm that in accordance to the policies set by the *Journal of Neuroscience Research*, this manuscript presents an accurate and transparent account of the study being reported and that all critical details describing the methods and results are present.

ACKNOWLEDGMENTS

GSDIM was performed at Sydney Microscopy and Microanalysis, Charles Perkins Centre, The University of Sydney. Human tissues were received from the New South Wales Brain Tissue Resource Centre at the University of Sydney which is supported by the National Institute of Alcohol Abuse and Alcoholism (NIH (NIAAA) AA012725). Parts of this work were supported by the Australian Research Council (ARC) grant, DP150104472. GTS is a University of Sydney SOAR Fellow.

CONFLICT OF INTEREST

The authors declare no conflict of interest.

AUTHOR CONTRIBUTIONS

PJP and SYFF performed research, analyzed data, and wrote the paper. PJP designed the co-localization study. SS, AJS, CVD, NFR, RMDH, JJK, TSB, RBB, and GTS performed research and analyzed data. MBG designed the study, performed research, analyzed data, and wrote the paper. All authors contributed to editing the manuscript.

PEER REVIEW

The peer review history for this article is available at <https://publons.com/publon/10.1002/jnr.24819>.

DATA AVAILABILITY STATEMENT

The data and code for raw data processing and statistical analysis that support the findings of this study are available from the corresponding author upon reasonable request.

REFERENCES

- Banati, R. B., Middleton, R. J., Chan, R., Hatty, C. R., Kam, W. W., Quin, C., Graeber, M. B., Parmar, A., Zahra, D., Callaghan, P., Fok, S., Howell, N. R., Gregoire, M., Szabo, A., Pham, T., Davis, E., & Liu, G.-J. (2014). Positron emission tomography and functional characterization of a complete PBR/TSPO knockout. *Nature Communications*, 5, 5452. <https://doi.org/10.1038/ncomms6452>
- Birk, U. J. (2019). Super-resolution microscopy of chromatin. *Genes*, 10(7), 493. <https://doi.org/10.3390/genes10070493>
- Blinzinger, K., & Kreutzberg, G. (1968). Displacement of synaptic terminals from regenerating motoneurons by microglial cells. *Zeitschrift Für Zellforschung Und Mikroskopische Anatomie*, 85(2), 145–157. <https://doi.org/10.1007/BF00325030>
- Bolte, S., & Cordelières, F. P. (2006). A guided tour into subcellular colocalization analysis in light microscopy. *Journal of Microscopy*, 224(Pt 3), 213–232. <https://doi.org/10.1111/j.1365-2818.2006.01706.x>
- Bretschneider, S., Eggeling, C., & Hell, S. W. (2007). Breaking the diffraction barrier in fluorescence microscopy by optical shelving. *Physical Review Letters*, 98(21), 218103. <https://doi.org/10.1103/PhysRevLett.98.218103>
- Chen, S. K., Tvrdik, P., Peden, E., Cho, S., Wu, S., Spangrude, G., & Capeocchi, M. R. (2010). Hematopoietic origin of pathological grooming in Hoxb8 mutant mice. *Cell*, 141(5), 775–785. <https://doi.org/10.1016/j.cell.2010.03.055>
- Cizeron, M., Qiu, Z., Koniaris, B., Gokhale, R., Komiyama, N. H., Fransén, E., & Grant, S. G. (2020). A brainwide atlas of synapses across the mouse life span. *Science*, 369(6501), 270–275.
- Coltharp, C., & Xiao, J. (2012). Superresolution microscopy for microbiology. *Cellular Microbiology*, 14(12), 1808–1818. <https://doi.org/10.1111/cmi.12024>
- Damisah, E. C., Hill, R. A., Rai, A., Chen, F., Rothlin, C. V., Ghosh, S., & Grutzendler, J. (2020). Astrocytes and microglia play orchestrated roles and respect phagocytic territories during neuronal corpse removal *in vivo*. *Science Advances*, 6(26), eaba3239. <https://doi.org/10.1126/sciadv.aba3239>
- Dani, A., Huang, B., Bergan, J., Dulac, C., & Zhuang, X. (2010). Superresolution imaging of chemical synapses in the brain. *Neuron*, 68(5), 843–856. <https://doi.org/10.1016/j.neuron.2010.11.021>
- Dickson, R. M., Cubitt, A. B., Tsien, R. Y., & Moerner, W. E. (1997). On/off blinking and switching behaviour of single molecules of green fluorescent protein. *Nature*, 388(6640), 355–358. <https://doi.org/10.1038/41048>
- Eugenin, E. A., Eckardt, D., Theis, M., Willecke, K., Bennett, M. V., & Saez, J. C. (2001). Microglia at brain stab wounds express connexin 43 and *in vitro* form functional gap junctions after treatment with interferon-gamma and tumor necrosis factor-alpha. *Proceedings of the National Academy of Sciences of the United States of America*, 98(7), 4190–4195.
- Fang, K., Chen, X., Li, X., Shen, Y., Sun, J., Czajkowsky, D. M., & Shao, Z. (2018). Super-resolution imaging of individual human subchromosomal regions *in situ* reveals nanoscopic building blocks of higher-order structure. *ACS Nano*, 12(5), 4909–4918.
- Fernandez-Suarez, M., & Ting, A. Y. (2008). Fluorescent probes for super-resolution imaging in living cells. *Nature Reviews Molecular Cell Biology*, 9(12), 929–943. <https://doi.org/10.1038/nrm2531>
- Fölling, J., Bossi, M., Bock, H., Medda, R., Wurm, C. A., Hein, B., Jakobs, S., Eggeling, C., & Hell, S. W. (2008). Fluorescence nanoscopy by ground-state depletion and single-molecule return. *Nature Methods*, 5(11), 943–945. <https://doi.org/10.1038/nmeth.1257>
- Galbraith, C. G., & Galbraith, J. A. (2011). Super-resolution microscopy at a glance. *Journal of Cell Science*, 124(Pt 10), 1607–1611. <https://doi.org/10.1242/jcs.080085>
- Garcia, A., Huang, D., Righolt, A., Righolt, C., Kalaw, M. C., Mathur, S., McAvoy, E., Anderson, J., Luedke, A., Itorralba, J., & Mai, S. (2017). Super-resolution structure of DNA significantly differs in buccal cells of controls and Alzheimer's patients. *Journal of Cellular Physiology*, 232(9), 2387–2395. <https://doi.org/10.1002/jcp.25751>
- Ginhoux, F., Lim, S., Hoeffel, G., Low, D., & Huber, T. (2013). Origin and differentiation of microglia. *Frontiers in Cellular Neuroscience*, 7, 45. <https://doi.org/10.3389/fncel.2013.00045>
- Giulian, D., Haverkamp, L. J., Yu, J. H., Karshin, W., Tom, D., Li, J., Kirkpatrick, J., Kuo, Y. M., & Roher, A. E. (1996). Specific domains of beta-amyloid from Alzheimer plaque elicit neuron killing in human microglia. *Journal of Neuroscience*, 16(19), 6021–6037.
- Gomez-Isla, T., Hollister, R., West, H., Mui, S., Growdon, J. H., Petersen, R. C., Parisi, J. E., & Hyman, B. T. (1997). Neuronal loss correlates with but exceeds neurofibrillary tangles in Alzheimer's disease. *Annals of Neurology*, 41(1), 17–24. <https://doi.org/10.1002/ana.410410106>
- Graeber, M. B. (2010). Changing face of microglia. *Science*, 330(6005), 783–788. <https://doi.org/10.1126/science.1190929>
- Graeber, M. B. (2014). Neuroinflammation: No rose by any other name. *Brain Pathology*, 24(6), 620–622. <https://doi.org/10.1111/bpa.12192>
- Graeber, M. B., Bise, K., & Mehraein, P. (1993). Synaptic stripping in the human facial nucleus. *Acta Neuropathologica*, 86(2), 179–181. <https://doi.org/10.1007/BF00334886>
- Graeber, M. B., & Kreutzberg, G. W. (1988). Delayed astrocyte reaction following facial nerve axotomy. *Journal of Neurocytology*, 17(2), 209–220. <https://doi.org/10.1007/BF01674208>
- Graeber, M. B., Streit, W. J., & Kreutzberg, G. W. (1988). Axotomy of the rat facial nerve leads to increased CR3 complement receptor expression by activated microglial cells. *Journal of Neuroscience Research*, 21(1), 18–24. <https://doi.org/10.1002/jnr.490210104>
- Hell, S. W. (2007). Far-field optical nanoscopy. *Science*, 316(5828), 1153–1158. <https://doi.org/10.1126/science.1137395>
- Helmuth, J. A., Paul, G., & Sbalzarini, I. F. (2010). Beyond co-localization: Inferring spatial interactions between sub-cellular structures from microscopy images. *BMC Bioinformatics*, 11, 372. <https://doi.org/10.1186/1471-2105-11-372>
- Hong, S., Beja-Glasser, V. F., Nfonoyim, B. M., Frouin, A., Li, S., Ramakrishnan, S., Merry, K. M., Shi, Q., Rosenthal, A., Barres, B. A., Lemere, C. A., Selkoe, D. J., & Stevens, B. (2016). Complement and microglia mediate early synapse loss in Alzheimer mouse models. *Science*, 352(6286), 712–716. <https://doi.org/10.1126/science.aad8373>
- Hyman, B. T., Phelps, C. H., Beach, T. G., Bigio, E. H., Cairns, N. J., Carrillo, M. C., Dickson, D. W., Duyckaerts, C., Frosch, M. P., Masliah, E., Mirra, S. S., Nelson, P. T., Schneider, J. A., Thal, D. R., Thies, B., Trojanowski, J. Q., Vinters, H. V., & Montine, T. J. (2012). National Institute on Aging-Alzheimer's Association guidelines for the neuropathologic assessment of Alzheimer's disease. *Alzheimer's & Dementia: the Journal of the Alzheimer's Association*, 8(1), 1–13. <https://doi.org/10.1016/j.jalz.2011.10.007>
- Ji, K., Akgul, G., Wollmuth, L. P., & Tsirka, S. E. (2013). Microglia actively regulate the number of functional synapses. *PLoS One*, 8(2), e56293. <https://doi.org/10.1371/journal.pone.0056293>
- Kreutzberg, G. W. (1996). Microglia: A sensor for pathological events in the CNS. *Trends in Neurosciences*, 19(8), 312–318. [https://doi.org/10.1016/0166-2236\(96\)10049-7](https://doi.org/10.1016/0166-2236(96)10049-7)
- Lalkens, B., Testa, I., Willig, K. I., & Hell, S. W. (2012). MRT letter: Nanoscopy of protein colocalization in living cells by STED and GSDIM. *Microscopy Research and Technique*, 75(1), 1–6. <https://doi.org/10.1002/jemt.21026>
- Lim, S. H., Park, E., You, B., Jung, Y., Park, A. R., Park, S. G., & Lee, J.-R. (2013). Neuronal synapse formation induced by microglia and

- interleukin 10. *PLoS One*, 8(11), e81218. <https://doi.org/10.1371/journal.pone.0081218>
- Liu, X. B., & Schumann, C. M. (2014). Optimization of electron microscopy for human brains with long-term fixation and fixed-frozen sections. *Acta Neuropathologica Communications*, 2, 42. <https://doi.org/10.1186/2051-5960-2-42>
- Miyamoto, A., Wake, H., Moorhouse, A. J., & Nabekura, J. (2013). Microglia and synapse interactions: Fine tuning neural circuits and candidate molecules. *Frontiers in Cellular Neuroscience*, 7, 70. <https://doi.org/10.3389/fncel.2013.00070>
- Mockl, L., Lamb, D. C., & Brauchle, C. (2014). Super-resolved fluorescence microscopy: Nobel Prize in Chemistry 2014 for Eric Betzig, Stefan Hell, and William E. Moerner. *Angewandte Chemie International Edition*, 53(51), 13972–13977.
- Moerner, W. E. (2012). Microscopy beyond the diffraction limit using actively controlled single molecules. *Journal of Microscopy*, 246(3), 213–220. <https://doi.org/10.1111/j.1365-2818.2012.03600.x>
- Montine, T. J., Phelps, C. H., Beach, T. G., Bigio, E. H., Cairns, N. J., Dickson, D. W., Duyckaerts, C., Frosch, M. P., Masliah, E., Mirra, S. S., Nelson, P. T., Schneider, J. A., Thal, D. R., Trojanowski, J. Q., Vinters, H. V., & Hyman, B. T. (2012). National Institute on Aging-Alzheimer's Association guidelines for the neuropathologic assessment of Alzheimer's disease: A practical approach. *Acta Neuropathologica*, 123(1), 1–11. <https://doi.org/10.1007/s00401-011-0910-3>
- Moran, L. B., & Graeber, M. B. (2004). The facial nerve axotomy model. *Brain Research. Brain Research Reviews*, 44(2–3), 154–178. <https://doi.org/10.1016/j.brainresrev.2003.11.004>
- Nimmerjahn, A., Kirchhoff, F., & Helmchen, F. (2005). Resting microglial cells are highly dynamic surveillants of brain parenchyma in vivo. *Science*, 308(5726), 1314–1318. <https://doi.org/10.1126/science.1110647>
- Paasila, P. J., Davies, D. S., Goldsbury, C., & Sutherland, G. T. (2020). Clustering of activated microglia occurs before the formation of dystrophic neurites in the evolution of A β plaques in Alzheimer's disease. *Free Neuropathology*, 1(20). <https://doi.org/10.17879/freeneuropathology-2020-2845>
- Paasila, P. J., Davies, D. S., Kril, J. J., Goldsbury, C., & Sutherland, G. T. (2019). The relationship between the morphological subtypes of microglia and Alzheimer's disease neuropathology. *Brain Pathology*, 29(6), 726–740. <https://doi.org/10.1111/bpa.12717>
- Paolicelli, R. C., Bolasco, G., Pagani, F., Maggi, L., Scianni, M., Panzanelli, P., Giustetto, M., Ferreira, T. A., Guiducci, E., Dumas, L., Ragozzino, D., & Gross, C. T. (2011). Synaptic pruning by microglia is necessary for normal brain development. *Science*, 333(6048), 1456–1458. <https://doi.org/10.1126/science.1202529>
- Paparelli, L., Corthout, N., Pavie, B., Wakefield, D. L., Sannerud, R., Jovanovic-Talman, T., Annaert, W., & Munck, S. (2016). Inhomogeneity based characterization of distribution patterns on the plasma membrane. *PLoS Computational Biology*, 12(9), e1005095. <https://doi.org/10.1371/journal.pcbi.1005095>
- Parkhurst, C. N., Yang, G., Ninan, I., Savas, J. N., Yates, J. R., 3rd, Lafaille, J. J., Hempstead, B. L., Littman, D. R., & Gan, W.-B. (2013). Microglia promote learning-dependent synapse formation through brain-derived neurotrophic factor. *Cell*, 155(7), 1596–1609. <https://doi.org/10.1016/j.cell.2013.11.030>
- Rankin, B. R., Moneron, G., Wurm, C. A., Nelson, J. C., Walter, A., Schwarzer, D., Schroeder, J., Colón-Ramos, D. A., & Hell, S. W. (2011). Nanoscopy in a living multicellular organism expressing GFP. *Biophysical Journal*, 100(12), L63–L65. <https://doi.org/10.1016/j.bpj.2011.05.020>
- Ries, J., Kaplan, C., Platonova, E., Eghlidi, H., & Ewers, H. (2012). A simple, versatile method for GFP-based super-resolution microscopy via nanobodies. *Nature Methods*, 9(6), 582–584. <https://doi.org/10.1038/nmeth.1991>
- Sajjan, S., Holsinger, R. M., Fok, S., Ebrahimkhani, S., Rollo, J. L., Banati, R. B., & Graeber, M. (2014). Up-regulation of matrix metalloproteinase 12 in motor neurons undergoing synaptic stripping. *Neuroscience*, 274, 331–340. <https://doi.org/10.1016/j.neuroscience.2014.05.052>
- Sarmiento, M. (2013). Use of confocal microscopy in the study of microglia in a brain metastasis model. *Methods in Molecular Biology*, 1041, 337–346.
- Schafer, D. P., Lehrman, E. K., Kautzman, A. G., Koyama, R., Mardinly, A. R., Yamasaki, R., Ransohoff, R. M., Greenberg, M. E., Barres, B. A., & Stevens, B. (2012). Microglia sculpt postnatal neural circuits in an activity and complement-dependent manner. *Neuron*, 74(4), 691–705. <https://doi.org/10.1016/j.neuron.2012.03.026>
- Schafer, D. P., Lehrman, E. K., & Stevens, B. (2013). The "quad-partite" synapse: Microglia-synapse interactions in the developing and mature CNS. *Glia*, 61(1), 24–36. <https://doi.org/10.1002/glia.22389>
- Schermelleh, L., Ferrand, A., Huser, T., Eggeling, C., Sauer, M., Biehlmair, O., & Drummen, G. P. (2019). Super-resolution microscopy demystified. *Nature Cell Biology*, 21(1), 72–84. <https://doi.org/10.1038/s41556-018-0251-8>
- Schermelleh, L., Heintzmann, R., & Leonhardt, H. (2010). A guide to super-resolution fluorescence microscopy. *Journal of Cell Biology*, 190(2), 165–175. <https://doi.org/10.1083/jcb.201002018>
- Shivanandan, A., Radenovic, A., & Sbalzarini, I. F. (2013). MosaicIA: An ImageJ/Fiji plugin for spatial pattern and interaction analysis. *BMC Bioinformatics*, 14, 349. <https://doi.org/10.1186/1471-2105-14-349>
- Sieben, C., Douglass, K. M., Guichard, P., & Manley, S. (2018). Super-resolution microscopy to decipher multi-molecular assemblies. *Current Opinion in Structural Biology*, 49, 169–176. <https://doi.org/10.1016/j.sbi.2018.03.017>
- Sigrist, S. J., & Sabatini, B. L. (2012). Optical super-resolution microscopy in neurobiology. *Current Opinion in Neurobiology*, 22(1), 86–93. <https://doi.org/10.1016/j.conb.2011.10.014>
- Sreedharan, S., Gill, M. R., Garcia, E., Saeed, H. K., Robinson, D., Byrne, A., Cadby, A., Keyes, T. E., Smythe, C., Pellett, P., Bernardino de la Serna, J., & Thomas, A. (2017). Multimodal super-resolution optical microscopy using a transition-metal-based probe provides unprecedented capabilities for imaging both nuclear chromatin and mitochondria. *Journal of the American Chemical Society*, 139(44), 15907–15913. <https://doi.org/10.1021/jacs.7b08772>
- Stracy, M., & Kapanidis, A. N. (2017). Single-molecule and super-resolution imaging of transcription in living bacteria. *Methods*, 120, 103–114. <https://doi.org/10.1016/j.ymeth.2017.04.001>
- Streit, W. J., Braak, H., Xue, Q. S., & Bechmann, I. (2009). Dystrophic (senescent) rather than activated microglial cells are associated with tau pathology and likely precede neurodegeneration in Alzheimer's disease. *Acta Neuropathologica*, 118(4), 475–485. <https://doi.org/10.1007/s00401-009-0556-6>
- Sutherland, G. T., Sheedy, D., Stevens, J., McCrossin, T., Smith, C. C., van Rooijen, M., & Kril, J. J. (2016). The NSW brain tissue resource centre: Banking for alcohol and major neuropsychiatric disorders research. *Alcohol*, 52, 33–39. <https://doi.org/10.1016/j.alcohol.2016.02.005>
- Svahn, A. J., Becker, T. S., & Graeber, M. B. (2014). Emergent properties of microglia. *Brain Pathology*, 24(6), 665–670. <https://doi.org/10.1111/bpa.12195>
- Svahn, A. J., Graeber, M. B., Ellett, F., Lieschke, G. J., Rinkwitz, S., Bennett, M. R., & Becker, T. S. (2013). Development of ramified microglia from early macrophages in the zebrafish optic tectum. *Developmental Neurobiology*, 73(1), 60–71. <https://doi.org/10.1002/dneu.22039>
- Terry, R. D., Masliah, E., Salmon, D. P., Butters, N., DeTeresa, R., Hill, R., Hansen, L. A., & Katzman, R. (1991). Physical basis of cognitive alterations in Alzheimer's disease: Synapse loss is the major correlate of cognitive impairment. *Annals of Neurology*, 30(4), 572–580. <https://doi.org/10.1002/ana.410300410>
- Thompson, M. A., Lew, M. D., & Moerner, W. E. (2012). Extending microscopic resolution with single-molecule imaging and active control.

- Annual Review of Biophysics*, 41, 321–342. <https://doi.org/10.1146/annurev-biophys-050511-102250>
- Tischer, J., Krueger, M., Mueller, W., Staszewski, O., Prinz, M., Streit, W. J., & Bechmann, I. (2016). Inhomogeneous distribution of Iba-1 characterizes microglial pathology in Alzheimer's disease. *Glia*, 64(9), 1562–1572. <https://doi.org/10.1002/glia.23024>
- Tremblay, M., Lowery, R. L., & Majewska, A. K. (2010). Microglial interactions with synapses are modulated by visual experience. *PLoS Biology*, 8(11), e1000527. <https://doi.org/10.1371/journal.pbio.1000527>
- Tzioras, M., Daniels, M. J. D., King, D., Popovic, K., Holloway, R. K., Stevenson, A. J., Tulloch, J., Kandasamy, J., Sokol, D., Latta, C., Rose, J., Smith, C., Miron, V. E., Henstridge, C., McColl, B. W., & Spires-Jones, T. L. (2019). Altered synaptic ingestion by human microglia in Alzheimer's disease. *bioRxiv*. <https://doi.org/10.1101/795930>
- van de Linde, S. (2019). Single-molecule localization microscopy analysis with ImageJ. *Journal of Physics. D. Applied Physics*, 52(20), 203002. <https://doi.org/10.1088/1361-6463/ab092f>
- Vasek, M. J., Garber, C., Dorsey, D., Durrant, D. M., Bollman, B., Soung, A., Yu, J., Perez-Torres, C., Frouin, A., Wilton, D. K., Funk, K., DeMasters, B. K., Jiang, X., Bowen, J. R., Mennerick, S., Robinson, J. K., Garbow, J. R., Tyler, K. L., Suthar, M. S., ... Klein, R. S. (2016). A complement-microglial axis drives synapse loss during virus-induced memory impairment. *Nature*, 534(7608), 538–543. <https://doi.org/10.1038/nature18283>
- Vaziri, A., Tang, J., Shroff, H., & Shank, C. V. (2008). Multilayer three-dimensional super resolution imaging of thick biological samples. *Proceedings of the National Academy of Sciences of the United States of America*, 105(51), 20221–20226. <https://doi.org/10.1073/pnas.0810636105>
- Wake, H., Moorhouse, A. J., Jinno, S., Kohsaka, S., & Nabekura, J. (2009). Resting microglia directly monitor the functional state of synapses *in vivo* and determine the fate of ischemic terminals. *Journal of Neuroscience*, 29(13), 3974–3980. <https://doi.org/10.1523/JNEUROSCI.4363-08.2009>
- Wang, C., Yue, H., Hu, Z., Shen, Y., Ma, J., Li, J., Wang, X.-D., Wang, L., Sun, B., Shi, P., Wang, L., & Gu, Y. (2020). Microglia mediate forgetting via complement-dependent synaptic elimination. *Science*, 367(6478), 688–694. <https://doi.org/10.1126/science.aaz2288>
- Wasseff, S. K., & Scherer, S. S. (2014). Activated microglia do not form functional gap junctions *in vivo*. *Journal of Neuroimmunology*, 269(1–2), 90–93. <https://doi.org/10.1016/j.jneuroim.2014.02.005>
- Watanabe, S., Lehmann, M., Hujber, E., Fetter, R. D., Richards, J., Söhl-Kielczynski, B., Felies, A., Rosenmund, C., Schmoranz, J., & Jorgensen, E. M. (2014). Nanometer-resolution fluorescence electron microscopy (nano-EM) in cultured cells. *Methods in Molecular Biology*, 1117, 503–526.
- Weinhard, L., di Bartolomei, G., Bolasco, G., Machado, P., Schieber, N. L., Neniskyte, U., Exiga, M., Vadiute, A., Raggioli, A., Schertel, A., Schwab, Y., & Gross, C. T. (2018). Microglia remodel synapses by presynaptic trogocytosis and spine head filopodia induction. *Nature Communications*, 9(1), 1228. <https://doi.org/10.1038/s41467-018-03566-5>
- Westerfield, M. (2000). *The zebrafish book: A guide for the laboratory use of zebrafish* (Danio rerio). University of Oregon.
- Wu, Y., Dissing-Olesen, L., MacVicar, B. A., & Stevens, B. (2015). Microglia: Dynamic mediators of synapse development and plasticity. *Trends in Immunology*, 36(10), 605–613. <https://doi.org/10.1016/j.it.2015.08.008>
- Xu, J., & Liu, Y. (2019). A guide to visualizing the spatial epigenome with super-resolution microscopy. *FEBS Journal*, 286(16), 3095–3109. <https://doi.org/10.1111/febs.14938>
- Yamamoto, S., Nakajima, K., & Kohsaka, S. (2010). Macrophage-colony stimulating factor as an inducer of microglial proliferation in axotomized rat facial nucleus. *Journal of Neurochemistry*, 115(4), 1057–1067. <https://doi.org/10.1111/j.1471-4159.2010.06996.x>
- Zhan, Y., Paolicelli, R. C., Sforzini, F., Weinhard, L., Bolasco, G., Pagani, F., Vyssotski, A. L., Bifone, A., Gozzi, A., Ragozzino, D., & Gross, C. T. (2014). Deficient neuron-microglia signaling results in impaired functional brain connectivity and social behavior. *Nature Neuroscience*, 17(3), 400–406. <https://doi.org/10.1038/nn.3641>

SUPPORTING INFORMATION

Additional supporting information may be found online in the Supporting Information section.

Supplementary Material

Transparent Science Questionnaire for Authors

Transparent Peer Review Report

How to cite this article: Paasila PJ, Fok SYY, Flores-Rodriguez N, et al. Ground state depletion microscopy as a tool for studying microglia–synapse interactions. *J Neurosci Res*. 2021;00:1–18. <https://doi.org/10.1002/jnr.24819>

4.4 Published supplementary material

The published supplementary material begins on the next page.

Supplementary Figure 1 Examples of widefield (left) and corresponding GSDIM reconstruction (right) composites of Iba1- (magenta) and Syp- (green) immunoreactivity in the superior frontal gyrus of a control case (Non-AD PC 1) fixed for 24 hrs only. *Scale bar = 2.5 μ m*

Supplementary Figure 2 Examples of widefield (left) and GSDIM reconstruction (right) composites of Iba1- (magenta) and Syp- (green) immunoreactivity in a human brain (Non-AD Control 2) fixed for 421 weeks. A few small white spots indicate signal co-localization in the GSDIM reconstructions. *Scale bar = 2.5 μ m*

Supplementary Figure 3 Widefield (left) and GSDIM reconstruction (right) composites of Iba1- (magenta) and Syp- (green) immunoreactivity in AD brain tissue (case AD 4) fixed for 3 weeks. White spots reveal areas of signal co-localization. The two asterisks (*) indicate partial profiles of blood vessel walls that can have perivascular microglia and/or perivascular cells (Iba1-immunoreactive macrophages) attached and which occasionally appeared in GSDIM reconstructions of the 532 nm channel. *Scale bar = 2.5 μ m*

Supplementary Figure 4 Chromatic aberration was negligible. Tests were performed before and after GSDIM experiments using TetraSpeckTM microspheres imaged using the 488 (green), 532 (red), and 642 (blue) nm laser lines. *Scale bar = 10 μ m*

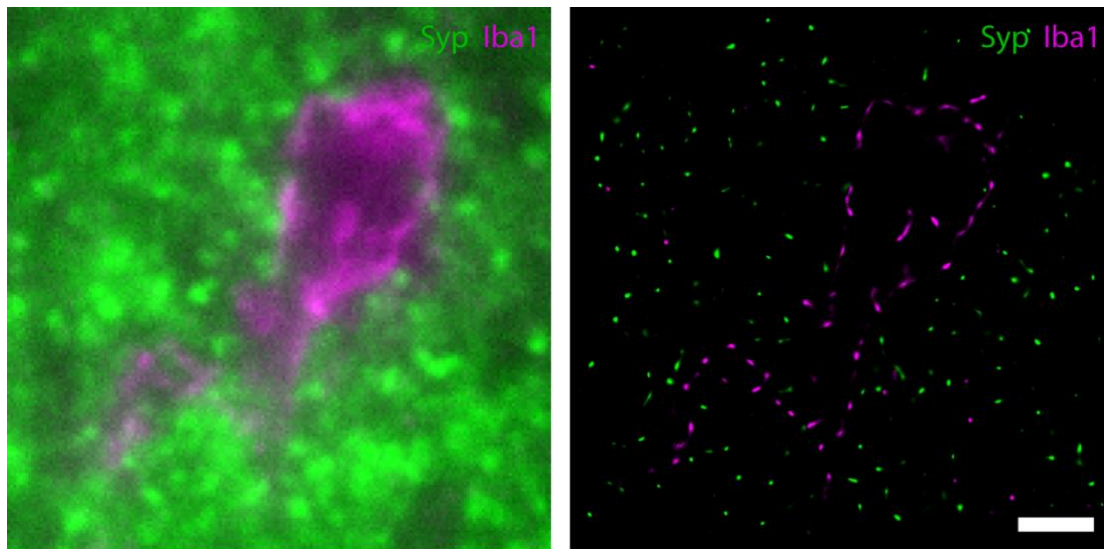
Supplementary Figure 5 Occasional profiles of Iba1-immunoreactive cells around blood vessels (including perivascular cells/macrophages) were useful as internal controls (arrows in **a**). These profiles did not affect the results of the Iba1/Syp co-localization study. **a–b** Widefield images of (**a**) Iba1 (magenta) and (**b**) Syp (green) immunolabelling are displayed as composites with their respective GSDIM reconstructions overlayed (red glow). The arrows in **a** indicate partial profiles of Iba1-immunoreactive cells around blood vessels, which are absent in the Syp-labelled channel. **c** Composite image of the GSDIM reconstructions of the Iba1 (magenta) and Syp (green) channels shown in red glow in **a** and **b**, respectively. *Scale bar in c = 5 μ m* (**c**), 10 μ m (**a**, **b**)

Supplementary Figure 6 Widefield (left) and GSDIM reconstruction (right) composites of Iba1 (magenta) and Syp (green) immunostaining of control tissue (Non-AD Control 1). Brain sections shown were treated with Sudan Black B to quench autofluorescence caused by

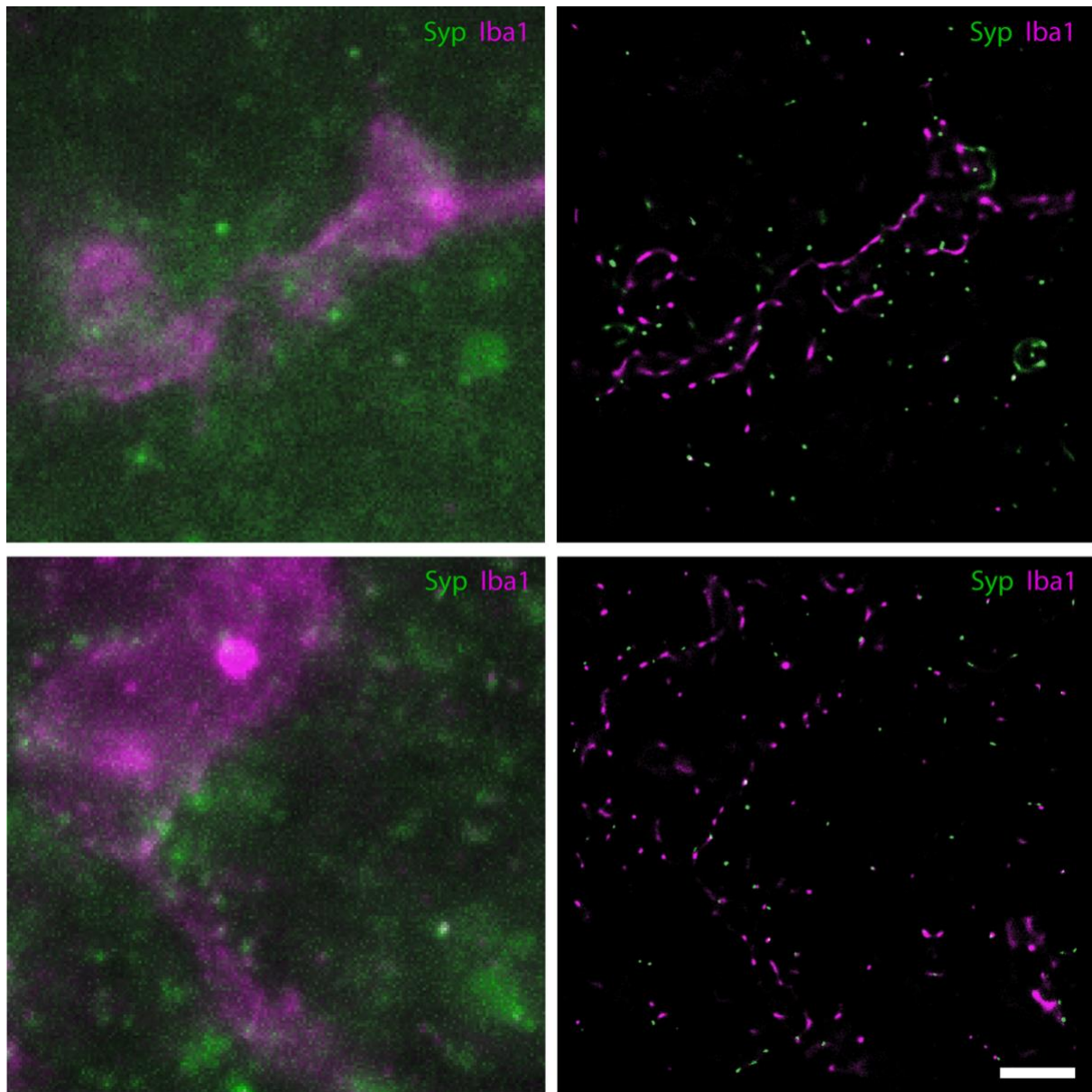
lipofuscin deposits. However, Sudan Black B significantly impaired photo-switching of fluorophores, particularly of AF 532. The latter reduced the localization precision of the LAS X software, leading to ‘smearing’ in GSDIM reconstructions. Therefore Sudan Black B was excluded from further use in experiments. *Scale bar* = 2.5 μm

Supplementary Movie 1 Merged 3D GSDIM projections of the region of interest seen in Figure 3 demonstrating co-localization of Iba1-immunolabelling (magenta) and Syp-immunolabelling (green). Arrow indicates the area of co-localization highlighted in Figure 3. *Scale bar* = 5 μm (first and last frame only). Available at <https://onlinelibrary.wiley.com/action/downloadSupplement?doi=10.1002%2Fjnr.24819&file=jnr24819-sup-0007-VideoS1.mp4>

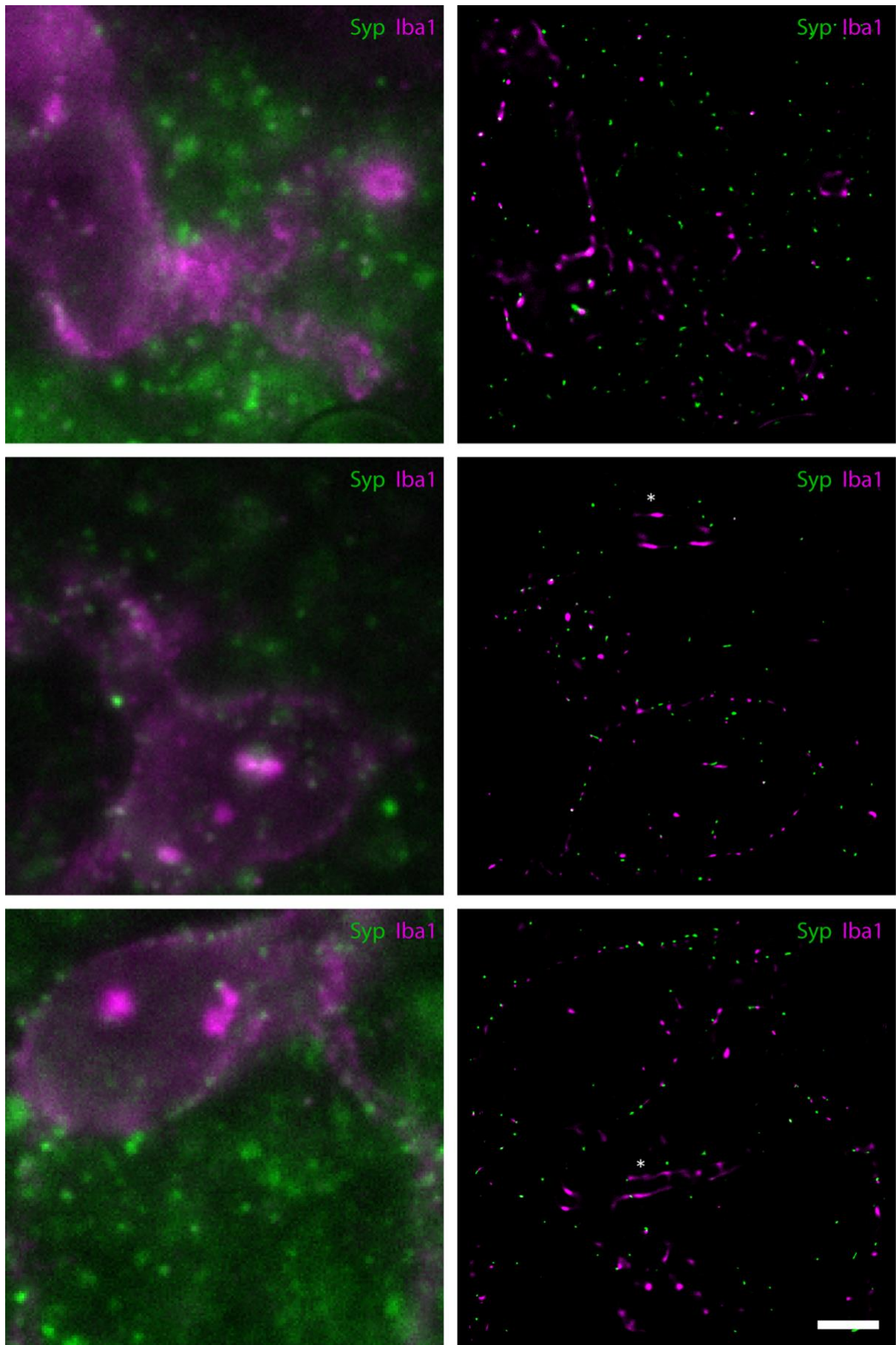
Supplementary Movie 2 Corresponding 3D widefield fluorescence projection of the microglial cell shown in Figure 3 and Supplementary Movie 1. Arrow indicates the area of co-localization confirmed using GSDIM shown in Figure 3 and Supplementary Movie 1. *Scale bar* = 10 μm (first and last frame only). Available at <https://onlinelibrary.wiley.com/action/downloadSupplement?doi=10.1002%2Fjnr.24819&file=jnr24819-sup-0008-VideoS2.mp4>



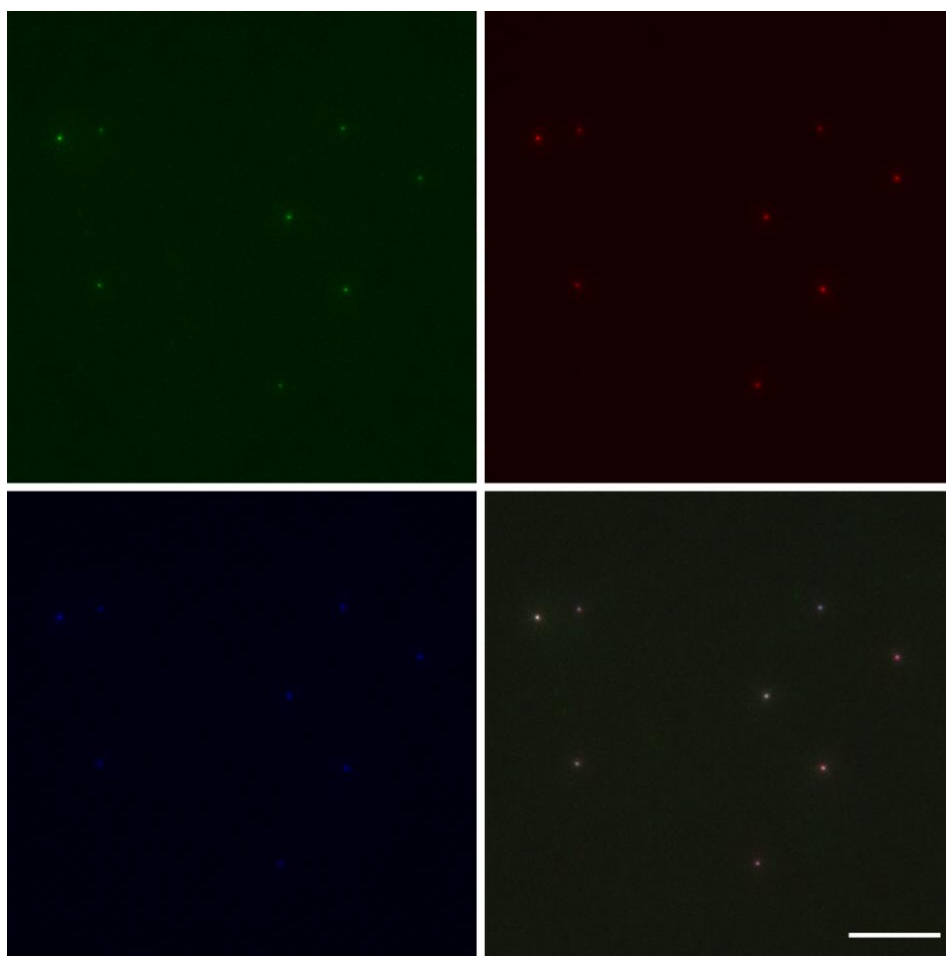
Supplementary Figure 1.



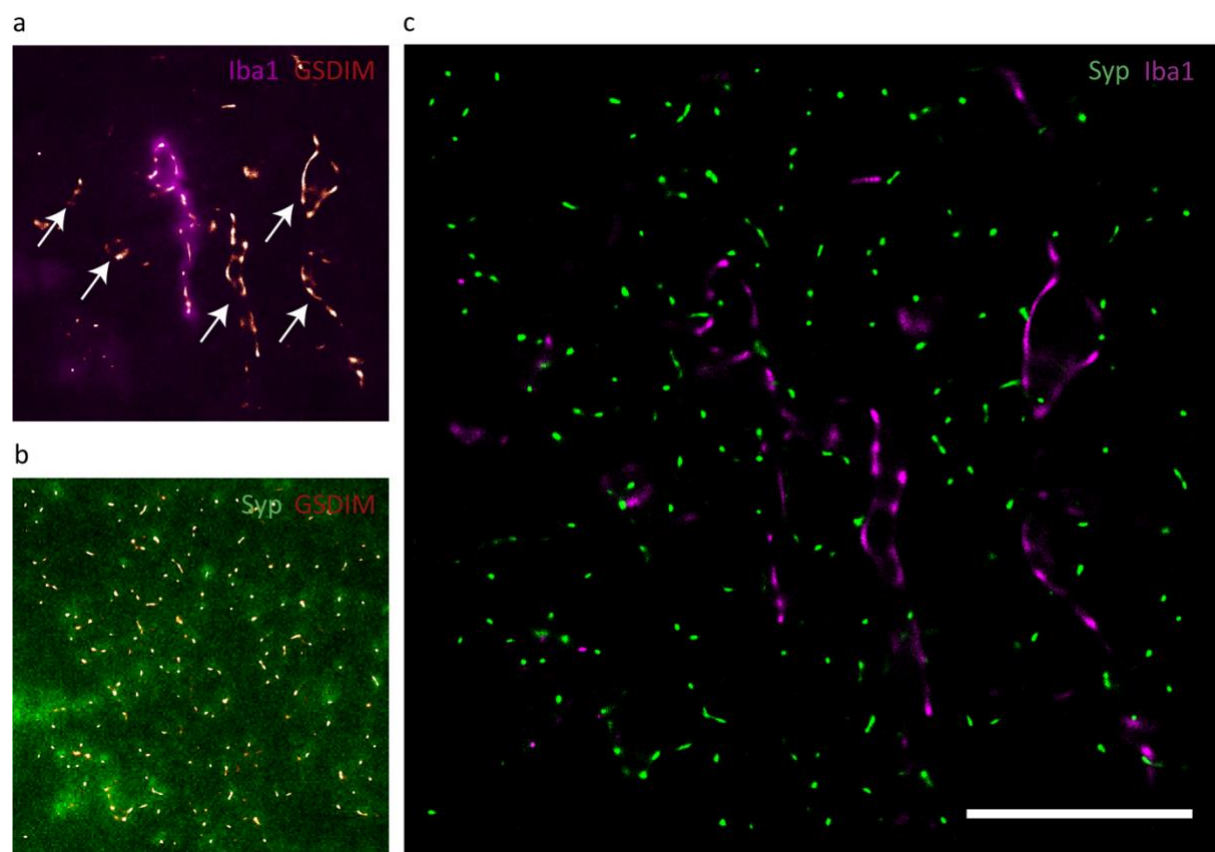
Supplementary Figure 2.



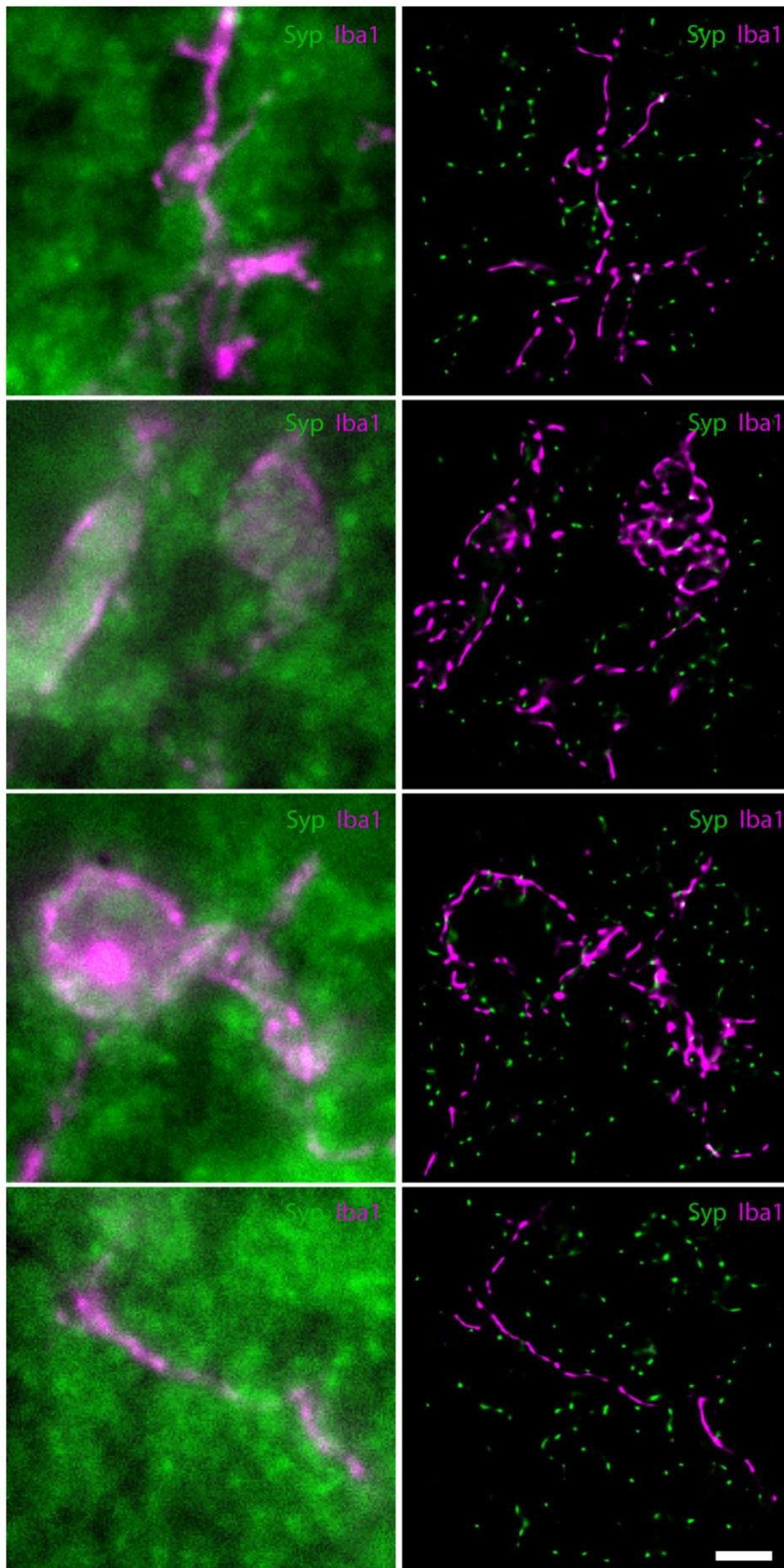
Supplementary Figure 3.



Supplementary Figure 4.



Supplementary Figure 5.



Supplementary Figure 6.

Step-by-step protocol for using GSDIM on archival paraffin-embedded human brain sections:

1 Materials and equipment required

1.1. Human brain tissue preparation

Neutral-buffered Formalin (15%) (POCD, LabTech Service & Supplies, 15NBF5L).

Agar (Grade J3, Gelita Australia).
Paraffin (Paraplast Plus, Leica, 39602004).
Uncoated glass coverslips (24 × 40 mm) (Grale Scientific, 471112440).

1.2. Immunofluorescence histochemistry

Dewaxing and rehydration:

Xylene.
Ethanol (EtOH) (100%, 95%, 70%, 50%).

Buffers

10 mM Tris/1 mM EDTA (TE; pH 8.5).
10 mM PBST (0.3% Tween-20; pH 7.4).
Fresh sodium borohydride (0.1% w/v).

Tissue staining

Primary antibodies (anti-Iba1; anti-Syp).
Secondary antibodies (AF 647; AF 532).

10% animal serum (preferably sourced from the host animal of secondary antibodies).

Equipment

Decloaking chamber (BioCare, DC2002).
6-well plates.
Fine tip paint brush.
Fridge (4°C for sample storage).

1.3. Preparation for GSDIM

100 mM β -mercaptoethylamine (MEA; pH 8.5)
Bondic® (or Twinsil®).

Equipment:

‘Ultracleaned’ high precision glass coverslips (#0107032, Marienfeld Superior).

Depression slides (neoLab, 1-6293).

Filter paper.
 Fine point forceps.
 Fine tip paint brush.
 N₂ outlet with pipe and nozzle.

1.4. ‘Ultracleaning’ coverslips High precision glass coverslips.
 MilliQ water.
 Acetone.
 100% EtOH.
 Nitric acid (note: appropriate PPE and chemical hood).
 N₂ outlet with pipe and nozzle.

1.5. Microscope setup The GSDIM setup at Sydney Microscopy and microanalysis (SMM) is built on an inverted Leica DMI6000B microscope equipped a 30 mW 405 nm diode laser (Coherent Scientific, USA) and the following continuous wave lasers (MPBC Inc., Canada): 500 mW 642 nm, 500 mW 532 nm, and 300 mW 488; for epifluorescence (EPI), Total Internal Reflection Fluorescence (TIRF) and GSDIM.

Filters:

	Excitation	Dichroic	Emission
642	642/10; 405/10	649	710/100; 450/50
532	532/10; 405/10	541	600/100; 450/50
488	488/10; 405/10	496	555/100; 450/50

For drift prevention the system uses the SUMO (Supress Motion) stage, which couples the objective to the sample holder. Additionally, the base of the microscope rests on a dynamic anti-vibration system (The Table Stable Ltd., TS-140-LP, Switzerland) on top of an isolation table (#11522154, Accurion, Germany).

For EPI- and TIRF-GSDIM, a Leica HCX PL APO 160×/1.43 NA CORR GSD oil-immersion objective is used. Images are acquired using an Andor iXon Ultra 897 EMCCD camera (Oxford Instruments Plc, UK). The microscope is also equipped with a HC PLAPO 10×/0.4 objective and a HCX PL FLUOTAR L 40×/0.6 objective for EPI imaging.

2.1. Human brain tissue preparation

The preparation of human brain tissue by the NSWBTRC has been previously published (1). Briefly, brains are hemisected, with one half fixed in formalin for three weeks, before being embedded in agar and sliced at 3 mm intervals. A series of tissue blocks are cut for paraffin embedding. Importantly, the remainder of the fixed slices remain stored in formalin indefinitely, and further blocks may be cut as required.

Extended periods of fixation may adversely affect antigen detection. However, we have been able to demonstrate the successful application of GSDIM across a range of fixation periods (see Table 1 in the main text) and from archived paraffin-embedded tissue sections.

Here, 7 μ m thick formalin-fixed paraffin-embedded sections from the superior frontal gyrus were prepared and mounted onto uncoated glass coverslips (24 \times 40 mm).

2.2. Immunofluorescence

Immunofluorescence immunohistochemistry was carried out as described in the main text. A step-by-step procedure is also provided here:

- i.* Dewax sections in xylene; 3 \times 5 mins.
- ii.* Rehydrate sections in graded ethanol solutions:
 - a. 100% EtOH; 3 \times 5 mins.
 - b. 95% EtOH; 3 mins.
 - c. 70% EtOH; 3 mins.
 - d. 50% EtOH; 3 mins.
 - e. ddH₂O; hold.
- iii.* Perform antigen retrieval: 1 \times TE; 110°C, 30 mins (decloaking chamber).
 - Equilibrate to room temperature (RT).
 - Sections will either detach from the uncoated glass coverslips or can be easily removed in a PBST bath using a fine-tip paint brush.
 - Transfer sections to PBST in a 6-well plate; sections are then treated free-floating.
 - A new 6-well plate is used for each wash to maximise the effectiveness of washing procedures; sections are transferred using a fine-tip paint brush.
- iv.* Rinse in PBS.

- v. Quench in sodium borohydride; 2× 5 mins.
- vi. Wash; 5× 5 mins (PBST).
- vii. Block: 10% normal goat serum in PBST; 1 hr.
- viii. Incubate in 1° antibody solution: anti-Iba1 (1:500; rabbit), anti-Syp (1:200; mouse); 20 hrs, 4°C.
 - Dilute antibodies in 1% blocking solution.
 - Apply gentle agitation using an orbital shaker.
 - See main text for antibody manufacturers and catalogues.
- ix. Wash; 5× 5 mins (PBST).
- x. Incubate in 2° antibodies: AlexaFluor 647 (anti-mouse), AlexaFluor 532 (anti-rabbit); 1:200; 20 hrs, 4°C, gentle agitation.
 - See main text for antibody manufacturers and catalogue numbers.
- xi. Wash; 5× 5 mins (PBS).
 - Wrap 6-well plate in aluminium foil; hold sections in PBS (4°C) until ready to image.
- xii. Image same day.

2.3. Sample preparation

For imaging of human brain sections:

- i. Mount section (in a 6-well plate or larger receptacle if needed) onto an ‘ultracleaned’ glass coverslip (18 × 18 mm; see section 2.4. for coverslip cleaning method) using fine tip forceps and paint brush.
- ii. Allow section to dry for ~ 10 mins (N₂ gas can be used to aid with drying).
- iii. Apply 80–100 µL MEA to depression slide.
- iv. Mount section onto depression slide using fine tip forceps.
- v. Remove excess MEA using filter paper
 - Bring the edge of the paper as close as possible to the space between the depression slide and coverslip.
 - Ensure no bubbles are present as these will oxidise the MEA and impair photoswitching.
 - Continue to apply filter paper until no more MEA is absorbed to ensure flatness of the section and coverslip.
- vi. Seal using Bondic[®] for best results (allows for storage overnight at 4°C with minimal

impact on photoswitching; Twinsil[®] is suitable for imaging < 2 hrs).

2.4. 'Ultracleaning' coverslips The following is a step-by-step procedure used for the preparation of glass coverslips for GSDIM:

- i. Sonicate in MilliQ water; 30 mins, RT.
- ii. Sonicate in acetone; 30 mins, RT.
- iii. Sonicate in 100% EtOH; 30 mins, RT.
- iv. 3× rinse with MilliQ water.
- v. Boil in nitric acid (85°C); 5 mins (wear appropriate PPE; perform under chemical hood); leave under hood overnight.
- vi. Decant nitric acid.
- vii. 4× rinse with MilliQ water.
- viii. Dry with compressed N₂ gas (do not autoclave).
- ix. Store coverslips in a sealed container to prevent contamination by moisture or airborne particles.

2.5. Imaging protocol

Sections were screened using the 10×/0.4 objective and mercury-halide light source. Regions of interest between cortical layers II–V were selected at random whilst visualising with the 532 channel using the 160×/1.43 objective. At least three regions of interest were imaged per case.

2.6. Acquisition settings

EPI imaging for reference images (51 µm × 51 µm or 18 µm × 18 µm; z-depth up to 7 µm):

- 532 channel:
 - a. Laser line: 532 nm.
 - b. Laser power: 0.5%.
 - c. Camera exposure: 50 ms.
 - d. Camera EM Gain: 100.
- 647 channel:
 - a. Laser line: 642 nm.
 - b. Laser power: 2.0%.
 - c. Camera exposure: 200 ms.
 - d. Camera EM Gain: 100.

2D GSDIM:

EPI mode

- 532 channel (imaged first):
 - a. Laser line: 532 nm.
 - b. Laser power: 2.0%.

- c. Camera exposure: 11.7 ms.
- d. Camera EM Gain: 200.
- e. Detection threshold: 20 photons/pixel.
- f. Pixel size: 20 nm (X, Y).
- g. Acquisition time: 3 mins.
- 647 nm channel (imaged second):
 - a. Laser line: 642 nm.
 - b. Laser power: 4.0%.
 - c. Camera exposure: 11.7 ms.
 - d. Camera EM Gain: 200.
 - e. Detection threshold: 20 photons/pixel.
 - f. Pixel size: 20 nm (X, Y).
 - g. Acquisition time: 3 mins.

TIRF mode

- Same settings as above.
- Penetration depth: 100 nm – 140 nm.
- Evanescent field direction: 0 or 90.

3D GSDIM:

- Uses the cylindrical astigmatism lens approach: 3D calibration files were generated using 80 nm gold nanoparticles following the LAS X wizard.
- Pixel size: 20 nm (X, Y), 50 nm (Z).
- Z-depth: 800 nm.
- Same acquisition settings as 2D GSDIM.
- No pumping or ‘back pumping’ with the 405 nm laser line was used in this study.

2.7. Post-processing

Perform all post-processing using the LAS X software suite for Windows operating systems. Remove the first 30 seconds of data for GSDIM reconstructions. Ensure the detection threshold is consistent between GSDIM reconstructions (here a threshold of 20–30 events/pixel was used). Also ensure that GSDIM reconstructions are visualised using a consistent dynamic range setting; here a range of 0–10 was used. Merged mark-ups of sequential GSDIM reconstructions of the 532 nm and 647 nm channels were visualised by applying false colour; here the 532 nm channel was assigned

magenta and the 647 nm channel was assigned green.

3 Notes

3.1. Optimisation

- Increasing washes decreased non-specific secondary antibody staining; here 5× 5 min washes were performed compared to more commonly employed 3× 5 min washes for confocal imaging.
- Aldehyde-related background fluorescence was reduced using freshly prepared NaBH₄, although this is more suited to glutaraldehyde-based fixation (2) and does not reduce lipofuscin autofluorescence. Sudan Black B (0.1%) treatment which removes lipofuscin autofluorescence was tested, but this significantly impaired photoswitching of both fluorophores used here.
- Adjustment of MEA pH 7.4 to pH 8.5 using HCl improved photoswitching of both the 647 and 532 fluorophores. MEA viability was maintained for much longer when sealing was done using Bondic[®], instead of Twinsil[®] which allowed for imaging of only up to two hours before the photoswitching of fluorophores was impaired. Bondic[®] also allowed for overnight storage at 4°C with minimal impact on photoswitching of both fluorophores.
- Lower laser power (2% for the 532 nm channel and 4% for the 647 nm channel) compared to traditional super-resolution acquisition settings significantly improved signal-to-noise ratio. Importantly, sufficient power was still achieved to satisfy the conditions for SMACM. The majority of background fluorescence seen during these experiments was collected within the first 30 seconds of imaging and could be omitted from the GSDIM reconstruction in post-processing.
- The TIRF capability significantly reduced background fluorescence by limiting the penetration depth of the excitation wavelength to 100–140 nm.
- Antibody titrations were performed to find optimal concentrations. As for confocal microscopy, an Iba1 concentration of 1:1000 was suitable for GSDIM. GSDIM imaging of Syp-immunostaining was significantly improved at a higher antibody concentration

(1:200) compared to the optimal concentration for confocal microscopy (1:500). Interestingly, reduced secondary antibody concentrations (1:500) compared to standard confocal imaging (1:200) significantly reduced background fluorescence generated by GSDIM.

3.2. Further considerations

- Corrections for drift and chromatic aberration may be necessary when performing super-resolution microscopy (3). Potential chromatic aberration occurs when performing multi-channel imaging of spectrally distant fluorophores and may require data transformation determined using multi-colour fluorescent beads. Here, chromatic aberration and drift was tested before and after GSDIM experiments using 100 nm TetraSpeck™ microspheres (T7279, ThermoFisher Scientific) which demonstrated negligible issues (Supplementary Figures) when imaged using the 488 nm, 532 nm, and 642 nm laser lines, and the same acquisition settings described for EPI imaging (see part 2.6.). An additional test for drift was also performed using 40 nm FluoSpheres™ (F8789, ThermoFisher Scientific) and the 642 nm laser line over ~6 mins and was found to be absent.
 - Here, 7 µm paraffin sections were imaged. Tests were also performed on 4 µm thick sections, but there was no significant improvement to background fluorescence. Notwithstanding this, further reduction of section thickness may improve signal-noise ratio. However handling of the sections during the labelling procedure may be more difficult.
 - Other buffer systems may be considered in order to increase the brightness and number of localised events for fluorophores of choice. For instance, BME is an alternative to MEA for AF 647 in particular (4).
 - GSDIM is compatible with many standard fluorophores. A study examining the photoswitching properties of fluorophores provides further information on the photoswitching characteristics of 26 different organic dyes (5).
-

References

1. Sutherland GT, Sheedy D, Stevens J, McCrossin T, Smith CC, van Roijen M, et al. The NSW brain tissue resource centre: Banking for alcohol and major neuropsychiatric disorders research. *Alcohol*. 2016;33-9.
2. Whelan DR, Bell TD. Image artifacts in single molecule localization microscopy: why optimization of sample preparation protocols matters. *Sci Rep*. 2015;5:7924.
3. Herrmannsdörfer F, Flottmann B, Nangneri S, Venkataramani V, Horstmann H, Kuner T, et al. 3D d STORM Imaging of Fixed Brain Tissue. *Methods Mol Biol*. 2017;1538:169-84.
4. Thevathasan JV, Kahnwald M, Cieśliński K, Hoess P, Peneti SK, Reitberger M, et al. Nuclear pores as versatile reference standards for quantitative superresolution microscopy. *Nature Methods*. 2019;16(10):1045-53.
5. Dempsey GT, Vaughan JC, Chen KH, Bates M, Zhuang X. Evaluation of fluorophores for optimal performance in localization-based super-resolution imaging. *Nat Methods*. 2011;8(12):1027-36.

Rigorous study design and transparent reporting of results are the cornerstones of science. By maximizing the information provided in a manuscript, factors that may contribute to irreproducibility will be mitigated. The *Journal of Neuroscience Research* promotes transparency in research by strongly encouraging authors to include all relevant information about their studies (see our [preprint](#) for details). To expedite reviewer monitoring of these factors, authors submitting original research articles must complete this questionnaire.

If the manuscript is accepted and all items within the checklist are present, we will include a declaration of transparency at the end of the manuscript. This declaration reads as follows:

The authors, reviewers and editors affirm that in accordance to the policies set by the Journal of Neuroscience Research, this manuscript presents an accurate and transparent account of the study being reported and that all critical details describing the methods and results are present.

To complete the checklist, fill in the right-hand column with the page and paragraph number (e.g., 'Page 3, Paragraph 2') corresponding to the checklist item. If a checklist item is not applicable to the study being reported or the authors are unable to provide that item, a reason must be supplied. Additional comments can be added at the end of the document. Upload the completed document as supplementary information for review.

Experimental and Study Design

1. Clearly state the primary and any secondary objective or hypothesis of the study	Abstract; Significance statement; Page 4, Paragraph 1, last sentence.
2. For each experiment, the study design must include:	2a
a. Number of experimental and control groups	Mouse: Page 6, Paragraph 2
b. Randomization and blinding procedures and/or steps to minimize subjective bias when allocating subjects to experimental groups	Zebrafish: Page 7, Paragraph 2
c. Precise details of all procedures, including housing and husbandry are carried out in the experiment	Human: Page 5, Paragraph 1
d. Is sex considered as a biological variable? See Editorial for details about proper reporting	2b
	Mouse: N/A
	Zebrafish: N/A
	Human: Page 5, Paragraph 1, Page 10 (Statistics)
	2c
	Mouse: Page 6, Paragraphs 1 & 2; Page 8, Paragraphs 1 & 2
	Zebrafish: Page 7, Paragraphs 1, 2, & 3; Page 8, Paragraph 2
	Human: Pages 5 & 9; Supplementary Methods
	2d
	Mouse: Page 6, Paragraph 2
	Zebrafish: Page 7, Paragraph 1
	Human: Pages 10, Statistics; 18, Conclusions; Table 1

Experimental Subjects

3. Specify the total number of subjects in each experiment, including the number of animals, sex and age in each group	3
a. Explain how the number of animals were arrived at and provide details of any sample size calculation, including power analysis	Mouse: Page 6, Paragraph 2
b. Indicate the number of independent replications of each experiment, when applicable	Zebrafish: Page 7, Paragraph 2

Human: Page 5, Page 9
Paragraph 2, Page 11
Paragraph 2

3a

Mouse: Page 6,
Paragraph 2 (*this was a
reproduction experiment;
the underlying paper has
more than 400 citations*)

Zebrafish: Page 7,
Paragraph 2

Human: Page 5, Page 9

3b

Mouse: Page 6,
Paragraph 2 (*probably
hundreds of times locally
and in the literature*)

Zebrafish: Page 7,
Paragraph 2

Human: Page 5; Page 11;
Table 1 (Page 24)

Data Handling

4. Indicate data collection start and stop rules:

- Define the criteria for data/subject inclusion and exclusion. If any outcome or condition measure used was not reported in the results section, authors must address this omission
- Specify reasons for any discrepancy between the number of animals at the beginning and end of the study
- Define and explain how outliers are handled and report if data are removed prior to analysis

4a

Mouse: Page 8,
Paragraphs 1 & 2

Zebrafish: Page 8,
Paragraph 2

Human: Page 9;
Supplementary Methods

4b

Zebrafish:
See Page 7 Paragraph 2

4c

Human:
Exclusion of case AD 4
(missing ABC score data)
& Non-AD Control 1
(tissue unavailable); see
Table 1.

Statistical Analysis and Depiction of Continuous Data

5. Provide details of the statistical methods used for each analysis

- State, define and justify the statistical analysis used and specify the unit of analysis for each dataset
- Describe and report methods used to assess whether data met the assumptions of the statistical approach and any adjustments for multiple comparisons
- Fully report statistics (including exact value of N, degrees of freedom, test value and exact P-value when >0.001) and we encourage the use of effect sizes and confidence intervals
- Disaggregated data are presented for males and females
- Data distribution is depicted with univariate scatterplots boxplots, violin plots, or kernel density plots when presenting **continuous data** (see Editorial [Publishing Transparent and Rigorous Scientific Research](#))

Page 9–10

"

"

"

"

e. Figures 5–7.

Discussion

- Comment on study limitations including any potential source of bias, limitations to the animal model, imprecisions associated with the results, and the inability for any reason to study possible sex influences where they may exist.
- Comment on possible translational implications and future research directions

Page 17–18 (Conclusions)

Page 14; Page 15;

Chapter 5: Gene amplification studies

5.1 Preamble

The first three Results chapters presented in this thesis were histopathological studies performed in post-mortem human brain tissues. Post-mortem investigations are retrospective studies which may be unable to distinguish cause and effect. Therefore, it was of interest to perform a prospective molecular study in order to gain greater clarity into gene expression responses to A β over time. A β was selected for investigation since the earlier post-mortem human studies suggested it represents the earliest pathological change in AD cortical tissue and showed better correlation to morphological markers of activation; contrasting with tau pathology which correlated better with degenerative changes. The molecular work was performed in mouse BSCs treated for eight or 72 hours with two or 10 μ M of synthetic preparations of monomeric or fibrillar species of A β . Published results from a gene amplification study in two regions of post-mortem human brain are also included (Guennewig et al., 2021). The overarching intention of this chapter was to characterise some of the changes to gene expression profiles at different timepoints in various models of disease. This work was done in collaboration with Dr Giuseppe D. Ciccotosto at The University of Melbourne, Dr Markus J. Hofer, and Barney Viengkhou both at The University of Sydney. GDC advised on handling of the A β peptides as well as dosage and culture durations.

5.2 Authorship attribution statement

This chapter contains material published in ‘Defining early changes in Alzheimer’s disease from RNA sequencing of brain regions differentially affected by pathology’ (Guennewig et al., 2021). The manuscript was authored by Boris Guennewig, Julia Lim, Lee Marshall, Andrew N. McCorkindale, Patrick J. Paasila, Ellis Patrick, Jillian J. Kril, Glenda M. Halliday, Antony A. Cooper, and Greg T. Sutherland (corresponding author). PJP performed the ddPCR assays and related analyses, the Methods for which appear here in sections 5.4.6, 5.4.7, and 5.4.8 and the Results in section 5.5.2 and Figure 7. The published manuscript appears in the Appendix of this thesis.

Attestation

In addition to the statement above, permission to include the published material has been granted by the corresponding author.

Patrick J. Paasila

Candidate

June 2021



Greg T. Sutherland

Corresponding author

June 2021

5.3 Introduction

The cellular and molecular complexity of the brain brings with it significant challenges to understanding chronic multifactorial diseases like AD. Organotypic BSCs have been increasingly used to better understand molecular mechanisms of health and disease of the CNS (Croft et al., 2019a; Humpel, 2015), especially given the distinct phenotypes displayed by microglia *in vivo* versus primary cell culture (Butovsky et al., 2014). A past study of hippocampal slice cultures used exogenous A β _{28, 25–35, 40} species to examine effects on neuronal health; where only A β ₄₀ appeared to produce neurodegenerative changes (Malouf, 1992). A later investigation was able to induce Thioflavin S-positive A β plaques in hippocampal slice cultures following seeding with brain extract from *APP* transgenic mice and continual supplementation with synthetic A β species (Novotny et al., 2016). Other BSC models using single *APP* mutants (Harwell & Coleman, 2016), transgenic mice with two fAD mutations (*APP* and *PSEN1*) and one *MAPT* mutation (3xTg mice) (Croft et al., 2017), or 5xTg mice (carrying a total of five mutations in *APP* and *PSEN1*) (Hellwig et al., 2016) have demonstrated small diffuse deposits of A β , but with tau abnormalities and gliosis which poorly mimic the human disease. The role of microglia in the clearance of A β plaques has also been studied using BSCs from rats (Fan & Tenner, 2004). Rat hippocampal BSCs treated with synthetic soluble or fibrillar A β ₄₂ showed uptake of the peptides by pyramidal neurons to cause an upregulation of C1q—which is associated with thioflavin-positive plaques and activated microglia in AD brains (Afagh et al., 1996). TREM2 deficiency has also been investigated in BSCs, in which microglia displayed an impaired migratory capacity in response to neuronal injury (Mazaheri et al., 2017).

The role of microglia in the pathogenesis of AD is increasingly appreciated due to findings from GWAS of AD which have demonstrated the enrichment of myeloid cell genes—particularly microglial—amongst common risk variants (Jones et al., 2015; Pimenova et al., 2018; Podleśny-Drabiniok et al., 2020). These genes include *Trem2* (Keren-Shaul et al., 2017; Krasemann et al., 2017) and *Cd68* (Castanho et al., 2020; Grubman et al., 2021), both involved in microglia-mediated phagocytosis and associated with A β plaques in AD mouse models. Interestingly, *Trem2* has been

implicated in the development of both neuroprotective DAM (Keren-Shaul et al., 2017) and neurodegenerative pro-inflammatory MGnD (Krasemann et al., 2017). As such, there remains critical work to be done to resolve the causes and effects of pro- or anti-inflammatory responses of microglia in AD.

In the work presented here, coronal BSCs of mouse cerebral hemispheres were used to characterise gene expression responses following treatment with different preparations of synthetic A β ₄₂. Genes of interest included those involved in phagocytosis such as *Trem2* and *Cd68* and those highly expressed by microglia such as *Itgam*, *Ptprc*, and *Aif1*—the lattermost also as a follow up from the Iba1 IHC studies in post-mortem human tissue. The suitability of BSCs for examining microglial responses were tested using IFN α and several IFN-stimulated genes, including *Eif2ak2* (Schoggins, 2019), *Isg15* (Zhang & Zhang, 2011), and *Oasl2* (Leisching et al., 2017). This also provided an opportunity to compare gene expression responses to A β with a broadly pro-inflammatory mediator. *Chrna7* was also selected for investigation as it encodes the α 7nAChR—an important anti-inflammatory mediator associated with protective polymorphisms among non-carriers of *APOE* ϵ 4 (Weng et al., 2016)—and a (potential) receptor for A β binding (Dineley, 2007). Finally this chapter sought to link the animal work here to subsequent findings of an RNA-Seq study of the PreC and PVC from AD and control brains (Guennewig et al., 2021).

5.4 Methods

5.4.1 Animal handling

All animal work carried out here was approved by the Animal Ethics Committee (AEC, #2017/1216), Research Integrity and Ethics Administration, The University of Sydney. Animal experiments complied with the Animal Research Act of NSW (1985) and the Australian code for the care and use of animals for scientific purposes (2013), National Health and Medical Research Council (NHMRC) of Australia. Mice were held in a secure licenced facility at the Molecular Bioscience Building (G08), The University of Sydney, Darlington NSW 2008. Three sets of

one male to three female mice were housed in a temperature-controlled room maintained on a 12-hour light-dark cycle. Food and water were made available to mice *ad libitum* as well as bedding and environmental enrichment. For BSCs, 24 three-day old neonates were required for two groups of eight experimental groups, each performed in triplicate.

5.4.2 Preparation of A β solutions

Monomerisation of peptides

Synthetic A β_{42} peptides were purchased from The ERI Amyloid Laboratory (Oxford, Connecticut, United States). All handling procedures for A β peptides were performed as previously published by a collaborator (Jana et al., 2016), but with minor modifications. Given their natural propensity to aggregate, monomerisation of the peptides was performed for two hours at RT with 1 mg/mL 1,1,1,3,3,3-hexafluoro-2-propanol (HFIP; >99%) (catalogue #105228, Sigma-Aldrich, Merck Group). Complete monomerisation of pre-aggregated A β can be visualised when the peptide-HFIP solution changes from cloudy to transparent. Monomerised solutions were aliquoted evenly into new tubes (~1 mg/tube) with screw-top lids fitted with rubber rings and placed open into a Genevac centrifugal solvent evaporator (EZ-2 series; SP Scientific, Harbour Group, Warminster, Pennsylvania, United States) for 30 minutes set to the ‘low boiling point’ programme for chemicals with a boiling point between 40–90°C (58.2°C, HFIP), where risk of bumping during evaporation is low. The tubes containing the dried A β monomers were closed, sealed with parafilm, and stored at –80°C until required.

Resuspension of peptides

Fresh solubilised A β solutions were prepared on ice before the experiment. Monomers were first dissolved in 130 μ L of sodium hydroxide (NaOH; 60 mM). The peptide-NaOH solutions were vortexed for 10 seconds, ultrasonicated in an iced water bath for 15 minutes, and then diluted with 455 μ L of water and 65 μ L of 10 \times phosphate buffered saline (PBS; pH 7.4) (final ratio of 2:1:7). The total volume of solvent for 1 mg peptide/tube was 650 μ L, yielding a theoretical concentration

of $\sim 340.8 \mu\text{M}$ A β_{42} per tube (the average molecular weight of the peptide as reported by the supplier was $4514.1043 \text{ g}\cdot\text{mol}^{-1}$). To accurately determine the concentration of monomers, the optical density (OD) at 214 nm (Figure 1a) of a 1/100 dilution of the peptide solution was measured in a 100 μL freshly cleaned (using 2% Hellmanex II detergent, water, then ethanol rinse) quartz cuvette using a DU[®] 800 UV/Visible Spectrophotometer (Beckman Coulter, Danaher Corporation, Washington D. C., United States). The sample concentration was calculated using a pathlength of 1 cm and a molar extinction coefficient of $75,887 \text{ L}\cdot\text{mol}^{-1}\text{cm}^{-1}$ (Ciccotosto et al., 2004; Jana et al., 2016).

SDS-PAGE electrophoresis

Samples were mixed with 4 \times Laemmli buffer (catalogue #1610747; Bio-Rad Laboratories, Hercules, California, United States) and heated at 95°C for 5 minutes followed by centrifugation for 10 seconds at 16,000g. A protein standard (catalogue #LC5925; Thermo Fisher Scientific) and samples were equilibrated to RT and then loaded into a 7.5% TGX Stain-Free[™] FastCast[™] gel (catalogue #1610181; Bio-Rad Laboratories). Gels were run at 200 V for 45 minutes in running buffer containing tris (25 mM), glycine (192 mM), and SDS (3.5 mM) and were then transferred to a PVDF membrane (catalogue #1704272; Bio-Rad Laboratories) pre-soaked in methanol (100%) and transfer buffer containing tris (25 mM), glycine (192 mM), and methanol (20%). Transfer was performed over 30 minutes with a Trans-Blot Turbo Transfer System (catalogue #1704150; Bio-Rad Laboratories).

Western blot

PVDF membranes were rinsed in water and washed with 1 \times tris buffered saline with 0.01% polysorbate 20 (TBST). Membranes were incubated in blocking buffer containing 5% skim milk diluted in 1 \times TBST for one hour at RT. Membranes were incubated in primary antibodies (either 6E10 monoclonal antibody, catalogue #803001, BioLegend, San Diego, California, United States; or an in-house W02 monoclonal antibody supplied by a collaborator, GDC) diluted in blocking buffer for 14 hours at 4°C. Membranes were rinsed once and then washed three times for five minutes in 1 \times TBST. Secondary incubation was performed with horseradish

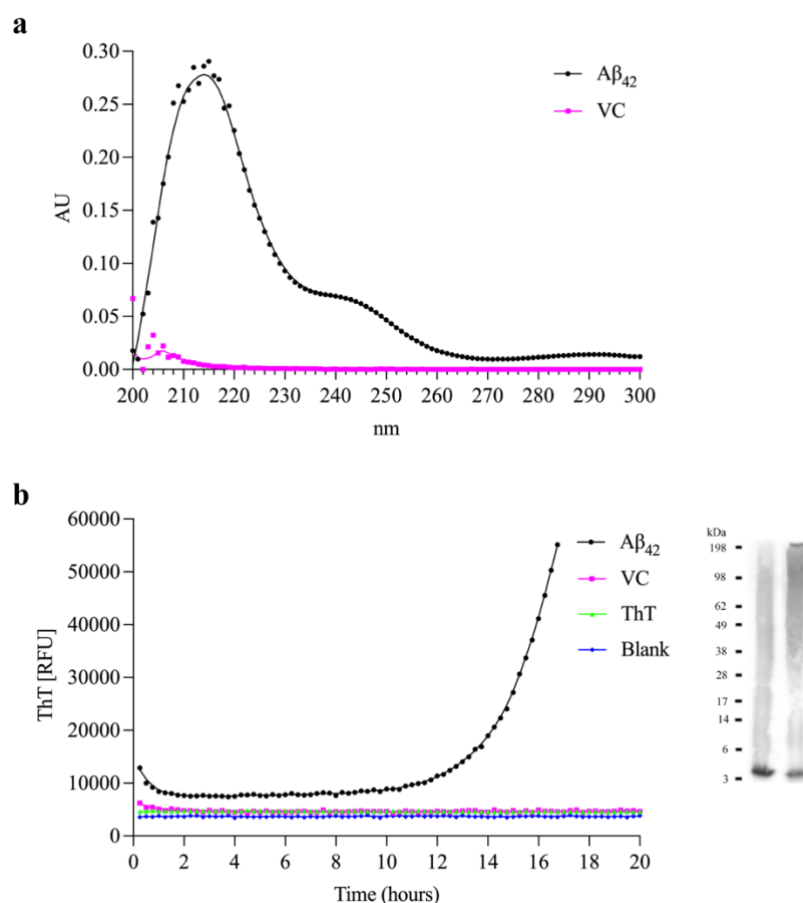


Figure 1. Preparations of A β_{42} peptides. **a** Absorbance over 200–300 nm of a 1 in 100 dilution of A β_{42} monomers and vehicle control (VC) fitted with a local regression line. OD₂₁₄ in the given exemplar corresponds to ~0.275 AU, equating to ~362.4 μ M. **b** ThT aggregation assay showing relative fluorescence of A β_{42} fibrillisation during incubation at 37°C for 20 hours. Western blots of A β_{42} aggregates were visualised using a 6E10 monoclonal antibody (left) and an in-house W02 monoclonal antibody (right). A prominent band at ~4.5 kDa is visible and represents A β_{42} monomers. Local regression curves are also provided for VC (magenta), ThT-only solution (green), and blank (blue).

peroxidase (HRP)-conjugated anti-mouse IgG antibodies (catalogue #7076; Cell Signaling Technology, Danvers, Massachusetts, United States) diluted 1:5000 in blocking buffer for two hours at RT followed by a rinse and three five-minute washes with 1 \times TBST. All incubations were performed with gentle agitation, ensuring complete submersion. Membranes were developed using Clarity Western enhanced chemiluminescence (ECL) Substrate (catalogue #1705060; Bio-Rad Laboratories) for five minutes. Imaging was performed using a ChemiDocTM XRS+ System (catalogue #1708265; Bio-Rad Laboratories) with an exposure time of one second.

A β ₄₂ fibrillisation and Thioflavin T (ThT) aggregation assay

A β ₄₂ fibrils were generated by incubating resuspend monomers for 20 hours at 37°C with gentle agitation (Jana, 2016). Fibrillisation kinetics were determined by quantification of Thioflavin (ThT) fluorescence (Biancalana & Koide, 2010; Younan & Viles, 2015) (catalogue #T3516; Sigma-Aldrich, Merck Group). ThT assays were performed with 100 μ L solutions containing 20 μ M monomers and 50 μ M ThT (diluted with water) in a clear flat-bottom 96-well polystyrene plate (catalogue #655161; Greiner Bio-One, Frickenhausen, Baden-Württemberg, Germany) sealed with cling wrap. Fluorescence was measured every 15 minutes immediately after five seconds of orbital agitation using an Infinite® M1000 Pro Plate Reader (catalogue #106061; Tecan Group, Männedorf, Kanton Zürich, Switzerland). An excitation wavelength of 450 nm and an emission filter set to 490 nm (5 nm bandwidth) were used during the assay. ThT-A β ₄₂ solutions were initially yellow in colour but changed to transparent after 20 hours of cycling. A vehicle-only, ThT only, and blank were included as controls (Figure 1b).

5.4.3 Isolation of brain slices

Isolation and culture of mouse brain slices were performed according to previously published work by a collaborator (Friedl et al., 2004) but with minor modifications. Neonates were decapitated as per recommendation and the brain removed (Figure 2). The brainstem and cerebellum were removed immediately, and the remaining tissue was placed in cold dissection media (~4°C) containing 48.75% Minimum Essential Medium α (catalogue #32561037; Thermo Fisher Scientific, Waltham, Massachusetts, United States); 48.75% Hanks' Balanced Salt Solution (catalogue #H6648; Sigma-Aldrich, Merck Group, Darmstadt, Hesse, Germany); and 2.5% HEPES (1M) (catalogue #15630106; Thermo Fisher Scientific). The cerebral hemispheres were separated and most of the meninges removed. Hemispheres were transferred onto a Teflon disc mounted on a tissue chopper in a rostrocaudal orientation (McIlwain Model TC752; Campden Instruments Limited, Loughborough, Leicestershire, United Kingdom). Between 14–16 coronal slices of 375 μ m thickness were isolated per hemisphere. All of the slices isolated from one hemisphere were placed onto one slice culture insert (Millicell® cell culture insert,

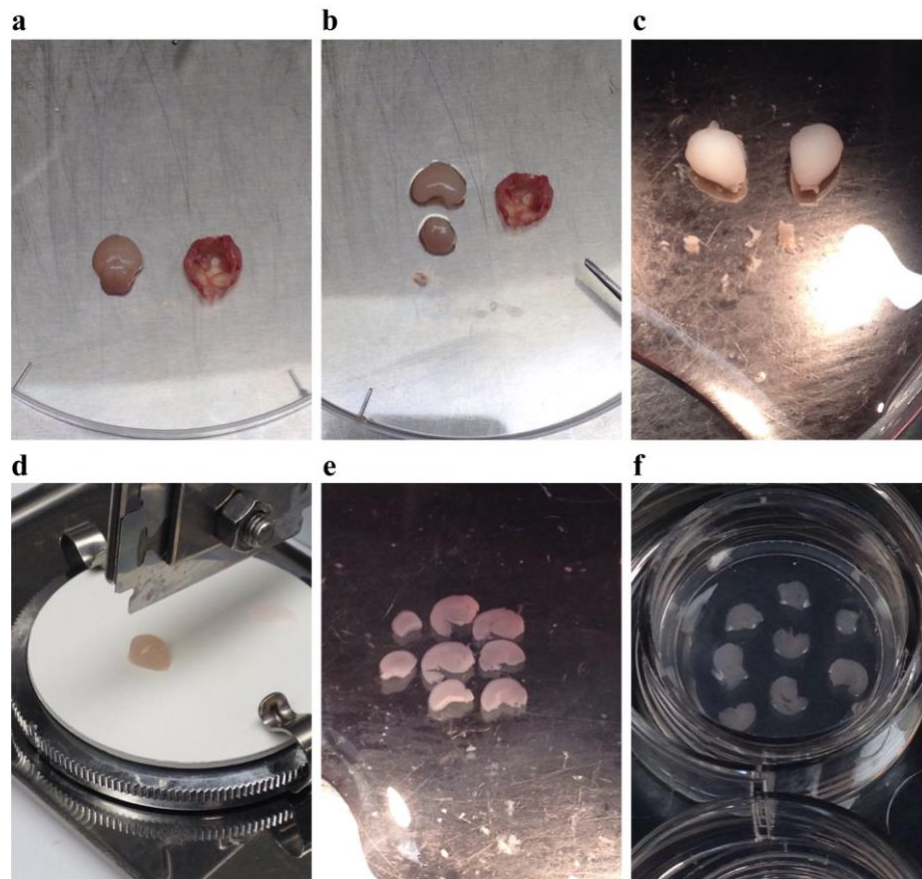


Figure 2. Isolation of neonatal mouse brain slice cultures. **a–b** The brain is removed from the caput (**a**) and the brainstem and cerebellum separated from the cerebrum and midbrain (**b**). **c** The brain is placed into cold dissection media and the hemispheres are separated. **d** The cerebral hemispheres are placed one at a time onto a Teflon disc mounted on a tissue chopper with an automatic chopping arm fixed with a blade. **e** The hemisphere is carefully collected with a spatula and transferred back to the dissection media and the slices are separated from each other. **f** The slices are then transferred to a 6-well plate containing culture inserts on 1.2 mL of incubation media.

catalogue #PICM03050 or equivalent #PICM0RG50; Millipore, Merck Group) over 1.2 mL incubation media containing 37.5% Minimum Essential Medium α ; 35% Hanks' Balanced Salt Solution; 25% heat inactivated horse serum (catalogue #H1138; Sigma-Aldrich, Merck Group); and 2.5% HEPES (1M).

5.4.4 Culture procedures

In total, 48 hemispheres from 24 neonates were divided into two groups of eight experimental groups, each in triplicate. Slices were cultured for 48 hours before experimentation, with one change of media at 24 hours. Group 1 were cultured for eight hours and Group 2 were cultured for 72 hours, without any further media

changes. The groups included: media control, vehicle control, A β monomers at 2 μ M and 10 μ M, fibrils at 2 μ M and 10 μ M, murine recombinant IFN α A (1 U/ μ L; catalogue #18782; Sigma-Aldrich, Merck Group) positive control, and H₂O₂ (0.1%) negative control. A β , IFN α A, and H₂O₂ solutions were all prepared with incubation media. Peptide concentrations and treatment lengths were based on previous work published by a collaborator, GDC, in which supraphysiological concentrations of A β ₄₂ (15 μ M) produced neurotoxic effects after 72 hours while lower concentrations (5 μ M) were well tolerated by cultured neurons (Jana et al., 2016).

5.4.5 ddPCR of mouse samples

RNA isolation and cDNA synthesis

RNA was extracted from each cultured hemisphere using TRIzol reagent (catalogue #T9424; Sigma-Aldrich, Merck Group) and the ISOLATE II RNA Mini Kit (catalogue #BIO-52072; Bioline, Meridian Bioscience, Cincinnati, Ohio, United States). DNase I treatment was also performed on columns for 15 minutes at RT. RNA was eluted with 40 μ L RNase free water and stored at -30°C until cDNA synthesis using the SensiFASTTM cDNA Synthesis Kit (catalogue #BIO-65053; Bioline, Meridian Bioscience). cDNA synthesis was performed using 500 ng of RNA. RNA concentration and RNA Integrity Number (RIN) was measured using a 2100 Bioanalyzer Instrument (catalogue #G2939BA; Agilent Technologies, Santa Clara, California, United States), nanochip, reagents (catalogue #5067-1511; Agilent Technologies), and ladder (catalogue #5067-1529; Agilent Technologies).

Conventional PCR (cPCR)

Primers for genes of interest (Table 1) were tested by cPCR before proceeding to ddPCR (Figure 3). cPCR was performed using the MyTaqTM DNA Polymerase Kit (catalogue #BIO-21105; Bioline, Meridian Bioscience). Reaction mixes (10 μ L, total) included 50 ng template (cDNA quantities listed in Table 1 pertain only to ddPCR assays), 1 \times reaction mix (including DNA polymerase), and 100 nM forward and reverse primers. Reaction mixes were cycled with the following conditions:

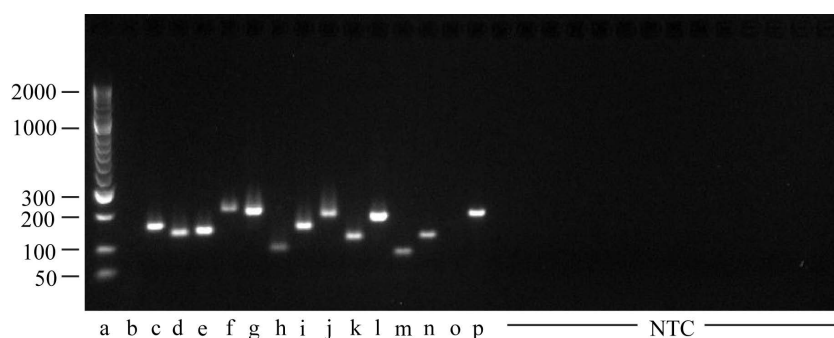


Figure 3. cPCR of genes of interest. Bands for each gene of interest occur at the expected level; a–ladder; b–no reverse transcriptase control; c–*Actb*; d–*Aif1*; e–*Cd68*; f–*Chrna7*; g–*Gapdh*; h–*Hprt*; i–*Itgam*; j–*Ptprc*; k–*Tbp*; l–*Trem2*; m–*Eif2ak2*; n–*Isg15*; o–*Mx1* (failed; excluded from further analysis); p–*Oasl2*; the remaining wells show negative results for the no template controls (NTC), which appear in the same order.

95°C (1 minute) → 35×[95°C (15 seconds) → 60°C (15 seconds) → 72°C (10 seconds)] → 4°C (hold). Samples were mixed with 2.5 µL of loading buffer and transferred to the gel with the HyperLadder™ 50bp molecular marker (catalogue #BIO-33054; Bioline, Meridian Bioscience). Electrophoresis using 2% agarose gels was performed at 100 V for one hour in 1×TBE running buffer. The agarose gel (100 mL) was pre-stained with Invitrogen™ SYBR™ Safe DNA Gel Stain (catalogue #S33102; Thermo Fisher Scientific) at a concentration of 1/10000. Gels were imaged using a ChemiDoc™ System (Bio-Rad Laboratories) with 2s exposure.

Table 1. Murine genes of interest.			
Gene name	Primer sequences	Amplicon (bp)	cDNA (ng)
Actin beta	Forward 5'-GGCTGTATTCCCCTCCATCG-3' Reverse 5'-CCAGTTGGTAACAATGCCATGT-3'	154	6.25
Allograft inflammatory factor 1	Forward 5'-CAGACTGCCAGCCTAAGACA-3' Reverse 5'-AGGAATTGCTTGTTGATCCC-3'	132	25
Cd68 molecule	Forward 5'-ACTTCGGGCCATGTTTCTCT-3' Reverse 5'-GCTGGTAGGTTGATTGTCGT-3'	138	25
Cholinergic receptor nicotinic alpha 7 subunit	Forward 5'-CCGTGTACTTCTCCCTGAGC-3' Reverse 5'-AAGCGTTCATCTGCACTGTTA-3'	211	50

Glyceraldehyde-3-phosphate dehydrogenase	Forward 5'-TGCGACTTCAACAGCAACTC-3' Reverse 5'-CTTGCTCAGTGTCTTGCTG-3'	199	6.25
Hypoxanthine guanine phosphoribosyl transferase	Forward 5'-AGTCCCAGCGTCGTGATTAG-3' Reverse 5'-TTCCAAATCCTCGGCATAATGA-3'	87	50
Integrin subunit alpha M	Forward 5'-CCATGACCTTCCAAGAGAATGC-3' Reverse 5'-ACCGGCTTGTGCTGTAGTC-3'	147	50
Protein tyrosine phosphatase receptor type C	Forward 5'-GTTTTGCTACATGACTGCACA-3' Reverse 5'-AGGTTGTCCAAGTACATCTTTC-3'	195	50
TATA-box binding protein	Forward 5'-CCTTGTACCCTTCACCAATGAC-3' Reverse 5'-ACAGCCAAGATTCACGGTAGA-3'	119	12.5
Triggering receptor expressed on myeloid cells 2	Forward 5'-CTGGAACCGTCACCATCACTC-3' Reverse 5'-CGAAACTCGATGACTCCTCGG-3'	183	12.5
Eukaryotic translation initiation factor 2 alpha kinase 2	Forward 5'-GTTGTTGGGAGGGAGTTGAC-3' Reverse 5'-AGAGGCACCGGGTTTTGTAT-3'	75	50
Interferon-stimulated gene 15	Forward 5'-GAGCTAGAGCCTGCAGCAAT-3' Reverse 5'-TTCTGGGCAATCTGCTTCTT-3'	122	50
2'-5' oligoadenylate synthetase-like 2	Forward 5'-GGATGCCTGGGAGAGAATCG-3' Reverse 5'-TCGCCTGCTCTTCGAAAC-3'	194	50

ddPCR assays

Reaction mixtures were made up to 20 μ L with final concentrations of 1 \times EvaGreen Supermix (catalogue # 1864034; Bio-Rad Laboratories), 100 nM of forward and reverse primers, and cDNA concentrations given in Table 1. Reaction mixtures were divided into droplets using the QX200 Droplet Generator (catalogue #1864002; Bio-Rad Laboratories) and cycled in a C1000 Touch™ Thermal Cycler (catalogue #1851197; Bio-Rad Laboratories) using the following conditions: 95°C (5 minutes) \rightarrow 40 \times [95°C (30 seconds) \rightarrow 60°C (1 minute)] \rightarrow 4°C (5 minutes) \rightarrow

90°C (5 minutes) → 4°C (hold); sample volume of 40 µL (which includes an additional 20 µL of oil from droplet generation); lid temperature of 105°C; and ramp rate of 2°C/second. Transcript abundance was measured using the FAM and HEX/VIC channels of the QX200 Droplet Reader (catalogue #1864003; Bio-Rad Laboratories). All primers were optimised before the main experiment to ensure clear separation of positive and negative droplet fractions (Figure 4). Primers were either retrieved from PrimerBank (Wang et al., 2012) (<https://pga.mgh.harvard.edu/primerbank/>) or designed using PrimerBlast (Ye et al., 2012) (<https://www.ncbi.nlm.nih.gov/tools/primer-blast/>) and were manufactured by Integrated DNA Technologies Australia Pty Ltd. The ddPCR system provides absolute quantification of transcripts based on a Poisson distribution of positive and negative EvaGreen fluorescence of droplets. Raw concentrations of transcripts were normalised as the quotient of genes of interest over *Tbp*. *Tbp* was selected empirically from three other potential reference genes, including *Actb*, *Gapdh*, and *Hprt*, as it showed greatest stability across treatment groups.

5.4.6 Human cohort

Results from the ddPCR assays of human genes of interest (Table 2) have been published previously (Guennewig et al., 2021). Use of human tissue was carried out in accordance with the Declaration of Helsinki and following ethics approval from Human Research Ethics Committee, The University of Sydney (HREC #2012/161). Deidentified samples were supplied by the New South Wales Brain Banks (NSWBB) which include the Sydney Brain Bank (SBB) at Neuroscience Research Australia (NeuRA) and the NSW Brain Tissue Resource Centre (NSWBTRC) at The University of Sydney following approval from their Scientific Advisory Committee. NSWBB provided information on age, sex, dementia status, CDR, neuropathological diagnostics (ABC score), cause of death, post-mortem interval (PMI), and brain pH. Formalin-fixed paraffin embedded (FFPE) sections (10 µm) and 100 mg frozen tissue from the contralateral hemisphere of the PreC and PVC were obtained from 26 Braak stage VI AD cases and 22 controls matched for age, sex, and *APOE* status.

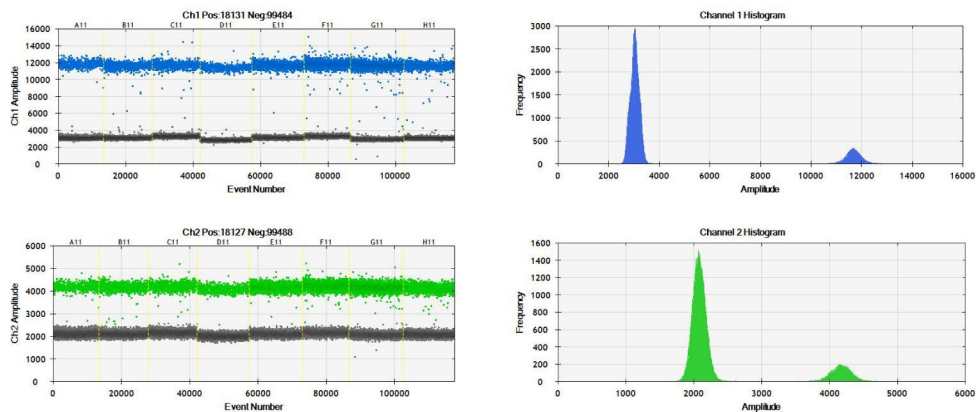


Figure 4. ddPCR assay output. An exemplar showing the clear separation of positive (coloured) and negative (dark grey) droplets in both the FAM (blue) and HEX/VIC (green) channels using EvaGreen Supermix and the QX200 ddPCR system (sample results are for *Aif1*).

5.4.7 ddPCR of human samples

RNA isolation and cDNA synthesis

RNA was isolated from 30 mg of brain tissue using TRIzol reagent and the Invitrogen™ PureLink™ RNA Mini Kit (catalogue #12183025; Life Technologies, Thermo Fisher Scientific). DNase I treatment was performed on columns for 15 minutes at RT. RNA was eluted with RNase free water and stored at -80°C until cDNA synthesis using the SensiFAST™ cDNA Synthesis Kit (catalogue #BIO-65053; Bioline, Meridian Bioscience). cDNA synthesis was performed using 1000 ng of RNA. RIN was measured using a 2100 Bioanalyzer Instrument, nanochip, reagents, and ladder (Agilent Technologies).

ddPCR assays

Reaction mixtures were made up to 20 μL with final concentrations of $1\times$ EvaGreen Supermix, 50 nM of forward and reverse primers, and 100 ng cDNA. Reaction mixtures were processed in the QX200 Droplet Generator and cycled in the C1000 Touch™ Thermal Cycler using the conditions described earlier. Transcript abundance was measured using the QX200 Droplet Reader. All primers were optimised before the main experiment to ensure clear separation of positive and

negative droplet fractions. Primers for the genes of interest (listed in Table 2) were selected based on the most significant differentially expressed genes (DEGs) in the RNA-Seq analysis of human PreC and PVC (Guennewig et al., 2021). Primers were designed using PrimerBlast (Ye et al., 2012) and were manufactured by Integrated DNA Technologies Australia Pty Ltd. *GAPDH* was empirically selected as a reference gene out of three others: *HMBS*, *HPRT1*, and *GFAP*. Positive correlations between *GAPDH* and the genes of interest with RIN were similar, thereby controlling for the effects of antemortem (agonal) factors, as previously described (Mills et al., 2014). As previously discussed by Mills et al. (2014) this approach attempts to deal with both the effects of varying RNA quality and agonal period-related gene expression. Raw concentrations of transcripts were normalised as the quotient of genes of interest over *GAPDH*.

Table 2. Human genes of interest.		
Gene name	Primer sequence	Amplicon (bp)
C-X-C motif chemokine receptor 4	Forward 5'-GAGTGCTCCAGTAGCCACC-3' Reverse 5'-GCCCATTTCTCCTCGGTGTAGT-3'	94
Glyceraldehyde 3-phosphate dehydrogenase	Forward 5'-AAATCAAGTGGGGCGATGCT-3' Reverse 5'-CAAATGAGCCCCAGCCTTCT-3'	86
Insulin receptor	Forward 5'-GGACCAGGCATCCTGTGAAA-3' Reverse 5'-GGGCCTCTTTGTAGAACAGCA-3'	143
Insulin-like growth factor 1 receptor	Forward 5'-AGGAATGAAGTCTGGCTCCG-3' Reverse 5'-CCGCAGATTTCTCCACTCGT-3'	105
Membrane spanning 4-domains A6A	Forward 5'-GCTGATTTGCACTCTGCTGG-3' Reverse 5'-GCAGGAAAAGTACACTCCCAGG-3'	101
Parvin gamma	Forward 5'-AAATGCTGCACAACGTCACC-3' Reverse 5'-AGGCAGTGAGGGTCAATTCTG-3'	200
Solute carrier family 7 member 2	Forward 5'-CCATTTTCCCAATGCCTCGTG-3' Reverse 5'-GAAAGGCCATCAAAGCTGCC-3'	144
Somatostatin	Forward 5'-ACCCAGACTCCGTCAGTTT-3' Reverse 5'-AGTACTTGGCCAGTTCCTGCT-3'	71
Triggering receptor expressed on myeloid cells 2	Forward 5'-TGCTGGCAGACCCCTG-3' Reverse 5'-GAAGGATGGAAGTGGGTGGG-3'	147

5.4.8 Statistics

Normal distribution was tested by Shapiro-Wilk test. For mouse BSCs, differences of means were tested using Welch's ANOVA with Brown-Forsythe test and Dunnett's T3 test for multiple comparisons. For human samples, differences of means were tested using Welch's T test for parametric data with F test of equality of variances or Mann-Whitney U test for non-parametric data. Spearman ρ was calculated for correlations with RIN, brain pH, and age. All statistical analyses and graphing were performed in GraphPad Prism (GraphPad Software; San Diego, California, United States).

5.5 Results

5.5.1 ddPCR of mouse BSCs

Reference genes

Tbp showed the greatest stability amongst the tested reference genes across the treatment groups (Figure 5). *Actb* and *Gapdh* showed reduced expression particularly in BSCs treated with monomeric A β (mA β ; 2 & 10 μ M) for 72 hours (hrs). *Hprt* showed increased expression following treatment with mA β (2 μ M, 8 hrs) and fibrillar A β (fA β ; 10 μ M, 72 hrs). Therefore, *Tbp* was used for the normalisation of the genes of interest. The mean RIN value for all BSC samples was 9.2 ± 0.5 (standard deviation; SD).

Genes of interest

The genes of interest included three myeloid markers expressed by microglia, genes involved in microglia-mediated phagocytosis, and three IFN stimulated genes (Figure 6). *Aif1* showed relatively stable expression, though was non-significantly reduced following 8 hrs treatment with mA β (10 μ M) and fA β (2 μ M). *Itgam* also showed relative stability, though trended lower with IFN α over 72 hrs. *Ptprc* showed increased expression in BSCs treated with 2 μ M fA β for 72 hrs compared

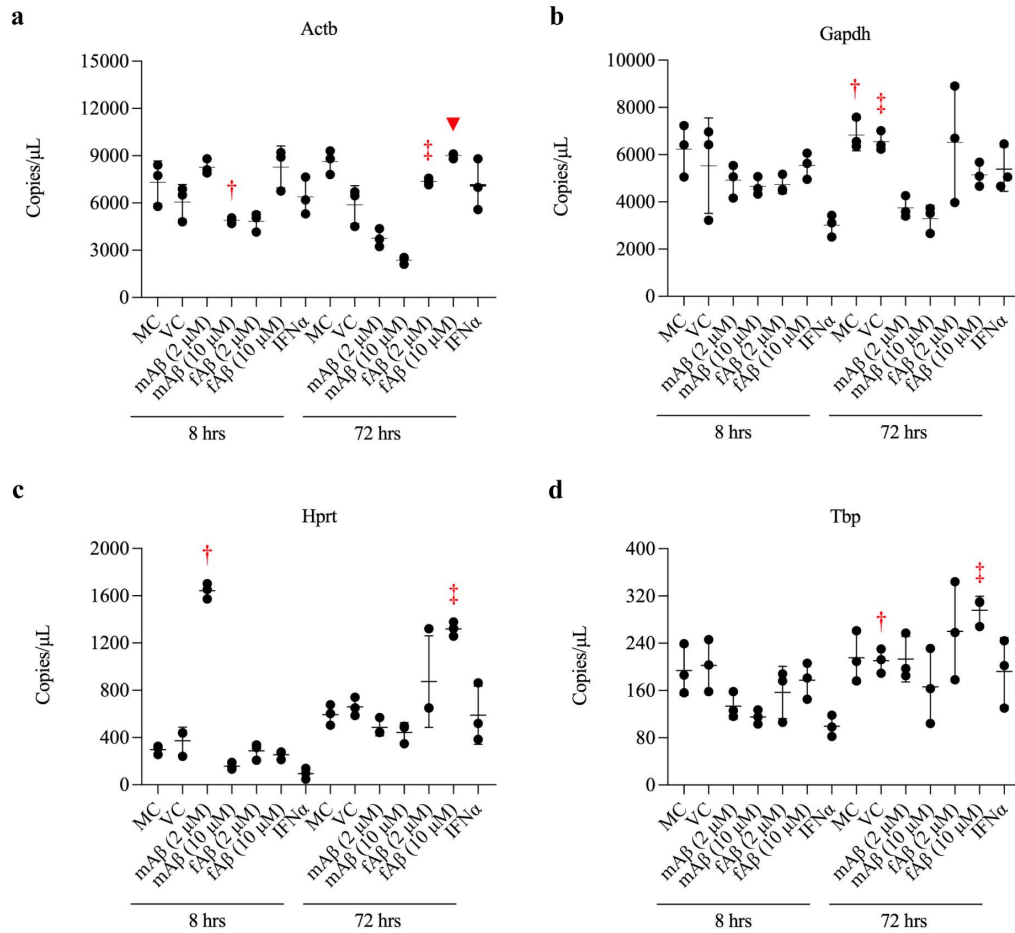
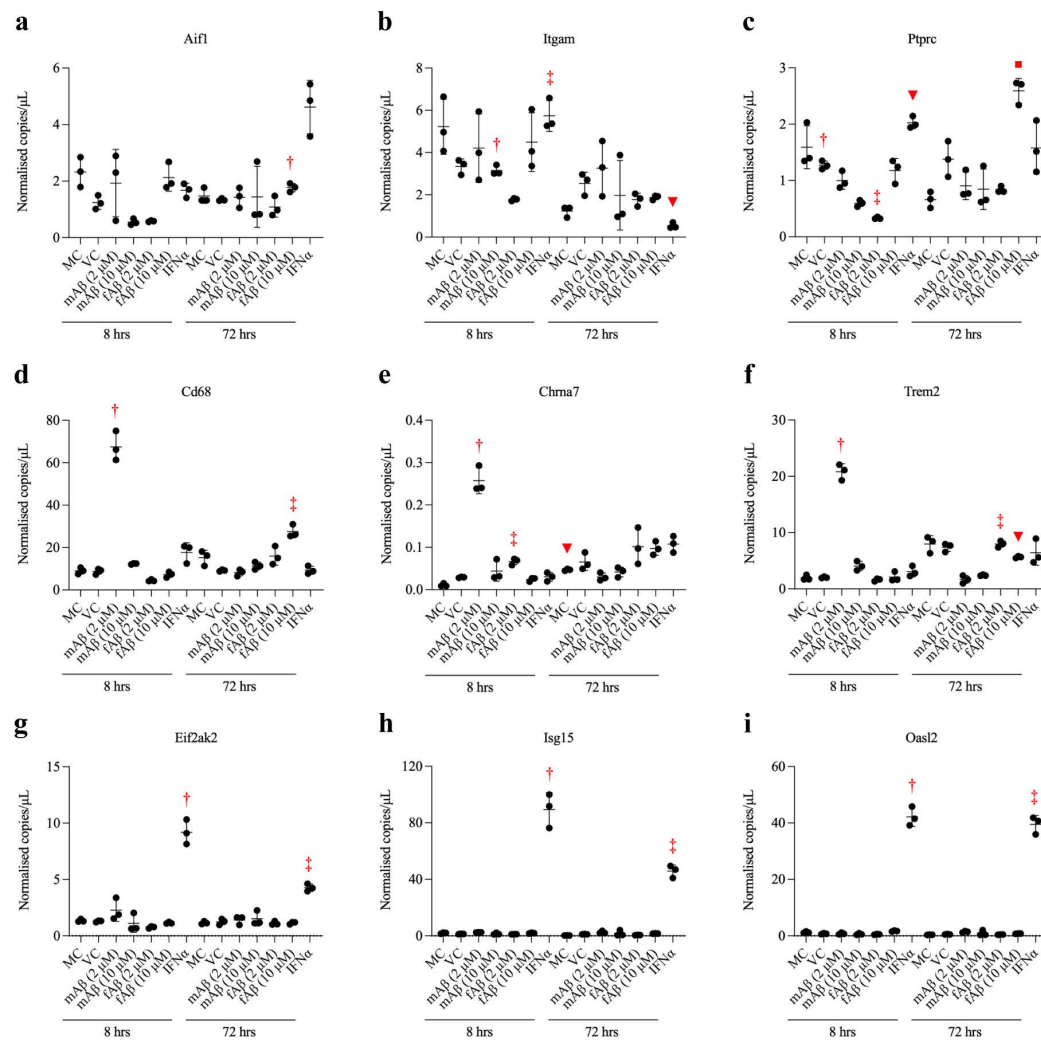


Figure 5. Reference genes for mouse BSCs. Number of copies per μL for media controls (MC), vehicle controls (VC), monomeric A β (mA β), fibrillar A β (fA β), and interferon α (IFN α) solutions over 8 and 72 hours (hrs). Error bars indicate mean and standard deviation of triplicates. **a–b** Both *Actb* (**a**) and *Gapdh* (**b**) showed some variability between treatments within each time group. **c** *Hprt* was significantly upregulated in response to 2 μM mA β for 8 hrs and 10 μM fA β for 72 hrs. **d** *Tbp* was selected as the reference gene for the normalisation of the genes of interest due to its relative stability within both time groups compared to *Actb*, *Gapdh*, and *Hprt*. Statistical comparisons: **a** *Actb*; † $p < 0.05$ compared to mA β (10 μM , 72 hrs); ‡mA β (10 μM , 8 hrs) and mA β (2 & 10 μM , 72 hrs); ▼mA β (10 μM , 8 hrs), mA β (2 & 10 μM , 72 hrs), and fA β (2 μM , 72 hrs); **b** *Gapdh*; † $p < 0.05$ compared to mA β (2 & 10 μM , 72 hrs); ‡mA β (2 & 10 μM , 72 hrs); **c** †*Hprt*; $p < 0.001$ compared to all other treatment groups (8 hrs); ‡ $p < 0.05$ compared to all other treatment groups (8 and 72 hrs), except fA β (2 μM , 72 hrs) and IFN α (72 hrs); **d** *Tbp*; † $p < 0.05$ compared to IFN α (8 hrs); ‡ $p < 0.05$ compared to mA β (2 & 10 μM , 8 hrs) and IFN α (8 hrs).

to 8 hrs. *Cd68* and *Trem2* showed similar expression patterns across treatment groups. Both showed control-level expression with fA β (2 or 10 μM) compared to decreased expression with mA β_{42} for 72 hrs. However, the strongest response for *Cd68* and *Trem2* expression was with 2 μM mA β for 8 hrs, which was also seen for



Chrna7 and *Hprt*. The IFN stimulated genes—*Eif2ak2*, *Isg15*, and *Oas12*—showed an expected upregulation following treatment with IFNα for 8 and 72 hrs. No RNA was extracted from the H₂O₂ (0.1%) treated BSCs. A summary of the key findings is also provided in Table 3.

5.5.2 ddPCR of human samples

The results from the ddPCR assays of post-mortem cortical homogenates from the PreC and PVC have been published previously Guennewig et al. (2021). The box plots are reproduced here (Figure 7) with permission, but with minor changes to formatting. The PreC showed increased expression of *INSR*, *IGF1R*, *CXCR4*, *MS4A6A*, *PARVG*, *SLC7A2*, and *TREM2* and decreased expression of *SST* in AD cases compared to controls. The PVC showed increased expression of *INSR*, *IGF1R*, *CXCR4*, *TREM2*, and *PARVG* and decreased expression of *SST* in AD cases

compared to controls. The mean PMI of human brain samples was 17.2 hrs \pm 13.6 (SD); mean RIN values appear in Table 8 of the appended manuscript.

5.6 Discussion

The hypotheses under investigation in this Chapter were (1) that myeloid/microglial constitutive markers would be upregulated in a dose and time dependent manner in murine BSCs following treatment with mAb β_{42} and (2) that phagocytic markers

←**Figure 6. Genes of interest for mouse BSCs.** Number of copies per μ L of the genes of interest were expressed as the quotient of raw counts over *Tbp* counts. Error bars indicate mean and standard deviation of triplicates. **a–c** The top panel shows markers of myeloid cells expressed by microglia. **a–b** *Aifl* (**a**) and *Itgam* (**b**) showed relatively stable expression across treatment groups over 8 and 72 hrs. **c** *Ptprc* showed significantly reduced expression in BSCs treated with 2 μ M fA β for 8 hrs compared to 72 hrs. **d–f** The middle panel shows additional genes of interest, including two phagocytic markers—*Cd68* and *Trem2*—highly expressed by microglia. **d** *Cd68* expression was significantly increased in mAb β (2 μ M, 8 hrs) compared to all other groups and was also increased in fA β (10 μ M, 72 hrs). **e** *Chrna7* expression was significantly increased in mAb β (2 μ M, 8 hrs), fA β (2 μ M, 8 hrs), MC samples incubated for 72 hrs. **f** *Trem2* expression was significantly increased in mAb β (2 μ M, 8 hrs) compared to all other groups and showed restored expression in BSCs treated with 2 & 10 μ M fA β compared to those treated with mAb β for 72 hrs. **g–i** The bottom panel shows IFN stimulated genes which were used as a positive control for cellular reactivity and BSC viability. **g** *Eif2ak2* showed increased expression in IFN α (8 hrs) compared to all other groups and in IFN α (72 hrs) compared most other groups. **h–i** Expression of *Isg15* (**h**) and *Oasl2* (**i**) was increased in IFN α treated BSCs compared to all other groups. Statistical comparisons: **a** *Aifl*; $^{\dagger}p < 0.05$ compared to mAb β (10 μ M, 8 hrs) and fA β (2 μ M, 8 hrs). **b** *Itgam*; $^{\dagger}p < 0.05$ compared to MC (72 hrs) and fA β (10 μ M, 72 hrs); $^{\ddagger}p < 0.05$ compared to MC (72 hrs) and fA β (2 μ M, 72 hrs); $^{\nabla}p < 0.05$ compared to VC (8 hrs), mAb β (10 μ M, 8 hrs), fA β (2 μ M, 8 hrs), IFN α (8 hrs), and fA β (10 μ M, 72 hrs). **c** *Ptprc*; $^{\dagger}p < 0.05$ compared to mAb β (10 μ M, 8 hrs) and fA β (2 μ M, 8 hrs); $^{\ddagger}p < 0.001$ compared to fA β (2 & 10 μ M, 72 hrs); $^{\nabla}p < 0.05$ compared to VC (8 hrs), mAb β (2 & 10 μ M, 8 hrs), fA β (2 μ M, 8 hrs), MC (72 hrs), and fA β (2 μ M, 72 hrs); $^{\blacksquare}p < 0.05$ compared to mAb β (2 & 10 μ M, 8 hrs), fA β (2 & 10 μ M, 8 hrs), MC (72 hrs), mAb β (2 μ M, 72 hrs), and fA β (2 μ M, 72 hrs). **d** *Cd68*; $^{\dagger}p < 0.05$ all other groups; $^{\ddagger}p < 0.05$ compared to fA β (2 & 10 μ M, 8 hrs), mAb β (2 & 10 μ M, 72 hrs), and IFN α (72 hrs). **e** *Chrna7*; $^{\dagger}p < 0.05$ compared to MC (8 hrs), VC (8 hrs), mAb β (10 μ M, 8 hrs), fA β (10 μ M, 8 hrs), and mAb β (2 & 10 μ M, 72 hrs); $^{\ddagger}p < 0.05$ compared to MC (8 hrs) and fA β (10 μ M, 8 hrs); $^{\nabla}p < 0.05$ compared to MC and VC (8 hrs). **f** *Trem2*; $^{\dagger}p < 0.05$ compared to all other groups; $^{\ddagger}p < 0.05$ compared to mAb β (10 μ M, 8 hrs), fA β (2 μ M, 8 hrs), and mAb β (2 & 10 μ M, 72 hrs); $^{\nabla}p < 0.01$ compared to fA β (2 μ M, 8 hrs) and mAb β (10 μ M, 72 hrs). **g** *Eif2ak2*; $^{\dagger}p < 0.05$ compared to all other groups; $^{\ddagger}p < 0.05$ compared to all other groups except mAb β (2 μ M, 8 hrs) and mAb β (10 μ M, 72 hrs). **h–i** *Isg15* (**h**) and *Oasl2* (**i**); $^{\ddagger}p < 0.05$ compared to all other groups.

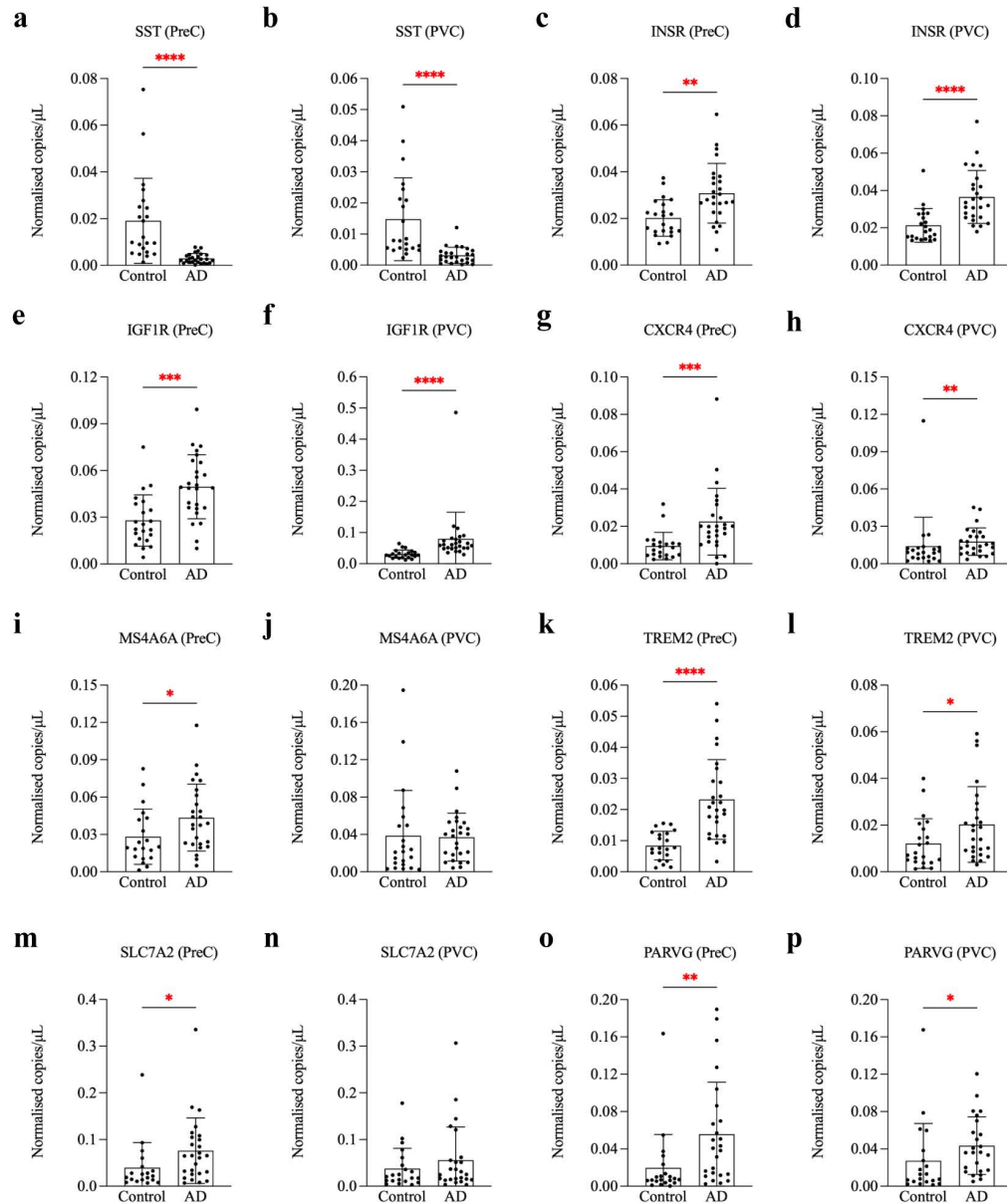


Figure 7. Gene amplification studies in the PreC and PVC of AD and control brains. Box plots showing the mean and standard deviation of the number of copies per μL of the genes of interest expressed as the quotient of raw counts over *GAPDH* counts. Genes under investigation included *SST* (a–b), *INSR* (c–d), *IGF1R* (e–f), *CXCR4* (g–h), *MS4A6A* (i–j), *TREM2* (k–l), *SLC7A2* (m–n), and *PARVG* (o–p). Statistical comparisons: * $p < 0.05$; ** $p < 0.01$; *** $p < 0.001$; **** $p < 0.0001$.

would be upregulated in a dose and time dependent manner in response to treatment with $\text{fA}\beta_{42}$. In human tissue, it was hypothesised that markers of immune activation and phagocytosis such as *TREM2*, *CXCR4*, and *MS4A6A* would be elevated in mild–moderately affected areas of the AD brain. The primary experimental aims of this Chapter were to quantify candidate gene expression changes in BSCs treated

with synthetic A β ₄₂ and differentially affected areas of post-mortem AD brains. In BSCs, the major outcome was a uniform upregulation of *Cd68*, *Chrna7*, and *Trem2* in response to 2 μ M mA β ₄₂ treatment for eight hrs without changes to other myeloid markers such as *Aif1*, *Itgam*, or *Ptprc*. In the post-mortem human brain studies, the major outcome was the validation of an RNA-Seq analysis which demonstrated a strong association between immune pathways and mild AD.

Table 3. Summary of key findings from ddPCR studies of mouse BSCs.	
Reference genes	
<i>Actb</i>	Upregulated in response to fA β (2 & 10 μ M, 72 hrs).
<i>Gapdh</i>	Downregulated to mA β (2 & 10 μ M, 72 hrs).
<i>Hprt</i>	Upregulated to mA β (2 μ M, 8 hrs) and fA β (10 μ M, 72 hrs).
<i>Tbp</i>	No changes across treatments within the 8 & 72 hr groups.
Markers of microglial activation	
<i>Aif1</i>	Non-significant downregulation to mA β (10 μ M, 8 hrs), fA β (2 μ M, 8 hrs), upregulation to IFN α (72 hrs).
<i>Itgam</i>	Downregulation to IFN α (72 hrs).
<i>Ptprc</i>	Downregulation to fA β (2 μ M, 8 hrs) and upregulation to fA β (10 μ M, 72 hrs).
Genes of interest	
<i>Cd68</i>	Upregulation to mA β (2 μ M, 8 hrs).
<i>Chrna7</i>	Upregulation to mA β (2 μ M, 8 hrs).
<i>Trem2</i>	Upregulation to mA β (2 μ M, 8 hrs).
Interferon regulated genes	
<i>Eif2ak2</i>	Upregulation to IFN α (8 & 72 hrs).
<i>Isg15</i>	Upregulation to IFN α (8 & 72 hrs).
<i>Oasl2</i>	Upregulation to IFN α (8 & 72 hrs).

The treatment of murine BSCs with synthetic preparations of A β yielded unexpected results. Evidence of microglial activation in PreAD in response to A β plaques presented in Chapters 2 and 3 lead to the hypothesis that the most basic form of A β , *i.e.* monomers, could cause increased expression of constitutive markers such as *Aif1*, *Itgam*, and *Ptprc*—particularly given their physiological (Puzzo et al., 2015), anti-microbial (Moir et al., 2018), and even protective effects during trophic deprivation through PI3K activation shown elsewhere (Giuffrida et al., 2009). However, this was not observed in BSCs treated with two or 10 μ M mA β ₄₂ over eight or 72 hrs. Unexpectedly, *Aif1* and *Itgam* exhibited relatively

stable expression across all treatment groups—with *Itgam* only trending towards reduced expression at 72 hrs compared to just eight hrs, but significantly reduced expression following exposure to IFN α over 72 hrs. *Ptprc* showed significantly reduced expression over eight hrs' treatment with 2 μ M fA β , but which markedly reversed after 72 hrs. Evidence of microglial phagocytic activity presented in Chapters 3 and 4 lead to the hypothesis that there would be an upregulation of phagocytic markers in response to fibrillar A β ₄₂. Interestingly, this was only seen as restored expression in BSCs treated with two or 10 μ M fA β ₄₂ for 72 hrs compared to the relatively reduced levels seen following treatment with mA β ₄₂ for 72 hrs. More notable however, was the increased expression of phagocytic markers—*Cd68* (an endolysosomal marker) and *Trem2* (a receptor involved in cellular activation and microglia-mediated phagocytosis)—in response to treatment with 2 μ M mA β ₄₂ for eight hrs. Additionally, *Chrna7* and even *Hprt*—one of the candidate reference genes—also showed significantly elevated expression after treatment with 2 μ M mA β ₄₂ for eight hrs. IFN α was used here as a positive control of transcriptional upregulation. Reassuringly, the expression of *Eif2ak2*, *Isg15*, and *Oasl2* increased substantially in BSCs treated with IFN α over eight and 72 hrs. Unfortunately, no RNA was salvaged from BSCs treated with H₂O₂ (0.1%) which was the designated negative control. Future work would ideally include a milder form cellular insult so as to ensure the collection of high enough quality RNA to serve as a negative control.

Two of the key findings from the murine BSC experiments were the upregulation of *Cd68* and *Trem2* in response to treatment with 2 μ M mA β ₄₂ for eight hrs. *Cd68* is a type I transmembrane glycoprotein (Holness & Simmons, 1993; Holness et al., 1993) mainly occurring in late endosomes, suggesting a role in antigen processing and peptide transportation (Barois et al., 2002). It is a scavenger receptor which is upregulated in myeloid cells responding to inflammatory stimuli and is capable of binding apoptotic cells, low-density lipoproteins, and phosphatidylserine (Chistiakov et al., 2017). It is commonly used as a marker of phagocytically active microglia (Walker & Lue, 2015) and appears to be increased in post-mortem AD brains (Hopperton et al., 2018) and decreased in A β ₄₂ immunised brains (Zotova et al., 2013). Further, co-culturing BSCs from aged APP/PS1 mice with those from young WT mice restored A β plaque clearance and was associated with boosted

levels of Cd68 (Daria et al., 2017). Here *Cd68* expression was not impacted by treatment with IFN α , whereas at least one study found that increased peripheral IFN α caused downregulation of *Cd68* in mice (Aw et al., 2020). Trem2 is a myeloid cell surface transmembrane glycoprotein with a V-set IgG extracellular domain and a cytoplasmic tail (Bouchon et al., 2000). *TREM2* is upregulated in human post-mortem AD hippocampus (Celarain et al., 2016) and cortex (Lue et al., 2015; Perez et al., 2017). It exerts its effects through intracellular TYROBP, including the recruitment of Syk kinase which activates the phosphoinositide 3-kinase (PI3K)/protein kinase B (Akt) system and MAPKs to increase intracellular Ca²⁺ (Chen et al., 2020a; Gratuze et al., 2018) and clearance of apoptotic neurons without necessarily triggering inflammatory pathways (Takahashi et al., 2005). *Trem2* is also upregulated in A β plaque associated microglia of aged APP mice (Frank et al., 2008) and attenuates inflammation (Jiang et al., 2018) and neuropathology (Jiang et al., 2014) in APP/PS1 mice. Thus the upregulation of these phagocytic markers in response to low-level A β monomers may represent a normal physiological pathway for the control of synaptic pruning.

The upregulation of *Chrna7* was another significant finding made here. *Chrna7* encodes the $\alpha 7$ subunit of the nAChR, itself a pentameric receptor comprised of either α , β , γ , δ , or ϵ subunits (Fujii et al., 2017). nAChRs occur in the peripheral nervous system at neuromuscular junctions and nerve ganglia and in the central nervous system, where they are expressed by neuronal and non-neuronal cells (Kalamida et al., 2007). The homomeric $\alpha 7$ nAChR shows particularly high Ca²⁺ permeability (even compared to glutamatergic NMDA receptors) on activation (Séguéla et al., 1993). Its activation produces potent anti-inflammatory effects in immune cells—particularly macrophages (Wang et al., 2003)—through both ionotropic and metabotropic pathways (Fujii et al., 2017). The ionotropic pathway involves a phosphorylation cascade governed by protein kinase C (PKC) which culminates in the activation of p38 MAPK signalling, PI3K/Akt pathway, translocation of nuclear factor erythroid 2-related factor 2 (Nrf2), and overexpression of haem oxygenase 1 (Corradi & Bouzat, 2016; de Jonge & Ulloa, 2007). Physiological concentrations (pico/nanomolar) of oligomeric species of A β_{42} have also been shown to activate $\alpha 7$ nAChRs in a lipid raft-dependent manner

in presynaptic terminals, resulting in increased intracellular Ca^{2+} (Khan et al., 2010).

Two DEGs identified in the BSC experiment included *Ptprc* and *Hprt*. Here *Ptprc* expression dropped in response to 2 μM $\text{fA}\beta_{42}$ over eight hrs, but increased following 10 μM $\text{fA}\beta_{42}$ over 72 hrs. It also increased in response to $\text{IFN}\alpha$ over 8 hrs, as has been observed in another study (Aw et al., 2020). PTPRC is a cell surface antigen expressed by most haematopoietic cells and is involved in cell division and differentiation. It is expressed by homeostatic and activated human microglia *ex vivo* (Becher & Antel, 1996). Post-mortem investigation have identified increased PTPRC-positive cells in different cortical regions and the hippocampus of AD cases, but with mixed results for overall expression levels (Hopperton et al., 2018). Interestingly, *Ptprc*-KO APP/PS1 mice show worsened soluble oligomeric and insoluble fibrillar $\text{A}\beta$ pathology, increased microglial neurotoxic cytokines, and greater neuronal loss compared to non-KO APP/PS1 mice (Zhu et al., 2011). The upregulation of *Hprt* in BSCs treated with 2 μM $\text{mA}\beta_{42}$ for eight hrs was unexpected. *Hprt* is involved in the salvage of purines, which may be overproduced in *Hprt* deficiency as seen in Lesch Nyhan syndrome (Nyhan, 2012) and gouty arthritis (Zoref-Shani et al., 2000). It is estimated that 90% of free purines are recycled through the HPRT-governed salvage pathway in humans (Stout & Caskey, 1985). It has historically been used as a reporter gene for evaluating mutational frequency in the development of cancer—in which it has an emerging role (Townsend et al., 2018). Epistasis of mutated *Hprt* and *App* has previously been reported (Nguyen, 2019), however the upregulation of *Hprt* in response to $\text{mA}\beta_{42}$ here is of unknown significance; potentially representing a feedback mechanism in the context of increased DNA degradation or elevated hypoxia inducible factor 1 α (HIF1 α) in response to increased energy demands or oxygen deprivation, a scenario which has been demonstrated in a model of cardiac ischaemia (Wu et al., 2015).

The amplification studies of candidate genes performed in the PreC and PVC of post-mortem AD brains broadly validated the findings made in the published RNA-Seq analysis (Guennewig et al., 2021) and supported the hypothesis that immune activation coincides with early phases of AD. Markers of immune activation which were elevated in both the PreC and PVC included *CXCR4* and *TREM2*. *MS4A6A*

was another upregulated immune-related gene, but only in the PreC. These three genes were amongst the most significantly upregulated DEGs in the RNA-Seq analysis of the PreC. Other DEGs in the PreC and PVC identified by the RNA-Seq analysis which were also validated by the ddPCR assays included the upregulation of *INSR*, *IGF1R*, and *PARVG*. *SLC7A2* showed upregulation in the PreC but not the PVC and *SST* showed downregulation in both regions of AD cases. Overall, the PreC showed significant differences between AD cases and controls for all of the genes of interest whereas the PVC showed differences for all genes except *MS4A6A* and *SLC7A2*.

The upregulation of immune-related genes such as *CXCR4*, *MS4A6A*, and *TREM2* in the RNA-Seq analysis and ddPCR validation study are consistent with previous bulk tissue RNA-Seq (Mostafavi et al., 2018), snRNA-Seq (Gerrits et al., 2021) and scRNA-Seq (Sobue et al., 2021), GWAS of AD (Efthymiou & Goate, 2017) and a later meta-analysis (Jansen et al., 2019). *CXCR4* and functionally related genes expressed by microglia, such as *CXCL12*, *TLR2*, *RALB*, and *CCR5*, are dysregulated in a number of neurodegenerative diseases, including AD (Bonham et al., 2018). *CXCR4* is a G protein-coupled chemokine receptor with wide ranging functions in brain development and immunity (Li & Wang, 2017). It has previously been shown to be elevated in AD (though decreased in a mouse model; Parachikova & Cotman, 2007) and associated with increased activation of PKC (Weeraratna et al., 2007). As previously discussed, *TREM2* is increased in AD—in which its loss of function is associated with increased risk (Guerreiro et al., 2013). *MS4A* family consists of 12 related genes in humans that function as accessory proteins to membrane receptors and channels through which they effect immune cell activation and support survival (Liang et al., 2001). These genes are highly expressed by myeloid cells—particularly M2 macrophages (Sanyal et al., 2017)—and are key regulators of soluble *TREM2* which is associated with AD pathological processes following A β deposition (Deming et al., 2019).

Other DEGs of interest included *INSR*, *IGF1R*, *PARVG*, *SLC7A2*, and *SST*. Diabetes mellitus is associated with increased risk of AD, but the precise mechanisms underlying this association remain unexplained. Potential explanations include the possibility that central insulin resistance leads to increased activity of

GSK3 β , a major tau kinase (Steen et al., 2005). Increased *INSR* and *IGF1R* may represent a compensatory feedback loop associated with increased PI3K/Akt signalling—which is increased in AD (Chami et al., 2016)—aimed at preserving insulin and IGF1 signalling in areas yet to sustain neuronal loss. The downregulation of *SST* in the PreC and PVC was of interest given early pathological studies showing somatostatin immunoreactive NPs (Morrison et al., 1985), NFTs in somatostatinergic neurons (Roberts et al., 1985), and reduced levels in AD brains (Davies et al., 1980) and a recent meta-analysis of microarray data (Bai et al., 2016). Somatostatinergic interneurons with long range connections modulate neuronal excitation through G protein-coupled receptors and are involved in motor and sensory activity, sleep, and cognition (Martel et al., 2012). Somatostatin dysfunction is also linked to GABAergic dysfunction which underlies widespread neuronal network and glial dysfunction in AD (Ambrad Giovannetti & Fuhrmann, 2019). The significance of *PARVG* and *SLC7A2* elevation in the context of AD is unknown. *PARVG* is relatively expressed by microglia and encodes γ -parvin which is a member of the parvin family of actin-binding focal adhesion proteins (Korenbaum et al., 2001). *SLC7A2* encodes the cationic amino acid transporter 2 which is an important modulator of T-cell mediated immunity (Thompson et al., 2008) and when deficient has been associated with spontaneous inflammation in the lungs of mice (Rothenberg et al., 2006).

BSCs represent a useful tool for studying complex cellular activities and interactions in a 3D setting. They are also cheaper and more readily available than other 3D models of biological tissues such as brain organoids grown from induced pluripotent stem cell, which hold promise but face many cost and technical hurdles (Arber et al., 2017; Ooi et al., 2020). Here BSCs treated with synthetic preparations of A β ₄₂ peptides demonstrated boosted phagocytic and anti-inflammatory markers in response to lower doses of monomeric peptides. Longer treatment times with fibrillar A β ₄₂ species showed restored levels of phagocytic markers compared to the relatively reduced levels observed following extended treatment with mA β ₄₂. This occurred in the absence of an upregulation of the *Chrna7*-dependent anti-inflammatory pathway. Ultimately, this may reflect a situation in which microglia display heightened phagocytic potential and anti-inflammatory characteristics early in the disease time course, but later exhibit a sustained phagocytic capability in the

absence of a critical anti-inflammatory pathway. *Aif1* remained relatively stable across the treatment groups which was surprising given that the results from Chapter 1 indicate marked reductions in *Iba1* in severe AD.

The work presented in this chapter on BSCs confirmed the hypothesis that microglia upregulate phagocytic markers, but not just in response to fibrillar A β , but also to the monomeric peptide. Future work might aim to include markers of viability, *e.g.* fluorescent dyes such as propidiumiodine, ethidiumbromide, Hoechst, DAPI, or annexin V, among others (Lossi et al., 2009). Further, the transcriptomes of human AD and mouse model brain tissues diverge in a number of key gene co-expression networks despite broad preservation of genetic make-up between the two species (Miller et al., 2010). Incidentally, Miller et al. (2010) demonstrated that the greatest differences occurred in the microglial gene modules. Therefore usual caution should be used when considering results from animal studies, especially given the poor record of translation of findings to viable therapeutics for AD (Vitek et al., 2021). For instance, human microglia show differential expression profiles for immune-related genes during ageing such as sialic acid binding immunoglobulin type lectins (SIGLECs) and MHCs (Galatro et al., 2017) which are important inducers of immune tolerance (Jurewicz & Stern, 2019; Lübbers et al., 2018)—a feature of immunity which has been associated with reduced A β pathology (Wendeln et al., 2018) and healthy ageing, *c.f.*, chronic inflammation (Rogovskii, 2020). More broadly these differences may represent key factors which have facilitated the relative longevity and low-turnover of microglia in humans (Réu et al., 2017). Another shortcoming of the present study was that monomeric peptides likely underwent fibrillisation over the 72 hrs incubation period. Future work might be improved by replacing incubation media every eighth hour—which reflects the amount of time that lapsed before the ThT aggregation assay showed significantly increased fluorescence (Figure 1). Finally, the gene amplification assays performed in the PreC and PVC of AD cases validated findings from an RNA-Seq analysis of these regions and confirmed the hypothesis that markers of immune activation are upregulated during early phases of AD. Genes of interest in the human study were based on an RNA-Seq analysis subsequent to the mouse BSCs. Harmonisation of genes of interest between the mouse and human work presented here might also be an aim of future work.

Chapter 6: Discussion

The major theme of the research presented here was to characterise the phenotypic changes in microglial populations in differentially affected areas of the PreAD and AD brain. Concurrently a quantitative analysis of AD neuropathological changes was carried out in order to better relate patterns of accumulation in different association and primary cortices of PreAD and AD cases to the microglial population. This also allowed for the determination as to which of A β or tau deposition was the more potent driver at relative ‘timepoints’ in the disease. The histopathological work finished on an examination of the emerging concept of aberrant microglia-mediated phagocytosis in AD using relatively recent advances in IF microscopy which have allowed for sub-diffraction limited light microscopy as a more rigorous method of assessing colocalisation of fluorescent signals. These studies were complemented by gene amplification studies in human AD brain and mouse BSCs treated with monomeric and fibrillar species of synthetic A β ₄₂ in order to characterise aspects of the molecular changes in microglia at different timepoints in the natural history of AD.

6.1 Summary of key findings

The key hypotheses under investigation here included: (1) microglial activation occurs in PreAD, whereas microglial degeneration coincides with symptomatic disease (dementia); (2) the activation of cortical microglia in PreAD follows the deposition of A β but precedes NFD; (3) there is increased phagocytosis of (pre-)synapses by microglia in AD; (4) microglia react to A β monomers by upregulating phagocytic genes and a major anti-inflammatory pathway; and (5) markers of immune activation and phagocytosis are upregulated in mild AD.

6.1.1 Activation of microglia in PreAD and loss of healthy microglia in AD

The first hypothesis—that the activation of microglia occurs in PreAD but degeneration occurs in symptomatic AD—was confirmed (Paasila et al., 2019). This study showed that in the earlier and severely affected ITC the activation of

microglia is most prominent in PreAD, whereas there is a loss of total microglia, made up almost entirely by the loss of ramified cells, in advanced disease. These findings were also corroborated by automated morphometric analyses performed *in silico*, which included determination of total branch length, number of junctions, number of branches, and territorial coverage by positive pixel fraction and convex hull analysis. Interestingly the study also highlighted that the clustering of microglia at sites of A β or TTau deposition incorporates only a small fraction of the total microglial population in both PreAD and AD. Interestingly, the belatedly and mildly affected PVC—which was spared of any neuronal loss or cortical atrophy—had the highest proportion of plaques with an associated cluster of microglia, followed by the intermediately affected SFC, and finally the severely affected ITC. Features of activation, such as clustering and shortening of processes tended to correlate with A β , but the loss of ramified microglia correlated with TTau. Finally, dystrophic microglia were most often associated with NPs with very dense collections of DNs compared to plaques with sparser DNs. However, dystrophic microglia correlated best with low brain pH rather than disease status.

6.1.2 Activation of microglia precedes NFD

The second hypothesis—that the activation of cortical microglia occurs after the deposition of A β but before NFD—was also confirmed (Paasila et al., 2020). This study compared A β , TTau, and microglial pathological changes in the PMC to the previously examined ITC. The PMC was unaffected by any neurodegenerative changes and showed an even sparser quantity of A β and TTau than the PVC. All individual control and CAC brains showed a very low level of TTau pathology in both regions which was not associated histopathologically with either A β or microglial clustering but correlated with age. In the belatedly affected PMC, controls and CAC differed only by the level of A β and clustering, indicative of a microglial reaction in response to A β in the absence of tau pathology. There was also evidence of the internalisation of A β by microglia. Overall, clustering of activated microglia was significantly higher in the PMC compared to the severely affected ITC of both CAC and AD brains. Therefore, it was concluded that the sequence of pathological events in the cortex of AD brains begins with A β , followed by clustering of activated microglia, and finally NFD.

6.1.3 Increased phagocytosis of (pre-)synapses in AD

The third hypothesis—that there is increased phagocytosis of presynapses in AD but not control or CAc—was confirmed (Paasila et al., 2021). This study used 3D GSDIM—a form of super-resolution light microscopy—to demonstrate internalisation of Syp-immunoreactive presynaptic elements by microglia in AD. Colocalisation of Iba1 and Syp signals were shown at a horizontal resolution of 20 nm/pixel and an axial resolution of 50 nm/pixel. Increased colocalisation was observed in AD cortex, but not CAc or control tissues.

6.1.4 Microglia react more potently to monomers than fibrils of A β

Part one of the fourth hypothesis—that BSCs treated with synthetic A β monomers would upregulate constitutive myeloid/microglial markers—was disconfirmed. Myeloid markers expressed by microglia, such as *Aif1*, *Itgam*, and *Ptprc*, all displayed relatively stable expression across treatment groups. Part two of the fourth hypothesis—that BSCs treated fA β would upregulate phagocytic markers—was confirmed, but with important caveats; that a relatively shorter period of treatment with A β monomers had a far more potent effect on the expression of phagocytic markers and that fA β only restored phagocytic potential following extended treatment with mA β . Notably, the increased expression of phagocytic markers in response to short treatment time with mA β was also accompanied by significantly increased expression of the *Chrna7* anti-inflammatory marker and the candidate reference gene *Hprt* which is involved in the salvage of purines for DNA and RNA synthesis.

6.1.5 Immune activation and phagocytosis coincides with mild AD

The fifth hypothesis—that markers of immune activation and phagocytosis would be upregulated in early phases of AD—was confirmed. The genes of interest here were selected based on an RNA-Seq analysis which found them to be amongst the highest DEGs in the PreC and PVC of post-mortem AD cases. The PreC showed increased expression of phagocytic and immune markers, including, *CXCR4*, *MS4A6A*, *SLC7A2*, and *TREM2*. The PVC was also showed increased *CXCR4* and

TREM2. Other DEGs identified in both regions included the upregulation of *INSR*, *IGF1R*, and *PARVG* and the downregulation of *SST*.

6.2 Contextualisation of findings

6.2.1 Neuropathology

A β plaques and tau pathology do not follow the same spatiotemporal pattern of accumulation (Arriagada et al., 1992; Braak & Braak, 1991; Mirra et al., 1991; Ohm et al., 1995; Thal et al., 2002). Unexpectedly, the regions first investigated in Chapter 2—including the ITC, SFC, and PVC—were found to have similar levels of AD neuropathological changes. A β deposition shows a relatively haphazard pattern of accumulation throughout the cerebral cortex and plateaus early during the disease course (Serrano-Pozo et al., 2011b), whereas NFD—including NPs—accrues in a more linear fashion, correlating with progressive cognitive impairment in AD (Nelson et al., 2012) across a number of allocortical and neocortical areas (Nelson et al., 2007). However, there have been several quantitative reports of striking inter-individual variability in the density of NFD across different regions of the brain (Berg et al., 1998; Bouras et al., 1994; Giannakopoulos et al., 1995; Nelson et al., 2009b; Vermersch et al., 1992)—with primary cortices generally carrying fewer NFTs. This supports the need for greater sampling of patient populations and brain regions when quantifying pathological changes in AD.

The similarities between the PVC and ITC prompted the inclusion of the PMC in the subsequent investigation. Reassuringly the PMC showed significantly reduced levels of A β and tau pathology than the ITC, as corroborated by several other studies (Arendt et al., 1998; Geula et al., 1998; Golaz et al., 1992; Murray et al., 2011; Petersen et al., 2019; Suva et al., 1999)—again however, there was a wide range of estimates for NFTs in these studies; from <5 to >60 tangles *per mm*². This to some extent is owed to differences in sampling methodologies, such as targeting the most susceptible cortical laminae (III & V) versus unbiased anatomical protocols. Like the PVC, the PMC showed no evidence of neurodegenerative changes despite carrying a higher than anticipated load of AD pathology. There

were no changes to cortical thickness, total neurons, or density of Betz cells. A comparison of the neuronal density estimates generated in control cases with two previously published reports suggests a potential underestimation of total neurons in the PMC by approximately 18% (Gredal et al., 2000) to 22% (Mochizuki et al., 2011). The presence of the large pyramidal upper motor neurons known as Betz cells which cluster in layer Vb and an attenuated granular layer IV are two characteristics of the PMC. Histologically, Betz cells may be identified by their large size, a conspicuous nucleolus, prominent somal lipofuscin deposits, and multiple dendritic shafts projecting asymmetrically from the entire circumference of the cell body. The size of Betz cells decreases gradually along a mediolateral gradient, with the largest cells occurring in the medial somatotopic zones subserving the hands and feet. The sections analysed here were derived from the superomedial area of the caudal aspect of the PMC which accounted for the slightly more prominent granular layer IV and the clusters of Betz cells that were triangular and round in shape, which contrasts with the more obscured granular layer and fusiform-shaped Betz cells in the rostral portions of the PMC (Rivara et al., 2003).

6.2.2 Relationships between microglia and AD neuropathology

Morphological changes

Here microglia which showed features of activation, including hypertrophy of the soma and primary processes (if present), either hyper-ramification (bushy) or de-ramification (amoeboid), with or without the presence of spheroidal swellings of cellular processes, were found to occur most prominently in the ITC of PreAD. In AD cases, these cells occurred more frequently in clusters around A β plaques, especially in more mildly affected regions such as the PVC and SFC. NPs with dense accumulations of DNs were associated with microglia displaying features of dystrophy, including the shortening of processes with significant tortuosities, blebbing, or fragmentation. These microglia also correlated significantly with lower brain pH. Future work might seek to determine if this represents a disease-associated effect or secondary to agonal events immediately preceding death. The concept of protective microglial activation early in the disease time course followed by degeneration associated with a loss of homeostatic function during end-stage

disease is increasingly appreciated (Chatila & Bradshaw, 2021; Navarro et al., 2018; Schwabe et al., 2020; Streit et al., 2009, 2020).

Microglia exhibit highly dynamic context-dependent responses to pathological stimuli (Prokop et al., 2013; Raivich et al., 1999). Direct correlations between morphological features of microglia with precise physiological or diseased states are not known (Dubbelaar et al., 2018). Gene inductions in culture can occur in the absence of obvious morphological transitions (Eskes et al., 2003) and certain morphologies can be experimentally induced *in vitro* even under conditions that would not ordinarily support these morphological features (Ilschner et al., 1996; Suzumura et al., 1991). Consequently, morphology is not necessarily a reliable reflection of functional orientation (Kettenmann et al., 2011; Richter et al., 2014). However, work that has come out from peripheral and central nerve axotomy tentatively suggests that the aforementioned morphological markers of activation represent neuroprotective or ‘proregenerative’ microglia (Streit, 2002, 2005). Overall, it appears that only a very small proportion of total microglia are actively involved in clustering at sites of AD pathological aggregates early in the disease and that this clustering response dissipates with the progression of disease. Further, the results presented here show no global differences in the morphological states of the microglial population when conducting a complete examination of all cortical laminae across different brain regions. Indeed, all morphologies can be found inhabiting the same cortical regions of healthy and AD cortex, as has previously been reported (Bachstetter et al., 2015; Torres-Platas et al., 2014). Next generation single-cell, single-nuclear sequencing, and spatial transcriptomics (Chen et al., 2020b) have an important role to more fully elucidate the molecular dynamics of microglial activity in AD (Hammond et al., 2019; Keren-Shaul et al., 2017; Krasemann et al., 2017; Masuda et al., 2019; Mathys et al., 2019; Sala Frigerio et al., 2019; Sankowski et al., 2019; Sousa et al., 2018; Tay et al., 2018; Thrupp et al., 2020).

Sequence of pathological changes

Inferring sequences of pathological changes from hierarchical involvement of differentially affected brain regions is an objective of experimental neuropathology.

Results presented in Chapter 3 suggest that the relative sequence of microglial and AD pathological changes in PreAD begins with the deposition of fibrillar A β , followed by the clustering of activated microglia, then by the formation of fibrillar tau pathology. This finding conflicts with a previous report which placed tau pathology first, followed by A β , then microglial activation (Streit et al., 2018). Notwithstanding this difference, both scenarios are compatible with the possibility that soluble phosphotau drives the degeneration of microglia (Sanchez-Mejias et al., 2016). It then appears that microglia are susceptible to an impaired clustering response with degenerative changes over the disease time course. Finally, a subset of viable cells display a re-emergent, but destructive phagocytosis (characterised by the targeting of synapses) which coincides with significant tau pathology as demonstrated in Chapter 4 by the increased internalisation of pre-synaptic elements by microglia observed in symptomatic cases only. This concept of biphasic activation is also supported by PET imaging studies (Fan et al., 2017; Ismail et al., 2020; Nordengen et al., 2019).

6.2.3 Immune activation and phagocytosis in mild AD

Murine BSCs

Cd68 and *Trem2* were two key genes involved in phagocytic pathways that were upregulated in BSCs treated with mA β for eight hours. These changes were also associated with a pronounced upregulation of *Chrna7*, a potent anti-inflammatory mediator. *Trem2* is also capable of exerting anti-inflammatory effects through the inhibition of NF- κ B at a point downstream of PKC (Yao et al., 2019), whereas *Cd68* does not appear to be involved in potentiating any major effects on a cell's inflammatory profile—as demonstrated in a KO mouse model (Song et al., 2011). Interestingly, extended treatment with fA β restored expression levels which were relatively depressed in BSCs treated with mA β ₄₂ (72 hours), but in the absence of *Chrna7* upregulation. This appears to be in general agreement with a biphasic pattern of microglial activation wherein the first peak is associated with a phagocytic, anti-inflammatory phenotype, but the second is characterised by destructive phagocytic activity on synapses (as shown by increased internalisation of Syp-positive synapses by microglia in AD) without inhibition of inflammatory

pathways likely characterised by NF- κ B activation (Ju Hwang et al., 2019). Future work might aim to increase the culture duration by another 24 hours to see if the expression levels continue to climb to significantly greater than those seen in the 72-hour media controls and monitor the inflammatory profile of cultures throughout.

Post-mortem cortical homogenates

The gene amplification studies performed in the PreC and PVC of AD cases demonstrated the coincidence of immune activation and phagocytosis with mild AD. These two regions were selected based on the staging schema, the previous IHC studies presented here (which included unpublished data on the PreC generated during the work done for Chapter 2), and volumetrics studies which suggested mild to intermediate involvement at relatively later stages of AD—thus representative of mild AD. Upregulated immune genes included *CXCR4*—a chemokine receptor associated with PKC activity; *MS4A6A*—a regulator of soluble TREM2; and *TREM2*. An important caveat with regard to early and late stage phagocytosis is that the former appears to be associated with microglial activation in the absence of inflammation (Graeber et al., 2011; Graeber, 2014) and the preservation of synaptic architecture whilst the latter is likely associated with impairment of the CHRNA7-related anti-inflammatory pathway and active targeting of synapses for phagocytosis (Hong et al., 2016). Further, the upregulation of metabolic regulators including *INSR* and *IGF1R* may even exert some level of anti-inflammatory activity as they are directly involved in PI3K/Akt signalling. The convergence of many of the aforementioned genes in the mouse and human studies on PI3K/Akt signalling may serve to potentiate immune activation and phagocytosis, but also cause the generation of phosphotau as a by-product of increased GSK3 β activity downstream of Akt.

6.3 Strengths and weaknesses

6.3.1 Post-mortem human brain tissue

The use of post-mortem human brain tissue presents with a number of benefits and drawbacks. The major importance of using human AD tissue is that it provides the essential definition of the disease. All the major working hypotheses and disease models in the field are secondary to the primary analysis of human tissues. Therefore, the observations made here are highly relevant in their description of AD pathophysiological processes. The major drawback is that the use of post-mortem tissue is inherently retrospective, which obscures cause and effect—conceptually like Heisenberg’s uncertainty principle. Further, human tissue is often subject to extended PMI which can adversely affect RIN values with potentially adverse, but not necessarily disqualifying, impacts on gene amplification studies (White et al., 2018). The effects of antemortem factors and PMI on RIN has been previously examined and at least partly resolved by normalising gene counts by a reference gene which shows a similar pattern of residual effects to potential confounders such as PMI (Mills et al., 2014). Extended fixation of post-mortem tissue also impacted the antigenicity of proteins targeted for IHC, IF, and GSDIM studies. Longer fixation times inversely correlated with the overall level of staining that was achievable, particularly for synaptic markers and the transmembrane glycoprotein CD68—which would have provided a more ideal marker for demonstrating the internalisation of synaptophysin by microglia given its position in the lysosomal/endosomal membrane in contrast to Iba1 which is an intracellular marker. Another drawback is the relative rarity of human brain tissue, which has a limiting effect on obtainable sample sizes. Future work would benefit greatly from larger sample sizes.

6.3.2 Quantitative neuropathology

One of the other major strengths of the IHC/IF investigations presented here were the automated and highly scalable quantitative analyses. This brings with it the prospect of rigorous statistical assessment and the possibility of making accurate

CPCs with which to inform future avenues of study. For instance, the inverse correlation between brain pH and dystrophic microglia was an unexpected finding which provokes further consideration as to whether this is simply an artefact of agonal effects or representative of a bona fide disease-related process. The use of automated procedures in future work could open the possibility of much larger sampling protocols of individual brains using whole slide scanning for high-throughput analyses. Lastly, machine or even deep learning for automated morphological subtyping would also be made possible provided large enough sample sizes are achieved—though may require cross-institutional collaborations.; with early attempts already having been made (Vizcarra et al., 2020).

6.3.3 Gene amplification studies

The study of genes highly expressed by microglia (though not all genes, *e.g.*, *CHRNA7*, *SST*, *INSR*, and *IGF1R*) provided some insight into the molecular characteristics of their activation in AD. The use of BSCs as a 3D biological setting with a comparable mix of cells seen *in vivo* allowed for mechanistic insight as to how microglia respond to challenge with A β ₄₂. BSCs were prepared according to a previously published protocol (Friedl et al., 2004), however there are several limitations which bear consideration (Croft & Noble, 2018; Humpel, 2015), including being subject to acute axotomy and loss of target innervation—this might be ameliorated by supplementing the culture medium with nerve growth factors and including a resting period of up to two weeks to allow for the acute effects of axotomy to resolve; the absence of a functional vascular system (however BSCs still have advantages over isolated primary cell cultures in this respect); the development of a layer of reactive astrocytes on the outer surface of the slice zone which requires time in culture to resolve (Benediktsson et al., 2005); and the flattening of cultured slices over time which causes minor alterations to anatomical structure—this can be partially reduced by using a high concentration of horse serum in the culture medium. One significant drawback of using murine BSCs is that mouse and human tissues are known to behave in disparate ways (Masuda et al., 2019; Schwabe et al., 2020). Additionally, synthetic A β fibrils have also been shown to assume a different conformation compared to those isolated from AD

patients (Kollmer et al., 2019) which might affect receptor affinities. To overcome these, future work might aim to derive pathological seeds from human patients and apply them to human BSCs (Andersson et al., 2016; Eugène et al., 2014; Lyman et al., 1991; Schwarz et al., 2019; Verwer et al., 2003)—although these would also be limited by PMI, tissue availability, and ethical considerations.

6.4 Conclusions

Here the observation of microglial activation in PreAD and mild AD were interpreted as neuroprotective processes as the activated cells shared features seen in proregenerative microglia in mouse axotomy models. Importantly, these activated cells were not implicated in the phagocytosis of pre-synaptic material in PreAD unlike end-stage disease. Further, gene amplification studies in mouse demonstrated enhancement of phagocytosis and anti-inflammatory pathways in response to mA β ₄₂ but restored phagocytosis without a similarly elevated level of a major anti-inflammatory pathway. This concept of immune activation in early or mild AD was also corroborated by gene studies performed in post-mortem AD cortical tissue. The findings here suggest that augmenting microglial function early in the disease may be key to prolonging cognitive function as opposed to the long held view that the correct therapeutic avenue lies in attenuating microgliosis.

References

- Abbracchio, M. P., Burnstock, G., Verkhratsky, A., & Zimmermann, H. (2009). Purinergic signalling in the nervous system: an overview. *Trends Neurosci*, 32(1), 19-29. doi:10.1016/j.tins.2008.10.001
- Afagh, A., Cummings, B. J., Cribbs, D. H., Cotman, C. W., & Tenner, A. J. (1996). Localization and cell association of C1q in Alzheimer's disease brain. *Exp Neurol*, 138(1), 22-32. doi:10.1006/exnr.1996.0043
- Aihara, M., Ishii, S., Kume, K., & Shimizu, T. (2000). Interaction between neurone and microglia mediated by platelet-activating factor. *Genes Cells*, 5(5), 397-406. doi:10.1046/j.1365-2443.2000.00333.x
- Ajami, B., Samusik, N., Wieghofer, P., Ho, P. P., Crotti, A., Bjornson, Z., Prinz, M., Fantl, W. J., Nolan, G. P., & Steinman, L. (2018). Single-cell mass cytometry reveals distinct populations of brain myeloid cells in mouse neuroinflammation and neurodegeneration models. *Nat Neurosci*, 21(4), 541-551. doi:10.1038/s41593-018-0100-x
- Akiyama, H., & McGeer, P. L. (1990). Brain microglia constitutively express β -2 integrins. *J Neuroimmunol*, 30(1), 81-93. doi:10.1016/0165-5728(90)90055-r
- Akiyama, H., Nishimura, T., Kondo, H., Ikeda, K., Hayashi, Y., & McGeer, P. L. (1994). Expression of the receptor for macrophage colony stimulating factor by brain microglia and its upregulation in brains of patients with Alzheimer's disease and amyotrophic lateral sclerosis. *Brain Res*, 639(1), 171-174. doi:10.1016/0006-8993(94)91779-5
- Akiyama, H., Barger, S., Barnum, S., Bradt, B., Bauer, J., Cole, G. M., Cooper, N. R., Eikelenboom, P., Emmerling, M., Fiebich, B. L., Finch, C. E., Frautschy, S., Griffin, W. S., Hampel, H., Hull, M., Landreth, G., Lue, L., Mrak, R., Mackenzie, I. R., McGeer, P. L., O'Banion, M. K., Pachter, J., Pasinetti, G., Plata-Salaman, C., Rogers, J., Rydel, R., Shen, Y., Streit, W., Strohmeyer, R., Tooyoma, I., Van Muiswinkel, F. L., Veerhuis, R., Walker, D., Webster, S., Wegrzyniak, B., Wenk, G., & Wyss-Coray, T. (2000). Inflammation and Alzheimer's disease. *Neurobiol Aging*, 21(3), 383-421. doi:10.1016/s0197-4580(00)00124-x
- Albert, M. S., DeKosky, S. T., Dickson, D., Dubois, B., Feldman, H. H., Fox, N. C., Gamst, A., Holtzman, D. M., Jagust, W. J., Petersen, R. C., Snyder, P. J., Carrillo, M. C., Thies, B., & Phelps, C. H. (2011). The diagnosis of mild cognitive impairment due to Alzheimer's disease: recommendations from the National Institute on Aging-Alzheimer's Association workgroups on diagnostic guidelines for Alzheimer's disease. *Alzheimers Dement*, 7(3), 270-279. doi:10.1016/j.jalz.2011.03.008
- Alexander, G. C., Emerson, S., & Kesselheim, A. S. (2021). Evaluation of aducanumab for Alzheimer disease: scientific evidence and regulatory review involving efficacy, safety, and futility. *Jama*, 325(17), 1717-1718. doi:10.1001/jama.2021.3854
- Alliot, F., Lecain, E., Grima, B., & Pessac, B. (1991). Microglial progenitors with a high proliferative potential in the embryonic and adult mouse brain. *Proc Natl Acad Sci USA*, 88(4), 1541-1545. doi:10.1073/pnas.88.4.1541

- Alliot, F., Godin, I., & Pessac, B. (1999). Microglia derive from progenitors, originating from the yolk sac, and which proliferate in the brain. *Brain Res Dev Brain Res*, 117(2), 145-152. doi:10.1016/s0165-3806(99)00113-3
- Allsop, D., Landon, M., & Kidd, M. (1983). The isolation and amino acid composition of senile plaque core protein. *Brain Res*, 259(2), 348-352. doi:10.1016/0006-8993(83)91273-8
- Almolda, B., González, B., & Castellano, B. (2013). Microglia detection by enzymatic histochemistry. *Methods Mol Biol*, 1041, 243-259. doi:10.1007/978-1-62703-520-0_22
- Aloisi, F. (2001). Immune function of microglia. *Glia*, 36(2), 165-179. doi:10.1002/glia.1106
- Alonso, A. d. C., Zaidi, T., Grundke-Iqbal, I., & Iqbal, K. (1994). Role of abnormally phosphorylated tau in the breakdown of microtubules in Alzheimer disease. *Proc Natl Acad Sci USA*, 91(12), 5562-5566. doi:10.1073/pnas.91.12.5562
- Alonso, A. d. C., Li, B., Grundke-Iqbal, I., & Iqbal, K. (2006). Polymerization of hyperphosphorylated tau into filaments eliminates its inhibitory activity. *Proc Natl Acad Sci USA*, 103(23), 8864-8869. doi:10.1073/pnas.0603214103
- Alzforum, a. Mutations: APP [Online Database]. Retrieved 2021, Apr 13, from <https://www.alzforum.org/mutations/app>
- Alzforum, b. Mutations: PSEN-1 [Online Database]. Retrieved 2021, Apr 13, from <https://www.alzforum.org/mutations/psen-1>
- Alzforum, c. Mutations: PSEN-2 [Online Database]. Retrieved 2021, Apr 13, from <https://www.alzforum.org/mutations/psen-2>
- Alzheimer's Association. (2020). 2020 Alzheimer's disease facts and figures. *Alzheimers Dement*, 16(3), 391-460. doi:10.1002/alz.12068
- Ambrad Giovannetti, E., & Fuhrmann, M. (2019). Unsupervised excitation: GABAergic dysfunctions in Alzheimer's disease. *Brain Res*, 1707, 216-226. doi:10.1016/j.brainres.2018.11.042
- Andersson, M., Avaliani, N., Svensson, A., Wickham, J., Pinborg, L. H., Jespersen, B., Christiansen, S. H., Bengzon, J., Woldbye, D. P., & Kokaia, M. (2016). Optogenetic control of human neurons in organotypic brain cultures. *Sci Rep*, 6, 24818. doi:10.1038/srep24818
- Andrews, S. J., Fulton-Howard, B., & Goate, A. (2020). Interpretation of risk loci from genome-wide association studies of Alzheimer's disease. *Lancet Neurol*, 19(4), 326-335. doi:10.1016/s1474-4422(19)30435-1
- Arber, C., Lovejoy, C., & Wray, S. (2017). Stem cell models of Alzheimer's disease: progress and challenges. *Alzheimers Res Ther*, 9(1), 42. doi:10.1186/s13195-017-0268-4
- Arboleda-Velasquez, J. F., Lopera, F., O'Hare, M., Delgado-Tirado, S., Marino, C., Chmielewska, N., Saez-Torres, K. L., Amarnani, D., Schultz, A. P., Sperling, R. A., Leyton-Cifuentes, D., Chen, K., Baena, A., Aguillon, D., Rios-Romenets, S., Giraldo, M., Guzmán-Vélez, E., Norton, D. J., Pardilla-Delgado, E., Artola, A., Sanchez, J. S., Acosta-Urbe, J., Lalli, M., Kosik, K. S., Huentelman, M. J., Zetterberg, H., Blennow, K., Reiman, R. A., Luo, J., Chen, Y., Thiyyagura, P., Su, Y., Jun, G. R., Naymik, M., Gai, X., Bootwalla, M., Ji, J., Shen, L., Miller, J. B., Kim, L. A., Tariot, P. N., Johnson, K. A., Reiman, E. M., & Quiroz, Y. T. (2019). Resistance to autosomal dominant Alzheimer's disease in an APOE3 Christchurch

- homozygote: a case report. *Nat Med*, 25(11), 1680-1683.
doi:10.1038/s41591-019-0611-3
- Arendt, T., Bruckner, M. K., Gertz, H. J., & Marcova, L. (1998). Cortical distribution of neurofibrillary tangles in Alzheimer's disease matches the pattern of neurons that retain their capacity of plastic remodelling in the adult brain. *Neuroscience*, 83(4), 991-1002. doi:10.1016/s0306-4522(97)00509-5
- Armstrong, R. A. (1998). β -Amyloid plaques: stages in life history or independent origin? *Dement Geriatr Cogn Disord*, 9(4), 227-238.
doi:10.1159/000017051
- Armstrong, R. A., Lantos, P. L., & Cairns, N. J. (2005). Overlap between neurodegenerative disorders. *Neuropathology*, 25(2), 111-124.
doi:10.1111/j.1440-1789.2005.00605.x
- Arndt, J. W., Qian, F., Smith, B. A., Quan, C., Kilambi, K. P., Bush, M. W., Walz, T., Pepinsky, R. B., Bussi re, T., Hamann, S., Cameron, T. O., & Weinreb, P. H. (2018). Structural and kinetic basis for the selectivity of aducanumab for aggregated forms of amyloid- β . *Sci Rep*, 8(1), 6412.
doi:10.1038/s41598-018-24501-0
- Arnold, S. E., Arvanitakis, Z., Macauley-Rambach, S. L., Koenig, A. M., Wang, H. Y., Ahima, R. S., Craft, S., Gandy, S., Buettner, C., Sto ckel, L. E., Holtzman, D. M., & Nathan, D. M. (2018). Brain insulin resistance in type 2 diabetes and Alzheimer disease: concepts and conundrums. *Nat Rev Neurol*, 14(3), 168-181. doi:10.1038/nrneurol.2017.185
- Arnsten, A. F. T., Datta, D., Tredici, K. D., & Braak, H. (2021). Hypothesis: tau pathology is an initiating factor in sporadic Alzheimer's disease. *Alzheimers Dement*, 17(1), 115-124. doi:10.1002/alz.12192
- Arranz, A., Abad, C., Juarranz, Y., Leceta, J., Martinez, C., & Gomariz, R. P. (2008). Vasoactive intestinal peptide as a healing mediator in Crohn's disease. *Neuroimmunomodulation*, 15(1), 46-53. doi:10.1159/000135623
- Arriagada, P. V., Growdon, J. H., Hedley-Whyte, E. T., & Hyman, B. T. (1992). Neurofibrillary tangles but not senile plaques parallel duration and severity of Alzheimer's disease. *Neurology*, 42(3 Pt 1), 631-639.
- Arvanitakis, Z., Leurgans, S. E., Wang, Z., Wilson, R. S., Bennett, D. A., & Schneider, J. A. (2011). Cerebral amyloid angiopathy pathology and cognitive domains in older persons. *Ann Neurol*, 69(2), 320-327.
doi:10.1002/ana.22112
- Ashwell, K. (1990). Microglia and cell death in the developing mouse cerebellum. *Brain Res Dev Brain Res*, 55(2), 219-230. doi:10.1016/0165-3806(90)90203-b
- Askew, K., Li, K., Olmos-Alonso, A., Garcia-Moreno, F., Liang, Y., Richardson, P., Tipton, T., Chapman, M. A., Riecken, K., Beccari, S., Sierra, A., Moln r, Z., Cragg, M. S., Garaschuk, O., Perry, V. H., & Gomez-Nicola, D. (2017). Coupled proliferation and apoptosis maintain the rapid turnover of microglia in the adult brain. *Cell Rep*, 18(2), 391-405.
doi:10.1016/j.celrep.2016.12.041
- Au, N. P. B., & Ma, C. H. E. (2017). Recent advances in the study of bipolar/rod-shaped microglia and their roles in neurodegeneration. *Front Aging Neurosci*, 9. doi:10.3389/fnagi.2017.00128
- Audrain, M., Haure-Mirande, J. V., Mleczko, J., Wang, M., Griffin, J. K., St George-Hyslop, P. H., Fraser, P., Zhang, B., Gandy, S., & Ehrlich, M. E.

- (2021). Reactive or transgenic increase in microglial TYROBP reveals a TREM2-independent TYROBP-APOE link in wild-type and Alzheimer's-related mice. *Alzheimers Dement*, 17(2), 149-163. doi:10.1002/alz.12256
- Australian Bureau of Statistics. (2019). *Australia's leading causes of death, 2018. Cat. No. 3303.0*. Canberra, Australia: ABS. Retrieved from <https://www.abs.gov.au/AUSSTATS/abs@.nsf/Lookup/3303.0Main+Features12018?OpenDocument>
- Australian Institute of Health and Welfare. (2019a). *Australian Burden of Disease Study: impact and causes of illness and death in Australia 2015. Australian Burden of Disease series No. 19. Cat. No. BOD 22*. Canberra, Australia: AIHW. Retrieved from <https://www.aihw.gov.au/getmedia/c076f42f-61ea-4348-9c0a-d996353e838f/aihw-bod-22.pdf.aspx?inline=true>
- Australian Institute of Health and Welfare. (2019b). *Hospital care for people with dementia 2016–17. Cat. No. AGE 94*. Canberra, Australia: AIHW. Retrieved from <https://www.aihw.gov.au/getmedia/34d3dd23-56be-4809-b61f-62b7697b9dc4/aihw-age-94.pdf.aspx?inline=true>
- Aw, E., Zhang, Y., & Carroll, M. (2020). Microglial responses to peripheral type 1 interferon. *J Neuroinflammation*, 17(1), 340. doi:10.1186/s12974-020-02003-z
- Bachstetter, A. D., Rowe, R. K., Kaneko, M., Goulding, D., Lifshitz, J., & Eldik, L. J. (2013). The p38 α MAPK regulates microglial responsiveness to diffuse traumatic brain injury. *J Neurosci*, 33. doi:10.1523/jneurosci.5399-12.2013
- Bachstetter, A. D., Van Eldik, L. J., Schmitt, F. A., Neltner, J. H., Ighodaro, E. T., Webster, S. J., Patel, E., Abner, E. L., Kryscio, R. J., & Nelson, P. T. (2015). Disease-related microglia heterogeneity in the hippocampus of Alzheimer's disease, dementia with Lewy bodies, and hippocampal sclerosis of aging. *Acta Neuropathol Commun*, 3, 32. doi:10.1186/s40478-015-0209-z
- Bachstetter, A. D., Ighodaro, E. T., Hassoun, Y., Aldeiri, D., Neltner, J. H., Patel, E., Abner, E. L., & Nelson, P. T. (2017). Rod-shaped microglia morphology is associated with aging in 2 human autopsy series. *Neurobiol Aging*, 52, 98-105. doi:10.1016/j.neurobiolaging.2016.12.028
- Badawi, Y., & Nishimune, H. (2020). Super-resolution microscopy for analyzing neuromuscular junctions and synapses. *Neurosci Lett*, 715, 134644. doi:10.1016/j.neulet.2019.134644
- Baggiolini, M., Dewald, B., & Moser, B. (1997). Human chemokines: an update. *Annu Rev Immunol*, 15, 675-705. doi:10.1146/annurev.immunol.15.1.675
- Bai, Z., Han, G., Xie, B., Wang, J., Song, F., Peng, X., & Lei, H. (2016). AlzBase: an integrative database for gene dysregulation in Alzheimer's disease. *Mol Neurobiol*, 53(1), 310-319. doi:10.1007/s12035-014-9011-3
- Bail, K., Goss, J., Draper, B., Berry, H., Karmel, R., & Gibson, D. (2015). The cost of hospital-acquired complications for older people with and without dementia; a retrospective cohort study. *BMC Health Serv Res*, 15, 91. doi:10.1186/s12913-015-0743-1
- Ballerini, P., Di Iorio, P., Ciccarelli, R., Caciagli, F., Poli, A., Beraudi, A., Buccella, S., D'Alimonte, I., D'Auro, M., Nargi, E., Patricelli, P., Visini, D., & Traversa, U. (2005). P2Y1 and cysteinyl leukotriene receptors mediate purine and cysteinyl leukotriene co-release in primary cultures of

- rat microglia. *Int J Immunopathol Pharmacol*, 18(2), 255-268.
doi:10.1177/039463200501800208
- Bancher, C., Jellinger, K., Lassmann, H., Fischer, P., & Leblhuber, F. (1996). Correlations between mental state and quantitative neuropathology in the Vienna Longitudinal Study on Dementia. *Eur Arch Psychiatry Clin Neurosci*, 246(3), 137-146. doi:10.1007/bf02189115
- Barclay, A. N., Wright, G. J., Brooke, G., & Brown, M. H. (2002). CD200 and membrane protein interactions in the control of myeloid cells. *Trends Immunol*, 23(6), 285-290. doi:10.1016/s1471-4906(02)02223-8
- Barger, S. W., & Basile, A. S. (2001). Activation of microglia by secreted amyloid precursor protein evokes release of glutamate by cystine exchange and attenuates synaptic function. *J Neurochem*, 76(3), 846-854. doi:10.1046/j.1471-4159.2001.00075.x
- Barger, S. W., Goodwin, M. E., Porter, M. M., & Beggs, M. L. (2007). Glutamate release from activated microglia requires the oxidative burst and lipid peroxidation. *J Neurochem*, 101(5), 1205-1213. doi:10.1111/j.1471-4159.2007.04487.x
- Barois, N., de Saint-Vis, B., Lebecque, S., Geuze, H. J., & Kleijmeer, M. J. (2002). MHC class II compartments in human dendritic cells undergo profound structural changes upon activation. *Traffic*, 3(12), 894-905. doi:10.1034/j.1600-0854.2002.31205.x
- Barthélemy, N. R., Horie, K., Sato, C., & Bateman, R. J. (2020a). Blood plasma phosphorylated-tau isoforms track CNS change in Alzheimer's disease. *J Exp Med*, 217(11). doi:10.1084/jem.20200861
- Barthélemy, N. R., Bateman, R. J., Hirtz, C., Marin, P., Becher, F., Sato, C., Gabelle, A., & Lehmann, S. (2020b). Cerebrospinal fluid phospho-tau T217 outperforms T181 as a biomarker for the differential diagnosis of Alzheimer's disease and PET amyloid-positive patient identification. *Alzheimers Res Ther*, 12(1), 26. doi:10.1186/s13195-020-00596-4
- Barthélemy, N. R., Li, Y., Joseph-Mathurin, N., Gordon, B. A., Hassenstab, J., Benzinger, T. L. S., Buckles, V., Fagan, A. M., Perrin, R. J., Goate, A. M., Morris, J. C., Karch, C. M., Xiong, C., Allegri, R., Mendez, P. C., Berman, S. B., Ikeuchi, T., Mori, H., Shimada, H., Shoji, M., Suzuki, K., Noble, J., Farlow, M., Chhatwal, J., Graff-Radford, N. R., Salloway, S., Schofield, P. R., Masters, C. L., Martins, R. N., O'Connor, A., Fox, N. C., Levin, J., Jucker, M., Gabelle, A., Lehmann, S., Sato, C., Bateman, R. J., & McDade, E. (2020c). A soluble phosphorylated tau signature links tau, amyloid and the evolution of stages of dominantly inherited Alzheimer's disease. *Nat Med*, 26(3), 398-407. doi:10.1038/s41591-020-0781-z
- Bartles, J. R. (2000). Parallel actin bundles and their multiple actin-bundling proteins. *Curr Opin Cell Biol*, 12(1), 72-78. doi:10.1016/s0955-0674(99)00059-9
- Bateman, R. J., Munsell, L. Y., Morris, J. C., Swarm, R., Yarasheski, K. E., & Holtzman, D. M. (2006). Human amyloid- β synthesis and clearance rates as measured in cerebrospinal fluid in vivo. *Nat Med*, 12(7), 856-861. doi:10.1038/nm1438
- Bateman, R. J., Xiong, C., Benzinger, T. L., Fagan, A. M., Goate, A., Fox, N. C., Marcus, D. S., Cairns, N. J., Xie, X., Blazey, T. M., Holtzman, D. M., Santacruz, A., Buckles, V., Oliver, A., Moulder, K., Aisen, P. S., Ghetti, B., Klunk, W. E., McDade, E., Martins, R. N., Masters, C. L., Mayeux, R.,

- Ringman, J. M., Rossor, M. N., Schofield, P. R., Sperling, R. A., Salloway, S., & Morris, J. C. (2012). Clinical and biomarker changes in dominantly inherited Alzheimer's disease. *N Engl J Med*, *367*(9), 795-804. doi:10.1056/NEJMoa1202753
- Beach, R. L., Bathgate, S. L., & Cotman, C. W. (1982). Identification of cell types in rat hippocampal slices maintained in organotypic cultures. *Brain Res*, *255*(1), 3-20. doi:10.1016/0165-3806(82)90071-2
- Becher, B., & Antel, J. P. (1996). Comparison of phenotypic and functional properties of immediately ex vivo and cultured human adult microglia. *Glia*, *18*(1), 1-10. doi:10.1002/(sici)1098-1136(199609)18:1<1::Aid-glia1>3.0.Co;2-6
- Benediktsson, A. M., Schachtele, S. J., Green, S. H., & Dailey, M. E. (2005). Ballistic labeling and dynamic imaging of astrocytes in organotypic hippocampal slice cultures. *J Neurosci Methods*, *141*(1), 41-53. doi:10.1016/j.jneumeth.2004.05.013
- Bennett, D. A., Cochran, E. J., Saper, C. B., Leverenz, J. B., Gilley, D. W., & Wilson, R. S. (1993). Pathological changes in frontal cortex from biopsy to autopsy in Alzheimer's disease. *Neurobiol Aging*, *14*(6), 589-596. doi:10.1016/0197-4580(93)90043-b
- Bennett, M. L., Bennett, F. C., Liddelow, S. A., Ajami, B., Zamanian, J. L., Fernhoff, N. B., Mulinyawe, S. B., Bohlen, C. J., Adil, A., Tucker, A., Weissman, I. L., Chang, E. F., Li, G., Grant, G. A., Hayden Gephart, M. G., & Barres, B. A. (2016). New tools for studying microglia in the mouse and human CNS. *Proc Natl Acad Sci USA*, *113*(12), E1738-1746. doi:10.1073/pnas.1525528113
- Benson, M. D., Buxbaum, J. N., Eisenberg, D. S., Merlini, G., Saraiva, M. J. M., Sekijima, Y., Sipe, J. D., & Westermarck, P. (2018). Amyloid nomenclature 2018: recommendations by the International Society of Amyloidosis (ISA) nomenclature committee. *Amyloid*, *25*(4), 215-219. doi:10.1080/13506129.2018.1549825
- Berg, L., McKeel, D. W., Jr., Miller, J. P., Storandt, M., Rubin, E. H., Morris, J. C., Baty, J., Coats, M., Norton, J., Goate, A. M., Price, J. L., Gearing, M., Mirra, S. S., & Saunders, A. M. (1998). Clinicopathologic studies in cognitively healthy aging and Alzheimer's disease: relation of histologic markers to dementia severity, age, sex, and apolipoprotein E genotype. *Arch Neurol*, *55*(3), 326-335. doi:10.1001/archneur.55.3.326
- Bertram, L., Lill, C. M., & Tanzi, R. E. (2010). The genetics of Alzheimer disease: back to the future. *Neuron*, *68*(2), 270-281. doi:10.1016/j.neuron.2010.10.013
- Bertram, L., & Tanzi, R. E. (2019). Alzheimer disease risk genes: 29 and counting. *Nat Rev Neurol*, *15*(4), 191-192. doi:10.1038/s41582-019-0158-4
- Biancalana, M., & Koide, S. (2010). Molecular mechanism of Thioflavin-T binding to amyloid fibrils. *Biochim Biophys Acta*, *1804*(7), 1405-1412. doi:10.1016/j.bbapap.2010.04.001
- Bianchi, M. E. (2007). DAMPs, PAMPs and alarmins: all we need to know about danger. *J Leukoc Biol*, *81*(1), 1-5. doi:10.1189/jlb.0306164
- Biber, K., Neumann, H., Inoue, K., & Boddeke, H. W. (2007). Neuronal 'On' and 'Off' signals control microglia. *Trends Neurosci*, *30*(11), 596-602. doi:10.1016/j.tins.2007.08.007

- Biber, K., Vinet, J., & Boddeke, H. W. (2008). Neuron-microglia signaling: chemokines as versatile messengers. *J Neuroimmunol*, 198(1-2), 69-74. doi:10.1016/j.jneuroim.2008.04.012
- Bisht, K., Sharma, K. P., Lecours, C., Sánchez, M. G., El Hajj, H., Milior, G., Olmos-Alonso, A., Gómez-Nicola, D., Luheshi, G., Vallières, L., Branchi, I., Maggi, L., Limatola, C., Butovsky, O., & Tremblay, M.-È. (2016). Dark microglia: A new phenotype predominantly associated with pathological states. *Glia*, 64(5), 826-839. doi:10.1002/glia.22966
- Björkqvist, M., Wild, E. J., & Tabrizi, S. J. (2009). Harnessing immune alterations in neurodegenerative diseases. *Neuron*, 64(1), 21-24. doi:10.1016/j.neuron.2009.09.034
- Black, J. A., Liu, S., & Waxman, S. G. (2009). Sodium channel activity modulates multiple functions in microglia. *Glia*, 57(10), 1072-1081. doi:10.1002/glia.20830
- Blanchard, J. W., Bula, M., Davila-Velderrain, J., Akay, L. A., Zhu, L., Frank, A., Victor, M. B., Bonner, J. M., Mathys, H., Lin, Y. T., Ko, T., Bennett, D. A., Cam, H. P., Kellis, M., & Tsai, L. H. (2020). Reconstruction of the human blood-brain barrier in vitro reveals a pathogenic mechanism of APOE4 in pericytes. *Nat Med*, 26(6), 952-963. doi:10.1038/s41591-020-0886-4
- Blanchoin, L., Boujemaa-Paterski, R., Sykes, C., & Plastino, J. (2014). Actin dynamics, architecture, and mechanics in cell motility. *Physiol Rev*, 94(1), 235-263. doi:10.1152/physrev.00018.2013
- Ble, A., Ranzini, M., Zurlo, A., Menozzi, L., Atti, A. R., Munari, M. R., Volpato, S., Scaramelli, G., Fellin, R., & Zuliani, G. (2006). Leukoaraiosis is associated with functional impairment in older patients with Alzheimer's disease but not vascular dementia. *J Nutr Health Aging*, 10(1), 31-35.
- Blinzinger, K., & Kreutzberg, G. (1968). Displacement of synaptic terminals from regenerating motoneurons by microglial cells. *Z Zellforsch Mikrosk Anat*, 85(2), 145-157. doi:10.1007/bf00325030
- Block, M. L., Zecca, L., & Hong, J. S. (2007). Microglia-mediated neurotoxicity: uncovering the molecular mechanisms. *Nat Rev Neurosci*, 8(1), 57-69. doi:10.1038/nrn2038
- Boche, D., Perry, V. H., & Nicoll, J. A. (2013). Review: activation patterns of microglia and their identification in the human brain. *Neuropathol Appl Neurobiol*, 39. doi:10.1111/nan.12011
- Bohnert, S., Seiffert, A., Trella, S., Bohnert, M., Distel, L., Ondruschka, B., & Monoranu, C. M. (2020). TMEM119 as a specific marker of microglia reaction in traumatic brain injury in postmortem examination. *Int J Legal Med*, 134(6), 2167-2176. doi:10.1007/s00414-020-02384-z
- Bolmont, T., Haiss, F., Eicke, D., Radde, R., Mathis, C. A., Klunk, W. E., Kohsaka, S., Jucker, M., & Calhoun, M. E. (2008). Dynamics of the microglial/amyloid interaction indicate a role in plaque maintenance. *J Neurosci*, 28(16), 4283-4292. doi:10.1523/jneurosci.4814-07.2008
- Bonham, L. W., Karch, C. M., Fan, C. C., Tan, C., Geier, E. G., Wang, Y., Wen, N., Broce, I. J., Li, Y., Barkovich, M. J., Ferrari, R., Hardy, J., Momeni, P., Höglinger, G., Müller, U., Hess, C. P., Sugrue, L. P., Dillon, W. P., Schellenberg, G. D., Miller, B. L., Andreassen, O. A., Dale, A. M., Barkovich, A. J., Yokoyama, J. S., & Desikan, R. S. (2018). CXCR4

- involvement in neurodegenerative diseases. *Transl Psychiatry*, 8(1), 73. doi:10.1038/s41398-017-0049-7
- Boon, B. D. C., Bulk, M., Jonker, A. J., Morrema, T. H. J., van den Berg, E., Popovic, M., Walter, J., Kumar, S., van der Lee, S. J., Holstege, H., Zhu, X., Van Nostrand, W. E., Natté, R., van der Weerd, L., Bouwman, F. H., van de Berg, W. D. J., Rozemuller, A. J. M., & Hoozemans, J. J. M. (2020). The coarse-grained plaque: a divergent A β plaque-type in early-onset Alzheimer's disease. *Acta Neuropathol*, 140(6), 811-830. doi:10.1007/s00401-020-02198-8
- Bordey, A., & Spencer, D. D. (2003). Chemokine modulation of high-conductance Ca(2+)-sensitive K(+) currents in microglia from human hippocampi. *Eur J Neurosci*, 18(10), 2893-2898. doi:10.1111/j.1460-9568.2003.03021.x
- Borges, M. K., Canevelli, M., Cesari, M., & Aprahamian, I. (2019). Frailty as a predictor of cognitive disorders: a systematic review and meta-analysis. *Front Med (Lausanne)*, 6, 26. doi:10.3389/fmed.2019.00026
- Böttcher, C., Schlickeiser, S., Sneeboer, M. A. M., Kunkel, D., Knop, A., Paza, E., Fidzinski, P., Kraus, L., Snijders, G. J. L., Kahn, R. S., Schulz, A. R., Mei, H. E., Hol, E. M., Siegmund, B., Glauben, R., Spruth, E. J., de Witte, L. D., & Priller, J. (2019). Human microglia regional heterogeneity and phenotypes determined by multiplexed single-cell mass cytometry. *Nat Neurosci*, 22(1), 78-90. doi:10.1038/s41593-018-0290-2
- Bouchon, A., Dietrich, J., & Colonna, M. (2000). Cutting edge: inflammatory responses can be triggered by TREM-1, a novel receptor expressed on neutrophils and monocytes. *J Immunol*, 164(10), 4991-4995. doi:10.4049/jimmunol.164.10.4991
- Boucsein, C., Kettenmann, H., & Nolte, C. (2000). Electrophysiological properties of microglial cells in normal and pathologic rat brain slices. *Eur J Neurosci*, 12(6), 2049-2058. doi:10.1046/j.1460-9568.2000.00100.x
- Bouras, C., Hof, P. R., Giannakopoulos, P., Michel, J. P., & Morrison, J. H. (1994). Regional distribution of neurofibrillary tangles and senile plaques in the cerebral cortex of elderly patients: a quantitative evaluation of a one-year autopsy population from a geriatric hospital. *Cereb Cortex*, 4(2), 138-150. doi:10.1093/cercor/4.2.138
- Bouvier, D. S., Jones, E. V., Quesseveur, G., Davoli, M. A., T, A. F., Quirion, R., Mechawar, N., & Murai, K. K. (2016). High resolution dissection of reactive glial nets in Alzheimer's disease. *Sci Rep*, 6, 24544. doi:10.1038/srep24544
- Boyle, P. A., Yu, L., Wilson, R. S., Leurgans, S. E., Schneider, J. A., & Bennett, D. A. (2018). Person-specific contribution of neuropathologies to cognitive loss in old age. *Ann Neurol*, 83(1), 74-83. doi:10.1002/ana.25123
- Bozzali, M., Serra, L., & Cercignani, M. (2016). Quantitative MRI to understand Alzheimer's disease pathophysiology. *Curr Opin Neurol*, 29(4), 437-444. doi:10.1097/wco.0000000000000345
- Braak, E., Braak, H., & Mandelkow, E. M. (1994). A sequence of cytoskeleton changes related to the formation of neurofibrillary tangles and neuropil threads. *Acta Neuropathol*, 87(6), 554-567.
- Braak, H., & Braak, E. (1988). Neuropil threads occur in dendrites of tangle-bearing nerve cells. *Neuropathol Appl Neurobiol*, 14(1), 39-44.

- Braak, H., & Braak, E. (1991). Neuropathological staging of Alzheimer-related changes. *Acta Neuropathol*, 82(4), 239-259.
- Braak, H., & Del Tredici, K. (2011). The pathological process underlying Alzheimer's disease in individuals under thirty. *Acta Neuropathol*, 121(2), 171-181. doi:10.1007/s00401-010-0789-4
- Braak, H., Thal, D. R., Ghebremedhin, E., & Del Tredici, K. (2011). Stages of the pathologic process in Alzheimer disease: age categories from 1 to 100 years. *J Neuropathol Exp Neurol*, 70(11), 960-969. doi:10.1097/NEN.0b013e318232a379
- Braak, H., & Del Tredici, K. (2015a). Neuroanatomy and pathology of sporadic Alzheimer's disease. *Adv Anat Embryol Cell Biol*, 215, 1-162.
- Braak, H., & Del Tredici, K. (2015b). The preclinical phase of the pathological process underlying sporadic Alzheimer's disease. *Brain*, 138(Pt 10), 2814-2833. doi:10.1093/brain/awv236
- Bradshaw, E. M., Chibnik, L. B., Keenan, B. T., Ottoboni, L., Raj, T., Tang, A., Rosenkrantz, L. L., Imboywa, S., Lee, M., Von Korff, A., Morris, M. C., Evans, D. A., Johnson, K., Sperling, R. A., Schneider, J. A., Bennett, D. A., & De Jager, P. L. (2013). CD33 Alzheimer's disease locus: altered monocyte function and amyloid biology. *Nat Neurosci*, 16(7), 848-850. doi:10.1038/nn.3435
- Brawek, B., Skok, M., & Garaschuk, O. (2021). Changing functional signatures of microglia along the axis of brain aging. *Int J Mol Sci*, 22(3). doi:10.3390/ijms22031091
- Brenowitz, W. D., Nelson, P. T., Besser, L. M., Heller, K. B., & Kukull, W. A. (2015). Cerebral amyloid angiopathy and its co-occurrence with Alzheimer's disease and other cerebrovascular neuropathologic changes. *Neurobiol Aging*, 36(10), 2702-2708. doi:10.1016/j.neurobiolaging.2015.06.028
- Brion, J. P., Couck, A. M., Passareiro, E., & Flament-Durand, J. (1985). Neurofibrillary tangles of Alzheimer's disease: an immunohistochemical study. *J Submicrosc Cytol*, 17(1), 89-96.
- Brooke, G., Holbrook, J. D., Brown, M. H., & Barclay, A. N. (2004). Human lymphocytes interact directly with CD47 through a novel member of the signal regulatory protein (SIRP) family. *J Immunol*, 173(4), 2562-2570. doi:10.4049/jimmunol.173.4.2562
- Brookmeyer, R., Evans, D. A., Hebert, L., Langa, K. M., Heeringa, S. G., Plassman, B. L., & Kukull, W. A. (2011). National estimates of the prevalence of Alzheimer's disease in the United States. *Alzheimers Dement*, 7(1), 61-73. doi:10.1016/j.jalz.2010.11.007
- Brouwers, N., Van Cauwenberghe, C., Engelborghs, S., Lambert, J. C., Bettens, K., Le Bastard, N., Pasquier, F., Montoya, A. G., Peeters, K., Mattheijssens, M., Vandenberghe, R., Deyn, P. P., Cruts, M., Amouyel, P., Sleegers, K., & Van Broeckhoven, C. (2012). Alzheimer risk associated with a copy number variation in the complement receptor 1 increasing C3b/C4b binding sites. *Mol Psychiatry*, 17(2), 223-233. doi:10.1038/mp.2011.24
- Brown, E. M., & MacLeod, R. J. (2001). Extracellular calcium sensing and extracellular calcium signaling. *Physiol Rev*, 81(1), 239-297. doi:10.1152/physrev.2001.81.1.239

- Brown, L., Hansnata, E., & La, H. A. (2017). *Economic Cost of Dementia in Australia 2016–2056*. Canberra, Australia: Institute for Governance & Policy Analysis, University of Canberra. Retrieved from <https://www.dementia.org.au/sites/default/files/NATIONAL/documents/The-economic-cost-of-dementia-in-Australia-2016-to-2056.pdf>
- Bruce, A. J., Boling, W., Kindy, M. S., Peschon, J., Kraemer, P. J., Carpenter, M. K., Holtzman, F. W., & Mattson, M. P. (1996). Altered neuronal and microglial responses to excitotoxic and ischemic brain injury in mice lacking TNF receptors. *Nat Med*, 2(7), 788-794. doi:10.1038/nm0796-788
- Buckner, R. L., Snyder, A. Z., Shannon, B. J., LaRossa, G., Sachs, R., Fotenos, A. F., Sheline, Y. I., Klunk, W. E., Mathis, C. A., Morris, J. C., & Mintun, M. A. (2005). Molecular, structural, and functional characterization of Alzheimer's disease: evidence for a relationship between default activity, amyloid, and memory. *J Neurosci*, 25(34), 7709-7717. doi:10.1523/jneurosci.2177-05.2005
- Buée, L., Hof, P. R., Bouras, C., Delacourte, A., Perl, D. P., Morrison, J. H., & Fillit, H. M. (1994). Pathological alterations of the cerebral microvasculature in Alzheimer's disease and related dementing disorders. *Acta Neuropathol*, 87(5), 469-480. doi:10.1007/bf00294173
- Buée, L., Bussière, T., Buée-Scherrer, V., Delacourte, A., & Hof, P. R. (2000). Tau protein isoforms, phosphorylation and role in neurodegenerative disorders. *Brain Res Brain Res Rev*, 33(1), 95-130. doi:10.1016/s0165-0173(00)00019-9
- Bunn, F., Burn, A. M., Goodman, C., Rait, G., Norton, S., Robinson, L., Schoeman, J., & Brayne, C. (2014). Comorbidity and dementia: a scoping review of the literature. *BMC Med*, 12, 192. doi:10.1186/s12916-014-0192-4
- Burkovetskaya, M. E., Small, R., Guo, L., Buch, S., & Guo, M. L. (2020). Cocaine self-administration differentially activates microglia in the mouse brain. *Neurosci Lett*, 728, 134951. doi:10.1016/j.neulet.2020.134951
- Bush, A. I., Pettingell, W. H., Multhaup, G., d Paradis, M., Vonsattel, J. P., Gusella, J. F., Beyreuther, K., Masters, C. L., & Tanzi, R. E. (1994). Rapid induction of Alzheimer A β amyloid formation by zinc. *Science*, 265(5177), 1464-1467. doi:10.1126/science.8073293
- Bussière, T., Gold, G., Kövari, E., Giannakopoulos, P., Bouras, C., Perl, D. P., Morrison, J. H., & Hof, P. R. (2003). Stereologic analysis of neurofibrillary tangle formation in prefrontal cortex area 9 in aging and Alzheimer's disease. *Neuroscience*, 117(3), 577-592. doi:10.1016/s0306-4522(02)00942-9
- Butovsky, O., Siddiqui, S., Gabriely, G., Lanser, A. J., Dake, B., Murugaiyan, G., Doykan, C. E., Wu, P. M., Gali, R. R., Iyer, L. K., Lawson, R., Berry, J., Krichevsky, A. M., Cudkowicz, M. E., & Weiner, H. L. (2012). Modulating inflammatory monocytes with a unique microRNA gene signature ameliorates murine ALS. *J Clin Invest*, 122(9), 3063-3087. doi:10.1172/jci62636
- Butovsky, O., Jedrychowski, M. P., Moore, C. S., Cialic, R., Lanser, A. J., Gabriely, G., Koeglsperger, T., Dake, B., Wu, P. M., Doykan, C. E., Fanek, Z., Liu, L., Chen, Z., Rothstein, J. D., Ransohoff, R. M., Gygi, S. P., Antel, J. P., & Weiner, H. L. (2014). Identification of a unique TGF- β –

- dependent molecular and functional signature in microglia. *Nat Neurosci*, 17. doi:10.1038/nn.3599
- Cabral, G. A., & Marciano-Cabral, F. (2005). Cannabinoid receptors in microglia of the central nervous system: immune functional relevance. *J Leukoc Biol*, 78(6), 1192-1197. doi:10.1189/jlb.0405216
- Calsolaro, V., & Edison, P. (2016). Neuroinflammation in Alzheimer's disease: current evidence and future directions. *Alzheimers Dement*, 12(6), 719-732. doi:10.1016/j.jalz.2016.02.010
- Camins, A., Verdaguer, E., Folch, J., Canudas, A. M., & Pallàs, M. (2006). The role of CDK5/P25 formation/inhibition in neurodegeneration. *Drug News Perspect*, 19(8), 453-460. doi:10.1358/dnp.2006.19.8.1043961
- Cao, T., Thomas, T. C., Ziebell, J. M., Pauly, J. R., & Lifshitz, J. (2012). Morphological and genetic activation of microglia after diffuse traumatic brain injury in the rat. *Neuroscience*, 225, 65-75. doi:10.1016/j.neuroscience.2012.08.058
- Caplan, H. W., Cardenas, F., Gudenkauf, F., Zelnick, P., Xue, H., Cox, C. S., & Bedi, S. S. (2020). Spatiotemporal distribution of microglia after traumatic brain injury in male mice. *ASN Neuro*, 12, 1759091420911770. doi:10.1177/1759091420911770
- Cardona, A. E., Pioro, E. P., Sasse, M. E., Kostenko, V., Cardona, S. M., Dijkstra, I. M., Huang, D., Kidd, G., Dombrowski, S., Dutta, R., Lee, J. C., Cook, D. N., Jung, S., Lira, S. A., Littman, D. R., & Ransohoff, R. M. (2006). Control of microglial neurotoxicity by the fractalkine receptor. *Nat Neurosci*, 9(7), 917-924. doi:10.1038/nn1715
- Carlson, M. C., Helms, M. J., Steffens, D. C., Burke, J. R., Potter, G. G., & Plassman, B. L. (2008). Midlife activity predicts risk of dementia in older male twin pairs. *Alzheimers Dement*, 4(5), 324-331. doi:10.1016/j.jalz.2008.07.002
- Carnevale, D., De Simone, R., & Minghetti, L. (2007). Microglia-neuron interaction in inflammatory and degenerative diseases: role of cholinergic and noradrenergic systems. *CNS Neurol Disord Drug Targets*, 6(6), 388-397. doi:10.2174/187152707783399193
- Carrier, E. J., Kearn, C. S., Barkmeier, A. J., Breese, N. M., Yang, W., Nithipatikom, K., Pfister, S. L., Campbell, W. B., & Hillard, C. J. (2004). Cultured rat microglial cells synthesize the endocannabinoid 2-arachidonylglycerol, which increases proliferation via a CB2 receptor-dependent mechanism. *Mol Pharmacol*, 65(4), 999-1007. doi:10.1124/mol.65.4.999
- Casanova, M. F., Starkstein, S. E., & Jellinger, K. A. (2011). Clinicopathological correlates of behavioral and psychological symptoms of dementia. *Acta Neuropathol*, 122(2), 117-135. doi:10.1007/s00401-011-0821-3
- Cascella, R., & Cecchi, C. (2021). Calcium Dyshomeostasis in Alzheimer's Disease Pathogenesis. *Int J Mol Sci*, 22(9). doi:10.3390/ijms22094914
- Case, R. M., Eisner, D., Gurney, A., Jones, O., Muallem, S., & Verkhratsky, A. (2007). Evolution of calcium homeostasis: from birth of the first cell to an omnipresent signalling system. *Cell Calcium*, 42(4-5), 345-350. doi:10.1016/j.ceca.2007.05.001
- Castanho, I., Murray, T. K., Hannon, E., Jeffries, A., Walker, E., Laing, E., Baulf, H., Harvey, J., Bradshaw, L., Randall, A., Moore, K., O'Neill, P., Lunnon, K., Collier, D. A., Ahmed, Z., O'Neill, M. J., & Mill, J. (2020).

- Transcriptional signatures of tau and amyloid neuropathology. *Cell Rep*, 30(6), 2040-2054.e2045. doi:10.1016/j.celrep.2020.01.063
- Castellani, R. J., Lee, H. G., Zhu, X., Perry, G., & Smith, M. A. (2008). Alzheimer disease pathology as a host response. *J Neuropathol Exp Neurol*, 67(6), 523-531. doi:10.1097/NEN.0b013e318177eaf4
- Castellani, R. J., & Smith, M. A. (2011). Compounding artefacts with uncertainty, and an amyloid cascade hypothesis that is 'too big to fail'. *J Pathol*, 224(2), 147-152. doi:10.1002/path.2885
- Celarain, N., Sánchez-Ruiz de Gordo, J., Zelaya, M. V., Roldán, M., Larumbe, R., Pulido, L., Echavarri, C., & Mendioroz, M. (2016). TREM2 upregulation correlates with 5-hydroxymethylcytosine enrichment in Alzheimer's disease hippocampus. *Clin Epigenetics*, 8, 37. doi:10.1186/s13148-016-0202-9
- Chami, B., Steel, A. J., De La Monte, S. M., & Sutherland, G. T. (2016). The rise and fall of insulin signaling in Alzheimer's disease. *Metab Brain Dis*, 31(3), 497-515. doi:10.1007/s11011-016-9806-1
- Chao, C. C., Gekker, G., Hu, S., Sheng, W. S., Shark, K. B., Bu, D. F., Archer, S., Bidlack, J. M., & Peterson, P. K. (1996). κ opioid receptors in human microglia downregulate human immunodeficiency virus 1 expression. *Proc Natl Acad Sci USA*, 93(15), 8051-8056. doi:10.1073/pnas.93.15.8051
- Chatila, Z. K., & Bradshaw, E. M. (2021). Alzheimer's disease genetics: a dampened microglial response? *Neuroscientist*, 10738584211024531. doi:10.1177/10738584211024531
- Chen, M., Maleski, J. J., & Sawmiller, D. R. (2011). Scientific truth or false hope? Understanding Alzheimer's disease from an aging perspective. *J Alzheimers Dis*, 24(1), 3-10. doi:10.3233/jad-2010-101638
- Chen, S., Peng, J., Sherchan, P., Ma, Y., Xiang, S., Yan, F., Zhao, H., Jiang, Y., Wang, N., Zhang, J. H., & Zhang, H. (2020a). TREM2 activation attenuates neuroinflammation and neuronal apoptosis via PI3K/Akt pathway after intracerebral hemorrhage in mice. *J Neuroinflammation*, 17(1), 168. doi:10.1186/s12974-020-01853-x
- Chen, W. T., Lu, A., Craessaerts, K., Pavie, B., Sala Frigerio, C., Corthout, N., Qian, X., Laláková, J., Kühnemund, M., Voytyuk, I., Wolfs, L., Mancuso, R., Salta, E., Balusu, S., Snellinx, A., Munck, S., Jurek, A., Fernandez Navarro, J., Saido, T. C., Huitinga, I., Lundberg, J., Fiers, M., & De Strooper, B. (2020b). Spatial Transcriptomics and In Situ Sequencing to Study Alzheimer's Disease. *Cell*, 182(4), 976-991.e919. doi:10.1016/j.cell.2020.06.038
- Chesser, A. S., Pritchard, S. M., & Johnson, G. V. (2013). Tau clearance mechanisms and their possible role in the pathogenesis of Alzheimer disease. *Front Neurol*, 4, 122. doi:10.3389/fneur.2013.00122
- Chiffolleau, E. (2018). C-Type lectin-like receptors as emerging orchestrators of sterile inflammation represent potential therapeutic targets. *Front Immunol*, 9, 227. doi:10.3389/fimmu.2018.00227
- Chistiakov, D. A., Killingsworth, M. C., Myasoedova, V. A., Orekhov, A. N., & Bobryshev, Y. V. (2017). CD68/macrosialin: not just a histochemical marker. *Lab Invest*, 97(1), 4-13. doi:10.1038/labinvest.2016.116
- Chiu, I. M., Morimoto, E. T., Goodarzi, H., Liao, J. T., O'Keeffe, S., Phatnani, H. P., Muratet, M., Carroll, M. C., Levy, S., Tavazoie, S., Myers, R. M., & Maniatis, T. (2013). A neurodegeneration-specific gene-expression

- signature of acutely isolated microglia from an amyotrophic lateral sclerosis mouse model. *Cell Rep*, 4(2), 385-401.
doi:10.1016/j.celrep.2013.06.018
- Cho, K., & Choi, G. E. (2017). Microglia: physiological functions revealed through morphological profiles. *Folia Biol (Praha)*, 63(3), 85-90.
- Christensen, R. N., Ha, B. K., Sun, F., Bresnahan, J. C., & Beattie, M. S. (2006). Kainate induces rapid redistribution of the actin cytoskeleton in amoeboid microglia. *J Neurosci Res*, 84(1), 170-181. doi:10.1002/jnr.20865
- Ciccotosto, G. D., Tew, D., Curtain, C. C., Smith, D., Carrington, D., Masters, C. L., Bush, A. I., Cherny, R. A., Cappai, R., & Barnham, K. J. (2004). Enhanced toxicity and cellular binding of a modified amyloid β peptide with a methionine to valine substitution. *J Biol Chem*, 279(41), 42528-42534. doi:10.1074/jbc.M406465200
- Clare, R., King, V. G., Wrenfeldt, M., & Vinters, H. V. (2010). Synapse loss in dementias. *J Neurosci Res*, 88(10), 2083-2090. doi:10.1002/jnr.22392
- Clark, R. F., Hutton, M., Fuldner, R. A., Froelich, S., Karran, E., Talbot, C., Crook, R., Lendon, C., Prihar, G., He, C., Korenblat, K., Martinez, A., Wragg, M., Busfield, F., Behrens, M. I., Myers, A., Norton, J., Morris, J., Mehta, N., Pearson, C., Lincoln, S., Baker, M., Duff, K., Zehr, C., Perez-Tur, J., Houlden, H., Ruiz, A., Ossa, J., Lopera, F., Arcos, M., Madrigal, L., Collinge, J., Humphreys, C., Ashworth, A., Sarnier, S., Fox, N., Harvey, R., Kennedy, A., Roques, P., Cline, R. T., Phillips, C. A., Venter, J. C., Forsell, L., Axelman, K., Lilius, L., Johnston, J., Cowburn, R., Vitanen, M., Winblad, B., Kosik, K., Haltia, M., Poyhonen, M., Dickson, D., Mann, D., Neary, D., Snowden, J., Lantos, P., Lannfelt, L., Rossor, M., Roberts, G. W., Adams, M. D., Hardy, J., & Goate, A. (1995). The structure of the presenilin 1 (S182) gene and identification of six novel mutations in early onset AD families. *Nat Genet*, 11(2), 219-222.
doi:10.1038/ng1095-219
- Cleveland, D. W., Hwo, S. Y., & Kirschner, M. W. (1977). Purification of tau, a microtubule-associated protein that induces assembly of microtubules from purified tubulin. *J Mol Biol*, 116(2), 207-225. doi:10.1016/0022-2836(77)90213-3
- Close, W., Neumann, M., Schmidt, A., Hora, M., Annamalai, K., Schmidt, M., Reif, B., Schmidt, V., Grigorieff, N., & Fändrich, M. (2018). Physical basis of amyloid fibril polymorphism. *Nat Commun*, 9(1), 699.
doi:10.1038/s41467-018-03164-5
- Coltharp, C., & Xiao, J. (2012). Superresolution microscopy for microbiology. *Cell Microbiol*, 14(12), 1808-1818. doi:10.1111/cmi.12024
- Congdon, E. E., Wu, J. W., Myeku, N., Figueroa, Y. H., Herman, M., Marinec, P. S., Gestwicki, J. E., Dickey, C. A., Yu, W. H., & Duff, K. E. (2012). Methylthioninium chloride (methylene blue) induces autophagy and attenuates tauopathy in vitro and in vivo. *Autophagy*, 8(4), 609-622.
doi:10.4161/auto.19048
- Cope, E. C., LaMarca, E. A., Monari, P. K., Olson, L. B., Martinez, S., Zych, A. D., Katchur, N. J., & Gould, E. (2018). Microglia play an active role in obesity-associated cognitive decline. *J Neurosci*, 38(41), 8889-8904.
doi:10.1523/jneurosci.0789-18.2018

- Corradi, J., & Bouzat, C. (2016). Understanding the bases of function and modulation of $\alpha 7$ nicotinic receptors: implications for drug discovery. *Mol Pharmacol*, 90(3), 288-299. doi:10.1124/mol.116.104240
- Craig-Schapiro, R., Fagan, A. M., & Holtzman, D. M. (2009). Biomarkers of Alzheimer's disease. *Neurobiol Dis*, 35(2), 128-140. doi:10.1016/j.nbd.2008.10.003
- Crehan, H., Hardy, J., & Pocock, J. (2012). Microglia, Alzheimer's disease, and complement. *Int J Alzheimers Dis*, 2012, 983640. doi:10.1155/2012/983640
- Cremonini, A. L., Caffa, I., Cea, M., Nencioni, A., Odetti, P., & Monacelli, F. (2019). Nutrients in the prevention of Alzheimer's disease. *Oxid Med Cell Longev*, 2019, 9874159. doi:10.1155/2019/9874159
- Croft, C. L., Wade, M. A., Kurbatskaya, K., Mastrandreas, P., Hughes, M. M., Phillips, E. C., Pooler, A. M., Perkinson, M. S., Hanger, D. P., & Noble, W. (2017). Membrane association and release of wild-type and pathological tau from organotypic brain slice cultures. *Cell Death Dis*, 8(3), e2671. doi:10.1038/cddis.2017.97
- Croft, C. L., & Noble, W. (2018). Preparation of organotypic brain slice cultures for the study of Alzheimer's disease. *F1000Res*, 7, 592. doi:10.12688/f1000research.14500.2
- Croft, C. L., Futch, H. S., Moore, B. D., & Golde, T. E. (2019a). Organotypic brain slice cultures to model neurodegenerative proteinopathies. *Mol Neurodegener*, 14(1), 45. doi:10.1186/s13024-019-0346-0
- Croft, C. L., Cruz, P. E., Ryu, D. H., Ceballos-Diaz, C., Strang, K. H., Woody, B. M., Lin, W. L., Deture, M., Rodríguez-Lebrón, E., Dickson, D. W., Chakrabarty, P., Levites, Y., Giasson, B. I., & Golde, T. E. (2019b). rAAV-based brain slice culture models of Alzheimer's and Parkinson's disease inclusion pathologies. *J Exp Med*, 216(3), 539-555. doi:10.1084/jem.20182184
- Crystal, H. A., Dickson, D. W., Sliwinski, M. J., Lipton, R. B., Grober, E., Marks-Nelson, H., & Antis, P. (1993). Pathological markers associated with normal aging and dementia in the elderly. *Ann Neurol*, 34(4), 566-573. doi:10.1002/ana.410340410
- Cuijpers, P. (2005). Depressive disorders in caregivers of dementia patients: a systematic review. *Aging Ment Health*, 9(4), 325-330. doi:10.1080/13607860500090078
- Cumano, A., & Godin, I. (2007). Ontogeny of the hematopoietic system. *Annu Rev Immunol*, 25, 745-785. doi:10.1146/annurev.immunol.25.022106.141538
- Cummings, J., Lee, G., Ritter, A., Sabbagh, M., & Zhong, K. (2019). Alzheimer's disease drug development pipeline: 2019. *Alzheimers Dement (NY)*, 5, 272-293. doi:10.1016/j.trci.2019.05.008
- Cummings, J., Aisen, P., Lemere, C., Atri, A., Sabbagh, M., & Salloway, S. (2021). Aducanumab produced a clinically meaningful benefit in association with amyloid lowering. *Alzheimers Res Ther*, 13(1), 98. doi:10.1186/s13195-021-00838-z
- Cummings, J. L., Morstorf, T., & Zhong, K. (2014). Alzheimer's disease drug-development pipeline: few candidates, frequent failures. *Alzheimers Res Ther*, 6(4), 37. doi:10.1186/alzrt269

- Da Mesquita, S., Louveau, A., Vaccari, A., Smirnov, I., Cornelison, R. C., Kingsmore, K. M., Contarino, C., Onengut-Gumuscu, S., Farber, E., Raper, D., Viar, K. E., Powell, R. D., Baker, W., Dabhi, N., Bai, R., Cao, R., Hu, S., Rich, S. S., Munson, J. M., Lopes, M. B., Overall, C. C., Acton, S. T., & Kipnis, J. (2018). Functional aspects of meningeal lymphatics in ageing and Alzheimer's disease. *Nature*, 560(7717), 185-191. doi:10.1038/s41586-018-0368-8
- Dai, M. H., Zheng, H., Zeng, L. D., & Zhang, Y. (2018). The genes associated with early-onset Alzheimer's disease. *Oncotarget*, 9(19), 15132-15143. doi:10.18632/oncotarget.23738
- Dani, A., Huang, B., Bergan, J., Dulac, C., & Zhuang, X. (2010). Superresolution imaging of chemical synapses in the brain. *Neuron*, 68(5), 843-856. doi:10.1016/j.neuron.2010.11.021
- Daria, A., Colombo, A., Llovera, G., Hampel, H., Willem, M., Liesz, A., Haass, C., & Tahirovic, S. (2017). Young microglia restore amyloid plaque clearance of aged microglia. *Embo j*, 36(5), 583-603. doi:10.15252/embj.201694591
- Das, G. D. (1976). Gitter cells and their relationship to macrophages in the developing cerebellum: an electron microscopic study. *Virchows Arch B Cell Pathol*, 20(4), 299-305. doi:10.1007/bf02890348
- Davalos, D., Grutzendler, J., Yang, G., Kim, J. V., Zuo, Y., Jung, S., Littman, D. R., Dustin, M. L., & Gan, W. B. (2005). ATP mediates rapid microglial response to local brain injury in vivo. *Nat Neurosci*, 8(6), 752-758. doi:10.1038/nn1472
- Davies, D. S., Ma, J., Jegathees, T., & Goldsbury, C. (2017). Microglia show altered morphology and reduced arborization in human brain during aging and Alzheimer's disease. *Brain Pathol*, 27(6), 795-808. doi:10.1111/bpa.12456
- Davies, L., Wolska, B., Hilbich, C., Multhaup, G., Martins, R., Simms, G., Beyreuther, K., & Masters, C. L. (1988). A4 amyloid protein deposition and the diagnosis of Alzheimer's disease: prevalence in aged brains determined by immunocytochemistry compared with conventional neuropathologic techniques. *Neurology*, 38(11), 1688-1693. doi:10.1212/wnl.38.11.1688
- Davies, P., & Maloney, A. J. (1976). Selective loss of central cholinergic neurons in Alzheimer's disease. *Lancet*, 2(8000), 1403. doi:10.1016/s0140-6736(76)91936-x
- Davies, P., Katzman, R., & Terry, R. D. (1980). Reduced somatostatin-like immunoreactivity in cerebral cortex from cases of Alzheimer disease and Alzheimer senile dementia. *Nature*, 288(5788), 279-280. doi:10.1038/288279a0
- Davis, B. M., Salinas-Navarro, M., Cordeiro, M. F., Moons, L., & De Groef, L. (2017). Characterizing microglia activation: a spatial statistics approach to maximize information extraction. *Sci Rep*, 7(1), 1576. doi:10.1038/s41598-017-01747-8
- Davis, D. G., Schmitt, F. A., Wekstein, D. R., & Markesbery, W. R. (1999). Alzheimer neuropathologic alterations in aged cognitively normal subjects. *J Neuropathol Exp Neurol*, 58(4), 376-388. doi:10.1097/00005072-199904000-00008

- De Felice, F. G., Vieira, M. N., Saraiva, L. M., Figueroa-Villar, J. D., Garcia-Abreu, J., Liu, R., Chang, L., Klein, W. L., & Ferreira, S. T. (2004). Targeting the neurotoxic species in Alzheimer's disease: inhibitors of A β oligomerization. *FASEB J*, 18(12), 1366-1372. doi:10.1096/fj.04-1764com
- De Felice, F. G., Wu, D., Lambert, M. P., Fernandez, S. J., Velasco, P. T., Lacor, P. N., Bigio, E. H., Jerecic, J., Acton, P. J., Shughrue, P. J., Chen-Dodson, E., Kinney, G. G., & Klein, W. L. (2008). Alzheimer's disease-type neuronal tau hyperphosphorylation induced by A β oligomers. *Neurobiol Aging*, 29(9), 1334-1347. doi:10.1016/j.neurobiolaging.2007.02.029
- de Jonge, W. J., & Ulloa, L. (2007). The $\alpha 7$ nicotinic acetylcholine receptor as a pharmacological target for inflammation. *Br J Pharmacol*, 151(7), 915-929. doi:10.1038/sj.bjp.0707264
- de la Monte, S. M. (2019). The full spectrum of Alzheimer's disease is rooted in metabolic derangements that drive type 3 diabetes. *Adv Exp Med Biol*, 1128, 45-83. doi:10.1007/978-981-13-3540-2_4
- De la Rosa, A., Olaso-Gonzalez, G., Arc-Chagnaud, C., Millan, F., Salvador-Pascual, A., García-Lucerga, C., Blasco-Lafarga, C., Garcia-Dominguez, E., Carretero, A., Correias, A. G., Viña, J., & Gomez-Cabrera, M. C. (2020). Physical exercise in the prevention and treatment of Alzheimer's disease. *J Sport Health Sci*, 9(5), 394-404. doi:10.1016/j.jshs.2020.01.004
- de la Torre, J. (2018). The vascular hypothesis of Alzheimer's disease: a key to preclinical prediction of dementia using neuroimaging. *J Alzheimers Dis*, 63(1), 35-52. doi:10.3233/jad-180004
- de Wilde, M. C., Overk, C. R., Sijben, J. W., & Masliah, E. (2016). Meta-analysis of synaptic pathology in Alzheimer's disease reveals selective molecular vesicular machinery vulnerability. *Alzheimers Dement*, 12(6), 633-644. doi:10.1016/j.jalz.2015.12.005
- DeKosky, S. T., & Scheff, S. W. (1990). Synapse loss in frontal cortex biopsies in Alzheimer's disease: correlation with cognitive severity. *Ann Neurol*, 27(5), 457-464. doi:10.1002/ana.410270502
- DeKosky, S. T., Scheff, S. W., & Styren, S. D. (1996). Structural correlates of cognition in dementia: quantification and assessment of synapse change. *Neurodegeneration*, 5(4), 417-421. doi:10.1006/neur.1996.0056
- del Rio, J. A., Heimrich, B., Soriano, E., Schwegler, H., & Frotscher, M. (1991). Proliferation and differentiation of glial fibrillary acidic protein-immunoreactive glial cells in organotypic slice cultures of rat hippocampus. *Neuroscience*, 43(2-3), 335-347. doi:10.1016/0306-4522(91)90298-3
- Delacourte, A. (2008). Tau pathology and neurodegeneration: an obvious but misunderstood link. *J Alzheimers Dis*, 14(4), 437-440. doi:10.3233/jad-2008-14412
- Delgado, M., Leceta, J., & Ganea, D. (2003). Vasoactive intestinal peptide and pituitary adenylate cyclase-activating polypeptide inhibit the production of inflammatory mediators by activated microglia. *J Leukoc Biol*, 73(1), 155-164. doi:10.1189/jlb.0702372
- Dementia Australia. (2018). *Dementia prevalence estimates, 2018-2058*. ACT, Australia: University of Canberra. Retrieved from <https://www.dementia.org.au/information/statistics/prevalence-data>
- Deming, Y., Filipello, F., Cignarella, F., Cantoni, C., Hsu, S., Mikesell, R., Li, Z., Del-Aguila, J. L., Dube, U., Farias, F. G., Bradley, J., Budde, J., Ibanez,

- L., Fernandez, M. V., Blennow, K., Zetterberg, H., Heslegrave, A., Johansson, P. M., Svensson, J., Nellgård, B., Lleo, A., Alcolea, D., Clarimon, J., Rami, L., Molinuevo, J. L., Suárez-Calvet, M., Morenas-Rodríguez, E., Kleinberger, G., Ewers, M., Harari, O., Haass, C., Brett, T. J., Benitez, B. A., Karch, C. M., Piccio, L., & Cruchaga, C. (2019). The MS4A gene cluster is a key modulator of soluble TREM2 and Alzheimer's disease risk. *Sci Transl Med*, *11*(505). doi:10.1126/scitranslmed.aau2291
- DeTure, M. A., & Dickson, D. W. (2019). The neuropathological diagnosis of Alzheimer's disease. *Mol Neurodegener*, *14*(1), 32. doi:10.1186/s13024-019-0333-5
- Dickson, D. W., Farlo, J., Davies, P., Crystal, H., Fuld, P., & Yen, S. H. (1988). Alzheimer's disease: a double-labeling immunohistochemical study of senile plaques. *Am J Pathol*, *132*(1), 86-101.
- Dickson, T. C., & Vickers, J. C. (2001). The morphological phenotype of β -amyloid plaques and associated neuritic changes in Alzheimer's disease. *Neuroscience*, *105*(1), 99-107.
- Dineley, K. T. (2007). β -amyloid peptide—nicotinic acetylcholine receptor interaction: the two faces of health and disease. *Front Biosci*, *12*, 5030-5038. doi:10.2741/2445
- Dobrenis, K., Makman, M. H., & Stefano, G. B. (1995). Occurrence of the opiate alkaloid-selective μ 3 receptor in mammalian microglia, astrocytes and Kupffer cells. *Brain Res*, *686*(2), 239-248. doi:10.1016/0006-8993(95)00452-v
- Doorn, K. J., Goudriaan, A., Blits-Huizinga, C., Bol, J. G., Rozemuller, A. J., Hoogland, P. V., Lucassen, P. J., Drukarch, B., van de Berg, W. D., & van Dam, A. M. (2014). Increased amoeboid microglial density in the olfactory bulb of Parkinson's and Alzheimer's patients. *Brain Pathol*, *24*(2), 152-165. doi:10.1111/bpa.12088
- Downey, C. L., Young, A., Burton, E. F., Graham, S. M., Macfarlane, R. J., Tsapakis, E. M., & Tsiridis, E. (2017). Dementia and osteoporosis in a geriatric population: is there a common link? *World J Orthop*, *8*(5), 412-423. doi:10.5312/wjo.v8.i5.412
- Dubbelaar, M. L., Kracht, L., Eggen, B. J. L., & Boddeke, E. (2018). The kaleidoscope of microglial phenotypes. *Front Immunol*, *9*. doi:10.3389/fimmu.2018.01753
- Dubois, B., Feldman, H. H., Jacova, C., Cummings, J. L., Dekosky, S. T., Barberger-Gateau, P., Delacourte, A., Frisoni, G., Fox, N. C., Galasko, D., Gauthier, S., Hampel, H., Jicha, G. A., Meguro, K., O'Brien, J., Pasquier, F., Robert, P., Rossor, M., Salloway, S., Sarazin, M., de Souza, L. C., Stern, Y., Visser, P. J., & Scheltens, P. (2010). Revising the definition of Alzheimer's disease: a new lexicon. *Lancet Neurol*, *9*(11), 1118-1127. doi:10.1016/s1474-4422(10)70223-4
- Duthie, A., Chew, D., & Soiza, R. L. (2011). Non-psychiatric comorbidity associated with Alzheimer's disease. *Qjm*, *104*(11), 913-920. doi:10.1093/qjmed/hcr118
- Duyckaerts, C., Delatour, B., & Potier, M. C. (2009). Classification and basic pathology of Alzheimer disease. *Acta Neuropathol*, *118*(1), 5-36. doi:10.1007/s00401-009-0532-1
- Dyrks, T., Weidemann, A., Multhaup, G., Salbaum, J. M., Lemaire, H. G., Kang, J., Müller-Hill, B., Masters, C. L., & Beyreuther, K. (1988). Identification,

- transmembrane orientation and biogenesis of the amyloid A4 precursor of Alzheimer's disease. *Embo j*, 7(4), 949-957.
- Efthymiou, A. G., & Goate, A. M. (2017). Late onset Alzheimer's disease genetics implicates microglial pathways in disease risk. *Mol Neurodegener*, 12(1), 43. doi:10.1186/s13024-017-0184-x
- Eid, R. S., Chaiton, J. A., Lieblich, S. E., Bodnar, T. S., Weinberg, J., & Galea, L. A. M. (2019). Early and late effects of maternal experience on hippocampal neurogenesis, microglia, and the circulating cytokine milieu. *Neurobiol Aging*, 78, 1-17. doi:10.1016/j.neurobiolaging.2019.01.021
- Eikelenboom, P., & Stam, F. C. (1982). Immunoglobulins and complement factors in senile plaques. An immunoperoxidase study. *Acta Neuropathol*, 57(2-3), 239-242. doi:10.1007/bf00685397
- Eikelenboom, P., Hack, C. E., Rozemuller, J. M., & Stam, F. C. (1989). Complement activation in amyloid plaques in Alzheimer's dementia. *Virchows Arch B Cell Pathol Incl Mol Pathol*, 56(4), 259-262. doi:10.1007/bf02890024
- Emamian, F., Khazaie, H., Tahmasian, M., Leschziner, G. D., Morrell, M. J., Hsiung, G. Y., Rosenzweig, I., & Sepehry, A. A. (2016). The association between obstructive sleep apnea and Alzheimer's disease: A meta-analysis perspective. *Front Aging Neurosci*, 8, 78. doi:10.3389/fnagi.2016.00078
- Eon Kuek, L., Leffler, M., Mackay, G. A., & Hulett, M. D. (2016). The MS4A family: counting past 1, 2 and 3. *Immunol Cell Biol*, 94(1), 11-23. doi:10.1038/icb.2015.48
- Esch, F. S., Keim, P. S., Beattie, E. C., Blacher, R. W., Culwell, A. R., Oltersdorf, T., McClure, D., & Ward, P. J. (1990). Cleavage of amyloid β peptide during constitutive processing of its precursor. *Science*, 248(4959), 1122-1124. doi:10.1126/science.2111583
- Escott-Price, V., Sims, R., Bannister, C., Harold, D., Vronskaya, M., Majounie, E., Badarinarayan, N., Morgan, K., Passmore, P., Holmes, C., Powell, J., Brayne, C., Gill, M., Mead, S., Goate, A., Cruchaga, C., Lambert, J. C., van Duijn, C., Maier, W., Ramirez, A., Holmans, P., Jones, L., Hardy, J., Seshadri, S., Schellenberg, G. D., Amouyel, P., & Williams, J. (2015). Common polygenic variation enhances risk prediction for Alzheimer's disease. *Brain*, 138(Pt 12), 3673-3684. doi:10.1093/brain/awv268
- Esques, C., Juillerat-Jeanneret, L., Leuba, G., Honegger, P., & Monnet-Tschudi, F. (2003). Involvement of microglia-neuron interactions in the tumor necrosis factor- α release, microglial activation, and neurodegeneration induced by trimethyltin. *J Neurosci Res*, 71(4), 583-590. doi:10.1002/jnr.10508
- Eugène, E., Cluzeaud, F., Cifuentes-Diaz, C., Fricker, D., Le Duigou, C., Clemenceau, S., Baulac, M., Poncer, J. C., & Miles, R. (2014). An organotypic brain slice preparation from adult patients with temporal lobe epilepsy. *J Neurosci Methods*, 235, 234-244. doi:10.1016/j.jneumeth.2014.07.009
- Eugenín, E. A., Eckardt, D., Theis, M., Willecke, K., Bennett, M. V., & Saez, J. C. (2001). Microglia at brain stab wounds express connexin 43 and in vitro form functional gap junctions after treatment with interferon- γ and tumor necrosis factor- α . *Proc Natl Acad Sci USA*, 98(7), 4190-4195. doi:10.1073/pnas.051634298

- Faff, L., Ohlemeyer, C., & Kettenmann, H. (1996). Intracellular pH regulation in cultured microglial cells from mouse brain. *J Neurosci Res*, 46(3), 294-304. doi:10.1002/(sici)1097-4547(19961101)46:3<294::Aid-jnr2>3.0.Co;2-f
- Fagan, A. M., Head, D., Shah, A. R., Marcus, D., Mintun, M., Morris, J. C., & Holtzman, D. M. (2009). Decreased cerebrospinal fluid A β (42) correlates with brain atrophy in cognitively normal elderly. *Ann Neurol*, 65(2), 176-183. doi:10.1002/ana.21559
- Fan, R., & Tenner, A. J. (2004). Complement C1q expression induced by A β in rat hippocampal organotypic slice cultures. *Exp Neurol*, 185(2), 241-253. doi:10.1016/j.expneurol.2003.09.023
- Fan, Z., Brooks, D. J., Okello, A., & Edison, P. (2017). An early and late peak in microglial activation in Alzheimer's disease trajectory. *Brain*, 140(3), 792-803. doi:10.1093/brain/aww349
- Fantin, A., Vieira, J. M., Gestri, G., Denti, L., Schwarz, Q., Prykhodzhiy, S., Peri, F., Wilson, S. W., & Ruhrberg, C. (2010). Tissue macrophages act as cellular chaperones for vascular anastomosis downstream of VEGF-mediated endothelial tip cell induction. *Blood*, 116(5), 829-840. doi:10.1182/blood-2009-12-257832
- Fantoni, E., Collij, L., Lopes Alves, I., Buckley, C., & Farrar, G. (2020). The spatial-temporal ordering of amyloid pathology and opportunities for PET imaging. *J Nucl Med*, 61(2), 166-171. doi:10.2967/jnumed.119.235879
- Färber, K., Pannasch, U., & Kettenmann, H. (2005). Dopamine and noradrenaline control distinct functions in rodent microglial cells. *Mol Cell Neurosci*, 29(1), 128-138. doi:10.1016/j.mcn.2005.01.003
- Färber, K., & Kettenmann, H. (2006). Purinergic signaling and microglia. *Pflugers Arch*, 452(5), 615-621. doi:10.1007/s00424-006-0064-7
- Farris, W., Mansourian, S., Chang, Y., Lindsley, L., Eckman, E. A., Frosch, M. P., Eckman, C. B., Tanzi, R. E., Selkoe, D. J., & Guenette, S. (2003). Insulin-degrading enzyme regulates the levels of insulin, amyloid β -protein, and the β -amyloid precursor protein intracellular domain in vivo. *Proc Natl Acad Sci USA*, 100(7), 4162-4167. doi:10.1073/pnas.0230450100
- Feindt, J., Schmidt, A., & Mentlein, R. (1998). Receptors and effects of the inhibitory neuropeptide somatostatin in microglial cells. *Brain Res Mol Brain Res*, 60(2), 228-233. doi:10.1016/s0169-328x(98)00184-3
- Fenn, A. M., Gensel, J. C., Huang, Y., Popovich, P. G., Lifshitz, J., & Godbout, J. P. (2014). Immune activation promotes depression 1 month after diffuse brain injury: a role for primed microglia. *Biol Psychiatry*, 76(7), 575-584. doi:10.1016/j.biopsych.2013.10.014
- Fern, R., Waxman, S. G., & Ransom, B. R. (1995). Endogenous GABA attenuates CNS white matter dysfunction following anoxia. *J Neurosci*, 15(1 Pt 2), 699-708. doi:10.1523/jneurosci.15-01-00699.1995
- Fernández-Arjona, M. D. M., Grondona, J. M., Fernández-Llebrez, P., & López-Ávalos, M. D. (2019). Microglial morphometric parameters correlate with the expression level of IL-1 β , and allow identifying different activated morphotypes. *Front Cell Neurosci*, 13, 472. doi:10.3389/fncel.2019.00472
- Ferreira, S. T., & Klein, W. L. (2011). The A β oligomer hypothesis for synapse failure and memory loss in Alzheimer's disease. *Neurobiol Learn Mem*, 96(4), 529-543. doi:10.1016/j.nlm.2011.08.003

- Fitzpatrick, A. W. P., Falcon, B., He, S., Murzin, A. G., Murshudov, G., Garringer, H. J., Crowther, R. A., Ghetti, B., Goedert, M., & Scheres, S. H. W. (2017). Cryo-EM structures of tau filaments from Alzheimer's disease. *Nature*, 547(7662), 185-190. doi:10.1038/nature23002
- Fleminger, S., Oliver, D. L., Lovestone, S., Rabe-Hesketh, S., & Giora, A. (2003). Head injury as a risk factor for Alzheimer's disease: the evidence 10 years on; a partial replication. *J Neurol Neurosurg Psychiatry*, 74(7), 857-862. doi:10.1136/jnnp.74.7.857
- Food and Drug Administration. (2020, Nov 6). Final summary minutes of the peripheral and central nervous system drugs advisory committee meeting [Summary of Minutes]. Retrieved 2021, Jun 9, from <https://www.fda.gov/media/145690/download>
- Food and Drug Administration. (2021, Jun 7). FDA grants accelerated approval for Alzheimer's drug [Press Release]. Retrieved 2021, Jun 9, from <https://www.fda.gov/news-events/press-announcements/fda-grants-accelerated-approval-alzheimers-drug>
- Forester, B. P., Patrick, R. E., & Harper, D. G. (2020). Setbacks and opportunities in disease-modifying therapies in Alzheimer disease. *JAMA Psychiatry*, 77(1), 7-8. doi:10.1001/jamapsychiatry.2019.2332
- Franco-Bocanegra, D. K., McAuley, C., Nicoll, J. A. R., & Boche, D. (2019). Molecular mechanisms of microglial motility: changes in ageing and Alzheimer's disease. *Cells*, 8(6). doi:10.3390/cells8060639
- Frank, S., Burbach, G. J., Bonin, M., Walter, M., Streit, W., Bechmann, I., & Deller, T. (2008). TREM2 is upregulated in amyloid plaque-associated microglia in aged APP23 transgenic mice. *Glia*, 56(13), 1438-1447. doi:10.1002/glia.20710
- Franz, G., Beer, R., Kampfl, A., Engelhardt, K., Schmutzhard, E., Ulmer, H., & Deisenhammer, F. (2003). Amyloid β 1-42 and tau in cerebrospinal fluid after severe traumatic brain injury. *Neurology*, 60(9), 1457-1461. doi:10.1212/01.wnl.0000063313.57292.00
- Fratiglioni, L., Paillard-Borg, S., & Winblad, B. (2004). An active and socially integrated lifestyle in late life might protect against dementia. *Lancet Neurol*, 3(6), 343-353. doi:10.1016/s1474-4422(04)00767-7
- Friedl, G., Hofer, M., Auber, B., Sauder, C., Hausmann, J., Staeheli, P., & Pagenstecher, A. (2004). Borna disease virus multiplication in mouse organotypic slice cultures is site-specifically inhibited by γ interferon but not by interleukin-12. *J Virol*, 78(3), 1212-1218. doi:10.1128/jvi.78.3.1212-1218.2004
- Fritz, J. H., Ferrero, R. L., Philpott, D. J., & Girardin, S. E. (2006). Nod-like proteins in immunity, inflammation and disease. *Nat Immunol*, 7(12), 1250-1257. doi:10.1038/ni1412
- Frost, B., Jacks, R. L., & Diamond, M. I. (2009). Propagation of tau misfolding from the outside to the inside of a cell. *J Biol Chem*, 284(19), 12845-12852. doi:10.1074/jbc.M808759200
- Frost, J. L., & Schafer, D. P. (2016). Microglia: architects of the developing nervous system. *Trends Cell Biol*, 26(8), 587-597. doi:10.1016/j.tcb.2016.02.006
- Fujii, T., Mashimo, M., Moriwaki, Y., Misawa, H., Ono, S., Horiguchi, K., & Kawashima, K. (2017). Expression and function of the cholinergic system in immune cells. *Front Immunol*, 8, 1085. doi:10.3389/fimmu.2017.01085

- Fujita, R., Ma, Y., & Ueda, H. (2008). Lysophosphatidic acid-induced membrane ruffling and brain-derived neurotrophic factor gene expression are mediated by ATP release in primary microglia. *J Neurochem*, 107(1), 152-160. doi:10.1111/j.1471-4159.2008.05599.x
- Galasko, D., Hansen, L. A., Katzman, R., Wiederholt, W., Masliah, E., Terry, R., Hill, L. R., Lessin, P., & Thal, L. J. (1994). Clinical-neuropathological correlations in Alzheimer's disease and related dementias. *Arch Neurol*, 51(9), 888-895. doi:10.1001/archneur.1994.00540210060013
- Galatro, T. F., Holtman, I. R., Lerario, A. M., Vainchtein, I. D., Brouwer, N., Sola, P. R., Veras, M. M., Pereira, T. F., Leite, R. E. P., Möller, T., Wes, P. D., Sogayar, M. C., Laman, J. D., den Dunnen, W., Pasqualucci, C. A., Oba-Shinjo, S. M., Boddeke, E., Marie, S. K. N., & Eggen, B. J. L. (2017). Transcriptomic analysis of purified human cortical microglia reveals age-associated changes. *Nat Neurosci*, 20(8), 1162-1171. doi:10.1038/nn.4597
- Galbraith, C. G., & Galbraith, J. A. (2011). Super-resolution microscopy at a glance. *J Cell Sci*, 124(Pt 10), 1607-1611. doi:10.1242/jcs.080085
- Galloway, P. G., Perry, G., Kosik, K. S., & Gambetti, P. (1987a). Hirano bodies contain tau protein. *Brain Res*, 403(2), 337-340. doi:10.1016/0006-8993(87)90071-0
- Galloway, P. G., Perry, G., & Gambetti, P. (1987b). Hirano body filaments contain actin and actin-associated proteins. *J Neuropathol Exp Neurol*, 46(2), 185-199. doi:10.1097/00005072-198703000-00006
- Ganguly, P., Thompson, V., Gildawie, K., & Brenhouse, H. C. (2018). Adolescent food restriction in rats alters prefrontal cortex microglia in an experience-dependent manner. *Stress*, 21(2), 162-168. doi:10.1080/10253890.2017.1423054
- Garcez, M. L., Falchetti, A. C., Mina, F., & Budni, J. (2015). Alzheimer's disease associated with psychiatric comorbidities. *An Acad Bras Cienc*, 87(2 Suppl), 1461-1473. doi:10.1590/0001-3765201520140716
- Gatz, M., Reynolds, C. A., Fratiglioni, L., Johansson, B., Mortimer, J. A., Berg, S., Fiske, A., & Pedersen, N. L. (2006). Role of genes and environments for explaining Alzheimer disease. *Arch Gen Psychiatry*, 63(2), 168-174. doi:10.1001/archpsyc.63.2.168
- Gautier, E. L., Shay, T., Miller, J., Greter, M., Jakubzick, C., Ivanov, S., Helft, J., Chow, A., Elpek, K. G., Gordonov, S., Mazloom, A. R., Ma'ayan, A., Chua, W. J., Hansen, T. H., Turley, S. J., Merad, M., & Randolph, G. J. (2012). Gene-expression profiles and transcriptional regulatory pathways that underlie the identity and diversity of mouse tissue macrophages. *Nat Immunol*, 13(11), 1118-1128. doi:10.1038/ni.2419
- Gebicke-Haerter, P. J., Spleiss, O., Ren, L. Q., Li, H., Dichmann, S., Norgauer, J., & Boddeke, H. W. (2001). Microglial chemokines and chemokine receptors. *Prog Brain Res*, 132, 525-532. doi:10.1016/s0079-6123(01)32100-3
- Geijtenbeek, T. B., & Gringhuis, S. I. (2009). Signalling through C-type lectin receptors: shaping immune responses. *Nat Rev Immunol*, 9(7), 465-479. doi:10.1038/nri2569
- Gerrits, E., Brouwer, N., Kooistra, S. M., Woodbury, M. E., Vermeiren, Y., Lambourne, M., Mulder, J., Kummer, M., Möller, T., Biber, K., Dunnen, W., De Deyn, P. P., Eggen, B. J. L., & Boddeke, E. (2021). Distinct

- amyloid- β and tau-associated microglia profiles in Alzheimer's disease. *Acta Neuropathol.* doi:10.1007/s00401-021-02263-w
- Geula, C., Mesulam, M. M., Saroff, D. M., & Wu, C. K. (1998). Relationship between plaques, tangles, and loss of cortical cholinergic fibers in Alzheimer disease. *J Neuropathol Exp Neurol*, 57(1), 63-75. doi:10.1097/00005072-199801000-00008
- Giannakopoulos, P., Hof, P. R., Giannakopoulos, A. S., Herrmann, F. R., Michel, J. P., & Bouras, C. (1995). Regional distribution of neurofibrillary tangles and senile plaques in the cerebral cortex of very old patients. *Arch Neurol*, 52(12), 1150-1159. doi:10.1001/archneur.1995.00540360028012
- Gibson, P. H., & Tomlinson, B. E. (1977). Numbers of Hirano bodies in the hippocampus of normal and demented people with Alzheimer's disease. *J Neurol Sci*, 33(1-2), 199-206. doi:10.1016/0022-510x(77)90193-9
- Ginhoux, F., Greter, M., Leboeuf, M., Nandi, S., See, P., Gokhan, S., Mehler, M. F., Conway, S. J., Ng, L. G., Stanley, E. R., Samokhvalov, I. M., & Merad, M. (2010). Fate mapping analysis reveals that adult microglia derive from primitive macrophages. *Science*, 330(6005), 841-845. doi:10.1126/science.1194637
- Ginhoux, F., Lim, S., Hoeffel, G., Low, D., & Huber, T. (2013). Origin and differentiation of microglia. *Front Cell Neurosci*, 7, 45. doi:10.3389/fncel.2013.00045
- Ginhoux, F., & Prinz, M. (2015). Origin of microglia: current concepts and past controversies. *Cold Spring Harb Perspect Biol*, 7(8), a020537. doi:10.1101/cshperspect.a020537
- Giordano, K. R., Denman, C. R., Dubisch, P. S., Akhter, M., & Lifshitz, J. (2021). An update on the rod microglia variant in experimental and clinical brain injury and disease. *Brain Commun*, 3(1), fcaa227. doi:10.1093/braincomms/fcaa227
- Giuffrida, M. L., Caraci, F., Pignataro, B., Cataldo, S., De Bona, P., Bruno, V., Molinaro, G., Pappalardo, G., Messina, A., Palmigiano, A., Garozzo, D., Nicoletti, F., Rizzarelli, E., & Copani, A. (2009). β -amyloid monomers are neuroprotective. *J Neurosci*, 29(34), 10582-10587. doi:10.1523/jneurosci.1736-09.2009
- Glass, C. K., Saijo, K., Winner, B., Marchetto, M. C., & Gage, F. H. (2010). Mechanisms underlying inflammation in neurodegeneration. *Cell*, 140(6), 918-934. doi:10.1016/j.cell.2010.02.016
- Glenner, G. G., & Wong, C. W. (1984a). Alzheimer's disease and Down's syndrome: sharing of a unique cerebrovascular amyloid fibril protein. *Biochem Biophys Res Commun*, 122(3), 1131-1135. doi:10.1016/0006-291x(84)91209-9
- Glenner, G. G., & Wong, C. W. (1984b). Alzheimer's disease: initial report of the purification and characterization of a novel cerebrovascular amyloid protein. *Biochem Biophys Res Commun*, 120(3), 885-890. doi:10.1016/s0006-291x(84)80190-4
- Goate, A., Chartier-Harlin, M. C., Mullan, M., Brown, J., Crawford, F., Fidani, L., Giuffra, L., Haynes, A., Irving, N., James, L., Mant, R., Newton, P., Rooke, K., Roques, P., Talbot, C., Pericak-Vance, M., Roses, A., Williamson, R., Rossor, M., Owen, M., & Hardy, J. (1991). Segregation of a missense mutation in the amyloid precursor protein gene with familial Alzheimer's disease. *Nature*, 349(6311), 704-706. doi:10.1038/349704a0

- Goedert, M., Wischik, C. M., Crowther, R. A., Walker, J. E., & Klug, A. (1988). Cloning and sequencing of the cDNA encoding a core protein of the paired helical filament of Alzheimer disease: identification as the microtubule-associated protein tau. *Proc Natl Acad Sci USA*, 85(11), 4051-4055. doi:10.1073/pnas.85.11.4051
- Goedert, M., Spillantini, M. G., Jakes, R., Rutherford, D., & Crowther, R. A. (1989). Multiple isoforms of human microtubule-associated protein tau: sequences and localization in neurofibrillary tangles of Alzheimer's disease. *Neuron*, 3(4), 519-526. doi:10.1016/0896-6273(89)90210-9
- Goedert, M. (2004). Tau protein and neurodegeneration. *Semin Cell Dev Biol*, 15(1), 45-49. doi:10.1016/j.semcdb.2003.12.015
- Golaz, J., Bouras, C., & Hof, P. R. (1992). Motor cortex involvement in presenile dementia: report of a case. *J Geriatr Psychiatry Neurol*, 5(2), 85-92. doi:10.1177/002383099200500205
- Goldsbury, C., Mocanu, M. M., Thies, E., Kaether, C., Haass, C., Keller, P., Biernat, J., Mandelkow, E., & Mandelkow, E. M. (2006). Inhibition of APP trafficking by tau protein does not increase the generation of amyloid- β peptides. *Traffic*, 7(7), 873-888. doi:10.1111/j.1600-0854.2006.00434.x
- Gomez, W., Morales, R., Maracaja-Coutinho, V., Parra, V., & Nassif, M. (2020). Down syndrome and Alzheimer's disease: common molecular traits beyond the amyloid precursor protein. *Aging (Albany NY)*, 12(1), 1011-1033. doi:10.18632/aging.102677
- Gomez-Isla, T., Price, J. L., McKeel, D. W., Jr., Morris, J. C., Growdon, J. H., & Hyman, B. T. (1996). Profound loss of layer II entorhinal cortex neurons occurs in very mild Alzheimer's disease. *J Neurosci*, 16(14), 4491-4500.
- Gomez-Isla, T., Hollister, R., West, H., Mui, S., Growdon, J. H., Petersen, R. C., Parisi, J. E., & Hyman, B. T. (1997). Neuronal loss correlates with but exceeds neurofibrillary tangles in Alzheimer's disease. *Ann Neurol*, 41(1), 17-24. doi:10.1002/ana.410410106
- Gomez-Nicola, D., & Boche, D. (2015). Post-mortem analysis of neuroinflammatory changes in human Alzheimer's disease. *Alzheimers Res Ther*, 7(1), 42. doi:10.1186/s13195-015-0126-1
- Gonzalez-Rey, E., & Delgado, M. (2008). Vasoactive intestinal peptide inhibits cyclooxygenase-2 expression in activated macrophages, microglia, and dendritic cells. *Brain Behav Immun*, 22(1), 35-41. doi:10.1016/j.bbi.2007.07.004
- Goodson, H. V., & Jonasson, E. M. (2018). Microtubules and microtubule-associated proteins. *Cold Spring Harb Perspect Biol*, 10(6). doi:10.1101/cshperspect.a022608
- Gosselin, D., Link, V. M., Romanoski, C. E., Fonseca, G. J., Eichenfield, D. Z., Spann, N. J., Stender, J. D., Chun, H. B., Garner, H., Geissmann, F., & Glass, C. K. (2014). Environment drives selection and function of enhancers controlling tissue-specific macrophage identities. *Cell*, 159(6), 1327-1340. doi:10.1016/j.cell.2014.11.023
- Gosselin, D., Skola, D., Coufal, N. G., Holtman, I. R., Schlachetzki, J. C. M., Sajti, E., Jaeger, B. N., O'Connor, C., Fitzpatrick, C., Pasillas, M. P., Pena, M., Adair, A., Gonda, D. D., Levy, M. L., Ransohoff, R. M., Gage, F. H., & Glass, C. K. (2017). An environment-dependent transcriptional network

- specifies human microglia identity. *Science*, 356(6344). doi:10.1126/science.aal3222
- Graeber, M. B. (2010). Changing face of microglia. *Science*, 330(6005), 783-788. doi:10.1126/science.1190929
- Graeber, M. B., Li, W., & Rodriguez, M. L. (2011). Role of microglia in CNS inflammation. *FEBS Lett*, 585(23), 3798-3805. doi:10.1016/j.febslet.2011.08.033
- Graeber, M. B. (2014). Neuroinflammation: no rose by any other name. *Brain Pathol*, 24(6), 620-622. doi:10.1111/bpa.12192
- Graham, L. C., Harder, J. M., Soto, I., de Vries, W. N., John, S. W., & Howell, G. R. (2016). Chronic consumption of a western diet induces robust glial activation in aging mice and in a mouse model of Alzheimer's disease. *Sci Rep*, 6, 21568. doi:10.1038/srep21568
- Grandbarbe, L., Michelucci, A., Heurtaux, T., Hemmer, K., Morga, E., & Heuschling, P. (2007). Notch signaling modulates the activation of microglial cells. *Glia*, 55(15), 1519-1530. doi:10.1002/glia.20553
- Gratuze, M., Leyns, C. E. G., & Holtzman, D. M. (2018). New insights into the role of TREM2 in Alzheimer's disease. *Mol Neurodegener*, 13(1), 66. doi:10.1186/s13024-018-0298-9
- Gredal, O., Pakkenberg, H., Karlsborg, M., & Pakkenberg, B. (2000). Unchanged total number of neurons in motor cortex and neocortex in amyotrophic lateral sclerosis: a stereological study. *J Neurosci Methods*, 95(2), 171-176. doi:10.1016/s0165-0270(99)00175-2
- Greenberg, S. M., Al-Shahi Salman, R., Biessels, G. J., van Buchem, M., Cordonnier, C., Lee, J. M., Montaner, J., Schneider, J. A., Smith, E. E., Vernooij, M., & Werring, D. J. (2014). Outcome markers for clinical trials in cerebral amyloid angiopathy. *Lancet Neurol*, 13(4), 419-428. doi:10.1016/s1474-4422(14)70003-1
- Greenberg, S. M., & Charidimou, A. (2018). Diagnosis of cerebral amyloid angiopathy: evolution of the Boston criteria. *Stroke*, 49(2), 491-497. doi:10.1161/strokeaha.117.016990
- Greenberg, S. M., Bacskaï, B. J., Hernandez-Guillamon, M., Pruzin, J., Sperling, R., & van Veluw, S. J. (2020). Cerebral amyloid angiopathy and Alzheimer disease - one peptide, two pathways. *Nat Rev Neurol*, 16(1), 30-42. doi:10.1038/s41582-019-0281-2
- Griciuc, A., Serrano-Pozo, A., Parrado, A. R., Lesinski, A. N., Asselin, C. N., Mullin, K., Hooli, B., Choi, S. H., Hyman, B. T., & Tanzi, R. E. (2013). Alzheimer's disease risk gene CD33 inhibits microglial uptake of amyloid β . *Neuron*, 78. doi:10.1016/j.neuron.2013.04.014
- Grinberg, L. T., Rub, U., Ferretti, R. E., Nitrini, R., Farfel, J. M., Polichiso, L., Gierga, K., Jacob-Filho, W., & Heinsen, H. (2009). The dorsal raphe nucleus shows phospho-tau neurofibrillary changes before the transentorhinal region in Alzheimer's disease. A precocious onset? *Neuropathol Appl Neurobiol*, 35(4), 406-416. doi:10.1111/j.1365-2990.2009.00997.x
- Grinberg, L. T., & Thal, D. R. (2010). Vascular pathology in the aged human brain. *Acta Neuropathol*, 119(3), 277-290. doi:10.1007/s00401-010-0652-7
- Grubman, A., Choo, X. Y., Chew, G., Ouyang, J. F., Sun, G., Croft, N. P., Rossello, F. J., Simmons, R., Buckberry, S., Landin, D. V., Pflueger, J.,

- Vandekolk, T. H., Abay, Z., Zhou, Y., Liu, X., Chen, J., Larcombe, M., Haynes, J. M., McLean, C., Williams, S., Chai, S. Y., Wilson, T., Lister, R., Pouton, C. W., Purcell, A. W., Rackham, O. J. L., Petretto, E., & Polo, J. M. (2021). Transcriptional signature in microglia associated with A β plaque phagocytosis. *Nat Commun*, 12(1), 3015. doi:10.1038/s41467-021-23111-1
- Grundke-Iqbal, I., Iqbal, K., Tung, Y. C., Quinlan, M., Wisniewski, H. M., & Binder, L. I. (1986). Abnormal phosphorylation of the microtubule-associated protein tau (tau) in Alzheimer cytoskeletal pathology. *Proc Natl Acad Sci USA*, 83(13), 4913-4917. doi:10.1073/pnas.83.13.4913
- Grundke-Iqbal, I., Fleming, J., Tung, Y. C., Lassmann, H., Iqbal, K., & Joshi, J. G. (1990). Ferritin is a component of the neuritic (senile) plaque in Alzheimer dementia. *Acta Neuropathol*, 81(2), 105-110. doi:10.1007/bf00334497
- Grzybowski, A., Pięta, A., & Pugaczewska, M. (2017). Teofil Simchowicz (1879-1957). *J Neurol*, 264(8), 1831-1832. doi:10.1007/s00415-017-8460-9
- Guennewig, B., Lim, J., Marshall, L., McCorkindale, A. N., Paasila, P. J., Patrick, E., Kril, J. J., Halliday, G. M., Cooper, A. A., & Sutherland, G. T. (2021). Defining early changes in Alzheimer's disease from RNA sequencing of brain regions differentially affected by pathology. *Sci Rep*, 11(1), 4865. doi:10.1038/s41598-021-83872-z
- Guerreiro, R., Wojtas, A., Bras, J., Carrasquillo, M., Rogaeva, E., Majounie, E., Cruchaga, C., Sassi, C., Kauwe, J. S., YOUNKIN, S., Hazrati, L., Collinge, J., Pocock, J., Lashley, T., Williams, J., Lambert, J. C., Amouyel, P., Goate, A., Rademakers, R., Morgan, K., Powell, J., St George-Hyslop, P., Singleton, A., Hardy, J., & Alzheimer Genetic Analysis, G. (2013). TREM2 variants in Alzheimer's disease. *N Engl J Med*, 368. doi:10.1056/NEJMoA1211851
- Guillozet, A. L., Weintraub, S., Mash, D. C., & Mesulam, M. M. (2003). Neurofibrillary tangles, amyloid, and memory in aging and mild cognitive impairment. *Arch Neurol*, 60(5), 729-736. doi:10.1001/archneur.60.5.729
- Gustke, N., Trinczek, B., Biernat, J., Mandelkow, E. M., & Mandelkow, E. (1994). Domains of tau protein and interactions with microtubules. *Biochemistry*, 33(32), 9511-9522. doi:10.1021/bi00198a017
- Ha, S., Furukawa, R., & Fechtner, M. (2011). Association of AICD and Fe65 with Hirano bodies reduces transcriptional activation and initiation of apoptosis. *Neurobiol Aging*, 32(12), 2287-2298. doi:10.1016/j.neurobiolaging.2010.01.003
- Haass, C., Hung, A. Y., Schlossmacher, M. G., Teplow, D. B., & Selkoe, D. J. (1993). β -amyloid peptide and a 3-kDa fragment are derived by distinct cellular mechanisms. *J Biol Chem*, 268(5), 3021-3024.
- Haass, C. (2004). Take five—BACE and the γ -secretase quartet conduct Alzheimer's amyloid β -peptide generation. *Embo j*, 23(3), 483-488. doi:10.1038/sj.emboj.7600061
- Haass, C., & Selkoe, D. J. (2007). Soluble protein oligomers in neurodegeneration: lessons from the Alzheimer's amyloid β -peptide. *Nat Rev Mol Cell Biol*, 8(2), 101-112. doi:10.1038/nrm2101
- Haass, C., Kaether, C., Thinakaran, G., & Sisodia, S. (2012). Trafficking and proteolytic processing of APP. *Cold Spring Harb Perspect Med*, 2(5), a006270. doi:10.1101/cshperspect.a006270

- Hagemeyer, N., Hanft, K. M., Akriditou, M. A., Unger, N., Park, E. S., Stanley, E. R., Staszewski, O., Dimou, L., & Prinz, M. (2017). Microglia contribute to normal myelinogenesis and to oligodendrocyte progenitor maintenance during adulthood. *Acta Neuropathol*, 134(3), 441-458. doi:10.1007/s00401-017-1747-1
- Hailer, N. P., Jarhult, J. D., & Nitsch, R. (1996). Resting microglial cells in vitro: analysis of morphology and adhesion molecule expression in organotypic hippocampal slice cultures. *Glia*, 18(4), 319-331. doi:10.1002/(sici)1098-1136(199612)18:4<319::aid-glia6>3.0.co;2-s
- Hall, A. A., Herrera, Y., Ajmo, C. T., Jr., Cuevas, J., & Pennypacker, K. R. (2009). Sigma receptors suppress multiple aspects of microglial activation. *Glia*, 57(7), 744-754. doi:10.1002/glia.20802
- Halle, A., Hornung, V., Petzold, G. C., Stewart, C. R., Monks, B. G., Reinheckel, T., Fitzgerald, K. A., Latz, E., Moore, K. J., & Golenbock, D. T. (2008). The NALP3 inflammasome is involved in the innate immune response to amyloid- β . *Nat Immunol*, 9(8), 857-865. doi:10.1038/ni.1636
- Halliday, G. M., Double, K. L., Macdonald, V., & Kril, J. J. (2003). Identifying severely atrophic cortical subregions in Alzheimer's disease. *Neurobiol Aging*, 24(6), 797-806. doi:10.1016/s0197-4580(02)00227-0
- Hamilton, R. L. (2000). Lewy bodies in Alzheimer's disease: a neuropathological review of 145 cases using α -synuclein immunohistochemistry. *Brain Pathol*, 10(3), 378-384. doi:10.1111/j.1750-3639.2000.tb00269.x
- Hammond, T. R., Dufort, C., Dissing-Olesen, L., Giera, S., Young, A., Wysoker, A., Walker, A. J., Gergits, F., Segel, M., Nemesh, J., Marsh, S. E., Saunders, A., Macosko, E., Ginhoux, F., Chen, J., Franklin, R. J. M., Piao, X., McCarroll, S. A., & Stevens, B. (2019). Single-cell RNA sequencing of microglia throughout the mouse lifespan and in the injured brain reveals complex cell-state changes. *Immunity*, 50(1), 253-271.e256. doi:10.1016/j.immuni.2018.11.004
- Hanisch, U.-K., & Kettenmann, H. (2007). Microglia: active sensor and versatile effector cells in the normal and pathologic brain. *Nat Neurosci*, 10(11), 1387-1394. doi:10.1038/nn1997
- Hanisch, U. K., Johnson, T. V., & Kipnis, J. (2008). Toll-like receptors: roles in neuroprotection? *Trends Neurosci*, 31(4), 176-182. doi:10.1016/j.tins.2008.01.005
- Hanslik, K. L., & Ulland, T. K. (2020). The role of microglia and the Nlrp3 inflammasome in Alzheimer's disease. *Front Neurol*, 11, 570711. doi:10.3389/fneur.2020.570711
- Hansson, G. K., & Edfeldt, K. (2005). Toll to be paid at the gateway to the vessel wall. *Arterioscler Thromb Vasc Biol*, 25(6), 1085-1087. doi:10.1161/01.Atv.0000168894.43759.47
- Hardy, J., & Allsop, D. (1991). Amyloid deposition as the central event in the aetiology of Alzheimer's disease. *Trends Pharmacol Sci*, 12(10), 383-388. doi:10.1016/0165-6147(91)90609-v
- Hardy, J., & Higgins, G. (1992). Alzheimer's disease: the amyloid cascade hypothesis. *Science*, 184. doi:10.1126/science.1566067
- Hardy, J., & Selkoe, D. J. (2002). The amyloid hypothesis of Alzheimer's disease: progress and problems on the road to therapeutics. *Science*, 297(5580), 353-356. doi:10.1126/science.1072994

- Harmeier, A., Wozny, C., Rost, B. R., Munter, L. M., Hua, H., Georgiev, O., Beyermann, M., Hildebrand, P. W., Weise, C., Schaffner, W., Schmitz, D., & Multhaup, G. (2009). Role of amyloid- β glycine 33 in oligomerization, toxicity, and neuronal plasticity. *J Neurosci*, 29(23), 7582-7590. doi:10.1523/jneurosci.1336-09.2009
- Harold, D., Abraham, R., Hollingworth, P., Sims, R., Gerrish, A., Hamshere, M. L., Pahwa, J. S., Moskvina, V., Dowzell, K., Williams, A., Jones, N., Thomas, C., Stretton, A., Morgan, A. R., Lovestone, S., Powell, J., Proitsi, P., Lupton, M. K., Brayne, C., Rubinsztein, D. C., Gill, M., Lawlor, B., Lynch, A., Morgan, K., Brown, K. S., Passmore, P. A., Craig, D., McGuinness, B., Todd, S., Holmes, C., Mann, D., Smith, A. D., Love, S., Kehoe, P. G., Hardy, J., Mead, S., Fox, N., Rossor, M., Collinge, J., Maier, W., Jessen, F., Schürmann, B., Heun, R., van den Bussche, H., Heuser, I., Kornhuber, J., Wiltfang, J., Dichgans, M., Frölich, L., Hampel, H., Hüll, M., Rujescu, D., Goate, A. M., Kauwe, J. S., Cruchaga, C., Nowotny, P., Morris, J. C., Mayo, K., Sleegers, K., Bettens, K., Engelborghs, S., De Deyn, P. P., Van Broeckhoven, C., Livingston, G., Bass, N. J., Gurling, H., McQuillin, A., Gwilliam, R., Deloukas, P., Al-Chalabi, A., Shaw, C. E., Tsolaki, M., Singleton, A. B., Guerreiro, R., Mühleisen, T. W., Nöthen, M. M., Moebus, S., Jöckel, K. H., Klopp, N., Wichmann, H. E., Carrasquillo, M. M., Pankratz, V. S., Younkin, S. G., Holmans, P. A., O'Donovan, M., Owen, M. J., & Williams, J. (2009). Genome-wide association study identifies variants at CLU and PICALM associated with Alzheimer's disease. *Nat Genet*, 41(10), 1088-1093. doi:10.1038/ng.440
- Harper, J. D., Wong, S. S., Lieber, C. M., & Lansbury, P. T., Jr. (1999). Assembly of A β amyloid protofibrils: an in vitro model for a possible early event in Alzheimer's disease. *Biochemistry*, 38(28), 8972-8980. doi:10.1021/bi9904149
- Harvey, L., Mitchell, R., Brodaty, H., Draper, B., & Close, J. (2017). The impact of dementia and other comorbidities on increased risk of subsequent hip fracture following hip fracture in Australia: a competing risk approach. *Int J Popul Data Sci*, 1:141(1), 1. doi:doi: 10.23889/ijpds.v1i1.160
- Harwell, C. S., & Coleman, M. P. (2016). Synaptophysin depletion and intraneuronal A β in organotypic hippocampal slice cultures from huAPP transgenic mice. *Mol Neurodegener*, 11(1), 44. doi:10.1186/s13024-016-0110-7
- Hashioka, S., Klegeris, A., & McGeer, P. L. (2009). Proton pump inhibitors exert anti-inflammatory effects and decrease human microglial and monocytic THP-1 cell neurotoxicity. *Exp Neurol*, 217(1), 177-183. doi:10.1016/j.expneurol.2009.02.002
- Hashioka, S., Wu, Z., & Klegeris, A. (2020). Glia-driven neuroinflammation and systemic inflammation in Alzheimer's disease. *Curr Neuroparmacol*. doi:10.2174/1570159x18666201111104509
- Hellwig, S., Brioschi, S., Dieni, S., Frings, L., Masuch, A., Blank, T., & Biber, K. (2016). Altered microglia morphology and higher resilience to stress-induced depression-like behavior in CX3CR1-deficient mice. *Brain Behav Immun*, 55, 126-137. doi:10.1016/j.bbi.2015.11.008
- Hendrickx, D. A. E., van Eden, C. G., Schuurman, K. G., Hamann, J., & Huitinga, I. (2017). Staining of HLA-DR, Iba1 and CD68 in human microglia reveals partially overlapping expression depending on cellular morphology

- and pathology. *J Neuroimmunol*, 309, 12-22.
doi:10.1016/j.jneuroim.2017.04.007
- Heneka, M. T., & O'Banion, M. K. (2007). Inflammatory processes in Alzheimer's disease. *J Neuroimmunol*, 184(1-2), 69-91.
doi:10.1016/j.jneuroim.2006.11.017
- Heneka, M. T., Nadrigny, F., Regen, T., Martinez-Hernandez, A., Dumitrescu-Ozimek, L., Terwel, D., Jardimhazy-Kurutz, D., Walter, J., Kirchhoff, F., Hanisch, U. K., & Kummer, M. P. (2010). Locus ceruleus controls Alzheimer's disease pathology by modulating microglial functions through norepinephrine. *Proc Natl Acad Sci USA*, 107(13), 6058-6063.
doi:10.1073/pnas.0909586107
- Heneka, M. T., Kummer, M. P., Stutz, A., Delekate, A., Schwartz, S., Vieira-Saecker, A., Griep, A., Axt, D., Remus, A., Tzeng, T. C., Gelpi, E., Halle, A., Korte, M., Latz, E., & Golenbock, D. T. (2013). NLRP3 is activated in Alzheimer's disease and contributes to pathology in APP/PS1 mice. *Nature*, 493(7434), 674-678. doi:10.1038/nature11729
- Heneka, M. T., Kummer, M. P., & Latz, E. (2014). Innate immune activation in neurodegenerative disease. *Nat Rev Immunol*, 14(7), 463-477.
doi:10.1038/nri3705
- Heneka, M. T., Golenbock, D. T., & Latz, E. (2015a). Innate immunity in Alzheimer's disease. *Nat Immunol*, 16(3), 229-236. doi:10.1038/ni.3102
- Heneka, M. T., Carson, M. J., El Khoury, J., Landreth, G. E., Brosseron, F., Feinstein, D. L., Jacobs, A. H., Wyss-Coray, T., Vitorica, J., Ransohoff, R. M., Herrup, K., Frautschy, S. A., Finsen, B., Brown, G. C., Verkhratsky, A., Yamanaka, K., Koistinaho, J., Latz, E., Halle, A., Petzold, G. C., Town, T., Morgan, D., Shinohara, M. L., Perry, V. H., Holmes, C., Bazan, N. G., Brooks, D. J., Hunot, S., Joseph, B., Deigendesch, N., Garaschuk, O., Boddeke, E., Dinarello, C. A., Breitner, J. C., Cole, G. M., Golenbock, D. T., & Kummer, M. P. (2015b). Neuroinflammation in Alzheimer's disease. *Lancet Neurol*, 14(4), 388-405. doi:10.1016/s1474-4422(15)70016-5
- Herrup, K. (2010). Reimagining Alzheimer's disease—an age-based hypothesis. *J Neurosci*, 30(50), 16755-16762. doi:10.1523/jneurosci.4521-10.2010
- Hickman, S., Izzy, S., Sen, P., Morsett, L., & El Khoury, J. (2018). Microglia in neurodegeneration. *Nat Neurosci*, 21(10), 1359-1369. doi:10.1038/s41593-018-0242-x
- Hickman, S. E., Kingery, N. D., Ohsumi, T. K., Borowsky, M. L., Wang, L. C., Means, T. K., & Khoury, J. (2013). The microglial sensome revealed by direct RNA sequencing. *Nat Neurosci*, 16. doi:10.1038/nn.3554
- Hillen, J. B., Vitry, A., & Caughey, G. E. (2017). Disease burden, comorbidity and geriatric syndromes in the Australian aged care population. *Australas J Ageing*, 36(2), E14-e19. doi:10.1111/ajag.12411
- Hiller, G., & Weber, K. (1978). Radioimmunoassay for tubulin: a quantitative comparison of the tubulin content of different established tissue culture cells and tissues. *Cell*, 14(4), 795-804. doi:10.1016/0092-8674(78)90335-5
- Hind, L. E., Vincent, W. J., & Huttenlocher, A. (2016). Leading from the back: the role of the uropod in neutrophil polarization and migration. *Dev Cell*, 38(2), 161-169. doi:10.1016/j.devcel.2016.06.031
- Hirano, A., Malamud, N., Elizan, T. S., & Kurland, L. T. (1966). Amyotrophic lateral sclerosis and Parkinsonism-dementia complex on Guam. Further

- pathologic studies. *Arch Neurol*, 15(1), 35-51.
doi:10.1001/archneur.1966.00470130039004
- Hirano, A., Dembitzer, H. M., Kurland, L. T., & Zimmerman, H. M. (1968). The fine structure of some intraganglionic alterations. Neurofibrillary tangles, granulovacuolar bodies and "rod-like" structures as seen in Guam amyotrophic lateral sclerosis and parkinsonism-dementia complex. *J Neuropathol Exp Neurol*, 27(2), 167-182.
- Hof, P. R., Glannakopoulos, P., & Bouras, C. (1996). The neuropathological changes associated with normal brain aging. *Histol Histopathol*, 11(4), 1075-1088.
- Hof, P. R., Bussière, T., Gold, G., Kövari, E., Giannakopoulos, P., Bouras, C., Perl, D. P., & Morrison, J. H. (2003). Stereologic evidence for persistence of viable neurons in layer II of the entorhinal cortex and the CA1 field in Alzheimer disease. *J Neuropathol Exp Neurol*, 62(1), 55-67.
doi:10.1093/jnen/62.1.55
- Hollingsworth, P., Harold, D., Sims, R., Gerrish, A., Lambert, J. C., Carrasquillo, M. M., Abraham, R., Hamshere, M. L., Pahwa, J. S., Moskva, V., Dowzell, K., Jones, N., Stretton, A., Thomas, C., Richards, A., Ivanov, D., Widdowson, C., Chapman, J., Lovestone, S., Powell, J., Proitsi, P., Lupton, M. K., Brayne, C., Rubinsztein, D. C., Gill, M., Lawlor, B., Lynch, A., Brown, K. S., Passmore, P. A., Craig, D., McGuinness, B., Todd, S., Holmes, C., Mann, D., Smith, A. D., Beaumont, H., Warden, D., Wilcock, G., Love, S., Kehoe, P. G., Hooper, N. M., Vardy, E. R., Hardy, J., Mead, S., Fox, N. C., Rossor, M., Collinge, J., Maier, W., Jessen, F., Rütter, E., Schürmann, B., Heun, R., Kölsch, H., van den Bussche, H., Heuser, I., Kornhuber, J., Wiltfang, J., Dichgans, M., Frölich, L., Hampel, H., Gallacher, J., Hüll, M., Rujescu, D., Giegling, I., Goate, A. M., Kauwe, J. S., Cruchaga, C., Nowotny, P., Morris, J. C., Mayo, K., Sleegers, K., Bettens, K., Engelborghs, S., De Deyn, P. P., Van Broeckhoven, C., Livingston, G., Bass, N. J., Gurling, H., McQuillin, A., Gwilliam, R., Deloukas, P., Al-Chalabi, A., Shaw, C. E., Tsolaki, M., Singleton, A. B., Guerreiro, R., Mühleisen, T. W., Nöthen, M. M., Moebus, S., Jöckel, K. H., Klopp, N., Wichmann, H. E., Pankratz, V. S., Sando, S. B., Aasly, J. O., Barcikowska, M., Wszolek, Z. K., Dickson, D. W., Graff-Radford, N. R., Petersen, R. C., van Duijn, C. M., Breteler, M. M., Ikram, M. A., DeStefano, A. L., Fitzpatrick, A. L., Lopez, O., Launer, L. J., Seshadri, S., Berr, C., Campion, D., Epelbaum, J., Dartigues, J. F., Tzourio, C., Alperovitch, A., Lathrop, M., Feulner, T. M., Friedrich, P., Riehle, C., Krawczak, M., Schreiber, S., Mayhaus, M., Nicolhaus, S., Wagenpfeil, S., Steinberg, S., Stefansson, H., Stefansson, K., Snaedal, J., Björnsson, S., Jonsson, P. V., Chouraki, V., Genier-Boley, B., Hiltunen, M., Soininen, H., Combarros, O., Zelenika, D., Delepine, M., Bullido, M. J., Pasquier, F., Mateo, I., Frank-Garcia, A., Porcellini, E., Hanon, O., Coto, E., Alvarez, V., Bosco, P., Siciliano, G., Mancuso, M., Panza, F., Solfrizzi, V., Nacmias, B., Sorbi, S., Bossù, P., Piccardi, P., Arosio, B., Annoni, G., Seripa, D., Pilotto, A., Scarpini, E., Galimberti, D., Brice, A., Hannequin, D., Licastro, F., Jones, L., Holmans, P. A., Jonsson, T., Riemenschneider, M., Morgan, K., Younkin, S. G., Owen, M. J., O'Donovan, M., Amouyel, P., & Williams, J. (2011). Common variants at ABCA7,

- MS4A6A/MS4A4E, EPHA1, CD33 and CD2AP are associated with Alzheimer's disease. *Nat Genet*, 43(5), 429-435. doi:10.1038/ng.803
- Holloway, O. G., Canty, A. J., King, A. E., & Ziebell, J. M. (2019). Rod microglia and their role in neurological diseases. *Semin Cell Dev Biol*, 94, 96-103. doi:10.1016/j.semcdb.2019.02.005
- Holloway, O. G., King, A. E., & Ziebell, J. M. (2020). Microglia demonstrate local mixed inflammation and a defined morphological shift in an APP/PS1 mouse model. *J Alzheimers Dis*, 77(4), 1765-1781. doi:10.3233/jad-200098
- Holmes, C., Boche, D., Wilkinson, D., Yadegarfar, G., Hopkins, V., Bayer, A., Jones, R. W., Bullock, R., Love, S., Neal, J. W., Zotova, E., & Nicoll, J. A. (2008). Long-term effects of A β 42 immunisation in Alzheimer's disease: follow-up of a randomised, placebo-controlled phase I trial. *Lancet*, 372(9634), 216-223. doi:10.1016/s0140-6736(08)61075-2
- Holness, C. L., da Silva, R. P., Fawcett, J., Gordon, S., & Simmons, D. L. (1993). Macrosialin, a mouse macrophage-restricted glycoprotein, is a member of the lamp/lgp family. *J Biol Chem*, 268(13), 9661-9666.
- Holness, C. L., & Simmons, D. L. (1993). Molecular cloning of CD68, a human macrophage marker related to lysosomal glycoproteins. *Blood*, 81(6), 1607-1613.
- Hong, S., Dissing-Olesen, L., & Stevens, B. (2016). New insights on the role of microglia in synaptic pruning in health and disease. *Curr Opin Neurobiol*, 36, 128-134. doi:10.1016/j.conb.2015.12.004
- Hopperton, K. E., Mohammad, D., Trepanier, M. O., Giuliano, V., & Bazinet, R. P. (2018). Markers of microglia in post-mortem brain samples from patients with Alzheimer's disease: a systematic review. *Mol Psychiatry*, 23(2), 177-198. doi:10.1038/mp.2017.246
- Horvath, R. J., & DeLeo, J. A. (2009). Morphine enhances microglial migration through modulation of P2X4 receptor signaling. *J Neurosci*, 29(4), 998-1005. doi:10.1523/jneurosci.4595-08.2009
- Houlden, H., Baker, M., McGowan, E., Lewis, P., Hutton, M., Crook, R., Wood, N. W., Kumar-Singh, S., Geddes, J., Swash, M., Scaravilli, F., Holton, J. L., Lashley, T., Tomita, T., Hashimoto, T., Verkkoniemi, A., Kalimo, H., Somer, M., Paetau, A., Martin, J. J., Van Broeckhoven, C., Golde, T., Hardy, J., Haltia, M., & Revesz, T. (2000). Variant Alzheimer's disease with spastic paraparesis and cotton wool plaques is caused by PS-1 mutations that lead to exceptionally high amyloid- β concentrations. *Ann Neurol*, 48(5), 806-808.
- Howie, A. J., Brewer, D. B., Howell, D., & Jones, A. P. (2008). Physical basis of colors seen in Congo red-stained amyloid in polarized light. *Lab Invest*, 88(3), 232-242. doi:10.1038/labinvest.3700714
- Hoyle, G. (1985). *Neurotransmitters, neuromodulators, and neurohormones*. In Neurobiology: Current Comparative Approaches Vol. 3 (R. Gilles & J. Balthazart Eds.). Heidelberg, Germany: Springer Berlin Heidelberg.
- Hristovska, I., & Pascual, O. (2015). Deciphering resting microglial morphology and process motility from a synaptic prospect. *Front Integr Neurosci*, 9, 73. doi:10.3389/fnint.2015.00073
- Hsu, J. C., Lee, Y. S., Chang, C. N., Ling, E. A., & Lan, C. T. (2003). Sleep deprivation prior to transient global cerebral ischemia attenuates glial

- reaction in the rat hippocampal formation. *Brain Res*, 984(1-2), 170-181. doi:10.1016/s0006-8993(03)03128-7
- Huang, K. L., Marcora, E., Pimenova, A. A., Di Narzo, A. F., Kapoor, M., Jin, S. C., Harari, O., Bertelsen, S., Fairfax, B. P., Czajkowski, J., Chouraki, V., Grenier-Boley, B., Bellenguez, C., Deming, Y., McKenzie, A., Raj, T., Renton, A. E., Budde, J., Smith, A., Fitzpatrick, A., Bis, J. C., DeStefano, A., Adams, H. H. H., Ikram, M. A., van der Lee, S., Del-Aguila, J. L., Fernandez, M. V., Ibañez, L., Sims, R., Escott-Price, V., Mayeux, R., Haines, J. L., Farrer, L. A., Pericak-Vance, M. A., Lambert, J. C., van Duijn, C., Launer, L., Seshadri, S., Williams, J., Amouyel, P., Schellenberg, G. D., Zhang, B., Borecki, I., Kauwe, J. S. K., Cruchaga, C., Hao, K., & Goate, A. M. (2017). A common haplotype lowers PU.1 expression in myeloid cells and delays onset of Alzheimer's disease. *Nat Neurosci*, 20(8), 1052-1061. doi:10.1038/nn.4587
- Huang, L. K., Chao, S. P., & Hu, C. J. (2020). Clinical trials of new drugs for Alzheimer disease. *J Biomed Sci*, 27(1), 18. doi:10.1186/s12929-019-0609-7
- Huang, Y., & Mahley, R. W. (2014). Apolipoprotein E: structure and function in lipid metabolism, neurobiology, and Alzheimer's diseases. *Neurobiol Dis*, 72 Pt A, 3-12. doi:10.1016/j.nbd.2014.08.025
- Huang, Y., Happonen, K. E., Burrola, P. G., O'Connor, C., Hah, N., Huang, L., Nimmerjahn, A., & Lemke, G. (2021). Microglia use TAM receptors to detect and engulf amyloid β plaques. *Nat Immunol*. doi:10.1038/s41590-021-00913-5
- Hui, C. W., St-Pierre, M.-K., Detuncq, J., Aumailley, L., Dubois, M.-J., Couture, V., Skuk, D., Marette, A., Tremblay, J. P., Lebel, M., & Tremblay, M.-È. (2018). Nonfunctional mutant Wrn protein leads to neurological deficits, neuronal stress, microglial alteration, and immune imbalance in a mouse model of Werner syndrome. *Brain Behav Immun*, 73, 450-469. doi:10.1016/j.bbi.2018.06.007
- Humpel, C. (2015). Organotypic brain slice cultures: A review. *Neuroscience*, 305, 86-98. doi:10.1016/j.neuroscience.2015.07.086
- Hutter-Schmid, B., Kniewallner, K. M., & Humpel, C. (2015). Organotypic brain slice cultures as a model to study angiogenesis of brain vessels. *Front Cell Dev Biol*, 3, 52. doi:10.3389/fcell.2015.00052
- Hutton, M., Lendon, C. L., Rizzu, P., Baker, M., Froelich, S., Houlden, H., Pickering-Brown, S., Chakraborty, S., Isaacs, A., Grover, A., Hackett, J., Adamson, J., Lincoln, S., Dickson, D., Davies, P., Petersen, R. C., Stevens, M., de Graaff, E., Wauters, E., van Baren, J., Hillebrand, M., Joosse, M., Kwon, J. M., Nowotny, P., Che, L. K., Norton, J., Morris, J. C., Reed, L. A., Trojanowski, J., Basun, H., Lannfelt, L., Neystat, M., Fahn, S., Dark, F., Tannenberg, T., Dodd, P. R., Hayward, N., Kwok, J. B., Schofield, P. R., Andreadis, A., Snowden, J., Craufurd, D., Neary, D., Owen, F., Oostra, B. A., Hardy, J., Goate, A., van Swieten, J., Mann, D., Lynch, T., & Heutink, P. (1998). Association of missense and 5'-splice-site mutations in tau with the inherited dementia FTDP-17. *Nature*, 393(6686), 702-705. doi:10.1038/31508
- Hyman, B. T., Phelps, C. H., Beach, T. G., Bigio, E. H., Cairns, N. J., Carrillo, M. C., Dickson, D. W., Duyckaerts, C., Frosch, M. P., Masliah, E., Mirra, S. S., Nelson, P. T., Schneider, J. A., Thal, D. R., Thies, B., Trojanowski, J.

- Q., Vinters, H. V., & Montine, T. J. (2012). National Institute on Aging-Alzheimer's Association guidelines for the neuropathologic assessment of Alzheimer's disease. *Alzheimers Dement*, 8(1), 1-13. doi:10.1016/j.jalz.2011.10.007
- Hyman, B. T., & Sorger, P. (2014). Failure analysis of clinical trials to test the amyloid hypothesis. *Ann Neurol*, 76(2), 159-161. doi:10.1002/ana.24227
- Iacobas, D. A., Iacobas, S., & Spray, D. C. (2007). Connexin-dependent transcellular transcriptomic networks in mouse brain. *Prog Biophys Mol Biol*, 94(1-2), 169-185. doi:10.1016/j.pbiomolbio.2007.03.015
- Iadecola, C. (2004). Neurovascular regulation in the normal brain and in Alzheimer's disease. *Nat Rev Neurosci*, 5(5), 347-360. doi:10.1038/nrn1387
- Ikeda, S., Allsop, D., & Glenner, G. G. (1989). Morphology and distribution of plaque and related deposits in the brains of Alzheimer's disease and control cases. An immunohistochemical study using amyloid β -protein antibody. *Lab Invest*, 60(1), 113-122.
- Ilshner, S., Nolte, C., & Kettenmann, H. (1996). Complement factor C5a and epidermal growth factor trigger the activation of outward potassium currents in cultured murine microglia. *Neuroscience*, 73(4), 1109-1120. doi:10.1016/0306-4522(96)00107-8
- Ingelsson, M., Fukumoto, H., Newell, K. L., Growdon, J. H., Hedley-Whyte, E. T., Frosch, M. P., Albert, M. S., Hyman, B. T., & Irizarry, M. C. (2004). Early A β accumulation and progressive synaptic loss, gliosis, and tangle formation in AD brain. *Neurology*, 62(6), 925-931. doi:10.1212/01.wnl.0000115115.98960.37
- Innocenti, G. M., Clarke, S., & Koppel, H. (1983). Transitory macrophages in the white matter of the developing visual cortex. II. Development and relations with axonal pathways. *Brain Res*, 313(1), 55-66. doi:10.1016/0165-3806(83)90201-8
- Institute for Clinical and Economic Review. (2021, May 5). Aducanumab for Alzheimer's disease: effectiveness and value [Draft Evidence Report]. Retrieved 2021, Jun 9, from https://icer.org/wp-content/uploads/2020/10/ICER_ALZ_Draft_Evidence_Report_050521.pdf
- Iqbal, K., Zaidi, T., Bancher, C., & Grundke-Iqbal, I. (1994). Alzheimer paired helical filaments: restoration of the biological activity by dephosphorylation. *FEBS Lett*, 349(1), 104-108. doi:10.1016/0014-5793(94)00650-4
- Iqbal, K., & Grundke-Iqbal, I. (2005). Metabolic/signal transduction hypothesis of Alzheimer's disease and other tauopathies. *Acta Neuropathol*, 109(1), 25-31. doi:10.1007/s00401-004-0951-y
- Iqbal, K., Liu, F., Gong, C. X., Alonso, A. d. C., & Grundke-Iqbal, I. (2009). Mechanisms of tau-induced neurodegeneration. *Acta Neuropathol*, 118(1), 53-69. doi:10.1007/s00401-009-0486-3
- Iqbal, K., Liu, F., Gong, C. X., & Grundke-Iqbal, I. (2010). Tau in Alzheimer disease and related tauopathies. *Curr Alzheimer Res*, 7(8), 656-664. doi:10.2174/156720510793611592
- Ismail, R., Parbo, P., Madsen, L. S., Hansen, A. K., Hansen, K. V., Schaldemose, J. L., Kjeldsen, P. L., Stokholm, M. G., Gottrup, H., Eskildsen, S. F., & Brooks, D. J. (2020). The relationships between neuroinflammation, β -

- amyloid and tau deposition in Alzheimer's disease: a longitudinal PET study. *J Neuroinflammation*, 17(1), 151. doi:10.1186/s12974-020-01820-6
- Itagaki, S., McGeer, P. L., Akiyama, H., Zhu, S., & Selkoe, D. (1989). Relationship of microglia and astrocytes to amyloid deposits of Alzheimer disease. *J Neuroimmunol*, 24(3), 173-182. doi:10.1016/0165-5728(89)90115-x
- Ito, D., Imai, Y., Ohsawa, K., Nakajima, K., Fukuuchi, Y., & Kohsaka, S. (1998). Microglia-specific localisation of a novel calcium binding protein, Iba1. *Brain Res Mol Brain Res*, 57(1), 1-9.
- Ito, D., Tanaka, K., Suzuki, S., Dembo, T., & Fukuuchi, Y. (2001). Enhanced expression of Iba1, ionized calcium-binding adapter molecule 1, after transient focal cerebral ischemia in rat brain. *Stroke*, 32(5), 1208-1215. doi:10.1161/01.str.32.5.1208
- Ittner, A., & Ittner, L. M. (2018). Dendritic tau in Alzheimer's disease. *Neuron*, 99(1), 13-27. doi:10.1016/j.neuron.2018.06.003
- Iwata, N., Tsubuki, S., Takaki, Y., Watanabe, K., Sekiguchi, M., Hosoki, E., Kawashima-Morishima, M., Lee, H. J., Hama, E., Sekine-Aizawa, Y., & Saido, T. C. (2000). Identification of the major A β 1-42-degrading catabolic pathway in brain parenchyma: suppression leads to biochemical and pathological deposition. *Nat Med*, 6(2), 143-150. doi:10.1038/72237
- Iwata, N., Mizukami, H., Shirotani, K., Takaki, Y., Muramatsu, S., Lu, B., Gerard, N. P., Gerard, C., Ozawa, K., & Saido, T. C. (2004). Presynaptic localization of neprilysin contributes to efficient clearance of amyloid- β peptide in mouse brain. *J Neurosci*, 24(4), 991-998. doi:10.1523/jneurosci.4792-03.2004
- Jack, C. R., Jr., Knopman, D. S., Jagust, W. J., Shaw, L. M., Aisen, P. S., Weiner, M. W., Petersen, R. C., & Trojanowski, J. Q. (2010). Hypothetical model of dynamic biomarkers of the Alzheimer's pathological cascade. *Lancet Neurol*, 9(1), 119-128. doi:10.1016/s1474-4422(09)70299-6
- Jack, C. R., Jr., Albert, M. S., Knopman, D. S., McKhann, G. M., Sperling, R. A., Carrillo, M. C., Thies, B., & Phelps, C. H. (2011). Introduction to the recommendations from the National Institute on Aging-Alzheimer's Association workgroups on diagnostic guidelines for Alzheimer's disease. *Alzheimers Dement*, 7(3), 257-262. doi:10.1016/j.jalz.2011.03.004
- Jana, M. K. (2016). *Identifying the key A β oligomer species by correlating cell neurotoxicity and binding properties*. (Doctoral dissertation). The University of Melbourne, Melbourne, Victoria, Australia. Retrieved from <https://minerva-access.unimelb.edu.au/handle/11343/116121>
- Jana, M. K., Cappai, R., Pham, C. L., & Ciccotosto, G. D. (2016). Membrane-bound tetramer and trimer A β oligomeric species correlate with toxicity towards cultured neurons. *J Neurochem*, 136(3), 594-608. doi:10.1111/jnc.13443
- Janelidze, S., Stomrud, E., Smith, R., Palmqvist, S., Mattsson, N., Airey, D. C., Proctor, N. K., Chai, X., Shcherbinin, S., Sims, J. R., Triana-Baltzer, G., Theunis, C., Slemmon, R., Mercken, M., Kolb, H., Dage, J. L., & Hansson, O. (2020). Cerebrospinal fluid p-tau217 performs better than p-tau181 as a biomarker of Alzheimer's disease. *Nat Commun*, 11(1), 1683. doi:10.1038/s41467-020-15436-0
- Jansen, I. E., Savage, J. E., Watanabe, K., Bryois, J., Williams, D. M., Steinberg, S., Sealock, J., Karlsson, I. K., Hägg, S., Athanasiu, L., Voyle, N., Proitsi,

- P., Witoelar, A., Stringer, S., Aarsland, D., Almdahl, I. S., Andersen, F., Bergh, S., Bettella, F., Bjornsson, S., Brækhus, A., Bråthen, G., de Leeuw, C., Desikan, R. S., Djurovic, S., Dumitrescu, L., Fladby, T., Hohman, T. J., Jonsson, P. V., Kiddle, S. J., Rongve, A., Saltvedt, I., Sando, S. B., Selbæk, G., Shoai, M., Skene, N. G., Snaedal, J., Stordal, E., Ulstein, I. D., Wang, Y., White, L. R., Hardy, J., Hjerling-Leffler, J., Sullivan, P. F., van der Flier, W. M., Dobson, R., Davis, L. K., Stefansson, H., Stefansson, K., Pedersen, N. L., Ripke, S., Andreassen, O. A., & Posthuma, D. (2019). Genome-wide meta-analysis identifies new loci and functional pathways influencing Alzheimer's disease risk. *Nat Genet*, *51*(3), 404-413. doi:10.1038/s41588-018-0311-9
- Jelistratova, I., Teipel, S. J., & Grothe, M. J. (2020). Longitudinal validity of PET-based staging of regional amyloid deposition. *Hum Brain Mapp*, *41*(15), 4219-4231. doi:10.1002/hbm.25121
- Jellinger, K. A. (2020). Neuropathological assessment of the Alzheimer spectrum. *J Neural Transm (Vienna)*, *127*(9), 1229-1256. doi:10.1007/s00702-020-02232-9
- Jiang, T., Tan, L., Zhu, X. C., Zhang, Q. Q., Cao, L., Tan, M. S., Gu, L. Z., Wang, H. F., Ding, Z. Z., Zhang, Y. D., & Yu, J. T. (2014). Upregulation of TREM2 ameliorates neuropathology and rescues spatial cognitive impairment in a transgenic mouse model of Alzheimer's disease. *Neuropsychopharmacology*, *39*(13), 2949-2962. doi:10.1038/npp.2014.164
- Jiang, Y., Li, Z., Ma, H., Cao, X., Liu, F., Tian, A., Sun, X., Li, X., & Wang, J. (2018). Upregulation of TREM2 ameliorates neuroinflammatory responses and improves cognitive deficits triggered by surgical trauma in APPswe/PS1dE9 mice. *Cell Physiol Biochem*, *46*(4), 1398-1411. doi:10.1159/000489155
- Jicha, G. A., Abner, E. L., Schmitt, F. A., Kryscio, R. J., Riley, K. P., Cooper, G. E., Stiles, N., Mendiondo, M. S., Smith, C. D., Van Eldik, L. J., & Nelson, P. T. (2012). Preclinical AD Workgroup staging: pathological correlates and potential challenges. *Neurobiol Aging*, *33*(3), 622.e621-622.e616. doi:10.1016/j.neurobiolaging.2011.02.018
- Jin, M. S., & Lee, J. O. (2008). Structures of the toll-like receptor family and its ligand complexes. *Immunity*, *29*(2), 182-191. doi:10.1016/j.immuni.2008.07.007
- Jin, X., & Yamashita, T. (2016). Microglia in central nervous system repair after injury. *J Biochem*, *159*(5), 491-496. doi:10.1093/jb/mvw009
- Johnson, G. V., & Stoothoff, W. H. (2004). Tau phosphorylation in neuronal cell function and dysfunction. *J Cell Sci*, *117*(Pt 24), 5721-5729. doi:10.1242/jcs.01558
- Johnson, J. W., & Kotermanski, S. E. (2006). Mechanism of action of memantine. *Curr Opin Pharmacol*, *6*(1), 61-67. doi:10.1016/j.coph.2005.09.007
- Joling, K. J., van Marwijk, H. W., Veldhuijzen, A. E., van der Horst, H. E., Scheltens, P., Smit, F., & van Hout, H. P. (2015). The two-year incidence of depression and anxiety disorders in spousal caregivers of persons with dementia: who is at the greatest risk? *Am J Geriatr Psychiatry*, *23*(3), 293-303. doi:10.1016/j.jagp.2014.05.005
- Jones, L., Lambert, J.-C., Wang, L.-S., Choi, S.-H., Harold, D., Vedernikov, A., Escott-Price, V., Stone, T., Richards, A., Bellenguez, C., Ibrahim-Verbaas,

- C. A., Naj, A. C., Sims, R., Gerrish, A., Jun, G., DeStefano, A. L., Bis, J. C., Beecham, G. W., Grenier-Boley, B., Russo, G., Thornton-Wells, T. A., Jones, N., Smith, A. V., Chouraki, V., Thomas, C., Ikram, M. A., Zelenika, D., Vardarajan, B. N., Kamatani, Y., Lin, C.-F., Schmidt, H., Kunkle, B. W., Dunstan, M. L., Ruiz, A., Bihoreau, M.-T., Reitz, C., Pasquier, F., Hollingworth, P., Hanon, O., Fitzpatrick, A. L., Buxbaum, J. D., Campion, D., Crane, P. K., Becker, T., Gudnason, V., Cruchaga, C., Craig, D., Amin, N., Berr, C., Lopez, O. L., De Jager, P. L., Deramecourt, V., Johnston, J. A., Evans, D., Lovestone, S., Letteneur, L., Kornhuber, J., Tárraga, L., Rubinsztein, D. C., Eiriksdottir, G., Sleegers, K., Goate, A. M., Fiévet, N., Huentelman, M. J., Gill, M., Emilsson, V., Brown, K., Kamboh, M. I., Keller, L., Barberger-Gateau, P., McGuinness, B., Larson, E. B., Myers, A. J., Dufouil, C., Todd, S., Wallon, D., Love, S., Kehoe, P., Rogaeva, E., Gallacher, J., St George-Hyslop, P., Clarimon, J., Lleò, A., Bayer, A., Tsuang, D. W., Yu, L., Tsolaki, M., Bossù, P., Spalletta, G., Proitsi, P., Collinge, J., Sorbi, S., Sanchez Garcia, F., Fox, N., Hardy, J., Deniz Naranjo, M. C., Razquin, C., Bosco, P., Clarke, R., Brayne, C., Galimberti, D., Mancuso, M., CFAS, M., Moebus, S., Mecocci, P., del Zompo, M., Maier, W., Hampel, H., Pilotto, A., Bullido, M., Panza, F., Caffarra, P., Nacmias, B., Gilbert, J. R., Mayhaus, M., Jessen, F., Dichgans, M., Lannfelt, L., Hakonarson, H., Pichler, S., Carrasquillo, M. M., Ingelsson, M., Beekly, D., Alavarez, V., Zou, F., Valladares, O., Younkin, S. G., Coto, E., Hamilton-Nelson, K. L., Mateo, I., Owen, M. J., Faber, K. M., Jonsson, P. V., Combarros, O., O'Donovan, M. C., Cantwell, L. B., Soininen, H., Blacker, D., Mead, S., Mosley Jr., T. H., Bennett, D. A., Harris, T. B., Fratiglioni, L., Holmes, C., de Bruijn, R. F. A. G., Passmore, P., Montine, T. J., Bettens, K., Rotter, J. I., Brice, A., Morgan, K., Foroud, T. M., Kukull, W. A., Hannequin, D., Powell, J. F., Nalls, M. A., Ritchie, K., Lunetta, K. L., Kauwe, J. S. K., Boerwinkle, E., Riemenschneider, M., Boada, M., Hiltunen, M., Martin, E. R., Pastor, P., Schmidt, R., Rujescu, D., Dartigues, J.-F., Mayeux, R., Tzourio, C., Hofman, A., Nöthen, M. M., Graff, C., Psaty, B. M., Haines, J. L., Lathrop, M., Pericak-Vance, M. A., Launer, L. J., Farrer, L. A., van Duijn, C. M., Van Broeckhoven, C., Ramirez, A., Schellenberg, G. D., Seshadri, S., Amouyel, P., Williams, J., & Holmans, P. A. (2015). Convergent genetic and expression data implicate immunity in Alzheimer's disease. *Alzheimer's & Dementia*, 11(6), 658-671. doi:10.1016/j.jalz.2014.05.1757
- Jones, P. M., & George, A. M. (2004). The ABC transporter structure and mechanism: perspectives on recent research. *Cell Mol Life Sci*, 61(6), 682-699. doi:10.1007/s00018-003-3336-9
- Jonsson, T., Atwal, J. K., Steinberg, S., Snaedal, J., Jonsson, P. V., Bjornsson, S., Stefansson, H., Sulem, P., Gudbjartsson, D., Maloney, J., Hoyte, K., Gustafson, A., Liu, Y., Lu, Y., Bhangale, T., Graham, R. R., Huttenlocher, J., Bjornsdottir, G., Andreassen, O. A., Jönsson, E. G., Palotie, A., Behrens, T. W., Magnusson, O. T., Kong, A., Thorsteinsdottir, U., Watts, R. J., & Stefansson, K. (2012). A mutation in APP protects against Alzheimer's disease and age-related cognitive decline. *Nature*, 488(7409), 96-99. doi:10.1038/nature11283
- Jonsson, T., Stefansson, H., Steinberg, S., Jonsdottir, I., Jonsson, P. V., Snaedal, J., Bjornsson, S., Huttenlocher, J., Levey, A. I., Lah, J. J., Rujescu, D.,

- Hampel, H., Giegling, I., Andreassen, O. A., Engedal, K., Ulstein, I., Djurovic, S., Ibrahim-Verbaas, C., Hofman, A., Ikram, M. A., Duijn, C. M., Thorsteinsdottir, U., Kong, A., & Stefansson, K. (2013). Variant of TREM2 associated with the risk of Alzheimer's disease. *N Engl J Med*, 368. doi:10.1056/NEJMoa1211103
- Jordan-Sciutto, K., Dragich, J., Walcott, D., & Bowser, R. (1998). The presence of FAC1 protein in Hirano bodies. *Neuropathol Appl Neurobiol*, 24(5), 359-366. doi:10.1046/j.1365-2990.1998.00140.x
- Josephs, K. A., Whitwell, J. L., Tosakulwong, N., Weigand, S. D., Murray, M. E., Liesinger, A. M., Petrucelli, L., Senjem, M. L., Ivnik, R. J., Parisi, J. E., Petersen, R. C., & Dickson, D. W. (2015). TAR DNA-binding protein 43 and pathological subtype of Alzheimer's disease impact clinical features. *Ann Neurol*, 78(5), 697-709. doi:10.1002/ana.24493
- Ju Hwang, C., Choi, D. Y., Park, M. H., & Hong, J. T. (2019). NF- κ B as a key mediator of brain inflammation in Alzheimer's disease. *CNS Neurol Disord Drug Targets*, 18(1), 3-10. doi:10.2174/1871527316666170807130011
- Jun, G., Naj, A. C., Beecham, G. W., Wang, L. S., Buross, J., Gallins, P. J., Buxbaum, J. D., Ertekin-Taner, N., Fallin, M. D., Friedland, R., Inzelberg, R., Kramer, P., Rogaeva, E., St George-Hyslop, P., Cantwell, L. B., Dombroski, B. A., Saykin, A. J., Reiman, E. M., Bennett, D. A., Morris, J. C., Lunetta, K. L., Martin, E. R., Montine, T. J., Goate, A. M., Blacker, D., Tsuang, D. W., Beekly, D., Cupples, L. A., Hakonarson, H., Kukull, W., Foroud, T. M., Haines, J., Mayeux, R., Farrer, L. A., Pericak-Vance, M. A., & Schellenberg, G. D. (2010). Meta-analysis confirms CR1, CLU, and PICALM as Alzheimer disease risk loci and reveals interactions with APOE genotypes. *Arch Neurol*, 67(12), 1473-1484. doi:10.1001/archneurol.2010.201
- Jurewicz, M. M., & Stern, L. J. (2019). Class II MHC antigen processing in immune tolerance and inflammation. *Immunogenetics*, 71(3), 171-187. doi:10.1007/s00251-018-1095-x
- Kalamida, D., Poulas, K., Avramopoulou, V., Fostieri, E., Lagoumintzis, G., Lazaridis, K., Sideri, A., Zouridakis, M., & Tzartos, S. J. (2007). Muscle and neuronal nicotinic acetylcholine receptors. Structure, function and pathogenicity. *Febs j*, 274(15), 3799-3845. doi:10.1111/j.1742-4658.2007.05935.x
- Kalaria, R. N. (2016). Neuropathological diagnosis of vascular cognitive impairment and vascular dementia with implications for Alzheimer's disease. *Acta Neuropathol*, 131(5), 659-685. doi:10.1007/s00401-016-1571-z
- Kamboj, M. I. (2018). A brief synopsis on the genetics of Alzheimer's disease. *Curr Genet Med Rep*, 6(4), 133-135. doi:10.1007/s40142-018-0155-8
- Kang, J., Lemaire, H. G., Unterbeck, A., Salbaum, J. M., Masters, C. L., Grzeschik, K. H., Multhaup, G., Beyreuther, K., & Müller-Hill, B. (1987). The precursor of Alzheimer's disease amyloid A4 protein resembles a cell-surface receptor. *Nature*, 325(6106), 733-736. doi:10.1038/325733a0
- Kantarci, K. (2007). 1H magnetic resonance spectroscopy in dementia. *Br J Radiol*, 80 Spec No 2, S146-152. doi:10.1259/bjr/60346217

- Kapasi, A., DeCarli, C., & Schneider, J. A. (2017). Impact of multiple pathologies on the threshold for clinically overt dementia. *Acta Neuropathol*, 134(2), 171-186. doi:10.1007/s00401-017-1717-7
- Kaplan, D. R., & Miller, F. D. (2000). Neurotrophin signal transduction in the nervous system. *Curr Opin Neurobiol*, 10(3), 381-391. doi:10.1016/s0959-4388(00)00092-1
- Karran, E., & Hardy, J. (2014). A critique of the drug discovery and phase 3 clinical programs targeting the amyloid hypothesis for Alzheimer disease. *Ann Neurol*, 76(2), 185-205. doi:10.1002/ana.24188
- Karunakaran, I., Alam, S., Jayagopi, S., Frohberger, S. J., Hansen, J. N., Kuehlwein, J., Hölbling, B. V., Schumak, B., Hübner, M. P., Gräler, M. H., Halle, A., & van Echten-Deckert, G. (2019). Neural sphingosine 1-phosphate accumulation activates microglia and links impaired autophagy and inflammation. *Glia*, 67(10), 1859-1872. doi:10.1002/glia.23663
- Kaur, C., Rathnasamy, G., & Ling, E. A. (2017). Biology of microglia in the developing brain. *J Neuropathol Exp Neurol*, 76(9), 736-753. doi:10.1093/jnen/nlx056
- Kaur, G., Han, S. J., Yang, I., & Crane, C. (2010). Microglia and central nervous system immunity. *Neurosurg Clin N Am*, 21(1), 43-51. doi:10.1016/j.nec.2009.08.009
- Kaushal, V., & Schlichter, L. C. (2008). Mechanisms of microglia-mediated neurotoxicity in a new model of the stroke penumbra. *J Neurosci*, 28(9), 2221-2230. doi:10.1523/jneurosci.5643-07.2008
- Kawasaki, T., & Kawai, T. (2014). Toll-like receptor signaling pathways. *Front Immunol*, 5, 461. doi:10.3389/fimmu.2014.00461
- Kayed, R., Pensalfini, A., Margol, L., Sokolov, Y., Sarsoza, F., Head, E., Hall, J., & Glabe, C. (2009). Annular protofibrils are a structurally and functionally distinct type of amyloid oligomer. *J Biol Chem*, 284(7), 4230-4237. doi:10.1074/jbc.M808591200
- Keating, S. E., Baran, M., & Bowie, A. G. (2011). Cytosolic DNA sensors regulating type I interferon induction. *Trends Immunol*, 32(12), 574-581. doi:10.1016/j.it.2011.08.004
- Keren-Shaul, H., Spinrad, A., Weiner, A., Matcovitch-Natan, O., Dvir-Szternfeld, R., Ulland, T. K., David, E., Baruch, K., Lara-Astaiso, D., Toth, B., Itzkovitz, S., Colonna, M., Schwartz, M., & Amit, I. (2017). A unique microglia type associated with restricting development of Alzheimer's disease. *Cell*, 169(7), 1276-1290.e1217. doi:10.1016/j.cell.2017.05.018
- Kettenmann, H., & Verkhratsky, A. (2008). Neuroglia: the 150 years after. *Trends Neurosci*, 31(12), 653-659. doi:10.1016/j.tins.2008.09.003
- Kettenmann, H., Hanisch, U. K., Noda, M., & Verkhratsky, A. (2011). Physiology of microglia. *Physiol Rev*, 91. doi:10.1152/physrev.00011.2010
- Khachaturian, Z. S. (1994). Calcium hypothesis of Alzheimer's disease and brain aging. *Ann NY Acad Sci*, 747, 1-11. doi:10.1111/j.1749-6632.1994.tb44398.x
- Khan, G. M., Tong, M., Jhun, M., Arora, K., & Nichols, R. A. (2010). β -amyloid activates presynaptic $\alpha 7$ nicotinic acetylcholine receptors reconstituted into a model nerve cell system: involvement of lipid rafts. *Eur J Neurosci*, 31(5), 788-796. doi:10.1111/j.1460-9568.2010.07116.x
- Khatoon, S., Grundke-Iqbal, I., & Iqbal, K. (1992). Brain levels of microtubule-associated protein tau are elevated in Alzheimer's disease: a radioimmuno-

- slot-blot assay for nanograms of the protein. *J Neurochem*, 59(2), 750-753. doi:10.1111/j.1471-4159.1992.tb09432.x
- Khatoon, S., Grundke-Iqbal, I., & Iqbal, K. (1994). Levels of normal and abnormally phosphorylated tau in different cellular and regional compartments of Alzheimer disease and control brains. *FEBS Lett*, 351(1), 80-84. doi:10.1016/0014-5793(94)00829-9
- Kielian, T. (2008). Glial connexins and gap junctions in CNS inflammation and disease. *J Neurochem*, 106(3), 1000-1016. doi:10.1111/j.1471-4159.2008.05405.x
- Kierdorf, K., Erny, D., Goldmann, T., Sander, V., Schulz, C., Perdiguero, E. G., Wieghofer, P., Heinrich, A., Riemke, P., Hölscher, C., Müller, D. N., Luckow, B., Bocker, T., Debowski, K., Fritz, G., Opdenakker, G., Diefenbach, A., Biber, K., Heikenwalder, M., Geissmann, F., Rosenbauer, F., & Prinz, M. (2013). Microglia emerge from erythromyeloid precursors via Pu.1- and Irf8-dependent pathways. *Nat Neurosci*, 16(3), 273-280. doi:10.1038/nn.3318
- Kierdorf, K., & Prinz, M. (2017). Microglia in steady state. *J Clin Invest*, 127(9), 3201-3209. doi:10.1172/jci90602
- Kim, W. K., Kan, Y., Ganea, D., Hart, R. P., Gozes, I., & Jonakait, G. M. (2000). Vasoactive intestinal peptide and pituitary adenylyl cyclase-activating polypeptide inhibit tumor necrosis factor- α production in injured spinal cord and in activated microglia via a cAMP-dependent pathway. *J Neurosci*, 20(10), 3622-3630. doi:10.1523/jneurosci.20-10-03622.2000
- Kins, S., Lauther, N., Szodorai, A., & Beyreuther, K. (2006). Subcellular trafficking of the amyloid precursor protein gene family and its pathogenic role in Alzheimer's disease. *Neurodegener Dis*, 3(4-5), 218-226. doi:10.1159/000095259
- Kirkitadze, M. D., Condron, M. M., & Teplow, D. B. (2001). Identification and characterization of key kinetic intermediates in amyloid β -protein fibrillogenesis. *J Mol Biol*, 312(5), 1103-1119. doi:10.1006/jmbi.2001.4970
- Kirkley, K. S., Popichak, K. A., Afzali, M. F., Legare, M. E., & Tjalkens, R. B. (2017). Microglia amplify inflammatory activation of astrocytes in manganese neurotoxicity. *J Neuroinflammation*, 14(1), 99. doi:10.1186/s12974-017-0871-0
- Knight, R., Khondoker, M., Magill, N., Stewart, R., & Landau, S. (2018). A systematic review and meta-analysis of the effectiveness of acetylcholinesterase inhibitors and memantine in treating the cognitive symptoms of dementia. *Dement Geriatr Cogn Disord*, 45(3-4), 131-151. doi:10.1159/000486546
- Knopman, D. S., Parisi, J. E., Salviati, A., Floriach-Robert, M., Boeve, B. F., Ivnik, R. J., Smith, G. E., Dickson, D. W., Johnson, K. A., Petersen, L. E., McDonald, W. C., Braak, H., & Petersen, R. C. (2003). Neuropathology of cognitively normal elderly. *J Neuropathol Exp Neurol*, 62(11), 1087-1095.
- Knopman, D. S., & Roberts, R. (2010). Vascular risk factors: imaging and neuropathologic correlates. *J Alzheimers Dis*, 20(3), 699-709. doi:10.3233/jad-2010-091555
- Knopman, D. S., Jones, D. T., & Greicius, M. D. (2021). Failure to demonstrate efficacy of aducanumab: an analysis of the EMERGE and ENGAGE trials

- as reported by Biogen, December 2019. *Alzheimers Dement*, 17(4), 696-701. doi:10.1002/alz.12213
- Kollmer, M., Close, W., Funk, L., Rasmussen, J., Bsoul, A., Schierhorn, A., Schmidt, M., Sigurdson, C. J., Jucker, M., & Fändrich, M. (2019). Cryo-EM structure and polymorphism of A β amyloid fibrils purified from Alzheimer's brain tissue. *Nat Commun*, 10(1), 4760. doi:10.1038/s41467-019-12683-8
- Kono, H., & Rock, K. L. (2008). How dying cells alert the immune system to danger. *Nature Reviews Immunology*, 8, 279. doi:10.1038/nri2215
- Koo, E. H., Sisodia, S. S., Archer, D. R., Martin, L. J., Weidemann, A., Beyreuther, K., Fischer, P., Masters, C. L., & Price, D. L. (1990). Precursor of amyloid protein in Alzheimer disease undergoes fast anterograde axonal transport. *Proc Natl Acad Sci USA*, 87(4), 1561-1565. doi:10.1073/pnas.87.4.1561
- Korenbaum, E., Olski, T. M., & Noegel, A. A. (2001). Genomic organization and expression profile of the parvin family of focal adhesion proteins in mice and humans. *Gene*, 279(1), 69-79. doi:10.1016/s0378-1119(01)00743-0
- Kosik, K. S., Joachim, C. L., & Selkoe, D. J. (1986). Microtubule-associated protein tau (tau) is a major antigenic component of paired helical filaments in Alzheimer disease. *Proc Natl Acad Sci USA*, 83(11), 4044-4048. doi:10.1073/pnas.83.11.4044
- Koushik, S. V., Wang, J., Rogers, R., Moskophidis, D., Lambert, N. A., Creazzo, T. L., & Conway, S. J. (2001). Targeted inactivation of the sodium-calcium exchanger (Ncx1) results in the lack of a heartbeat and abnormal myofibrillar organization. *Faseb j*, 15(7), 1209-1211. doi:10.1096/fj.00-0696fje
- Kraft, A. D., McPherson, C. A., & Harry, G. J. (2016). Association between microglia, inflammatory factors, and complement with loss of hippocampal mossy fiber synapses induced by trimethyltin. *Neurotox Res*, 30(1), 53-66. doi:10.1007/s12640-016-9606-8
- Krasemann, S., Madore, C., Cialic, R., Baufeld, C., Calcagno, N., El Fatimy, R., Beckers, L., O'Loughlin, E., Xu, Y., Fanek, Z., Greco, D. J., Smith, S. T., Tweet, G., Humulock, Z., Zrzavy, T., Conde-Sanroman, P., Gacias, M., Weng, Z., Chen, H., Tjon, E., Mazaheri, F., Hartmann, K., Madi, A., Ulrich, J. D., Glatzel, M., Worthmann, A., Heeren, J., Budnik, B., Lemere, C., Ikezu, T., Heppner, F. L., Litvak, V., Holtzman, D. M., Lassmann, H., Weiner, H. L., Ochando, J., Haass, C., & Butovsky, O. (2017). The TREM2-APOE pathway drives the transcriptional phenotype of dysfunctional microglia in neurodegenerative diseases. *Immunity*, 47(3), 566-581.e569. doi:10.1016/j.immuni.2017.08.008
- Kreisel, T., Frank, M. G., Licht, T., Reshef, R., Ben-Menachem-Zidon, O., Baratta, M. V., Maier, S. F., & Yirmiya, R. (2014). Dynamic microglial alterations underlie stress-induced depressive-like behavior and suppressed neurogenesis. *Mol Psychiatry*, 19(6), 699-709. doi:10.1038/mp.2013.155
- Kuhn, S. A., van Landeghem, F. K., Zacharias, R., Färber, K., Rappert, A., Pavlovic, S., Hoffmann, A., Nolte, C., & Kettenmann, H. (2004). Microglia express GABA(B) receptors to modulate interleukin release. *Mol Cell Neurosci*, 25(2), 312-322. doi:10.1016/j.mcn.2003.10.023
- Kuller, L. H., & Lopez, O. L. (2021). ENGAGE and EMERGE: truth and consequences? *Alzheimers Dement*, 17(4), 692-695. doi:10.1002/alz.12286

- Kummer, M. P., Hermes, M., Delekarte, A., Hammerschmidt, T., Kumar, S., Terwel, D., Walter, J., Pape, H. C., König, S., Roeber, S., Jessen, F., Klockgether, T., Korte, M., & Heneka, M. T. (2011). Nitration of tyrosine 10 critically enhances amyloid β aggregation and plaque formation. *Neuron*, 71(5), 833-844. doi:10.1016/j.neuron.2011.07.001
- Kummer, M. P., & Heneka, M. T. (2014). Truncated and modified amyloid- β species. *Alzheimers Res Ther*, 6(3), 28. doi:10.1186/alzrt258
- Kunkle, B. W., Grenier-Boley, B., Sims, R., Bis, J. C., Damotte, V., Naj, A. C., Boland, A., Vronskaya, M., van der Lee, S. J., Amlie-Wolf, A., Bellenguez, C., Frizatti, A., Chouraki, V., Martin, E. R., Sleegers, K., Badarinarayan, N., Jakobsdottir, J., Hamilton-Nelson, K. L., Moreno-Grau, S., Olasso, R., Raybould, R., Chen, Y., Kuzma, A. B., Hiltunen, M., Morgan, T., Ahmad, S., Vardarajan, B. N., Epelbaum, J., Hoffmann, P., Boada, M., Beecham, G. W., Garnier, J. G., Harold, D., Fitzpatrick, A. L., Valladares, O., Moutet, M. L., Gerrish, A., Smith, A. V., Qu, L., Bacq, D., Denning, N., Jian, X., Zhao, Y., Del Zompo, M., Fox, N. C., Choi, S. H., Mateo, I., Hughes, J. T., Adams, H. H., Malamon, J., Sanchez-Garcia, F., Patel, Y., Brody, J. A., Dombroski, B. A., Naranjo, M. C. D., Daniilidou, M., Eiriksdottir, G., Mukherjee, S., Wallon, D., Uphill, J., Aspelund, T., Cantwell, L. B., Garzia, F., Galimberti, D., Hofer, E., Butkiewicz, M., Fin, B., Scarpini, E., Sarnowski, C., Bush, W. S., Meslage, S., Kornhuber, J., White, C. C., Song, Y., Barber, R. C., Engelborghs, S., Sordon, S., Voijnovic, D., Adams, P. M., Vandenberghe, R., Mayhaus, M., Cupples, L. A., Albert, M. S., De Deyn, P. P., Gu, W., Himali, J. J., Beekly, D., Squassina, A., Hartmann, A. M., Orellana, A., Blacker, D., Rodriguez-Rodriguez, E., Lovestone, S., Garcia, M. E., Doody, R. S., Munoz-Fernandez, C., Sussams, R., Lin, H., Fairchild, T. J., Benito, Y. A., Holmes, C., Karamujic-Comic, H., Frosch, M. P., Thonberg, H., Maier, W., Roshchupkin, G., Ghetti, B., Giedraitis, V., Kawalia, A., Li, S., Huebinger, R. M., Kilander, L., Moebus, S., Hernández, I., Kamboh, M. I., Brundin, R., Turton, J., Yang, Q., Katz, M. J., Concari, L., Lord, J., Beiser, A. S., Keene, C. D., Helisalmi, S., Kloszewska, I., Kukull, W. A., Koivisto, A. M., Lynch, A., Tarraga, L., Larson, E. B., Haapasalo, A., Lawlor, B., Mosley, T. H., Lipton, R. B., Solfrizzi, V., Gill, M., Longstreth, W. T., Jr., Montine, T. J., Frisardi, V., Diez-Fairen, M., Rivadeneira, F., Petersen, R. C., Deramecourt, V., Alvarez, I., Salani, F., Ciarrella, A., Boerwinkle, E., Reiman, E. M., Fievet, N., Rotter, J. I., Reisch, J. S., Hanon, O., Cupidi, C., Andre Uitterlinden, A. G., Royall, D. R., Dufouil, C., Maletta, R. G., de Rojas, I., Sano, M., Brice, A., Cecchetti, R., George-Hyslop, P. S., Ritchie, K., Tsolaki, M., Tsuang, D. W., Dubois, B., Craig, D., Wu, C. K., Soininen, H., Avramidou, D., Albin, R. L., Fratiglioni, L., Germanou, A., Apostolova, L. G., Keller, L., Koutroumani, M., Arnold, S. E., Panza, F., Gkatzima, O., Asthana, S., Hannequin, D., Whitehead, P., Atwood, C. S., Caffarra, P., Hampel, H., Quintela, I., Carracedo, Á., Lannfelt, L., Rubinsztein, D. C., Barnes, L. L., Pasquier, F., Frölich, L., Barral, S., McGuinness, B., Beach, T. G., Johnston, J. A., Becker, J. T., Passmore, P., Bigio, E. H., Schott, J. M., Bird, T. D., Warren, J. D., Boeve, B. F., Lupton, M. K., Bowen, J. D., Proitsi, P., Boxer, A., Powell, J. F., Burke, J. R., Kauwe, J. S. K., Burns, J. M., Mancuso, M., Buxbaum, J. D., Bonuccelli, U., Cairns, N. J., McQuillin, A., Cao, C., Livingston, G.,

Carlson, C. S., Bass, N. J., Carlsson, C. M., Hardy, J., Carney, R. M., Bras, J., Carrasquillo, M. M., Guerreiro, R., Allen, M., Chui, H. C., Fisher, E., Masullo, C., Crocco, E. A., DeCarli, C., Bisceglia, G., Dick, M., Ma, L., Duara, R., Graff-Radford, N. R., Evans, D. A., Hodges, A., Faber, K. M., Scherer, M., Fallon, K. B., Riemenschneider, M., Fardo, D. W., Heun, R., Farlow, M. R., Kölsch, H., Ferris, S., Leber, M., Foroud, T. M., Heuser, I., Galasko, D. R., Giegling, I., Gearing, M., Hüll, M., Geschwind, D. H., Gilbert, J. R., Morris, J., Green, R. C., Mayo, K., Growdon, J. H., Feulner, T., Hamilton, R. L., Harrell, L. E., Drichel, D., Honig, L. S., Cushion, T. D., Huentelman, M. J., Hollingworth, P., Hulette, C. M., Hyman, B. T., Marshall, R., Jarvik, G. P., Meggy, A., Abner, E., Menzies, G. E., Jin, L. W., Leonenko, G., Real, L. M., Jun, G. R., Baldwin, C. T., Grozeva, D., Karydas, A., Russo, G., Kaye, J. A., Kim, R., Jessen, F., Kowall, N. W., Vellas, B., Kramer, J. H., Vardy, E., LaFerla, F. M., Jöckel, K. H., Lah, J. J., Dichgans, M., Leverenz, J. B., Mann, D., Levey, A. I., Pickering-Brown, S., Lieberman, A. P., Klopp, N., Lunetta, K. L., Wichmann, H. E., Lyketsos, C. G., Morgan, K., Marson, D. C., Brown, K., Martiniuk, F., Medway, C., Mash, D. C., Nöthen, M. M., Masliah, E., Hooper, N. M., McCormick, W. C., Daniele, A., McCurry, S. M., Bayer, A., McDavid, A. N., Gallacher, J., McKee, A. C., van den Bussche, H., Mesulam, M., Brayne, C., Miller, B. L., Riedel-Heller, S., Miller, C. A., Miller, J. W., Al-Chalabi, A., Morris, J. C., Shaw, C. E., Myers, A. J., Wiltfang, J., O'Bryant, S., Olichney, J. M., Alvarez, V., Parisi, J. E., Singleton, A. B., Paulson, H. L., Collinge, J., Perry, W. R., Mead, S., Peskind, E., Cribbs, D. H., Rossor, M., Pierce, A., Ryan, N. S., Poon, W. W., Nacmias, B., Potter, H., Sorbi, S., Quinn, J. F., Sacchinelli, E., Raj, A., Spalletta, G., Raskind, M., Caltagirone, C., Bossù, P., Orfei, M. D., Reisberg, B., Clarke, R., Reitz, C., Smith, A. D., Ringman, J. M., Warden, D., Roberson, E. D., Wilcock, G., Rogaeva, E., Bruni, A. C., Rosen, H. J., Gallo, M., Rosenberg, R. N., Ben-Shlomo, Y., Sager, M. A., Mecocci, P., Saykin, A. J., Pastor, P., Cuccaro, M. L., Vance, J. M., Schneider, J. A., Schneider, L. S., Slifer, S., Seeley, W. W., Smith, A. G., Sonnen, J. A., Spina, S., Stern, R. A., Swerdlow, R. H., Tang, M., Tanzi, R. E., Trojanowski, J. Q., Troncoso, J. C., Van Deerlin, V. M., Van Eldik, L. J., Vinters, H. V., Vonsattel, J. P., Weintraub, S., Welsh-Bohmer, K. A., Wilhelmsen, K. C., Williamson, J., Wingo, T. S., Woltjer, R. L., Wright, C. B., Yu, C. E., Yu, L., Saba, Y., Pilotto, A., Bullido, M. J., Peters, O., Crane, P. K., Bennett, D., Bosco, P., Coto, E., Boccardi, V., De Jager, P. L., Lleo, A., Warner, N., Lopez, O. L., Ingelsson, M., Deloukas, P., Cruchaga, C., Graff, C., Gwilliam, R., Fornage, M., Goate, A. M., Sanchez-Juan, P., Kehoe, P. G., Amin, N., Ertekin-Taner, N., Berr, C., Dobbie, S., Love, S., Launer, L. J., Younkin, S. G., Dartigues, J. F., Corcoran, C., Ikram, M. A., Dickson, D. W., Nicolas, G., Campion, D., Tschanz, J., Schmidt, H., Hakonarson, H., Clarimon, J., Munger, R., Schmidt, R., Farrer, L. A., Van Broeckhoven, C., M, C. O. D., DeStefano, A. L., Jones, L., Haines, J. L., Deleuze, J. F., Owen, M. J., Gudnason, V., Mayeux, R., Escott-Price, V., Psaty, B. M., Ramirez, A., Wang, L. S., Ruiz, A., van Duijn, C. M., Holmans, P. A., Seshadri, S., Williams, J., Amouyel, P., Schellenberg, G. D., Lambert, J. C., & Pericak-Vance, M. A. (2019). Genetic meta-analysis of diagnosed Alzheimer's disease identifies

- new risk loci and implicates A β , tau, immunity and lipid processing. *Nat Genet*, 51(3), 414-430. doi:10.1038/s41588-019-0358-2
- Kuno, R., Wang, J., Kawanokuchi, J., Takeuchi, H., Mizuno, T., & Suzumura, A. (2005). Autocrine activation of microglia by tumor necrosis factor- α . *J Neuroimmunol*, 162(1-2), 89-96. doi:10.1016/j.jneuroim.2005.01.015
- Ladeby, R., Wirenfeldt, M., Garcia-Ovejero, D., Fenger, C., Dissing-Olesen, L., Dalmau, I., & Finsen, B. (2005). Microglial cell population dynamics in the injured adult central nervous system. *Brain Res Brain Res Rev*, 48(2), 196-206. doi:10.1016/j.brainresrev.2004.12.009
- Lalkens, B., Testa, I., Willig, K. I., & Hell, S. W. (2012). MRT letter: nanoscopy of protein colocalization in living cells by STED and GSDIM. *Microsc Res Tech*, 75(1), 1-6. doi:10.1002/jemt.21026
- Lambert, J.-C., Heath, S., Even, G., Campion, D., Sleegers, K., Hiltunen, M., Combarros, O., Zelenika, D., Bullido, M. J., Tavernier, B., Letenneur, L., Bettens, K., Berr, C., Pasquier, F., Fiévet, N., Barberger-Gateau, P., Engelborghs, S., De Deyn, P., Mateo, I., Franck, A., Helisalmi, S., Porcellini, E., Hanon, O., de Pancorbo, M. M., Lendon, C., Dufouil, C., Jaillard, C., Leveillard, T., Alvarez, V., Bosco, P., Mancuso, M., Panza, F., Nacmias, B., Bossù, P., Piccardi, P., Annoni, G., Seripa, D., Galimberti, D., Hannequin, D., Licastro, F., Soininen, H., Ritchie, K., Blanché, H., Dartigues, J. F., Tzourio, C., Gut, I., Van Broeckhoven, C., Alperovitch, A., Lathrop, M., & Amouyel, P. (2009). Genome-wide association study identifies variants at CLU and CR1 associated with Alzheimer's disease. *Nat Genet*, 41(10), 1094-1099. doi:10.1038/ng.439
- Lambert, J.-C., Ibrahim-Verbaas, C. A., Harold, D., Naj, A. C., Sims, R., Bellenguez, C., DeStafano, A. L., Bis, J. C., Beecham, G. W., Grenier-Boley, B., Russo, G., Thorton-Wells, T. A., Jones, N., Smith, A. V., Chouraki, V., Thomas, C., Ikram, M. A., Zelenika, D., Vardarajan, B. N., Kamatani, Y., Lin, C. F., Gerrish, A., Schmidt, H., Kunkle, B., Dunstan, M. L., Ruiz, A., Bihoreau, M. T., Choi, S. H., Reitz, C., Pasquier, F., Cruchaga, C., Craig, D., Amin, N., Berr, C., Lopez, O. L., De Jager, P. L., Deramecourt, V., Johnston, J. A., Evans, D., Lovestone, S., Letenneur, L., Morón, F. J., Rubinsztein, D. C., Eiriksdottir, G., Sleegers, K., Goate, A. M., Fiévet, N., Huentelman, M. W., Gill, M., Brown, K., Kamboh, M. I., Keller, L., Barberger-Gateau, P., McGuinness, B., Larson, E. B., Green, R., Myers, A. J., Dufouil, C., Todd, S., Wallon, D., Love, S., Rogaeva, E., Gallacher, J., St George-Hyslop, P., Clarimon, J., Lleo, A., Bayer, A., Tsuang, D. W., Yu, L., Tsolaki, M., Bossù, P., Spalletta, G., Proitsi, P., Collinge, J., Sorbi, S., Sanchez-Garcia, F., Fox, N. C., Hardy, J., Deniz Naranjo, M. C., Bosco, P., Clarke, R., Brayne, C., Galimberti, D., Mancuso, M., Matthews, F., Moebus, S., Mecocci, P., Del Zompo, M., Maier, W., Hampel, H., Pilotto, A., Bullido, M., Panza, F., Caffarra, P., Nacmias, B., Gilbert, J. R., Mayhaus, M., Lannefelt, L., Hakonarson, H., Pichler, S., Carrasquillo, M. M., Ingelsson, M., Beekly, D., Alvarez, V., Zou, F., Valladares, O., Younkin, S. G., Coto, E., Hamilton-Nelson, K. L., Gu, W., Razquin, C., Pastor, P., Mateo, I., Owen, M. J., Faber, K. M., Jonsson, P. V., Combarros, O., O'Donovan, M. C., Cantwell, L. B., Soininen, H., Blacker, D., Mead, S., Mosley, T. H., Jr., Bennett, D. A., Harris, T. B., Fratiglioni, L., Holmes, C., de Bruijn, R. F., Passmore, P., Montine, T. J., Bettens, K., Rotter, J. I., Brice, A., Morgan, K., Foroud, T.

- M., Kukull, W. A., Hannequin, D., Powell, J. F., Nalls, M. A., Ritchie, K., Lunetta, K. L., Kauwe, J. S., Boerwinkle, E., Riemenschneider, M., Boada, M., Hiltunen, M., Martin, E. R., Schmidt, R., Rujescu, D., Wang, L. S., Dartigues, J. F., Mayeux, R., Tzourio, C., Hofman, A., Nöthen, M. M., Graff, C., Psaty, B. M., Jones, L., Haines, J. L., Holmans, P. A., Lathrop, M., Pericak-Vance, M. A., Launer, L. J., Farrer, L. A., van Duijn, C. M., Van Broeckhoven, C., Moskvin, V., Seshadri, S., Williams, J., Schellenberg, G. D., & Amouyel, P. (2013). Meta-analysis of 74,046 individuals identifies 11 new susceptibility loci for Alzheimer's disease. *Nat Genet*, 45(12), 1452-1458. doi:10.1038/ng.2802
- Lamy, C., Duyckaerts, C., Delaere, P., Payan, C., Fermanian, J., Poulain, V., & Hauw, J. J. (1989). Comparison of seven staining methods for senile plaques and neurofibrillary tangles in a prospective series of 15 elderly patients. *Neuropathol Appl Neurobiol*, 15(6), 563-578. doi:10.1111/j.1365-2990.1989.tb01255.x
- Lane, C. A., Hardy, J., & Schott, J. M. (2018). Alzheimer's disease. *Eur J Neurol*, 25(1), 59-70. doi:10.1111/ene.13439
- Lanoiselée, H. M., Nicolas, G., Wallon, D., Rovelet-Lecrux, A., Lacour, M., Rousseau, S., Richard, A. C., Pasquier, F., Rollin-Sillaire, A., Martinaud, O., Quillard-Muraine, M., de la Sayette, V., Boutoleau-Bretonniere, C., Etcharry-Bouyx, F., Chauviré, V., Sarazin, M., le Ber, I., Epelbaum, S., Jonveaux, T., Rouaud, O., Ceccaldi, M., Félician, O., Godefroy, O., Formaglio, M., Croisile, B., Auriacombe, S., Chamard, L., Vincent, J. L., Sauvé, M., Marelli-Tosi, C., Gabelle, A., Oksa, C., Pariente, J., Paquet, C., Hannequin, D., & Campion, D. (2017). APP, PSEN1, and PSEN2 mutations in early-onset Alzheimer disease: A genetic screening study of familial and sporadic cases. *PLoS Med*, 14(3), e1002270. doi:10.1371/journal.pmed.1002270
- Larson, M. E., & Lesné, S. E. (2012). Soluble A β oligomer production and toxicity. *J Neurochem*, 120 Suppl 1(Suppl 1), 125-139. doi:10.1111/j.1471-4159.2011.07478.x
- Lasagna-Reeves, C. A., Castillo-Carranza, D. L., Sengupta, U., Sarmiento, J., Troncoso, J., Jackson, G. R., & Kaye, R. (2012). Identification of oligomers at early stages of tau aggregation in Alzheimer's disease. *FASEB J*, 26(5), 1946-1959. doi:10.1096/fj.11-199851
- Lauwers, E., Lalli, G., Brandner, S., Collinge, J., Compennolle, V., Duyckaerts, C., Edgren, G., Haïk, S., Hardy, J., Helmy, A., Iverson, A. J., Jaunmuktane, Z., Jucker, M., Knight, R., Lemmens, R., Lin, I. C., Love, S., Mead, S., Perry, V. H., Pickett, J., Poppy, G., Radford, S. E., Rousseau, F., Routledge, C., Schiavo, G., Schymkowitz, J., Selkoe, D. J., Smith, C., Thal, D. R., Theys, T., Tiberghien, P., van den Burg, P., Vandekerckhove, P., Walton, C., Zaijier, H. L., Zetterberg, H., & De Strooper, B. (2020). Potential human transmission of amyloid β pathology: surveillance and risks. *Lancet Neurol*, 19(10), 872-878. doi:10.1016/s1474-4422(20)30238-6
- Lavin, Y., Winter, D., Blecher-Gonen, R., David, E., Keren-Shaul, H., Merad, M., Jung, S., & Amit, I. (2014). Tissue-resident macrophage enhancer landscapes are shaped by the local microenvironment. *Cell*, 159(6), 1312-1326. doi:10.1016/j.cell.2014.11.018

- Lawson, L. J., Perry, V. H., Dri, P., & Gordon, S. (1990). Heterogeneity in the distribution and morphology of microglia in the normal adult mouse brain. *Neuroscience*, 39(1), 151-170. doi:10.1016/0306-4522(90)90229-w
- Lawson, L. J., Perry, V. H., & Gordon, S. (1992). Turnover of resident microglia in the normal adult mouse brain. *Neuroscience*, 48(2), 405-415. doi:10.1016/0306-4522(92)90500-2
- Leceta, J., Gomariz, R. P., Martinez, C., Carrión, M., Arranz, A., & Juarranz, Y. (2007). Vasoactive intestinal peptide regulates Th17 function in autoimmune inflammation. *Neuroimmunomodulation*, 14(3-4), 134-138. doi:10.1159/000110636
- Lee, H. G., Castellani, R. J., Zhu, X., Perry, G., & Smith, M. A. (2005). Amyloid- β in Alzheimer's disease: the horse or the cart? Pathogenic or protective? *Int J Exp Pathol*, 86(3), 133-138. doi:10.1111/j.0959-9673.2005.00429.x
- Lee, M. J., Lee, J. H., & Rubinsztein, D. C. (2013). Tau degradation: the ubiquitin-proteasome system versus the autophagy-lysosome system. *Prog Neurobiol*, 105, 49-59. doi:10.1016/j.pneurobio.2013.03.001
- Lee, Y. B., Nagai, A., & Kim, S. U. (2002). Cytokines, chemokines, and cytokine receptors in human microglia. *J Neurosci Res*, 69(1), 94-103. doi:10.1002/jnr.10253
- Lehmenkühler, A., Syková, E., Svoboda, J., Zilles, K., & Nicholson, C. (1993). Extracellular space parameters in the rat neocortex and subcortical white matter during postnatal development determined by diffusion analysis. *Neuroscience*, 55(2), 339-351. doi:10.1016/0306-4522(93)90503-8
- Lehnardt, S. (2010). Innate immunity and neuroinflammation in the CNS: the role of microglia in Toll-like receptor-mediated neuronal injury. *Glia*, 58(3), 253-263. doi:10.1002/glia.20928
- Leisching, G., Wiid, I., & Baker, B. (2017). The association of OASL and type I interferons in the pathogenesis and survival of intracellular replicating bacterial species. *Front Cell Infect Microbiol*, 7, 196. doi:10.3389/fcimb.2017.00196
- Leissring, M. A., Farris, W., Chang, A. Y., Walsh, D. M., Wu, X., Sun, X., Frosch, M. P., & Selkoe, D. J. (2003). Enhanced proteolysis of β -amyloid in APP transgenic mice prevents plaque formation, secondary pathology, and premature death. *Neuron*, 40(6), 1087-1093. doi:10.1016/s0896-6273(03)00787-6
- Lenz, K. M., Nugent, B. M., Haliyur, R., & McCarthy, M. M. (2013). Microglia are essential to masculinization of brain and behavior. *J Neurosci*, 33(7), 2761-2772. doi:10.1523/jneurosci.1268-12.2013
- Lenz, K. M., & Nelson, L. H. (2018). Microglia and beyond: innate immune cells As regulators of brain development and behavioral function. *Front Immunol*, 9, 698. doi:10.3389/fimmu.2018.00698
- Lesné, S., Koh, M. T., Kotilinek, L., Kaye, R., Glabe, C. G., Yang, A., Gallagher, M., & Ashe, K. H. (2006). A specific amyloid- β protein assembly in the brain impairs memory. *Nature*, 440(7082), 352-357. doi:10.1038/nature04533
- Levtova, N., Healy, L. M., Gonczi, C. M. C., Stopnicki, B., Blain, M., Kennedy, T. E., Moore, C. S., Antel, J. P., & Darlington, P. J. (2017). Comparative morphology and phagocytic capacity of primary human adult microglia with time-lapse imaging. *J Neuroimmunol*, 310, 143-149. doi:10.1016/j.jneuroim.2017.05.012

- Li, H., & Wang, R. (2017). A focus on CXCR4 in Alzheimer's disease. *Brain Circ*, 3(4), 199-203. doi:10.4103/bc.bc_13_17
- Li, Q., Cheng, Z., Zhou, L., Darmanis, S., Neff, N. F., Okamoto, J., Gulati, G., Bennett, M. L., Sun, L. O., Clarke, L. E., Marschallinger, J., Yu, G., Quake, S. R., Wyss-Coray, T., & Barres, B. A. (2019). Developmental heterogeneity of microglia and brain myeloid cells revealed by deep single-cell RNA sequencing. *Neuron*, 101(2), 207-223.e210. doi:10.1016/j.neuron.2018.12.006
- Li, Y., Du, X. F., Liu, C. S., Wen, Z. L., & Du, J. L. (2012). Reciprocal regulation between resting microglial dynamics and neuronal activity in vivo. *Dev Cell*, 23(6), 1189-1202. doi:10.1016/j.devcel.2012.10.027
- Liang, Y., Buckley, T. R., Tu, L., Langdon, S. D., & Tedder, T. F. (2001). Structural organization of the human MS4A gene cluster on chromosome 11q12. *Immunogenetics*, 53(5), 357-368. doi:10.1007/s002510100339
- Lichtenthaler, S. F., Haass, C., & Steiner, H. (2011). Regulated intramembrane proteolysis—lessons from amyloid precursor protein processing. *J Neurochem*, 117(5), 779-796. doi:10.1111/j.1471-4159.2011.07248.x
- Lim, A., Tsuang, D., Kukull, W., Nochlin, D., Leverenz, J., McCormick, W., Bowen, J., Teri, L., Thompson, J., Peskind, E. R., Raskind, M., & Larson, E. B. (1999). Clinico-neuropathological correlation of Alzheimer's disease in a community-based case series. *J Am Geriatr Soc*, 47(5), 564-569. doi:10.1111/j.1532-5415.1999.tb02571.x
- Ling, E. A., & Wong, W. C. (1993). The origin and nature of ramified and amoeboid microglia: a historical review and current concepts. *Glia*, 7(1), 9-18. doi:10.1002/glia.440070105
- Liu, J., Chang, L., Song, Y., Li, H., & Wu, Y. (2019b). The role of NMDA receptors in Alzheimer's disease. *Front Neurosci*, 13, 43. doi:10.3389/fnins.2019.00043
- Liu, K. Y., Schneider, L. S., & Howard, R. (2021). The need to show minimum clinically important differences in Alzheimer's disease trials. *Lancet Psychiatry*. doi:10.1016/s2215-0366(21)00197-8
- Liu, P.-P., Xie, Y., Meng, X. Y., & Kang, J. S. (2019a). History and progress of hypotheses and clinical trials for Alzheimer's disease. *Signal Transduct Target Ther*, 4, 29. doi:10.1038/s41392-019-0063-8
- Liu, Y., Shenouda, D., Bilfinger, T. V., Stefano, M. L., Magazine, H. I., & Stefano, G. B. (1996). Morphine stimulates nitric oxide release from invertebrate microglia. *Brain Res*, 722(1-2), 125-131. doi:10.1016/0006-8993(96)00204-1
- Livingston, G., Huntley, J., Sommerlad, A., Ames, D., Ballard, C., Banerjee, S., Brayne, C., Burns, A., Cohen-Mansfield, J., Cooper, C., Costafreda, S. G., Dias, A., Fox, N., Gitlin, L. N., Howard, R., Kales, H. C., Kivimäki, M., Larson, E. B., Ogunniyi, A., Orgeta, V., Ritchie, K., Rockwood, K., Sampson, E. L., Samus, Q., Schneider, L. S., Selbæk, G., Teri, L., & Mukadam, N. (2020). Dementia prevention, intervention, and care: 2020 report of the Lancet Commission. *Lancet*, 396(10248), 413-446. doi:10.1016/s0140-6736(20)30367-6
- Lorente-Gea, L., García, B., Martín, C., Quirós, L. M., & Fernández-Vega, I. (2017). Heparan sulfate proteoglycans and heparanases in Alzheimer's disease: current outlook and potential therapeutic targets. *Neural Regen Res*, 12(6), 914-915. doi:10.4103/1673-5374.208571

- Lossi, L., Alasia, S., Salio, C., & Merighi, A. (2009). Cell death and proliferation in acute slices and organotypic cultures of mammalian CNS. *Prog Neurobiol*, 88(4), 221-245. doi:10.1016/j.pneurobio.2009.01.002
- Lübbbers, J., Rodríguez, E., & van Kooyk, Y. (2018). Modulation of immune tolerance via siglec-sialic acid interactions. *Front Immunol*, 9, 2807. doi:10.3389/fimmu.2018.02807
- Lue, L. F., Brachova, L., Civin, W. H., & Rogers, J. (1996). Inflammation, A β deposition, and neurofibrillary tangle formation as correlates of Alzheimer's disease neurodegeneration. *J Neuropathol Exp Neurol*, 55(10), 1083-1088.
- Lue, L. F., Schmitz, C. T., Serrano, G., Sue, L. I., Beach, T. G., & Walker, D. G. (2015). TREM2 protein expression changes correlate with Alzheimer's disease neurodegenerative pathologies in post-mortem temporal cortices. *Brain Pathol*, 25(4), 469-480. doi:10.1111/bpa.12190
- Lyman, W. D., Tricoche, M., Hatch, W. C., Kress, Y., Chiu, F. C., & Rashbaum, W. K. (1991). Human fetal central nervous system organotypic cultures. *Brain Res Dev Brain Res*, 60(2), 155-160. doi:10.1016/0165-3806(91)90044-j
- Ma, B., Buckalew, R., Du, Y., Kiyoshi, C. M., Alford, C. C., Wang, W., McTigue, D. M., Enyeart, J. J., Terman, D., & Zhou, M. (2016). Gap junction coupling confers isopotentiality on astrocyte syncytium. *Glia*, 64(2), 214-226. doi:10.1002/glia.22924
- MacEwan, D. J. (2002). TNF ligands and receptors – a matter of life and death. *Br J Pharmacol*, 135(4), 855-875. doi:10.1038/sj.bjp.0704549
- Madry, C., & Attwell, D. (2015). Receptors, ion channels, and signaling mechanisms underlying microglial dynamics. *J Biol Chem*, 290(20), 12443-12450. doi:10.1074/jbc.R115.637157
- Maeda, S., Sahara, N., Saito, Y., Murayama, M., Yoshiike, Y., Kim, H., Miyasaka, T., Murayama, S., Ikai, A., & Takashima, A. (2007). Granular tau oligomers as intermediates of tau filaments. *Biochemistry*, 46(12), 3856-3861. doi:10.1021/bi061359o
- Mah, V. H., Eskin, T. A., Kazee, A. M., Lapham, L., & Higgins, G. A. (1992). In situ hybridization of calcium/calmodulin dependent protein kinase II and tau mRNAs; species differences and relative preservation in Alzheimer's disease. *Brain Res Mol Brain Res*, 12(1-3), 85-94. doi:10.1016/0169-328x(92)90071-i
- Majumder, S., Richardson, A., Strong, R., & Oddo, S. (2011). Inducing autophagy by rapamycin before, but not after, the formation of plaques and tangles ameliorates cognitive deficits. *PLoS One*, 6(9), e25416. doi:10.1371/journal.pone.0025416
- Makrides, V., Massie, M. R., Feinstein, S. C., & Lew, J. (2004). Evidence for two distinct binding sites for tau on microtubules. *Proc Natl Acad Sci USA*, 101(17), 6746-6751. doi:10.1073/pnas.0400992101
- Malouf, A. T. (1992). Effect of β amyloid peptides on neurons in hippocampal slice cultures. *Neurobiol Aging*, 13(5), 543-551. doi:10.1016/0197-4580(92)90054-2
- Maltsev, A. V., Bystryak, S., & Galzitskaya, O. V. (2011). The role of β -amyloid peptide in neurodegenerative diseases. *Ageing Res Rev*, 10(4), 440-452. doi:10.1016/j.arr.2011.03.002

- Mancino, R., Martucci, A., Cesareo, M., Giannini, C., Corasaniti, M. T., Bagetta, G., & Nucci, C. (2018). Glaucoma and Alzheimer disease: one age-related neurodegenerative disease of the brain. *Curr Neuroparmacol*, 16(7), 971-977. doi:10.2174/1570159x16666171206144045
- Mandelkow, E., von Bergen, M., Biernat, J., & Mandelkow, E. M. (2007). Structural principles of tau and the paired helical filaments of Alzheimer's disease. *Brain Pathol*, 17(1), 83-90. doi:10.1111/j.1750-3639.2007.00053.x
- Mandelkow, E. M., & Mandelkow, E. (2012). Biochemistry and cell biology of tau protein in neurofibrillary degeneration. *Cold Spring Harb Perspect Med*, 2(7), a006247. doi:10.1101/cshperspect.a006247
- Manolio, T. A., Collins, F. S., Cox, N. J., Goldstein, D. B., Hindorff, L. A., Hunter, D. J., McCarthy, M. I., Ramos, E. M., Cardon, L. R., Chakravarti, A., Cho, J. H., Guttmacher, A. E., Kong, A., Kruglyak, L., Mardis, E., Rotimi, C. N., Slatkin, M., Valle, D., Whittemore, A. S., Boehnke, M., Clark, A. G., Eichler, E. E., Gibson, G., Haines, J. L., Mackay, T. F., McCarroll, S. A., & Visscher, P. M. (2009). Finding the missing heritability of complex diseases. *Nature*, 461(7265), 747-753. doi:10.1038/nature08494
- Marshall, S. A., McClain, J. A., Wooden, J. I., & Nixon, K. (2020). Microglia dystrophy following binge-like alcohol exposure in adolescent and adult male rats. *Front Neuroanat*, 14, 52. doi:10.3389/fnana.2020.00052
- Martel, G., Dutar, P., Epelbaum, J., & Viollet, C. (2012). Somatostatinergic systems: an update on brain functions in normal and pathological aging. *Front Endocrinol (Lausanne)*, 3, 154. doi:10.3389/fendo.2012.00154
- Martin, F. C., Anton, P. A., Gornbein, J. A., Shanahan, F., & Merrill, J. E. (1993). Production of interleukin-1 by microglia in response to substance P: role for a non-classical NK-1 receptor. *J Neuroimmunol*, 42(1), 53-60. doi:10.1016/0165-5728(93)90212-h
- Masliah, E., Terry, R. D., DeTeresa, R. M., & Hansen, L. A. (1989). Immunohistochemical quantification of the synapse-related protein synaptophysin in Alzheimer disease. *Neurosci Lett*, 103(2), 234-239. doi:10.1016/0304-3940(89)90582-x
- Masliah, E., Hansen, L., Albright, T., Mallory, M., & Terry, R. D. (1991). Immunoelectron microscopic study of synaptic pathology in Alzheimer's disease. *Acta Neuropathol*, 81(4), 428-433. doi:10.1007/bf00293464
- Masliah, E., Mallory, M., Alford, M., DeTeresa, R., Hansen, L. A., McKeel, D. W., Jr., & Morris, J. C. (2001). Altered expression of synaptic proteins occurs early during progression of Alzheimer's disease. *Neurology*, 56(1), 127-129. doi:10.1212/wnl.56.1.127
- Mass, E., Jacome-Galarza, C. E., Blank, T., Lazarov, T., Durham, B. H., Ozkaya, N., Pastore, A., Schwabenland, M., Chung, Y. R., Rosenblum, M. K., Prinz, M., Abdel-Wahab, O., & Geissmann, F. (2017). A somatic mutation in erythro-myeloid progenitors causes neurodegenerative disease. *Nature*, 549(7672), 389-393. doi:10.1038/nature23672
- Masters, C. L., Simms, G., Weinman, N. A., Multhaup, G., McDonald, B. L., & Beyreuther, K. (1985). Amyloid plaque core protein in Alzheimer disease and Down syndrome. *Proc Natl Acad Sci USA*, 82(12), 4245-4249. doi:10.1073/pnas.82.12.4245

- Masters, C. L., & Selkoe, D. J. (2012). Biochemistry of amyloid β -protein and amyloid deposits in Alzheimer disease. *Cold Spring Harb Perspect Med*, 2(6), a006262. doi:10.1101/cshperspect.a006262
- Masuda, T., Sankowski, R., Staszewski, O., Böttcher, C., Amann, L., Sagar, Scheiwe, C., Nessler, S., Kunz, P., van Loo, G., Coenen, V. A., Reinacher, P. C., Michel, A., Sure, U., Gold, R., Grün, D., Priller, J., Stadelmann, C., & Prinz, M. (2019). Spatial and temporal heterogeneity of mouse and human microglia at single-cell resolution. *Nature*, 566(7744), 388-392. doi:10.1038/s41586-019-0924-x
- Matcovitch-Natan, O., Winter, D. R., Giladi, A., Vargas Aguilar, S., Spinrad, A., Sarrazin, S., Ben-Yehuda, H., David, E., Zelada González, F., Perrin, P., Keren-Shaul, H., Gury, M., Lara-Astaiso, D., Thaiss, C. A., Cohen, M., Bahar Halpern, K., Baruch, K., Deczkowska, A., Lorenzo-Vivas, E., Itzkovitz, S., Elinav, E., Sieweke, M. H., Schwartz, M., & Amit, I. (2016). Microglia development follows a stepwise program to regulate brain homeostasis. *Science*, 353(6301), aad8670. doi:10.1126/science.aad8670
- Mathys, H., Adaikkan, C., Gao, F., Young, J. Z., Manet, E., Hemberg, M., De Jager, P. L., Ransohoff, R. M., Regev, A., & Tsai, L. H. (2017). Temporal tracking of microglia activation in neurodegeneration at single-cell resolution. *Cell Rep*, 21(2), 366-380. doi:10.1016/j.celrep.2017.09.039
- Mathys, H., Davila-Velderrain, J., Peng, Z., Gao, F., Mohammadi, S., Young, J. Z., Menon, M., He, L., Abdurrob, F., Jiang, X., Martorell, A. J., Ransohoff, R. M., Hafler, B. P., Bennett, D. A., Kellis, M., & Tsai, L. H. (2019). Single-cell transcriptomic analysis of Alzheimer's disease. *Nature*, 570(7761), 332-337. doi:10.1038/s41586-019-1195-2
- Mattson, M. P. (2004). Pathways towards and away from Alzheimer's disease. *Nature*, 430(7000), 631-639. doi:10.1038/nature02621
- Mattsson-Carlsson, N., Andersson, E., Janelidze, S., Ossenkoppele, R., Insel, P., Strandberg, O., Zetterberg, H., Rosen, H. J., Rabinovici, G., Chai, X., Blennow, K., Dage, J. L., Stomrud, E., Smith, R., Palmqvist, S., & Hansson, O. (2020). A β deposition is associated with increases in soluble and phosphorylated tau that precede a positive tau PET in Alzheimer's disease. *Sci Adv*, 6(16), eaaz2387. doi:10.1126/sciadv.aaz2387
- Matzinger, P. (2007). Friendly and dangerous signals: is the tissue in control? *Nat Immunol*, 8(1), 11-13. doi:10.1038/ni0107-11
- Mawuenyega, K. G., Sigurdson, W., Ovod, V., Munsell, L., Kasten, T., Morris, J. C., Yarasheski, K. E., & Bateman, R. J. (2010). Decreased clearance of CNS β -amyloid in Alzheimer's disease. *Science*, 330(6012), 1774. doi:10.1126/science.1197623
- Mayeux, R., & Stern, Y. (2012). Epidemiology of Alzheimer disease. *Cold Spring Harb Perspect Med*, 2(8). doi:10.1101/cshperspect.a006239
- Mazaheri, F., Snaidero, N., Kleinberger, G., Madore, C., Daria, A., Werner, G., Krasemann, S., Capell, A., Trümbach, D., Wurst, W., Brunner, B., Bultmann, S., Tahirovic, S., Kerschensteiner, M., Misgeld, T., Butovsky, O., & Haass, C. (2017). TREM2 deficiency impairs chemotaxis and microglial responses to neuronal injury. *EMBO Rep*, 18(7), 1186-1198. doi:10.15252/embr.201743922
- Mc Donald, J. M., Savva, G. M., Brayne, C., Welzel, A. T., Forster, G., Shankar, G. M., Selkoe, D. J., Ince, P. G., & Walsh, D. M. (2010). The presence of sodium dodecyl sulphate-stable A β dimers is strongly associated with

- Alzheimer-type dementia. *Brain*, 133(Pt 5), 1328-1341.
doi:10.1093/brain/awq065
- McAleese, K. E., Colloby, S., Attems, J., Thomas, A., & Francis, P. T. (2020). Mixed brain pathologies account for most dementia in the Brains for Dementia Research cohort (abstract). *Neuropathol Appl Neurobiol*, 46(Suppl. 1), 24. doi:10.1111/nan.12605
- McCarthy, S., Das, S., Kretzschmar, W., Delaneau, O., Wood, A. R., Teumer, A., Kang, H. M., Fuchsberger, C., Danecek, P., Sharp, K., Luo, Y., Sidore, C., Kwong, A., Timpson, N., Koskinen, S., Vrieze, S., Scott, L. J., Zhang, H., Mahajan, A., Veldink, J., Peters, U., Pato, C., van Duijn, C. M., Gillies, C. E., Gandin, I., Mezzavilla, M., Gilly, A., Cocca, M., Traglia, M., Angius, A., Barrett, J. C., Boomsma, D., Branham, K., Breen, G., Brummett, C. M., Busonero, F., Campbell, H., Chan, A., Chen, S., Chew, E., Collins, F. S., Corbin, L. J., Smith, G. D., Dedoussis, G., Dorr, M., Farmaki, A. E., Ferrucci, L., Forer, L., Fraser, R. M., Gabriel, S., Levy, S., Groop, L., Harrison, T., Hattersley, A., Holmen, O. L., Hveem, K., Kretzler, M., Lee, J. C., McGue, M., Meitinger, T., Melzer, D., Min, J. L., Mohlke, K. L., Vincent, J. B., Nauck, M., Nickerson, D., Palotie, A., Pato, M., Pirastu, N., McInnis, M., Richards, J. B., Sala, C., Salomaa, V., Schlessinger, D., Schoenherr, S., Slagboom, P. E., Small, K., Spector, T., Stambolian, D., Tuke, M., Tuomilehto, J., Van den Berg, L. H., Van Rheenen, W., Volker, U., Wijmenga, C., Toniolo, D., Zeggini, E., Gasparini, P., Sampson, M. G., Wilson, J. F., Frayling, T., de Bakker, P. I., Swertz, M. A., McCarroll, S., Kooperberg, C., Dekker, A., Altshuler, D., Willer, C., Iacono, W., Ripatti, S., Soranzo, N., Walter, K., Swaroop, A., Cucca, F., Anderson, C. A., Myers, R. M., Boehnke, M., McCarthy, M. I., & Durbin, R. (2016). A reference panel of 64,976 haplotypes for genotype imputation. *Nat Genet*, 48(10), 1279-1283. doi:10.1038/ng.3643
- McGeer, P. L., Akiyama, H., Itagaki, S., & McGeer, E. G. (1989). Immune system response in Alzheimer's disease. *Can J Neurol Sci*, 16(4 Suppl), 516-527. doi:10.1017/s0317167100029863
- McGeer, P. L., Rogers, J., & McGeer, E. G. (2016). Inflammation, anti-inflammatory agents, and Alzheimer's disease: the last 22 years. *J Alzheimers Dis*, 54(3), 853-857. doi:10.3233/jad-160488
- McKee, A. C., Kosik, K. S., & Kowall, N. W. (1991). Neuritic pathology and dementia in Alzheimer's disease. *Ann Neurol*, 30(2), 156-165. doi:10.1002/ana.410300206
- McKhann, G. M., Drachman, D., Folstein, M., Katzman, R., Price, D., & Stadlan, E. M. (1984). Clinical diagnosis of Alzheimer's disease: report of the NINCDS-ADRDA Work Group under the auspices of Department of Health and Human Services Task Force on Alzheimer's Disease. *Neurology*, 34(7), 939-944. doi:10.1212/wnl.34.7.939
- McKhann, G. M., Knopman, D. S., Chertkow, H., Hyman, B. T., Jack, C. R., Jr., Kawas, C. H., Klunk, W. E., Koroshetz, W. J., Manly, J. J., Mayeux, R., Mohs, R. C., Morris, J. C., Rossor, M. N., Scheltens, P., Carrillo, M. C., Thies, B., Weintraub, S., & Phelps, C. H. (2011). The diagnosis of dementia due to Alzheimer's disease: recommendations from the National Institute on Aging-Alzheimer's Association workgroups on diagnostic guidelines for Alzheimer's disease. *Alzheimers Dement*, 7(3), 263-269. doi:10.1016/j.jalz.2011.03.005

- McLarnon, J. G., Xu, R., Lee, Y. B., & Kim, S. U. (1997). Ion channels of human microglia in culture. *Neuroscience*, 78(4), 1217-1228. doi:10.1016/s0306-4522(96)00680-x
- McLean, C. A., Cherny, R. A., Fraser, F. W., Fuller, S. J., Smith, M. J., Beyreuther, K., Bush, A. I., & Masters, C. L. (1999). Soluble pool of A β amyloid as a determinant of severity of neurodegeneration in Alzheimer's disease. *Ann Neurol*, 46(6), 860-866. doi:10.1002/1531-8249(199912)46:6<860::aid-ana8>3.0.co;2-m
- Meltzer, C. C., Smith, G., DeKosky, S. T., Pollock, B. G., Mathis, C. A., Moore, R. Y., Kupfer, D. J., & Reynolds, C. F., 3rd. (1998). Serotonin in aging, late-life depression, and Alzheimer's disease: the emerging role of functional imaging. *Neuropsychopharmacology*, 18(6), 407-430. doi:10.1016/s0893-133x(97)00194-2
- Mendez, M. F. (2017). Early-onset Alzheimer disease. *Neurol Clin*, 35(2), 263-281. doi:10.1016/j.ncl.2017.01.005
- Meng, Q., Lin, M. S., & Tzeng, I. S. (2020). Relationship between exercise and Alzheimer's disease: a narrative literature review. *Front Neurosci*, 14, 131. doi:10.3389/fnins.2020.00131
- Mentis, A. A., Dardiotis, E., & Chrousos, G. P. (2021). Apolipoprotein E4 and meningeal lymphatics in Alzheimer disease: a conceptual framework. *Mol Psychiatry*, 26(4), 1075-1097. doi:10.1038/s41380-020-0731-7
- Mildner, A., Schmidt, H., Nitsche, M., Merkler, D., Hanisch, U. K., Mack, M., Heikenwalder, M., Brück, W., Priller, J., & Prinz, M. (2007). Microglia in the adult brain arise from Ly-6ChiCCR2+ monocytes only under defined host conditions. *Nat Neurosci*, 10(12), 1544-1553. doi:10.1038/nn2015
- Miller, J. A., Horvath, S., & Geschwind, D. H. (2010). Divergence of human and mouse brain transcriptome highlights Alzheimer disease pathways. *Proc Natl Acad Sci USA*, 107(28), 12698-12703. doi:10.1073/pnas.0914257107
- Mills, J. D., Sheahan, P. J., Lai, D., Kril, J. J., Janitz, M., & Sutherland, G. T. (2014). The alternative splicing of the apolipoprotein E gene is unperturbed in the brains of Alzheimer's disease patients. *Mol Biol Rep*, 41(10), 6365-6376. doi:10.1007/s11033-014-3516-8
- Minett, T., Classey, J., Matthews, F. E., Fahrenhold, M., Taga, M., Brayne, C., Ince, P. G., Nicoll, J. A., & Boche, D. (2016). Microglial immunophenotype in dementia with Alzheimer's pathology. *J Neuroinflammation*, 13(1), 135. doi:10.1186/s12974-016-0601-z
- Mirra, S. S., Heyman, A., McKeel, D., Sumi, S. M., Crain, B. J., Brownlee, L. M., Vogel, F. S., Hughes, J. P., van Belle, G., & Berg, L. (1991). The Consortium to Establish a Registry for Alzheimer's Disease (CERAD); part II: standardization of the neuropathologic assessment of Alzheimer's disease. *Neurology*, 41(4), 479-486.
- Mitchell, R. J., Harvey, L. A., Brodaty, H., Draper, B., & Close, J. C. (2015). Dementia and intentional and unintentional poisoning in older people: a 10 year review of hospitalization records in New South Wales, Australia. *Int Psychogeriatr*, 27(11), 1757-1768. doi:10.1017/s1041610215001258
- Mitrasinovic, O. M., & Murphy, G. M., Jr. (2003). Microglial overexpression of the M-CSF receptor augments phagocytosis of opsonized A β . *Neurobiol Aging*, 24(6), 807-815. doi:10.1016/s0197-4580(02)00237-3

- Mittal, K., Mani, R. J., & Katare, D. P. (2016). Type 3 diabetes: cross talk between differentially regulated proteins of type 2 diabetes mellitus and Alzheimer's disease. *Sci Rep*, 6, 25589. doi:10.1038/srep25589
- Miyoshi, M., Miyano, K., Moriyama, N., Taniguchi, M., & Watanabe, T. (2008). Angiotensin type 1 receptor antagonist inhibits lipopolysaccharide-induced stimulation of rat microglial cells by suppressing nuclear factor κ B and activator protein-1 activation. *Eur J Neurosci*, 27(2), 343-351. doi:10.1111/j.1460-9568.2007.06014.x
- Mizoguchi, Y., Monji, A., Kato, T., Seki, Y., Gotoh, L., Horikawa, H., Suzuki, S. O., Iwaki, T., Yonaha, M., Hashioka, S., & Kanba, S. (2009). Brain-derived neurotrophic factor induces sustained elevation of intracellular Ca^{2+} in rodent microglia. *J Immunol*, 183(12), 7778-7786. doi:10.4049/jimmunol.0901326
- Mocanu, M. M., Nissen, A., Eckermann, K., Khlistunova, I., Biernat, J., Drexler, D., Petrova, O., Schönig, K., Bujard, H., Mandelkow, E., Zhou, L., Rune, G., & Mandelkow, E. M. (2008). The potential for β -structure in the repeat domain of tau protein determines aggregation, synaptic decay, neuronal loss, and coassembly with endogenous tau in inducible mouse models of tauopathy. *J Neurosci*, 28(3), 737-748. doi:10.1523/jneurosci.2824-07.2008
- Mochizuki, Y., Mizutani, T., Shimizu, T., & Kawata, A. (2011). Proportional neuronal loss between the primary motor and sensory cortex in amyotrophic lateral sclerosis. *Neurosci Lett*, 503(1), 73-75. doi:10.1016/j.neulet.2011.08.014
- Moir, R. D., Lathe, R., & Tanzi, R. E. (2018). The antimicrobial protection hypothesis of Alzheimer's disease. *Alzheimers Dement*, 14(12), 1602-1614. doi:10.1016/j.jalz.2018.06.3040
- Möller, T., Kann, O., Verkhratsky, A., & Kettenmann, H. (2000a). Activation of mouse microglial cells affects P2 receptor signaling. *Brain Res*, 853(1), 49-59. doi:10.1016/s0006-8993(99)02244-1
- Möller, T., Hanisch, U. K., & Ransom, B. R. (2000b). Thrombin-induced activation of cultured rodent microglia. *J Neurochem*, 75(4), 1539-1547. doi:10.1046/j.1471-4159.2000.0751539.x
- Mondragón-Rodríguez, S., Basurto-Islas, G., Lee, H. G., Perry, G., Zhu, X., Castellani, R. J., & Smith, M. A. (2010). Causes versus effects: the increasing complexities of Alzheimer's disease pathogenesis. *Expert Rev Neurother*, 10(5), 683-691. doi:10.1586/ern.10.27
- Monif, M., Reid, C. A., Powell, K. L., Drummond, K. J., O'Brien, T. J., & Williams, D. A. (2016). Interleukin-1 β has trophic effects in microglia and its release is mediated by P2X7R pore. *J Neuroinflammation*, 13(1), 173. doi:10.1186/s12974-016-0621-8
- Montine, T. J., Phelps, C. H., Beach, T. G., Bigio, E. H., Cairns, N. J., Dickson, D. W., Duyckaerts, C., Frosch, M. P., Masliah, E., Mirra, S. S., Nelson, P. T., Schneider, J. A., Thal, D. R., Trojanowski, J. Q., Vinters, H. V., & Hyman, B. T. (2012). National Institute on Aging-Alzheimer's Association guidelines for the neuropathologic assessment of Alzheimer's disease: a practical approach. *Acta Neuropathol*, 123(1), 1-11. doi:10.1007/s00401-011-0910-3
- Moreira, T. J., Pierre, K., Maekawa, F., Repond, C., Cebere, A., Liljequist, S., & Pellerin, L. (2009). Enhanced cerebral expression of MCT1 and MCT2 in

- a rat ischemia model occurs in activated microglial cells. *J Cereb Blood Flow Metab*, 29(7), 1273-1283. doi:10.1038/jcbfm.2009.50
- Moro, M. L., Phillips, A. S., Gaimster, K., Paul, C., Mudher, A., Nicoll, J. A. R., & Boche, D. (2018). Pyroglutamate and isoaspartate modified amyloid- β in ageing and Alzheimer's disease. *Acta Neuropathol Commun*, 6(1), 3. doi:10.1186/s40478-017-0505-x
- Morris, G. P., Clark, I. A., & Vissel, B. (2018). Questions concerning the role of amyloid- β in the definition, aetiology and diagnosis of Alzheimer's disease. *Acta Neuropathol*, 136(5), 663-689. doi:10.1007/s00401-018-1918-8
- Morrison, H. W., & Filosa, J. A. (2013). A quantitative spatiotemporal analysis of microglia morphology during ischemic stroke and reperfusion. *J Neuroinflammation*, 10, 4. doi:10.1186/1742-2094-10-4
- Morrison, J. H., Rogers, J., Scherr, S., Benoit, R., & Bloom, F. E. (1985). Somatostatin immunoreactivity in neuritic plaques of Alzheimer's patients. *Nature*, 314(6006), 90-92. doi:10.1038/314090a0
- Mostafavi, S., Gaiteri, C., Sullivan, S. E., White, C. C., Tasaki, S., Xu, J., Taga, M., Klein, H. U., Patrick, E., Komashko, V., McCabe, C., Smith, R., Bradshaw, E. M., Root, D. E., Regev, A., Yu, L., Chibnik, L. B., Schneider, J. A., Young-Pearse, T. L., Bennett, D. A., & De Jager, P. L. (2018). A molecular network of the aging human brain provides insights into the pathology and cognitive decline of Alzheimer's disease. *Nat Neurosci*, 21(6), 811-819. doi:10.1038/s41593-018-0154-9
- Mrdjen, D., Pavlovic, A., Hartmann, F. J., Schreiner, B., Utz, S. G., Leung, B. P., Lelios, I., Heppner, F. L., Kipnis, J., Merkler, D., Greter, M., & Becher, B. (2018). High-dimensional single-cell mapping of central nervous system immune cells reveals distinct myeloid subsets in health, aging, and disease. *Immunity*, 48(2), 380-395.e386. doi:10.1016/j.immuni.2018.01.011
- Muliyala, K. P., & Varghese, M. (2010). The complex relationship between depression and dementia. *Ann Indian Acad Neurol*, 13(Suppl 2), S69-73. doi:10.4103/0972-2327.74248
- Murray, M. E., Graff-Radford, N. R., Ross, O. A., Petersen, R. C., Duara, R., & Dickson, D. W. (2011). Neuropathologically defined subtypes of Alzheimer's disease with distinct clinical characteristics: a retrospective study. *Lancet Neurol*, 10(9), 785-796. doi:10.1016/s1474-4422(11)70156-9
- Murray, M. E., Cannon, A., Graff-Radford, N. R., Liesinger, A. M., Rutherford, N. J., Ross, O. A., Duara, R., Carrasquillo, M. M., Rademakers, R., & Dickson, D. W. (2014). Differential clinicopathologic and genetic features of late-onset amnesic dementias. *Acta Neuropathol*, 128(3), 411-421. doi:10.1007/s00401-014-1302-2
- Nagano, T., Kimura, S. H., Takai, E., Matsuda, T., & Takemura, M. (2006). Lipopolysaccharide sensitizes microglia toward Ca(2+)-induced cell death: mode of cell death shifts from apoptosis to necrosis. *Glia*, 53(1), 67-73. doi:10.1002/glia.20260
- Naj, A. C., Jun, G., Beecham, G. W., Wang, L. S., Vardarajan, B. N., Buross, J., Gallins, P. J., Buxbaum, J. D., Jarvik, G. P., Crane, P. K., Larson, E. B., Bird, T. D., Boeve, B. F., Graff-Radford, N. R., De Jager, P. L., Evans, D., Schneider, J. A., Carrasquillo, M. M., Ertekin-Taner, N., Younkin, S. G.,

- Cruchaga, C., Kauwe, J. S., Nowotny, P., Kramer, P., Hardy, J., Huentelman, M. J., Myers, A. J., Barmada, M. M., Demirci, F. Y., Baldwin, C. T., Green, R. C., Rogaeva, E., St George-Hyslop, P., Arnold, S. E., Barber, R., Beach, T., Bigio, E. H., Bowen, J. D., Boxer, A., Burke, J. R., Cairns, N. J., Carlson, C. S., Carney, R. M., Carroll, S. L., Chui, H. C., Clark, D. G., Corneveaux, J., Cotman, C. W., Cummings, J. L., DeCarli, C., DeKosky, S. T., Diaz-Arrastia, R., Dick, M., Dickson, D. W., Ellis, W. G., Faber, K. M., Fallon, K. B., Farlow, M. R., Ferris, S., Frosch, M. P., Galasko, D. R., Ganguli, M., Gearing, M., Geschwind, D. H., Ghetti, B., Gilbert, J. R., Gilman, S., Giordani, B., Glass, J. D., Growdon, J. H., Hamilton, R. L., Harrell, L. E., Head, E., Honig, L. S., Hulette, C. M., Hyman, B. T., Jicha, G. A., Jin, L. W., Johnson, N., Karlawish, J., Karydas, A., Kaye, J. A., Kim, R., Koo, E. H., Kowall, N. W., Lah, J. J., Levey, A. I., Lieberman, A. P., Lopez, O. L., Mack, W. J., Marson, D. C., Martiniuk, F., Mash, D. C., Masliah, E., McCormick, W. C., McCurry, S. M., McDavid, A. N., McKee, A. C., Mesulam, M., Miller, B. L., Miller, C. A., Miller, J. W., Parisi, J. E., Perl, D. P., Peskind, E., Petersen, R. C., Poon, W. W., Quinn, J. F., Rajbhandary, R. A., Raskind, M., Reisberg, B., Ringman, J. M., Roberson, E. D., Rosenberg, R. N., Sano, M., Schneider, L. S., Seeley, W., Shelanski, M. L., Slifer, M. A., Smith, C. D., Sonnen, J. A., Spina, S., Stern, R. A., Tanzi, R. E., Trojanowski, J. Q., Troncoso, J. C., Van Deerlin, V. M., Vinters, H. V., Vonsattel, J. P., Weintraub, S., Welsh-Bohmer, K. A., Williamson, J., Woltjer, R. L., Cantwell, L. B., Dombroski, B. A., Beekly, D., Lunetta, K. L., Martin, E. R., Kamboh, M. I., Saykin, A. J., Reiman, E. M., Bennett, D. A., Morris, J. C., Montine, T. J., Goate, A. M., Blacker, D., Tsuang, D. W., Hakonarson, H., Kukull, W. A., Foroud, T. M., Haines, J. L., Mayeux, R., Pericak-Vance, M. A., Farrer, L. A., & Schellenberg, G. D. (2011). Common variants at MS4A4/MS4A6E, CD2AP, CD33 and EPHA1 are associated with late-onset Alzheimer's disease. *Nat Genet*, 43(5), 436-441. doi:10.1038/ng.801
- Nakanishi, H., Ni, J., Nonaka, S., & Hayashi, Y. (2021). Microglial circadian clock regulation of microglial structural complexity, dendritic spine density and inflammatory response. *Neurochem Int*, 142, 104905. doi:10.1016/j.neuint.2020.104905
- Navarro, V., Sanchez-Mejias, E., Jimenez, S., Muñoz-Castro, C., Sanchez-Varo, R., Davila, J. C., Vizuete, M., Gutierrez, A., & Vitorica, J. (2018). Microglia in Alzheimer's disease: activated, dysfunctional or degenerative. *Front Aging Neurosci*, 10, 140. doi:10.3389/fnagi.2018.00140
- Nelis, S. M., Wu, Y. T., Matthews, F. E., Martyr, A., Quinn, C., Rippon, I., Rusted, J., Thom, J. M., Kopelman, M. D., Hindle, J. V., Jones, R. W., & Clare, L. (2019). The impact of co-morbidity on the quality of life of people with dementia: findings from the IDEAL study. *Age Ageing*, 48(3), 361-367. doi:10.1093/ageing/afy155
- Nelson, P. T., Jicha, G. A., Schmitt, F. A., Liu, H., Davis, D. G., Mendiondo, M. S., Abner, E. L., & Markesbery, W. R. (2007). Clinicopathologic correlations in a large Alzheimer disease center autopsy cohort: neuritic plaques and neurofibrillary tangles "do count" when staging disease severity. *J Neuropathol Exp Neurol*, 66(12), 1136-1146. doi:10.1097/nen.0b013e31815c5efb

- Nelson, P. T., Braak, H., & Markesbery, W. R. (2009a). Neuropathology and cognitive impairment in Alzheimer disease: a complex but coherent relationship. *J Neuropathol Exp Neurol*, 68(1), 1-14. doi:10.1097/NEN.0b013e3181919a48
- Nelson, P. T., Abner, E. L., Scheff, S. W., Schmitt, F. A., Kryscio, R. J., Jicha, G. A., Smith, C. D., Patel, E., & Markesbery, W. R. (2009b). Alzheimer's-type neuropathology in the precuneus is not increased relative to other areas of neocortex across a range of cognitive impairment. *Neurosci Lett*, 450(3), 336-339. doi:10.1016/j.neulet.2008.11.006
- Nelson, P. T., Head, E., Schmitt, F. A., Davis, P. R., Neltner, J. H., Jicha, G. A., Abner, E. L., Smith, C. D., Van Eldik, L. J., Kryscio, R. J., & Scheff, S. W. (2011). Alzheimer's disease is not "brain aging": neuropathological, genetic, and epidemiological human studies. *Acta Neuropathol*, 121(5), 571-587. doi:10.1007/s00401-011-0826-y
- Nelson, P. T., Alafuzoff, I., Bigio, E. H., Bouras, C., Braak, H., Cairns, N. J., Castellani, R. J., Crain, B. J., Davies, P., Tredici, K., Duyckaerts, C., Frosch, M. P., Haroutunian, V., Hof, P. R., Hulette, C. M., Hyman, B. T., Iwatsubo, T., Jellinger, K. A., Jicha, G. A., Kovari, E., Kukull, W. A., Leverenz, J. B., Love, S., Mackenzie, I. R., Mann, D. M., Masliah, E., McKee, A. C., Montine, T. J., Morris, J. C., Schneider, J. A., Sonnen, J. A., Thal, D. R., Trojanowski, J. Q., Troncoso, J. C., Wisniewski, T., Woltjer, R. L., & Beach, T. G. (2012). Correlation of Alzheimer disease neuropathologic changes with cognitive status: a review of the literature. *J Neuropathol Exp Neurol*, 71. doi:10.1097/NEN.0b013e31825018f7
- Neniskyte, U., Neher, J. J., & Brown, G. C. (2011). Neuronal death induced by nanomolar amyloid β is mediated by primary phagocytosis of neurons by microglia. *J Biol Chem*, 286(46), 39904-39913. doi:10.1074/jbc.M111.267583
- Nguyen, K. V. (2019). β -Amyloid precursor protein (APP) and the human diseases. *AIMS Neurosci*, 6(4), 273-281. doi:10.3934/Neuroscience.2019.4.273
- Nichols, E., Szoek, C. E. I., Vollset, S. E., Abbasi, N., Abd-Allah, F., Abdela, J., Aichour, M. T. E., Akinyemi, R. O., Alahdab, F., Asgedom, S. W., Awasthi, A., Barker-Collo, S. L., Baune, B. T., Béjot, Y., Belachew, A. B., Bennett, D. A., Biadgo, B., Bijani, A., Bin Sayeed, M. S., Brayne, C., Carpenter, D. O., Carvalho, F., Catalá-López, F., Cerin, E., Choi, J.-Y. J., Dang, A. K., Degefa, M. G., Djalalinia, S., Dubey, M., Duken, E. E., Edvardsson, D., Endres, M., Eskandarieh, S., Faro, A., Farzadfar, F., Fereshtehnejad, S.-M., Fernandes, E., Filip, I., Fischer, F., Gebre, A. K., Geremew, D., Ghasemi-Kasman, M., Gnedovskaya, E. V., Gupta, R., Hachinski, V., Hagos, T. B., Hamidi, S., Hankey, G. J., Haro, J. M., Hay, S. I., Irvani, S. S. N., Jha, R. P., Jonas, J. B., Kalani, R., Karch, A., Kasaeian, A., Khader, Y. S., Khalil, I. A., Khan, E. A., Khanna, T., Khoja, T. A. M., Khubchandani, J., Kisa, A., Kissimova-Skarbek, K., Kivimäki, M., Koyanagi, A., Krohn, K. J., Logroscino, G., Lorkowski, S., Majdan, M., Malekzadeh, R., März, W., Massano, J., Mengistu, G., Meretoja, A., Mohammadi, M., Mohammadi-Khanaposhtani, M., Mokdad, A. H., Mondello, S., Moradi, G., Nagel, G., Naghavi, M., Naik, G., Nguyen, L. H., Nguyen, T. H., Nirayo, Y. L., Nixon, M. R., Ofori-Asenso, R., Ogbo, F. A., Olagunju, A. T., Owolabi, M. O., Panda-Jonas, S., Passos, V. M. d.

- A., Pereira, D. M., Pinilla-Monsalve, G. D., Piradov, M. A., Pond, C. D., Poustchi, H., Qorbani, M., Radfar, A., Reiner, R. C., Jr., Robinson, S. R., Roshandel, G., Rostami, A., Russ, T. C., Sachdev, P. S., Safari, H., Safiri, S., Sahathevan, R., Salimi, Y., Satpathy, M., Sawhney, M., Saylan, M., Sepanlou, S. G., Shafieesabet, A., Shaikh, M. A., Sahraian, M. A., Shigematsu, M., Shiri, R., Shiue, I., Silva, J. P., Smith, M., Sobhani, S., Stein, D. J., Tabarés-Seisdedos, R., Tovani-Palone, M. R., Tran, B. X., Tran, T. T., Tsegay, A. T., Ullah, I., Venketasubramanian, N., Vlassov, V., Wang, Y.-P., Weiss, J., Westerman, R., Wijeratne, T., Wyper, G. M. A., Yano, Y., Yimer, E. M., Yonemoto, N., Yousefifard, M., Zaidi, Z., Zare, Z., Vos, T., Feigin, V. L., & Murray, C. J. L. (2019). Global, regional, and national burden of Alzheimer's disease and other dementias, 1990–2016: a systematic analysis for the Global Burden of Disease Study 2016. *Lancet Neurol*, 18(1), 88-106. doi:10.1016/S1474-4422(18)30403-4
- Nicotera, P., Petersen, O. H., Melino, G., & Verkhatsky, A. (2007). Janus a god with two faces: death and survival utilise same mechanisms conserved by evolution. *Cell Death Differ*, 14(7), 1235-1236. doi:10.1038/sj.cdd.4402161
- Nimmerjahn, A., Kirchhoff, F., & Helmchen, F. (2005). Resting microglial cells are highly dynamic surveillants of brain parenchyma in vivo. *Science*, 308(5726), 1314-1318. doi:10.1126/science.1110647
- Noble, W., Hanger, D. P., Miller, C. C., & Lovestone, S. (2013). The importance of tau phosphorylation for neurodegenerative diseases. *Front Neurol*, 4, 83. doi:10.3389/fneur.2013.00083
- Noda, M., Kariura, Y., Pannasch, U., Nishikawa, K., Wang, L., Seike, T., Ifuku, M., Kosai, Y., Wang, B., Nolte, C., Aoki, S., Kettenmann, H., & Wada, K. (2007). Neuroprotective role of bradykinin because of the attenuation of pro-inflammatory cytokine release from activated microglia. *J Neurochem*, 101(2), 397-410. doi:10.1111/j.1471-4159.2006.04339.x
- Nolte, C., Kirchhoff, F., & Kettenmann, H. (1997). Epidermal growth factor is a motility factor for microglial cells in vitro: evidence for EGF receptor expression. *Eur J Neurosci*, 9(8), 1690-1698. doi:10.1111/j.1460-9568.1997.tb01526.x
- Norden, D. M., Trojanowski, P. J., Villanueva, E., Navarro, E., & Godbout, J. P. (2016). Sequential activation of microglia and astrocyte cytokine expression precedes increased Iba-1 or GFAP immunoreactivity following systemic immune challenge. *Glia*, 64(2), 300-316. doi:10.1002/glia.22930
- Nordengen, K., Kirsebom, B. E., Henjum, K., Selnes, P., Gísladóttir, B., Wettergreen, M., Torsetnes, S. B., Grøntvedt, G. R., Waterloo, K. K., Aarsland, D., Nilsson, L. N. G., & Fladby, T. (2019). Glial activation and inflammation along the Alzheimer's disease continuum. *J Neuroinflammation*, 16(1), 46. doi:10.1186/s12974-019-1399-2
- Novotny, R., Langer, F., Mahler, J., Skodras, A., Vlachos, A., Wegenast-Braun, B. M., Kaeser, S. A., Neher, J. J., Eisele, Y. S., Pietrowski, M. J., Nilsson, K. P., Deller, T., Staufenbiel, M., Heimrich, B., & Jucker, M. (2016). Conversion of synthetic A β to in vivo active seeds and amyloid plaque formation in a hippocampal slice culture model. *J Neurosci*, 36(18), 5084-5093. doi:10.1523/jneurosci.0258-16.2016

- Nyhan, W. L. (2012). Lesch–Nyhan syndrome. In *eLS*. Chichester, United Kingdom: John Wiley & Sons.
doi:10.1002/9780470015902.a0001457.pub2
- Ogata, J., Budzilovich, G. N., & Cravioto, H. (1972). A study of rod-like structures (Hirano bodies) in 240 normal and pathological brains. *Acta Neuropathol*, 21(1), 61-67. doi:10.1007/bf00688000
- Ohgomori, T., Yamada, J., Takeuchi, H., Kadomatsu, K., & Jinno, S. (2016). Comparative morphometric analysis of microglia in the spinal cord of SOD1(G93A) transgenic mouse model of amyotrophic lateral sclerosis. *Eur J Neurosci*, 43(10), 1340-1351. doi:10.1111/ejn.13227
- Ohm, T. G., Müller, H., Braak, H., & Bohl, J. (1995). Close-meshed prevalence rates of different stages as a tool to uncover the rate of Alzheimer's disease-related neurofibrillary changes. *Neuroscience*, 64(1), 209-217. doi:10.1016/0306-4522(95)90397-p
- Ohsawa, K., Imai, Y., Kanazawa, H., Sasaki, Y., & Kohsaka, S. (2000). Involvement of Iba1 in membrane ruffling and phagocytosis of macrophages/microglia. *J Cell Sci*, 113 (Pt 17), 3073-3084.
- Ohsawa, K., Imai, Y., Sasaki, Y., & Kohsaka, S. (2004). Microglia/macrophage-specific protein Iba1 binds to fimbrin and enhances its actin-bundling activity. *J Neurochem*, 88(4), 844-856. doi:10.1046/j.1471-4159.2003.02213.x
- Oide, T., Kinoshita, T., & Arima, K. (2006). Regression stage senile plaques in the natural course of Alzheimer's disease. *Neuropathol Appl Neurobiol*, 32(5), 539-556. doi:10.1111/j.1365-2990.2006.00767.x
- Ono, K., Condrón, M. M., & Teplow, D. B. (2009). Structure-neurotoxicity relationships of amyloid β -protein oligomers. *Proc Natl Acad Sci USA*, 106(35), 14745-14750. doi:10.1073/pnas.0905127106
- Ooi, L., Dottori, M., Cook, A. L., Engel, M., Gautam, V., Grubman, A., Hernández, D., King, A. E., Maksour, S., Targa Dias Anastacio, H., Balez, R., Pébay, A., Pouton, C., Valenzuela, M., White, A., & Williamson, R. (2020). If human brain organoids are the answer to understanding dementia, what are the questions? *Neuroscientist*, 26(5-6), 438-454. doi:10.1177/1073858420912404
- Orkin, S. H., & Zon, L. I. (2008). Hematopoiesis: an evolving paradigm for stem cell biology. *Cell*, 132(4), 631-644. doi:10.1016/j.cell.2008.01.025
- Overk, C. R., & Masliah, E. (2014). Pathogenesis of synaptic degeneration in Alzheimer's disease and Lewy body disease. *Biochem Pharmacol*, 88(4), 508-516. doi:10.1016/j.bcp.2014.01.015
- Ownby, R. L., Crocco, E., Acevedo, A., John, V., & Loewenstein, D. (2006). Depression and risk for Alzheimer disease: systematic review, meta-analysis, and metaregression analysis. *Arch Gen Psychiatry*, 63(5), 530-538. doi:10.1001/archpsyc.63.5.530
- Paasila, P. J., Davies, D. S., Kril, J. J., Goldsberry, C., & Sutherland, G. T. (2019). The relationship between the morphological subtypes of microglia and Alzheimer's disease neuropathology. *Brain Pathol*. doi:10.1111/bpa.12717
- Paasila, P. J., Davies, D. S., Goldsberry, C., & Sutherland, G. T. (2020). Clustering of activated microglia occurs before the formation of dystrophic neurites in the evolution of A β plaques in Alzheimer's disease. *Free Neuropathol*. doi:10.17879/freeneuropathology-2020-2845

- Paasila, P. J., Fok, S. Y. Y., Flores-Rodriguez, N., Sajjan, S., Svahn, A. J., Dennis, C. V., Holsinger, R. M. D., Kril, J. J., Becker, T. S., Banati, R. B., Sutherland, G. T., & Graeber, M. B. (2021). Ground state depletion microscopy as a tool for studying microglia-synapse interactions. *J Neurosci Res*. doi:10.1002/jnr.24819
- Padovan, E., Landmann, R. M., & De Libero, G. (2007). How pattern recognition receptor triggering influences T cell responses: a new look into the system. *Trends Immunol*, 28(7), 308-314. doi:10.1016/j.it.2007.05.002
- Palm, N. W., & Medzhitov, R. (2009). Pattern recognition receptors and control of adaptive immunity. *Immunol Rev*, 227(1), 221-233. doi:10.1111/j.1600-065X.2008.00731.x
- Palmqvist, S., Janelidze, S., Quiroz, Y. T., Zetterberg, H., Lopera, F., Stomrud, E., Su, Y., Chen, Y., Serrano, G. E., Leuzy, A., Mattsson-Carlsson, N., Strandberg, O., Smith, R., Villegas, A., Sepulveda-Falla, D., Chai, X., Proctor, N. K., Beach, T. G., Blennow, K., Dage, J. L., Reiman, E. M., & Hansson, O. (2020). Discriminative accuracy of plasma phospho-tau217 for Alzheimer disease vs other neurodegenerative disorders. *Jama*, 324(8), 772-781. doi:10.1001/jama.2020.12134
- Panza, F., Lozupone, M., Logroscino, G., & Imbimbo, B. P. (2019). A critical appraisal of amyloid- β -targeting therapies for Alzheimer disease. *Nat Rev Neurol*, 15(2), 73-88. doi:10.1038/s41582-018-0116-6
- Paolicelli, R. C., Bolasco, G., Pagani, F., Maggi, L., Scianni, M., Panzanelli, P., Giustetto, M., Ferreira, T. A., Guiducci, E., Dumas, L., Ragozzino, D., & Gross, C. T. (2011). Synaptic pruning by microglia is necessary for normal brain development. *Science*, 333(6048), 1456-1458. doi:10.1126/science.1202529
- Parachikova, A., & Cotman, C. W. (2007). Reduced CXCL12/CXCR4 results in impaired learning and is downregulated in a mouse model of Alzheimer disease. *Neurobiol Dis*, 28(2), 143-153. doi:10.1016/j.nbd.2007.07.001
- Park, S. A., Han, S. M., & Kim, C. E. (2020). New fluid biomarkers tracking non-amyloid- β and non-tau pathology in Alzheimer's disease. *Exp Mol Med*, 52(4), 556-568. doi:10.1038/s12276-020-0418-9
- Parkhurst, C. N., Yang, G., Ninan, I., Savas, J. N., Yates, J. R., 3rd, Lafaille, J. J., Hempstead, B. L., Littman, D. R., & Gan, W. B. (2013). Microglia promote learning-dependent synapse formation through brain-derived neurotrophic factor. *Cell*, 155(7), 1596-1609. doi:10.1016/j.cell.2013.11.030
- Patapoutian, A., & Reichardt, L. F. (2001). Trk receptors: mediators of neurotrophin action. *Curr Opin Neurobiol*, 11(3), 272-280. doi:10.1016/s0959-4388(00)00208-7
- Payne, J., Maher, F., Simpson, I., Mattice, L., & Davies, P. (1997). Glucose transporter Glut 5 expression in microglial cells. *Glia*, 21(3), 327-331. doi:10.1002/(sici)1098-1136(199711)21:3<327::aid-glia7>3.0.co;2-1
- Peacock, M. L., Warren, J. T., Jr., Roses, A. D., & Fink, J. K. (1993). Novel polymorphism in the A4 region of the amyloid precursor protein gene in a patient without Alzheimer's disease. *Neurology*, 43(6), 1254-1256. doi:10.1212/wnl.43.6.1254
- Pei, J. J., Sjögren, M., & Winblad, B. (2008). Neurofibrillary degeneration in Alzheimer's disease: from molecular mechanisms to identification of drug

- targets. *Curr Opin Psychiatry*, 21(6), 555-561.
doi:10.1097/YCO.0b013e328314b78b
- Perez, S. E., Nadeem, M., He, B., Miguel, J. C., Malek-Ahmadi, M. H., Chen, K., & Mufson, E. J. (2017). Neocortical and hippocampal TREM2 protein levels during the progression of Alzheimer's disease. *Neurobiol Aging*, 54, 133-143. doi:10.1016/j.neurobiolaging.2017.02.012
- Perl, D. P. (2010). Neuropathology of Alzheimer's disease. *Mt Sinai J Med*, 77(1), 32-42. doi:10.1002/msj.20157
- Perlmuter, L. S., Barron, E., & Chui, H. C. (1990). Morphologic association between microglia and senile plaque amyloid in Alzheimer's disease. *Neurosci Lett*, 119(1), 32-36. doi:10.1016/0304-3940(90)90748-x
- Perrin, R. J., Fagan, A. M., & Holtzman, D. M. (2009). Multimodal techniques for diagnosis and prognosis of Alzheimer's disease. *Nature*, 461(7266), 916-922. doi:10.1038/nature08538
- Perry, V. H., Hume, D. A., & Gordon, S. (1985). Immunohistochemical localization of macrophages and microglia in the adult and developing mouse brain. *Neuroscience*, 15(2), 313-326. doi:10.1016/0306-4522(85)90215-5
- Perry, V. H. (2016). Microglia. *Microbiol Spectr*, 4(3). doi:10.1128/microbiolspec.MCHD-0003-2015
- Persson, M., Sandberg, M., Hansson, E., & Rönnbäck, L. (2006). Microglial glutamate uptake is coupled to glutathione synthesis and glutamate release. *Eur J Neurosci*, 24(4), 1063-1070. doi:10.1111/j.1460-9568.2006.04974.x
- Petersen, C., Nolan, A. L., de Paula Franca Resende, E., Miller, Z., Ehrenberg, A. J., Gorno-Tempini, M. L., Rosen, H. J., Kramer, J. H., Spina, S., Rabinovici, G. D., Miller, B. L., Seeley, W. W., Heinsen, H., & Grinberg, L. T. (2019). Alzheimer's disease clinical variants show distinct regional patterns of neurofibrillary tangle accumulation. *Acta Neuropathol*, 138(4), 597-612. doi:10.1007/s00401-019-02036-6
- Petersen, O. H., Michalak, M., & Verkhratsky, A. (2005). Calcium signalling: past, present and future. *Cell Calcium*, 38(3-4), 161-169. doi:10.1016/j.ceca.2005.06.023
- Petersson, S. D., & Philippou, E. (2016). Mediterranean diet, cognitive function, and dementia: a systematic review of the evidence. *Adv Nutr*, 7(5), 889-904. doi:10.3945/an.116.012138
- Pey, P., Pearce, R. K., Kalaitzakis, M. E., Griffin, W. S., & Gentleman, S. M. (2014). Phenotypic profile of alternative activation marker CD163 is different in Alzheimer's and Parkinson's disease. *Acta Neuropathol Commun*, 2, 21. doi:10.1186/2051-5960-2-21
- Pickett, J., Bird, C., Ballard, C., Banerjee, S., Brayne, C., Cowan, K., Clare, L., Comas-Herrera, A., Corner, L., Daley, S., Knapp, M., Lafortune, L., Livingston, G., Manthorpe, J., Marchant, N., Moriarty, J., Robinson, L., van Lynden, C., Windle, G., Woods, B., Gray, K., & Walton, C. (2018). A roadmap to advance dementia research in prevention, diagnosis, intervention, and care by 2025. *Int J Geriatr Psychiatry*, 33(7), 900-906. doi:10.1002/gps.4868
- Pierre, K., & Pellerin, L. (2005). Monocarboxylate transporters in the central nervous system: distribution, regulation and function. *J Neurochem*, 94(1), 1-14. doi:10.1111/j.1471-4159.2005.03168.x

- Piguet, O., Double, K. L., Kril, J. J., Harasty, J., Macdonald, V., McRitchie, D. A., & Halliday, G. M. (2009). White matter loss in healthy ageing: a postmortem analysis. *Neurobiol Aging*, 30(8), 1288-1295. doi:10.1016/j.neurobiolaging.2007.10.015
- Pimenova, A. A., Raj, T., & Goate, A. M. (2018). Untangling genetic risk for Alzheimer's disease. *Biol Psychiatry*, 83(4), 300-310. doi:10.1016/j.biopsych.2017.05.014
- Pintaux, E., Parker, L. C., Rothwell, N. J., & Luheshi, G. N. (2002). Expression of interleukin-1 receptors and their role in interleukin-1 actions in murine microglial cells. *J Neurochem*, 83(4), 754-763. doi:10.1046/j.1471-4159.2002.01184.x
- Podleśny-Drabiniok, A., Marcora, E., & Goate, A. M. (2020). Microglial phagocytosis: a disease-associated process emerging from Alzheimer's disease genetics. *Trends Neurosci*. doi:10.1016/j.tins.2020.10.002
- Poppek, D., Keck, S., Ermak, G., Jung, T., Stolzing, A., Ullrich, O., Davies, K. J., & Grune, T. (2006). Phosphorylation inhibits turnover of the tau protein by the proteasome: influence of RCAN1 and oxidative stress. *Biochem J*, 400(3), 511-520. doi:10.1042/bj20060463
- Prelli, F., Castaño, E., Glenner, G. G., & Frangione, B. (1988). Differences between vascular and plaque core amyloid in Alzheimer's disease. *J Neurochem*, 51(2), 648-651. doi:10.1111/j.1471-4159.1988.tb01087.x
- Price, J. L., McKeel, D. W., Jr., Buckles, V. D., Roe, C. M., Xiong, C., Grundman, M., Hansen, L. A., Petersen, R. C., Parisi, J. E., Dickson, D. W., Smith, C. D., Davis, D. G., Schmitt, F. A., Markesbery, W. R., Kaye, J., Kurlan, R., Hulette, C., Kurland, B. F., Higdon, R., Kukull, W., & Morris, J. C. (2009). Neuropathology of nondemented aging: presumptive evidence for preclinical Alzheimer disease. *Neurobiol Aging*, 30(7), 1026-1036. doi:10.1016/j.neurobiolaging.2009.04.002
- Prince, M., Ali, G. C., Guerchet, M., Prina, A. M., Albanese, E., & Wu, Y. T. (2016). Recent global trends in the prevalence and incidence of dementia, and survival with dementia. *Alzheimers Res Ther*, 8(1), 23. doi:10.1186/s13195-016-0188-8
- Prinz, M., & Priller, J. (2010). Tickets to the brain: role of CCR2 and CX3CR1 in myeloid cell entry in the CNS. *J Neuroimmunol*, 224(1-2), 80-84. doi:10.1016/j.jneuroim.2010.05.015
- Prinz, M., & Mildner, A. (2011). Microglia in the CNS: immigrants from another world. *Glia*, 59(2), 177-187. doi:10.1002/glia.21104
- Prinz, M., & Priller, J. (2014). Microglia and brain macrophages in the molecular age: from origin to neuropsychiatric disease. *Nat Rev Neurosci*, 15(5), 300-312. doi:10.1038/nrn3722
- Prinz, M., Tay, T. L., Wolf, Y., & Jung, S. (2014). Microglia: unique and common features with other tissue macrophages. *Acta Neuropathol*, 128(3), 319-331. doi:10.1007/s00401-014-1267-1
- Prinz, M., Jung, S., & Priller, J. (2019). Microglia biology: one century of evolving concepts. *Cell*, 179(2), 292-311. doi:10.1016/j.cell.2019.08.053
- Pritchard, S. M., Dolan, P. J., Vitkus, A., & Johnson, G. V. (2011). The toxicity of tau in Alzheimer disease: turnover, targets and potential therapeutics. *J Cell Mol Med*, 15(8), 1621-1635. doi:10.1111/j.1582-4934.2011.01273.x

- Prokop, S., Miller, K. R., & Heppner, F. L. (2013). Microglia actions in Alzheimer's disease. *Acta Neuropathol*, 126(4), 461-477. doi:10.1007/s00401-013-1182-x
- Puzzo, D., Gulisano, W., Arancio, O., & Palmeri, A. (2015). The keystone of Alzheimer pathogenesis might be sought in A β physiology. *Neuroscience*, 307, 26-36. doi:10.1016/j.neuroscience.2015.08.039
- Qin, S., Colin, C., Hinnens, I., Gervais, A., Cheret, C., & Mallat, M. (2006). System Xc⁻ and apolipoprotein E expressed by microglia have opposite effects on the neurotoxicity of amyloid- β peptide 1–40. *J Neurosci*, 26(12), 3345-3356. doi:10.1523/jneurosci.5186-05.2006
- Qiu, W. Y., Yang, Q., Zhang, W., Wang, N., Zhang, D., Huang, Y., & Ma, C. (2018). The correlations between postmortem brain pathologies and cognitive dysfunction in aging and Alzheimer's disease. *Curr Alzheimer Res*, 15(5), 462-473. doi:10.2174/1567205014666171106150915
- Qizilbash, N., Gregson, J., Johnson, M. E., Pearce, N., Douglas, I., Wing, K., Evans, S. J. W., & Pocock, S. J. (2015). BMI and risk of dementia in two million people over two decades: a retrospective cohort study. *Lancet Diabetes Endocrinol*, 3(6), 431-436. doi:10.1016/s2213-8587(15)00033-9
- Rabinovici, G. D., & Miller, B. L. (2010). Frontotemporal lobar degeneration: epidemiology, pathophysiology, diagnosis and management. *CNS Drugs*, 24(5), 375-398. doi:10.2165/11533100-000000000-00000
- Rahimi, J., & Kovacs, G. G. (2014). Prevalence of mixed pathologies in the aging brain. *Alzheimers Res Ther*, 6(9), 82. doi:10.1186/s13195-014-0082-1
- Raivich, G., Bohatschek, M., Kloss, C. U., Werner, A., Jones, L. L., & Kreutzberg, G. W. (1999). Neuroglial activation repertoire in the injured brain: graded response, molecular mechanisms and cues to physiological function. *Brain Res Brain Res Rev*, 30(1), 77-105. doi:10.1016/s0165-0173(99)00007-7
- Ramaekers, F. C., & Bosman, F. T. (2004). The cytoskeleton and disease. *J Pathol*, 204(4), 351-354. doi:10.1002/path.1665
- Rasley, A., Bost, K. L., Olson, J. K., Miller, S. D., & Marriott, I. (2002). Expression of functional NK-1 receptors in murine microglia. *Glia*, 37(3), 258-267. doi:10.1002/glia.10034
- Rasley, A., Marriott, I., Halberstadt, C. R., Bost, K. L., & Anguita, J. (2004). Substance P augments Borrelia burgdorferi-induced prostaglandin E2 production by murine microglia. *J Immunol*, 172(9), 5707-5713. doi:10.4049/jimmunol.172.9.5707
- Rasmussen, J., Jucker, M., & Walker, L. C. (2017). A β seeds and prions: How close the fit? *Prion*, 11(4), 215-225. doi:10.1080/19336896.2017.1334029
- Reddy, P. H., Mani, G., Park, B. S., Jacques, J., Murdoch, G., Whetsell, W., Jr., Kaye, J., & Manczak, M. (2005). Differential loss of synaptic proteins in Alzheimer's disease: implications for synaptic dysfunction. *J Alzheimers Dis*, 7(2), 103-117; discussion 173-180. doi:10.3233/jad-2005-7203
- Reeves, B. C., Karimy, J. K., Kundishora, A. J., Mestre, H., Cerci, H. M., Matouk, C., Alper, S. L., Lundgaard, I., Nedergaard, M., & Kahle, K. T. (2020). Glymphatic system impairment in Alzheimer's disease and idiopathic normal pressure hydrocephalus. *Trends Mol Med*, 26(3), 285-295. doi:10.1016/j.molmed.2019.11.008

- Rehwinkel, J., & Gack, M. U. (2020). RIG-I-like receptors: their regulation and roles in RNA sensing. *Nat Rev Immunol*, 20(9), 537-551. doi:10.1038/s41577-020-0288-3
- Reiman, E. M., Arboleda-Velasquez, J. F., Quiroz, Y. T., Huentelman, M. J., Beach, T. G., Caselli, R. J., Chen, Y., Su, Y., Myers, A. J., Hardy, J., Paul Vonsattel, J., Younkin, S. G., Bennett, D. A., De Jager, P. L., Larson, E. B., Crane, P. K., Keene, C. D., Kamboh, M. I., Kofler, J. K., Duque, L., Gilbert, J. R., Gwirtsman, H. E., Buxbaum, J. D., Dickson, D. W., Frosch, M. P., Ghetti, B. F., Lunetta, K. L., Wang, L. S., Hyman, B. T., Kukull, W. A., Foroud, T., Haines, J. L., Mayeux, R. P., Pericak-Vance, M. A., Schneider, J. A., Trojanowski, J. Q., Farrer, L. A., Schellenberg, G. D., Beecham, G. W., Montine, T. J., & Jun, G. R. (2020). Exceptionally low likelihood of Alzheimer's dementia in APOE2 homozygotes from a 5,000-person neuropathological study. *Nat Commun*, 11(1), 667. doi:10.1038/s41467-019-14279-8
- Reitz, C., & Mayeux, R. (2014). Alzheimer disease: epidemiology, diagnostic criteria, risk factors and biomarkers. *Biochem Pharmacol*, 88(4), 640-651. doi:10.1016/j.bcp.2013.12.024
- Réu, P., Khosravi, A., Bernard, S., Mold, J. E., Salehpour, M., Alkass, K., Perl, S., Tisdale, J., Possnert, G., Druid, H., & Frisén, J. (2017). The lifespan and turnover of microglia in the human brain. *Cell Rep*, 20(4), 779-784. doi:10.1016/j.celrep.2017.07.004
- Reyes-Ortega, P., Ragu Varman, D., Rodríguez, V. M., & Reyes-Haro, D. (2020). Anorexia induces a microglial associated pro-inflammatory environment and correlates with neurodegeneration in the prefrontal cortex of young female rats. *Behav Brain Res*, 392, 112606. doi:10.1016/j.bbr.2020.112606
- Rezaie, P., & Male, D. (2002). Mesoglia & microglia – a historical review of the concept of mononuclear phagocytes within the central nervous system. *J Hist Neurosci*, 11(4), 325-374. doi:10.1076/jhin.11.4.325.8531
- Richter, N., Wendt, S., Georgieva, P. B., Hambardzumyan, D., Nolte, C., & Kettenmann, H. (2014). Glioma-associated microglia and macrophages/monocytes display distinct electrophysiological properties and do not communicate via gap junctions. *Neurosci Lett*, 583, 130-135. doi:10.1016/j.neulet.2014.09.035
- Ridge, P. G., Hoyt, K. B., Boehme, K., Mukherjee, S., Crane, P. K., Haines, J. L., Mayeux, R., Farrer, L. A., Pericak-Vance, M. A., Schellenberg, G. D., & Kauwe, J. S. K. (2016). Assessment of the genetic variance of late-onset Alzheimer's disease. *Neurobiol Aging*, 41, 200.e213-200.e220. doi:10.1016/j.neurobiolaging.2016.02.024
- Río Hortega, P. d. (1919). El tercer elemento de los centros nerviosos. I. La microglia en estados normal. II. Intervencio de la microglia en los procesos patologicas. III. Naturaleza probable de la microglia. *Bol Soc Espanola Biol*, 9, 69-120.
- Río Hortega, P. d. (1939). The Microglia. *Lancet*, 233(6036), 1023-1026. doi:10.1016/S0140-6736(00)60571-8
- Rivara, C. B., Sherwood, C. C., Bouras, C., & Hof, P. R. (2003). Stereologic characterization and spatial distribution patterns of Betz cells in the human primary motor cortex. *Anat Rec A Discov Mol Cell Evol Biol*, 270(2), 137-151. doi:10.1002/ar.a.10015

- Rivest, S. (2009). Regulation of innate immune responses in the brain. *Nat Rev Immunol*, 9(6), 429-439. doi:10.1038/nri2565
- Roberts, G. W., Crow, T. J., & Polak, J. M. (1985). Location of neuronal tangles in somatostatin neurones in Alzheimer's disease. *Nature*, 314(6006), 92-94. doi:10.1038/314092a0
- Rodríguez García, P. L., & Rodríguez García, D. (2015). Diagnosis of vascular cognitive impairment and its main categories. *Neurologia*, 30(4), 223-239. doi:10.1016/j.nrl.2011.12.014
- Roehr, S., Pabst, A., Luck, T., & Riedel-Heller, S. G. (2018). Is dementia incidence declining in high-income countries? A systematic review and meta-analysis. *Clin Epidemiol*, 10, 1233-1247. doi:10.2147/clep.S163649
- Rogaev, E. I., Sherrington, R., Rogaeva, E. A., Levesque, G., Ikeda, M., Liang, Y., Chi, H., Lin, C., Holman, K., Tsuda, T., Mar, L., Sorbi, S., Nacmias, B., Pacentini, S., Amaducci, L., Chumakov, I., Cohen, D., Lannfelt, L., Fraser, P. E., Rommens, J. M., & St George-Hyslop, P. H. (1995). Familial Alzheimer's disease in kindreds with missense mutations in a gene on chromosome 1 related to the Alzheimer's disease type 3 gene. *Nature*, 376(6543), 775-778. doi:10.1038/376775a0
- Rogovskii, V. (2020). Immune tolerance as the physiologic counterpart of chronic inflammation. *Front Immunol*, 11, 2061. doi:10.3389/fimmu.2020.02061
- Rosness, T. A., Strand, B. H., Bergem, A. L., Nafstad, P., Langballe, E. M., Engedal, K., Tambs, K., & Bjertness, E. (2016). Association of psychological distress late in life and dementia-related mortality. *Aging Ment Health*, 20(6), 603-610. doi:10.1080/13607863.2015.1031639
- Rothenberg, M. E., Doepker, M. P., Lewkowich, I. P., Chiaramonte, M. G., Stringer, K. F., Finkelman, F. D., MacLeod, C. L., Ellies, L. G., & Zimmermann, N. (2006). Cationic amino acid transporter 2 regulates inflammatory homeostasis in the lung. *Proc Natl Acad Sci USA*, 103(40), 14895-14900. doi:10.1073/pnas.0605478103
- Rowe, R. K., Harrison, J. L., Morrison, H. W., Subbian, V., Murphy, S. M., & Lifshitz, J. (2019). Acute post-traumatic sleep may define vulnerability to a second traumatic brain injury in mice. *J Neurotrauma*, 36(8), 1318-1334. doi:10.1089/neu.2018.5980
- Rowson, S. A., Harrell, C. S., Bekhbat, M., Gangavelli, A., Wu, M. J., Kelly, S. D., Reddy, R., & Neigh, G. N. (2016). Neuroinflammation and behavior in HIV-1 transgenic rats exposed to chronic adolescent stress. *Front Psychiatry*, 7, 102. doi:10.3389/fpsy.2016.00102
- Russell-Williams, J., Jaroudi, W., Perich, T., Hoscheidt, S., El Haj, M., & Moustafa, A. A. (2018). Mindfulness and meditation: treating cognitive impairment and reducing stress in dementia. *Rev Neurosci*, 29(7), 791-804. doi:10.1515/revneuro-2017-0066
- Saido, T., & Leissring, M. A. (2012). Proteolytic degradation of amyloid β -protein. *Cold Spring Harb Perspect Med*, 2(6), a006379. doi:10.1101/cshperspect.a006379
- Saito, T., Suemoto, T., Brouwers, N., Sleegers, K., Funamoto, S., Mihira, N., Matsuba, Y., Yamada, K., Nilsson, P., Takano, J., Nishimura, M., Iwata, N., Van Broeckhoven, C., Ihara, Y., & Saido, T. C. (2011). Potent amyloidogenicity and pathogenicity of A β 43. *Nat Neurosci*, 14(8), 1023-1032. doi:10.1038/nn.2858

- Sala Frigerio, C., Wolfs, L., Fattorelli, N., Thrupp, N., Voytyuk, I., Schmidt, I., Mancuso, R., Chen, W. T., Woodbury, M. E., Srivastava, G., Möller, T., Hudry, E., Das, S., Saido, T., Karran, E., Hyman, B., Perry, V. H., Fiers, M., & De Strooper, B. (2019). The major risk factors for Alzheimer's disease: age, sex, and genes modulate the microglia response to A β plaques. *Cell Rep*, 27(4), 1293-1306.e1296. doi:10.1016/j.celrep.2019.03.099
- Salamanca, L., Mechawar, N., Murai, K. K., Balling, R., Bouvier, D. S., & Skupin, A. (2019). MIC-MAC: an automated pipeline for high-throughput characterization and classification of three-dimensional microglia morphologies in mouse and human postmortem brain samples. *Glia*, 67(8), 1496-1509. doi:10.1002/glia.23623
- Salloway, S. P., Sevingy, J., Budur, K., Pederson, J. T., DeMattos, R. B., Von Rosenstiel, P., Paez, A., Evans, R., Weber, C. J., Hendrix, J. A., Worley, S., Bain, L. J., & Carrillo, M. C. (2020). Advancing combination therapy for Alzheimer's disease. *Alzheimers Dement (NY)*, 6(1), e12073. doi:10.1002/trc2.12073
- Salminen, A., Ojala, J., Kauppinen, A., Kaarniranta, K., & Suuronen, T. (2009). Inflammation in Alzheimer's disease: amyloid- β oligomers trigger innate immunity defence via pattern recognition receptors. *Prog Neurobiol*, 87(3), 181-194.
- Sanchez-Mejias, E., Navarro, V., Jimenez, S., Sanchez-Mico, M., Sanchez-Varo, R., Nunez-Diaz, C., Trujillo-Estrada, L., Davila, J. C., Vizuet, M., Gutierrez, A., & Vitorica, J. (2016). Soluble phospho-tau from Alzheimer's disease hippocampus drives microglial degeneration. *Acta Neuropathol*, 132(6), 897-916. doi:10.1007/s00401-016-1630-5
- Sankowski, R., Böttcher, C., Masuda, T., Geirsdottir, L., Sagar, Sindram, E., Seredenina, T., Muhs, A., Scheiwe, C., Shah, M. J., Heiland, D. H., Schnell, O., Grün, D., Priller, J., & Prinz, M. (2019). Mapping microglia states in the human brain through the integration of high-dimensional techniques. *Nat Neurosci*, 22(12), 2098-2110. doi:10.1038/s41593-019-0532-y
- Sanyal, R., Polyak, M. J., Zuccolo, J., Puri, M., Deng, L., Roberts, L., Zuba, A., Storek, J., Luider, J. M., Sundberg, E. M., Mansoor, A., Baigorri, E., Chu, M. P., Belch, A. R., Pilarski, L. M., & Deans, J. P. (2017). MS4A4A: a novel cell surface marker for M2 macrophages and plasma cells. *Immunol Cell Biol*, 95(7), 611-619. doi:10.1038/icb.2017.18
- Sasaki, A., Yamaguchi, H., Ogawa, A., Sugihara, S., & Nakazato, Y. (1997). Microglial activation in early stages of amyloid β protein deposition. *Acta Neuropathol*, 94(4), 316-322.
- Sasaki, Y., Ohsawa, K., Kanazawa, H., Kohsaka, S., & Imai, Y. (2001). Iba1 is an actin-cross-linking protein in macrophages/microglia. *Biochem Biophys Res Commun*, 286(2), 292-297. doi:10.1006/bbrc.2001.5388
- Satoh, J., Kino, Y., Asahina, N., Takitani, M., Miyoshi, J., Ishida, T., & Saito, Y. (2016). TMEM119 marks a subset of microglia in the human brain. *Neuropathology*, 36(1), 39-49. doi:10.1111/neup.12235
- Savage, J. C., Picard, K., González-Ibáñez, F., & Tremblay, M.-È. (2018). A brief history of microglial ultrastructure: distinctive features, phenotypes, and functions discovered over the past 60 years by electron microscopy. *Front Immunol*, 9, 803. doi:10.3389/fimmu.2018.00803

- Savage, J. C., Carrier, M., & Tremblay, M.-È. (2019). Morphology of microglia across contexts of health and disease. *Methods Mol Biol*, 2034, 13-26. doi:10.1007/978-1-4939-9658-2_2
- Sawada, M., Suzumura, A., & Marunouchi, T. (1995). Induction of functional interleukin-2 receptor in mouse microglia. *J Neurochem*, 64(5), 1973-1979. doi:10.1046/j.1471-4159.1995.64051973.x
- Sawada, M., Suzumura, A., Hosoya, H., Marunouchi, T., & Nagatsu, T. (1999). Interleukin-10 inhibits both production of cytokines and expression of cytokine receptors in microglia. *J Neurochem*, 72(4), 1466-1471. doi:10.1046/j.1471-4159.1999.721466.x
- Scandol, J. P., Toson, B., & Close, J. C. (2013). Fall-related hip fracture hospitalisations and the prevalence of dementia within older people in New South Wales, Australia: an analysis of linked data. *Injury*, 44(6), 776-783. doi:10.1016/j.injury.2012.11.023
- Schaeffer, V., Lavenir, I., Ozelik, S., Tolnay, M., Winkler, D. T., & Goedert, M. (2012). Stimulation of autophagy reduces neurodegeneration in a mouse model of human tauopathy. *Brain*, 135(Pt 7), 2169-2177. doi:10.1093/brain/aws143
- Schaffert, L. N., & Carter, W. G. (2020). Do post-translational modifications influence protein aggregation in neurodegenerative diseases: a systematic review. *Brain Sci*, 10(4). doi:10.3390/brainsci10040232
- Scheff, S. W., DeKosky, S. T., & Price, D. A. (1990). Quantitative assessment of cortical synaptic density in Alzheimer's disease. *Neurobiol Aging*, 11(1), 29-37.
- Scheff, S. W., Sparks, L., & Price, D. A. (1993). Quantitative assessment of synaptic density in the entorhinal cortex in Alzheimer's disease. *Ann Neurol*, 34(3), 356-361. doi:10.1002/ana.410340309
- Scheff, S. W., & Price, D. A. (1993). Synapse loss in the temporal lobe in Alzheimer's disease. *Ann Neurol*, 33(2), 190-199. doi:10.1002/ana.410330209
- Scheff, S. W., Price, D. A., & Sparks, D. L. (2001). Quantitative assessment of possible age-related change in synaptic numbers in the human frontal cortex. *Neurobiol Aging*, 22(3), 355-365. doi:10.1016/s0197-4580(01)00222-6
- Scheff, S. W., & Price, D. A. (2006). Alzheimer's disease-related alterations in synaptic density: neocortex and hippocampus. *J Alzheimers Dis*, 9(3 Suppl), 101-115. doi:10.3233/jad-2006-9s312
- Scheff, S. W., Price, D. A., Schmitt, F. A., & Mufson, E. J. (2006). Hippocampal synaptic loss in early Alzheimer's disease and mild cognitive impairment. *Neurobiol Aging*, 27(10), 1372-1384. doi:10.1016/j.neurobiolaging.2005.09.012
- Scheff, S. W., Price, D. A., Schmitt, F. A., DeKosky, S. T., & Mufson, E. J. (2007). Synaptic alterations in CA1 in mild Alzheimer disease and mild cognitive impairment. *Neurology*, 68(18), 1501-1508. doi:10.1212/01.wnl.0000260698.46517.8f
- Scheff, S. W., Neltner, J. H., & Nelson, P. T. (2014). Is synaptic loss a unique hallmark of Alzheimer's disease? *Biochem Pharmacol*, 88(4), 517-528. doi:10.1016/j.bcp.2013.12.028
- Scheffer, S., Hermkens, D. M. A., van der Weerd, L., de Vries, H. E., & Daemen, M. (2021). Vascular hypothesis of Alzheimer disease: topical review of

- mouse models. *Arterioscler Thromb Vasc Biol*, 41(4), 1265-1283.
doi:10.1161/atvbaha.120.311911
- Schneider, J. A., Arvanitakis, Z., Bang, W., & Bennett, D. A. (2007). Mixed brain pathologies account for most dementia cases in community-dwelling older persons. *Neurology*, 69(24), 2197-2204.
doi:10.1212/01.wnl.0000271090.28148.24
- Schoggins, J. W. (2019). Interferon-stimulated genes: what do they all do? *Annu Rev Virol*, 6(1), 567-584. doi:10.1146/annurev-virology-092818-015756
- Schöll, M., Lockhart, S. N., Schonhaut, D. R., O'Neil, J. P., Janabi, M., Ossenkoppele, R., Baker, S. L., Vogel, J. W., Faria, J., Schwimmer, H. D., Rabinovici, G. D., & Jagust, W. J. (2016). PET imaging of tau deposition in the aging human brain. *Neuron*, 89(5), 971-982.
doi:10.1016/j.neuron.2016.01.028
- Schulz, C., Gomez Perdiguero, E., Chorro, L., Szabo-Rogers, H., Cagnard, N., Kierdorf, K., Prinz, M., Wu, B., Jacobsen, S. E., Pollard, J. W., Frampton, J., Liu, K. J., & Geissmann, F. (2012). A lineage of myeloid cells independent of Myb and hematopoietic stem cells. *Science*, 336(6077), 86-90. doi:10.1126/science.1219179
- Schwabe, T., Srinivasan, K., & Rhinn, H. (2020). Shifting paradigms: the central role of microglia in Alzheimer's disease. *Neurobiol Dis*, 143, 104962.
doi:10.1016/j.nbd.2020.104962
- Schwarz, A. J., Yu, P., Miller, B. B., Shcherbinin, S., Dickson, J., Navitsky, M., Joshi, A. D., Devous, M. D., Sr., & Mintun, M. S. (2016). Regional profiles of the candidate tau PET ligand 18F-AV-1451 recapitulate key features of Braak histopathological stages. *Brain*, 139(Pt 5), 1539-1550.
doi:10.1093/brain/aww023
- Schwarz, N., Uysal, B., Welzer, M., Bahr, J. C., Layer, N., Löffler, H., Stanaitis, K., Pa, H., Weber, Y. G., Hedrich, U. B., Honegger, J. B., Skodras, A., Becker, A. J., Wuttke, T. V., & Koch, H. (2019). Long-term adult human brain slice cultures as a model system to study human CNS circuitry and disease. *Elife*, 8. doi:10.7554/eLife.48417
- Schweers, O., Schönbrunn-Hanebeck, E., Marx, A., & Mandelkow, E. (1994). Structural studies of tau protein and Alzheimer paired helical filaments show no evidence for β -structure. *J Biol Chem*, 269(39), 24290-24297.
- Seaks, C. E., & Wilcock, D. M. (2020). Infectious hypothesis of Alzheimer disease. *PLoS Pathog*, 16(11), e1008596.
doi:10.1371/journal.ppat.1008596
- Sebastiani, P., Gurinovich, A., Nygaard, M., Sasaki, T., Sweigart, B., Bae, H., Andersen, S. L., Villa, F., Atzmon, G., Christensen, K., Arai, Y., Barzilai, N., Puca, A., Christiansen, L., Hirose, N., & Perls, T. T. (2019). APOE alleles and extreme human longevity. *J Gerontol A Biol Sci Med Sci*, 74(1), 44-51. doi:10.1093/gerona/gly174
- Séguéla, P., Wadiche, J., Dineley-Miller, K., Dani, J. A., & Patrick, J. W. (1993). Molecular cloning, functional properties, and distribution of rat brain $\alpha 7$: a nicotinic cation channel highly permeable to calcium. *J Neurosci*, 13(2), 596-604. doi:10.1523/jneurosci.13-02-00596.1993
- Selkoe, D. J., Abraham, C. R., Podlisny, M. B., & Duffy, L. K. (1986). Isolation of low-molecular-weight proteins from amyloid plaque fibers in Alzheimer's disease. *J Neurochem*, 46(6), 1820-1834. doi:10.1111/j.1471-4159.1986.tb08501.x

- Selkoe, D. J. (1991). The molecular pathology of Alzheimer's disease. *Neuron*, 6(4), 487-498. doi:10.1016/0896-6273(91)90052-2
- Selkoe, D. J., & Hardy, J. (2016). The amyloid hypothesis of Alzheimer's disease at 25 years. *EMBO Mol Med*, 8(6), 595-608. doi:10.15252/emmm.201606210
- Selkoe, D. J. (2019). Alzheimer disease and aducanumab: adjusting our approach. *Nat Rev Neurol*, 15(7), 365-366. doi:10.1038/s41582-019-0205-1
- Sengoku, R. (2020). Aging and Alzheimer's disease pathology. *Neuropathology*, 40(1), 22-29. doi:10.1111/neup.12626
- Serrano-Pozo, A., Frosch, M. P., Masliah, E., & Hyman, B. T. (2011a). Neuropathological alterations in Alzheimer disease. *Cold Spring Harb Perspect Med*, 1(1). doi:10.1101/cshperspect.a006189
- Serrano-Pozo, A., Mielke, M. L., Gomez-Isla, T., Betensky, R. A., Growdon, J. H., Frosch, M. P., & Hyman, B. T. (2011b). Reactive glia not only associates with plaques but also parallels tangles in Alzheimer's disease. *Am J Pathol*, 179(3), 1373-1384. doi:10.1016/j.ajpath.2011.05.047
- Serrano-Pozo, A., Gómez-Isla, T., Growdon, J. H., Frosch, M. P., & Hyman, B. T. (2013). A phenotypic change but not proliferation underlies glial responses in Alzheimer disease. *Am J Pathol*, 182(6), 2332-2344. doi:10.1016/j.ajpath.2013.02.031
- Serrano-Pozo, A., Das, S., & Hyman, B. T. (2021). APOE and Alzheimer's disease: advances in genetics, pathophysiology, and therapeutic approaches. *Lancet Neurol*, 20(1), 68-80. doi:10.1016/s1474-4422(20)30412-9
- Serrats, J., Schiltz, J. C., García-Bueno, B., van Rooijen, N., Reyes, T. M., & Sawchenko, P. E. (2010). Dual roles for perivascular macrophages in immune-to-brain signaling. *Neuron*, 65(1), 94-106. doi:10.1016/j.neuron.2009.11.032
- Seyfried, N. T., Dammer, E. B., Swarup, V., Nandakumar, D., Duong, D. M., Yin, L., Deng, Q., Nguyen, T., Hales, C. M., Wingo, T., Glass, J., Gearing, M., Thambisetty, M., Troncoso, J. C., Geschwind, D. H., Lah, J. J., & Levey, A. I. (2017). A multi-network approach identifies protein-specific co-expression in asymptomatic and symptomatic Alzheimer's disease. *Cell Syst*, 4(1), 60-72.e64. doi:10.1016/j.cels.2016.11.006
- Shankar, G. M., Li, S., Mehta, T. H., Garcia-Munoz, A., Shepardson, N. E., Smith, I., Brett, F. M., Farrell, M. A., Rowan, M. J., Lemere, C. A., Regan, C. M., Walsh, D. M., Sabatini, B. L., & Selkoe, D. J. (2008). Amyloid- β protein dimers isolated directly from Alzheimer's brains impair synaptic plasticity and memory. *Nat Med*, 14(8), 837-842. doi:10.1038/nm1782
- Sharp, E. S., & Gatz, M. (2011). Relationship between education and dementia: an updated systematic review. *Alzheimer Dis Assoc Disord*, 25(4), 289-304. doi:10.1097/WAD.0b013e318211c83c
- Shemer, A., Erny, D., Jung, S., & Prinz, M. (2015). Microglia plasticity during health and disease: an immunological perspective. *Trends Immunol*, 36(10), 614-624. doi:10.1016/j.it.2015.08.003
- Sheng, J. G., Mrak, R. E., & Griffin, W. S. (1997). Neuritic plaque evolution in Alzheimer's disease is accompanied by transition of activated microglia from primed to enlarged to phagocytic forms. *Acta Neuropathol*, 94(1), 1-5.

- Shi, Y. B., Tu, T., Jiang, J., Zhang, Q. L., Ai, J. Q., Pan, A., Manavis, J., Tu, E., & Yan, X. X. (2020). Early dendritic dystrophy in human brains with primary age-related tauopathy. *Front Aging Neurosci*, 12, 596894. doi:10.3389/fnagi.2020.596894
- Shim, Y. S., & Morris, J. C. (2011). Biomarkers predicting Alzheimer's disease in cognitively normal aging. *J Clin Neurol*, 7(2), 60-68. doi:10.3988/jcn.2011.7.2.60
- Shimada, K., Motoi, Y., Ishiguro, K., Kambe, T., Matsumoto, S. E., Itaya, M., Kunichika, M., Mori, H., Shinohara, A., Chiba, M., Mizuno, Y., Ueno, T., & Hattori, N. (2012). Long-term oral lithium treatment attenuates motor disturbance in tauopathy model mice: implications of autophagy promotion. *Neurobiol Dis*, 46(1), 101-108. doi:10.1016/j.nbd.2011.12.050
- Shirihai, O., Smith, P., Hammar, K., & Dagan, D. (1998). Microglia generate external proton and potassium ion gradients utilizing a member of the H/K ATPase family. *Glia*, 23(4), 339-348.
- Shytle, R. D., Mori, T., Townsend, K., Vendrame, M., Sun, N., Zeng, J., Ehrhart, J., Silver, A. A., Sanberg, P. R., & Tan, J. (2004). Cholinergic modulation of microglial activation by $\alpha 7$ nicotinic receptors. *J Neurochem*, 89(2), 337-343. doi:10.1046/j.1471-4159.2004.02347.x
- Sierra, A., Encinas, J. M., Deudero, J. J., Chancey, J. H., Enikolopov, G., Overstreet-Wadiche, L. S., Tsirka, S. E., & Maletic-Savatic, M. (2010). Microglia shape adult hippocampal neurogenesis through apoptosis-coupled phagocytosis. *Cell Stem Cell*, 7(4), 483-495. doi:10.1016/j.stem.2010.08.014
- Sierra, A., Abiega, O., Shahraz, A., & Neumann, H. (2013). Janus-faced microglia: beneficial and detrimental consequences of microglial phagocytosis. *Front Cell Neurosci*, 7, 6. doi:10.3389/fncel.2013.00006
- Sigrist, S. J., & Sabatini, B. L. (2012). Optical super-resolution microscopy in neurobiology. *Curr Opin Neurobiol*, 22(1), 86-93. doi:10.1016/j.conb.2011.10.014
- Simchowicz, T. (1911). *Histologische Studien über die senile Demenz*. In *Histologische und histopathologische Arbeiten über die Grosshirnrinde mit besonderer Berücksichtigung der pathologischen Anatomie der Geisteskrankheiten Vol. 4* (A. Alzheimer & F. A. Nissl Eds.). Jena, Germany: Fischer Verlag.
- Simic, G., Stanic, G., Mladinov, M., Jovanov-Milosevic, N., Kostovic, I., & Hof, P. R. (2009). Does Alzheimer's disease begin in the brainstem? *Neuropathol Appl Neurobiol*, 35(6), 532-554. doi:10.1111/j.1365-2990.2009.01038.x
- Sindi, S., Kåreholt, I., Johansson, L., Skoog, J., Sjöberg, L., Wang, H.-X., Johansson, B., Fratiglioni, L., Soininen, H., Solomon, A., Skoog, I., & Kivipelto, M. (2018). Sleep disturbances and dementia risk: a multicenter study. *Alzheimers Dement*, 14(10), 1235-1242. doi:10.1016/j.jalz.2018.05.012
- Sisodia, S. S., Koo, E. H., Beyreuther, K., Unterbeck, A., & Price, D. L. (1990). Evidence that β -amyloid protein in Alzheimer's disease is not derived by normal processing. *Science*, 248(4954), 492-495. doi:10.1126/science.1691865
- Sisodia, S. S., Koo, E. H., Hoffman, P. N., Perry, G., & Price, D. L. (1993). Identification and transport of full-length amyloid precursor proteins in rat

- peripheral nervous system. *J Neurosci*, 13(7), 3136-3142.
doi:10.1523/jneurosci.13-07-03136.1993
- Sjogren, T., Sjogren, H., & Lindgren, A. G. (1952). Morbus Alzheimer and morbus Pick; a genetic, clinical and patho-anatomical study. *Acta Psychiatr Neurol Scand Suppl*, 82, 1-152.
- Skogen, J. C., Bergh, S., Stewart, R., Knudsen, A. K., & Bjerkeset, O. (2015). Midlife mental distress and risk for dementia up to 27 years later: the Nord-Trøndelag Health Study (HUNT) in linkage with a dementia registry in Norway. *BMC Geriatr*, 15, 23. doi:10.1186/s12877-015-0020-5
- Small, S. A., & Duff, K. (2008). Linking A β and tau in late-onset Alzheimer's disease: a dual pathway hypothesis. *Neuron*, 60(4), 534-542.
doi:10.1016/j.neuron.2008.11.007
- Snow, A. D., Sekiguchi, R. T., Nochlin, D., Kalaria, R. N., & Kimata, K. (1994). Heparan sulfate proteoglycan in diffuse plaques of hippocampus but not of cerebellum in Alzheimer's disease brain. *Am J Pathol*, 144(2), 337-347.
- Sobue, A., Komine, O., Hara, Y., Endo, F., Mizoguchi, H., Watanabe, S., Murayama, S., Saito, T., Saido, T. C., Sahara, N., Higuchi, M., Ogi, T., & Yamanaka, K. (2021). Microglial gene signature reveals loss of homeostatic microglia associated with neurodegeneration of Alzheimer's disease. *Acta Neuropathol Commun*, 9(1), 1. doi:10.1186/s40478-020-01099-x
- Sochocka, M., Zwolińska, K., & Leszek, J. (2017). The infectious etiology of Alzheimer's disease. *Curr Neuropharmacol*, 15(7), 996-1009.
doi:10.2174/1570159x15666170313122937
- Soltys, Z., Ziaja, M., Pawliński, R., Setkowicz, Z., & Janeczko, K. (2001). Morphology of reactive microglia in the injured cerebral cortex: fractal analysis and complementary quantitative methods. *J Neurosci Res*, 63(1), 90-97. doi:10.1002/1097-4547(20010101)63:1<90::Aid-jnr11>3.0.Co;2-9
- Song, L., Lee, C., & Schindler, C. (2011). Deletion of the murine scavenger receptor CD68. *J Lipid Res*, 52(8), 1542-1550. doi:10.1194/jlr.M015412
- Sousa, C., Golebiewska, A., Poovathingal, S. K., Kaoma, T., Pires-Afonso, Y., Martina, S., Coowar, D., Azuaje, F., Skupin, A., Balling, R., Biber, K., Niclou, S. P., & Michelucci, A. (2018). Single-cell transcriptomics reveals distinct inflammation-induced microglia signatures. *EMBO Rep*, 19(11). doi:10.15252/embr.201846171
- Spears, W., Furgerson, M., Sweetnam, J. M., Evans, P., Gearing, M., Fechtmeier, M., & Furukawa, R. (2014). Hirano bodies differentially modulate cell death induced by tau and the amyloid precursor protein intracellular domain. *BMC Neurosci*, 15, 74. doi:10.1186/1471-2202-15-74
- Sperling, R. A., Aisen, P. S., Beckett, L. A., Bennett, D. A., Craft, S., Fagan, A. M., Iwatsubo, T., Jack, C. R., Jr., Kaye, J., Montine, T. J., Park, D. C., Reiman, E. M., Rowe, C. C., Siemers, E., Stern, Y., Yaffe, K., Carrillo, M. C., Thies, B., Morrison-Bogorad, M., Wagster, M. V., & Phelps, C. H. (2011). Toward defining the preclinical stages of Alzheimer's disease: recommendations from the National Institute on Aging-Alzheimer's Association workgroups on diagnostic guidelines for Alzheimer's disease. *Alzheimers Dement*, 7(3), 280-292. doi:10.1016/j.jalz.2011.03.003
- Spinello, A., Bonsignore, R., Barone, G., Keppler, B. K., & Terenzi, A. (2016). Metal ions and metal complexes in Alzheimer's disease. *Curr Pharm Des*, 22(26), 3996-4010. doi:10.2174/1381612822666160520115248

- Staal, J. A., Alexander, S. R., Liu, Y., Dickson, T. D., & Vickers, J. C. (2011). Characterization of cortical neuronal and glial alterations during culture of organotypic whole brain slices from neonatal and mature mice. *PLoS One*, 6(7), e22040. doi:10.1371/journal.pone.0022040
- Starkstein, S. E., Mizrahi, R., & Power, B. D. (2008). Depression in Alzheimer's disease: phenomenology, clinical correlates and treatment. *Int Rev Psychiatry*, 20(4), 382-388. doi:10.1080/09540260802094480
- Steen, E., Terry, B. M., Rivera, E. J., Cannon, J. L., Neely, T. R., Tavares, R., Xu, X. J., Wands, J. R., & de la Monte, S. M. (2005). Impaired insulin and insulin-like growth factor expression and signaling mechanisms in Alzheimer's disease--is this type 3 diabetes? *J Alzheimers Dis*, 7(1), 63-80. doi:10.3233/jad-2005-7107
- Stella, N. (2009). Endocannabinoid signaling in microglial cells. *Neuropharmacology*, 56 Suppl 1(Suppl 1), 244-253. doi:10.1016/j.neuropharm.2008.07.037
- Stella, N. (2010). Cannabinoid and cannabinoid-like receptors in microglia, astrocytes, and astrocytomas. *Glia*, 58(9), 1017-1030. doi:10.1002/glia.20983
- Stephan, B. C. M., Birdi, R., Tang, E. Y. H., Cosco, T. D., Donini, L. M., Licher, S., Ikram, M. A., Siervo, M., & Robinson, L. (2018). Secular trends in dementia prevalence and incidence worldwide: a systematic review. *J Alzheimers Dis*, 66(2), 653-680. doi:10.3233/jad-180375
- Stout, J. T., & Caskey, C. T. (1985). HPRT: gene structure, expression, and mutation. *Annu Rev Genet*, 19, 127-148. doi:10.1146/annurev.ge.19.120185.001015
- Streit, W. J., & Sparks, D. L. (1997). Activation of microglia in the brains of humans with heart disease and hypercholesterolemic rabbits. *J Mol Med (Berl)*, 75(2), 130-138. doi:10.1007/s001090050097
- Streit, W. J., Walter, S. A., & Pennell, N. A. (1999). Reactive microgliosis. *Prog Neurobiol*, 57(6), 563-581. doi:10.1016/s0301-0082(98)00069-0
- Streit, W. J. (2002). Microglia as neuroprotective, immunocompetent cells of the CNS. *Glia*, 40(2), 133-139. doi:10.1002/glia.10154
- Streit, W. J., Sammons, N. W., Kuhns, A. J., & Sparks, D. L. (2004). Dystrophic microglia in the aging human brain. *Glia*, 45(2), 208-212. doi:10.1002/glia.10319
- Streit, W. J. (2005). Microglia and neuroprotection: implications for Alzheimer's disease. *Brain Res Brain Res Rev*, 48(2), 234-239. doi:10.1016/j.brainresrev.2004.12.013
- Streit, W. J. (2006). Microglial senescence: does the brain's immune system have an expiration date? *Trends Neurosci*, 29(9), 506-510. doi:10.1016/j.tins.2006.07.001
- Streit, W. J., Braak, H., Xue, Q. S., & Bechmann, I. (2009). Dystrophic (senescent) rather than activated microglial cells are associated with tau pathology and likely precede neurodegeneration in Alzheimer's disease. *Acta Neuropathol*, 118(4), 475-485. doi:10.1007/s00401-009-0556-6
- Streit, W. J., Xue, Q. S., Tischer, J., & Bechmann, I. (2014). Microglial pathology. *Acta Neuropathol Commun*, 2, 142. doi:10.1186/s40478-014-0142-6
- Streit, W. J., Braak, H., Del Tredici, K., Leyh, J., Lier, J., Khoshbouei, H., Eisenloffel, C., Muller, W., & Bechmann, I. (2018). Microglial activation

- occurs late during preclinical Alzheimer's disease. *Glia*, 66(12), 2550-2562. doi:10.1002/glia.23510
- Streit, W. J., Khoshbouei, H., & Bechmann, I. (2020). Dystrophic microglia in late-onset Alzheimer's disease. *Glia*. doi:10.1002/glia.23782
- Sutherland, G. T., Janitz, M., & Kril, J. J. (2011). Understanding the pathogenesis of Alzheimer's disease: will RNA-Seq realize the promise of transcriptomics? *J Neurochem*, 116(6), 937-946. doi:10.1111/j.1471-4159.2010.07157.x
- Suva, D., Favre, I., Kraftsik, R., Esteban, M., Lobrinus, A., & Miklossy, J. (1999). Primary motor cortex involvement in Alzheimer disease. *J Neuropathol Exp Neurol*, 58(11), 1125-1134. doi:10.1097/00005072-199911000-00002
- Suzuki, N., Iwatsubo, T., Odaka, A., Ishibashi, Y., Kitada, C., & Ihara, Y. (1994). High tissue content of soluble β 1-40 is linked to cerebral amyloid angiopathy. *Am J Pathol*, 145(2), 452-460.
- Suzumura, A., Marunouchi, T., & Yamamoto, H. (1991). Morphological transformation of microglia in vitro. *Brain Res*, 545(1-2), 301-306. doi:10.1016/0006-8993(91)91302-h
- Svahn, A. J., Becker, T. S., & Graeber, M. B. (2014). Emergent properties of microglia. *Brain Pathol*, 24(6), 665-670. doi:10.1111/bpa.12195
- Swanson, M. E. V., Scotter, E. L., Smyth, L. C. D., Murray, H. C., Ryan, B., Turner, C., Faull, R. L. M., Dragunow, M., & Curtis, M. A. (2020). Identification of a dysfunctional microglial population in human Alzheimer's disease cortex using novel single-cell histology image analysis. *Acta Neuropathol Commun*, 8(1), 170. doi:10.1186/s40478-020-01047-9
- Swerdlow, R. H., & Khan, S. M. (2004). A "mitochondrial cascade hypothesis" for sporadic Alzheimer's disease. *Med Hypotheses*, 63(1), 8-20. doi:10.1016/j.mehy.2003.12.045
- Takahashi, K., Rochford, C. D., & Neumann, H. (2005). Clearance of apoptotic neurons without inflammation by microglial triggering receptor expressed on myeloid cells-2. *J Exp Med*, 201(4), 647-657. doi:10.1084/jem.20041611
- Takashima, A. (2008). Hyperphosphorylated tau is a cause of neuronal dysfunction in tauopathy. *J Alzheimers Dis*, 14(4), 371-375. doi:10.3233/jad-2008-14403
- Tam, W. Y., & Ma, C. H. (2014). Bipolar/rod-shaped microglia are proliferating microglia with distinct M1/M2 phenotypes. *Sci Rep*, 4, 7279. doi:10.1038/srep07279
- Tan, Z. S., & Vasan, R. S. (2009). Thyroid function and Alzheimer's disease. *J Alzheimers Dis*, 16(3), 503-507. doi:10.3233/jad-2009-0991
- Tanaka, J., Fujita, H., Matsuda, S., Toku, K., Sakanaka, M., & Maeda, N. (1997). Glucocorticoid- and mineralocorticoid receptors in microglial cells: the two receptors mediate differential effects of corticosteroids. *Glia*, 20(1), 23-37.
- Tang, M., Harrison, J., Deaton, C. A., & Johnson, G. V. W. (2019). Tau clearance mechanisms. *Adv Exp Med Biol*, 1184, 57-68. doi:10.1007/978-981-32-9358-8_5
- Tarkowski, E., Andreasen, N., Tarkowski, A., & Blennow, K. (2003). Intrathecal inflammation precedes development of Alzheimer's disease. *J Neurol Neurosurg Psychiatry*, 74(9), 1200-1205. doi:10.1136/jnnp.74.9.1200

- Tay, T. L., Béchade, C., D'Andrea, I., St-Pierre, M. K., Henry, M. S., Roumier, A., & Tremblay, M.-È. (2017a). Microglia gone rogue: impacts on psychiatric disorders across the lifespan. *Front Mol Neurosci*, 10, 421. doi:10.3389/fnmol.2017.00421
- Tay, T. L., Mai, D., Dautzenberg, J., Fernández-Klett, F., Lin, G., Sagar, Datta, M., Drougard, A., Stempf, T., Ardura-Fabregat, A., Staszewski, O., Margineanu, A., Sporbert, A., Steinmetz, L. M., Pospisilik, J. A., Jung, S., Priller, J., Grün, D., Ronneberger, O., & Prinz, M. (2017b). A new fate mapping system reveals context-dependent random or clonal expansion of microglia. *Nat Neurosci*, 20(6), 793-803. doi:10.1038/nn.4547
- Tay, T. L., Sagar, Dautzenberg, J., Grün, D., & Prinz, M. (2018). Unique microglia recovery population revealed by single-cell RNAseq following neurodegeneration. *Acta Neuropathol Commun*, 6(1), 87. doi:10.1186/s40478-018-0584-3
- Taylor, S. E., Morganti-Kossmann, C., Lifshitz, J., & Ziebell, J. M. (2014). Rod microglia: a morphological definition. *PLoS One*, 9. doi:10.1371/journal.pone.0097096
- Terry, R. D., Masliah, E., Salmon, D. P., Butters, N., DeTeresa, R., Hill, R., Hansen, L. A., & Katzman, R. (1991). Physical basis of cognitive alterations in Alzheimer's disease: synapse loss is the major correlate of cognitive impairment. *Ann Neurol*, 30(4), 572-580. doi:10.1002/ana.410300410
- Thal, D. R., Rüb, U., Schultz, C., Sassin, I., Ghebremedhin, E., Del Tredici, K., Braak, E., & Braak, H. (2000). Sequence of A β -protein deposition in the human medial temporal lobe. *J Neuropathol Exp Neurol*, 59(8), 733-748. doi:10.1093/jnen/59.8.733
- Thal, D. R., Rub, U., Orantes, M., & Braak, H. (2002). Phases of A β -deposition in the human brain and its relevance for the development of AD. *Neurology*, 58(12), 1791-1800.
- Thal, D. R., Capetillo-Zarate, E., Del Tredici, K., & Braak, H. (2006). The development of amyloid β protein deposits in the aged brain. *Sci Aging Knowledge Environ*, 2006(6), re1. doi:10.1126/sageke.2006.6.re1
- Thomas, D. X., Bajaj, S., McRae-McKee, K., Hadjichrysanthou, C., Anderson, R. M., & Collinge, J. (2020). Association of TDP-43 proteinopathy, cerebral amyloid angiopathy, and Lewy bodies with cognitive impairment in individuals with or without Alzheimer's disease neuropathology. *Sci Rep*, 10(1), 14579. doi:10.1038/s41598-020-71305-2
- Thompson, R. W., Pesce, J. T., Ramalingam, T., Wilson, M. S., White, S., Cheever, A. W., Ricklefs, S. M., Porcella, S. F., Li, L., Ellies, L. G., & Wynn, T. A. (2008). Cationic amino acid transporter-2 regulates immunity by modulating arginase activity. *PLoS Pathog*, 4(3), e1000023. doi:10.1371/journal.ppat.1000023
- Thrupp, N., Sala Frigerio, C., Wolfs, L., Skene, N. G., Fattorelli, N., Poovathingal, S., Fourné, Y., Matthews, P. M., Theys, T., Mancuso, R., de Strooper, B., & Fiers, M. (2020). Single-nucleus RNA-Seq Is not suitable for detection of microglial activation genes in humans. *Cell Rep*, 32(13), 108189. doi:10.1016/j.celrep.2020.108189
- Tiffany, H. L., Lavigne, M. C., Cui, Y. H., Wang, J. M., Leto, T. L., Gao, J. L., & Murphy, P. M. (2001). Amyloid- β induces chemotaxis and oxidant stress by acting at formylpeptide receptor 2, a G protein-coupled receptor

- expressed in phagocytes and brain. *J Biol Chem*, 276(26), 23645-23652. doi:10.1074/jbc.M101031200
- Tiraboschi, P., Hansen, L. A., Thal, L. J., & Corey-Bloom, J. (2004). The importance of neuritic plaques and tangles to the development and evolution of AD. *Neurology*, 62(11), 1984-1989. doi:10.1212/01.wnl.0000129697.01779.0a
- Tischer, J., Krueger, M., Mueller, W., Staszewski, O., Prinz, M., Streit, W. J., & Bechmann, I. (2016). Inhomogeneous distribution of Iba-1 characterizes microglial pathology in Alzheimer's disease. *Glia*, 64(9), 1562-1572. doi:10.1002/glia.23024
- Tomás-Camardiel, M., Venero, J. L., de Pablos, R. M., Rite, I., Machado, A., & Cano, J. (2004). In vivo expression of aquaporin-4 by reactive microglia. *J Neurochem*, 91(4), 891-899. doi:10.1111/j.1471-4159.2004.02759.x
- Tomlinson, B. E., & Kitchener, D. (1972). Granulovacuolar degeneration of hippocampal pyramidal cells. *J Pathol*, 106(3), 165-185. doi:10.1002/path.1711060305
- Tooyama, I., Kimura, H., Akiyama, H., & McGeer, P. L. (1990). Reactive microglia express class I and class II major histocompatibility complex antigens in Alzheimer's disease. *Brain Res*, 523(2), 273-280. doi:10.1016/0006-8993(90)91496-4
- Torres-Platas, S. G., Comeau, S., Rachalski, A., Bo, G. D., Cruceanu, C., Turecki, G., Giros, B., & Mechawar, N. (2014). Morphometric characterization of microglial phenotypes in human cerebral cortex. *J Neuroinflammation*, 11, 12. doi:10.1186/1742-2094-11-12
- Townsend, M., Shankar, G. M., Mehta, T., Walsh, D. M., & Selkoe, D. J. (2006). Effects of secreted oligomers of amyloid β -protein on hippocampal synaptic plasticity: a potent role for trimers. *J Physiol*, 572(Pt 2), 477-492. doi:10.1113/jphysiol.2005.103754
- Townsend, M. H., Robison, R. A., & O'Neill, K. L. (2018). A review of HPRT and its emerging role in cancer. *Med Oncol*, 35(6), 89. doi:10.1007/s12032-018-1144-1
- Tremblay, M.-È. (2011). The role of microglia at synapses in the healthy CNS: novel insights from recent imaging studies. *Neuron Glia Biol*, 7(1), 67-76. doi:10.1017/s1740925x12000038
- Tremblay, M.-È., Stevens, B., Sierra, A., Wake, H., Bessis, A., & Nimmerjahn, A. (2011). The role of microglia in the healthy brain. *J Neurosci*, 31(45), 16064-16069. doi:10.1523/jneurosci.4158-11.2011
- Tremblay, M.-È., Zettel, M. L., Ison, J. R., Allen, P. D., & Majewska, A. K. (2012). Effects of aging and sensory loss on glial cells in mouse visual and auditory cortices. *Glia*, 60(4), 541-558. doi:10.1002/glia.22287
- Tynan, R. J., Naicker, S., Hinwood, M., Nalivaiko, E., Buller, K. M., Pow, D. V., Day, T. A., & Walker, F. R. (2010). Chronic stress alters the density and morphology of microglia in a subset of stress-responsive brain regions. *Brain Behav Immun*, 24(7), 1058-1068. doi:10.1016/j.bbi.2010.02.001
- Uchihara, T., Duyckaerts, C., He, Y., Kobayashi, K., Seilhean, D., Amouyel, P., & Haww, J. J. (1995). ApoE immunoreactivity and microglial cells in Alzheimer's disease brain. *Neurosci Lett*, 195(1), 5-8. doi:10.1016/0304-3940(95)11763-m

- Uchihara, T. (2007). Silver diagnosis in neuropathology: principles, practice and revised interpretation. *Acta Neuropathol*, 113(5), 483-499. doi:10.1007/s00401-007-0200-2
- Uehara, Y., Yamada, T., Baba, Y., Miura, S., Abe, S., Kitajima, K., Higuchi, M. A., Iwamoto, T., & Saku, K. (2008). ATP-binding cassette transporter G4 is highly expressed in microglia in Alzheimer's brain. *Brain Res*, 1217, 239-246. doi:10.1016/j.brainres.2008.04.048
- Valli eres, L., & Sawchenko, P. E. (2003). Bone marrow-derived cells that populate the adult mouse brain preserve their hematopoietic identity. *J Neurosci*, 23(12), 5197-5207. doi:10.1523/jneurosci.23-12-05197.2003
- van Helmond, Z., Miners, J. S., Kehoe, P. G., & Love, S. (2010). Higher soluble amyloid β concentration in frontal cortex of young adults than in normal elderly or Alzheimer's disease. *Brain Pathol*, 20(4), 787-793. doi:10.1111/j.1750-3639.2010.00374.x
- Van Vickle, G. D., Esh, C. L., Kokjohn, T. A., Patton, R. L., Kalback, W. M., Luehrs, D. C., Beach, T. G., Newel, A. J., Lopera, F., Ghetti, B., Vidal, R., Casta o, E. M., & Roher, A. E. (2008). Presenilin-1 280Glu \rightarrow Ala mutation alters c-terminal APP processing yielding longer A β peptides: implications for Alzheimer's disease. *Mol Med*, 14(3-4), 184-194. doi:10.2119/2007-00094.vanvickle
- Vaquer-Alicea, J., & Diamond, M. I. (2019). Propagation of protein aggregation in neurodegenerative diseases. *Annu Rev Biochem*, 88, 785-810. doi:10.1146/annurev-biochem-061516-045049
- Varol, D., Mildner, A., Blank, T., Shemer, A., Barashi, N., Yona, S., David, E., Boura-Halfon, S., Segal-Hayoun, Y., Chappell-Maor, L., Keren-Shaul, H., Leshkowitz, D., Hornstein, E., Fuhrmann, M., Amit, I., Maggio, N., Prinz, M., & Jung, S. (2017). Dicer deficiency differentially impacts microglia of the developing and adult brain. *Immunity*, 46(6), 1030-1044.e1038. doi:10.1016/j.immuni.2017.05.003
- Vassar, P. S., & Culling, C. F. (1959). Fluorescent stains, with special reference to amyloid and connective tissues. *Arch Pathol*, 68, 487-498.
- Vaziri, A., Tang, J., Shroff, H., & Shank, C. V. (2008). Multilayer three-dimensional super resolution imaging of thick biological samples. *Proc Natl Acad Sci USA*, 105(51), 20221-20226. doi:10.1073/pnas.0810636105
- Vecchio, F., Miraglia, F., Iberite, F., Lacidogna, G., Guglielmi, V., Marra, C., Pasqualetti, P., Tiziano, F. D., & Rossini, P. M. (2018). Sustainable method for Alzheimer dementia prediction in mild cognitive impairment: electroencephalographic connectivity and graph theory combined with apolipoprotein E. *Ann Neurol*, 84(2), 302-314. doi:10.1002/ana.25289
- Vela, J. M., Dalmau, I., Gonz lez, B., & Castellano, B. (1995). Morphology and distribution of microglial cells in the young and adult mouse cerebellum. *J Comp Neurol*, 361(4), 602-616. doi:10.1002/cne.903610405
- Verdonk, F., Roux, P., Flamant, P., Fiette, L., Bozza, F. A., Simard, S., Lemaire, M., Plaud, B., Shorte, S. L., Sharshar, T., Chr tien, F., & Danckaert, A. (2016). Phenotypic clustering: a novel method for microglial morphology analysis. *J Neuroinflammation*, 13(1), 153. doi:10.1186/s12974-016-0614-7
- Verghese, P. B., Castellano, J. M., & Holtzman, D. M. (2011). Apolipoprotein E in Alzheimer's disease and other neurological disorders. *Lancet Neurol*, 10(3), 241-252. doi:10.1016/s1474-4422(10)70325-2

- Verkman, A. S. (2009). Knock-out models reveal new aquaporin functions. *Handb Exp Pharmacol*(190), 359-381. doi:10.1007/978-3-540-79885-9_18
- Vermersch, P., Frigard, B., & Delacourte, A. (1992). Mapping of neurofibrillary degeneration in Alzheimer's disease: evaluation of heterogeneity using the quantification of abnormal tau proteins. *Acta Neuropathol*, 85(1), 48-54.
- Verwer, R. W., Baker, R. E., Boiten, E. F., Dubelaar, E. J., van Ginkel, C. J., Sluiter, A. A., & Swaab, D. F. (2003). Post-mortem brain tissue cultures from elderly control subjects and patients with a neurodegenerative disease. *Exp Gerontol*, 38(1-2), 167-172. doi:10.1016/s0531-5565(02)00154-7
- Villegas-Llerena, C., Phillips, A., Garcia-Reitboeck, P., Hardy, J., & Pocock, J. M. (2016). Microglial genes regulating neuroinflammation in the progression of Alzheimer's disease. *Curr Opin Neurobiol*, 36, 74-81. doi:10.1016/j.conb.2015.10.004
- Villemagne, V. L., Perez, K. A., Pike, K. E., Kok, W. M., Rowe, C. C., White, A. R., Bourgeat, P., Salvado, O., Bedo, J., Hutton, C. A., Faux, N. G., Masters, C. L., & Barnham, K. J. (2010). Blood-borne amyloid- β dimer correlates with clinical markers of Alzheimer's disease. *J Neurosci*, 30(18), 6315-6322. doi:10.1523/jneurosci.5180-09.2010
- Vitek, M. P., Araujo, J. A., Fossel, M., Greenberg, B. D., Howell, G. R., Rizzo, S. J. S., Seyfried, N. T., Tenner, A. J., Territo, P. R., Windisch, M., Bain, L. J., Ross, A., Carrillo, M. C., Lamb, B. T., & Edelmayer, R. M. (2021). Translational animal models for Alzheimer's disease: An Alzheimer's Association Business Consortium Think Tank. *Alzheimers Dement (NY)*, 6(1), e12114. doi:10.1002/trc2.12114
- Vizcarra, J. C., Gearing, M., Keiser, M. J., Glass, J. D., Dugger, B. N., & Gutman, D. A. (2020). Validation of machine learning models to detect amyloid pathologies across institutions. *Acta Neuropathol Commun*, 8(1), 59. doi:10.1186/s40478-020-00927-4
- von Bergen, M., Friedhoff, P., Biernat, J., Heberle, J., Mandelkow, E. M., & Mandelkow, E. (2000). Assembly of τ protein into Alzheimer paired helical filaments depends on a local sequence motif ((306)VQIVYK(311)) forming β structure. *Proc Natl Acad Sci USA*, 97(10), 5129-5134. doi:10.1073/pnas.97.10.5129
- von Rotz, R. C., Kohli, B. M., Bosset, J., Meier, M., Suzuki, T., Nitsch, R. M., & Konietzko, U. (2004). The APP intracellular domain forms nuclear multiprotein complexes and regulates the transcription of its own precursor. *J Cell Sci*, 117(Pt 19), 4435-4448. doi:10.1242/jcs.01323
- von Zahn, J., Möller, T., Kettenmann, H., & Nolte, C. (1997). Microglial phagocytosis is modulated by pro- and anti-inflammatory cytokines. *Neuroreport*, 8(18), 3851-3856. doi:10.1097/00001756-199712220-00003
- Wadhwa, M., Kumari, P., Chauhan, G., Roy, K., Alam, S., Kishore, K., Ray, K., & Panjwani, U. (2017). Sleep deprivation induces spatial memory impairment by altered hippocampus neuroinflammatory responses and glial cells activation in rats. *J Neuroimmunol*, 312, 38-48. doi:10.1016/j.jneuroim.2017.09.003
- Walker, D. G., Whetzel, A. M., Serrano, G., Sue, L. I., Beach, T. G., & Lue, L. F. (2015). Association of CD33 polymorphism rs3865444 with Alzheimer's disease pathology and CD33 expression in human cerebral cortex.

- Neurobiol Aging*, 36(2), 571-582.
doi:10.1016/j.neurobiolaging.2014.09.023
- Walker, D. G., & Lue, L. F. (2015). Immune phenotypes of microglia in human neurodegenerative disease: challenges to detecting microglial polarization in human brains. *Alzheimers Res Ther*, 7(1). doi:10.1186/s13195-015-0139-9
- Walker, D. G., Tang, T. M., & Lue, L. F. (2018). Increased expression of toll-like receptor 3, an anti-viral signaling molecule, and related genes in Alzheimer's disease brains. *Exp Neurol*, 309, 91-106.
doi:10.1016/j.expneurol.2018.07.016
- Walker, D. G., Tang, T. M., Mendsaikhan, A., Tooyama, I., Serrano, G. E., Sue, L. I., Beach, T. G., & Lue, L. F. (2020a). Patterns of expression of purinergic receptor P2RY12, a putative marker for non-activated microglia, in aged and Alzheimer's disease brains. *Int J Mol Sci*, 21(2). doi:10.3390/ijms21020678
- Walker, D. G. (2020b). Defining activation states of microglia in human brain tissue: an unresolved issue for Alzheimer's disease. *Neuroimmunol Neuroinflammation*, 7(3), 194-214. doi:10.20517/2347-8659.2020.09
- Walker, L. C., Schelle, J., & Jucker, M. (2016). The prion-like properties of amyloid- β assemblies: implications for Alzheimer's disease. *Cold Spring Harb Perspect Med*, 6(7). doi:10.1101/cshperspect.a024398
- Walker, L. C. (2020). A β plaques. *Free Neuropathol*, 1(31). doi:10.17879/freeneuropathology-2020-3025
- Wang, H., Yu, M., Ochani, M., Amella, C. A., Tanovic, M., Susarla, S., Li, J. H., Wang, H., Yang, H., Ulloa, L., Al-Abed, Y., Czura, C. J., & Tracey, K. J. (2003). Nicotinic acetylcholine receptor $\alpha 7$ subunit is an essential regulator of inflammation. *Nature*, 421(6921), 384-388.
doi:10.1038/nature01339
- Wang, R., & Reddy, P. H. (2017). Role of glutamate and NMDA receptors in Alzheimer's disease. *J Alzheimers Dis*, 57(4), 1041-1048. doi:10.3233/jad-160763
- Wang, X., Spandidos, A., Wang, H., & Seed, B. (2012). PrimerBank: a PCR primer database for quantitative gene expression analysis, 2012 update. *Nucleic Acids Res*, 40(Database issue), D1144-1149.
doi:10.1093/nar/gkr1013
- Wang, X. J., Ye, M., Zhang, Y. H., & Chen, S. D. (2007). CD200-CD200R regulation of microglia activation in the pathogenesis of Parkinson's disease. *J Neuroimmune Pharmacol*, 2(3), 259-264. doi:10.1007/s11481-007-9075-1
- Ward, S. M., Himmelstein, D. S., Lancia, J. K., & Binder, L. I. (2012). Tau oligomers and tau toxicity in neurodegenerative disease. *Biochem Soc Trans*, 40(4), 667-671. doi:10.1042/bst20120134
- Wasseff, S. K., & Scherer, S. S. (2014). Activated microglia do not form functional gap junctions in vivo. *J Neuroimmunol*, 269(1-2), 90-93.
doi:10.1016/j.jneuroim.2014.02.005
- Weeraratna, A. T., Kalehua, A., Deleon, I., Bertak, D., Maher, G., Wade, M. S., Lustig, A., Becker, K. G., Wood, W., 3rd, Walker, D. G., Beach, T. G., & Taub, D. D. (2007). Alterations in immunological and neurological gene expression patterns in Alzheimer's disease tissues. *Exp Cell Res*, 313(3), 450-461. doi:10.1016/j.yexcr.2006.10.028

- Weingarten, M. D., Lockwood, A. H., Hwo, S. Y., & Kirschner, M. W. (1975). A protein factor essential for microtubule assembly. *Proc Natl Acad Sci USA*, 72(5), 1858-1862. doi:10.1073/pnas.72.5.1858
- Wendeln, A. C., Degenhardt, K., Kaurani, L., Gertig, M., Ulas, T., Jain, G., Wagner, J., Häslér, L. M., Wild, K., Skodras, A., Blank, T., Staszewski, O., Datta, M., Centeno, T. P., Capece, V., Islam, M. R., Kerimoglu, C., Staufenbiel, M., Schultze, J. L., Beyer, M., Prinz, M., Jucker, M., Fischer, A., & Neher, J. J. (2018). Innate immune memory in the brain shapes neurological disease hallmarks. *Nature*, 556(7701), 332-338. doi:10.1038/s41586-018-0023-4
- Weng, P. H., Chen, J. H., Chen, T. F., Sun, Y., Wen, L. L., Yip, P. K., Chu, Y. M., & Chen, Y. C. (2016). CHRNA7 polymorphisms and dementia risk: interactions with apolipoprotein ϵ 4 and cigarette smoking. *Sci Rep*, 6, 27231. doi:10.1038/srep27231
- White, K., Yang, P., Li, L., Farshori, A., Medina, A. E., & Zielke, H. R. (2018). Effect of postmortem interval and years in storage on RNA quality of tissue at a repository of the NIH NeuroBioBank. *Biopreserv Biobank*, 16(2), 148-157. doi:10.1089/bio.2017.0099
- Whitehouse, P. J., George, D. R., & D'Alton, S. (2011). Describing the dying days of "Alzheimer's disease". *J Alzheimers Dis*, 24(1), 11-13. doi:10.3233/JAD-2010-101639
- Wiersma, V. I., Hoozemans, J. J. M., & Scheper, W. (2020). Untangling the origin and function of granulovacuolar degeneration bodies in neurodegenerative proteinopathies. *Acta Neuropathol Commun*, 8(1), 153. doi:10.1186/s40478-020-00996-5
- Wilson, M. A., & Molliver, M. E. (1994). Microglial response to degeneration of serotonergic axon terminals. *Glia*, 11(1), 18-34. doi:10.1002/glia.440110105
- Wilson, R. S., Barnes, L. L., Aggarwal, N. T., Boyle, P. A., Hebert, L. E., Mendes de Leon, C. F., & Evans, D. A. (2010). Cognitive activity and the cognitive morbidity of Alzheimer disease. *Neurology*, 75(11), 990-996. doi:10.1212/WNL.0b013e3181f25b5e
- Wimo, A., Jönsson, L., Bond, J., Prince, M., & Winblad, B. (2013). The worldwide economic impact of dementia 2010. *Alzheimers Dement*, 9(1), 1-11.e13. doi:10.1016/j.jalz.2012.11.006
- Wimo, A., Guerchet, M., Ali, G. C., Wu, Y. T., Prina, A. M., Winblad, B., Jonsson, L., Liu, Z., & Prince, M. (2017). The worldwide costs of dementia 2015 and comparisons with 2010. *Alzheimers Dement*, 13(1), 1-7. doi:10.1016/j.jalz.2016.07.150
- Wimo, A., Handels, R., Winblad, B., Black, C. M., Johansson, G., Salomonsson, S., Eriksdotter, M., & Khandker, R. K. (2020). Quantifying and describing the natural history and costs of Alzheimer's disease and effects of hypothetical interventions. *J Alzheimers Dis*, 75(3), 891-902. doi:10.3233/jad-191055
- Wirenfeldt, M., Clare, R., Tung, S., Bottini, A., Mathern, G. W., & Vinters, H. V. (2009). Increased activation of Iba1+ microglia in pediatric epilepsy patients with Rasmussen's encephalitis compared with cortical dysplasia and tuberous sclerosis complex. *Neurobiol Dis*, 34(3), 432-440. doi:10.1016/j.nbd.2009.02.015

- Wirths, O., & Bayer, T. A. (2010). Neuron loss in transgenic mouse models of Alzheimer's disease. *Int J Alzheimers Dis*, 2010. doi:10.4061/2010/723782
- Wisniewski, H. M., Bancher, C., Barcikowska, M., Wen, G. Y., & Currie, J. (1989). Spectrum of morphological appearance of amyloid deposits in Alzheimer's disease. *Acta Neuropathol*, 78(4), 337-347. doi:10.1007/bf00688170
- Wisniewski, H. M., Sadowski, M., Jakubowska-Sadowska, K., Tarnawski, M., & Wegiel, J. (1998). Diffuse, lake-like amyloid- β deposits in the paraventricular layer of the presubiculum in Alzheimer disease. *J Neuropathol Exp Neurol*, 57(7), 674-683. doi:10.1097/00005072-199807000-00004
- Wlodarczyk, A., Holtman, I. R., Krueger, M., Yogev, N., Bruttger, J., Khoroshii, R., Benmamar-Badel, A., de Boer-Bergsma, J. J., Martin, N. A., Karam, K., Kramer, I., Boddeke, E. W., Waisman, A., Eggen, B. J., & Owens, T. (2017). A novel microglial subset plays a key role in myelinogenesis in developing brain. *Embo j*, 36(22), 3292-3308. doi:10.15252/embj.201696056
- Wohleb, E. S., Hanke, M. L., Corona, A. W., Powell, N. D., Stiner, L. M., Bailey, M. T., Nelson, R. J., Godbout, J. P., & Sheridan, J. F. (2011). β -adrenergic receptor antagonism prevents anxiety-like behavior and microglial reactivity induced by repeated social defeat. *J Neurosci*, 31(17), 6277-6288. doi:10.1523/jneurosci.0450-11.2011
- Wohleb, E. S., McKim, D. B., Shea, D. T., Powell, N. D., Tarr, A. J., Sheridan, J. F., & Godbout, J. P. (2014). Re-establishment of anxiety in stress-sensitized mice is caused by monocyte trafficking from the spleen to the brain. *Biol Psychiatry*, 75(12), 970-981. doi:10.1016/j.biopsych.2013.11.029
- Wood, J. G., Mirra, S. S., Pollock, N. J., & Binder, L. I. (1986). Neurofibrillary tangles of Alzheimer disease share antigenic determinants with the axonal microtubule-associated protein tau (tau). *Proc Natl Acad Sci USA*, 83(11), 4040-4043. doi:10.1073/pnas.83.11.4040
- Wright, G. J., Cherwinski, H., Foster-Cuevas, M., Brooke, G., Puklavec, M. J., Bigler, M., Song, Y., Jenmalm, M., Gorman, D., McClanahan, T., Liu, M. R., Brown, M. H., Sedgwick, J. D., Phillips, J. H., & Barclay, A. N. (2003). Characterization of the CD200 receptor family in mice and humans and their interactions with CD200. *J Immunol*, 171(6), 3034-3046. doi:10.4049/jimmunol.171.6.3034
- Wu, J., Bond, C., Chen, P., Chen, M., Li, Y., Shohet, R. V., & Wright, G. (2015). HIF-1 α in the heart: remodeling nucleotide metabolism. *J Mol Cell Cardiol*, 82, 194-200. doi:10.1016/j.yjmcc.2015.01.014
- Wu, Y. T., Beiser, A. S., Breteler, M. M. B., Fratiglioni, L., Helmer, C., Hendrie, H. C., Honda, H., Ikram, M. A., Langa, K. M., Lobo, A., Matthews, F. E., Ohara, T., Pérès, K., Qiu, C., Seshadri, S., Sjölund, B. M., Skoog, I., & Brayne, C. (2017). The changing prevalence and incidence of dementia over time - current evidence. *Nat Rev Neurol*, 13(6), 327-339. doi:10.1038/nrneurol.2017.63
- Xekardaki, A., Kovari, E., Gold, G., Papadimitropoulou, A., Giacobini, E., Herrmann, F., Giannakopoulos, P., & Bouras, C. (2015). Neuropathological changes in aging brain. *Adv Exp Med Biol*, 821, 11-17. doi:10.1007/978-3-319-08939-3_6

- Yakupova, E. I., Bobyleva, L. G., Vikhlyantsev, I. M., & Bobylev, A. G. (2019). Congo Red and amyloids: history and relationship. *Biosci Rep*, 39(1). doi:10.1042/bsr20181415
- Yamada, J., & Jinno, S. (2013). Novel objective classification of reactive microglia following hypoglossal axotomy using hierarchical cluster analysis. *J Comp Neurol*, 521(5), 1184-1201. doi:10.1002/cne.23228
- Yamaguchi, H., Hirai, S., Morimatsu, M., Shoji, M., & Ihara, Y. (1988). A variety of cerebral amyloid deposits in the brains of the Alzheimer-type dementia demonstrated by β protein immunostaining. *Acta Neuropathol*, 76(6), 541-549. doi:10.1007/bf00689591
- Yamaguchi, H., Nakazato, Y., Shoji, M., Ihara, Y., & Hirai, S. (1990). Ultrastructure of the neuropil threads in the Alzheimer brain: their dendritic origin and accumulation in the senile plaques. *Acta Neuropathol*, 80(4), 368-374. doi:10.1007/bf00307689
- Yang, G. J., Liu, H., Ma, D. L., & Leung, C. H. (2019). Rebalancing metal dyshomeostasis for Alzheimer's disease therapy. *J Biol Inorg Chem*, 24(8), 1159-1170. doi:10.1007/s00775-019-01712-y
- Yang, I., Han, S. J., Kaur, G., Crane, C., & Parsa, A. T. (2010). The role of microglia in central nervous system immunity and glioma immunology. *J Clin Neurosci*, 17(1), 6-10. doi:10.1016/j.jocn.2009.05.006
- Yankner, B. A., Duffy, L. K., & Kirschner, D. A. (1990). Neurotrophic and neurotoxic effects of amyloid β protein: reversal by tachykinin neuropeptides. *Science*, 250(4978), 279-282. doi:10.1126/science.2218531
- Yao, H., Coppola, K., Schweig, J. E., Crawford, F., Mullan, M., & Paris, D. (2019). Distinct signaling pathways regulate TREM2 phagocytic and NF κ B antagonistic activities. *Front Cell Neurosci*, 13, 457. doi:10.3389/fncel.2019.00457
- Yasuhara, O., Kawamata, T., Aimi, Y., McGeer, E. G., & McGeer, P. L. (1994). Two types of dystrophic neurites in senile plaques of Alzheimer disease and elderly non-demented cases. *Neurosci Lett*, 171(1-2), 73-76.
- Ye, J., Coulouris, G., Zaretskaya, I., Cutcutache, I., Rozen, S., & Madden, T. L. (2012). Primer-BLAST: a tool to design target-specific primers for polymerase chain reaction. *BMC Bioinformatics*, 13, 134. doi:10.1186/1471-2105-13-134
- Yeh, F. L., Wang, Y., Tom, I., Gonzalez, L. C., & Sheng, M. (2016). TREM2 binds to apolipoproteins, including APOE and CLU/APOJ, and thereby facilitates uptake of amyloid- β by microglia. *Neuron*, 91(2), 328-340. doi:10.1016/j.neuron.2016.06.015
- Younan, N. D., & Viles, J. H. (2015). A comparison of three fluorophores for the detection of amyloid fibers and prefibrillar oligomeric assemblies: ThT (thioflavin t); ANS (1-anilinonaphthalene-8-sulfonic acid); and bisANS (4,4'-dianilino-1,1'-binaphthyl-5,5'-disulfonic acid). *Biochemistry*, 54(28), 4297-4306. doi:10.1021/acs.biochem.5b00309
- Yusufov, M., Weyandt, L. L., & Piryatinsky, I. (2017). Alzheimer's disease and diet: a systematic review. *Int J Neurosci*, 127(2), 161-175. doi:10.3109/00207454.2016.1155572
- Zetter, M. A., Hernández, V. S., Roque, A., Hernández-Pérez, O. R., Gómora, M. J., Ruiz-Velasco, S., Eiden, L. E., & Zhang, L. (2021). Microglial synaptic pruning on axon initial segment spines of dentate granule cells: sexually

- dimorphic effects of early-life stress and consequences for adult fear response. *J Neuroendocrinol*, e12969. doi:10.1111/jne.12969
- Zhan, X., Kim, C., & Sharp, F. R. (2008). Very brief focal ischemia simulating transient ischemic attacks (TIAs) can injure brain and induce Hsp70 protein. *Brain Res*, 1234, 183-197. doi:10.1016/j.brainres.2008.07.094
- Zhan, Y., Paolicelli, R. C., Sforazzini, F., Weinhard, L., Bolasco, G., Pagani, F., Vyssotski, A. L., Bifone, A., Gozzi, A., Ragozzino, D., & Gross, C. T. (2014). Deficient neuron-microglia signaling results in impaired functional brain connectivity and social behavior. *Nat Neurosci*, 17(3), 400-406. doi:10.1038/nn.3641
- Zhang, B., Gaiteri, C., Bodea, L. G., Wang, Z., McElwee, J., Podtelezhnikov, A. A., Zhang, C., Xie, T., Tran, L., Dobrin, R., Fluder, E., Clurman, B., Melquist, S., Narayanan, M., Suver, C., Shah, H., Mahajan, M., Gillis, T., Mysore, J., MacDonald, M. E., Lamb, J. R., Bennett, D. A., Molony, C., Stone, D. J., Gudnason, V., Myers, A. J., Schadt, E. E., Neumann, H., Zhu, J., & Emilsson, V. (2013). Integrated systems approach identifies genetic nodes and networks in late-onset Alzheimer's disease. *Cell*, 153(3), 707-720. doi:10.1016/j.cell.2013.03.030
- Zhang, D., & Zhang, D. E. (2011). Interferon-stimulated gene 15 and the protein ISGylation system. *J Interferon Cytokine Res*, 31(1), 119-130. doi:10.1089/jir.2010.0110
- Zhao, X., Liao, Y., Morgan, S., Mathur, R., Feustel, P., Mazurkiewicz, J., Qian, J., Chang, J., Mathern, G. W., Adamo, M. A., Ritaccio, A. L., Gruenthal, M., Zhu, X., & Huang, Y. (2018). Noninflammatory changes of microglia are sufficient to cause epilepsy. *Cell Rep*, 22(8), 2080-2093. doi:10.1016/j.celrep.2018.02.004
- Zhu, X. C., Tan, L., Wang, H. F., Jiang, T., Cao, L., Wang, C., Wang, J., Tan, C. C., Meng, X. F., & Yu, J. T. (2015). Rate of early onset Alzheimer's disease: a systematic review and meta-analysis. *Ann Transl Med*, 3(3), 38. doi:10.3978/j.issn.2305-5839.2015.01.19
- Zhu, Y., Hou, H., Rezai-Zadeh, K., Giunta, B., Ruscini, A., Gemma, C., Jin, J., Dragicevic, N., Bradshaw, P., Rasool, S., Glabe, C. G., Ehrhart, J., Bickford, P., Mori, T., Obregon, D., Town, T., & Tan, J. (2011). CD45 deficiency drives amyloid- β peptide oligomers and neuronal loss in Alzheimer's disease mice. *J Neurosci*, 31(4), 1355-1365. doi:10.1523/jneurosci.3268-10.2011
- Ziebell, J. M., Taylor, S. E., Cao, T., Harrison, J. L., & Lifshitz, J. (2012). Rod microglia: elongation, alignment, and coupling to form trains across the somatosensory cortex after experimental diffuse brain injury. *J Neuroinflammation*, 9, 247. doi:10.1186/1742-2094-9-247
- Ziebell, J. M., Ray-Jones, H., & Lifshitz, J. (2017). Nogo presence is inversely associated with shifts in cortical microglial morphology following experimental diffuse brain injury. *Neuroscience*, 359, 209-223. doi:10.1016/j.neuroscience.2017.07.027
- Zierler, S., Frei, E., Grissmer, S., & Kerschbaum, H. H. (2008). Chloride influx provokes lamellipodium formation in microglial cells. *Cell Physiol Biochem*, 21(1-3), 55-62. doi:10.1159/000113747
- Zlokovic, B. V. (2005). Neurovascular mechanisms of Alzheimer's neurodegeneration. *Trends Neurosci*, 28(4), 202-208. doi:10.1016/j.tins.2005.02.001

- Zoref-Shani, E., Feinstein, S., Frishberg, Y., Bromberg, Y., & Sperling, O. (2000). Kelley-Seegmiller syndrome due to a unique variant of hypoxanthine-guanine phosphoribosyltransferase: reduced affinity for 5-phosphoribosyl-1-pyrophosphate manifested only at low, physiological substrate concentrations. *Biochim Biophys Acta*, 1500(2), 197-203. doi:10.1016/s0925-4439(99)00103-9
- Zotova, E., Bharambe, V., Cheaveau, M., Morgan, W., Holmes, C., Harris, S., Neal, J. W., Love, S., Nicoll, J. A., & Boche, D. (2013). Inflammatory components in human Alzheimer's disease and after active amyloid- β 42 immunization. *Brain*, 136(Pt 9), 2677-2696. doi:10.1093/brain/awt210
- Zou, K., Gong, J. S., Yanagisawa, K., & Michikawa, M. (2002). A novel function of monomeric amyloid β -protein serving as an antioxidant molecule against metal-induced oxidative damage. *J Neurosci*, 22(12), 4833-4841. doi:10.1523/jneurosci.22-12-04833.2002
- Zou, K., Kim, D., Kakio, A., Byun, K., Gong, J. S., Kim, J., Kim, M., Sawamura, N., Nishimoto, S., Matsuzaki, K., Lee, B., Yanagisawa, K., & Michikawa, M. (2003). Amyloid β -protein ($A\beta$)1-40 protects neurons from damage induced by $A\beta$ 1-42 in culture and in rat brain. *J Neurochem*, 87(3), 609-619. doi:10.1046/j.1471-4159.2003.02018.x

Appendix

Appended here with permission is the manuscript by Guennewig et al. (2021) in which elements of Chapter 5 of this thesis are published. The manuscript begins on the next page.



OPEN

Defining early changes in Alzheimer's disease from RNA sequencing of brain regions differentially affected by pathology

Boris Guennewig^{1,6}, Julia Lim^{2,6}, Lee Marshall^{3,4}, Andrew N. McCorkindale², Patrick J. Paasila², Ellis Patrick⁵, Jillian J. Kril², Glenda M. Halliday¹, Antony A. Cooper^{3,4} & Greg T. Sutherland²✉

Tau pathology in Alzheimer's disease (AD) spreads in a predictable pattern that corresponds with disease symptoms and severity. At post-mortem there are cortical regions that range from mildly to severely affected by tau pathology and neuronal loss. A comparison of the molecular signatures of these differentially affected areas within cases and between cases and controls may allow the temporal modelling of disease progression. Here we used RNA sequencing to explore differential gene expression in the mildly affected primary visual cortex and moderately affected precuneus of ten age-, gender- and RNA quality-matched post-mortem brains from AD patients and healthy controls. The two regions in AD cases had similar transcriptomic signatures but there were broader abnormalities in the precuneus consistent with the greater tau load. Both regions were characterised by upregulation of immune-related genes such as those encoding triggering receptor expressed on myeloid cells 2 and membrane spanning 4-domains A6A and milder changes in insulin/IGF1 signalling. The precuneus in AD was also characterised by changes in vesicle secretion and downregulation of the interneuronal subtype marker, somatostatin. The 'early' AD transcriptome is characterised by perturbations in synaptic vesicle secretion on a background of neuroimmune dysfunction. In particular, the synaptic deficits that characterise AD may begin with the somatostatin division of inhibitory neurotransmission.

Alzheimer's disease (AD) is the most common neurodegenerative disorder and is predicted to become the most impactful health issue for Western countries by 2050 due to an ageing population and the lack of disease-modifying treatments¹. AD commonly manifests clinically in the eighth decade of life but imaging studies suggest that the disease develops at least 20 years before symptoms are detected². The neuropathology of AD is characterised by widescale atrophy, regional neuronal loss, gliosis and two pathognomonic entities; extracellular plaques, made up primarily of peptides called beta-amyloid (A β) and neurofibrillary tangles (NFT) made up chiefly of filaments of hyperphosphorylated microtubule-associated protein tau (tau). A pathological diagnosis is based on a qualitative assessment of NFTs, diffuse and neuritic plaques that prioritises the spread of these entities rather than the degree of pathology in any particular region. As both tau and A β pathology commonly occur in aged non-demented individuals³ a diagnosis of AD is probabilistic with no clear threshold of pathology that, above which, dementia is conferred.

Given that neuronal loss is synonymous with symptoms in AD and irreversible, any disease-modifying drug needs to be implemented before such loss occurs. The popular amyloid (cascade) hypothesis (ACH) states that the pathogenesis of common forms of AD is precipitated by accumulation of neurotoxic and soluble A β oligomers

¹Brain and Mind Centre and School of Medical Sciences, Faculty of Medicine and Health, The University of Sydney, Camperdown, NSW 2006, Australia. ²Discipline of Pathology and Charles Perkins Centre, School of Medical Sciences, Faculty of Medicine and Health, Rm 6211 Level 6W, The University of Sydney, Sydney, NSW 2006, Australia. ³St. Vincent's Clinical School and School of Biotechnology and Biomolecular Sciences, University of New South Wales, Kensington, NSW 2052, Australia. ⁴Garvan Institute of Medical Research, Darlinghurst, NSW 2010, Australia. ⁵School of Mathematics and Statistics, Faculty of Science, The University of Sydney, Camperdown, NSW 2006, Australia. ⁶These authors contributed equally: Boris Guennewig and Julia Lim. ✉email: g.sutherland@sydney.edu.au

in the brain parenchyma⁴. It further proposes a linear process where A β oligomers cause neuronal dysfunction that ultimately results in NFT formation, neuron dysfunction and death. ACH is based on the phenotypic similarities between rare familial and sporadic forms of AD and supported by positive emission tomography (PET) studies that show A β load in presymptomatic individuals⁵. In particular, PET imaging of asymptomatic mutation carriers suggests that the A β accumulation in the precuneus region is a key early event in disease progression⁶. It is unclear how amyloid and tau are in this cascade but one hypothesis is that A β attenuates central insulin signalling and AD has been called ‘Type 3 Diabetes’^{7,8}. The subsequent downregulation of the associated PI3K/AKT pathway is proposed to lead to excessive activity by major tau kinases, primarily glycogen synthase Kinase 3 β (GSK3 β) that is normally inhibited by insulin to enable glycogen synthase activity in cells⁹.

The findings from pathological studies in AD do not entirely support the linear process proposed by the ACH. A β pathology begins widely in the neocortex, particularly the ventral neocortex, before spreading to subcortical regions, the brainstem and cerebellum¹⁰. A β pathology shows more variation between cases than tau pathology and it plateaus in many regions early in the disease¹¹. Staging studies suggest that tau pathology has a more predictable pattern, beginning in the transentorhinal cortex before spreading through the limbic system and into the neocortex with relative sparing of the primary cortices such as the primary visual cortex¹². There are various forms of tau or neurofibrillary pathology such as dystrophic neurites¹³, neuritic threads and astroglial pathology¹⁴ but staging schema concentrate on neurofibrillary tangles (NFTs). AD symptoms are correlated with irreversible neuronal loss and this in turn is correlated to the spread of NFTs rather than A β pathology^{12,15}.

There are also a number of challenges in understanding the course of events within the ACH. Firstly, the long prodrome and disease duration would be consistent with a subtle pathogenic mechanism¹⁶. Second, mechanistic studies are best performed in animal models, but the human brain is more complex than any other organ relative to that found in lower mammals. In particular, the human brain transcriptome correlates closely with advanced human cognition¹⁷. As expected, there is little concordance between brain transcriptomic data from human AD brain and AD animal models^{18,19}.

Post-mortem tissue, the only consistently available source of human brain tissue, appears unsuitable for mechanistic studies. In neurodegenerative diseases, the most severely affected regions of the brain display considerable neuronal loss²⁰, making it challenging to interpret how case–control differences in gene expression from these areas relate to the disease process. A possible compromise is to utilise regions that are affected by the disease, with plaques and, or NFTs, but yet to experience neuronal loss at post-mortem. A putative scenario would see ‘sick’ neurons contributing maximally to the bulk tissue AD transcriptome. In reality, this model is likely to focus on tau-related pathomechanisms given its more predictable spread across the neocortex. By comparing areas mildly and moderately affected by tau pathology within the same AD brains, as well as traditional case–control comparisons, the natural history of the disease might be modelled²¹.

The development of new pre-symptomatic diagnostics and therapeutics in AD is hindered by our lack of understanding of the events promoting and connecting the various stages of the ACH²². We hypothesize that early pathogenic changes can be determined from observing gene expression profiles in less severely affected cortical regions of the AD brain at post-mortem. Here we report the pathomechanisms related to early tau deposition from comparing the moderately affected precuneus (PREC) to the mildly affected primary visual cortex (VIC).

Methods

Tissue. This study was carried out following ethical approval from The University of Sydney’s Human Research Ethics Committee (HREC#2012/161) with all experiments with human tissue performed in accordance with the Declaration of Helsinki. De-identified tissue was supplied by New South Wales Brain Banks (NSWBB) including the Sydney Brain Bank at Neuroscience Research Australia and the New South Wales Brain Tissue Resource Centre (NSWBTRC) at The University of Sydney following approval from their Scientific Advisory Committee. Informed consent was previously obtained from the participants (or next-of-kin at time of death) by NSWBB, who also provided information on age, gender, dementia status (yes/no) clinical dementia rating (CDR; non-demented = 0; MCI = 0.5; demented > 0.5), AD pathological diagnosis according to latest ‘ABC’ criteria³, cause of death, *post-mortem* interval (PMI), and brain pH (Supplementary Table 1 for details with RNA sequencing samples in bold type). 10 μ m formalin-fixed paraffin-embedded (FFPE) sections and 100 mg frozen tissue from the contralateral hemisphere of the VIC and PREC were obtained from 26 cases and 22 age-, gender- and APOE ϵ 4-matched neurologically normal controls.

RNA-Seq. Our overall aim was to explore the plausibility of using differentially affected areas of the *post-mortem* AD brain to model disease progression. As a ‘proof of concept’ study five cases and five controls were selected for RNA sequencing (RNA-Seq) following matching for age, gender, APOE ϵ 4 genotype and RNA quality (RNA integrity number; RIN). RINs had been derived from the superior temporal gyrus (STG) of all donors for a previous study²³. All cases had been designated with high likelihood of AD (‘ABC’ score) according to the latest pathological diagnostic criteria and all were Braak stage VI³ (Supplementary Table 1 for full clinical and pathological data). RNA was extracted from 30 mg frozen tissue from the PREC and VIC using TRIzol (Life Technologies, Thermo Fisher Scientific, Carlsbad, CA 92008, USA) including an on-column DNase I treatment. 500 ng of RNase H ribodepleted total RNA was used for library preparation with the TruSeq Stranded Total RNA Sample Prep Kit (Illumina, USA). Mixes of External RNA Controls Consortium (ERCC) Spike-Ins (Thermo Fisher Scientific) with different molar ratios were added to control (Mix 1) and AD samples (Mix 2). The libraries were sequenced using the Illumina HiSeq2500 at the Kinghorn Centre for Clinical Genomics, Garvan Institute of Medical Research, Sydney, Australia.

Gene name	Primer sequences	Primer concentration (nM)
Somatostatin	Forward 5'-ACCCCAGACTCCGTAGTTT-3' Reverse 5'-AGTACTTGGCCAGTTCCTGCT-3'	125
Insulin receptor	Forward 5'-GGACCAGGCATCCTGTGAAA-3' Reverse 5'-GGGCTCTTTGTAGAACAGCA-3'	125
Insulin-like growth factor 1 receptor	Forward 5'-AGGAATGAAGTCTGGTCCG-3' Reverse 5'-CCGCAGATTCTCCACTCGT-3'	125
Glyceraldehyde 3-phosphate dehydrogenase	Forward 5'-AAATCAAGTGGGGCGATGCT-3' Reverse 5'-CAAATGAGCCCCAGCCTTCT-3'	50
C-X-C motif chemokine receptor 4	Forward 5'-GAGTGTCTCCAGTAGCCACC-3' Reverse 5'-GCCCATTTCTCTCGGTAGT-3'	50
Membrane spanning 4-domains A6A	Forward 5'-GCTGATTGCACTCTGCTGG Reverse 5'-GCAGGAAAAGTACACTCCCAGG-3'	50
Triggering receptor expressed on myeloid cells 2	Forward 5'-TGCTGGCAGACCCCTG-3' Reverse 5'-GAAGGATGGAAGTGGGTGGG-3'	50
Parvin gamma	Forward 5'-AAATGCTGCACAACGTCACC-3' Reverse 5'-AGGCAGTGAGGGTCAATTCTG-3'	50
Solute carrier family 7 member 2	Forward 5'-CCATTTTCCCAATGCCTCGTG-3' Reverse 5'-GAAAGGCCATCAAAGCTGCC-3'	50

Table 1. Droplet digital PCR primer details.

RNA-Seq data analysis. All data analyses were carried out within the R project environment as previously described²⁴. Reads were mapped to GRCh38.p5 reference genome using STAR (version 2.5.1a)²⁵. Known GENCODE genes (version 24) were quantified by RSEM (version 1.3.0)²⁶. The complete code and supplementary quality metrics can be found at: https://github.com/gboris/AD_RNA-Seq. Trimmed mean of M values (TMM) normalization and filtering according to abundance of reads in the either case or control, were carried out in edgeR²⁷. An exploratory ANOVA of all RNA-Seq data (both regions), based on all filtered normalised gene counts, was used to identify potential covariates for inclusion in the subsequent differential gene expression analysis for each region (Additional Fig. 1). Status, region, age, gender, post-mortem interval (PMI), brain pH (occipital lobe), and STG-RIN²³ were included as covariates in the model to derive differentially expressed genes (DEG) with 'edgeR'²⁸. Significance was set at a false discovery rate (FDR)-adjusted p value ≤ 0.05 . Gene enrichment analysis was performed using various databases including: Gene Ontology (GO) sets of molecular functions (MF), biological processes (BP), and cellular components (CC). General concordance between gene associations in the two regions was explored by correlation analysis fold-changes.

Quantitative neuropathology. The VIC and PREC of all 26 cases and 22 controls were quantified for tau (AT8-tau)-immunopositive neurons [AT8-tau monoclonal antibody (1:500, #MN1020, Thermo Fisher Scientific, Rockford, IL 61105, USA); Phospho-Tau (Ser202, Thr205)], the areal fraction of A β immunopositivity [Beta Amyloid, 1–16 (6E10) monoclonal antibody (1:500, #SIG-39320-200, BioLegend, San Diego, CA 92121, USA)] and the total number of cortical neurons. Briefly, immunopositive neurons or all cortical neurons were counted manually in three cortical strips (cortical surface to grey matter/white matter boundary) from a 10 μ m section of either PREC or VIC with an eyepiece graticule. AT8-tau immunopositive (+ve) and cortical neuron counts were converted into cells per mm² value by dividing total neurons by the number of graticules across the three strips, while A β immunopositivity was calculated as an areal fraction. The mean density/areal fraction for each individual region was calculated and normalised for potential atrophy by multiplying by a correction factor (mean cortical width/mean cortical width of gender-matched controls) (Supplementary Table 1 for full quantitative neuropathology data).

RNA-Seq validation—droplet digital PCR. RNA was further isolated from 30 mg human brain tissue of all 26 cases and 22 controls including additional tissue from those individuals previously sampled for RNA-Seq. Here RNA was extracted using TRIzol reagent in combination with the PureLink RNA Isolation Kit (Life Technologies, Thermo Fisher Scientific) including an on-column DNase I treatment. RNA was eluted with RNase free water and stored at -80°C until use. cDNA was synthesised using the sensiFAST cDNA kit (Bioline, Sydney, NSW 2015, Australia) and diluted to 100 ng prior to amplification by droplet digital polymerase chain reaction (ddPCR). Transcript abundance was measured using the Bio-Rad QX200 Droplet Digital PCR System (Bio-Rad Life Science, Hercules, California 94547, USA) at the Molecular Biology Facility, Bosch Institute, The University of Sydney. Primers for genes of interest (GOI) were designed using PrimerBlast (<https://www.ncbi.nlm.nih.gov/tools/primer-blast/>) and manufactured by Integrated DNA Technologies Australia Pty Ltd (Table 1 for sequence information). A preliminary experiment in the five RNA-Seq controls only was carried out with SST and four potential housekeeping genes: glyceraldehyde-3-phosphate dehydrogenase (*GAPDH*), hydroxymethylbilane synthase (*HMBS*), hypoxanthine phosphoribosyltransferase 1 (*HPRT1*) and glial fibrillary acidic protein (*GFAP*) as previously described²³. All assays were optimised such that there was a clear differentiation of positive and negative droplets as per manufacturer's instructions. *GAPDH* was selected as the reference genes based on a similar positive correlation with RIN in the controls to SST, to minimise potential premortem effects on disease-specific differential expression as previously described²³. ddPCR was then extended to the full cohort with cDNA at 100 ng except for *GAPDH* (12.5 ng) with data normalised as GOI/*GAPDH*. An ANOVA was used to determine group differences for both regions. As GOIs, other than SST, did not necessary correlate with

Mean (S.D.)	AD (n = 5)	Control (n = 5)	p value
Age (years)	76 (14)	78 (9)	0.8
Post-mortem interval (hours)	11 (12)	18 (18)	0.3
Brain pH (occipital lobe)	6.5 (0.2)	6.6 (0.2)	0.1
RIN (STG for matching)	6.9 (0.3)	6.9 (0.4)	0.9
RIN (PREC)	5.2 (0.3)	5.5 (0.3)	0.5
RIN (VIC)	5.3 (0.2)	5.3 (0.2)	1

Table 2. Demographics and clinicopathological information.

RIN in the controls similarly to *GAPDH*, F ratios were also adjusted for age-, gender- and region-specific RIN by logistic regression. Correlations between normalised GOI expression and neuropathology (AT8-tau positive neurons, areal A β fraction and residual neurons) were also explored in the cases only and adjusted as above. All statistical analyses were carried out in JMP10.0.0 (SAS Institute Inc., Cary, North Carolina, USA).

RNA-Seq validation—ROSMAP study data. Permission was obtained to access the Religious Orders Study and Memory and Aging Project (ROSMAP) study data from the Rush Alzheimer's Disease Center and hosted by Sage Bionetworks—Synapse system (<https://www.synapse.org/#!Synapse:syn3219045>). RNA-Seq data was from the dorsal lateral prefrontal cortex of participants who had undergone comprehensive neuropsychological assessment to assign cognitive status as previously described²⁹. ROSMAP participants were classified as cognitively normal, having mild cognitive impairment or demented. The ROSMAP study is unique in that quantitative neuropathological examination has been performed across multiple brain regions³⁰ in combination with the semi-quantitative and probabilistic standard AD diagnostic criteria which classifies individuals with low, intermediate or high likelihood that their dementia is primarily due to AD³¹. A whole genome co-expression network analysis of the RNA-seq data on 478 individuals has been previously reported³² but was re-analysed here by comparing the most disparate groups—non-demented controls with no or low AD pathology (n = 117) versus demented individuals with intermediate or high AD pathology (n = 195)—using the same differential expression method described above.

Comparison with GWAS data. Seyfried and colleagues previously described a strategy for determining if protein products of GWAS targets are enriched in gene expression data³³. Using data from International Genomics of Alzheimer's Project³⁴ they used the gene set analysis program called MAGMA³⁵ to derive 1234 GWAS (AD risk) genes. A Chi-square test was used to determine if the DEGs in the AD-PREC or AD-VIC were significantly over-represented among their AD risk genes.

Ethics approval and consent to participate. Ethics approval for the use of de-identified post-mortem human tissue has been described in the Methods section, Paragraph 1.

Results

RNA sequencing (RNA-Seq) was carried out on samples from the PREC and VIC brain regions of five AD cases and five controls matched for age, gender, APOE genotype and RIN and selected from a previously described cohort²³ (Table 2 and Supplementary Table 1 for full data).

All AD cases had been previously classified as Braak stage VI according to current diagnostic criteria³ although one case (IS18), a 100 old female, had a relatively low tau load in her PREC (7.1 immunopositive cells/mm²) (Supplementary Table 1 for all details). The regional pathology in the AD cases was consistent with the expected pattern of tau pathology across the neocortex with relative sparing of VIC and generalised A β deposition across the entire neocortex (including VIC and PREC) early in the disease course^{12,15}. Neither region showed any difference in neuronal density between cases and controls, but both were characterised by higher A β areal fractions in the cases (Table 3). In contrast, only the PREC of AD cases (AD-PREC) had more AT8-tau + ve neurons compared to controls. Among the cases, A β areal fractions were similar in both regions ($p = 0.5$) but AT8-tau + ve neurons trended towards being higher in the PREC ($p = 0.08$) (Supplementary Table 1 for all quantitative neuropathology data; RNA-Seq samples in bold type).

RNA sequencing. RNA sequencing was carried using 125 bp paired-end approach at an average sequencing depth of 25 million reads per sample. Transcripts that had less than five reads in two or less samples were filtered out prior to differential expression analysis. In order of magnitude data variance was due to: RIN, age, brain region, pH, gender and then disease status (Additional Fig. 1). Excluding region, all these factors were included in linear regression models to generate the DEGs for the VIC and PREC. Hierarchical clustering of the DEGs from both regions demonstrated that control and case samples largely segregated with each other (Fig. 1). Two controls, IS43 and IS44, segregated with the cases and this could not be explained by a common APOE genotype ($\epsilon 3/\epsilon 4$ and $\epsilon 3/\epsilon 3$ respectively) or other available clinical data (Supplementary Table 1 for full details).

Precuneus (PREC). The AD-PREC was characterised by 559 DEGs (462 protein-coding) (FDR ≤ 0.05 ; Supplementary Table 2). The ERCC subgroup A transcripts that had been spiked-in to the AD samples at a fourfold

Mean (S.D.)	AD (n = 5)	Control (n = 5)	p value
PREC—AT8-tau + ve neuron density (mm ²)	29 (13)	0	0.001
PREC—Areal Aβ fraction	0.09 (0.05)	0	0.006
PREC—Neuronal density (mm ²)	303 (31)	269 (64)	0.31
VIC—AT8-tau + ve neuron density	13 (13)	0	0.06
VIC—areal Aβ fraction	0.07 (0.05)	0	0.01
VIC—neuronal density	306 (35)	262 (74)	0.26
	PREC	VIC	p value
Inter-regional comparisons (cases only)			
Areal Aβ fraction	0.09 (0.05)	0.07 (0.05)	0.5
AT8-tau + ve neuron density	29 (13)	13 (13)	0.08

Table 3. Quantification of AD neuropathology in the RNA-Seq cohort.

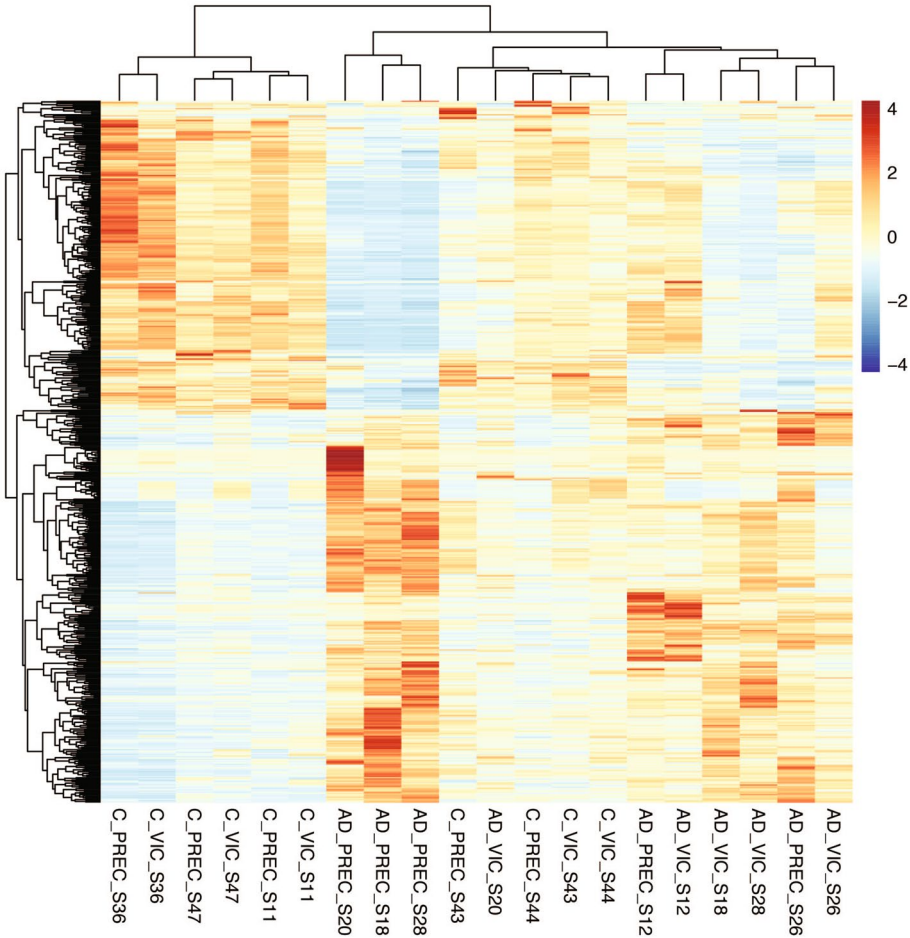


Figure 1. Hierarchical clustering of samples. A heatmap shows the clustering of the 20 Alzheimer’s disease (AD) and neurologically normal control (control) brain tissue samples based on their differential gene (transcript) expression (z-values). Samples are from the primary visual cortex (VIC) and precuneus (PREC); regions that are mildly- and moderately affected by tau pathology respectively in the AD brain at post-mortem. The colour scale shows transcripts that are upregulated (red) or downregulated (blue) relative to mean expression of all samples. Four control samples (PREC and VIC regions from IS43 and IS44) cluster with the cases.

Rank	GENCODE #	Gene symbol	Gene name	Log FC	p value (FDR adjusted)
1	ENSG00000185710	Non-coding	SMG1P4; SMG1 pseudogene 4	− 6.4	1.29E−19
2	ENSG00000226259	Non-coding	GTF2H2B; General transcription factor IIH subunit 2B	4.6	1.17E−12
3	ENSG00000275954	<i>TBC1D3F</i>	TBC1 domain family member 3F	− 10.5	2.13E−09
4	ENSG0000003989	<i>SLC7A2</i>	Solute carrier family 7, member 2	1.8	2.86E−09
5	ENSG00000138964	<i>PARVG</i>	Parvin gamma	1.4	3.93E−07
6	ENSG00000110077	<i>MS4A6A</i>	Membrane-spanning 4-domains, subfamily A, member 6A	1.4	1.27E−06
7	ENSG00000275830	Non-coding	AL355974.2	2.1	1.43E−06
8	ENSG00000211592	<i>IGKC</i>	Immunoglobulin kappa constant	3.9	1.43E−06
9	ENSG00000235833	Non-coding	AC017099.1	− 4.1	1.89E−06
10	ENSG00000152049	<i>KCNE4</i>	Potassium voltage-gated channel subfamily E regulatory subunit 4	1.6	2.2443E−06

Table 4. Top 10 most differentially expressed genes in the AD-PREC.

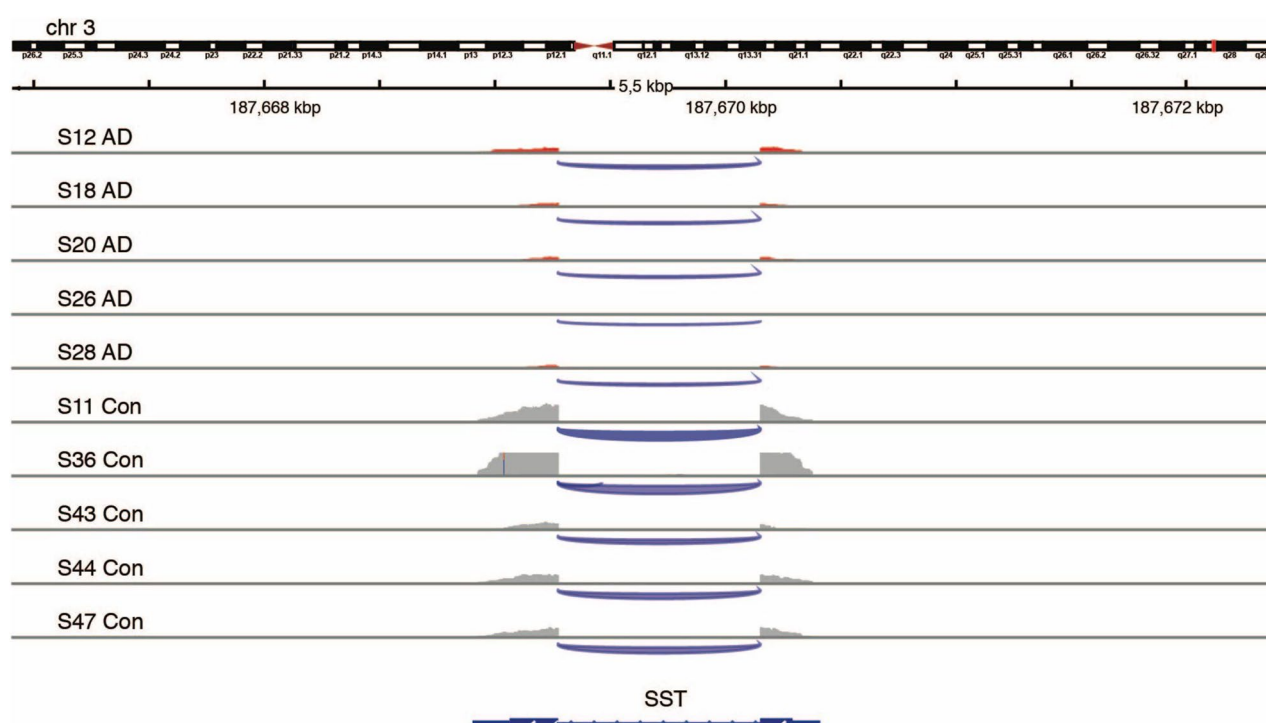


Figure 2. Downregulation of somatostatin gene expression in the precuneus of Alzheimer's disease brains. An Integrative Genomics Viewer (IGV)-derived image shows the comparative levels of reads from the two-exon somatostatin (*SST*)-encoding gene within the precuneus region of post-mortem brains from four Alzheimer's disease (AD) cases (upper tracks) and four controls (Con; lower tracks). (IGV ver. 2.3.91; Broad Institute).

molar ratio were prominent among the top DEGs and removed from further analysis. The top ten most significant DEGs in the AD-PREC included protein-coding transcripts: immunoglobulin kappa constant (*IGKC*), the cationic amino acid transporter (*SLC7A2*), parvin gamma (*PARVG*) and membrane-spanning 4-domains, subfamily A, member 6A (*MS4A6A*), a probable chemosensor expressed by microglia³⁶ (Table 4). *SST*, encoding the interneuron subtype marker somatostatin, was also downregulated in AD-PREC (ranked 14th, log FC = − 2.2, FDR adjusted *p* value = 6.9×10^{-6} (Fig. 2) consistent with immunohistochemical deficits in the AD brain³⁷.

Up- and down-regulated genes were combined for gene ontology (GO) analyses and this revealed two major themes among the enriched Biological Pathways (GO-BP): exocytosis and immune function (Table 5; Supplementary Table 3 for full list). Genes involved in exocytosis included *STXBP2*, encoding syntaxin binding protein 2 (log FC = 1.0, adj. *p* value = 0.02) and *NSF*, encoding protein N-ethylmaleimide-sensitive factor (log FC = − 1.1, adj. *p* value = 0.006) that are involved in SNARE complex assembly and disassembly respectively.

Primary visual cortex (VIC). There were 71 total and 44 protein-coding DEGs in the AD-VIC (adjusted *p* value < 0.05 Table 6; Supplementary Table 4 for full list). 40/71 DEGs in the AD-VIC brain region were differentially expressed in the same direction as in the AD-PREC suggesting similar responses to the presence of

GO term	Biological pathway	p value
GO:0006887	exocytosis	1.6E-12
GO:0032940	secretion by cell	6.2E-12
GO:0045055	regulated exocytosis	4.3E-11
GO:0046903	secretion	6.4E-11
GO:0042119	neutrophil activation	5.8E-09
GO:0002274	myeloid leukocyte activation	6.2E-09
GO:0036230	granulocyte activation	7.5E-09
GO:0043312	neutrophil degranulation	1.1E-08
GO:0002283	neutrophil activation involved in immune response	1.2E-08
GO:0006810	transport	2.1E-08

Table 5. Overrepresented gene ontology biological pathways in the AD-PREC.

Rank	GENCODE #	Gene symbol	Gene name	Log FC	p value (FDR adjusted)
1	ENSG00000185710	Non-coding	SMG1 pseudogene 4	-6.3	4.3E-18*
2	ENSG00000275954	<i>TBC1D3F</i>	TBC1 domain family member 3F	-13.3	3.1E-15*
3	ENSG00000205632	Non-coding	LINC01310	-2.0	2.6E-07
4	ENSG00000197728	<i>RPS26</i>	ribosomal protein S26	-1.2	3.5E-07
5	ENSG00000226259	Non-coding	General transcription factor IIH subunit 2B (pseudogene)	3.5	3.5E-07*
6	ENSG00000275830	Non-coding	AL355974.2	2.1	7.8E-06
7	ENSG00000116031	<i>CD207</i>	CD207 molecule, langerin	-5.8	1.4E-04
8	ENSG00000250770	Non-coding	AC005865.2	-1.5	1.5E-04
9	ENSG00000254269	Non-coding	CTD-2281E23.2	-1.9	1.5E-04
10	ENSG00000134201	<i>GSTM5</i>	Glutathione S-transferase mu 5	-1.4	1.6 E-04

Table 6. Top 10 most differentially expressed genes in the AD-VIC. *DEG in AD-PREC.

AD pathology. Overall, there was a high correlation between the direction of associations of all genes in the AD-PREC versus the AD-VIC ($r^2=0.35$) (Fig. 3). 27/462 protein coding genes were in common between the two regions including *TBC1D3F*, encoding TBC1 domain family member 3F, *RPS26* and *CD207*. There is little known about the putative oncogene *TBC1D3F*, while *CD207*, a receptor on antigen-presenting Langerhans cells in the skin, has very low expression in the brain. Other DEGs here included the microglial *PARVG* and *MS4A6A* ranked 5th and 6th among the PREC DEGs respectively.

Four immune-related GO-BPs in the AD-PREC were similarly among the top ten overrepresented pathways seen in the AD-VIC (Table 7; Supplementary Table 5 for full list).

With a 2.5-fold greater tau load compared to the AD-VIC, it was hypothesized that AD-PREC DEGs would include upregulated tau kinases and downregulated tau phosphatases³⁸. In particular, AD as a putative form of ‘Type 3 diabetes’⁷ would be consistent with impaired central insulin (PIK3-AKT) signalling and increased glycogen synthase kinase 3beta (GSK3 β) levels³⁹. Contrary to these hypotheses, *CDK5R2*, encoding a neuron-specific activator of the tau kinase cyclin dependent kinase 5, was downregulated, while the genes, phosphoinositide-3-kinase adaptor protein 1 (*PIK3AP1*) and phosphoinositide-3-kinase regulatory subunit 5 (*PIK3R5*), whose products promote PI3K activity, were both upregulated. Similarly, *INSR*, encoding the insulin receptor, and *IGF1R*, encoding the major IGF1 receptor, approached higher expression in the AD-PREC (unadjusted *p* values = 0.06 and 0.01 respectively).

Non-coding RNAs. 97/559 DEGs in the AD-PREC and 27/71 in AD-VIC were long non-coding transcripts included two of most significant DEGs in both regions: SMG1 pseudogene 4 (*SMG1P4*; ENSG00000185710; logFC = -6.4; FDR = 1.3×10^{-19}) and general transcription factor IIH subunit 2B (*GTF2H2B*; pseudogene; ENSG00000226259; logFC = 6.4; FDR = 1.2×10^{-12}).

ddPCR replication in a larger cohort. We selected eight protein-coding DEGs from the RNA-Seq study for validation in the full cohort of 26 AD cases and 22 controls: *SST*, *SLC7A2*, *TREM2*, *CXCR4* and *MS4A6A* and *PARVG*, *INSR* and *IGF1R*. As for the RNA-Seq cohort there was no difference in neuronal density between cases and controls for either region. However, both regions were characterised by higher A β areal fractions and more AT8-tau + ve neurons in the cases (Table 8). Among the cases, A β areal fractions were similar for both regions ($p=0.5$) but AT8-tau + ve neurons were higher in the PREC ($p=0.0009$) (Supplementary Table 1 for all quantitative neuropathology data; RNA-Seq samples in bold type).

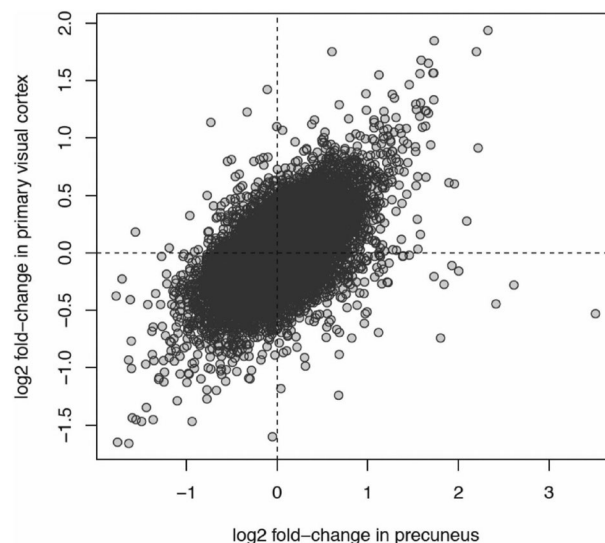


Figure 3. Correlation between Alzheimer's disease-associated genes in the precuneus versus the primary visual cortex. A scatter plot displays the positive correlation between differential expression of all transcripts in Alzheimer's disease and control post-mortem brains for the primary visual cortex (y-axis) versus the precuneus (x-axis). Each data point is a gene. The x-axis is the relative log₂ fold-change in mean expression between AD and control samples for the precuneus region. The y-axis is the relative log₂ fold-change in mean expression between AD and control samples for the primary visual cortex region. A gene with a positive fold-change has higher expression in AD samples. Genes in the upper-right and bottom-left quadrants of the plot have concordant changes in expression between AD and controls. The correlation between the fold-changes in both regions is $r^2 = 0.35$.

GO term	Biological Pathway	p value
GO:0002252	Immune effector process	1E-06
GO:0006952	Defense response	4E-06
GO:0050727	Regulation of inflammatory response	2E-05
GO:0006955	Immune response	6E-05
GO:0043312	Neutrophil degranulation	1E-04
GO:0002283	Neutrophil activation involved in immune response	1E-04
GO:0070613	Regulation of protein processing	1E-04
GO:0042119	Neutrophil activation	1E-04
GO:0002446	Neutrophil mediated immunity	1E-04
GO:1903317	Regulation of protein maturation	1E-04

Table 7. Top 10 overrepresented gene ontology biological pathways in AD_VIC.

Unlike the RNA sequencing samples, the mean RIN was significantly lower in the cases in both the PREC (mean RIN 4.1 ± 0.9 v. 5.2 ± 1.0 , $p = 0.0001$) and the VIC (AD mean RIN 4.2 ± 0.9 v controls mean RIN = 5.1 ± 1.21 ; $p = 0.003$) and required normalisation using the reference gene *GAPDH* and further adjustment for regional RIN using logistic regression. *SST* was significantly lower in the AD-PREC ($p < 0.0001$) while *TREM2* ($p < 0.0001$), *MS4A6A* ($p = 0.0004$) and *CXCR4* ($p = 0.003$) were higher in AD cases consistent with the RNA-Seq results (Fig. 4). Similar to RNA-Seq data, *SST* was lower in the AD-VIC ($p = 0.0001$), but neither *MS4A6A* nor *PARVG* were upregulated in the full cohort although *MS4A6A* was highly correlated with age ($p = 0.001$). In contrast to RNA-Seq results, both *INSR* ($p = 0.001$ and $p = 0.0001$) and *IGF1R* ($p = 0.0002$ and $p = 0.01$) were higher in the AD-PREC and AD-VIC respectively (Fig. 4) (Fig. 4). In the AD-VIC, *IGF1R* ($r^2 = 0.35$, $p = 0.002$), *SST* ($r^2 = 0.21$, $p = 0.02$) expression was correlated with tau-positive neurons; *PARVG* ($r^2 = 0.25$, $p = 0.02$) were correlated with residual neurons and *CXCR4* ($r^2 = 0.28$, $p = 0.007$) was correlated with A β areal fraction. There were no correlations between AD pathology and GOIs in the AD-PREC.

RNA-Seq validation—ROSMAP study data. The DEGs from the AD-PREC were compared with a recently published dataset from the Religious Orders Study and Memory and Aging Project (ROSMAP) study. The ROSMAP RNA-Seq data was from the dorsolateral prefrontal cortex from 478 individuals of varying cog-

Mean (S.D.)	AD (n = 26)	Control (n = 22)	p value
PREC—AT8-tau + ve neuron density (mm ²)	20 (14)	0	<0.0001
PREC—areal Aβ fraction	0.07 (0.05)	0.008 (0.008)	<0.0001
PREC—neuronal density (mm ²)	276 (56)	283 (63)	0.7
VIC—AT8-tau + ve neuron density (mm ²)	8 (9)	0	0.0003
VIC—areal Aβ fraction	0.07 (0.05)	0.002 (0.007)	<0.0001
VIC—neuronal density (mm ²)	309 (41)	278 (62)	0.06
PREC—RIN	4.1 (0.9)	5.2 (1.0)	0.0001
VIC—RIN	4.2 (0.9)	5.1 (1.2)	0.003
	PREC	VIC	p value
Inter-regional comparisons (cases only)			
Areal Aβ fraction	0.07 (0.05)	0.07 (0.05)	0.8
AT8-tau + ve neuron density	20 (14)	8 (9)	0.0009

Table 8. Quantification of AD neuropathology in the RNA-Seq cohort.

nitive function and pathological diagnoses including probable AD were originally analysed by a co-expression network technique³². Here we restricted the re-analysis to their two most disparate groups: Non-demented controls with no or low AD-type pathology (n = 117) versus demented individuals with intermediate or high AD pathology (n = 195). This revealed 3904 DEGs (3132 protein-coding) of which 203 were among the 462 protein-coding DEGs seen in the AD-PREC here. *SST* was downregulated and *INSR*, *CXCR4*, *SLC7A2* and *NFKB1A* were upregulated, respectively but *IGF1R*, *TREM2* and *MS4A6A* was not significantly different. The most prominent GO-BPs included ‘positive regulation of nucleic acid-templated transcription’ and ‘neurogenesis’ but there were no immune-related pathways affected.

Overlap with AD risk genes. Seyfried and colleagues previously described a strategy for determining if protein products of GWAS targets are enriched in gene expression data using the gene set analysis program called MAGMA³³. They reported 1234 that reached MAGMA GWAS significance using International Genomics of Alzheimer’s Project data³⁴. A chi-square analysis showed that AD-PREC DEGs were over-represented among their AD risk genes (overlap = 32; $p = 0.02$) but not in the AD-VIC (overlap = 3). Two GWAS targets, *MS4A6A* and *HLA-DRB5*, were in common to both regions (Supplementary Table 6).

Discussion

Pathological studies suggest that Aβ pathology develops concurrently across most cortical areas and plateaus early in the disease course¹⁰. In contrast, the severity of tau pathology is known to differ widely across the cortex, sparing the primary cortices¹², as demonstrated here by mildly-affected VIC versus the moderately-affected PREC. A comparison between such regions both within cases and between cases and controls may reveal the specific expression patterns associated with tau deposition.

Immune pathways strongly associate with mild AD. The upregulation of immune-related pathways and microglia-expressed genes such as *TREM2* and *MS4A6A*, along with *NFKB1A* (encoding NFKB inhibitor alpha) and *CXCR4* (encoding C-X-C motif chemokine receptor 4) here are consistent with both GWAS and transcriptomic studies^{40,41}. Specific gene changes were replicated by ddPCR in the AD-PREC but not the AD-VIC, although *MS4A6A* was correlated with age in the latter.

Similarly AD-PREC DEGs were significantly over-represented among known AD risk genes from GWAS³³ with immune-related *HLA-DRB5* and *MS4A6A* also among were among the 45 protein-coding DEGs in the AD-VIC. This overlaps suggests that both *HLA-DRB5* and *MS4A6A* influence AD pathogenesis through fine tuning of their gene expression levels. The ROSMAP study RNA-Seq data from the prefrontal cortex was mostly confirmatory with RNA-Seq results from the PREC here although *MS4A6A* or *TREM2* were not differentially expressed. In the original gene co-expression analysis of the ROSMAP RNA-Seq the reported ‘microglial module’, that did include *TREM2* and *MS4A6A*, was associated with age but not AD pathology or dementia status³². The module most associated with cognitive decline was enriched for genes involved in the ‘positive regulation of RNA metabolic process’. A similar pathway, ‘positive regulation of nucleic acid-templated transcription’ was the most enriched among the DEGs from our re-analysis of the ROSMAP data here.

This association between immune dysfunction and ageing, rather than AD status is consistent with our previous immunohistochemical studies of microglia morphology in the VIC, the superior frontal gyrus and the inferior temporal gyrus (ITG)⁴². This study, that also included one case here (IS38; Supplementary Table 1 for details) showed that activated microglia in the VIC and SFG, were associated with age but not disease status while the severely affected ITG in AD was characterised by a loss of normal (ramified) microglia. Although not reported, the PREC was also examined and showed the same associations between activated morphologies and age⁴². In contrast, controls with sufficient AD-type pathology to satisfy an intermediate likelihood of disease (according to current diagnostic criteria³) did have significantly more activated microglia than controls. Given the similarities in Aβ accumulation between the two regions it seems that disease-specific immune dysfunction may be more related to tau pathology as has been reported elsewhere for *TREM2* and *MS4A6A*⁴³. In contrast,

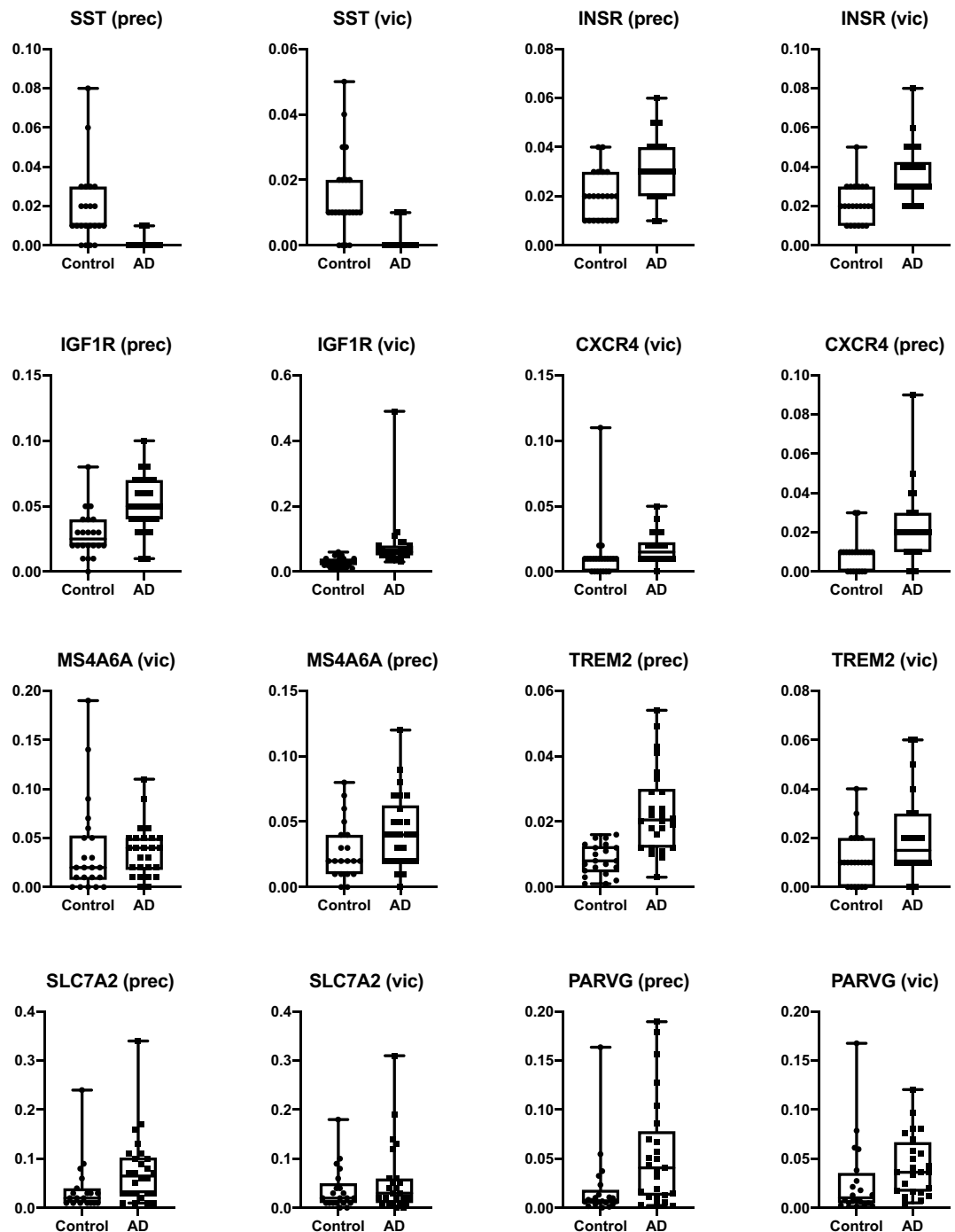


Figure 4. Validation of somatostatin and insulin/IGF1 signalling genes. Histograms show the differential expression, quantified by droplet digital (dd) PCR, of protein encoding genes that were differentially expressed in RNA-Seq: somatostatin (*SST*), insulin receptor (*INSR*), insulin-like growth factor 1 receptor (*IGF1R*), C-X-C motif chemokine receptor 4 (*CXCR4*), membrane spanning 4-domains A6A (*M4A6A*), triggering receptor expressed on myeloid cells 2 (*TREM2*), solute carrier family 7 member 2 (*SLC7A2*), parvin gamma (*PARVG*), in the precuneus (PREC) and primary visual cortex (VIC) of post-mortem brains from 26 Alzheimer's disease (AD) cases and 22 neurologically normal controls. This includes resampling of all individuals (n = 10) assayed by RNA-Seq.

the down regulation of *SST*, and upregulation of the insulin/IGF1 signalling pathway appear to be some of the earliest changes in the AD brain, or at least changes that prevent or limit tau pathology.

One of our major interests is to match the molecular findings from frozen post-mortem brain tissue to the immunohistochemical findings gathered from the mirror region in the contralateral hemisphere. This allows disease-specific changes to be further nuanced as either A β - or tau-related or related to residual neurons. Here correlations with pathology were only seen in the AD-VIC where the microglial- expressed *CXCR4* was related to A β load. *TREM2* and *IGF1* were associated with residual neurons and with tau pathology respectively but given that most neurons remain in the AD-VIC and tau-positive neurons are rare these correlations may prove to be spurious findings.

Transcriptomic support for dysfunctional exocytosis. Synaptic dynamics, another major theme from GWAS of AD, was also prominent in the AD-PREC but not AD-VIC⁴⁴. DEGs included *MEF2C* (encoding myocyte enhancer factor 2C)³⁴, which normally limits excessive synapse formation, and it was downregulated here. Similarly, DEGs included regulatory components of the SNARE (soluble NSF attachment protein receptor) protein complex, that facilitates membrane fusion of vesicles⁴⁵. *STXBP2*, whose encoded product, syntaxin binding protein 2, docks vesicles to membranes⁴⁶ was increased in AD-PREC, while N-ethylmaleimide-sensitive factor (NSF), a neuronally expressed ATP-ase³⁶ involved in disassembling docked vesicles⁴⁵ was reduced in AD-PREC. This is consistent with the increase of extracellular vesicles in AD brain⁴⁷ and increased synaptic activity enhancing tau propagation and tau pathology⁴⁸.

Genes associated with tau deposition. The major hypothesis tested in this study was that the combination of tau and A β pathology in the absence of neuronal loss meant that 'sick' or dysfunctional neurons would contribute substantially to the disease transcriptomic signature. A second hypothesis was that the greater tau load in the AD-PREC would result in greater changes in gene expression than those observed in the AD-VIC. More specifically, genes involved in tau hyperphosphorylation and NFT formation would be differentially expressed in the AD-PREC only or to a greater magnitude than seen in the AD-VIC. In support of our second hypothesis there were eightfold more DEGs in the AD-PREC, but on a background of similar changes in gene expression as indicated by the strong correlation between genes associated with AD in both areas. The differential expression of subunits of tau kinases CDK5 and PI3K are potentially consistent with the greater pathological tau load in the AD-PREC, although the direction of change for subunits of CDK5 (down) and PI3K (up) were opposite to what would have been predicted to result in the hyperphosphorylation of tau. In particular, the increase in PI3K components is consistent with increased PI3K/AKT signalling pathway and inhibition of another tau kinase, GSK3 β . Alternatively, these changes could represent efforts by residual cells to counter tau-related neurodegeneration. Liang et al.⁴⁹ came to this conclusion based on their microarray analysis of non-NFT bearing cortical neurons from the AD-VIC and five other regions of the AD brain. While they did not investigate the PREC, they reported more DEGs in areas with greater tau and A β pathology including entorhinal, hippocampal, middle temporal, superior frontal and posterior cingulate cortices. Specifically, they showed that *CDK5* was downregulated in all regions apart from the AD-VIC.

Insulin/IGF1 signalling upregulated early. It is not clear how diabetes modifies AD risk but it has been proposed that central insulin resistance in the AD brain, coined type 3 diabetes, leads to increased activity of the major tau kinase, GSK3 β ⁷. Furthermore, a rat study suggests that IGF1 infusion can rescue A β -dependent deficits in the hippocampal somatostatinergic system⁵⁰. Although not surviving correction for multiple comparisons in our RNA-Seq data, *INSR* and *IGF1R*, were upregulated in both regions of the AD brain according to ddPCR. *INSR*, but not *IGF1R*, was also differentially expressed in our re-analysis of the ROSMAP dataset. Yet an upregulation of insulin/IGF1 signalling machinery appears contrary to the idea of central insulin resistance or it represents a compensatory mechanism that is bolstering neuroprotection in areas of the AD brain yet to experience neuronal loss. Indeed a recent review of all *post-mortem* tissue studies favours an increase in PI3K/AKT activity which is consistent with a neuroprotective but ultimately inadequate response to the disease process³⁹.

Somatostatin—back to the future. The downregulation of the gene encoding somatostatin (*SST*) was particularly interesting given that early pathological studies have shown that both mRNA and protein levels were low across the AD brain^{37,51,52}. Somatostatin levels were also correlated with the reduction in choline acetyltransferase activity in AD and somatostatin-positive neurites have been reported within neuritic plaques⁵¹. From this work, somatostatin replacement therapy for AD was suggested in 1991⁵³, although it would be the augmentation of cholinergic activity through the use of acetylcholine esterase inhibitors that would ultimately reach the clinic⁵⁴. The lower *SST* levels reported here are also consistent with a recent meta-analysis of microarray data⁵⁵. Somatostatin is expressed by 30% of cortical interneurons, one of the three main GABAergic interneuron types in human cerebral cortex, the others expressing either parvalbumin (40%) or the serotonin receptor 5HT3a (30%)⁵⁶. Experiments in *SST* knock-out mice suggest that somatostatin-positive interneurons in the medial entorhinal cortex synapse with the dendrites of grid cells to maintain periodic spatial firing⁵⁷. Somatostatin-positive interneurons modulate excitatory input to principal neurons and are postulated to play a role in experience-dependent activity. Paradoxically, in an amyotrophic lateral sclerosis (ALS) and frontotemporal dementia (FTD) mouse model, hyperactive somatostatin interneurons led to disinhibition of layer 5 pyramidal neurons and excitotoxicity⁵⁸. The mechanism proposed was through the inhibition of nearby parvalbumin-positive interneurons. This disinhibitory circuit has also been shown to operate in layer 4 of the somatosensory cortex, in contrast to the direct inhibitory role of somatostatin interneurons towards layer 2/3 pyramidal cells⁵⁹. Although there are relatively few quantitative studies describing neuronal loss in the AD cortex the earliest neuronal loss probably occurs in layer 2/3^{60,61}. The downregulation of the gene encoding complexin 1 (*CPLX1*) and other molecules

involved in GABA neurotransmission such as those encoding the glutamic acid decarboxylases, *GAD1* and *GAD2*, seen in the AD-PREC is consistent a loss of inhibitory input⁶².

Non-coding RNAs. Two of the three most significant DEGs here were the non-coding transcripts *SMG1P4* and *GTF2H2B*. Although there are no known brain-specific data on these transcripts, SMG1 is also known as nonsense-mediated mRNA decay-associated PI3K-related kinase suggesting that *SMG1P4* might act in a regulatory capacity⁶³ similar to, and potentially affecting the same pathway as, the PTEN pseudogene, *PTENP1*⁶⁴. A downregulation of the *SMG1P4* would reduce SMG1 levels and promote PI3K/AKT activity. Alternatively, given the emerging role of splicing defects in AD including in tau, nonsense-mediated decay of mRNA may be a critical quality control mechanism^{65,66}. As more information is gained on lncRNAs and incorporated into databases the 'Pathway analysis' presented here and similar studies may be transformed.

Conclusion

These results suggest that 'early' responses to A β accumulation are relatively well tolerated and characterised by aberrant neuroimmune signalling. This same process is seen in the AD-PREC and AD-VIC with 27/44 protein-coding genes in common between the two regions all differentially expressed in the same direction and to the same degree. However, the presence of greater tau pathology in the AD-PREC is synonymous with an upregulation of vesicle exocytosis and we hypothesize that this represents increased excitatory activity as a result of dysfunction and probable loss of somatostatin-positive, inhibitory interneurons. While GABA-ergic function did not feature among these enriched pathways, *SST*, along with glutamate decarboxylases, *GAD1* and *GAD2*, *NSF* and *CPLX1* were all downregulated in the AD-PREC. Alternatively, the downregulation of *SST* in AD may represent the functional loss of an A β -interacting molecule that normally reduces the production of neurotoxic A β oligomeric species^{67,68}.

The hypothesis tested here was that case-control comparisons across differentially-affected areas of the AD brain that have plaques and NFTs but no, or minor neuronal loss, may allow early pathomechanisms to be elucidated from gene expression data. An alternative interpretation is that rather than being differentially affected by AD these two areas are differentially resistant to neuronal loss. The latter view is supported by the presence of supposedly dementia-stage cored plaques, neuritic plaques and NFTs in the 'spared' VIC¹³. If this latter interpretation is correct then the upregulation of immune function and downregulation of GABA-ergic, or specifically somatostatinergic transmission, seen here may be neuroprotective. Certainly our recent work showing that activated microglia are most prominent in non-demented high pathology controls is consistent with the latter⁴².

Differentiating between these two scenarios would be improved by a larger cohort and more regions, although it is not entirely clear whether the probable likelihood of one of these two competing scenarios could be determined by further post-mortem tissue studies alone. For example, the detection of broader and more extensive gene expression changes in severely affected regions of the AD brain will be complicated by relative neuronal loss. The inclusion of tissue from persons with MCI and subjective memory complaints from 'susceptible areas' like the entorhinal cortex as recently reported by Patel and colleagues could also be useful particularly if a neuroprotective interpretation is favoured⁶⁹. In their study, the transcriptome of high pathology controls in regions such as the entorhinal cortex was characterised by "overactivation" of the "glutamate-glutamine cycle" and disruption of the innate immune system and brain energy metabolism. Importantly, therapies based on either (promoting) a neuroprotective or (attenuating) a neurotoxic scenario must be linked to early detection, when augmenting or attenuating these processes can prevent the irreversible neuronal loss that characterises the symptomatic stages of AD.

Data availability

All data supporting the results in found within the Manuscript and accompanying Figures or in Supplementary Tables 1–6. All summary data generated in this study are included in this published article (and supplementary information files). The raw data has been submitted to the Sequence Read Archive (NCBI-SRA; <https://www.ncbi.nlm.nih.gov/sra>). The detailed scripts for all analyses are available at: https://github.com/gboris/AD_RNA-Seq.

Received: 15 March 2020; Accepted: 3 February 2021

Published online: 01 March 2021

References

1. Access Economics. Keeping Dementia Front of Mind: Incidence and Prevalence 2009–2050. Report for Alzheimer's Australia. (Canberra, 2009)
2. Jack, C. R. Jr. *et al.* Introduction to the recommendations from the National Institute on Aging-Alzheimer's Association workgroups on diagnostic guidelines for Alzheimer's disease. *Alzheimers Dement.* **7**, 257–262. <https://doi.org/10.1016/j.jalz.2011.03.004> (2011).
3. Montine, T. J. *et al.* National Institute on Aging-Alzheimer's Association guidelines for the neuropathologic assessment of Alzheimer's disease: A practical approach. *Acta Neuropathol.* **123**, 1–11. <https://doi.org/10.1007/s00401-011-0910-3> (2012).
4. Hardy, J. & Selkoe, D. J. The amyloid hypothesis of Alzheimer's disease: Progress and problems on the road to therapeutics. *Science* **297**, 353–356. <https://doi.org/10.1126/science.1072994> (2002).
5. Dubois, B. *et al.* Preclinical Alzheimer's disease: Definition, natural history, and diagnostic criteria. *Alzheimers Dement.* **12**, 292–323. <https://doi.org/10.1016/j.jalz.2016.02.002> (2016).
6. Gordon, B. A. *et al.* Spatial patterns of neuroimaging biomarker change in individuals from families with autosomal dominant Alzheimer's disease: A longitudinal study. *Lancet Neurol.* **17**, 241–250. [https://doi.org/10.1016/S1474-4422\(18\)30028-0](https://doi.org/10.1016/S1474-4422(18)30028-0) (2018).
7. Steen, E. *et al.* Impaired insulin and insulin-like growth factor expression and signaling mechanisms in Alzheimer's disease—is this type 3 diabetes?. *J. Alzheimers Dis.* **7**, 63–80 (2005).
8. de la Monte, S. M. Type 3 diabetes is sporadic Alzheimer's disease: Mini-review. *Eur. Neuropsychopharmacol.* **24**, 1954–1960. <https://doi.org/10.1016/j.euroneuro.2014.06.008> (2014).

9. Cross, D. A., Alessi, D. R., Cohen, P., Andjelkovich, M. & Hemmings, B. A. Inhibition of glycogen synthase kinase-3 by insulin mediated by protein kinase B. *Nature* **378**, 785–789. <https://doi.org/10.1038/378785a0> (1995).
10. Thal, D. R., Rub, U., Orantes, M. & Braak, H. Phases of A beta-deposition in the human brain and its relevance for the development of AD. *Neurology* **58**, 1791–1800 (2002).
11. Serrano-Pozo, A., Frosch, M. P., Masliah, E. & Hyman, B. T. Neuropathological alterations in Alzheimer disease. *Cold Spring Harb. Perspect. Med.* **1**, a006189. <https://doi.org/10.1101/cshperspect.a006189> (2011).
12. Braak, H. & Braak, E. Neuropathological staging of Alzheimer-related changes. *Acta Neuropathol. (Berl)* **82**, 239–259 (1991).
13. Dickson, T. C. & Vickers, J. C. The morphological phenotype of beta-amyloid plaques and associated neuritic changes in Alzheimer's disease. *Neuroscience* **105**, 99–107 (2001).
14. Wharton, S. B. *et al.* Epidemiological pathology of Tau in the ageing brain: application of staging for neurofibrillary tangles (BrainNet Europe protocol) to the MRC cognitive function and ageing brain study. *Acta Neuropathol. Commun.* **4**, 11. <https://doi.org/10.1186/s40478-016-0275-x> (2016).
15. Arriagada, P. V., Growdon, J. H., Hedley-Whyte, E. T. & Hyman, B. T. Neurofibrillary tangles but not senile plaques parallel duration and severity of Alzheimer's disease. *Neurology* **42**, 631–639 (1992).
16. Sutherland, G. T., Siebert, G. A., Kril, J. J. & Mellick, G. D. Knowing me, knowing you: Can a knowledge of risk factors for Alzheimer's disease prove useful in understanding the pathogenesis of Parkinson's disease? *J. Alzheimers Dis.* **25**, 395–415. <https://doi.org/10.3233/JAD-2011-110026> (2011).
17. Qureshi, I. A., Mattick, J. S. & Mehler, M. F. Long non-coding RNAs in nervous system function and disease. *Brain Res.* **1338**, 20–35. <https://doi.org/10.1016/j.brainres.2010.03.110> (2010).
18. Hargis, K. E. & Blalock, E. M. Transcriptional signatures of brain aging and Alzheimer's disease: What are our rodent models telling us? *Behav. Brain Res.* <https://doi.org/10.1016/j.bbr.2016.05.007> (2016).
19. Bai, B. *et al.* Deep multilayer brain proteomics identifies molecular networks in Alzheimer's disease progression. *Neuron* <https://doi.org/10.1016/j.neuron.2019.12.015> (2020).
20. Halliday, G. M., Double, K. L., Macdonald, V. & Kril, J. J. Identifying severely atrophic cortical subregions in Alzheimer's disease. *Neurobiol. Aging* **24**, 797–806 (2003).
21. Sutherland, G. T., Janitz, M. & Kril, J. J. Understanding the pathogenesis of Alzheimer's disease: Will RNA-Seq realize the promise of transcriptomics? *J. Neurochem.* **116**, 937–946. <https://doi.org/10.1111/j.1471-4159.2010.07157.x> (2011).
22. Mullane, K. & Williams, M. Alzheimer's disease (AD) therapeutics—2: Beyond amyloid—Re-defining AD and its causality to discover effective therapeutics. *Biochem. Pharmacol.* **158**, 376–401. <https://doi.org/10.1016/j.bcp.2018.09.027> (2018).
23. Mills, J. D. *et al.* The alternative splicing of the apolipoprotein E gene is unperturbed in the brains of Alzheimer's disease patients. *Mol. Biol. Rep.* **41**, 6365–6376. <https://doi.org/10.1007/s11033-014-3516-8> (2014).
24. Roussos, P., Guennewig, B., Kaczorowski, D. C., Barry, G. & Brennand, K. J. Activity-dependent changes in gene expression in schizophrenia human-induced pluripotent stem cell neurons. *JAMA Psychiatry* **73**, 1180–1188. <https://doi.org/10.1001/jamapsychiatry.2016.2575> (2016).
25. Dobin, A. & Gingeras, T. R. Mapping RNA-seq Reads with STAR. *Curr. Protoc. Bioinform.* **51**, 11–14. <https://doi.org/10.1002/0471250953.bi1114s51> (2015).
26. Li, B. & Dewey, C. N. RSEM: Accurate transcript quantification from RNA-Seq data with or without a reference genome. *BMC Bioinform.* **12**, 323. <https://doi.org/10.1186/1471-2105-12-323> (2011).
27. Robinson, M. D. & Oshlack, A. A scaling normalization method for differential expression analysis of RNA-seq data. *Genome Biol.* **11**, R25. <https://doi.org/10.1186/gb-2010-11-3-r25> (2010).
28. Robinson, M. D., McCarthy, D. J. & Smyth, G. K. edgeR: A Bioconductor package for differential expression analysis of digital gene expression data. *Bioinformatics* **26**, 139–140. <https://doi.org/10.1093/bioinformatics/btp616> (2010).
29. Bennett, D. A., Schneider, J. A., Arvanitakis, Z. & Wilson, R. S. Overview and findings from the religious orders study. *Curr. Alzheimer Res.* **9**, 628–645 (2012).
30. Boyle, P. A., Yu, L., Wilson, R. S., Schneider, J. A. & Bennett, D. A. Relation of neuropathology with cognitive decline among older persons without dementia. *Front Aging Neurosci.* **5**, 50. <https://doi.org/10.3389/fnagi.2013.00050> (2013).
31. NIA-Reagan Institute Working Group. Consensus recommendations for the postmortem diagnosis of Alzheimer's disease. The National Institute on Aging, and Reagan Institute Working Group on Diagnostic Criteria for the Neuropathological Assessment of Alzheimer's Disease. *Neurobiol. Aging* **18**, S1–2 (1997).
32. Mostafavi, S. *et al.* A molecular network of the aging human brain provides insights into the pathology and cognitive decline of Alzheimer's disease. *Nat. Neurosci.* **21**, 811–819. <https://doi.org/10.1038/s41593-018-0154-9> (2018).
33. Seyfried, N. T. *et al.* A multi-network approach identifies protein-specific co-expression in asymptomatic and symptomatic Alzheimer's disease. *Cell Syst.* **4**, 60–72. <https://doi.org/10.1016/j.cels.2016.11.006> (2016).
34. Lambert, J. C. *et al.* Meta-analysis of 74,046 individuals identifies 11 new susceptibility loci for Alzheimer's disease. *Nat. Genet.* **45**, 1452–1458. <https://doi.org/10.1038/ng.2802> (2013).
35. de Leeuw, C. A., Mooij, J. M., Heskes, T. & Posthuma, D. MAGMA: Generalized gene-set analysis of GWAS data. *PLoS Comput. Biol.* **11**, e1004219. <https://doi.org/10.1371/journal.pcbi.1004219> (2015).
36. Zhang, Y. *et al.* Purification and characterization of progenitor and mature human astrocytes reveals transcriptional and functional differences with mouse. *Neuron* **89**, 37–53. <https://doi.org/10.1016/j.neuron.2015.11.013> (2016).
37. Davies, P., Katzman, R. & Terry, R. D. Reduced somatostatin-like immunoreactivity in cerebral cortex from cases of Alzheimer disease and Alzheimer senile dementia. *Nature* **288**, 279–280 (1980).
38. Wang, J. Z., Xia, Y. Y., Grundke-Iqbal, I. & Iqbal, K. Abnormal hyperphosphorylation of tau: Sites, regulation, and molecular mechanism of neurofibrillary degeneration. *J. Alzheimers Dis.* **33**(Suppl 1), S123–139. <https://doi.org/10.3233/JAD-2012-129031> (2013).
39. Chami, B., Steel, A. J., De La Monte, S. M. & Sutherland, G. T. The rise and fall of insulin signaling in Alzheimer's disease. *Metab. Brain Dis.* <https://doi.org/10.1007/s11011-016-9806-1> (2016).
40. Efthymiou, A. G. & Goate, A. M. Late onset Alzheimer's disease genetics implicates microglial pathways in disease risk. *Mol. Neurodegener.* **12**, 43. <https://doi.org/10.1186/s13024-017-0184-x> (2017).
41. Jansen, I. E. *et al.* Genome-wide meta-analysis identifies new loci and functional pathways influencing Alzheimer's disease risk. *Nat. Genet.* **51**, 404–413. <https://doi.org/10.1038/s41588-018-0311-9> (2019).
42. Paasilta, P. J., Davies, D. S., Kril, J. J., Goldsburly, C. & Sutherland, G. T. The relationship between the morphological subtypes of microglia and Alzheimer's disease neuropathology. *Brain Pathol.* <https://doi.org/10.1111/bpa.12717> (2019).
43. Martiskainen, H. *et al.* Transcriptomics and mechanistic elucidation of Alzheimer's disease risk genes in the brain and in vitro models. *Neurobiol. Aging* **36**(1221), e1215–1228. <https://doi.org/10.1016/j.neurobiolaging.2014.09.003> (2015).
44. Dourlen, P., Kilinc, D., Malmanche, N., Chapuis, J. & Lambert, J. C. The new genetic landscape of Alzheimer's disease: From amyloid cascade to genetically driven synaptic failure hypothesis? *Acta Neuropathol.* <https://doi.org/10.1007/s00401-019-02004-0> (2019).
45. Cipriano, D. J. *et al.* Processive ATP-driven substrate disassembly by the N-ethylmaleimide-sensitive factor (NSF) molecular machine. *J. Biol. Chem.* **288**, 23436–23445. <https://doi.org/10.1074/jbc.M113.476705> (2013).
46. Borisovska, M. Syntaxins on granules promote docking of granules via interactions with munc18. *Sci. Rep.* **8**, 193. <https://doi.org/10.1038/s41598-017-18597-z> (2018).

47. Musunuri, S. *et al.* Increased levels of extracellular microvesicle markers and decreased levels of endocytic/exocytic proteins in the Alzheimer's disease brain. *J. Alzheimers Dis.* **54**, 1671–1686. <https://doi.org/10.3233/JAD-160271> (2016).
48. Wu, J. W. *et al.* Neuronal activity enhances tau propagation and tau pathology in vivo. *Nat. Neurosci.* **19**, 1085–1092. <https://doi.org/10.1038/nn.4328> (2016).
49. Liang, W. S. *et al.* Altered neuronal gene expression in brain regions differentially affected by Alzheimer's disease: A reference data set. *Physiol. Genomics* **33**, 240–256 (2008).
50. Aguado-Llera, D. *et al.* The protective effects of IGF-I against beta-Amyloid-related downregulation of hippocampal somatostatinergic system involve activation of akt and protein kinase A. *Neuroscience* **374**, 104–118. <https://doi.org/10.1016/j.neuroscience.2018.01.041> (2018).
51. Morrison, J. H., Rogers, J., Scherr, S., Benoit, R. & Bloom, F. E. Somatostatin immunoreactivity in neuritic plaques of Alzheimer's patients. *Nature* **314**, 90–92 (1985).
52. Roberts, G. W., Crow, T. J. & Polak, J. M. Location of neuronal tangles in somatostatin neurones in Alzheimer's disease. *Nature* **314**, 92–94 (1985).
53. Mouradian, M. M. *et al.* Somatostatin replacement therapy for Alzheimer dementia. *Ann. Neurol.* **30**, 610–613. <https://doi.org/10.1002/ana.410300415> (1991).
54. Douchamps, V. & Mathis, C. A second wind for the cholinergic system in Alzheimer's therapy. *Behav. Pharmacol.* **28**, 112–123. <https://doi.org/10.1097/FBP.0000000000000300> (2017).
55. Bai, Z. *et al.* AlzBase: An integrative database for gene dysregulation in Alzheimer's disease. *Mol. Neurobiol.* **53**, 310–319. <https://doi.org/10.1007/s12035-014-9011-3> (2016).
56. Rudy, B., Fishell, G., Lee, S. & Hjerling-Lefler, J. Three groups of interneurons account for nearly 100% of neocortical GABAergic neurons. *Dev. Neurobiol.* **71**, 45–61. <https://doi.org/10.1002/dneu.20853> (2011).
57. Miao, C., Cao, Q., Moser, M. & Moser, E. I. Parvalbumin and somatostatin interneurons control different space-coding networks in the medial entorhinal cortex. *Cell* <https://doi.org/10.1016/j.cell.2017.08.050> (2017).
58. Zhang, W. *et al.* Hyperactive somatostatin interneurons contribute to excitotoxicity in neurodegenerative disorders. *Nat. Neurosci.* **19**, 557–559. <https://doi.org/10.1038/nn.4257> (2016).
59. Xu, H., Jeong, H. Y., Tremblay, R. & Rudy, B. Neocortical somatostatin-expressing GABAergic interneurons disinhibit the thalamo-recipient layer 4. *Neuron* **77**, 155–167. <https://doi.org/10.1016/j.neuron.2012.11.004> (2013).
60. Gomez-Isla, T. *et al.* Neuronal loss correlates with but exceeds neurofibrillary tangles in Alzheimer's disease. *Ann. Neurol.* **41**, 17–24 (1997).
61. van de Nes, J. A., Nafe, R. & Schlote, W. Non-tau based neuronal degeneration in Alzheimer's disease—An immunocytochemical and quantitative study in the supragranular layers of the middle temporal neocortex. *Brain Res.* **1213**, 152–165. <https://doi.org/10.1016/j.brainres.2008.03.043> (2008).
62. Ramos-Miguel, A. *et al.* Presynaptic proteins complexin-I and complexin-II differentially influence cognitive function in early and late stages of Alzheimer's disease. *Acta Neuropathol.* **133**, 395–407. <https://doi.org/10.1007/s00401-016-1647-9> (2017).
63. Pink, R. C. *et al.* Pseudogenes: Pseudo-functional or key regulators in health and disease?. *RNA* **17**, 792–798. <https://doi.org/10.1261/rna.2658311> (2011).
64. Haddadi, N. *et al.* PTEN/PTENP1: 'Regulating the regulator of RTK-dependent PI3K/Akt signalling', new targets for cancer therapy. *Mol. Cancer* **17**, 37. <https://doi.org/10.1186/s12943-018-0803-3> (2018).
65. Bai, B. *et al.* U1 small nuclear ribonucleoprotein complex and RNA splicing alterations in Alzheimer's disease. *Proc. Natl. Acad. Sci. U S A* **110**, 16562–16567. <https://doi.org/10.1073/pnas.1310249110> (2013).
66. Hsieh, Y. C. *et al.* Tau-mediated disruption of the spliceosome triggers cryptic RNA splicing and neurodegeneration in Alzheimer's disease. *Cell Rep.* **29**, 301–316e310. <https://doi.org/10.1016/j.celrep.2019.08.104> (2019).
67. Wang, H. *et al.* Somatostatin binds to the human amyloid beta peptide and favors the formation of distinct oligomers. *Elife* <https://doi.org/10.7554/eLife.28401> (2017).
68. Solarski, M., Wang, H., Wille, H. & Schmitt-Ulms, G. Somatostatin in Alzheimer's disease: A new role for an old player. *Prion* **12**, 1–8. <https://doi.org/10.1080/19336896.2017.1405207> (2018).
69. Patel, H. *et al.* Transcriptomic analysis of probable asymptomatic and symptomatic Alzheimer brains. *Brain Behav. Immun.* <https://doi.org/10.1016/j.bbi.2019.05.009> (2019).

Acknowledgements

The authors would like to thank the brain donors and their families for their kind gift that has made this research possible. Tissues were received from the New South Wales Brain Banks (NSWBB) consisting of the NSW Brain Tissue Resource Centre at The University of Sydney and the Sydney Brain Bank at Neuroscience Research Australia which are supported by The University of New South Wales, Neuroscience Research Australia and the National Institute on Alcohol Abuse and Alcoholism of the National Institutes of Health under Award Number R28AA012725. Validation study data were provided by the Rush Alzheimer's Disease Center, Rush University Medical Center, Chicago. Data collection was supported through funding by NIA Grants: P30AG10161, R01AG15819, R01AG17917, R01AG30146, R01AG36836, U01AG32984, U01AG46152, the Illinois Department of Public Health, and the Translational Genomics Research Institute.

Author contributions

B.G. and J.L. contributed equally to the work. G.S., A.C. and B.G. designed the study, in conjunction with J.K. and G.H. L.M. prepared the libraries for sequencing. J.L. and P.P. performed the ddPCR assays and analyses. B.G. and A.M. performed primary and secondary analysis of RNA sequencing data. E.P., B.G. and G.S. performed the statistical analysis. B.G., J.L. and G.S. wrote the draft manuscript. All authors read, edited and approved the final manuscript.

Funding

GS was partly funded by a Sydney Medical School Foundation Fellowship.

Competing interests

The authors declare that they have no known competing interests. B.G. is a director of Pacific Analytics PTY LTD & SMRTR PTY LTD, Australia; a founding member of the International Cerebral Palsy Genetics Consortium and a member of the Australian Genomics Health Alliance.

Additional information

Supplementary Information The online version contains supplementary material available at <https://doi.org/10.1038/s41598-021-83872-z>.

Correspondence and requests for materials should be addressed to G.T.S.

Reprints and permissions information is available at www.nature.com/reprints.

Publisher's note Springer Nature remains neutral with regard to jurisdictional claims in published maps and institutional affiliations.



Open Access This article is licensed under a Creative Commons Attribution 4.0 International License, which permits use, sharing, adaptation, distribution and reproduction in any medium or format, as long as you give appropriate credit to the original author(s) and the source, provide a link to the Creative Commons licence, and indicate if changes were made. The images or other third party material in this article are included in the article's Creative Commons licence, unless indicated otherwise in a credit line to the material. If material is not included in the article's Creative Commons licence and your intended use is not permitted by statutory regulation or exceeds the permitted use, you will need to obtain permission directly from the copyright holder. To view a copy of this licence, visit <http://creativecommons.org/licenses/by/4.0/>.

© The Author(s) 2021